Establishment of Human Amniotic Fluid and Urine as Sources for Mesenchymal Stem Cells of Renal Origin with Versatile Regenerative Potential

Inaugural dissertation

for the attainment of the title of doctor
in the Faculty of Mathematics and Natural Sciences
at the Heinrich Heine University Düsseldorf

presented by

Md Shaifur Rahman
from Pabna, Bangladesh

Düsseldorf, November 2020

from the institute for Stem Cell Research and Regenerative Medicine
at the Heinrich Heine University Düsseldorf

Published by permission of the
Faculty of Mathematics and Natural Sciences at
Heinrich Heine University Düsseldorf

Supervisor: Professor Dr. James Adjaye
Co-supervisor: Professor Dr. Constantin Czekelius

Date of the oral examination: 24/03/2021

HEINRICH-HEINE-UNIVERSITÄT DÜSSELDORF

Abstract

Mathematisch-Naturwissenschaftliche Fakultät
Institut für Stammzellforschung und Regenerative Medizin
Doctor rerum naturalium

Establishment of Human Amniotic Fluid and Urine as Sources for Mesenchymal Stem Cells of Renal Origin with Versatile Regenerative Potential

by Md Shaifur Rahman

Investigations on stem cells and cell-based therapies are rising as an alternative of conventional treatment options. Amongst all cells, multipotent stem cells have been established as most promising for clinical uses. For instance, human mesenchymal stem cells (MSCs) have already been extensively examined in clinical trials and already have found their way into the clinic to a certain extend. MSCs are immune-privileged, able to self-renew, highly proliferative, and have a broad differentiation potential. Bone marrow (BM), adipose and early trimester amniotic fluid (AF) are well-established sources of MSCs with broad regenerative potential. However, shortage of donors and invasive collection procedures- are the limitations associated with risks and pain. Since numerous Caesarean sections are done each year, we used this opportunity to collect amniotic fluid without any additional risk for the mother and the foetus. Subsequently we isolated AF cells, cultured and characterized them. It could be shown that these cells fulfil the criteria for MSCs set by the International Society for Cellular Therapy (ISCT). Characteristically AF-MSCs able to adhere on plastic, possess fibroblastoid morphology, express cell surface markers CD73, CD90, and CD105, they are positive for Vimentin, CD133 and negative for E-Cadherin. *In vitro* AF-MSCs differentiate into bone, fat and cartilage cells. Furthermore, transcriptome analyses revealed similarities with foetal BM-derived MSCs. Thus, we confirmed third trimester AF as a non-invasive source of MSCs with regenerative potential for clinical applications.

Before using these cells in clinic, it is necessary to solve the controversial issues related to the exact origin of AF-MSCs; which was the focus in the second part of this work. We know that AF is mostly composed of foetal urine; logically we postulated that AF cells were exfoliated from foetal renal system and deposited in amniotic sac. Irrespective of media used, subpopulations of AF-MSCs were observed morphologically alike renal progenitors and expressed pluripotency-associated markers such as SSEA4, TRA-1-60, TRA-1-81 and c-KIT. Importantly, AF-MSCs express the key renal stem cell proteins SIX2 and CITED1, together with other renal markers when compared to commercially available kidney biopsy-derived renal cells (HREpCs). We also observed AF-MSCs have renal cell transporter functionality. Transcriptome analyses of AF-MSCs revealed more similarities with human kidney cells than with foetal MSCs, and the GO terms identified biological processes associated with kidney morphogenesis. Gene expression and semi-qPCR analysis indicated an increasing expression level and number of renal genes with gestational time, which reflects a synergistic relationship between renal gene expression and foetal nephrogenesis with pregnancy periods. To understand how self-renewal and gene-regulation maintenance of these cells is controlled in vitro, we activated WNT signaling using the GSK3ß inhibitor (CHIR99201). Upon this disruption of self-renewal, AF-MSCs were elongated in

morphology and had decreased c-KIT, SIX2 and CD133 expression. Taken above context together, third-trimester amniotic fluid could serve as a novel source of renal progenitor cells.

Increasing number of patients with kidney-associated dysfunctions urge for stem cell-based therapeutic options. Due to insufficient access to renal progenitor cells, finding alternatives sources of these cells is very important for not only cell-based therapeutic purpose but also for *in vitro* renal disease modelling and drug screening. Based on this need, the purpose of the third part of this thesis were investigations on adult human urine as a possible solution. It could be shown that adult human urine represents a non-invasive, repetitive, inexpensive and robust source of renal stem cells originating from the kidney. Like full term AF-MSCs, urine-derived renal progenitor cells (UdRPCs) are multipotent MSCs and express a subset of pluripotency-related proteins. Remarkably, UdRPCs express renal stem cell markers such as SIX2, CITED1, WT1 and show transporter functionality. Unmethylated CpG islands within the vicinity of *SIX2* 5′- regulatory region further denote their progenitor status. Transcriptome based cluster analysis revealed a clear-cut separation between undifferentiated UdRPCs and differentiated HREpCs. Differentiation of UdRPCs using CHIR99021 showed upregulation of WNT-associated genes- *AXIN2*, *JUN* and *NKD1*. In the self-renewal disrupted UdRPCs, a suppression of *FGF2*, *FGF7* and overexpression of *BMP7*, *BMP4* were identified at transcriptome level. To validate, downregulation of *SIX2* were detected in CHIR99021 treated as well as SU5402 (FGFR inhibitor) treated cells. Further analyses indicated that self-renewal of UdRPCs *in vitro* is sustained through FGF2-driven TGFβ-SMAD2/3 pathway. These SIX2+UdRPCs with known CYP2D6 status represents as a potential stem cell types which might be applicable for modelling renal-associated diseases, nephrotoxicity studies, drug screening and in future cell-replacement therapy.

Like full-term AF-MSCs, UdRPCs' are not pluripotent but express a subset of pluripotency-associated proteins which could facilitated swift converting of these cells into induced pluripotent stem cells (iPSCs). We generated stable AF-iPSCs and UdRPCs-iPSCs using nucleofection of episomal-based plasmids containing OCT4, SOX2, c-MYC, LIN28, and KLF4 without perturbations of TGFβ, MEK and GSK3β pathways. AF-iPSCs and UdRPCs-iPSCs can be used for renal disease modelling and 3D kidney organoid development.

In addition to the research on AF and urine-derived stem cells, we investigated the potential of iPSCs to generate cell types which are valuable for regenerative therapies. Primary MSCs obtained from adult donors are largely associated with several disadvantages such as ageing, limited autologous cell number and limited replicative potential in culture. To overcome this, the differentiated iPSCs into MSCs (iMSCs) could serve as an alternative of native MSCs. Induced MSCs possess all the criteria of bon-fide MSCs and overcome the ageing signature as it was derived through iPSCs. Upon transplantation of iMSCs together with the scaffold material CPG (calcium phosphate granule) into a proximal tibia defect of pigs a beneficial regenerative effect was identified which was similar to the treatment with autologous BMC (Bone marrow concentrate) together with CPG.

There is increasing interest on the fabrication of 3D scaffolds from naturally available osteo-conductive materials to mimic the structural support for bone defect improvement. Therefore, we engineered biocompatible porous scaffolds consist of hydroxyapatite, collagen and chitosan (Ha-Col1-Cs); and were found to improve defected maxillofacial mandible bone of rat upon grafting. For optimal and more

effective bone healing, a combination of AF-MSCs or uMSCs or iMSCs and Ha-Col1-Cs scaffolds need to be experimented for the repair of large bone defects.

As a further use of naturally available biomaterial, gels formulated from amnion, collagen and *Aloe vera* in different combinations and tested for their wound healing potency using an induced burn wound rat model. Application of the different gels could show a significant improved healing of the wound. Potentially these gels could be combined with stem cell derived skin cells to increase treatment effects. To study this, we were able to differentiate the full-term AF-MSCs into keratinocyte like cells (AF-KC) expressing epidermal markers- K5, K14 and K10.

Taken all together this study shows a broad range of stem cells sources and versatile application thereof. The findings of this study can contribute to drive forward regenerative medicine in various fields.

Zusammenfassung

Als Alternativen zu konventionellen Therapieansätzen besteht ein wachsendes Interesse an Stammzell- und zelluläre Therapien. Hierbei stellen multipotente Stammzellen die am besten etablierten Zellen für den Einsatz in der Klinik dar. Humane mesenchymale Zellen (MSCs) wurden bereits sehr umfassend in klinischen Studien analysiert und werden zu einem gewissen Maß schon im klinischen Alltag genutzt. MSCs sind immunprivilegiert, können sich selbst erneuern, sind hoch proliferativ und haben ein breites Differenzierungsspektrum. Knochenmark (BM), Fettgewebe und Fruchtwasser (AF) aus dem frühen Trimester sind etablierte Quellen für MSCs mit breitem regenerativem Potenzial. Jedoch sind diese Quellen mit einigen Limitierungen und Risiken verbunden, wie zum Beispiel die geringe Anzahl an Spendern und den nötigen invasiven Gewinnungsmethoden. Da jedes Jahr zahlreiche Geburten per Kaiserschnitt durchgeführt werden, haben wir während dieser Eingriffe Fruchtwasser ohne zusätzliches Risiko für die Mutter oder das Kind gewonnen. Anschließend haben wir Zellen aus dem Fruchtwasser isoliert, kultiviert und charakterisiert. Es konnte gezeigt werden, dass diese Zellen die Kriterien für MSCs von der Internationalen Gesellschaft für Zelluläre Therapie (ISCT) erfüllen. Diese AF-MSCs sind in der Lage auf Plastikoberflächen zu adhärieren, weisen eine fibroblastoide Morphologie auf, exprimieren Zelloberflächenmarker CD73, CD90 und CD105, sind positiv für Vimentin und CD133 und negativ für E-Cadherin. *In vitro* sind AF-MSCs in der Lage sich in Knochen-, Fett- und Knorpelzellen zu entwickeln. Zudem konnten Transkriptomanalysen Ähnlichkeiten zu fötalen MSCs aus dem Knochenmark zeigen. Somit konnten wir bestätigen, dass Fruchtwasser aus dem dritten Trimester als nicht-invasive Quelle für MSCs mit regenerativem Potenzial für klinische Applikationen genutzt werden kann.

Bevor diese Zellen in der Klinik eingesetzt werden können, ist es nötig die widersprüchlichen Berichte zur Herkunft dieser Zellen zu klären; dies stand im Fokus des zweiten Teils dieser Arbeit. Es ist bekannt, dass Fruchtwasser überwiegend aus fötalem Urin besteht. Daher haben wir logischerweise postuliert, dass Fruchtwasser Zellen aus dem fötalen renalen System ausgetreten sind und sich in der Fruchtblase angereichert haben. Unabhängig vom benutzten Medium waren die Populationen der AF-MSCs morphologisch ähnlich zu Nierenvorläuferzellen und exprimierten Pluripotenz-assoziierte Faktoren wie zum Beispiel SSEA4, TRA-1-60, TRA-1-81 und c-KIT. Besonders wichtig in diesem Zusammenhang ist, dass AF-MSCs die Schlüsselmarker von Nierenstammzellen, SIX2 und CITED1, exprimieren und zusätzlich weitere Nieren-spezifische Marker exprimieren; vergleichbar zu kommerziell verfügbaren Nierenzellen (HREpCs), die durch eine Nierenbiopsie gewonnen wurden. Zudem haben wir beobachtet, dass AF-MSCs nierenspezifische Transporter-Funktionen besitzen. Transkriptomanalysen von AF-MSCs zeigten mehr Ähnlichkeiten zu humanen Nierenzellen als zu fötalen MSCs und die GO Analyse identifizierte biologische Prozesse, die mit Nieren-Morphogenese assoziiert sind. Genexpressions- und qPCR-Analysen zeigten eine ansteigende Expression von nierenspezifischen Genen mit zunehmender Schwangerschaftsdauer, was die synergistische Beziehung von fötaler Nephrogenese und dem Schwangerschaftszeitpunkt unterstreicht. Um zu verstehen, wie die Aufrechterhaltung des Stammzellstatus und die Genregulation dieser Zellen *in vitro* kontrolliert wird, haben wir den WNT Signalweg durch die Zugabe des GSK3ß Inhibitors CHIR99201 angeregt. Durch diese Unterbrechung der Selbsterneuerungsfähigkeit der Zellen, wiesen AF-MSCs eine elongierte Morphologie auf und zeigten eine verringerte Expression von c-KIT, SIX2 und CD133. Zusammenfassend konnte somit gezeigt werden, dass Fruchtwasser aus dem dritten Trimester als neue Quelle für Nierenvorläuferzellen dienen kann.

Die steigende Anzahl an Patienten mit Nierenerkrankungen macht die Notwendigkeit von stammzellbasierten Therapien deutlich. Durch den unzureichenden Zugang zu Nierenvorläuferzellen, ist es wichtig alternative Quellen für diese Zellen zu finden. Dies ist nicht nur für die zelluläre Therapie,

sondern auch für die Modellierung von Krankheiten und die Medikamentenentwicklung wichtig. Basierend auf diesem Bedarf war das Ziel des dritten Teils dieser Arbeit, humanen Urin als mögliche alternative Zellquelle zu untersuchen. Es konnte gezeigt werden, dass Urin von Erwachsenen eine nicht-invasive, unbegrenzt-verfügbare und robuste Quelle für Stammzellen aus der Niere darstellt. Wie AF-MSCs aus dem Fruchtwasser, sind renale Vorläuferzellen aus dem Urin (UdRPCs) multipotente MSCs, die einige Pluripotenz-assoziierte Proteine exprimieren. Erstaunlicherweise exprimieren UdRPCs Nierenstammzellmarker SIX2, CITED1, WT1 und zeigen Transporter-Funktionalität. Unmethylierte CpG Inseln in der Nähe der *SIX2* 5‘ regulatorischen Region unterstreichen ebenfalls ihren Vorläuferzell-Status. Die auf Transkriptom-Analysen basierten Cluster- Analysen, zeigten eine klare Trennung zwischen undifferenzierten UdRPCs und den differenzierten HREpCs. Die Differenzierung von UdRPCs durch den Einsatz von CHIR99021 resultierte in einer Hochregulation von WNT-assoziierten Genen- *AXIN2*, *JUN* und *NKD1*. Ebenfalls wurde in den UdRPCs, in denen die Selbsterneuerungsfähigkeit gestört wurde, eine Suppression von *FGF2*, *FGF7* und eine Überexpression von *BMP7*, *BMP4* auf Transkriptom-Ebene festgestellt. Als ein weiterer Beweis wurde die SIX2-Runterregulierung nicht nur in CHIR99021 behandelten Zellen, sondern auch in Zellen festgestellt, die mit dem FGFR Inhibitor SU5402 behandelt wurden. Weitere Analysen gaben Hinweis darauf, dass die Selbsterneuerung von UdRPCs *in vitro* durch den FGF2 angetriebenen TGFβ-SMAD2/3 Signalweg aufrechterhalten wird. Diese $SIX2^+$ UdRPCs repräsentieren einen Stammzelltyp, der sich für den Einsatz in der Modellierung von Erkrankungen die mit der Niere assoziierten sind, sowie in Nephrotoxizitäts-Studien, Medikamenten Screenings und für zelluläre Therapien der Niere eignen könnte.

Genau wie AF-MSCs sind UdRPCs nicht pluripotent. Allerdings exprimieren sie jedoch einige Pluripotenz-assoziierten Proteinen, die es ermöglichen, diese Zellen schneller und effizienter in induzierte pluripotente Stammzellen (iPSCs) zu reprogrammieren. So haben wir stabile AF-iPSCs und UdRPC-iPSCs durch die Nukleofektion mit episomalen Plasmiden, mit den Genen OCT4, SOX2, c-MYC, LIN28, und KLF4 ohne Modifikationen von TGFβ-, MEK- und GSK3β-Signalwegen, generiert. AF-iPSCs und UdRPC-iPSCs können für das Modellieren von Nierenkrankheiten und die Entwicklung von 3D-Nieren-Organoiden eingesetzt werden.

Zusätzlich zu der Forschung an Stammzellen aus dem Fruchtwasser und aus dem Urin, haben wir iPSCs auf ihr Potenzial zur Generierung anderer Zelltypen, die für regenerative Therapien interessant sein könnten, hin untersucht. Primäre MSCs von erwachsenen Spendern sind mit einer Vielzahl von Einschränkungen assoziiert, wie etwa Alterung, limitierte autologe Zellmenge und dem limitierten Wachstumspotenzial in Kultur. Um diese Einschränkungen zu überwinden, können iPSCs in MSCs (iMSCs) differenziert werden. Induzierte MSCs besitzen allen Kriterien von *bona fide* MSCs und überwinden die einschränkende Alterungssignatur. Durch die Transplantation von iMSCs mit dem Trägermaterial CPG (Kalzium Phosphat Granulat) in einen proximalen Tibia Defekt konnte ein regenerativer Effekt in Schweinen gezeigt werden, dieser war vergleichbar mit der Behandlung von CPG kombiniert mit autologen Knochenmarkkonzentrat (BMC).

Es gibt steigendes Interesse an der Herstellung von 3D Trägermaterialien von natürlich verfügbaren osteokonduktiven Materialien, um strukturelle Unterstützung für die Verbesserung der Heilung eines Knochendefekts zu bewirken. Dafür haben wir biokompatible, poröse Trägermaterialien bestehend aus Hydroxyapatit, Kollagen und Chitosan (Ha-Col1-Cs) hergestellt. Wir konnten zeigen, dass der Einsatz dieses Trägermaterials die Regeneration eines maxillofazialen, mandibulären Knochendefektes in Ratten begünstigte. Für eine noch bessere Regeneration von Defekten an großen Knochen sollte eine Kombination aus AF-MSCs, uMSCs oder iMSCs und dem Trägermaterial Ha-Col1-Cs untersucht werden.

Als weitere Einsatzmöglichkeit von natürlich verfügbaren Biomaterialien wurden Gele aus Amnion, Kollagen und *Aloe Vera* in verschiedenen Kombinationen auf ihre Fähigkeit zur Wundheilung in einem Modell in Ratten eingesetzt. Der Einsatz der verschiedenen Gele konnte eine verbesserte Heilung zeigen. Die Kombination dieser Gele mit Hautzellen, welche aus Stammzellen differenziert wurden, könnte den Therapieerfolg erhöhen. Um dies zu untersuchen, haben wir AF-MSCs in Keratinozyten-ähnliche Zellen (AF-KC) differenziert, die die epidermalen Marker K5, K14 und K10 exprimierten.

Zusammengenommen zeigt diese Arbeit ein breites Spektrum an Stammzell-Quellen und deren vielfältigen Einsatzmöglichkeiten. Die Ergebnisse dieser Arbeit könnten dabei helfen, die regenerative Medizin in den verschiedensten Feldern voranzubringen.

Table of Contents

List of Tables

1. Introduction

2. Results- Publications

2.5 Stem cell therapy

2.9 Characterization of burn wound healing gel prepared from human amniotic membrane and *Aloe vera* extract

2.10 Amnion and collagen-based blended hydrogel improves burn healing efficacy on a rat skin wound model in the presence of wound dressing biomembrane

List of Figures

1. Introduction

2. Results - Publications

2.1 Isolation and molecular characterization of amniotic fluid-derived mesenchymal stem cells obtained from Caesarean sections

2.2 The presence of human mesenchymal stem cells of renal origin in amniotic fluid increases with gestational time

2.3 Urine-derived stem cells as innovative platform for drug testing and disease modelling

2.4 The FGF, TGFβ and WNT axis modulate self-renewal of human $SIX2^+$ urine derived renal progenitor cells

Abbreviations

AD-MSCs	Adipose-derived mesenchymal stem cells
AF	Amniotic fluid
AFCs	Amniotic fluid cells
AF-MSCs	Amniotic fluid mesenchymal stem cells
AFSC-K	Amniotic fluid stem cells derived keratinocyte
AF-MSCs-K	Amniotic fluid mesenchymal stem cells derived keratinocyte
AFP	α-Fetoprotein
AFSCs	Amniotic fluid stem cells
AKI	Acute kidney injury
ALK	Activin receptor-like kinase
AM	Amniotic membrane
Ang	Angiopoietin
ATF2	Activating transcription factor 2
ATMPs	Advanced therapy medicinal products
AXIN2	Axis inhibition protein 2
AV	*Aloe vera*
αMEM	Alfa modified eagles medium
BD	Beta defensins
bFGF/FGF2	Basic fibroblast growth factor
BMC	Bone marrow concentrate
BM-MSC	Bone marrow-derived mesenchymal stem cell
BMP7	Bone Morphogenetic Protein 7
BRN1	POU class 3 homeobox 3
BSA	Bovine serum albumin
CAS9	CRISPR-Associated endonuclease 9
CB-MSCs	Cord blood-derived mesenchymal stem cells
CCL2	C-C motif chemokine ligand 2
CD	Cluster of differentiation
CD2AP	CD2-associated protein
cDNA	Complementary deoxyribonucleic acid
CDKN1C	Cyclin Dependent Kinase Inhibitor 1C
CHIR 99021	6-((2-((4-(2,4-Dichlorophenyl)-5-(4-methyl-1H-imidazol-2-yl) pyrimidin-2-yl) amino) ethyl) amino) nicotinonitrile
CITED1	Cbp/p300-interacting transactivator 1
CK18	Cytokeratin 18
CK19	Cytokeratin 19
CKD	Chronic kidney disease
c-Myc	Myelocytomatosis viral oncogene homologue
CNS	Central nervous system
COVID-19	Coronavirus disease 2019
CPG	Calcium phosphate granules
CpG	5'-Cytosine-phosphate-Guanine-3'

CRISPR	Clustered regularly interspaced short palindromic repeats
C-section	Caesarean section
CTNNB1	Catenin Beta 1
CXCL	C-X-C motif chemokine ligand
CYP	Cytochromes P450
CYP2D6	Cytochrome P450 family 2 subfamily D member 6
DAB	3, 3'-Diaminobenzidine
DAVID	Database for Annotation, Visualization and Integrated Discovery
DE	Definitive endoderm
DNA	Deoxyribonucleic acid
DNMT3B	DNA Methyltransferase 3 Beta
EB	Embryoid Body
E-Cad	Epithelial Cadherin
EGF	Epidermal growth factor
EMT	Epithelial-to-mesenchymal transition
ESCs	Embryonic stem cells
et al.	et alia (and others)
FACS	Fluorescence-activated cell sorting
FGF	Fibroblast growth factor
FISH	Fluorescence in situ hybridization
fMSCs	Fetal mesenchymal stem cells
GATA2	GATA Binding Protein 2
GCNT2	Glucosaminyl (N-Acetyl) Transferase 2
GEO	Gene Expression Omnibus
GM-CSF	Granulocyte-macrophage colony-stimulating factor
GMP	Good manufacturing practice
GO	Gene ontology
GSK-3ß	Glycogen synthase kinase 3 beta (serine/threonine kinase glycogen synthase kinase-3 beta)
GvHD	Graft versus Host Disease
Ha-Col1-Cs	Hydroxyapatite-collagen 1-chitosan
HaCaT	Ha = human adult, Ca = calcium, T = temperature
HFF	Human foreskin fibroblasts
HGF	Hepatocyte growth factor
HLA	Human leukocyte antigen
HLA-DR	Human Leukocyte Antigen – DR isotype
HLCs	Hepatocyte-like cells
HREpCs	Human renal epithelial cell
ICAM	Intercellular adhesion molecule
IDO	Indoleamine 2,3-dioxygenase
IFNγ	Interferon-γ
IGF	Insulin like growth factor
IL	Interleukin
iMSCs	iPSC-derived mesenchymal stem cells

INHBE	Inhibin Subunit Beta E
IP-10	CXCL10
iPSCs	Induced pluripotent stem cells
ISCT	International society for cellular therapy
ISRM	Institut für Stammzellforschung und Regenerative Medizin
JNK	c-Jun N-terminal kinases
JUN	Jun Proto-Oncogene AP-1 Transcription Factor Subunit
K	cytokeratin
KEGG	Kyoto Encyclopaedia of Genes and Genomes
KLF4	Krueppel-like factor 4
kPMSC	Kidney progenitor mesenchymal stem cell
LATS2	Large tumor suppressor kinase 2
LHX1	LIM homeobox 1
LIN28	Lin-28 homologue A (*C. elegans*)
LL37	Human cathelicidin
MAPK	Mitogen-activated protein kinase
MCP	Monocyte chemoattractant protein
MEK	Mitogen-activated protein kinase
MET	Mesenchymal-to-epithelial transition
MHC	Major histocompatibility complex
MIF	Macrophage migration inhibitory factor
mRNA	Messenger ribonucleic acid
MSC	Mesenchymal stem cell
NANOG	Nanog homeobox
NCT	Number on Clinical Trial
NKD1	Naked cuticle 1 (NKD Inhibitor of WNT Signaling Pathway 1)
NO	Nitric oxide
NPHS2	Nephrotic syndrome type 2 (Nephrosis 2)
OCT4	Octamer-binding protein 4/POU class 5 homeobox 1
OXPHOS	Oxidative phosphorylation
OSR1	Odd-Skipped Related Transcription Factor 1
PAN	Protein association network
PAX2	Paired box gene 2
PAX8	Paired-Box-Protein 8
PBS	Phosphate buffered saline
PCR	Polymerase chain reaction
PDGF	Platelet-derived growth factor
PD0325901	N-[(2R)-2,3-dihydroxypropoxy]-3,4-difluoro-2-[(2-fluoro-4 iodophenyl) amino]-benzamide (Mirdametinib)
PGE2	Prostaglandin E2
PODXL	Podocalyxin-like protein 1
POU5F1B	POU class 5 homeobox 1B
PPI	Protein protein interaction
PSC	Pluripotent stem cell

qRT-PCR	Quantitative real time PCR
RA	Retinoic acid
RCM	Renal cell medium
REGM	Renal epithelial growth medium
RNA	Ribonucleic acid
ROS	Reactive oxygen species
RT	Room temperature
RUNX2	Runt-related transcription factor 2
SARS-CoV-2	Severe acute respiratory syndrome coronavirus 2
SB431542	4-[4-(1,3-benzodioxol-5-yl)-5-(2-pyridinyl)-1H-imidazol-2-yl] benzamide
SDF-1	Stromal cell-derived factor 1
SERPINE1	Serine protease inhibitor 1
SIX2	Sine oculis homeobox homolog 2
SMAD	Small Mothers Against Decapentaplegic
SOX2	Sex-determining region Y (SRY)-box 2
srRNA	Small regulatory RNA
SRY	Sex determining region Y
SSEA4	Stage-specific embryonic antigen 4
STAT3	Signal transducer and activator of transcription 3
SU5402	2-[(1,2-Dihydro-2-oxo-3H-indol-3-ylidene) methyl]-4-methyl-1H-pyrrole-3-propanoic acid
T1	First trimester
T2	Second trimester
T3	Third trimester
T18	Trisomy on chromosome 18
T20	Trisomy on chromosome 20
TGFβ	Transforming growth factor beta
TNF-α	Tumor necrosis factor α
TRA-1-60	Tumor-related antigen-1-60
TRA-1-81	Tumor-related antigen-1-81
UC-MSCs	Umbilical cord-derived mesenchymal stem cell
uMSCs	Urine-derived mesenchymal stem cells
UdRPCs	Urine-derived renal progenitor cells
UK	United Kingdom
UM51	Urine male age 51
USA	United States of America
USCs	Urine stem cells
VEGF	Vascular endothelial growth factor
WNT	Wingless-related integration site
WNT3a	Wingless-type MMTV integration site family, member
WT1	Wilms' tumor protein 1

1. Introduction

1.1 Stem Cells

The cell is a small, structural, and functional biological entity that contains the molecular basis of life. Multicellular organism such as humans contain various cell types, which differ from each other based on morphology, functional characteristics and tissue or organ specific localization [Dubich and Wirth, 2018; Bianconi *et al*., 2013]. These distinct cells are generated from an unspecialized cell type called stem cells, which differentiate spatiotemporally during early development and finally build up the fully functional organism. Later in adult life, stem cells can replenish injured, damaged, and dysfunctional tissues and play vital roles to maintain tissue/ organ specific functionality and homeostasis [Atala and Lanza, 2012] (Figure 1A). Through asymmetric cell division, one stem cell can give rise to a differentiated cell and an undifferentiated stem cell on another branch with identical characteristics of the mother cell, or stem cells can self-renew by symmetrical division pattern where they produce two undifferentiated stem cells [Morrison and Kimble, 2006; Barui and Datta, 2019]. Stem cells reside in a specialized dynamic microenvironment within the tissue, called the stem cell niche, where they interact with other cell types in addition to fate regulating molecular factors. A plethora of cellular and acellular molecular cues within the stem cell niche play important roles to sustain the undifferentiated highly plastic self-renewable state and promote their proliferation and differentiation potential [Donnelly *et al*., 2018; Chacón-Martínez *et al*., 2018; Morrison and Spradling, 2008].

In terms of differentiation potential, stem cells are broadly classified into three major groups. There are totipotent stem cells, which are sourced from early development from fertilized egg-zygote or early morula. These stem cells can differentiate into any of the 220 cell types found in human body including the extraembryonic tissues [Mitalipov and Wolf, 2009]. Stem cells can also be pluripotent. This type of stem cells is capable of forming all the three germ layers; ectoderm endoderm and mesoderm. The pluripotent stem cells (PSCs) can be isolated from inner cell mass of the blastocyst (embryonic stem cells, ESCs) or by *in vitro* reprogramming (inserting transcription factors OCT4, KLF4, NANOG, C-MYC, and SOX2) of adult cells into induced pluripotent stem cells (iPSCs) to regain the properties of ESCs [Takahashi and Yamanaka, 2006; Takahashi et al., 2007] (Figure 1B). Multipotent stem cells can develop into a limited range with a very specialized cell lineage. Researchers have discovered several sources of the lineage-restricted multipotent stem cells, and in general, named after their tissue of origin [Sobhani *et al*., 2017]. Unless triggered intrinsically to differentiate for specific biological

function in a tissue/organ system whenever required, adult stem cells can persist in an undifferentiated quiescent state throughout adult life [Cheung and Rando *et al*., 2013].

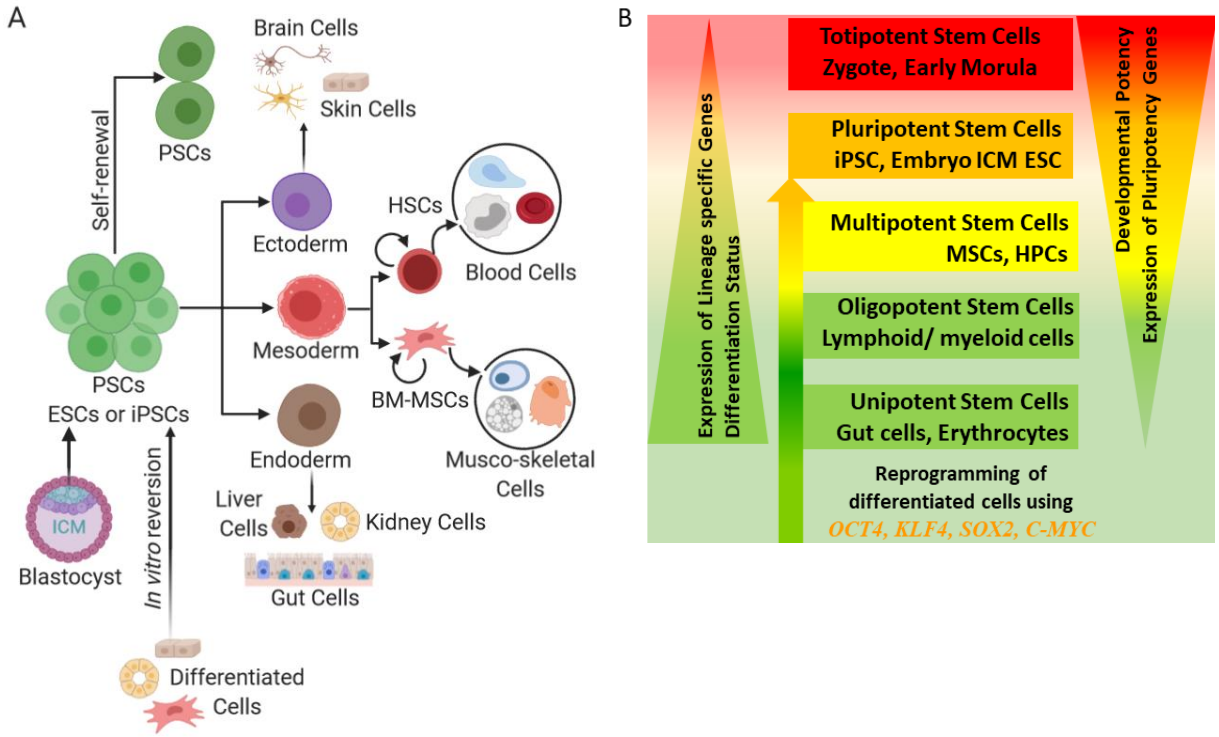

Figure 1: Stem cell self–renewal/ differentiation potential and hierarchical classification based on plasticity. [A] Pluripotent stem cells (ESC- present in the inner cell mass (ICM) of blastocyst stage) or iPSCs (*in vitro* reversion of differentiated cells into PSC) can self-renew via symmetric or asymmetric division. During differentiation, PSC become specialized at each step (step 1: Formation of the ectodermal, endodermal, and mesodermal lineages excluding placenta) and they maintain their own progeny (self-renewal). Later on, these tri-lineage germ lines can develop into a specialized cell lineage called multipotent stem cells, and/ or finally, these cells differentiate into tissue or organ specific functional cell types. For example, Ectodermal lines provide brain cells-neuron, astrocytes, and skin cells-keratinocytes; Mesodermal lineage can differentiate into blood cells-RBC, lymphocytes or musculoskeletal cells-osteocyte, chondrocyte; and Endoderm can become renal cells, tubular cells, liver cells-hepatocyte, lung epithelial cells. Figure 1A was prepared using the BioRender platform [https://biorender.com]. **[B]** Hierarchical comparison between stem cell types based on their level of potency including examples. The highest potent cells are totipotent stem cells, which can be found in early morula. The least potent or terminally differentiated stem cells are uni-potent stem cells such as red blood cells or gut cells. The highest potential means highest developmental potency and is associated with elevated expression levels of the pluripotency factors whereas minimal expression of lineage specific genes.

Due to ethical issues, the use of multipotent stem cells in research and therapy is a more accepted approach than using ESCs, because the derivation of multipotent cell does not require the destruction of an embryo. Multipotent stem cells are present in the human body at all stages of foetal, young and adult life (Figure 2). For example, amniotic fluid and umbilical cord are notable sources of foetal stem cells, which are multipotent**.** Adult/ somatic multipotent cells can be found in most of the human tissues/organ such as kidney and musculoskeletal system. Bone marrow and adipose tissue are two well-known sources of multipotent adult somatic stem cells

[Petrenko *et al*., 2020; Berebichez-Fridman and Montero-Olvera, 2018]. Among all multipotent stem cells, mesenchymal stem cells (MSCs) are considered the most promising candidate for future clinical applications in regenerative cell-based therapeutics.

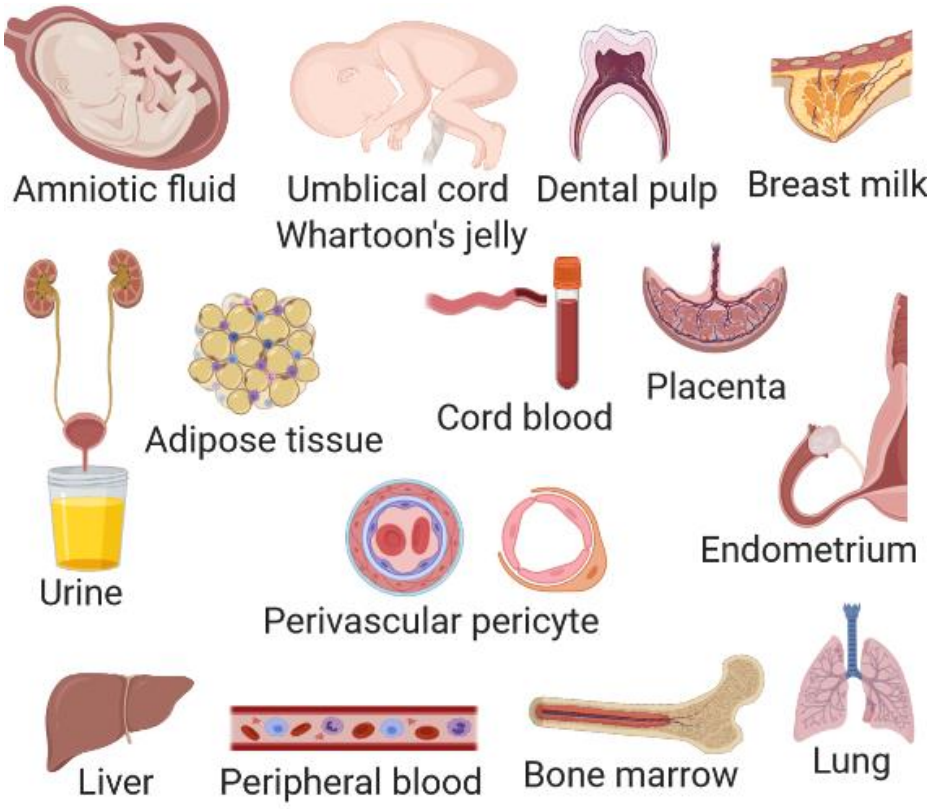

Figure 2: The most common sources of multipotent stem cells. Multipotent cells can be isolated from amniotic fluid, umbilical cord, Wharton's jelly, adipose tissue, cord blood, endometrium, bone marrow, placenta, urine, lung, kidney, liver, peripheral blood, perivascular pericytes, dental pulp and breast milk. Figure designed on BioRender platform [https://biorender.com].

1.2 Mesenchymal Stem Cells (MSCs)

Mesenchymal stem cells (MSCs) are plastic-adherent, spindle-shaped fibroblastoid cells which can be found in the foetal, in children and in the tissues of adults. Characteristically, these self-renewing stem cells have a high plasticity, and show their multipotency by terminally differentiating into cells of the mesoderm lineage; bone (osteoblasts), cartilage (chondrocytes) and fat cells (adipocytes) [Ullah *et al*., 2015]. In contrast to epithelial progenitors, MSCs are Vimentin positive and negative for the typical epithelial protein E-Cadherin [Spitzhorn *et al*., 2017]. Historically, in 1924, morphologist Alexander A. Maximov first reported a fibroblast like precursor cell within bone marrow and described it as hematopoietic supportive cells [Sell, 2013]. Later, in 1970, Friendenstein and his colleagues isolated fibroblastic mesenchymal cells from mouse bone marrow and showed its ability to grow on plastic plates with high proliferative potential. Additionally, they demonstrated the cells' differentiation capability into bone *in vitro* [Friedenstein *et al*., 1976]. Arnold I. Caplan in the 1990 has coined the term "mesenchymal

stem cells" (MSCs) to refer to these cells [Caplan, 1991]. Interestingly, these cells express cluster of differentiation CD105, CD73, CD90 but not hematopoietic antigens. MSCs have an inherent immunomodulatory nature such as anti-inflammatory properties, escape immune recognition and have immunosuppressive effects [Ankrum *et al*., 2014]. Pro-inflammatory cytokines such as IFN-γ, TNF-α, IL-1α or IL-1β stimulate MSCs to induce the secretion of TGF-β1, COX-2, PGE2, HGF, IDO, NO and IL-10 are reported to convey their immunosuppressive effect [Noronha *et al*., 2019]. MSCs support regeneration processes by the release of distinct biomolecules- VEGF-A, IL, and PDGF. Furthermore, MSCs can migrate into sites of inflammation or injury to support the healing process by interacting with the factors released within the injured niche [Ullah *et al*., 2019]. Moreover, MSCs secrete several antibacterial peptides such as human cathelicidin, β-defensins, lipocalin 2 and hepcidin [Alcayaga-Miranda *et al*., 2017]. These functional properties make these cells very attractive for cell-based therapy (Figure 3), and thereby enhancing the clinical interest of human multipotent MSCs. Although human MSCs were generally isolated from bone marrow, perivascular derived pericytes and adventitial progenitor cells; a plethora human tissue including adipose, muscle, umbilical cord, Wharton's jelly, placenta, amniotic fluid, urine, breast milk, synovial membrane, and molar tooth root have been reported to harbour MSCs [Berebichez-Fridman *et al*., 2018; Fan *et al*., 2010; Patki *et al*., 2010; Zhang *et al*., 2008].

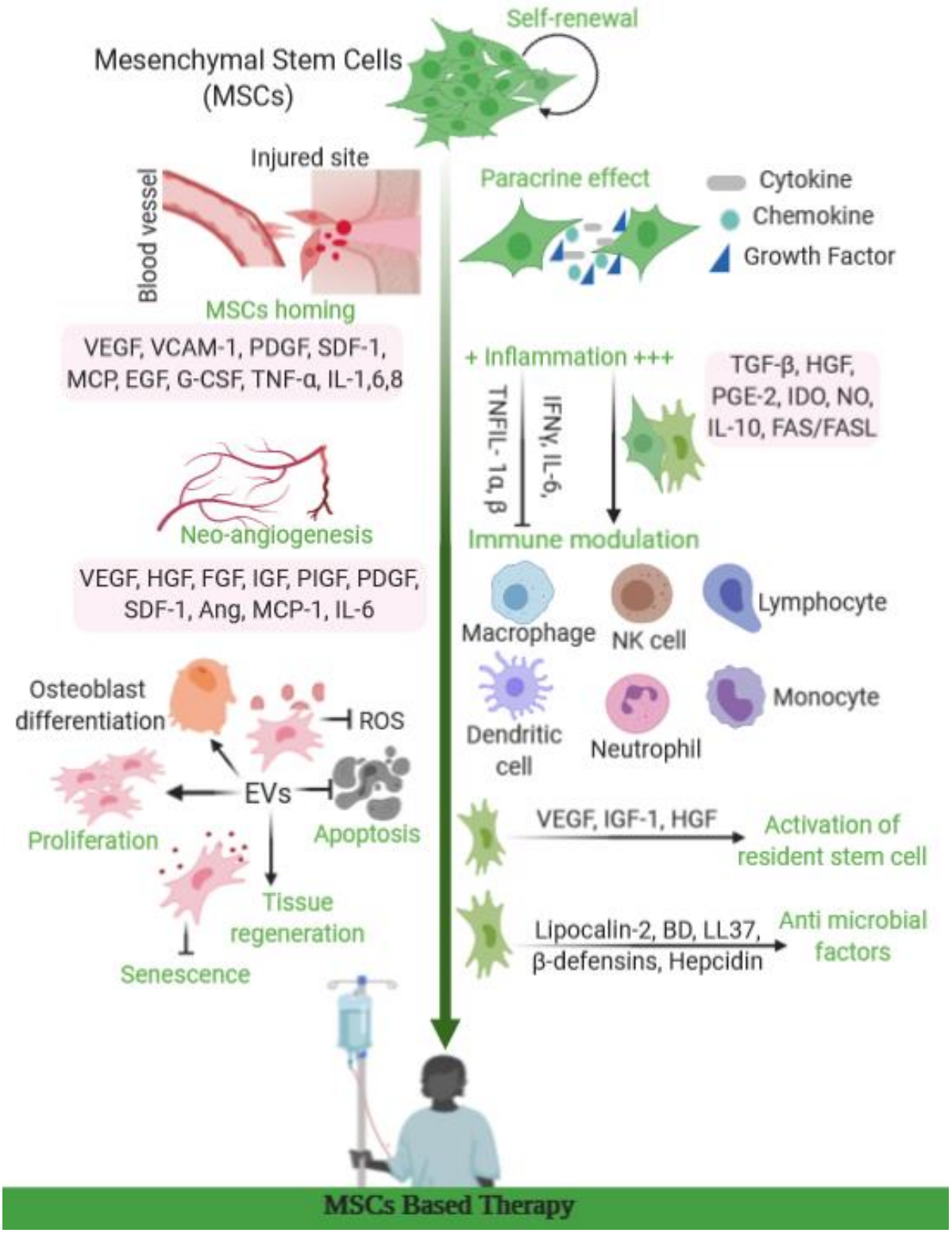

Figure 3: Summary of the functional characteristics of MSCs with respect to tissue regeneration and repair. The functional properties of MSCs include paracrine signalling, neo-vascularization, extracellular vesicle (EVs) secretion, immune suppression, activation of injured site resident cells etcetera. For instance, mechanistically, through chemotaxis, MSCs can migrate to the injured site and infiltrate to initiate repair in association with factors such as VEGF, MCP, IL-1,6,8 etc. MSCs-EVs can protect injured cells apoptosis; inhibit ROS production and cellular senescence. MSCs secretes numerous anti-microbial molecules, such as Lipocalin-2, which can inhibit bacterial load by disrupting bacterial membranes. This artwork was prepared on BioRender platform [https://biorender.com].

Mesenchymal stem cells obtained from different human tissues exhibit heterogeneity in characteristics, thereby leading to a disparity in their therapeutic outcomes [Sipp *et al*., 2018]. The quality of the isolated MSCs varies by the donor's age and culture conditions [Liu *et al*., 2019]. The Mesenchymal and Tissue Stem Cell Committee of the International Society for Cellular Therapy (ISCT) recognized this heterogeneity as problems for future therapeutic use thereby leading to the formulation of the set of minimal criteria, to which MSCs should fulfil [Dominici *et al*., 2006]. These criteria include plastic adherence, fibroblast-like morphology, phenotypic expression of immune cluster of differentials- CD73, CD90, CD105 but not CD11b, CD14, CD19, CD34, CD45, CD79a and HLA (human leucocyte antigen)-DR surface markers. In addition, MSCs must be able to differentiate into osteogenic, adipogenic and chondrogenic lineages *ex vivo*. Until now, MSCs are the most common cell type used in clinical trials for cell-based therapy [Pittenger *et al*., 2019], and are the most studied cells within the scientific literature.

1.3 Amniotic Fluid Derived Mesenchymal Stem Cells (AF-MSCs)

Physiologically, amniotic fluid (AF) serves as a protective liquid for the foetus and is confined within the amniotic sac. Functionally, AF provides mechanical support for the growing foetus, and expedites the interchange of nutrients, fluid, and biomolecules between mother and unborn baby [Underwood *et al*., 2005]. For prenatal disease diagnosis and karyotyping purpose, AF is collected using real-time ultrasound guided amniocentesis as a routine procedure. Recently, this medically discarded fluid -AF has been reported as an alternative and rich source of stem cells of foetal origin [Loukogeorgakis and De Coppi, 2017]. In 2007, Atala and his co-workers isolated and characterized human amniotic fluid-derived stem cells (AFSCs) and further demonstrated their therapeutic potential [De Coppi *et al*., 2007]. Morphologically, amniotic fluid cells are fibroblast-like and spindle-shaped, which easily adhere to plastic surfaces and have high proliferative capacity in culture [Noronha *et al*., 2011]. Because of their low immunogenicity, anti-inflammatory properties, high differentiation capacity *in vitro*, and reduced carcinogenesis potential, AFSCs are amenable for clinical application and tissue engineering. Additionally, AFSCs were demonstrated to have paracrine activity. The AF cells-conditioned media contain cytokines, which have a profound effect on vasculogenesis, neo-angiogenesis, and osteogenesis [Teodelinda *et al*., 2011; Mirabella *et al*., 2013; Ranzoni *et al*., 2016].

Nevertheless, there are some discrepancies regarding the type of cells present in amniotic fluid obtained from distinct phases of gestational time, and heterogeneous populations of differentiated and undifferentiated progenitor cells [Simoni and Colognato, 2009]. For instance, Torricelli et al. [1993] described the presence of hematopoietic progenitor populations in AF. Various investigators also reported that, a subpopulation of AFSCs express the key pluripotency-regulating transcription factors; OCT4, NANOG, SOX2 and KLF4; and cell surface makers- SSEA4, CD133, and c-KIT [Moschidou *et al*., 2013; Koike *et al*., 2014]. However, it is yet to be demonstrated the functionality of these factors in AFSCs as already observed in human pluripotent stem cells. To address these controversies, it was reported in 2019 that, AFSCs lack the transcription factor OCT4 [Vlahova *et al*., 2019]. Besides all the complexities, the Adjaye group (ISRM, Düsseldorf, Germany) demonstrated that second and third-trimester AF could harbour an unspecialized subpopulation of multipotent cells with the typical mesenchymal characteristics [Spitzhorn *et al*., 2017], hereafter; the cells were referred to as amniotic fluid derived mesenchymal stem cells (AF-MSCs).

AF-MSCs fulfil the minimal criteria set by ISCT, and show similarities to MSCs sourced from bone marrow, adipose tissue, umbilical cord, and first and second term AF. Furthermore, they are able to differentiate into mesodermal lineages such as osteoblasts, chondrocytes, and adipocytes [Rahman *et al*., 2018] *in vitro*. Invariably, the challenge of getting a bone marrow donor, adipose tissue donor, decreased differentiation potency and proliferation capacity of BM-MSCs as they age has been a major drawback for these cells, coupled with the methods of obtaining these cells such as the invasive BM aspiration and liposuction methods [Cooper and Viswanathan, 2009].

AF-MSCs of the two early trimesters of gestation are advantageous in terms of cellular potency but the collection of AF using the amniocentesis method is also invasive and can result in the risk of miscarriage for pregnant women, foetal injury and complications such respiratory distress, postural deformities, and chorioamnionitis of the mother [Tara *et al*., 2016]. Even more, some countries have imposed legal restrictions on amniocentesis. Full term C-section-derived AF is medically discarded biomaterial in practice, and few studies have fully characterized AF-MSCs obtained at this stage. Understanding full-term AF derived concerning MSCs characteristics like first, second trimester-derived AFSCs could open up an alternative source of MSCs.

Despite having cell-based therapeutic potentials as bona fide MSCs, before launching any clinical application, it is always important to solve the debateable origin of AF-MSCs [Loukogeorgakis and De Coppi, 2017]. Antonucci *et al.* described the epiblast as the probable origin of 1st term AFSCs by comparing the gene expression of primordial germ cells and AFSCs [Antonucci *et al*., 2014]. Beforehand, Perin *et al.* showed a possible link to the kidney since it was shown that 2nd term AF-MSCs could be differentiated into embryonic kidney structures *in vitro* [Perin *et al*., 2007]. Other studies showed that second term AF-MSCs expressed renal podocyte markers such as CD2AP and NPHS2 [Siegel *et al*., 2009]. Furthermore, the potentially of AF-MSCs to become renal cells has been demonstrated through the formation of chimeric renal organoid formation composed of murine embryonic kidney cells and human AF-MSCs [Siegel *et al*., 2010]. Several other groups have shown that human AF-MSCs can promote kidney regeneration in acute renal injured animal model [Hauser *et al*., 2010]. Of note, neonatal human urine was described as a source of kidney progenitor cells [Arcolino *et al*., 2016]. It is important to mention, that third trimester amniotic fluid mostly consists of foetal urine (produced by the kidneys) [Underwood *et al*., 2005]. Considering these examples, it is logical to contemplate and investigate that AF-MSCs could be exfoliated from the foetal kidney and accumulate in the AF.

1.4 Urine Derived Mesenchymal Stem Cells

In current times, urine has been identified as a source for obtaining mesenchymal stem cells. This offers a cheap, ethically uncomplicated, and safe approach to obtain mesenchymal stem cells [Chen *et al*., 2019]. Urine approximately contains 2,000 to 7,000 cells including epithelial cells, transitional cells, multipotent stem cells, and glomerular parietal cells. In 1972, Sutherland and Bain for the first time reported a successful isolation and culture of cells from urine of a neonate [Sutherland and Bain, 1972]. Later, Linder and Herz *et al.* described the culture of urine cells from adults, independently [Linder, 1976; Herz *et al*., 1979]. However, after the work of Zhang *et al.* and follow-up studies on urine-derived stem cells [Zhang *et al*., 2008; Bento *et al*., 2020], the existence of urine-derived stem cells (USC) has been gradually accepted, reproduced and refined.

Similar to adipose tissue-derived, bone marrow-derived and amniotic fluid-derived MSCs, USCs were shown to express surface markers such as CD29, CD44, CD73, CD90, and CD105 but not the hematopoietic stem cell markers CD14, CD31, CD34 and CD45 [Bharadwaj *et al*., 2013]. Furthermore, they are able to multi-differentiate into endodermal (e.g. podocytes and urothelial cells), and mesodermal lineages (e.g. endothelial cells, osteocytes, chondrocytes, and

adipocytes), respectively [Manaph *et al*., 2018], under appropriate culture environment. Additionally, these cells also express a subset of pluripotency-associated proteins such as TRA-1-60, TRA-1-81, SSEA4, C-KIT, CD133 and SSEA4; and possess high proliferation capacity with telomerase activity [Bharadwaj *et al*., 2013; Manaph *et al*., 2018]. Due to the MSC characteristics- Vimentin (+), E-Cad (-) and plastic adherent; USCs could have versatile applicable potential to treat different tissue defects and diseases. Considering it as a non-invasive and repetative cell source, it is suited for autologous transplantation which would allow to bypass immune rejection. Logically, stem cells originated from the genitourinary system, for instance renal stem cells, and can be the most promising candidate for renal tissue repair, and other for studies on kidney development, nephrotoxicity tests, disease modelling, and drug screening.

Renal stem cells are multipotent mesenchymal cells which can maintain self-renew and are able to differentiate into various cell types of the kidney [Huling and Yoo, 2017]. In developing foetal kidney, abundant amount of CD24 (renal progenitor marker) and CD133 (stem cell self-renewal marker) positive renal stem are detectable [Lazzeri *et al*., 2007; Sagrinati *et al*., 2006]. Gradually the presence of renal stem cell in the renal system decreases with age. However, in adults, very few renal stem cells are found in renal tubules and capsules. The renal progenitor cells reside in the Bowman's capsule and expresses CD106 in addition to CD24 and CD133. This $CD24^{+}CD133^{+}CD106^{+}$ progenitors are able to give rise to a variety of cell types of the renal tissue including podocytes [Angelotti *et al*., 2012; Huling and Yoo, 2017]. The rise in renal system dysfunctional diseases pushes present day research focus on renal stem cells as the most promising candidate to develop cell-based therapeutic, kidney disease modelling and drug development. Unfortunately, the isolation of cells from kidney using the invasive biopsy or lacking of altruistic kidney donor for research purpose are still a practical hurdle.

Strikingly, a subpopulation of cells were isolated and cultured from urine which express the renal stem cell surface markers CD24, CD106 and CD133 [Lazzeri *et al.,* 2015]. These progenitor cells are also positive for the renal stem cell transcription factors- SIX2, CITED1 and WT1 [Shukuya *et al.,* 2017; Arcolino *et al.,* 2016]. Studies using mice models, have shown that Osr1, Six2, Wnt and Wt1 are critical factors for sustaining renal progenitor cells [Mari and Winyard, 2015; O'Brien *et al*., 2018]. For this instance, Osr1 plays a crucial role in Six2-dependent maintenance of mouse nephron progenitors by antagonizing Wnt-directed differentiation, whereas Wt1 maintains self-renewal by modulating Fgf signal [Motamedi *et al*.,

2014]. Activation of Wnt were also reported during differentiation and disruption of the self-renewal of $Six2^{+}Cited1^{+}$ renal stem cells [Mari and Winyard, 2015]. Several signalling pathways including Wnt, Fgf, Tgfβ and Notch have been described to have an influential impact in the milieu of renal stem cell maintenance and differentiation in small lab animals [Lawlor *et al*., 2019; Little and Kairath, 2017]. However in human, it is unclear how renal stem cells maintain their self renewal/differentiation.

Recently, a divergent renal gene expression was identified in mouse and human nephrogenesis [Lindström *et al*., 2018]. Due to the lack of human renal stem cell models, several groups are working to generate kidney organoids using human pluripotent stem cells as starter. *In vitro*, stimulated WNT (using a GSK3β inhibitor- CHIR99021), FGF9, Activin A, Retinoic acid (RA) and BMP7 were described as useful signals which could help differentiate human PSCs into various cell types of the renal system such as podocytes, proximal renal tubules, and glomeruli [Little and Kairath, 2017; Rauch *et al*., 2018; Hariharan *et al*., 2019]. Due to the inconsistencies between the protocols and levels of gene expression at various phases of the differentiation and maturation during organoid development [Phipson *et al*., 2019; Wu *et al*., 2018], native urine derived renal stem cells may circumvent the practical pitfalls, and can be used as alternative model for the study of nephrogenesis.

1.5 Induced Pluripotent Stem Cells (iPSCs)

As mentioned earlier, PSCs are unspecialized cells that endow indefinite self-renewal and potency to give rise to cells of all the three primary germ cell layers-ectoderm, mesoderm and endoderm except the placenta. Embryonic stem cells and induced PSCs are the exemplary evidence of PSCs. In 1981, Evans and Kaufman reported, for the first time, the existence of ESCs in mouse embryo from the University of Cambridge, UK [Evans and Kaufman, 1981]. In the same year, Martin (USA) isolated and cultured mouse ESCs *in vitro*; and termed these cells, as we know now "Embryonic Stem Cell" [Martin, 1981]. Prof. Jones and his team, in 1998, reported a ground-breaking work on the derivation and characterization of ESC lines obtained from human blastocysts [Thomson *et al*., 1998].

The pluripotent traits essentially make these cells interesting and enormous potential cell type in the scientific and clinical fields with respect to cell replacement therapies, genetic disorder modelling and tissue engineering. For instance, to treat Parkinson's disease, dopamine-producing cells (neurons) that are differentiated from ESCs [Perrier *et al*., 2004] are already under clinical trials [Barker *et al*., 2017]. However, ESCs research and clinical interventions

are challenged with many controversial issues such as ethical problems, tumour formation upon transplantation, and the immaturity of differentiated cells *in vitro* [Knoepfler, 2009; King and Perrin, 2014]. These challenges fuelled the quest for stem cell biologists to discover other sources of pluripotent stem cells. In 2006, the Japanese scientists Yamanaka and Takashi revolutionized stem-cell research by reprogramming mouse somatic cells into pluripotent cells termed induced-pluripotent stem cells (iPSCs) [Takahashi and Yamanaka, 2006]. These cells are seemingly identical to ESCs and bypass most of the moral and ethical controversies.

In the following year, the Yamanaka group described the generation of human iPSCs from dermal fibroblast using same methods [Takahashi *et al*., 2007]. Practically, iPSCs were generated by infecting the fibroblast cells with viral vectors containing four transcription factors- *OCT4*, *SOX2*, *c-MYC*, and *Klf4* (Figure 4). Mechanistically, the transformation of somatic cells into pluripotent ones braces numerous regulatory incidents. For example, switching the morphology from mesenchymal into epithelial (MET), increasing level of ROS, over expression of *p53*, alteration of mitochondrial metabolic pathway into glycolysis (The Warburg effect) from OXPHOS, and at epigenetic level; changes in CpG islands methylation and histone modification [Prigione *et al*., 2015; Bukowiecki *et al*., 2014; Prigione and Adjaye, 2014; Prigione *et al*., 2010]. Although the seminal discovery of Yamanaka is reproducible, the low efficiency and the requirement of viral vectors is still under scrutiny. Follow up studies on the reprogramming of various cells to iPSCs have been refined and improved.

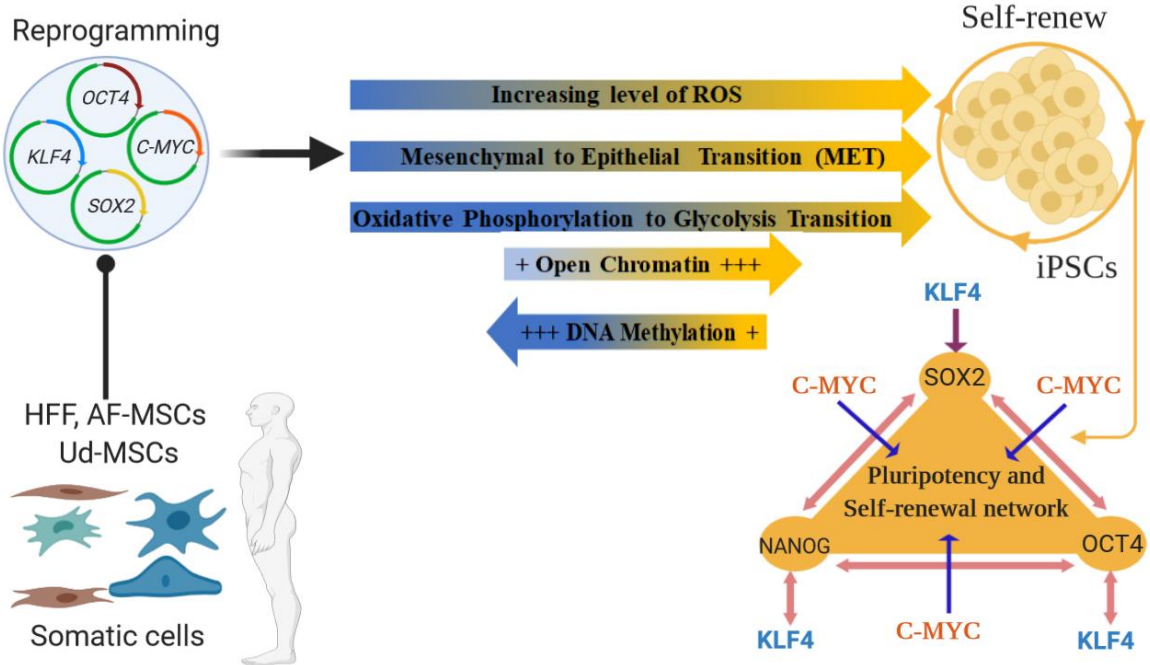

Figure 4: Reprogramming of somatic cells into iPSCs. Irrespective of age of the donor, somatic cells (HFF, AF-MSCs, uMSC) can be reprogrammed into pluripotent stem cells (iPSC) once infection or nucleofection the differentiated cells with the vectors containing four transcription factors- *OCT4*,

SOX2, *c-MYC*, and *Klf4* has taken place. The switching of somatic cells into iPSCs associated with increasing level of ROS, at epigenetic level and an increase in DNA demethylation and chromatin opening. Induced PSCs maintain self-renewal and pluripotency via an intricate interactive network among OCT4, SOX2, c-MYC, and Klf4. Figure was prepared on BioRender platform [https://biorender.com] and Microsoft power point.

To increase the efficiency, the pathways inhibitor small molecules such as ALK inhibitor SB431542, MEK inhibitor PD0325901 and GSK3β inhibitor CHIR99021 were reported [Greenberg, 2015; Lin and Wu, 2015]. To avoid tumour formation probability, it is important to use non-integrating adeno-virus, mRNA, srRNA and mini circular DNA based reprogramming [Hu, 2014; Steinle *et al*., 2019]. In contrast, electroporation of episomal based plasmids containing the transcription factors *OCT4, SOX2, NANOG, LIN28, c-MYC* and *KLF-4* were shown to be a robust option for reprogramming. The episomal vector-based reprogramming is integration free and this method omits pathway (TGFβ, MEK and GSK3β) inhibition [Matz and Adjaye, 2016; Megges *et al*., 2016]. Currently, numerous cell types obtained from different sources are used to generate iPSCs. AF derived AF-MSCs and urine derived MSCs are of high plasticity and easily reprogrammable as our studies demonstrated which could serve as original cells for disease-specific iPSCs [Bohndorf *et al*., 2017; Drews *et al*., 2015].

1.6 Generation of Mesenchymal Stem Cells from Induced Pluripotent Stem Cells (iPSCs)

MSCs for research and clinical applications were initially obtained from bone marrow of adults or children. Later on, other possible sources of MSC such as from fat, dental pulp, umbilical cord, and placenta were extensively studied. Recently, urine derived and amniotic fluid derived mesenchymal stem investigation is on the rise. Despite these available sources of MSC, heterogeneities among cell population, limited proliferative and differentiation capacity *in vitro* are still issues of concern [Wagner *et al*., 2008; Wagner *et al*., 2009; Duscher *et al*., 2014]. Furthermore, increasing level of DNA damage, genomic instabilities, ROS production, cellular senescence, telomere shortening, and age-related DNA methylation patterns have been reported in MSCs obtained from aged individual [Zhou *et al*., 2008; Moskalev *et al*., 2013; Reuter *et al*., 2010; Brink *et al*., 2009]. In contrast, MSCs from younger donors could avoid the age-related occurrences but there is an inconsistency in immunosuppression activity as donor-to-donor differences are reported [Wagner *et al*., 2008; Wagner *et al*., 2009; Wagner *et al*., 2010]. To tackle these shortcomings of parental MSCs, human ESC or iPSCs derived MSCs were demonstrated as an ideal candidate [Frobel *et al*., 2014]. Technically, it is possible to reprogram somatic cell into iPSCs, and then back to MSCs under specific culture condition [Chen *et al*.,

2012] (Figure 5). By definition, iMSCs (induced Mesenchymal Stem Cells) are multipotent cells like BM-MSCs but are generated from ESCs or iPSCs *in vitro*.

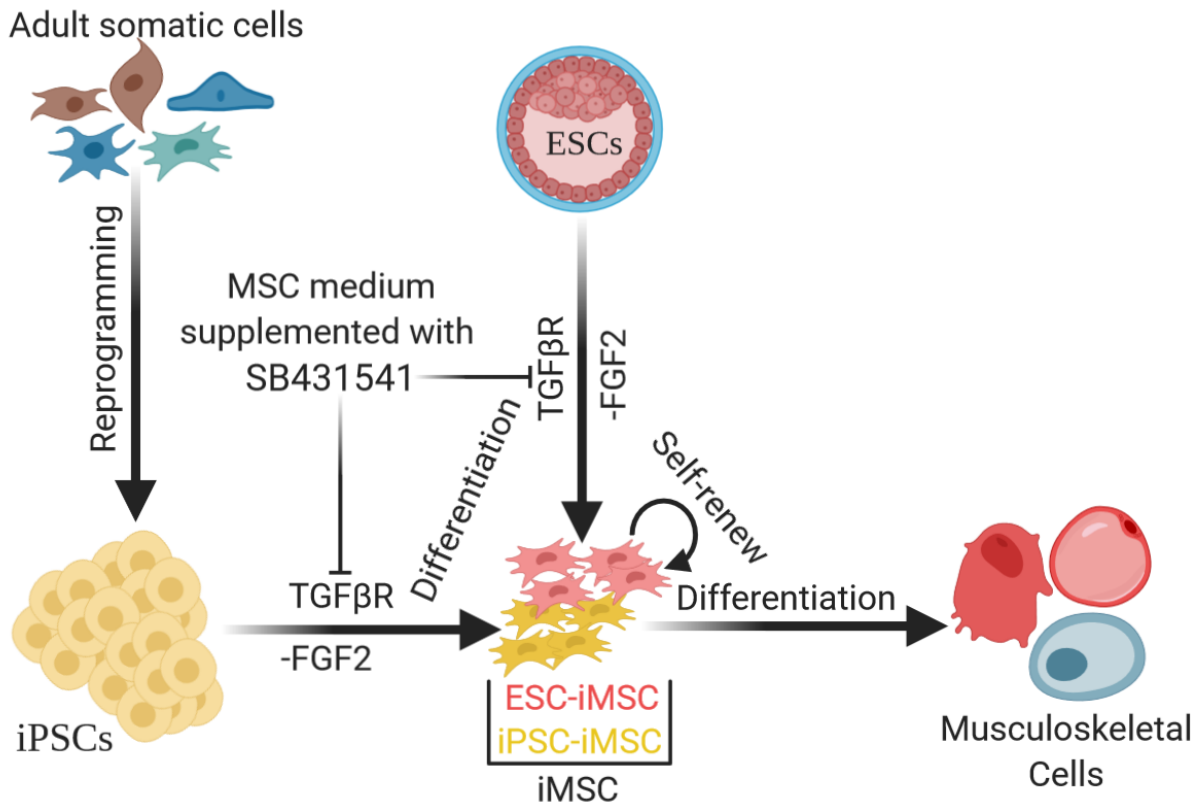

Figure 5: Generation of iMSCs from ESC or adults HFF-iPSCs. The differentiation ESCs or iPSCs into MSCs (iMSCs) can be achieved by inhibiting TGF-ß receptor using SB431541, which in turn convert the cell morphology to mesenchymal from epithelial. These iMSCs are capable to differentiate into Osteo-, adipo-, and chondrocytes. Figure was prepared on BioRender platform [https://biorender.com] and Microsoft power point.

Compared with primary MSCs, irrespective of donor age, human iMSCs has been revealed to have similar morphology, mesenchymal marker-Vimentin expression, transcriptomes and *in vitro* differentiation potential with limited occurrence of senescence [Umrath *et al*., 2020; Lian *et al*., 2010; Spitzhorn *et al*., 2018]. Importantly, iMSCs fulfil the MSC criteria of ISCT but are less sensitive to pro-inflammatory IFN-γ-induced HLA-II expression [Sun *et al*., 2015]. Induced MSCs were observed with less DNA damage and more resistant to stressors such as mitomycin-C [data not published]. In addition, iMSC regained rejuvenation gene signatures and demonstrated improved immunomodulatory properties by suppressing proliferation of NK cells, lymphocytes, CD4+ T, and CD8+ T cells [de Witte *et al*., 2016]. Heterogeneities and risk of transformation can be avoided when MSC are differentiated from a single cell iPSC colony [Steens and Klein, 2018]. Taken all these contexts together, human iMSCs offer an unlimited source of noninvasive production of MSCs with robust proliferation, cell survival and regeneration potential.

1.7 Clinical Application of Mesenchymal Stem Cells (MSCs)

The discoveries of ESC, iPSCs, various sources of MSCs; and the promising outcomes from preclinical stem cell-based investigations for treating fatal diseases have fueled scientists' interest vastly. Of note, MSCs is the most widely utilized cell-based therapeutics in the preclinic and clinic to treat a variety of diseases by replacing defective cells/tissues with healthy ones [Pittenger *et al*., 2019; Galipeau and Sensébé, 2018]. Due to the non-tumorigenicity of MSCs and low levels of HLA, MSCs could be employed in allogeneic transplantation even without matching HLA type [Kot *et al*., 2019]. In 1995, Lazarus *et al.* clinically used MSCs for the first time in human as cell-based therapeutics [Lazarus *et al*., 1995]. Up until today, on 30.05.2020, precisely 1114 clinical trials (registered, ongoing or completed) have been enlisted on https://clinicaltrials.gov server using MSCs. So far, most of the MSCs based trials have been undertaken in university hospitals, with most trials reported from china (350 clinical trials) (Figure 6A). Throughout Europe, about 200 MSCs-based clinical trials have been conducted with Germany participating in only 20 (Figure 6B, Table 1). The most recent example is the ongoing NCT04377334 clinical trial using allogeneic BM-MSCs to treat COVID-19 patients at the Tübingen university hospital.

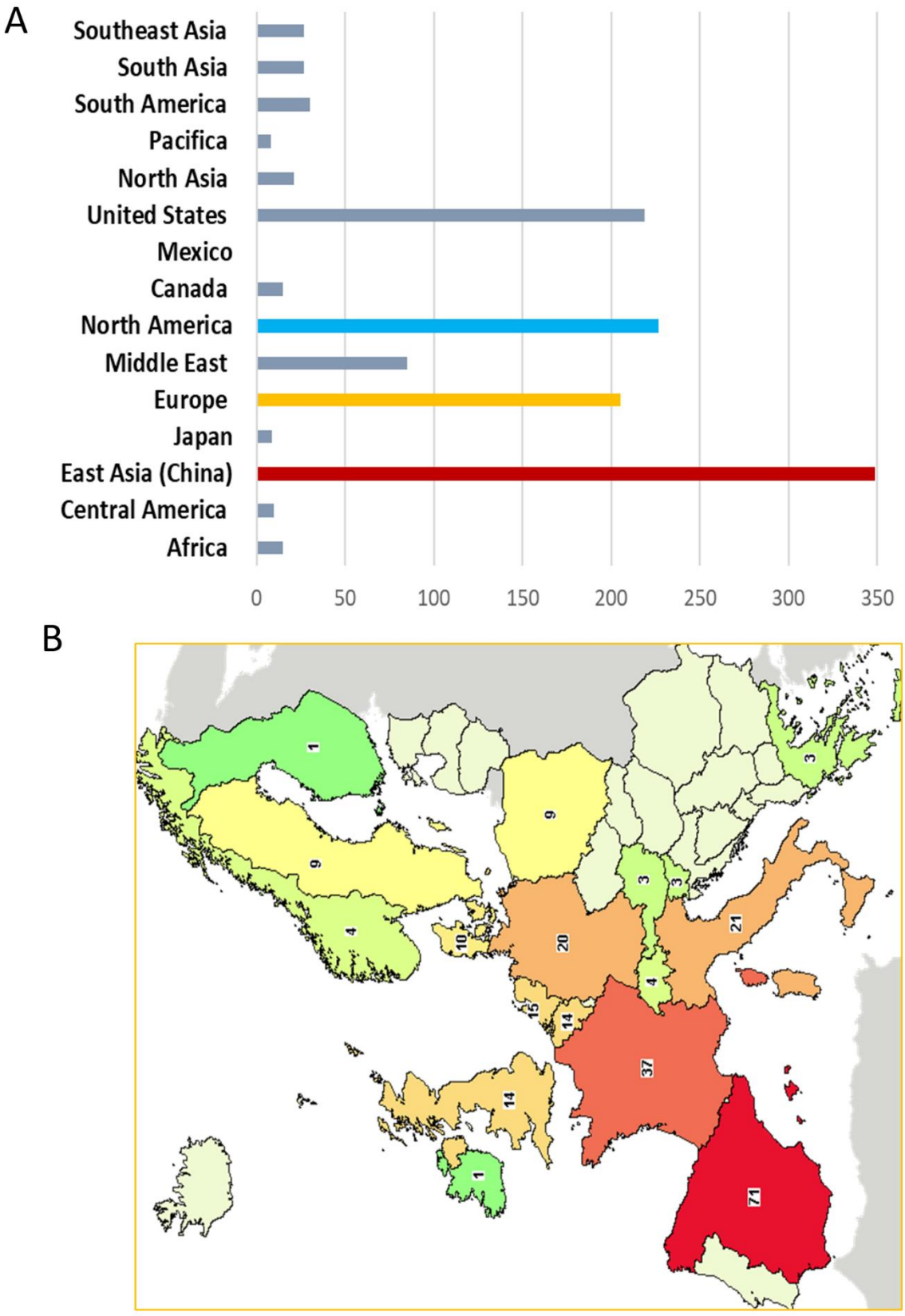

Figure 6. Region wise distribution of the cell based clinical trials using MSCs. **[A]** Bar diagram showing in country-wise global distribution of MSCs based-cellular therapies under trials. **[B]** European map shows the number of clinical studies in the particular country. All the data were annotated from ClinicalTrials.gov (https://ClinicalTrials.gov, Access date 30.05.2020). The data of the European map were adapted from https://ClinicalTrials.gov.

Table 1: Ongoing clinical trials reported from Germany (solely investigated in Germany or as a collaboration with partners) using MSCs enlisted at https://clinicaltrials.gov/ in May 2020

NCT number	Conditions	Interventions	Locations	Phase
NCT02957552	Pediatric Liver Transplantation	Donor-specific BM-MSCs	Tübingen	Phase 1
NCT04377334	ARDS, COVID-19	Allogeneic BM-MSCs	Tübingen	Phase 2
NCT01351610	Critical Limb Ischemia	PTA + Infusion of MSC_Apceth	Munich	Phase 1
NCT03860155	Acute-On-Chronic Liver Failure	Allogenic ABCB5$^+$ MSCs	Dresden, Mannheim, Essen, Magdeburg	Phase 1
NCT00710411	Musco-skeletal Trauma	MSCs	Ulm	NM*
NCT01065337	Diabetic Foot Ulcer	Autologus CD90$^+$ BM-MSCs	Bad Oeynhausen	Phase 2
NCT02065167	Necrosis of the Femoral Head	Autologous BM-MSCs	Tübingen	Phase 2
NCT03325504	Non Union Fracture	Autologous BM-MSCs + Biomaterial	Frankfurt, Freiburg, Munich, Tübingen, Ulm	Phase 3
NCT03529877	Epidermolysis Bullosa	Allogeneic ABCB5$^+$ MSCs	Freiburg	Phase 2
NCT03339973	Arterial Occlusive Disease	Allogeneic ABCB5$^+$ MSCs	Kiel	Phase 2
NCT03267784	Diabetic Neuropathic Ulcer	Allogeneic ABCB5$^+$ MSCs	Greifswald, Heidelberg, Leipzig, Ludwigshafen	Phase 2
NCT03257098	Chronic Venous Ulcers	Allogeneic ABCB5$^+$ MSCs	Bochum, Ulm, Erlangen, Hamburg, Kiel, Münster, Schwerin, Würzburg	Phase 2
NCT02742844	Non healing Ulcers	ABCB5$^+$ MSCs	Bochum, Würzburg	Phase 2
NCT02829216	GvHD	MSCs	Dresden	
NCT01842477	Fracture of Humerus, Tibial or Femur	Autologous MSCs + Biomaterial	Ulm	Phase 2
NCT01585857	Osteoarthritis	Autologous AD-MSCs	Würzburg	Phase 1
NCT01541579	Fistulizing Crohn's Disease	Autologous AD-MSCs	Berlin, Frankfurt Braunschweig	Phase 3
NCT01529008	Osteonecrosis of the Femoral Head	Autologous osteoblastic cells	Dresden, Köln, Eisenberg, Würzburg, Hannover	Phase 3
NCT01298830	Intracerebral Hemorrhage	Allogenic MSCs in alginate microcapsules	Heidelberg, Erlangen, München, Hannover	Phase 2
NCT01038596	Osteoarthritis	BM-MSCs	Dresden	NM*

NM denotes Not mentioned*.

Of the total MSCs based clinical trials analysed within the context of targeted clinical conditions, there are about 900 clinical indications. Musculo-skeletal diseases represented highest number out of the total number of trials followed by cardiovascular and immune system related disorders (Figure 7A). The sources of MSCs used for the clinical trials also compiled and revealed that most widely used source of MSCs were bone marrow (BM) followed by the umbilical cord tissue, adipose tissue, and cord blood (Figure 7B). However, AF-MSCs has been used only in 4 investigations, urine derived cells; 2 cases, and iPSCs derived MSCs (iMSCs); 2 cases.

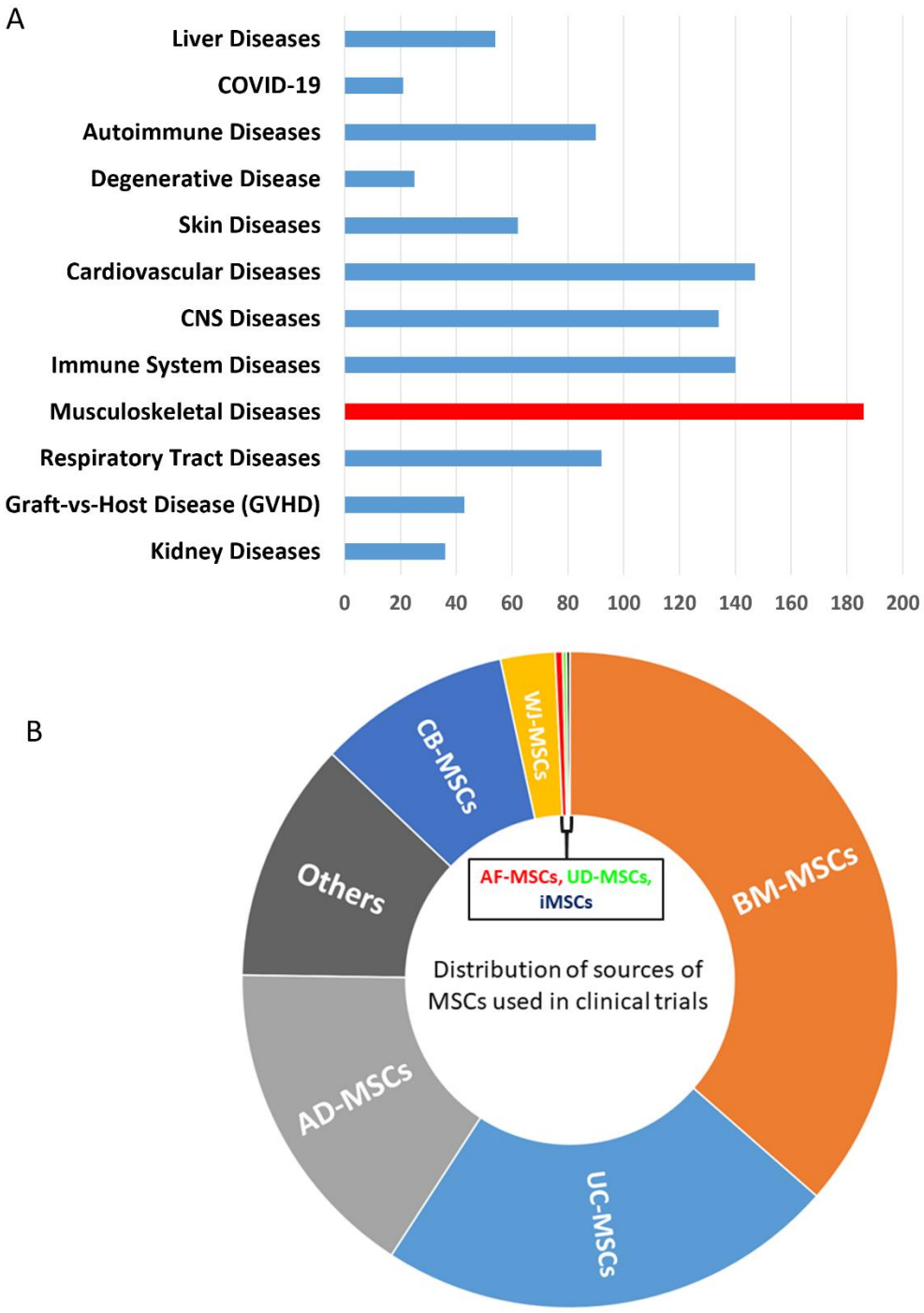

Figure 7. Medical conditions targeted by MSC therapy and the sources of MSCs. [A] Bar diagram representing the distributions of the clinical interventions by proportion of trials. **[B]** Distribution of the sources of MSCs so far used for the clinical investigation. Data was retrieved from ClinicalTrials.gov website using the mesenchymal stem cells as a search keyword for all MSCs clinical investigations that reflected the respective associated clinical conditions as well as the sources of the MSCs. Figures were prepared on MS excel.

Although many MSC-based clinical trials are ongoing currently, only a few products (so far 10) are permitted for clinical application [Graffmann *et al*., 2020] (Figure 8). In 2010, South Korea first approved autologous AD-MSCs based therapy to treat connective tissue disorder, and remains the top country in regards to the number of clinically permitted MSCs products. In the

context of cell source, autologous BM-MSC is the most widely used clinically approved MSCs. Graft versus Host disease (GvHD) is one of the most frequent clinical condition considered for MSCs therapy [Lukomska *et al*., 2019]. Because of the immunosuppressive nature of MSCs, with the intension to reduce organ rejection or suppress immune inflammation, and to enhance post organ transplantation safety [Galipeau and Sensébé, 2018].

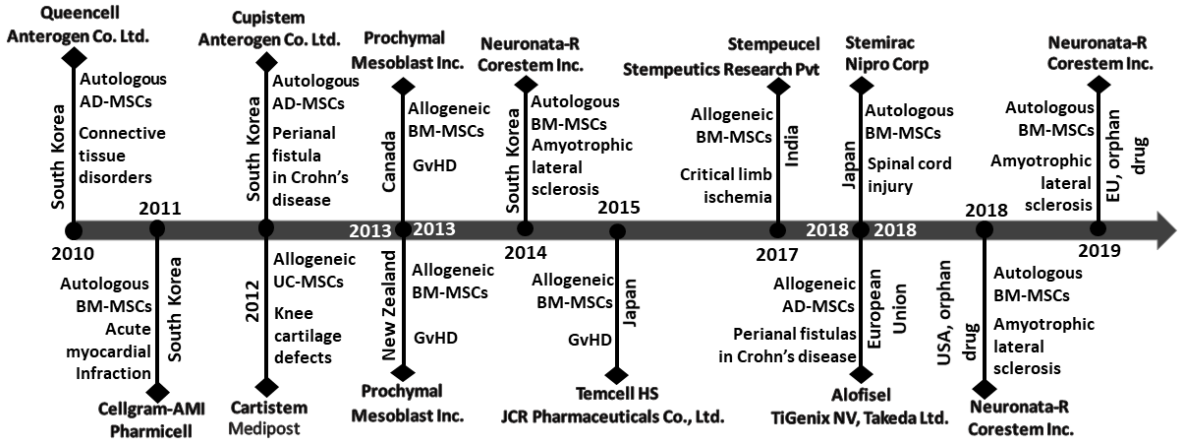

Figure 8: Clinically approved and commercially available MSCs based therapeutics. South Korea is the leading country in terms of number of approvals MSCs based therapeutics, and South Korea first approved MSCs based therapy for clinical application in 2010. Autologous BM-MSCs are the most widely clinical used MSCs.

1.8 Clinical Application of MSCs-based Cell Therapy for Covid-19

COVID-19 is a novel coronavirus β-SARS-CoV-2 (respiratory diseases) which primarily affects the respiratory tract. In severe conditions, patients experience bilateral pneumonia, which ultimately leads to lung failure and death [Yuki *et al.,* 2020]. Currently, there is no specific treatment to alleviate this life-threatening virus. MSC-based cellular or MSC-EV-based therapies have been utilised in preclinical studies and trials and seen to improve healing of the virus infected pulmonary injury and dysfunction [Behnke *et al*., 2020; Khoury *et al*., 2020; Bulut and Gürsel, 2020]. More than 35 clinical trials on COVID-19 patients are now running using MSC from different sources during the COVID-19 pandemic (https://clinicaltrials.gov, May 2020) (Figure 9). Furthermore, several other approaches are currently being investigated in china, incorporating MSCs, MSC-derived CM and MSC- EVs [Khoury *et al*., 2020; Chrzanowski *et al*., 2020]. The results from these trials are yet to be published.

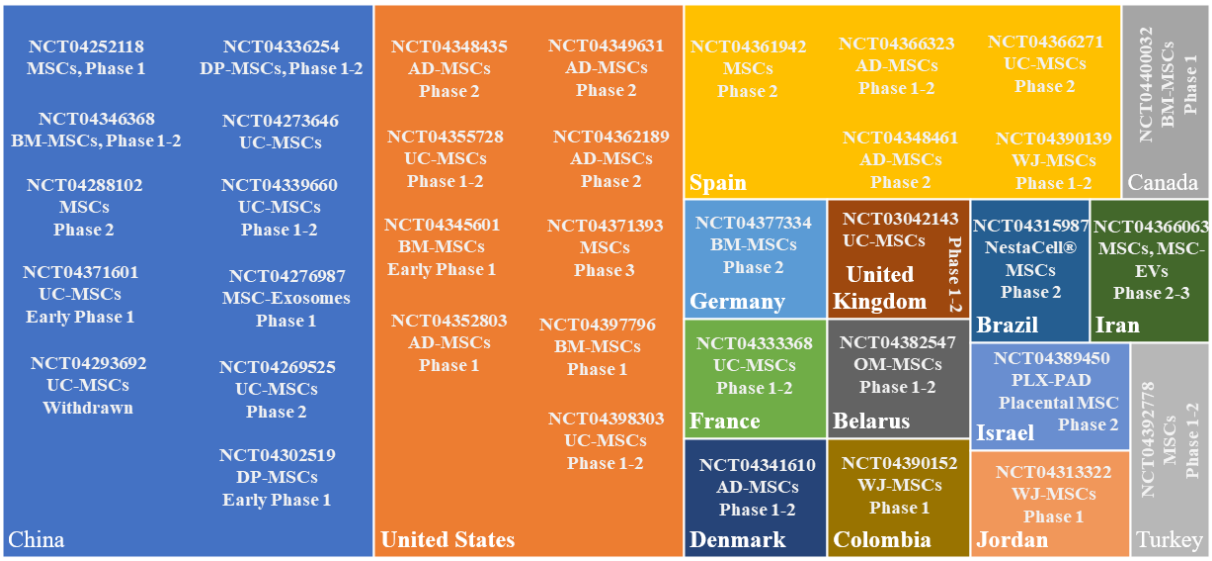

Figure 9: A list of all 38 clinical trials of the MSC based therapies to treat COVID-19. Data were retrieved from clinicalTrials.gov on 02.06.2020 and chart were prepared on Microsoft excel.

1.9 Preclinical and Clinical Application of iMSCs-based Cell Therapy

IMSCs ever since their derivation has affirmed their rejuvenation gene expressions, MSC phenotype properties and their status as being non-tumorigenic. Several preclinical studies have shown promising results following iMSC utilisation. For instance, Adjaye's group demonstrated that CPG loaded HFF-iMSC improved bone defects in mini-pig in similar fashion as of BMC + CPG transplantation [Jungbluth *et al*., 2019]. The group further reported in another study how iMSCs could take participate in the healing process for liver regeneration in Gunn Rats [Spitzhorn *et al*., 2018]. Additionally, preclinical applications of iMSCs were observed to have engraftment and immunomodulation effect on mouse pulmonary arterial hypertension, broncho-alveolar and nasal lavage [Sun *et al*., 2012]. So far, two clinical trials have been performed using iMSCs. In May 2017, the first clinical trial (NCT02923375) using iMSC was initiated to treat steroid-resistant acute GvHD in the UK and Australia, a trial funded by Cynata Therapeutics Ltd. (Australia). The second clinical trial (NCT03839238) of ESC-derived MSCs (iMSCs) is currently under joint investigation by the Tongji Hospital and Chinese Academy of Sciences in China, with the intention to treat meniscus injury [Graffmann *et al*., 2020].

1.10 Application of Amniotic Fluid derived Mesenchymal Cells (AF-MSCs)

Preclinical studies on AF-MSCs has revealed the potential of these cells in regenerative medicine. As AF-MSCs are genitourinary system originated cells, they were widely investigated to treat renal system affiliated problems such as mouse acute tubular necrosis and urethral obstruction [Hauser *et al*., 2010; Tran *et al*., 2015; Morigi and De Coppi, 2014; George

et al., 2019; Liang *et al*., 2017]. Besides, a recent study reported that AF-MSCs are able to reduce pulmonary fibrosis by inhibiting lung B-cell proliferation and maturation in mice [Cargnoni *et al*., 2020]. A reduction of bone fragility in mouse were demonstrated upon intraperitoneal injection of AF-MSCs mediated by suppressing TNFα and TGFβ signalling [Ranzoni *et al*., 2016]. Preclinical transplantation of AF-MSCs performed on Alport syndrome mouse model revealed an increased survival duration and a decrease in the progression of pathological conditions [Sedrakyan *et al*., 2012]. In-terms of combined tissue-engineered therapeutics, AF-MSCs has gained much attention in stem cell research. For instance, an acceleration of new bone formation in a sheep model of sinus augmentation were reported upon transplantation of AF-MSCs loaded magnesium-hydroxyapatite-collagen scaffold [Barboni *et al*., 2013]. Critical-sized calvarial defect reconstruction has also been reported in rat when AF-MSCs embedded collagen type I was implanted [Zavatti *et al*., 2015]. Recently, the usefulness of scaffolds developed from naturally available materials such as hydroxyapatite, collagen, and chitosan have increased significantly for bone tissue replacement therapy [Rahman *et al*., 2019]. These scaffolds in combination with AFSCs could accelerate bone defect healing faster by providing a suitable microenvironment and regeneration.

AFSCs were investigated to differentiate into skin keratinocyte cells, which expressed epidermal markers- K5, K14, K10 and involucrin. When AFSCs were transplanted *in vivo* in mouse wound model, it was observed that AFSCs initiated and contributed in early stages of skin wound healing process [Sun *et al*., 2015]. The transplantation of AF cells in combination with medically accepted biomaterial such as amniotic membrane and / or collagen gel [Murphy *et al*., 2017; Rana *et al*., 2020] need to be tested for managing wound.

Several clinical trials and investigations are now underway using AF-MSCs, AF or Amnion derived tissue containing AF-MSCs in the treatment of lupus nephritis (LN) using peripheral intravenous infusion of allogeneic AF-MSCs (Phase 1 clinical trial, NCT04318600). In Japan (UMIN000029945), AF-MSCs has been used in treating patients with steroid-refractory aGvHD after allogeneic HSCs transplantation [Yamahara, 2019]. In the USA, the FDA approved the use of AF-MSCs in clinical studies (Phase 2/3; NCT03390920) as therapeutics products for managing several musculoskeletal indications such as osteoarthritis, tendinitis, sports injury, degenerative disc disease, degenerative arthritis, ligament injury, neuropathy, and pelvic pain. The company- R3 stem cells from USA are also conducting clinical trials (NCT03899298) with amniotic and umbilical cord tissue therapy for numerous medical

conditions including orthopaedic disorder, erectile dysfunction, autoimmune diseases, renal diseases, cardiomyopathies, pulmonary disease-COPD, Alzheimer disease and peripheral arthritis.

1.11 Application of Urine derived Mesenchymal Stem Cells

Recently, the number of *in vivo* studies using urine derived MSCs as a non-invasive source for multipotent stem cells is continuously rising. Urine stem cells has been shown to increase vascularisation by angiogenesis, thereby suggesting a promising future for the treatment of kidney diseases [Pavathuparambil Abdul Manaph *et al*., 2018]. Several preclinical studies have been reported with promising outcomes upon transplantation of urine-derived cells or urine-derived cell secreted EVs. Example includes but not limited to, improvement of type 2 diabetic erectile dysfunction in rat models, enhanced bone regeneration, and urethral tissue reconstruction have been described using urine stem cell [Ouyang *et al*., 2014; Ouyang *et al*., 2018; Guan *et al*., 2015; Wu *et al*., 2019; Liu *et al*., 2017]. Furthermore, the urine cell-based TreaT-Assay for the diagnosis of complicacy related to kidney transplantation is another example of the usefulness of these cells in vitro [Thieme *et al*., 2019]. Extracellular vesicles secreted from urine stem cells has been observed to have a profound positive effect in repairing hind-limb ischemia in mouse [Zhu *et al*., 2018]. Other studies also demonstrated that urine cell secreted extracellular vesicles could inhibit osteoporosis via CTHRC1 and OPG [Chen *et al*., 2019].

Despite these advances with urine derived MSC-based preclinical investigations, so far only three clinical trials are under considerations worldwide. They include modelling of genetic diseases using urine cell derived iPSCs (NCT03612310), functionality assay of ABCC6 transporter using urine derived cells (NCT03364504) and finally, clinical assay to diagnosis bladder cancer utilising urine stem cells (NCT02735512).

2. Aims of This Thesis

Investigations on mesenchymal stem cells (MSCs)-based therapies are rising as an alternative of conventional treatment options. However, to overcome the shortage of donors and invasive collection procedures of MSCs- this thesis aimed to isolate and characterize MSCs from full term amniotic fluid and urine as non-invasive sources. This work also focused to address the controversial issues related to the origin of the amniotic fluid and urine-derived MSCs. An additional purpose of this thesis was to analyse, how self-renewal and differentiation of these cells are controlled *in vitro*. To get valuable insights for possible regenerative therapy options, investigations on the reprogramming potential of these cells into induced pluripotent stem cells (iPSCs), and the differentiation potential of amniotic fluid cells into keratinocyte-like cells also were performed. Furthermore, the differentiation capacity of iPSCs into MSCs (iMSCs) was experimented which could serve as an alternative to native MSCs. To understand the clinical value of iMSCs as cell-based therapeutic, iMSCs were trialled *in vivo* using a proximal tibia defect model in mini pigs. Further aims of this work were the fabrication of a biocompatible scaffold to be used in bone defects, and the formulation of a gel for ectopic treatment of burn wounds. Taken all together, this thesis aimed to demonstrate new ways of MSC sourcing, investigate versatile applications of these cells and to gain knowledge about the underlying molecular mechanisms influencing the cells' fate.

3. Results - Publications

Part A: Sources and Origin (Renal Identity) of Amniotic Fluid-derived Mesenchymal Stem Cells (AF-MSCs)

3.1 Isolation and Molecular Characterization of Amniotic Fluid-derived Mesenchymal Stem Cells obtained from Caesarean Sections

Lucas-Sebastian Spitzhorn*, Md Shaifur Rahman*, Laura Schwindt, Huyen-Tran Ho, Wasco Wruck, Martina Bohndorf, Silke Wehrmeyer, Audrey Ncube, Ines Beyer, Carsten Hagenbeck, Percy Balan, Tanja Fehm and James Adjaye

*These authors contributed equally to this work.

Abstract

Human amniotic fluid cells are immune-privileged with low immunogenicity and anti-inflammatory properties. They are able to self-renew, are highly proliferative, and have a broad differentiation potential, making them amenable for cell-based therapies. Amniotic fluid (AF) is routinely obtained via amniocentesis, and contains heterogeneous populations of foetal-derived progenitor cells including mesenchymal stem cells (MSCs). In this study, we isolated human MSCs from AF (AF-MSCs) obtained during Caesarean sections (C-sections) and characterized them. These AF-MSCs showed typical MSC characteristics such as morphology, *in vitro* differentiation potential, surface marker expression, and secreted factors. Besides Vimentin and the stem cell marker CD133, subpopulations of AF-MSCs expressed pluripotency-associated markers such as SSEA4, c-Kit, TRA-1-60, and TRA-1-81. The secretome and related gene ontology (GO) terms underline their immune modulatory properties. Furthermore, transcriptome analyses revealed similarities with native foetal bone marrow-derived MSCs. Significant KEGG pathways as well as GO terms are mostly related to immune function, embryonic skeletal system, and TGFβ-signalling. An AF-MSC-enriched gene set included putative AF-MSC markers PSG5, EMX-2, and EVR-3. In essence, C-section-derived AF-MSCs can be routinely obtained and are amenable for personalized cell therapies and disease modelling.

Approximated total share of contribution: 40%

Publication Status: Published in Stem Cells Int. 2017; 2017:5932706.

Impact Factor: 3.90

Authors' contributions on experimental design, realization and publication: JA, TF, MSR, LSS conceived the idea and designed the experiments. IB, CH and PB collected the third trimester C-section derived amniotic fluid samples. WW and JA did the bioinformatic analysis. MSR and LSS isolated the AF-MSCs from third trimester AF and characterized the AF-MSCs (marker protein expression, secretome and in vitro differentiation potential). MSR and LSS prepared the figures and wrote the manuscript and finally JA edited it. The manuscript including all figures were subsequently reviewed, amended and approved by all co-authors.

Pubmed link: https://www.ncbi.nlm.nih.gov/pubmed/29225627
Journal link: https://www.hindawi.com/journals/sci/2017/5932706/

Hindawi
Stem Cells International
Volume 2017, Article ID 5932706, 15 pages
https://doi.org/10.1155/2017/5932706

Research Article

Isolation and Molecular Characterization of Amniotic Fluid-Derived Mesenchymal Stem Cells Obtained from Caesarean Sections

Lucas-Sebastian Spitzhorn,[1] Md Shaifur Rahman,[1] Laura Schwindt,[1] Huyen-Tran Ho,[1] Wasco Wruck,[1] Martina Bohndorf,[1] Silke Wehrmeyer,[1] Audrey Ncube,[1] Ines Beyer,[2] Carsten Hagenbeck,[2] Percy Balan,[2] Tanja Fehm,[2] and James Adjaye[1]

[1]*Institute for Stem Cell Research and Regenerative Medicine, Heinrich Heine University Düsseldorf, Moorenstr. 5, 40225 Düsseldorf, Germany*
[2]*Department of Obstetrics and Gynaecology, Heinrich Heine University Düsseldorf, Moorenstr. 5, 40225 Düsseldorf, Germany*

Correspondence should be addressed to James Adjaye; james.adjaye@med.uni-duesseldorf.de

Lucas-Sebastian Spitzhorn and Md Shaifur Rahman contributed equally to this work.

Received 29 June 2017; Revised 13 September 2017; Accepted 1 October 2017; Published 31 October 2017

Academic Editor: Valentina Russo

Human amniotic fluid cells are immune-privileged with low immunogenicity and anti-inflammatory properties. They are able to self-renew, are highly proliferative, and have a broad differentiation potential, making them amenable for cell-based therapies. Amniotic fluid (AF) is routinely obtained via amniocentesis and contains heterogeneous populations of foetal-derived progenitor cells including mesenchymal stem cells (MSCs). In this study, we isolated human MSCs from AF (AF-MSCs) obtained during Caesarean sections (C-sections) and characterized them. These AF-MSCs showed typical MSC characteristics such as morphology, *in vitro* differentiation potential, surface marker expression, and secreted factors. Besides vimentin and the stem cell marker CD133, subpopulations of AF-MSCs expressed pluripotency-associated markers such as SSEA4, c-Kit, TRA-1-60, and TRA-1-81. The secretome and related gene ontology (GO) terms underline their immune modulatory properties. Furthermore, transcriptome analyses revealed similarities with native foetal bone marrow-derived MSCs. Significant KEGG pathways as well as GO terms are mostly related to immune function, embryonic skeletal system, and TGFβ-signalling. An AF-MSC-enriched gene set included putative AF-MSC markers *PSG5*, *EMX-2*, and *EVR-3*. In essence, C-section-derived AF-MSCs can be routinely obtained and are amenable for personalized cell therapies and disease modelling.

1. Introduction

Recent human AF research has shown that stem cells from the first and second trimester can be collected during amniocentesis (an invasive method of prenatal diagnosis of chromosomal abnormalities and foetal infections) [1]. The therapeutic potential including *in vitro* characterization of human amniotic fluid-derived stem cells (AFSCs) was first reported by the Atala group [2]. Because of their low immunogenicity, anti-inflammatory properties, and high proliferative and differentiation capacity *in vitro*, AFSCs are amenable for clinical application and tissue engineering. Furthermore, they lack carcinogenesis after transplantation in nude mice and have the ability to create embryoid body-like structures after specific treatments. Their possible origin from epiblast, demonstrated by the presence of common features with primordial germ cells, is also under discussion [2, 3]. The AFSC populations are heterogeneous in nature, of foetal-derived-differentiated and undifferentiated progenitor cells [4]. In 1993, Torricelli and coworkers first reported a subpopulation of hematopoietic progenitor cells in AF [5]. Interestingly, in 2003, it was reported that a small subpopulation of AFSCs expresses the pluripotency-regulating marker, octamer-binding transcription factor 4 (OCT4) [6]. Later, Moschidou

coworkers reported that AFSCs isolated from the first trimester express other pluripotent stem cell-associated markers such as NANOG, sex-determining region Y-box 2 (SOX2), Krüppel-like factor 4 (KLF4), stage-specific embryonic antigen-4 (SSEA4), CD133, and c-Kit [7, 8]. Their self-renewal capabilities were also confirmed, thus indicating that AFSCs are of high plasticity and easily reprogrammable as our previous studies demonstrated [9, 10]. At the transcription level, it has also been shown that a subpopulation of AFSCs has high overlap with human ESCs as they share about 82% of transcriptome identity [11]. Additionally, AFSCs were found to be paracrine active as their conditioned media contain cytokines which have a profound effect on vasculogenesis, angiogenesis, and osteogenesis [12–14]. AFSCs have the potential for use in clinical applications as shown for example by keratinocyte differentiation and subsequent improvement of wound healing [15].

Mesenchymal stem cells (MSCs) are multipotent stromal stem cells [16, 17]. Morphologically, they are fibroblast-like and spindle-shaped cells. *In vitro*, these clonogenic cells easily adhere to plastic surfaces and have high-replicative capacity [17, 18]. Several sources are reported from adult and foetal tissues from which these types of MSCs can be obtained, for example, bone marrow (BM) and adipose tissue [19] and extraembryonic tissues such as umbilical cord blood [20, 21] and placental tissues such as amnion and decidua and furthermore from second and term amniotic fluid [22]. *In vitro* and *in vivo* MSCs differentiate into mesodermal cell types such as fibroblasts, osteoblasts, chondrocytes, and adipocytes [16, 23]. The International Society for Cellular Therapy (ISCT) postulated that for transplantation and cellular therapy, MSCs should not differentiate into blood cells and therefore not express any markers of hematopoietic lineage such as the surface markers CD14, CD34, and CD45. In contrast to this, bone marrow MSCs should express CD73, CD90, and CD105 referring to their minimal characterization criteria [24]. MSCs have been widely used for therapies such as graft versus host disease, precisely in over 700 clinical trials till date (https://clinicaltrials.gov). The frequency and differentiation capacity as well as proliferation potential from BM-MSCs has been shown to decrease with age [25].

A subpopulation of AFSCs with mesenchymal characteristics has been isolated from second and third-trimester AF and thus referred to as amniotic fluid mesenchymal stem cells (AF-MSCs). They were isolated based upon their plastic adherence and similar cell surface marker composition as MSCs from other sources. Furthermore, they were also able to differentiate into bone, cartilage, and fat cells *in vitro* [23, 26–28]. Various studies have shown that these AF-MSCs also express OCT4 [27, 28]; however, this is still controversial since no one has yet defined the self-renewal function of OCT4 in AF-MSCs as has been shown in human embryonic stem cells [29].

AF-MSCs are advantageous in terms of developmental stages but problematic with respect to the invasiveness of the collection procedures—amniocentesis and foetal infections. Therefore, C-section-derived AF could be an alternative source for these cells. However, the amniotic fluid is merely discarded during this procedure that is why few studies have isolated AFSCs at this stage of gestation. The question remains as to whether full-term AF harbours AF-MSCs of similar potency as cells obtained in the first and second trimesters of pregnancy.

In this study, we characterized human AF-MSCs obtained from C-sections (third trimester) and tested their multilineage differentiation capacity *in vitro*, immunophenotype, expression of mesenchymal markers, multipotency markers, transcriptome, and their secretome. Our data suggests that AF obtained from C-sections may represent a promising source for stem cells of mesenchymal origin. Presently, the most common source of MSCs is the bone marrow (BM). However, harvesting and processing of BM-MSCs have major drawbacks and limitations. Thus, it is significant that AF collected during C-sections is an alternative source of AF-MSCs that are immature and possess high plasticity making them useful for clinical applications.

2. Materials and Methods

2.1. Preparation of Amniotic Fluid. Three amniotic fluid samples from healthy human donors were collected during full-term C-sections from the Obstetrics and Gynaecology faculty, Heinrich Heine University Düsseldorf, Germany, with patient consent as well as institutional ethical approval and kept at 4°C until processed. In general, the time between collection and processing was kept as short as possible to minimize cell death. First, AF was washed with PBS (Gibco; Thermo Fisher Scientific, Darmstadt, Germany) and centrifuged at 300 ×g for 5 min. The supernatant was discarded, and the pellet washed again with PBS and was dissolved in Ammonium chloride (University Hospital Düsseldorf; Pharmacy) to lyse the remaining erythrocytes. Thereafter, the cell solution was incubated at 4°C for 20 min and centrifuged again. This procedure was repeated until the pellet had a clear colour. Afterwards, the cells were cultured in Chang C Medium (Irvine Scientific, CA, USA) containing 88% αMEM (Minimum Essential Medium Eagle Alpha Modification; Sigma) with 10% FBS, 1% GlutaMAX, 1% penicillin/streptomycin (all Gibco), 10% Chang B Basal Medium, and 2% Chang C supplement (Irvine Scientific) at 37°C and 5% CO_2. Once attached, the cells were visible after 4–7 days and the medium was changed. Upon attainment of 90% confluency, the cells were detached using TrypLE Express (Thermo Fisher Scientific) and seeded into other plate formats or frozen.

2.2. Flow Cytometric Analysis of Amniotic Fluid Cells. The immunophenotyping of three independent AF preparations was done using the human MSC phenotyping kit (Miltenyi Biotec GmbH, Bergisch Gladbach, Germany) was done according to manufacturer's instructions. After harvesting, 2×10^5 AF-MSCs were transferred into two test tubes. 2 ml PBS was added to each tube and centrifuged at 300 ×g for 5 min. The supernatant was discarded and the pellet resuspended in 100 μl PBS within the tubes. In one of the tubes, 0.5 μl of the MSC phenotyping cocktail and the other tube 0.5 μl of the isotype control cocktail were added and vortexed. The MSC phenotyping cocktail contained fluorochrome-conjugated monoclonal antibodies CD14-PerCP, CD20-PerCP, CD34-PerCP, CD45-PerCP,

CD73-APC, CD90-FITC, and CD105-PE. The isotype phenotyping cocktail contained fluorochrome-conjugated antibodies that should not specifically detect human antigens and was therefore used as a negative control. The tubes were incubated at 4°C for 10 min in the dark. To washout nonbinding antibodies, 1 ml PBS was added and centrifugation at 300 ×g for 5 min was performed. Afterwards, the cell pellet was fixed using 4% paraformaldehyde (PFA; Polysciences Inc., PA, USA). For flow cytometric analysis of the AF-MSCs for pluripotency-associated markers, TRA-1-60, TRA-1-81, and SSEA4 dye-coupled antibodies were used (anti-TRA-1-60-PE, human (clone: REA157), number 130-100-347; anti-TRA-1-81-PE, human (clone: REA246), number 130-101-410, and anti-SSEA-4-PE, human (clone: REA101), number 130-098-369; Miltenyi Biotec GmbH). The staining procedure was carried out as described above.

The cells were stored at 4°C in the dark until flow cytometric analysis via BD FACSCanto (BD Biosciences, Heidelberg, Germany) and CyAn ADP (Beckman Coulter, CA, USA) was done. Histograms were created using the FCSalyzer software version 0.9.3.

2.3. Immunofluorescence Staining. To analyse the cells for specific markers, AF-MSCs were cultured in 12- or 24-well plates. At 60–80% confluency, the cells were washed and subsequently fixed using 4% PFA for 15 min at room temperature (RT) on a rocking platform. The fixed cells were treated with 1% Triton X-100 (Carl Roth GmbH & Co. KG, Karlsruhe, Germany) for 5 min and blocking buffer was added to the cells. For intracellular staining, this buffer contained 10% normal goat serum (NGS; Sigma), 0.5% Triton X-100, 1% BSA (Sigma), and 0.05% Tween 20 (Sigma), all dissolved in PBS. If extracellular structures were to be stained, Triton and Tween were omitted. After blocking for 2 h at RT, the first antibodies OCT-4A (C30A3) rabbit mAb number 2840, SSEA4 (MC813) mouse mAb number 4755, E-cadherin (24E10) rabbit mAb number 3195, vimentin (5G3F10) mouse mAb number 3390, TRA-1-60 mouse mAb number 4746, TRA-1-81 mouse mAb number 4745 (Cell Signalling Technology, MA, USA), CD133 PA2049 (Boster Bio, PA, USA), and c-Kit (H-300) rabbit polyclonal IgG (Tebu Bio, Offenbach, Germany) were diluted in blocking buffer/PBS and added to the cells with an incubation time of 1 h at RT. After washing for three times with 0.05% Tween 20 in PBS, the appropriate secondary Cy3- or Alexa Fluor 488-labelled antibodies (Thermo Fisher Scientific) and Hoechst 33258 dye (Sigma-Aldrich Chemie GmbH, Taufkirchen, Germany, 1 : 5000 in blocking buffer) were applied for visualization of the primary antibodies and cell nuclei, respectively. Images were taken with a fluorescence microscope (LSM700; Zeiss, Oberkochen, Germany).

2.4. In Vitro Differentiation into Adipogenic, Chondrogenic, and Osteogenic Lineage. The differentiation of the AF-MSCs from passages 5 to 6 was carried out using the StemPro Adipogenesis differentiation Kit, StemPro Chondrogenesis differentiation Kit, and StemPro Osteogenesis differentiation Kit (Gibco, Life Technologies, CA, USA). The differentiation media were formulated by mixing 90 ml of the respective basal media with 10 ml of their corresponding supplements and 1.1 ml of penicillin/streptomycin. At 60–70% confluency, cultivation of the cells in the differentiation media or Chang C media (control wells) was initiated. The medium was replaced every 2-3 days for three weeks. After this period, the medium was removed, and the cells were washed with PBS and fixed with 4% PFA for 30 min at RT on a rocking platform. Subsequently, the cells were stained for distinct developed structures.

2.5. Oil Red O Staining for Adipocytes. Fixed cells were washed with 50% ethanol and then 0.2% Oil Red O working solution was added to the wells and incubated for 30 min at RT on a rocking platform. This solution stained the developed fat vacuoles. The 0.2% Oil Red O working solution was prepared by diluting the 0.5% Oil Red O stock solution (Sigma) with distilled water and filtering it. After washing twice with 50% ethanol and at least 3 times with distilled water until all the excess Oil Red O solution was removed, cells were kept in PBS and images were taken with a light microscope.

2.6. Alcian Blue Staining of Chondrocytes. After fixation, cells should be stained with alcian blue which turns sulfated proteoglycans deposits in chondrocytes visibly blue. Cells were first washed with PBS and 1% alcian blue 8GX (Sigma) solution, prepared in 0.1 N hydrochloric acid (HCl), was added. The cells were stained for 30 min at RT on a rocking platform. Afterwards, the cells were washed three times with 0.1 N HCl solution and with distilled water until the alcian blue solution was completely removed. Cells were then kept in PBS for microscopic imaging.

2.7. Alizarin Red S Staining for Osteoblasts. Alizarin red S (Sigma) which specifically stains developed calcium deposits was used to stain the cells after osteogenic differentiation. Cells were washed after fixation with PBS, and 2% alizarin red S solution in distilled water was added. After 30 min incubation at RT on a rocking platform, the cells were washed with distilled water and then with PBS to remove the remaining dye. For light microscopic analysis, the cells were kept in PBS.

2.8. Secretome Analysis. For the detection of cytokines secreted by the AF-MSCs, the Proteome Profiler Human Cytokine Array Panel A (R&D Systems, MA, USA) was performed according to the manufacturer's instructions. Initially, 1.5 ml of conditioned medium (pooled equal volumes from the three independent AF-MSC samples used for this study) was used. The array was evaluated by detection of the emitted chemiluminescence. The pixel density of each spotted cytokine was analysed using the software ImageJ. All spots on the membrane including reference and negative control spots were measured separately. Correlation variations and p values were calculated based on the pixel density. The pixel density value of 50 was set as the threshold.

2.9. RNA Isolation. After incubation with TRIzol (Thermo Fisher) for 5 min at RT on a rocking platform, the cells were detached and frozen within this solution at −80°C.

The RNA was then isolated by using the Direct-zol RNA MiniPrep Kit (Zymo Research, CA, USA) which already contains DNase. The resulting RNA was dissolved in RNA/DNAse free water and analysed using the NanoDrop 2000 (Thermo Fisher) spectrophotometer.

2.10. Transcriptome Analysis. Microarray experiments were performed on the PrimeView Human Gene Expression Array (Affymetrix, Thermo Fisher Scientific) for two samples of AF-MSCs (AF-MSC1, AF-MSC2), foetal bone marrow-derived MSCs (fMSC), and embryonic stem cells (H1, H9) as well as human foreskin fibroblast-derived induced pluripotent stem cells (iPSCs) and are provided online at the National Center of Biotechnology Information (NCBI) Gene Expression Omnibus (https://www.ncbi.nlm.nih.gov/geo/query/acc.cgi?acc=GSE100448). The unnormalized bead summary data was further processed via the R/Bioconductor [30] environment using the package affy (http://bioconductor.org/packages/release/bioc/html/affy.html) [31]. The obtained data was background-corrected, transformed to a logarithmic scale (to the base 2), and normalized by employing the Robust Multiarray Average method. Heatmaps and cluster analysis were generated using the heatmap.2 function from the gplots package, and the correlation coefficients were measured using Pearson correlation as similarity measure (http://CRAN.R-project.org/package=gplots).

2.11. Gene Ontology, KEGG Pathway, and STRING Network Analysis. After transcriptome analysis gene ontology terms and associated KEGG pathways [32] for the different gene sets were generated using the DAVID tool (https://david.ncifcrf.gov/) [33], the STRING network tool was used for network cluster analysis (https://string-db.org/) [34].

3. Results

3.1. Isolation and Culture of C-Section-Derived AF-MSCs. During C-sections at full-term gestation, AF was collected using a syringe (Figure 1(a)) and transferred into 50 ml tubes. The red colour of the fluid indicates the presence of erythrocytes. The AF was washed twice with PBS (Figures 1(b) and 1(c)) then the remaining erythrocytes were lysed by resuspending the cell pellet in ammonium chloride (Figure 1(d)). After additional washing, the pellet had a whitish colour indicating successful removal of the remaining blood cells (Figure 1(e)). Microscopic analysis directly after the purification displayed a heterogeneous mixture of different cell types (Figure 1(f)). First, attached cells were visible after 4 to 7 days. After passaging them twice, the heterogeneous morphology of the cells (Figure 1(g)) became more homogeneous with spindle-shaped fibroblast-like forms (Figure 1(h)). Cells were cultured until they all showed a homogeneous MSC morphology and then used for further experiments.

3.2. In Vitro Differentiation Capacity and Cell Surface Marker Expression. To investigate their multipotent differentiation capacity, AF-MSCs from three independent preparations were challenged to differentiate into adipogenic, chondrogenic, and osteogenic directions by employing distinct differentiation media for 3 weeks. Successful differentiation into adipocytes was observed by staining of emerging fat droplets with Oil Red O solution (Figure 2(a), A1). The fat vacuoles surrounded the cell nuclei. During chondrogenic differentiation, the cells aggregated and alcian blue staining showed the presence of emerged proteoglycans within the developed cell clusters of chondrocytes (Figure 2(a), A2) and osteogenic lineage differentiation was shown by alizarin red S staining of developed calcium deposits (Figure 2(a), A3). The visual mineralization of the cells started after the first week. Cells of the control wells remained fibroblast-like. Cells from all preparations showed a higher propensity to differentiate into the osteogenic lineage than into the other two investigated lineages as evidenced by differentiated areas within the cell culture dish of about 90%.

3.3. Flow Cytometric Analysis for Cell Surface Marker Expression. To analyse the cell surface marker presence on the AF-MSCs, the human MSC phenotyping kit (Miltenyi Biotec GmbH, Bergisch Gladbach, Germany) was used which contained antibodies against MSC-related markers CD73, CD90, and CD105 separately and antibodies against haematopoietic markers CD14, CD20, CD34, and CD45 in a combined cocktail. After staining, the cells were analysed using a flow cytometer. Within the three independent AF-MSC preparations, the presence of CD73, CD90, and CD105 positive cells was up to 90%. As expected, all cell preparations were devoid of the haematopoietic markers CD14, CD20, CD34, and CD45 (Figure 2(b)). Furthermore, AF-MSCs were analysed for the expression of pluripotency-associated cell surface markers. A subpopulation of approximately 33% of the cells was positive for SSEA4 whereas 14% of the cells was positive for TRA-1-60 and 8% was positive for TRA-1-81 (Figure 3(b), B1, B2, and B3).

3.4. Immunofluorescent-Based Analysis of Stem Cell Marker Expression in AF-MSCs. AF-MSCs had a spindle-shaped morphology and expressed the type III intermediate filament vimentin (Figure 3(a), A1) which is expressed by mesenchymal cells and widely used as a mesenchymal indicator [35]. In parallel, these cells were negative for E-cadherin (Figure 3(a), A2) as a marker for epithelial cells. The expression of CD133/prominin-1 (Figure 3(a), A3), a marker for multipotent progenitor cells including MSCs [36, 37], was detected. The populations we isolated did not express OCT4 or NANOG (Figure 3(a), A5 and A6). However, the AF-MSCs expressed c-Kit, SSEA4, TRA-1-60, and TRA-1-81 (Figure 3(a), A4, A7, A8, and A9). The percentage of cells positive for the investigated markers was consistent with the flow cytometric data.

3.5. Secretome Analysis. The ability of AF-MSCs to secrete cytokines was investigated employing a cytokine array. To achieve this, cell culture supernatants from three distinct AF-MSC preparations were pooled and analysed using the cytokine array. This revealed the presence of chemokine (C-C motif), ligand 2 (CCL2; MCP-1), C-X-C motif chemokine 1 (CXCL1; GROα), CXCL12 (SDF-1), colony stimulating factor 2 (CSF2; GM-CSF), intercellular adhesion molecule 1 (ICAM1; CD54), interleukin-6 (IL-6), IL-8,

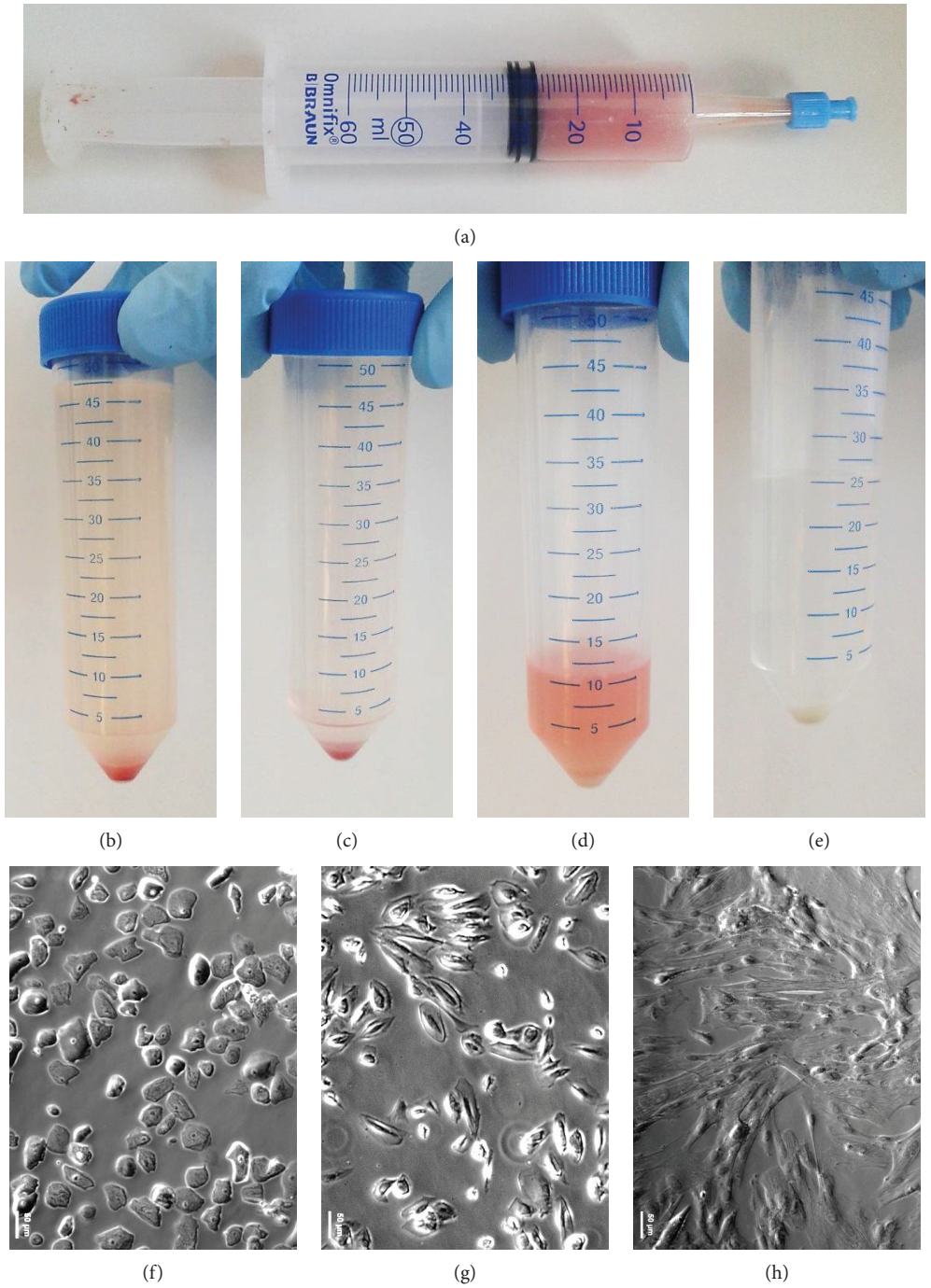

Figure 1: Amniotic fluid cell preparation. Amniotic fluid was collected during Caesarean sections using a 60 ml syringe (a). The AF was washed with PBS and centrifuged resulting in a reddish pellet (b, c). The red colour indicated the presence of erythrocytes which were then lysed using ammonium chloride at 4°C. The resulting white cell pellet (d, e) was transferred to cell culture vessels showing high level of heterogeneity (f). After, prolonged *in vitro* culture and passaging heterogeneous cell morphology (g) became uniform showing spindle-shaped fibroblast-like morphology (h).

IL-21, macrophage migration inhibitory factor (MIF), and plasminogen activator inhibitor-1 (PAI-1; SERPINE1) at distinct levels which were above background expression (Figures 4(a) and 4(b)). CCL2, CXCL1, IL-6, and IL-8 were the highest secreted cytokines. Average levels of secretion were found for CSF2, ICAM1, MIF, and SERPINE (PAI-1) whereas CXCL12 and IL-21 were expressed at the lowest levels. Gene ontology term analysis of the secreted cytokines revealed terms associated with immune modulatory properties such as "immune response," "chemotaxis," and "inflammatory response" (Figure 4(c)).

3.6. Overlapping, Distinct Gene Expression, Associated Gene Ontologies, and Pathways. Hierarchical clustering

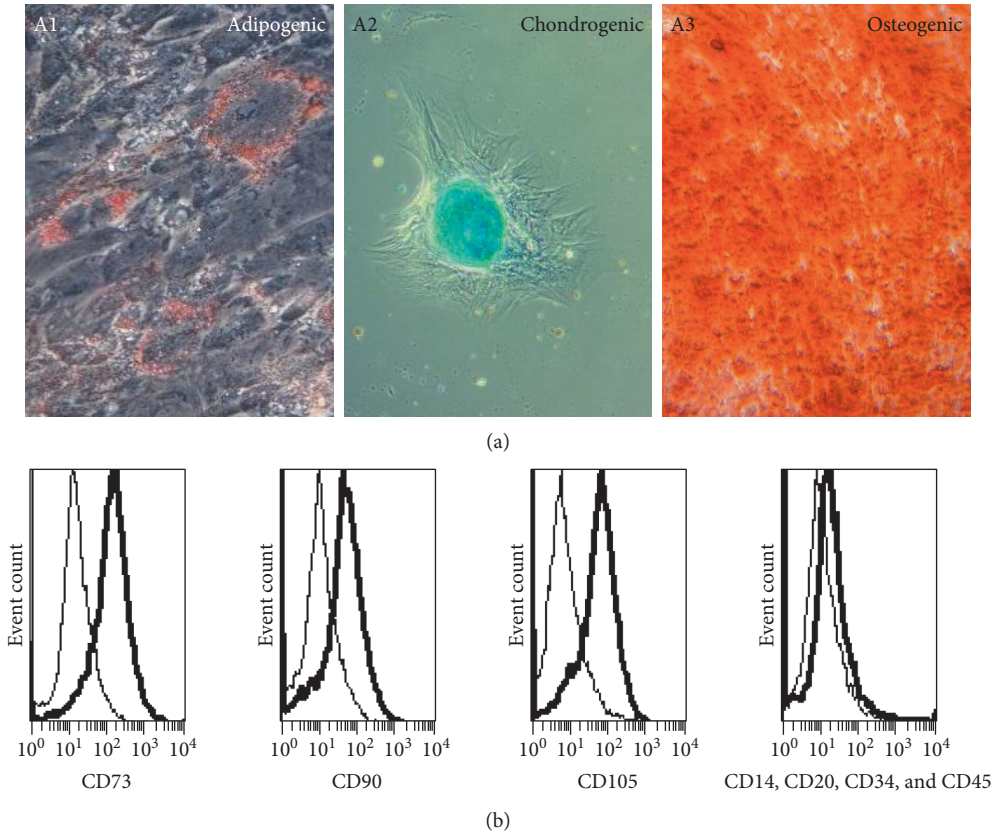

Figure 2: *In vitro* differentiation potential and immunophenotype of AF-MSCs. Multilineage differentiation potential of AF-MSCs was investigated by applying adipocyte, chondrocyte, and osteoblast differentiation media to the cells for 3 weeks. Staining of Oil Red O showed successful differentiation into adipogenic lineage with developed fat vacuoles surrounding the cell nucleus (A1). Chondrogenic differentiation was shown to be present by alcian blue staining of cell aggregates containing proteoglycan (A2). Osteoblast formation by AF-MSCs was indicated by alizarin red S staining of calcium deposits (A3). Flow cytometry was used for the analysis of cell surface marker expression. Histograms showed that MSC markers CD73, CD90, and CD105 were detected as cell surface proteins on AF-MSCs preparation derived from C-sections whereas hematopoietic marker expressions CD14, CD20, CD34, and CD45 were low (bold lines) (b). Antibody isotype controls are represented by thin lines.

(Figure 5(a)) based on the transcriptome profiles of AF-MSCs, fMSCs, and pluripotent stem cells (H1, H9, and iPSCs) revealed a closer relationship of AF-MSC1 and AF-MSC2 to native fMSCs than to pluripotent stem cells. The heatmap derived from the transcriptome data (Figure 5(b)) shows that the cells from both AF preparations are closer to fMSCs. The heatmap consists of 17 genes commonly up- and downregulated between AF-MSCs, fMSCs, and pluripotent cells. Genes which were expressed predominantly in AF-MSCs and fMSCs were vimentin *(VIM)*, *CD44*, *CD73*, *CD105*, and *SERPINE1* as well as osteogenic markers runt-related transcription factor 2 (*RUNX2*) and growth/differentiation factor 5 (*GDF5*). In contrast to this, AF-MSCs and fMSCs were devoid of *E-Cadherin* and pluripotency markers *OCT4*, *SOX2*, and *NANOG*. Venn diagram analysis (Figure 5(c)) revealed an overlap of 11,148 genes among all cell types. Interestingly, AF-MSCs shared more genes (489) with pluripotent stem cells than with fMSCs (442). KEGG pathway analysis of genes shared between pluripotent stem cells and AF-MSCs showed the involvement of phosphatidylinositol pathway and Notch signalling (Supplementary Figure S1 available online at https://doi.org/10.1155/2017/5932706). However, AF-MSCs distinctly expressed 181 genes.

Pearson correlation analysis of the transcriptome data (Figure 5(d)) revealed a high correlation (0.89 and 0.90) between AF-MSC1 and AF-MSC2 and fMSCs but low correlation (0.78–0.81) with the pluripotent cells. The significant KEGG pathways as well as gene ontology terms related to the shared genes between AF samples and fMSCs were related to immune function, skeletal development, and TGFβ-signalling (Figure S2).

3.7. AF-MSC-Specific Gene Expression Analysis. A heatmap was derived using the 181 AF-MSC exclusive gene set (Figure 6(a)). One subset of these genes could be used to identify possible AF-MSC marker genes (Figure 6(b)) including *PSG5*, *C4orf26*, *C8orf4*, *EVR-3*, *EMX-2*, and *C15orf37*. Furthermore, gene ontology analysis focusing on biological processes (Figure 6(c)) showed the involvement of genes associated with skeletal system development and patterning. Tissue-specific gene distribution analysis (Figure 6(d))

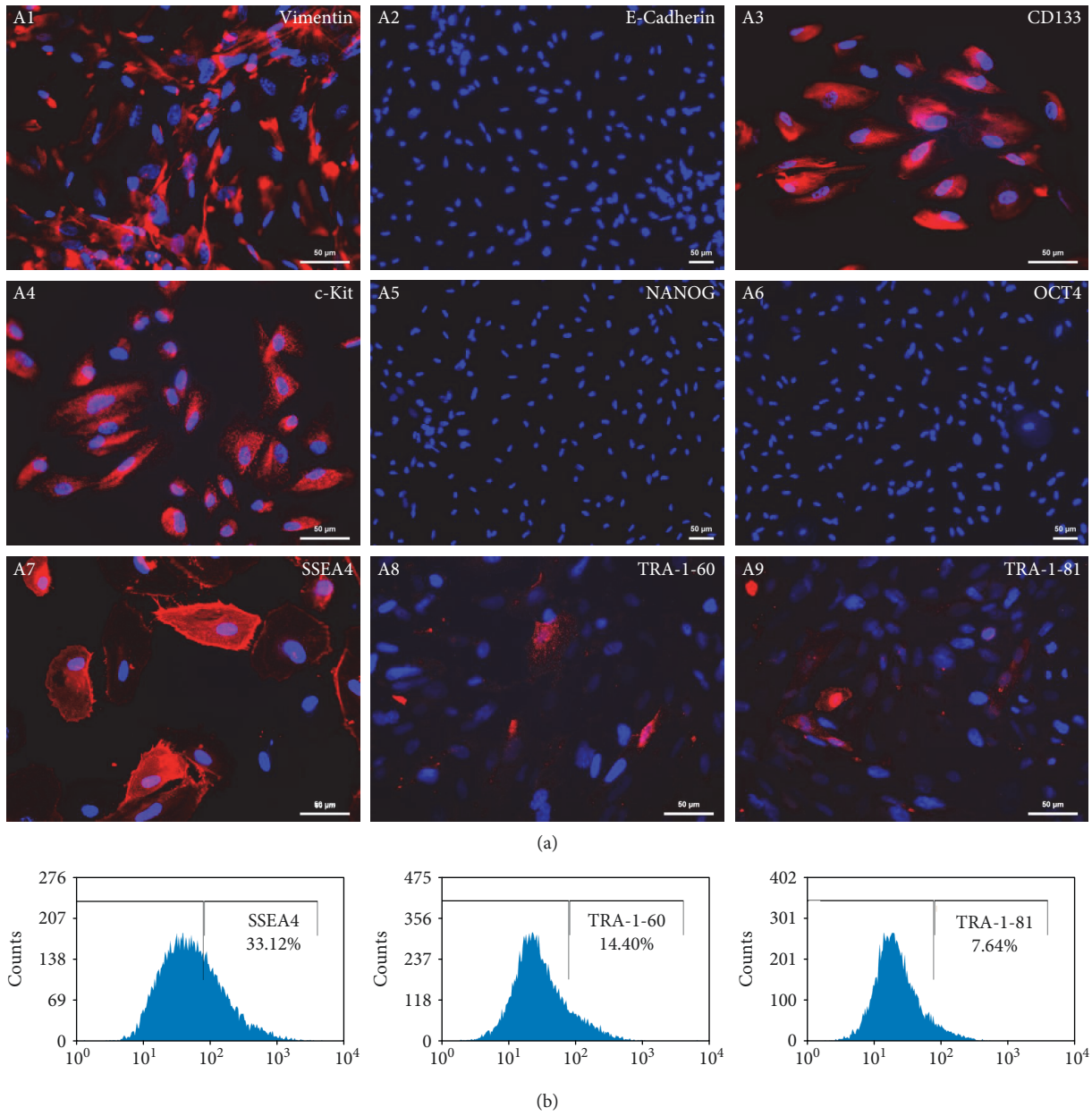

Figure 3: Protein expression analysis of AF-MSCs. (a) By immunofluorescent staining, AF-MSCs were found to express vimentin (A1), CD133 (A3), c-Kit (A4), SSEA4 (A7), TRA-1-60 (A8), and TRA-1-81 (A9) and by parallel absence of E-cadherin (A2), NANOG (A5), and OCT4 (A6). Cell nuclei were stained using Hoechst. (b) Flow cytometric analysis confirmed cell surface expression of SSEA4 (B1), TRA 1-60 (B2), and TRA-1-81 (B3).

revealed the relationship between the 181 AF-MSC-specific genes and the different embryonic tissues. The most prominent tissues were the testis, kidney, and hypothalamus. The rest of the genes were distributed among the other organs. The AF-MSC-specific gene set (181 genes) was further compared to an already published transcriptome dataset of third-trimester AFSCs [11] and visualized with a Venn diagram (Figure 6(e)). 25 genes including *HOXB7*, *APBB1IP*, *HOXB8*, *PTHLH*, and *ZPLD1* were found to be expressed in common between these two gene sets. Referring to the associated gene ontology terms, these genes are mostly associated with embryonic skeletal system morphogenesis, positive regulation of branching involved in ureteric bud morphogenesis, skeletal system development, and regulation of mesonephros development as well as anterior/posterior pattern specification.

3.8. Network Analysis of 181 AF-MSC Exclusive Genes. The network analysis of the 181 AF-MSC-specific genes was done using the STRING tool and predicted 4 different clusters (Figure 7): cluster 1 displayed the patterning and embryonic development related HOX genes such as the homeobox B7 (*HOXB7*), cluster 2 contained the immunity-related gene (e.g., *CSF2*), and cluster 3 included the extracellular matrix- (ECM-) related gene set (e.g., laminin subunit

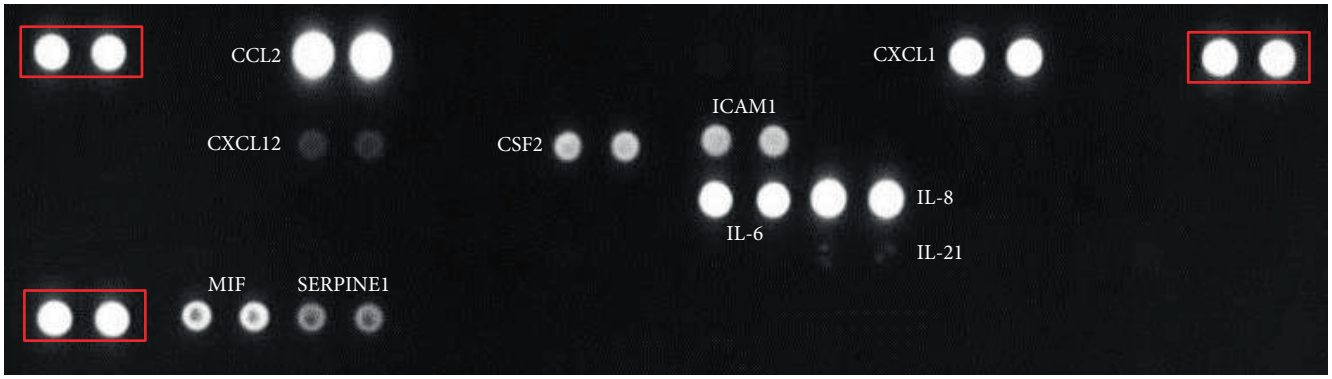

(a)

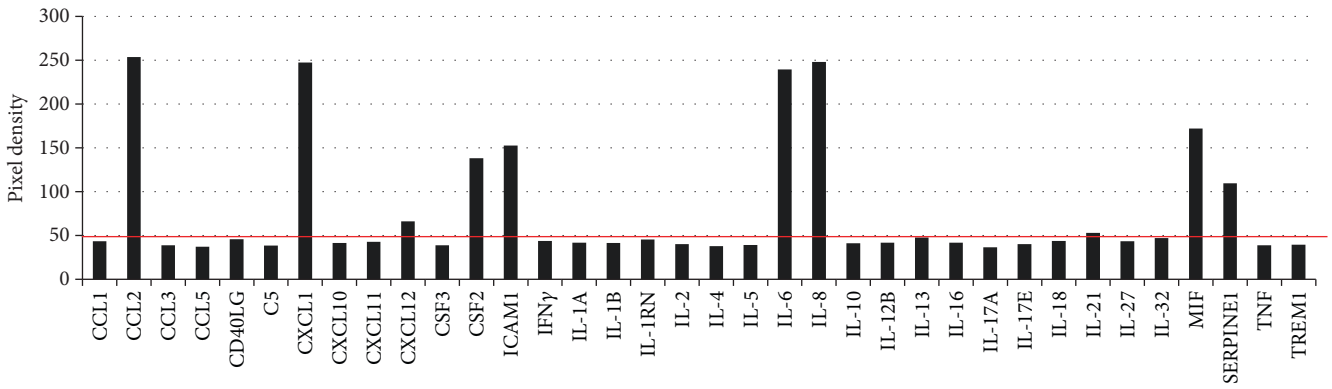

(b)

Category	Term	*p* value	Genes
GOTERM_CC_DIRECT	GO:0005615~extracellular space	8,74E-10	CXCL1, CSF2, ICAM1, IL6, CCL2, SERPINE1, IL21, CXCL12, and MIF
GOTERM_BP_DIRECT	GO:0071222~cellular response to lipopolysaccharide	1,33E-07	CSF2, ICAM1, IL6, CCL2, and SERPINE1
GOTERM_BP_DIRECT	GO:0006955~immune response	5,09E-07	CXCL1, CSF2, IL6, CCL2, IL21, and CXCL12
GOTERM_CC_DIRECT	GO:0005576~extracellular region	1,13E-05	CXCL1, CSF2, IL6, CCL2, SERPINE1, CXCL12, and MIF
GOTERM_MF_DIRECT	GO:0005102~receptor binding	1,23E-05	CXCL1, CCL2, SERPINE1, CXCL12, and MIF
GOTERM_BP_DIRECT	GO:0006954~inflammatory response	1,66E-05	CXCL1, IL6, CCL2, CXCL12, and MIF
GOTERM_BP_DIRECT	GO:0090026~positive regulation of monocyte chemotaxis	2,38E-05	CCL2, SERPINE1, and CXCL12
GOTERM_MF_DIRECT	GO:0008083~growth factor activity	4,69E-05	CXCL1, CSF2, IL6, and CXCL12
GOTERM_BP_DIRECT	GO:0070374~positive regulation of ERK1 and ERK2 cascade	6,00E-05	ICAM1, IL6, CCL2, and MIF
GOTERM_MF_DIRECT	GO:0005125~cytokine activity	6,00E-05	CSF2, IL6, IL21, and MIF
GOTERM_BP_DIRECT	GO:0043200~response to amino acid	9,17E-05	ICAM1, IL6, and CCL2
GOTERM_BP_DIRECT	GO:0009408~response to heat	2,22E-04	IL6, CCL2, and CXCL12
GOTERM_MF_DIRECT	GO:0008009~chemokine activity	2,29E-04	CXCL1, CCL2, and CXCL12
GOTERM_BP_DIRECT	GO:0060326~cell chemotaxis	4,07E-04	CXCL1, CCL2, and CXCL12

(c)

Figure 4: Secretome analysis of AF-MSCs. The cytokines CCL2, CXCL1, CXCL12, CSF2, ICAM, IL-6, IL-8, IL-21, MIF, and SERPINE1 were detected by protein arrays in cell culture supernatant from AF-MSCs. A membrane with spotted antibodies was used for detection. The three red-boxed spot pairs in the corners represent protein array quality controls (a). Densitometric analysis revealed specific pixel densities; the pixel density of 50 represents the threshold (red line) (b). Gene ontology analysis of secreted cytokines revealed the shown top 14 results with *p* values below 0.0005 (c).

alpha 3 (*LAMA 3*)) whereas cluster 4 showed the WNT pathway and signalling-related gene set which includes *WNT10A*. The network analysis also revealed functional biological process (BP) enrichment of regionalization, anterior/posterior pattern specification, chordate embryonic development, embryonic organ development, and embryonic skeletal system morphogenesis.

4. Discussion

In comparison to our results, it was shown that MSCs derived from the bone marrow attached to the cell culture dish within three days after plating whereas umbilical cord and adipose tissue-derived MSCs attached within the first 24 h [38]. The prolonged attachment time of the AF-MSCs

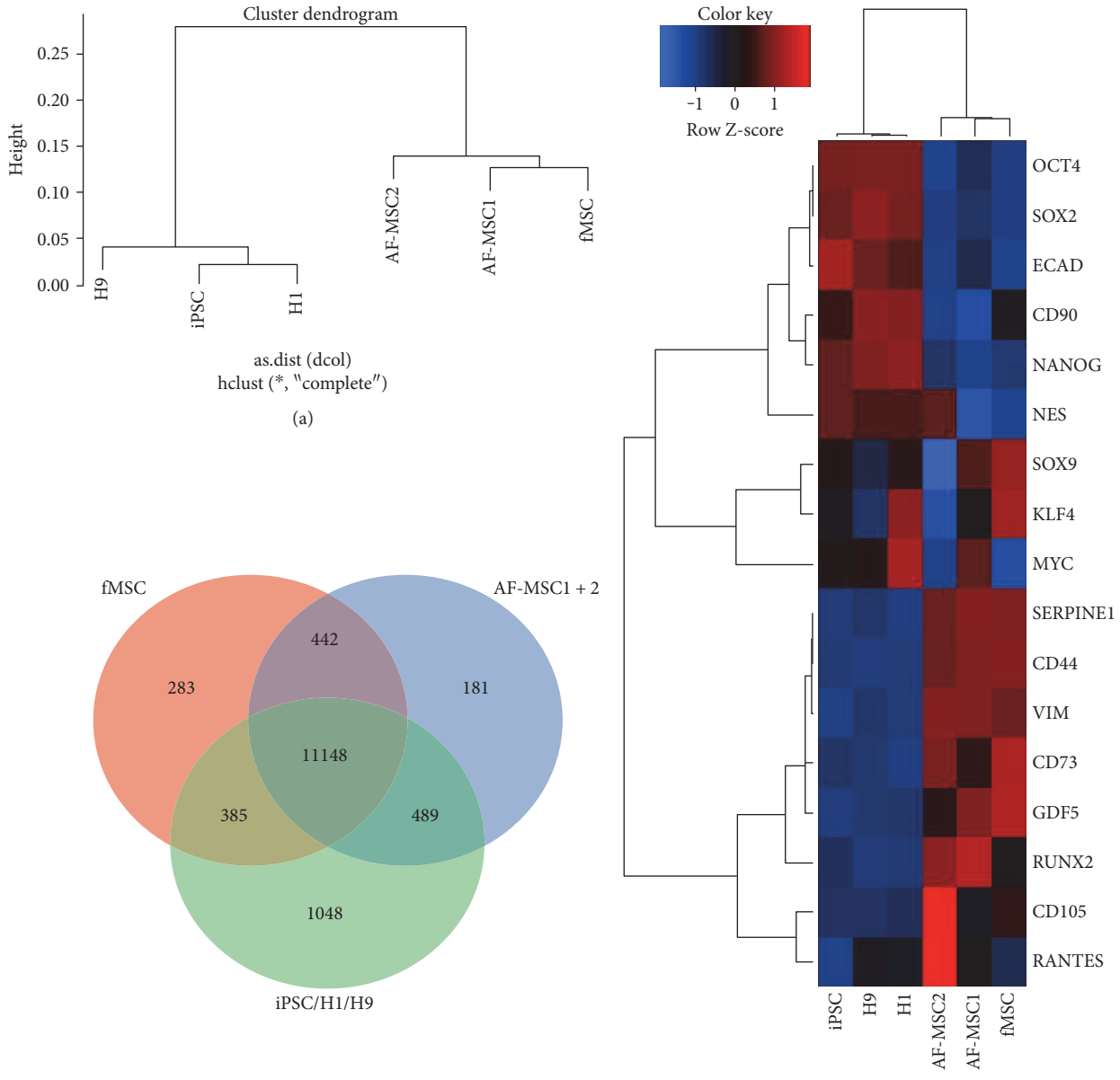

Sample	AF-MSC1	AF-MSC2	fMSC	iPSC	H1	H9
AF-MSC1	1.00	0.89	0.90	0.79	0.79	0.81
AF-MSC2	0.89	1.00	0.89	0.78	0.78	0.79
fMSC	0.90	0.89	1.00	0.84	0.83	0.87
iPSC	0.79	0.78	0.84	1.00	0.98	0.98
H1	0.79	0.78	0.83	0.98	1.00	0.97
H9	0.81	0.79	0.87	0.98	0.97	1.00

(d)

Figure 5: Overlapping and distinct gene expression in AF-MSCs. Dendrogram resulting from hierarchical clustering (a) of global gene expression profiles of AF-MSCs, fMSCs, and established pluripotent stem cells (H1, H9, and iPSCs). Transcriptomes of AF-MSC1 and AF-MSC2 cluster with fMSC while those of the H1, H9, and iPSCs cluster separately. The heatmap of 17 commonly up- or downregulated genes (b) shows similar gene expression of AF-MSCs and fMSCs. Venn diagram analysis revealed shared gene expression between fMSC, AF-MSCs, and pluripotent stem cells (c). Pearson's correlation coefficient was calculated based on the transcription data (d). Each replicate was pairwise compared with each other replicate. A value of 1 indicates perfect linear correlation while a value of 0 implies no correlation. Pearson correlation analysis of transcriptome data revealed a high correlation (green) of both AF-MSC1 and AF-MSC2 with fMSCs but low correlation (red) with pluripotent cells.

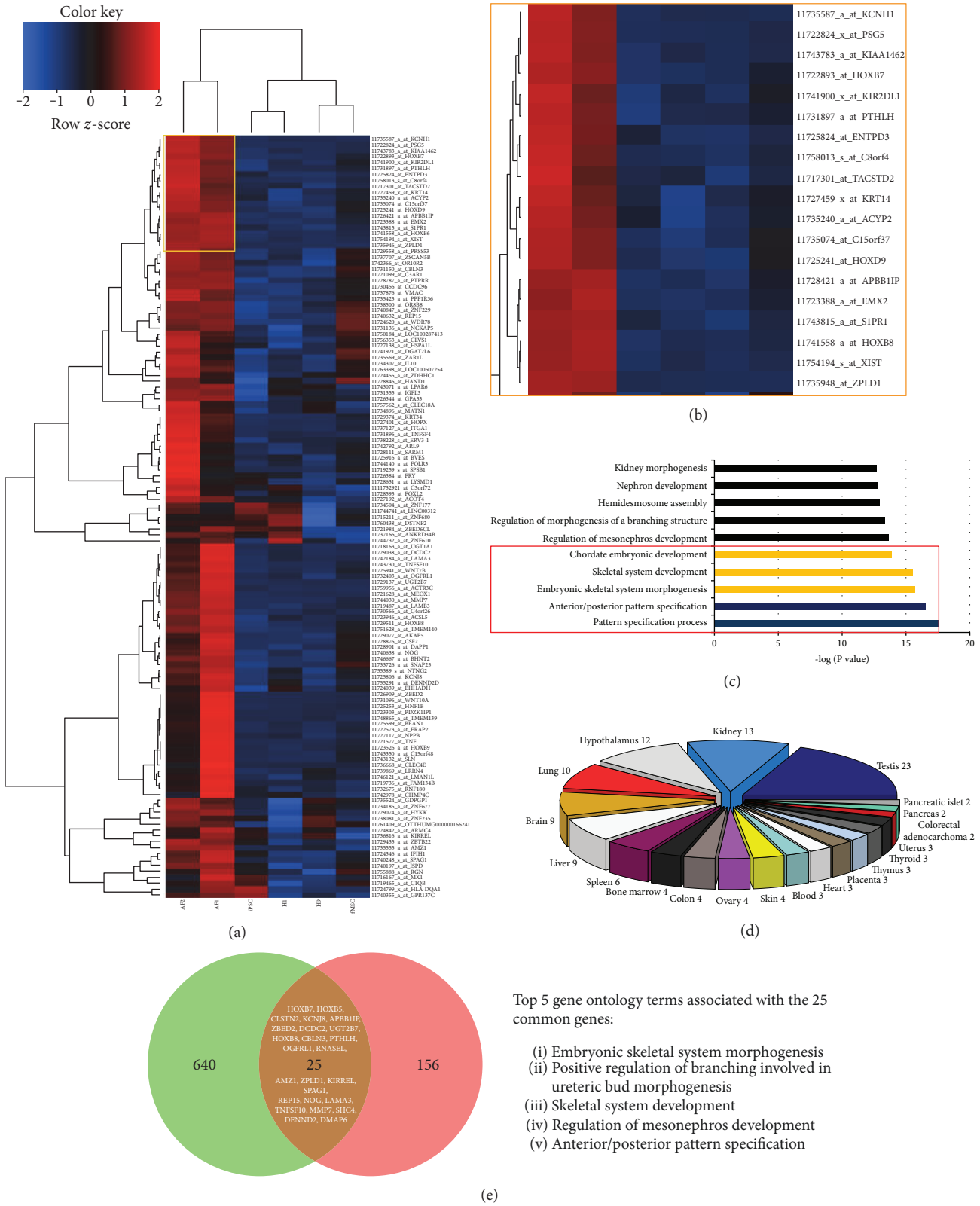

Figure 6: AF-MSC-specific genes. (a) Heatmap and clustering of the 181 genes exclusive for AF-MSCs (see Figure 5(c)). Zoom in on one cluster of the heatmap (b) showed possible AF-MSC markers (yellow box). Gene ontology (GO) analysis of the 181 AF-MSC exclusive genes using the DAVID tool for the GO terms associated with biological processes (c) with a maximum p value of 0.05. Significantly enriched GO terms for each category are shown with the −log of their p values. (d) Tissue distribution of the 181 exclusive AF-MSC-related genes. (e) Comparative analysis of 181 AF-MSC-specific genes and an already published data set of 665 AFSC-specific genes [11] via Venn diagram uncovered a common set of 25 genes.

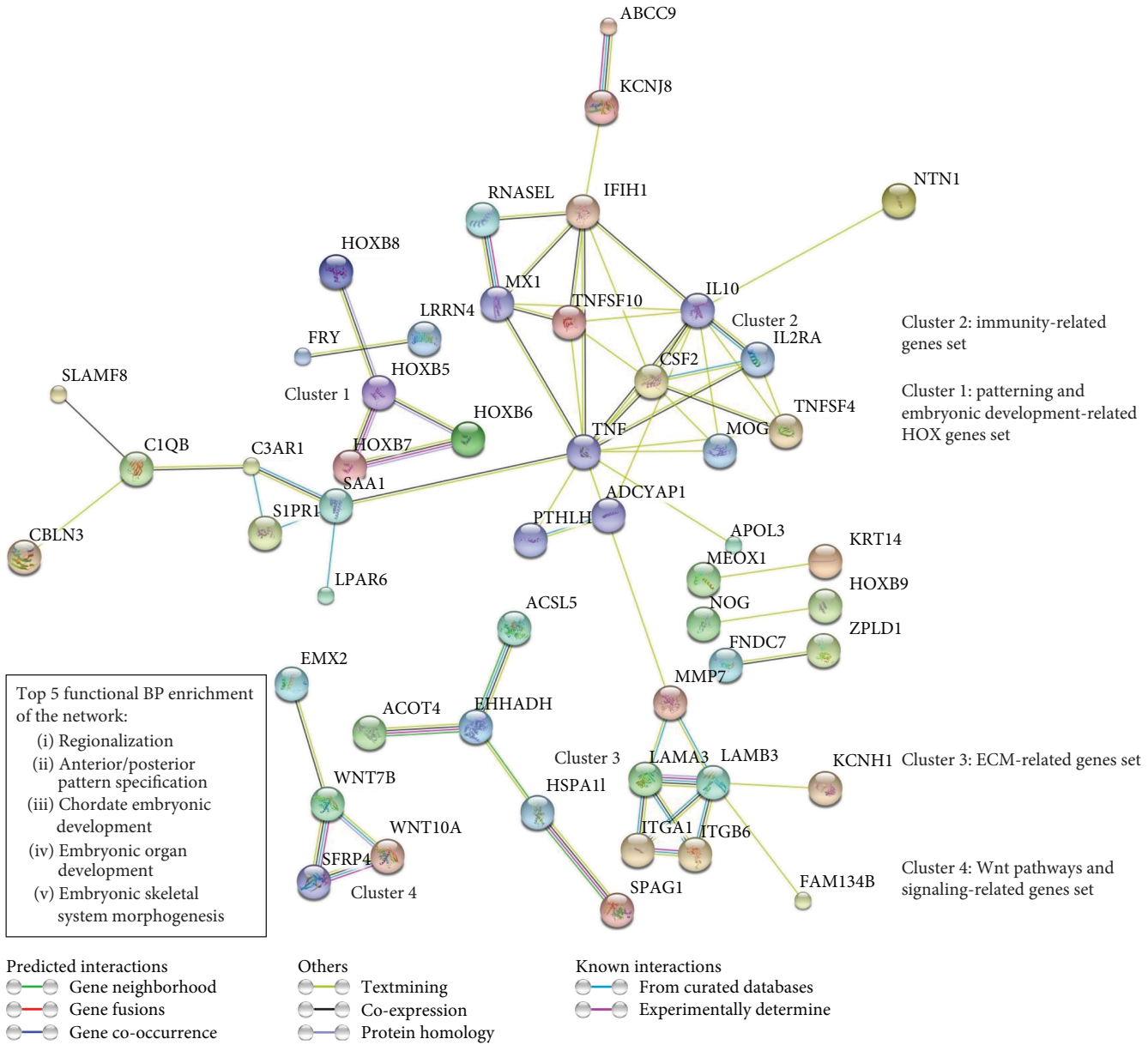

Figure 7: Network analysis of the 181 AF-MSC-specific genes. STRING network analysis revealed 4 distinct clusters: cluster 1 represents the genes involved in patterning and embryonic development which mainly involves the HOX genes. Cluster 2 contains genes related to immunity (e.g., TNF and IL-10). Extracellular matrix- (ECM-) related genes are found in cluster 3, and cluster 4 shows genes related to WNT signalling.

could be explained by the change of environment (micro-environment of amnion with distinct chemicals), the high heterogeneity of the cells, and a lower prevalence of stem cells within at term amniotic fluid when compared to the first and second-trimester amniotic fluid. In addition to the fibroblast-like cells, other cell morphologies were present in the AF preparation but these diluted out with time and increasing passage numbers (Figure 1). The remaining cells were of mesenchymal morphology and expressed vimentin and were devoid of E-cadherin (Figure 2(a), A1 and A2). Wolfrum et al. reported epithelial-like morphologies in senescent AFSCs [11]. Hoehn et al. similarly recognized different populations in second-trimester AF that either possessed fibroblast-like or epithelial-like morphologies [39, 40]. Comparable proliferative capabilities of the populations, long-lasting ex vivo culture of the fibroblast-like cells which proliferated over 30 passages and the epithelial-like morphologies have also been observed. Nevertheless, most of the studies obtained AFSCs from amniocentesis. This procedure has restricted access to the fluid with a certain level of risk to the foetus and mother [41]. The collection of AF from full-term pregnancies or during deliveries as done in the present study could be a possible alternative option with higher prevalence of healthy diploid foetuses as compared to first- and second-trimester-derived AF.

The exhibited multilineage differentiation potential into bone, fat, and cartilage cells of the C-section-derived AF-MSCs (Figure 2(a), A1, A2, and A3) was also previously described for AFSCs derived from amniocentesis. The chondrogenic differentiation potential of AF-MSCs derived from amniocentesis has been reported [42] and especially osteogenic differentiation potential and further use in bone defect models underlines the potency of these cells to build up osteoblasts [43] and thus could be used for future bone related therapies.

The AF-MSCs obtained during C-sections showed the typical MSC cell surface marker expression of CD73, CD90, and CD105 by parallel absence of the haematopoietic markers CD14, CD20, CD34, and CD45 (Figure 2(b)) as described by the ISCT [24]. However, as shown in previous studies, different individuals and origins of MSCs, respectively, can lead to altered cell surface maker expressions [23].

The transcription factor OCT4 in association with NANOG and SOX2 has been shown to be the key driver of pluripotency [29]. However, the majority of AFSC studies published so far have focused on only expression but not function.

In contrast to other studies describing OCT4 and NANOG expression in third-trimester AF-derived cells, our analysis revealed these markers to be negative for caesarean-derived AF-MSCs [27, 28, 41]. In our case, we identified singular cytoplasmic OCT4 positive-expressing cells at passages 1-2, but after a few more passaging, these cells were diluted out (data not shown). This variability could be due to the number of passages, different protocols, culture methods, and media used.

It was previously shown that a subpopulation of AFSCs from the first and second trimester expresses the pluripotency markers OCT4, NANOG, SOX2, c-MYC, and KLF4 [6, 7, 10] thus indicating that first and second-trimester AFSCs are multipotent and express pluripotency-associated markers. Although, Prusa et al. claimed OCT4 expression by 5 out of 11 independent AF-MSCs (no passage numbers stated) as indicated by real-time PCR. Additionally, they only showed a single cell of their AF preparations being positive for OCT4. Furthermore, the functionality of this OCT4 positivity was not addressed [6].

However, first-trimester c-Kit-positive AFSCs were converted to a pluripotent state by supplementation with valproic acid in pluripotency supporting media and matrix. [10]. While valproic acid could induce pluripotency, these cells were distinct from hESCs as evidenced by microarray analysis [9]. Additional results [7] further support our observation that developmental potential of AFSCs decreases with gestation time. Also shown in our current study, transcriptome cluster analysis revealed clear separation between AFSCs and hESCs [7]. Thus it can be concluded that subpopulations of early term AFSCs are more susceptible for reprogramming events but are not pluripotent.

In this study, we have demonstrated the expression of SSEA4, an early embryonic glycolipid antigen by immunofluorescent and flow cytometric analysis (Figures 3(a), A7 and 3(b), B1). This protein does not play a critical role in maintaining pluripotency and has also been shown to be expressed in adult BM-MSCs [44, 45]. Furthermore, the cells were found to be c-Kit positive (Figure 3(a), A4), which is essential for the maintenance and differentiation of hematopoietic stem cells and multipotent progenitor cells [46]. It has been reported that c-Kit-expressing cells show a subpopulation of MSCs derived from adipose tissue that possess a higher telomerase expression and differentiation potential [47]. Moreover, a subpopulation of the AF-MSCs from C-sections also expresses TRA-1-60 and TRA-1-81 as shown by immunofluorescent-based stainings as well as flow cytometric analysis (Figures 3(a), A8 and A9 and 3(b), B2 and B3). This relates to already existing studies of midtrimester AF preparations [48].

Chemokines and their correspondent receptors are important for attraction and homing of leukocytes to infections, injury, or inflammation sites [49]. MSCs express these receptors, and thus it has been shown that chemokines and growth factors are chemotactic for bone marrow-derived MSCs [50]. Due to their immune modulatory properties, MSCs are widely used in clinical application in graft versus host disease [51]. In accordance with our secretome data (Figure 3) revealing the release of at least 9 distinct cytokines from AF-MSCs, Mirabella et al. analysed AFSC-conditioned media and identified the presence of known proangiogenic and antiangiogenic factors such as vascular endothelial growth factor (VEGF), CXCL12, IL-8, CCL2, two angiogenesis inhibitors interferon gamma (IFNγ), and CXCL10 and IP-10 as secreted proteins [13]. Besides angiogenesis, AFSCs also contribute to osteogenesis either directly or indirectly by secreting distinct cytokines [14].

The therapeutic potential of AF-MSCs and their secreted molecules in mice with acute hepatic failure has been analysed, and numerous proinflammatory mediators, regulating cytokines and growth factors in AF-MSC-conditioned media such as IL-10, IL-27, IL-17E, IL-12p70, IL-1β, and IL-1ra, were observed. Some tissue repair promoting factors, namely, SERPINE1, MCP-1, and SDF-1, were also identified [52]. Our results agree with the previous comparison of cytokines released from MSCs originating from the bone marrow, cord blood, and placenta. The pool of cytokines previously investigated was the same as that of our work. MIF, IL-8, SERPINE1, GROα, and IL-6 were secreted by MSCs from all the investigated sources. Placental MSCs expressed ICAM-1 (CD54), and MCP-1 (CCL2) and bone marrow MSCs secreted MCP-1 (CCL2), and SDF-1 (CXCL12) in addition [53]. Other studies that investigated a larger pool of cytokines showed additional expression of RANTES, INFγ, IL-1α, TGFβ, angiogenin, and oncostatin M [54]. The trophic factors released by AF-MSCs are and will be of great importance for future therapies.

Cluster dendrogram analysis clearly demonstrated that the transcriptomes of the two AF-MSC samples clustered together with the fMSC sample while the pluripotent iPSCs and ESCs (H1, H9) clustered in a separate group (Figure 5(a)). Both AF-MSC preparations acquired the expression profile of native foetal MSCs (Figures 5(b) and 5(d)). They were devoid of pluripotency-associated markers *OCT4*, *NANOG*, and *SOX2* but express the MSC markers *CD44*, *CD73*, *CD105*, and *vimentin*.

Recent studies investigating the gene expression pattern of AFSCs at different passages by illumina microarray detected 1970 differentially expressed genes and classified the expression profile into 9 distinct clusters. Genes with gradually increasing expression and higher passages included *CXCL12*, *CDH6*, and *FOLR3*. On the other hand, the important downregulated genes were *CCND2*, *K8*, *IGF2*, *BNP-B*, and *CRABPII* [55]. The Venn diagram of the analysed data sets in the present study showed a group of genes which are exclusively expressed by the AF-MSC samples (Figure 5(c)). From the heatmap of the 181 AF-MSC-specific genes (Figure 6(a)) identified by transcriptome analysis, a group of potential AF-MSC marker genes was extracted. This group contained *PSG5*, *C4orf26*, *C8orf4*, *EVR-3*, *EMX-2*, and *C15orf37* amongst others (Figure 6(b)), of which some such as *C8orf4* have not been characterized yet. Using these 181 genes, gene ontology analysis was conducted and most of the terms within the top 10 results of the biological processes were related to bone and skeletal development (Figure 6(c)). Global gene expression of AFSCs compared with AF-iPSCs and ESCs revealed genes related to self-renewal and pluripotency (1299 genes, e.g., *POU5F1*, *SOX2*, *NANOG*, and *microRNA-binding protein LIN28*) as well as AFSC-specific genes (665 genes, e.g., *OXTR*, *HHAT*, *RGS5*, *NF2*, *CD59*, *TNFSF10*, and *NT5E*) were identified in AFSCs [11]. The AF-MSC-specific genes from our study were further investigated using the STRING tool which built up 4 different clusters (Figure 7): patterning and embryonic development-related HOX genes, immunity-related genes, ECM-related genes, and a WNT pathway and signalling-related gene set which is in line with the KEGG pathway analysis (Figure S3). Compared to the previous identified 665 AFSC-specific genes, we could show an overlap of 25 genes (Figure 6(e)) which include *HOXB7*, *APBB1IP*, *HOXB8*, *PTHLH*, and *ZPLD1* which were also present within the highest expressed genes within our samples (Figure 6(b)). These genes are mainly involved in skeletal development (Figure 6(e) and Table S1). This subset of genes represents putative marker genes for AF-MSC selection procedures in the future.

5. Conclusion

In this study, we have demonstrated that a subpopulation of human AFSCs (AF-MSCs) isolated from AF collected during C-sections is indeed MSCs meeting the accepted criteria and definition [16]. In addition, we show that the transcriptomes of AF-MSCs are more similar to that of BM-MSCs (Pearson's correlation of 0.9) than to bona fide pluripotent stem cells (human embryonic stem cell lines H1 and H9 and a dermal fibroblast-derived iPSC line) even though they express well-known pluripotency-associated markers. We finally demonstrated their ability to secrete a plethora of cytokines and growth factors crucial for paracrine signalling. Overall, Caesarean section-derived amniotic fluid which in contrast to that obtained from amniocentesis is of no risk to the foetus and contain AF-MSCs with great potential for clinical applications.

Conflicts of Interest

The authors declare that there is no conflict of interest regarding the publication of this paper.

Authors' Contributions

Lucas-Sebastian Spitzhorn and Md Shaifur Rahman contributed equally to this work.

Acknowledgments

Professor Dr. James Adjaye and Professor Dr. Tanja Fehm acknowledge support from the Medical Faculty, Heinrich-Heine-Universität Düsseldorf. In addition, Professor Dr. James Adjaye acknowledges support from the German Academic Exchange Service (DAAD) (91607303).

References

[1] M. C. Renda, E. Fecarotta, G. Schillaci et al., "Mesenchymal fetal stem cells (FMSC) from amniotic fluid (AF): expansion and phenotypic characterization," *Blood*, vol. 126, p. 4758, 2015.

[2] P. de Coppi, G. Bartsch Jr., M. M. Siddiqui et al., "Isolation of amniotic stem cell lines with potential for therapy," *Nature Biotechnology*, vol. 25, no. 1, pp. 100–106, 2007.

[3] I. Antonucci, R. Di Pietro, M. Alfonsi et al., "Human second trimester amniotic fluid cells are able to create embryoid body-like structures in vitro and to show typical expression profiles of embryonic and primordial germ cells," *Cell Transplantation*, vol. 23, no. 12, pp. 1501–1515, 2014.

[4] G. Simoni and R. Colognato, "The amniotic fluid-derived cells: the biomedical challenge for the third millennium," *Journal of Prenatal Medicine*, vol. 3, no. 3, pp. 34–36, 2009.

[5] F. Torricelli, L. Brizzi, P. A. Bernabei et al., "Identification of hematopoietic progenitor cells in human amniotic fluid before the 12th week of gestation," *Italian Journal of Anatomy and Embryology*, vol. 98, no. 2, pp. 119–126, 1993.

[6] A. R. Prusa, E. Marton, M. Rosner, G. Bernaschek, and M. Hengstschläger, "Oct-4-expressing cells in human amniotic fluid: a new source for stem cell research?," *Human Reproduction*, vol. 18, no. 7, pp. 1489–1493, 2003.

[7] D. Moschidou, K. Drews, A. Eddaoudi, J. Adjaye, P. de Coppi, and P. V. Guillot, "Molecular signature of human amniotic fluid stem cells during fetal development," *Current Stem Cell Research & Therapy*, vol. 8, no. 1, pp. 73–81, 2013.

[8] C. Koike, K. Zhou, Y. Takeda et al., "Characterization of amniotic stem cells," *Cellular Reprogramming*, vol. 16, no. 4, pp. 298–305, 2014.

[9] K. E. Hawkins, D. Moschidou, D. Faccenda et al., "Human amniocytes are receptive to chemically induced reprogramming to pluripotency," *Molecular Therapy*, vol. 25, no. 2, pp. 427–442, 2017.

[10] D. Moschidou, S. Mukherjee, M. P. Blundell et al., "Valproic acid confers functional pluripotency to human amniotic fluid stem cells in a transgene-free approach," *Molecular Therapy*, vol. 20, no. 10, pp. 1953–1967, 2012.

[11] K. Wolfrum, Y. Wang, A. Prigione, K. Sperling, H. Lehrach, and J. Adjaye, "The LARGE principle of cellular reprogramming: lost, acquired and retained gene expression in foreskin

and amniotic fluid-derived human iPS cells," *PLoS One*, vol. 5, no. 10, article e13703, 2010.

[12] M. Teodelinda, C. Michele, C. Sebastiano, C. Ranieri, and G. Chiara, "Amniotic liquid derived stem cells as reservoir of secreted angiogenic factors capable of stimulating neo-arteriogenesis in an ischemic model," *Biomaterials*, vol. 32, no. 15, pp. 3689–3699, 2011.

[13] T. Mirabella, C. Gentili, A. Daga, and R. Cancedda, "Amniotic fluid stem cells in a bone microenvironment: driving host angiogenic response," *Stem Cell Research*, vol. 11, no. 1, pp. 540–551, 2013.

[14] A. M. Ranzoni, M. Corcelli, K. L. Hau et al., "Counteracting bone fragility with human amniotic mesenchymal stem cells," *Scientific Reports*, vol. 6, no. 6, article 39656, 2016.

[15] Q. Sun, F. Li, H. Li et al., "Amniotic fluid stem cells provide considerable advantages in epidermal regeneration: B7H4 creates a moderate inflammation microenvironment to promote wound repair," *Scientific Reports*, vol. 5, article 11560, 2015.

[16] M. F. Pittenger, A. M. Mackay, S. C. Beck et al., "Multilineage potential of adult human mesenchymal stem cells," *Science*, vol. 284, no. 5411, pp. 143–147, 1999.

[17] A. J. Friedenstein, I. I. Piatetzky-Shapiro, and K. V. Petrakova, "Osteogenesis in transplants of bone marrow cells," *Journal of Embryology and Experimental Morphology*, vol. 16, no. 3, pp. 381–390, 1966.

[18] A. J. Friedenstein, U. F. Deriglasova, N. N. Kulagina et al., "Precursors for fibroblasts in different populations of hematopoietic cells as detected by the in vitro colony assay method," *Experimental Hematololgy*, vol. 2, pp. 83–92, 1974.

[19] M. Mimeault and S. K. Batra, "Concise review: recent advances on the significance of stem cells in tissue regeneration and cancer therapies," *Stem Cells*, vol. 24, no. 11, pp. 2319–2345, 2006.

[20] K. Bieback, S. Kern, H. Kluter, and H. Eichler, "Critical parameters for the isolation of mesenchymal stem cells from umbilical cord blood," *Stem Cells*, vol. 22, no. 4, pp. 625–634, 2004.

[21] J. W. Kim, S. Y. Kim, S. Y. Park et al., "Mesenchymal progenitor cells in the human umbilical cord," *Annals of Hematology*, vol. 83, no. 12, pp. 733–738, 2004.

[22] P. S. In 't Anker, S. A. Scherjon, C. Kleijburg-van der Keur et al., "Isolation of mesenchymal stem cells of fetal or maternal origin from human placenta," *Stem Cells*, vol. 22, no. 7, pp. 1338–1345, 2004.

[23] M. S. Tsai, S. M. Hwang, K. D. Chen et al., "Functional network analysis of the transcriptomes of mesenchymal stem cells derived from amniotic fluid, amniotic membrane, cord blood, and bone marrow," *Stem Cells*, vol. 25, no. 10, pp. 2511–2523, 2007.

[24] M. Dominici, K. Le Blanc, I. Mueller et al., "Minimal criteria for defining multipotent mesenchymal stromal cells. The International Society for Cellular Therapy position statement," *Cytotherapy*, vol. 8, no. 4, pp. 315–317, 2006.

[25] A. Stolzing, E. Jones, D. McGonagle, and A. Scutt, "Age-related changes in human bone marrow-derived mesenchymal stem cells: consequences for cell therapies," *Mechanisms of Ageing and Development*, vol. 129, no. 3, pp. 163–173, 2008.

[26] J. Savickiene, G. Treigyte, S. Baronaite et al., "Human amniotic fluid mesenchymal stem cells from second- and third-trimester amniocentesis: differentiation potential, molecular signature, and proteome analysis," *Stem Cells International*, vol. 2015, Article ID 319238, 15 pages, 2015.

[27] Q. You, X. Tong, Y. Guan et al., "The biological characteristics of human third trimester amniotic fluid stem cells," *The Journal of International Medical Research*, vol. 37, no. 1, pp. 105–112, 2009.

[28] M. S. Tsai, J. L. Lee, Y. J. Chang, and S. M. Hwang, "Isolation of human multipotent mesenchymal stem cells from second-trimester amniotic fluid using a novel two-stage culture protocol," *Human Reproduction*, vol. 19, no. 6, pp. 1450–1456, 2004.

[29] Y. Babaie, R. Herwig, B. Greber et al., "Analysis of Oct4-dependent transcriptional networks regulating self-renewal and pluripotency in human embryonic stem cells," *Stem Cells*, vol. 25, no. 2, pp. 500–510, 2007.

[30] R. C. Gentleman, V. J. Carey, D. M. Bates et al., "Bioconductor: open software development for computational biology and bioinformatics," *Genome Biology*, vol. 5, no. 10, article R80, 2004.

[31] L. Gautier, L. Cope, B. M. Bolstad, and R. A. Irizarry, "affy—analysis of *Affymetrix GeneChip* data at the probe level," *Bioinformatics*, vol. 20, no. 3, pp. 307–315, 2004.

[32] M. Kanehisa, M. Furumichi, M. Tanabe, Y. Sato, and K. Morishima, "KEGG: new perspectives on genomes, pathways, diseases and drugs," *Nucleic Acids Research*, vol. 45, no. D1, pp. D353–D361, 2017.

[33] D. W. Huang, B. T. Sherman, and R. A. Lempicki, "Systematic and integrative analysis of large gene lists using DAVID bioinformatics resources," *Nature Protocols*, vol. 4, no. 1, pp. 44–57, 2009.

[34] D. Szklarczyk, A. Franceschini, S. Wyder et al., "STRING v10: protein–protein interaction networks, integrated over the tree of life," *Nucleic Acids Research*, vol. 43, no. D1, Database issue, pp. D447–D452, 2015.

[35] M. G. Mendez, S. Kojima, and R. D. Goldman, "Vimentin induces changes in cell shape, motility, and adhesion during the epithelial to mesenchymal transition," *FASEB Journal*, vol. 24, no. 6, pp. 1838–1851, 2010.

[36] A. B. Balaji, K. Jamil, G. M. Ram, and G. S. Raju, "Pluripotent lineage of CD133 stem cells isolated from human skin samples," *Indian Journal of Experimental Biology*, vol. 51, no. 2, pp. 107–115, 2013.

[37] T. Tondreau, N. Meuleman, A. Delforge et al., "Mesenchymal stem cells derived from CD133-positive cells in mobilized peripheral blood and cord blood: proliferation, Oct4 expression, and plasticity," *Stem Cells*, vol. 23, no. 8, pp. 1105–1112, 2005.

[38] S. Kern, H. Eichler, J. Stoeve, H. Kluter, and K. Bieback, "Comparative analysis of mesenchymal stem cells from bone marrow, umbilical cord blood, or adipose tissue," *Stem Cells*, vol. 24, no. 5, pp. 1294–1301, 2006.

[39] H. Hoehn, E. M. Bryant, L. E. Karp, and G. M. Martin, "Cultivated cells from diagnostic amniocentesis in second trimester pregnancies. I. Clonal morphology and growth potential," *Pediatric Research*, vol. 8, no. 8, pp. 746–754, 1974.

[40] H. Hoehn and D. Salk, "Chapter 2. Morphological and biochemical heterogeneity of amniotic fluid cells in culture," *Methods in Cell Biology*, vol. 26, pp. 11–34, 1982.

[41] A. A. Hamid, M. K. Joharry, H. Mun-Fun et al., "Highly potent stem cells from full-term amniotic fluid: a realistic perspective," *Reproductive Biology*, vol. 17, no. 1, pp. 9–18, 2017.

[42] J. S. Park, M. S. Shim, S. H. Shim et al., "Chondrogenic potential of stem cells derived from amniotic fluid, adipose tissue, or

bone marrow encapsulated in fibrin gels containing TGF-β3," *Biomaterials*, vol. 32, no. 32, pp. 8139–8149, 2011.

[43] K. M. Dupont, K. Sharma, H. Y. Stevens, J. D. Boerckel, A. J. García, and R. E. Guldberg, "Human stem cell delivery for treatment of large segmental bone defects," *Proceedings of the National Academy of Sciences of the United States of America*, vol. 107, no. 8, pp. 3305–3310, 2010.

[44] S. N. Brimble, E. S. Sherrer, E. W. Uhl et al., "The cell surface glycosphingolipids SSEA-3 and SSEA-4 are not essential for human ESC pluripotency," *Stem Cells*, vol. 25, no. 1, pp. 54–62, 2007.

[45] E. J. Gang, D. Bosnakovski, C. A. Figueiredo, J. W. Visser, and R. C. Perlingeiro, "SSEA-4 identifies mesenchymal stem cells from bone marrow," *Blood*, vol. 109, no. 4, pp. 1743–1751, 2007.

[46] J. Zayas, D. S. Spassov, R. G. Nachtman, and R. Jurecic, "Murine hematopoietic stem cells and multipotent progenitors express truncated intracellular form of c-kit receptor," *Stem Cells and Development*, vol. 17, no. 2, pp. 343–353, 2008.

[47] A. Blazquez-Martinez, M. Chiesa, F. Arnalich, J. Fernandez-Delgado, M. Nistal, and M. P. de Miguel, "c-Kit identifies a subpopulation of mesenchymal stem cells in adipose tissue with higher telomerase expression and differentiation potential," *Differentiation*, vol. 87, no. 3-4, pp. 147–160, 2014.

[48] D. Moschidou, S. Mukherjee, M. P. Blundell et al., "Human mid-trimester amniotic fluid stem cells cultured under embryonic stem cell conditions with valproic acid acquire pluripotent characteristics," *Stem Cells and Development*, vol. 22, no. 3, pp. 444–458, 2013.

[49] M. Miyasaka and T. Tanaka, "Lymphocyte trafficking across high endothelial venules: dogmas and enigmas," *Nature Reviews Immunology*, vol. 4, no. 5, pp. 360–370, 2004.

[50] J. F. Ji, B. P. He, S. T. Dheen, and S. S. Tay, "Interactions of chemokines and chemokine receptors mediate the migration of mesenchymal stem cells to the impaired site in the brain after hypoglossal nerve injury," *Stem Cells*, vol. 22, no. 3, pp. 415–427, 2004.

[51] C. Balbi, M. Piccoli, L. Barile et al., "First characterization of human amniotic fluid stem cell extracellular vesicles as a powerful paracrine tool endowed with regenerative potential," *Stem Cells Translational Medicine*, vol. 6, no. 5, pp. 1340–1355, 2017.

[52] D. S. Zagoura, M. G. Roubelakis, V. Bitsika et al., "Therapeutic potential of a distinct population of human amniotic fluid mesenchymal stem cells and their secreted molecules in mice with acute hepatic failure," *Gut*, vol. 61, no. 6, pp. 894–906, 2012.

[53] J. H. Hwang, S. S. Shim, O. S. Seok et al., "Comparison of cytokine expression in mesenchymal stem cells from human placenta, cord blood, and bone marrow," *Journal of Korean Medical Science*, vol. 24, no. 4, pp. 547–554, 2009.

[54] J. A. Potian, H. Aviv, N. M. Ponzio, J. S. Harrison, and P. Rameshwar, "Veto-like activity of mesenchymal stem cells: functional discrimination between cellular responses to alloantigens and recall antigens," *Journal of Immunology*, vol. 171, no. 7, pp. 426–434, 2003.

[55] Y. W. Kim, H. J. Kim, S. M. Bae et al., "Time-course transcriptional profiling of human amniotic fluid-derived stem cells using microarray," *Cancer Research and Treatment*, vol. 42, no. 2, pp. 82–94, 2010.

3.2 The Presence of Human Mesenchymal Stem Cells of Renal Origin in Amniotic Fluid Increases with Gestational Time

Md Shaifur Rahman*, Lucas-Sebastian Spitzhorn*, Wasco Wruck, Carsten Hagenbeck, Percy Balan, Nina Graffmann, Martina Bohndorf, Audrey Ncube, Pascale V. Guillot, Tanja Fehm and James Adjaye

*These authors contributed equally.

Abstract

Background: Established therapies for managing kidney dysfunction such as kidney dialysis and transplantation are limited due to the shortage of compatible donated organs and high costs. Stem cell-based therapies are currently under investigation as an alternative treatment option. As amniotic fluid is composed of fetal urine harbouring mesenchymal stem cells (AF-MSCs), we hypothesized that third-trimester amniotic fluid could be a novel source of renal progenitor and differentiated cells.

Methods: Human third-trimester amniotic fluid cells (AFCs) were isolated and cultured in distinct media. These cells were characterized as renal progenitor cells with respect to cell morphology, cell surface marker expression, transcriptome and differentiation into chondrocytes, osteoblasts and adipocytes. To test for renal function, a comparative albumin endocytosis assay was performed using AF-MSCs and commercially available renal cells derived from kidney biopsies. Comparative transcriptome analyses of first, second and third trimester-derived AF-MSCs were conducted to monitor expression of renal-related genes.

Results: Regardless of the media used, AFCs showed expression of pluripotency associated markers such as SSEA4, TRA-1-60, TRA-1-81 and C-Kit. They also express the mesenchymal marker Vimentin. Immuno-phenotyping confirmed that third-trimester AFCs are bona fide MSCs. AF-MSCs expressed the master renal progenitor markers SIX2 and CITED1, in addition to typical renal proteins such as PODXL, LHX1, BRN1 and PAX8. Albumin endocytosis assays demonstrated the functionality of AF-MSCs as renal cells. Additionally, upregulated expression of *BMP7* and downregulation of WT1, CD133, SIX2 and C-Kit were observed upon activation of WNT signaling by treatment with the GSK-3 inhibitor CHIR99201. Transcriptome analysis and semi-quantitative PCR revealed increasing expression levels of renal-specific genes (e.g., *SALL1, HNF4B, SIX2*) with gestational time. Moreover, AF-MSCs shared more genes with human kidney

cells than with native MSCs and gene ontology terms revealed involvement of biological processes associated with kidney morphogenesis.
Conclusions: Third-trimester amniotic fluid contains AF-MSCs of renal origin and this novel source of kidney progenitors may have enormous future potentials for disease modelling, renal repair and drug screening.

Impact Factor: 4.62
This article is reproduced with permission.
Approximated total share of contribution: 40%
Publication Status: Published in Stem Cell Res Ther. 2018 Apr 25;9(1):113.

Authors' contributions on experimental design, realization and publication: JA, TF, MSR and LSS conceived the idea and designed the experiments. CH and PB collected third-trimester amniotic fluid samples. PVG collected first and second-trimester amniotic fluid samples and prepared the corresponding RNA. MB performed immunofluorescence staining of the HREpCs, and designed the renal specific primers. NG performed real-time PCR analysis. WW performed bioinformatic analysis. AN performed analysis of the CHIR99021-treated AF-MSCs and HREpCs. MSR and LSS isolated the AF-MSCs from third-trimester AF and characterized the AF-MSCs. MSR and LSS wrote the manuscript and JA edited it. All authors read and approved the manuscript.

Pubmed link: https://www.ncbi.nlm.nih.gov/pubmed/29695308
Journal link: https://stemcellres.biomedcentral.com/articles/10.1186/s13287-018-0864-7

Rahman et al. Stem Cell Research & Therapy (2018) 9:113
https://doi.org/10.1186/s13287-018-0864-7

Stem Cell Research & Therapy

RESEARCH Open Access

The presence of human mesenchymal stem cells of renal origin in amniotic fluid increases with gestational time

Md Shaifur Rahman[1†], Lucas-Sebastian Spitzhorn[1†], Wasco Wruck[1], Carsten Hagenbeck[2], Percy Balan[2], Nina Graffmann[1], Martina Bohndorf[1], Audrey Ncube[1], Pascale V. Guillot[3], Tanja Fehm[2] and James Adjaye[1*]

Abstract

Background: Established therapies for managing kidney dysfunction such as kidney dialysis and transplantation are limited due to the shortage of compatible donated organs and high costs. Stem cell-based therapies are currently under investigation as an alternative treatment option. As amniotic fluid is composed of fetal urine harboring mesenchymal stem cells (AF-MSCs), we hypothesized that third-trimester amniotic fluid could be a novel source of renal progenitor and differentiated cells.

Methods: Human third-trimester amniotic fluid cells (AFCs) were isolated and cultured in distinct media. These cells were characterized as renal progenitor cells with respect to cell morphology, cell surface marker expression, transcriptome and differentiation into chondrocytes, osteoblasts and adipocytes. To test for renal function, a comparative albumin endocytosis assay was performed using AF-MSCs and commercially available renal cells derived from kidney biopsies. Comparative transcriptome analyses of first, second and third trimester-derived AF-MSCs were conducted to monitor expression of renal-related genes.

Results: Regardless of the media used, AFCs showed expression of pluripotency-associated markers such as SSEA4, TRA-1-60, TRA-1-81 and C-Kit. They also express the mesenchymal marker Vimentin. Immunophenotyping confirmed that third-trimester AFCs are bona fide MSCs. AF-MSCs expressed the master renal progenitor markers SIX2 and CITED1, in addition to typical renal proteins such as PODXL, LHX1, BRN1 and PAX8. Albumin endocytosis assays demonstrated the functionality of AF-MSCs as renal cells. Additionally, upregulated expression of *BMP7* and downregulation of *WT1*, *CD133*, *SIX2* and C-Kit were observed upon activation of WNT signaling by treatment with the GSK-3 inhibitor CHIR99201. Transcriptome analysis and semiquantitative PCR revealed increasing expression levels of renal-specific genes (e.g., *SALL1*, *HNF4B*, *SIX2*) with gestational time. Moreover, AF-MSCs shared more genes with human kidney cells than with native MSCs and gene ontology terms revealed involvement of biological processes associated with kidney morphogenesis.

Conclusions: Third-trimester amniotic fluid contains AF-MSCs of renal origin and this novel source of kidney progenitors may have enormous future potentials for disease modeling, renal repair and drug screening.

Keywords: Amniotic fluid, Kidney, Renal progenitor cells, SIX2, Mesenchymal stem cells, Albumin endocytosis, Third trimester

* Correspondence: james.adjaye@med.uni-duesseldorf.de
†Equal contributors
[1]Institute for Stem Cell Research and Regenerative Medicine, Medical Faculty, Heinrich Heine University, Moorenstraße 5, 40225 Düsseldorf, Germany
Full list of author information is available at the end of the article

Background

A functional kidney is essential for healthy living due to its major role in toxin and drug filtration. Globally, each year millions of patients require rapid kidney transplantation or dialysis to restore renal function [1, 2]. But the shortage of compatible organs, donor-associated diseases, ageing-associated factors and high cost of transplantation/dialysis are major hurdles [3]. Kidney-associated dysfunctions are now a prioritized health concern and research area. A potential alternative source of renal cells are those derived from embryonic and induced pluripotent stem cells (ESCs and iPSCs) [4–9]. Clinical applications of pluripotent stem cell technologies are constrained by the risk of tumor formation, immunological rejection, legal as well as ethical concerns. In light of this, it is therefore important to find other sources of stem cells which are not tumorigenic, bear a broad differentiation potential and have a high renal regenerative potential.

The architecture and organization of the kidney is very complex and consists of numerous cell types [10] which can interchange identities by a very complex reciprocal interplay and interactions of stromal and epithelial cell lineages [9, 11]. Kidney mesenchymal cells have been demonstrated to express SIX2 and Cbp/p300-interacting transactivator 1 (*CITED1*) which are crucial for the self-renewing capability [11, 12]. Furthermore, the main kidney nephron-regulatory genes have been described, such as SALL1, PAX2, WT1, Cytokeratin 19 (CK19), CD133, Podocalyxin-like protein 1 (*PODXL*), *HOXD11*, *HNF1B*, BRN1, Lhx1 and Pax8 [13–18]. Adult and fetal bone marrow-derived mesenchymal stem cells (BM-MSCs) have been shown to be capable of repairing renal function deficits [19, 20]. BM-MSCs have potent immunosuppressive properties and their potential application in acute kidney injury animal models has been studied recently [21]. However, the use of adult BM-MSCs has some limitations such as the low number of MSCs in adult bone marrow, expression of ageing-associated factors, slow expansion rate, early senescence, inactive telomerase, shorter telomeres and restricted differentiation potential [22]. Due to the increasing number of patients with kidney diseases and limited cell-based therapeutic options, alternative renal progenitor cells and sources are clearly in need [23]. Amniotic fluid contains fetal-derived differentiated and undifferentiated progenitor cells. In vitro, they can be expanded in distinct media formulations and exhibit a heterogeneous morphology with a preponderance of epithelioid and fibroblastoid mesenchymal-like cell shape [24]. In 2007, Perin et al. [25] demonstrated the potency of second-trimester amniotic fluid-derived MSCs (AF-MSCs) to form embryonic kidney structures in vitro. Later, they also showed that human AF-MSCs help in regenerating kidneys undergoing acute tubular necrosis in a rodent model [26–28]. In an animal model of acute renal injury, Camussi's research group confirmed these results and could show comparable efficacy between BM-MSCs and AF-MSCs [29]. Remarkably, the renal differentiation potential of AF-MSCs was demonstrated by producing chimeric organotypic renal structures from murine embryonic kidney cells and human AF-MSCs [30]. Although properties of human amniotic fluid cells such as the lack of immunogenicity and tumorigenicity, their anti-inflammatory properties and their high proliferative and differentiation potential are well described [31, 32], the exact origin of AF-MSCs is still unknown and controversial [33]. Before use in clinical applications, it is mandatory to elucidate the origin of AF-MSCs. Due to the fact that term amniotic fluid consists mostly of fetal urine [34], we hypothesized that AF-MSCs originate from the kidney and accumulate in the AF during fetal nephrogenesis.

Adult and neonatal human urine has been described as a source of kidney progenitor cells [35, 36]. Second-trimester AFCs have been described as an alternative source of podocytes [37] which express mesenchymal markers as well as the podocyte markers CD2AP and NPHS2 [25, 38]. In this study we isolated third-trimester human AF-MSCs and cultured them in distinct supporting media. AF-MSCs were characterized as a multipotent population of renal cells. By combining cellular, molecular, functional and transcriptome data, we conclude that third-trimester amniotic fluid harbors MSCs originating from the fetal kidney. These cells should be considered promising sources for studies on kidney development, nephrotoxicity tests, disease modeling, drug screening and future kidney-related cellular therapies.

Methods

Isolation and culture of human amniotic fluidic cells

Healthy donors who provided the first and second-trimester amniotic fluid in this study provided written informed consent in accordance with the Declaration of Helsinki. Ethical approval was given by the Research Ethics Committees of Hammersmith & Queen Charlotte's Hospitals (2001/6234) in compliance with UK national guidelines (Review of the Guidance on the Research Use of Fetuses and Fetal Material (1989), also known as the Polkinghorne Guidelines, Her Majesty's Stationery Office, London, 1989: Cm762) for the collection of fetal tissue for research. Third-trimester amniotic fluid samples from healthy donors were collected from the Department of Obstetrics and Gynaecology, Medical Faculty, Heinrich Heine University Düsseldorf, Germany, with informed patient consent as well as institutional ethical approval. Amniotic fluids were processed and AF-MSCs were isolated as described previously [32]. In

brief, the cells were cultured in Prime XV or Chang C Medium (both Irvine Scientific, CA, USA), αMEM (Minimum Essential Medium Eagle Alpha Modification; Sigma) containing 10% FBS, 1% GlutaMAX and 1% penicillin/streptomycin (Penstrep), MG30 (Cell Lines Service, Germany) or renal cell medium (RCM) consisting of high-glucose Dulbecco's Modified Eagle's Medium (DMEM) supplemented with 1% Penstrep, 1% glutamine, 10% FBS and SingleQuot Kit CC-4127 REGM at 37 °C, 5% CO_2 and 5% O_2 (Lonza) [39, 40].

After the appearance of initially attached cells (days 4–7), the medium was changed and cells grew until reaching almost full confluency. The cells were then detached using TrypLE Express (Thermo Fisher Scientific) and prepared for further passaging and experiments. Urine-derived kidney progenitor cells and corresponding iPSCs (UM51, ISRM-UM51 [40]) and human renal epithelial cells from a biopsy (HREpCs; PromoCell, Heidelberg, Germany) were used as control cells.

Immunofluorescence staining

To analyze the cells for pluripotency, mesenchymal stem cell and renal cell specific markers, AF-MSCs were cultured in 12-well plates. After a washing step using PBS (Gibco), 4% paraformaldehyde (PFA; Polysciences Inc., PA, USA) was used to fix the cells for 15 min at room temperature (RT). To increase the cell membranes' permeability, 1% Triton X-100 (Carl Roth GmbH & Co. KG, Karlsruhe, Germany) was applied to the fixed cells for 5 min followed by blocking of unspecific binding sites for 2 h. For staining of intracellular proteins, this blocking buffer contained 10% normal goat serum (NGS; Sigma), 0.5% Triton X-100, 1% BSA (Sigma) and 0.05% Tween 20 (Sigma), all dissolved in PBS. Triton and Tween were omitted when extracellular proteins were stained. Afterward, the primary antibodies (presented in Additional file 1: Table S1) were diluted in blocking buffer/PBS and incubated with the cells for 1 h at RT followed by several washing steps using 0.05% Tween 20 in PBS. The corresponding secondary Cy3-labeled or Alexa Fluor 488-labeled antibodies (Thermo Fisher Scientific) and Hoechst 33,258 dye (Sigma-Aldrich Chemie GmbH, Taufkirchen, Germany) or DAPI (Southern Biotech) were added under light exclusion. For the actin filament staining, the toxin phalloidin 488 (A12370; Life Technologies) was used in a dilution of 1:200. A fluorescence microscope (LSM700; Zeiss, Oberkochen, Germany) was used for taking the pictures. All pictures were processed with the ZenBlue 2012 Software Version 1.1.2.0. (Carl Zeiss Microscopy GmbH, Jena, Germany).

In-vitro differentiation assay

In-vitro differentiation of the AF-MSCs into adipocytes, chondrocytes and osteoblasts was done employing the StemPro Adipogenesis, Chondrogenesis, and Osteogenesis differentiation Kits (Gibco, Life Technologies, CA, USA). Media were replaced 2–3 times per week for 3 weeks, and the formation of intracellular lipid droplets (adipocytes), calcium mineralization (osteoblasts) and cellular aggregation toward clusters (chondrocytes) was observed from 14 to 21 days. After the differentiation process, fixation of the cells was done using 4% PFA for 30 min at RT. Subsequently, the cells were stained with Oil Red O for adipocytes, Alcian Blue for chondrocytes, and Alizarin Red S for osteoblasts as described previously [32]. A light microscope was used for imaging.

Flow cytometric analysis

The human MSC phenotyping kit (Miltenyi Biotec GmbH, Bergisch Gladbach, Germany) was used to analyze the cell surface marker composition of the AF-MSC samples (2×10^5 cells were used for each analysis), according to the manufacturer's instructions. The cells were washed with PBS and centrifuged at 300 × *g* for 5 min. After resuspending the pellet in 100 μl PBS, 0.5 μl of the MSC phenotyping cocktail or of the isotype control cocktail were added and the tubes were mixed thoroughly. The MSC phenotyping cocktail is composed of a mixture of fluorochrome-coupled antibodies against various cell surface proteins (CD14-PerCP, CD20-PerCP, CD34-PerCP, CD45-PerCP, CD73-APC, CD90-FITC and CD105-PE). The isotype phenotyping cocktail served as a negative control. The antibody binding took place at 4 °C for 10 min in the dark. Nonbound antibodies were washed out using 1 ml PBS. After centrifugation at 300 × *g* for 5 min, cell fixation using 4% PFA was done.

To analyze the AF-MSCs for pluripotency-associated cell surface markers (TRA-1-60, TRA-1-81, stage-specific embryonic antigen 4 (SSEA4)), corresponding prelabeled antibodies (anti-TRA-1-60-PE, human (clone REA157), number 130-100-347; anti-TRA-1-81-PE, human (clone REA246), number 130-101-410, and anti-SSEA-4-PE, human (clone REA101), number 130-098-369; Miltenyi Biotec GmbH, Bergisch Gladbach, Germany) were used. The staining procedure was carried out as already described. Until analysis via BD FACSCanto (BD Biosciences, Heidelberg, Germany) and CyAn ADP (Beckman Coulter, CA, USA), stained cells were kept at 4 °C in the dark. The FCSalyzer software version 0.9.3 and Summit 4.3 software were used for data analysis.

RNA isolation and quantitative PCR

After single washing with PBS, TRIzol (Thermo Fisher) was added to the cells for 5 min at RT, and the cells were scraped off and stored at − 80 °C. For isolation of the RNA, the Direct-zol RNA Miniprep Kit (Zymo Research, CA, USA) was used according to the manufacturer's instructions. All of the primers used were

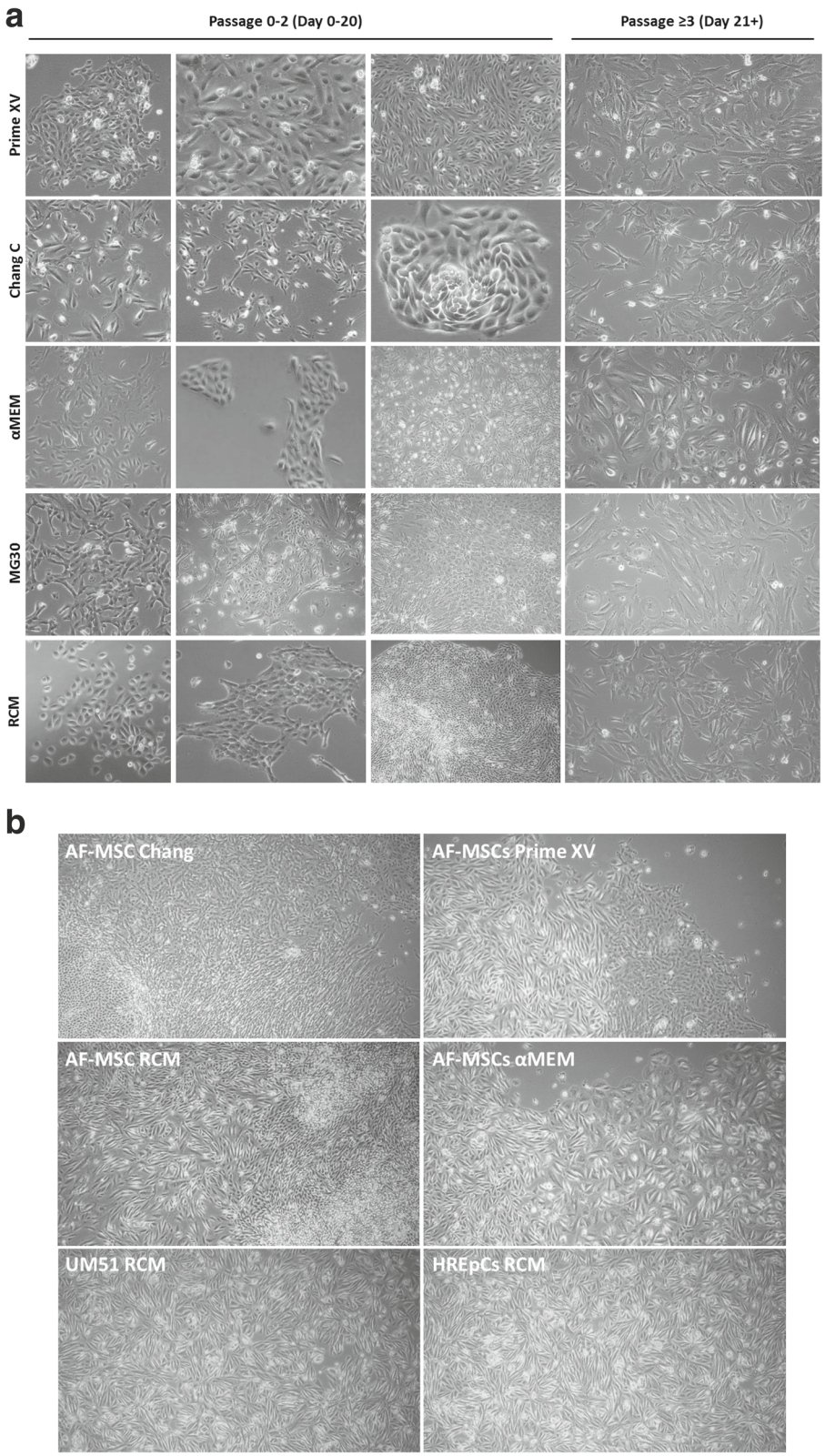

Fig. 1 (See legend on next page.)

(See figure on previous page.)
Fig. 1 Initially attached heterogeneous AFCs display homogeneous cell morphology upon passaging and include typical kidney cell morphologies. Phenotypical complexity of AFCs observed, regardless of culture media composition within first two passages. Upon further passaging, cells became homogeneous with fibroblast-like morphology (**a**). During culture, subpopulation of cells observed which had similar morphology to distinct renal-originated progenitor cells UM51 and HREpCs (**b**). AF-MSC amniotic fluid mesenchymal stem cell, HREpC human renal epithelial cell, αMEM minimum essential medium alpha modification, RCM renal cell medium

purchased from MWG (primer sequences and predicted sizes of amplicons presented in Additional file 1: Table S2). After checking the quality of mRNA, complementary DNA (cDNA) was synthesized with the TaqMan Reverse Transcription Kit (Applied Biosystems). A sample of 500 ng of RNA was used for cDNA synthesis. The prepared mix of 20 μl per sample consisted of 7.70 μl H_2O, 2 μl reverse transcriptase buffer, 4.4 μl $MgCl_2$ (25 mM), 1 μl Oligo (dT)/random hexamer (50 μM), 4 μl dNTP mix (10 mM), 0.4 μl RNase inhibitor (20 U/μl) and 0.5 μl reverse transcriptase (50 U/μl). For semi-qPCR, a mixture of 25 μl per sample contained the following: 11.375 μl H_2O, 5 μl of 1× Go-Taq G2 Hot Start Green PCR buffer, 4 μl of 4 mM $MgCl_2$, 0.5 μl dNTP-Mix (10 mM each), 1 μl forward primer (0.3 μM), 1 μl reverse primer (0.3 μM), 0.125 μl (0.625 U) Hotstart Taq polymerase (5 U/μl) and 2 μl cDNA. A PCR thermal cycler (PEQLAB, Erlangen Germany) was employed. After an initial denaturation step at 95 °C for 2 min, 30 cycles followed with a denaturation step at 95 °C for 30 s, an annealing step at the temperature specific for each primer (ranging from 55 to 63 °C) for 30–35 s and an extension step at 72 °C for 30–40 s. Detection of semi-qPCR amplification products was performed by size fractionation on 2% agarose gel electrophoresis. Real-time quantitative PCR was performed in technical triplicates with Power SYBR Green Master Mix (Life Technologies) on a VIIA7 (Life Technologies) machine. Mean values were normalized to levels of the housekeeping gene ribosomal protein L37A. Results are depicted as mean values (% of untreated control) with 95% confidence interval.

Albumin endocytosis assay

To analyze the functional ability of the AF-MSCs to endocytose exogenous albumin, cells were plated at a density of 30% in 12-well plates without coating. After 2 days, media were supplemented with 10 μM CHIR dissolved in DMSO or the same volume of DMSO alone and the cells were allowed to differentiate for 2 days. After this time period the cells were washed once with PBS and incubated in new medium supplemented with 20 μg/ml of albumin from bovine serum (BSA), Alexa Fluor™ 488 conjugate (catalog no. A13100; Thermo Fischer) for 1 h. As endocytosis is an energy-dependent process, incubations were performed at 37 °C. After 1 h of incubation, however, cells were washed three times with ice-cold PBS and fixed with 4% PFA for 15 min. Cell-associated fluorescence was analyzed using an excitation wavelength of 488 nm and an emission wavelength of 540 nm and imaged using a florescence microscope (LSM700; Zeiss, Oberkochen, Germany). All pictures were analyzed with ZenBlue 2012 Software Version 1.1.2.0. (Carl Zeiss Microscopy GmbH, Jena, Germany). Human fetal foreskin cell line HFF1 (SCRC-1041; ATCC) and fMSCs (kindly gifted from Prof. Richard O. C. Oreffo, Southampton, UK) served as control.

Transcriptome analysis

PrimeView Human Gene Expression Array Chips (Affymetrix; Thermo Fisher Scientific) were used for microarray experiments (conducted by Biologisch-Medizinisches Forschungszentrum, Düsseldorf, Germany). The gene expression profile for AF-MSCs, HREpCs, fMSCs, UM51 and ISRM-UM51 are provided online at the National Center of Biotechnology Information Gene Expression Omnibus. The affy package of the R/Bioconductor environment [41, 42] was used for further processing of the unnormalized bead summary data. After background correction, the data were transformed to a logarithmic scale (to base 2), and normalized by employing the robust multiarray average method. The heatmap.2 function from the gplots package (http://CRAN.R-project.org/package=gplots) was employed to create cluster analysis and heatmaps. The correlation coefficients were calculated with Pearson correlation as a similarity measure (http://CRAN.R-project.org/package=gplots). Based on the results of the transcriptome analysis, the DAVID tool (https://david.ncifcrf.gov/) [43] was used to generate gene ontology terms and associated KEGG pathways [44] for the distinct gene sets.

Results

AFCs become homogeneous after several passages and contain a renal cell-like subpopulation

In-vitro growth of AFCs in monolayers preserves diversity of cell types irrespective of media, in particular within the first two passages. AFCs were isolated and expanded in various media (RCM, Prime XV, Chang C, MG30, αMEM) under hypoxic conditions. Bright-field microscopic observation revealed a mixture of distinct cell types with a morphology of mesenchymal-like, epithelioid, spindle, cobble-stone and tubular shapes, of fetal-derived differentiated and undifferentiated progenitor cells (Fig. 1a). After

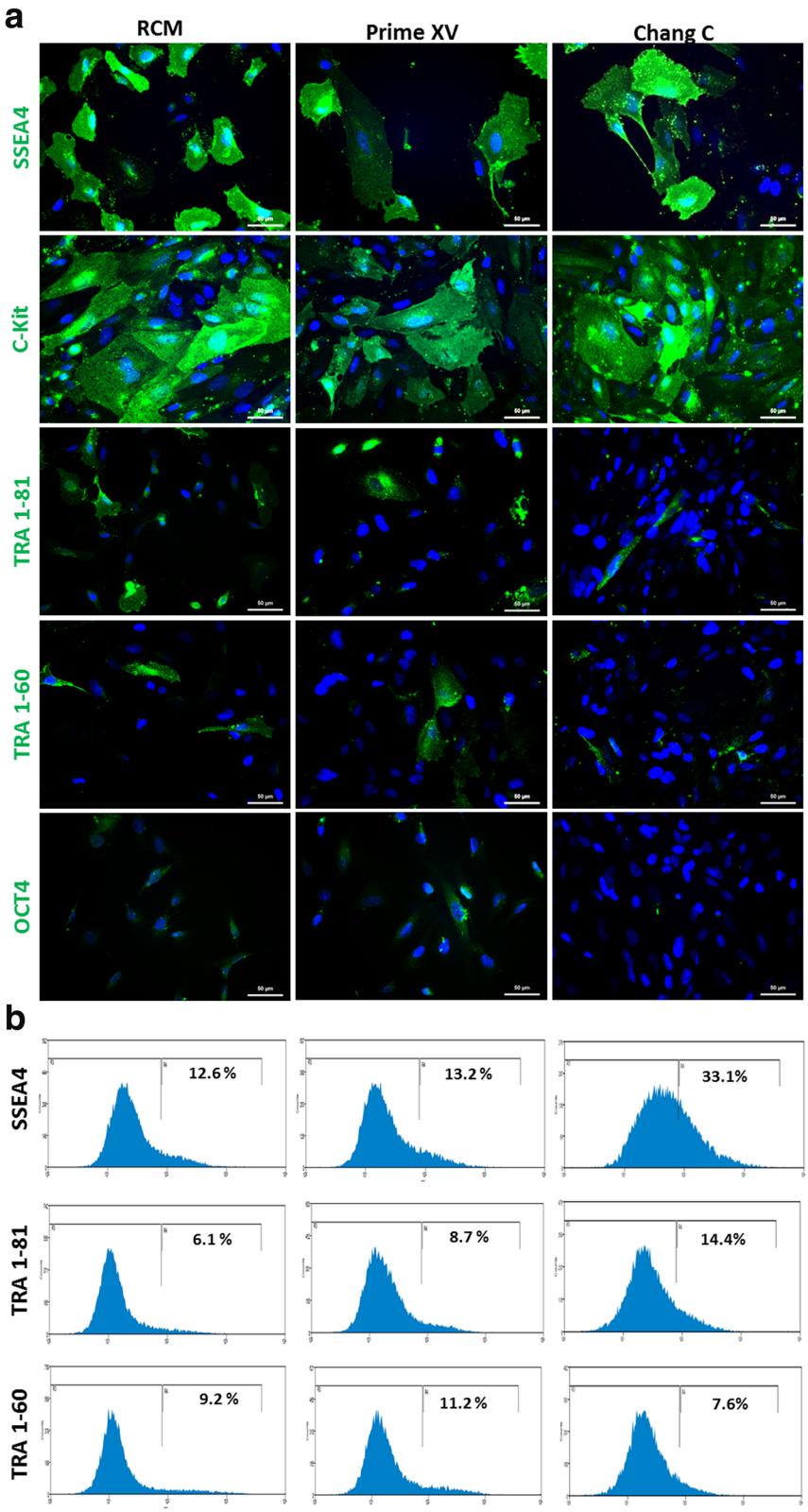

Fig. 2 (See legend on next page.)

(See figure on previous page.)
Fig. 2 Pluripotency-associated stem cell marker expression of AFCs in distinct media. Immunofluorescent-based staining showed similar stem cell-related protein expression in all three media conditions (RCM, Prime XV, Chang C). AFCs express SSEA4, C-Kit, TRA-1-60 and TRA-1-81. Cell nuclei stained using Hoechst (**a**). Flow cytometric analysis confirmed cell surface expression of SSEA4, TRA-1-60 and TRA-1-81 (**b**). RCM renal cell medium

passaging 3–4 times, the cells became more homogeneous with fibroblastic mesenchymal-like morphologies in all media except αMEM and MG30. In αMEM and MG30, cells attained an oval/egg-shaped morphology and had significantly decreased growth rates (Fig. 1a). Based on morphology, renal progenitor, undifferentiated and differentiated cell types were observed as subpopulations. The commercially available human kidney cell line HREpC as well as urine-derived renal cells (UM51) served as controls (Fig. 1b).

AFCs express pluripotency-associated proteins

To analyze the presence of pluripotent stem cell-associated markers in AFCs, both immunofluorescence staining and flow cytometry were performed. The AFC populations cultured in RCM, Prime XV and Chang C media were found to express SSEA4, C-Kit, TRA-1-60 and TRA-1-81. Expression of cytoplasmic and no nuclear octamer-binding transcription factor 4 (OCT4) was observed at early passages in RCM and Prime XV (Fig. 2a). However, the percentages of cells positive for the investigated markers (SSEA4, C-Kit, TRA-1-60 and TRA-1-81) were consistent with the flow cytometric data. Approximately 13% of the RCM cultured cells were positive for SSEA4, 9% for TRA-1-60 and 6% for TRA-1-81. AFCs cultured in Prime XV showed positivity rates of 13.2% for SSEA4, 8.7% for TRA-1-60 and 11.2% for TRA-1-81. Previously performed flow cytometric analysis for cells cultured in Chang C media revealed 33.1% SSEA4, 14.4% TRA-1-60 and 7.6% TRA-1-81 positive cells [32] (Fig. 2b).

AFCs express proteins related to MSCs as well as CK19 and show multilineage differentiation potential in vitro

AFCs cultured in all three media compositions (RCM, Prime XV and Chang C) expressed the typical mesenchymal marker Vimentin and not E-Cadherin. Additionally, subpopulations of the cells were positive for CK19, a marker for renal epithelial cells. The expression of CD133/Prominin-1, as a marker for multipotent progenitor cells, was also observed in all conditions. HREpCs, derived from kidney biopsies, were used as renal reference cells and also showed positivity for Vimentin, CD133 and CK19 (Fig. 3a). To analyze the typical MSC surface marker expression in AFCs, flow cytometric analysis was conducted. The presence of CD73, CD90 and CD105 could be identified in all cases; interestingly, cells in RCM had the highest level of expression. However, all cell preparations were devoid of the hematopoietic markers CD14, CD20, CD34 and CD45 (Fig. 3b, [32]). These features establish and confirm these cells as bona fide AF-MSCs.

To investigate the differentiation capacity of the AFCs, the cells were subjected to adipocyte, chondrocyte and osteoblast differentiation for 3 weeks. Successful differentiation into adipocytes was observed by Oil Red O staining of emerging fat droplets surrounding the cell nuclei. During chondrogenic differentiation the cells aggregated, and Alcian Blue staining showed the presence of emerged proteoglycans within the developed cell clusters. Osteogenic lineage differentiation was shown by Alizarin Red S staining of developed calcium deposits (Fig. 3c).

AF-MSCs express renal markers irrespective of in-vitro culture media composition

To validate our hypothesis that third-trimester AF-MSCs harbor renal progenitor cells, we analyzed AF-MSCs cultured in RCM, which is a medium formulated for kidney cells, for the expression of kidney-associated markers SIX2, CITED1, LHX1, PODXL, BRN1 and Paired-Box-Protein 8 (PAX8)—these were positive. Prime XV and Chang C, specialized for AFC culture, also supported expression of the renal markers. The commercially bought human kidney cells HREpCs served as a positive control. These results imply that AF-MSCs are of nephrogenic origin and the phenotype is maintained irrespective of the media used (Fig. 4).

AF-MSCs are able to transport albumin

Albumin endocytosis is a criterion defining renal cells. To analyze the ability of AF-MSCs to take up and release albumin, fluorescent dye-coupled Alexa Fluor™ 488-labeled albumin was used. It could be shown that the temperature-dependent (37 °C) uptake of albumin (1 h incubation) by AF-MSCs was higher in comparison to fetal MSCs (fMSCs) and human fetal foreskin cell HFF1. This held true for both progenitor and differentiated cells (Fig. 5a). To differentiate AF-MSCs, we treated the cells with 10 μM CHIR99021 (WNT pathway activation by GSK3 inhibition) for 2 days and observed morphological changes from fibroblastic to elongated tubular shape (Fig. 5b), resulting in decreased expression of progenitor markers C-Kit and SIX2. The expression and localization of WT1 switched from nuclear to cytoplasmic upon CHIR99021 treatment whereas Nephrin (NPHS1) expression was stable (Fig. 5c) as detected at

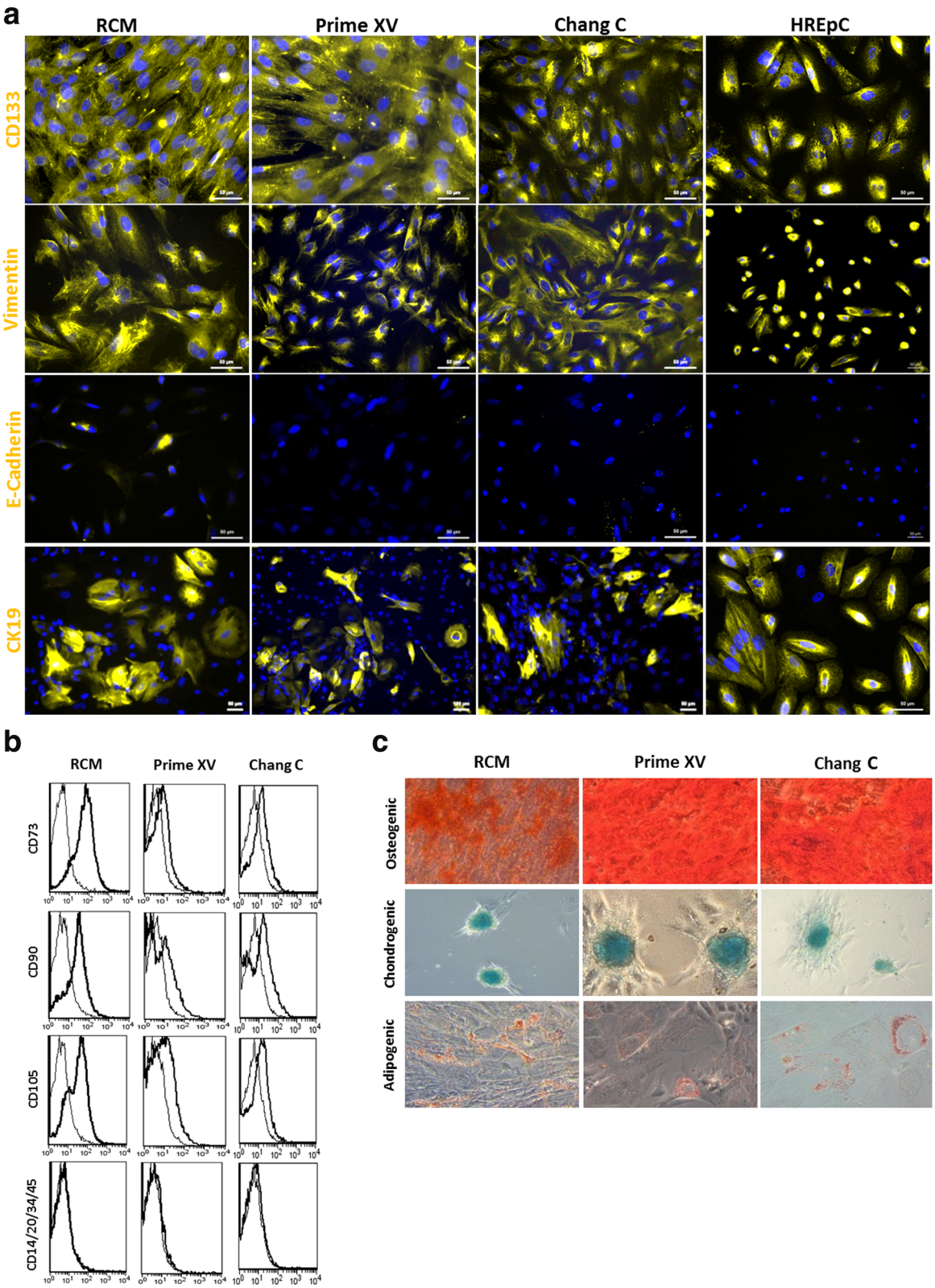

Fig. 3 (See legend on next page.)

(See figure on previous page.)
Fig. 3 AFCs express typical MSC-associated proteins as well as CK19 and show multilineage differentiation potential in vitro. AFCs cultured in distinct media compositions stained positive for Vimentin and CD133 but negative for E-Cadherin. CK19, an established kidney epithelial marker, also expressed. Cell nuclei stained using Hoechst/DAPI (**a**). Flow cytometry-based analysis confirmed expression of MSC markers CD73, CD90 and CD105, and negativity for hematopoietic markers CD14, CD20, CD34 and CD45 (antibody isotype controls represented by thin lines; bold lines indicate histograms of distinct proteins) (**b**). Analysis of multilineage differentiation capacity of AF-MSCs revealed Alizarin Red staining of osteoid matrix-like structure in osteogenic medium, Alcian Blue staining of proteoglycans in chondrogenic media and lipid droplet formation around the cells in adipogenic media (**c**). HREpC human renal epithelial cell, RCM renal cell medium

the protein level via immunofluorescent-based staining. Real-time RT PCR revealed downregulation of *SIX2*, *WT1* and *CD133* and activation of kidney-associated bone morphogenic protein 7 (*BMP7*) (Fig. 5d). Based on our experimental data we derive a scheme describing CHIR99021-mediated WNT activation and its influence on differentiation or self-renewal (Fig. 6). Self-renewal (inactive WNT signaling) is maintained by elevated expression of the renal progenitor markers *SIX2*, *WT1* and *CD133* (stem cell proliferation marker) and downregulated expression of *BMP7*. In contrast, upon activation of canonical WNT signaling by GSK3β inhibition with CHIR99021, AF-MSCs exit self-renewal and differentiate as a consequence of elevated *BMP7* expression and downregulation of *SIX2*, *WT1* and *CD133* respectively.

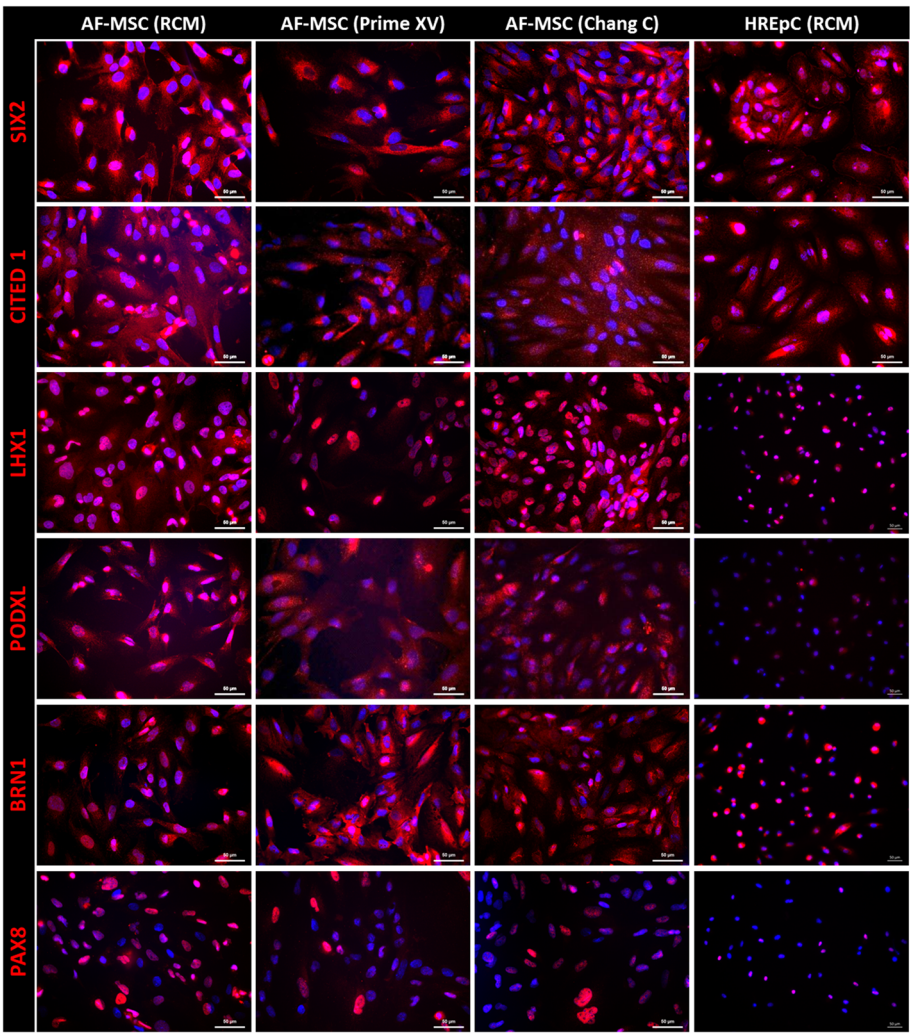

Fig. 4 Renal-specific marker expression in AF-MSCs. Immunofluorescent-based images showing expression and localization of SIX2, CITED1, PAX8, BRN1, PODXL and LHX1 in AF-MSCs cultured in either RCM, PrimeXV or Chang C. HREpCs cells served as positive control. Cell nuclei stained using Hoechst/DAPI. AF-MSC amniotic fluid mesenchymal stem cell, HREpC human renal epithelial cell, RCM renal cell medium

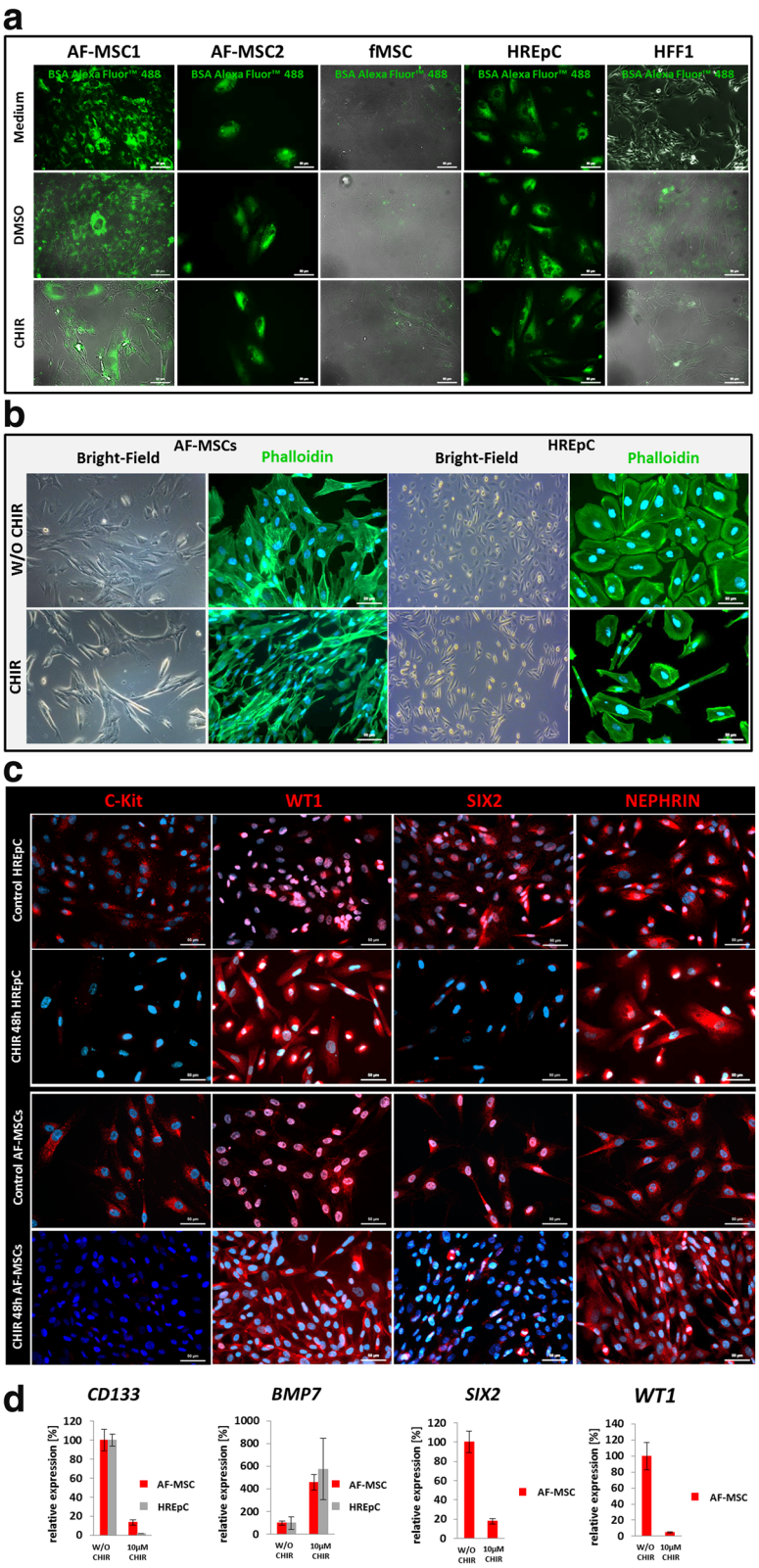

Fig. 5 (See legend on next page.)

(See figure on previous page.)
Fig. 5 Functional characterization of AF-MSCs as renal cells. Regardless of differentiated or undifferentiated AF-MSC status, functional albumin endocytosis observed at significantly higher levels than in HFF1 and fetal MSCs (fMSC) when cells incubated with albumin at 37 °C (**a**). Activation of WNT signaling by supplementation with GSK3-inhibitor CHIR99021 led to differentiation into tubular looking cells, shown by phalloidin staining (**b**). WT1 localization switch from nucleus to cytoplasm, Nephrin expression retained and C-Kit and SIX2 expression decreased (**c**). Cell nuclei stained using Hoechst/DAPI. qRT-PCR of CHIR differentiated cells clearly showed downregulation of renal undifferentiated progenitor markers *CD133*, *SIX2* and *WT1* and upregulation of the differentiation marker *BMP7* (**d**). AF-MSC amniotic fluid mesenchymal stem cell, DMSO dimethylsulfoxide, fMSC fetal mesenchymal stem cell, HFF human foreskin fibroblast, HREpC human renal epithelial cell, w/o without

Increased appearance of renal-associated genes in AFCs correlates with gestational time

Taking advantage of previously published transcriptome data [45], related to renal system development from first and second-trimester AFCs, we analyzed gene set enrichments and related GOs from T1 (first trimester), T2 (second trimester) and T3 (third trimester). Interestingly, the number of expressed kidney-associated genes increased with gestational time. From the predictions based on the datasets, we observed that most of the renal developmental-related genes (eight genes) were expressed in the third trimester. Subsequently, only four genes were identified to be present in the second trimester and none was predicted to be expressed in the first trimester. In line with this, no kidney development-related GO terms were found for AFC samples from the first trimester, 10 GOs were shown for the second and 12 GOs in the third trimester, thus implying an increasing renal expression pattern during fetal kidney development which is also shown in a heatmap generated from the transcriptome data (Fig. 7a–c). These data were validated by semi-qPCR of cDNA samples obtained from the mRNA of AFCs/AF-MSCs from the first, second, early third and late third trimesters. We did not detect renal gene expression from the first-trimester samples; in contrast, *PAX8* and *SALL1* could be detected in the second and third-trimester samples. In contrast to this, third-trimester cells exclusively expressed *SIX2*, *PAX2*, *LHX1*, *WT1*, *HNF1B*, *BRN1*, *NPHS1* and *SALL4* (Fig. 7d).

Transcriptome analysis of third-trimester AF-MSCs reveals involvement in kidney specific biological processes

To reveal the AF-MSC identity, the cells' transcriptomes were compared to HREpCs, UM51 (urine-derived SIX2-positive renal cells) and UM51-derived iPSCs (ISRM-UM51). Using cluster dendrogram analysis, AF-MSCs were shown to cluster together with two different kidney cells and apart from the iPSCs (Fig. 8a). This is also shown by Pearson correlation coefficient calculation (Fig. 8b), revealing a value of 0.9095 for AF-MSC 1 and UM51 and a value of 0.955 for AF-MSC 1 and HREpCs. Next, we wanted to focus on genes shared amongst the AF-MSCs and the other two renal cell types. Since UM51, HREpCs and AF-MSCs showed expression of MSC markers, a sample of bone marrow-derived fetal MSCs was included in the Venn diagram, to allow focus on commonly expressed genes in AF-MSCs, UM51 and HREpCs but not in fMSCs (409 genes) (Fig. 8c). Using these genes, a GO term analysis was conducted. Among the top 20 GOs (Fig. 8d), 11 GOs were connected to kidney development-related biological processes such as "renal tubule development" and "nephron epithelium development". The significant KEGG pathways resulting from the 409 shared genes are shown in Fig. 8e, revealing stem cell-related pathways such as "TGF-beta signaling pathway" and "Hedgehog signaling pathway". The complete gene lists, GOs (BP, CC, MF) and the KEGG pathways for each single group as well as for a group

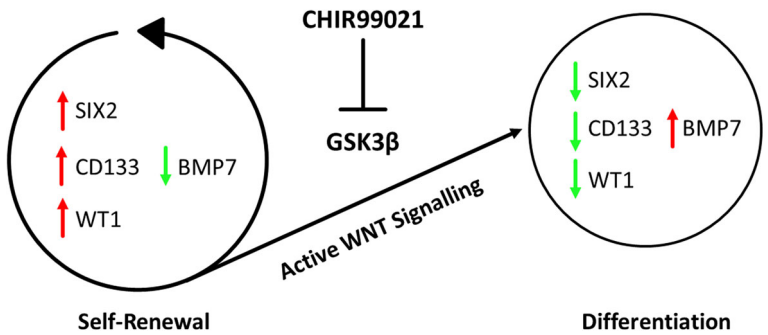

Fig. 6 WNT mediated cell fate decisions in AF-MSCs. Self-renewal renal progenitor cells maintained when WNT signaling is inactive due to sustained upregulated expression of *SIX2*, *WT1* and *CD133* and downregulation of *BMP7* on mRNA level. Upon activation of canonical WNT signaling (i.e., CHIR99021-mediated GSK3β inhibition) there is an exit of self-renewal, due to upregulated expression of *BMP7*, but downregulation of *WT1*, *SIX2* and *CD133* expression on mRNA level

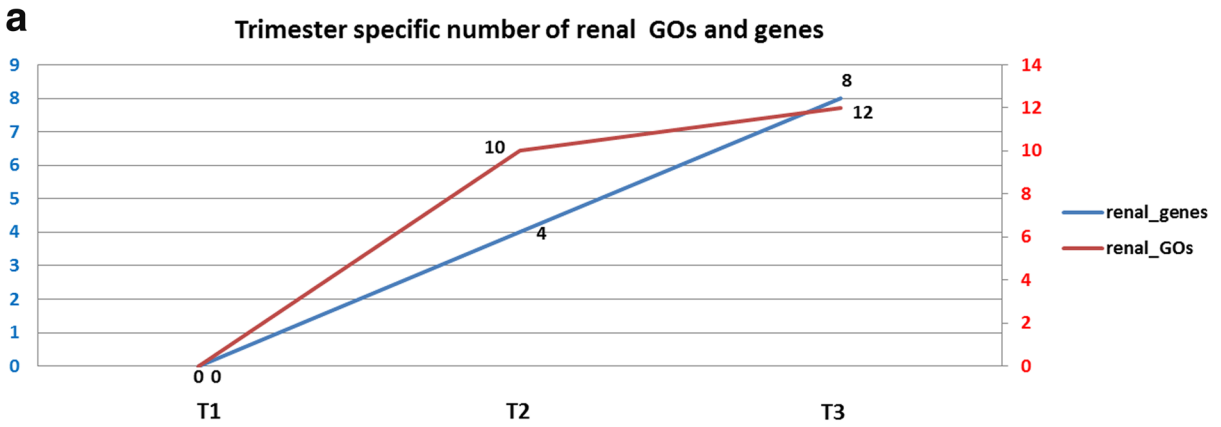

b

trimester	GO_term	genes
T2	metanephric distal convoluted tubule development	PAX2,UMOD
T2	nephric duct development	LHX1,PAX2
T2	regulation of epithelial cell differentiation involved in kidney development	LHX1,PAX2
T2	metanephric glomerulus development	LHX1,PAX2
T2	metanephric renal vesicle morphogenesis	LHX1,PAX2
T2	renal vesicle development	LHX1,PAX2
T2	metanephric tubule development	PAX2,UMOD
T2	metanephric nephron epithelium development	PAX2,UMOD
T2	renal tubule development	HOXD11,LHX1,PAX2,UMOD
T2	regulation of mesonephros development	LHX1,PAX2
T3	paramesonephric duct development	STRA6,WNT4
T3	regulation of kidney development	C3AR1,HNF1B,NOG,SALL1,WNT4
T3	mesenchymal stem cell maintenance involved in nephron morphogenesis	HNF1B,SALL1
T3	mesonephric tubule morphogenesis	ADAMTS16,HNF1B,NOG,SALL1,WNT4
T3	renal vesicle formation	SALL1,WNT4
T3	negative regulation of metanephros development	HNF1B,SALL1
T3	mesonephric epithelium development	ADAMTS16,EPCAM,HNF1B,NOG,SALL1,WNT4
T3	adrenal gland development	SALL1,STRA6,WNT4
T3	nephron epithelium morphogenesis	ADAMTS16,HNF1B,NOG,SALL1,WNT4
T3	renal tubule morphogenesis	ADAMTS16,HNF1B,NOG,SALL1,WNT4
T3	kidney morphogenesis	ADAMTS16,HNF1B,NOG,SALL1,WNT4
T3	nephron development	ADAMTS16,C3AR1,HNF1B,NOG,SALL1,WNT4

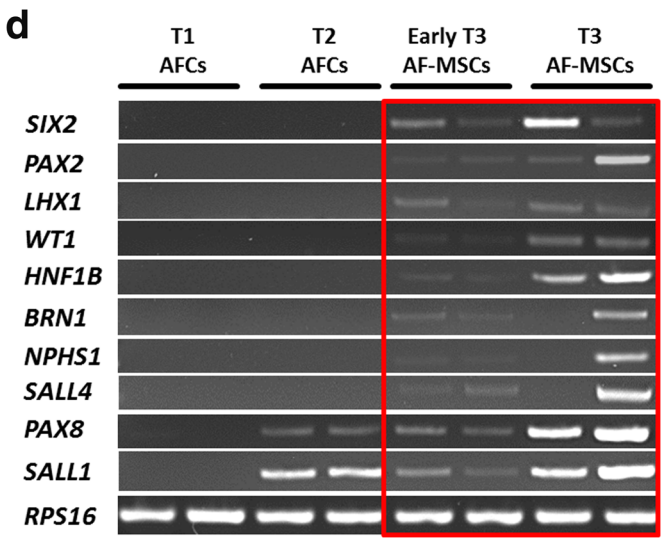

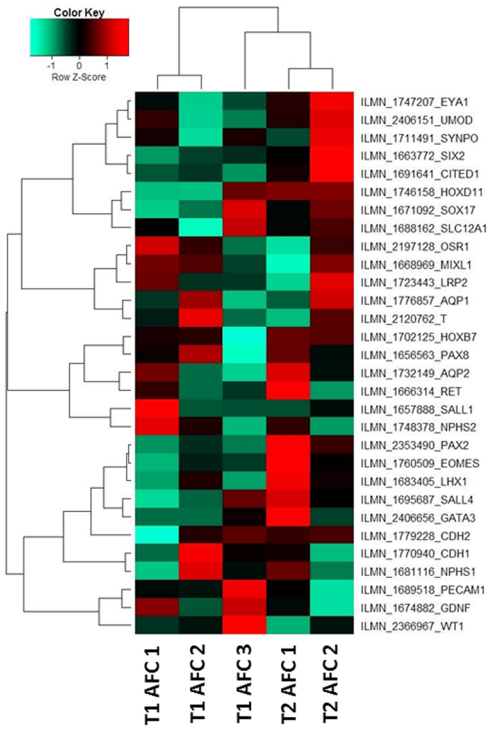

Fig. 7 (See legend on next page.)

(See figure on previous page.)
Fig. 7 Expression levels of renal-specific genes in AFCs increase with gestational time. Number of renal-enriched genes (blue line) and GOs of trimester-specific AFCs (red line) indicates increasing pattern during fetal kidney development (**a**). Differentially expressed genes involved in nephron development in second and third-trimester AFCs. Gene-set enrichment analysis revealed expression of genes from different renal developmental compartments such as metanephros development (*ADAMTS16*, *EPCAM*, *HNF1B*, *NOG*, *SALL1*, *WNT4*), metanephric mesenchyme development (*HNF1B*, *SALL1*), renal tubule development (*HOXD11*, *LHX1*, *PAX2*, *UMOD*), metanephric nephron and tubule development (*PAX2*, *UMOD*), and metanephric glomerulus and mesonephros development (*LHX1*, *PAX2*) (**b**). Heatmap showing relative expression of genes involved in nephrogenesis from existing published data of AFCs from first and second trimester (**c**). Semi-qPCR of renal genes in AFC/AF-MSC samples from first, second, early third and late third trimester. Gel bands indicating enriched expression of renal genes in third trimester boxed in red (**d**). AFC amniotic fluid cell, AF-MSC amniotic fluid mesenchymal stem cell, GO gene ontology, T1 first trimester, T2 second trimester, T3 third trimester

consisting of AF-MSCs, UM51 and HREpCs are provided in Additional files 2, 3 and 4.

Discussion

Amniotic fluid cells display a spectrum of morphologies (Fig. 1a) depicting their composition of fetal-derived differentiated and undifferentiated progenitor cells [24, 33]. In the majority of studies, the heterogeneity of AF-derived cells has led to conflicting results and uncertainty regarding the identity of the cell population, in particular the origin of the third-trimester AFCs [37]. In our earlier work it could be shown that first-trimester AFCs have a germ cell origin [45]. Remarkably, we observed that third-trimester AFCs have similar morphologies when compared to urine-derived cells and human kidney biopsy-derived cells (Fig. 1b), as shown by others [46–50]. It is well known that AF contains various cell types which originate mostly from fetal urine [34, 51] and the appearance of cells in the amniotic fluid/fetal urine increases in number with gestational age. Furthermore, it has also been shown recently that urine cells have a kidney origin [35–37, 40]. In studies on full-term male fetal AF-MSC transcriptomes, we and others found that most of the expressed genes were related to kidney and skeletal system development [32, 37]. Nevertheless, the phenotypes of AFCs obtained during culture were dictated by culture conditions [52] and by the passage number. Initially, we cultured the cells in five distinct media, namely RCM, Prime XV, Chang C, MG30 and αMEM. Regardless of the media used, homogeneous spindle-shaped mesenchymal like cells were observed after a few passages, except for αMEM and MG30 which also led to decreased growth rates. So, these media were excluded from further analysis.

In this study, the third-trimester AFCs were shown to maintain expression of pluripotency-associated stem cell markers C-Kit, SSEA4, TRA-1-60 and TRA-1-81 but not nuclear OCT4 (Fig. 2a), which has also been shown for a subpopulation of urine-derived stem cells [46, 48]. C-kit was also identified to be expressed at the loop of Henley and distal tubules of murine kidney [53]. Second-trimester human nephron progenitor cells were shown to have elevated expression of NANOG and OCT4 [14]. These data suggests that pluripotency-associated gene/protein expression decreases with gestational time.

Third-trimester AFCs investigated in the present work expressed the mesenchymal marker Vimentin, typical MSC cell surface markers CD73, CD90, and CD105 as well as the stem cell marker CD133. Furthermore, the cells differentiated into adipocytes, osteocytes and chondrocytes (Fig. 3a–c), which has also been reported for cells derived from human kidneys [13], and hence we refer to the cells as AF-MSCs. In support of our findings, AFCs as well as cells derived from preterm neonatal urine were described to be positive for Vimentin and CD133 but negative for hematopoietic cell markers [35], which also was confirmed for fetal and adult kidney-derived cells [13, 14, 54]. In addition, our AF-MSCs also express CK19 (Fig. 3a) as shown previously for human kidney cells [53]. It has been described that subpopulations of renal cells exist with MSC-specific morphology and marker expression (CD73, CD105) which additionally express metanephric mesenchyme markers such as SIX2, CITED1 and PAX2 [37, 54].

As the AF-MSCs share similar properties with neonatal urine cells and human renal cells with respect to pluripotency-associated and mesenchymal marker expression, and multipotent differentiation potential, we assumed, as shown in the 1970s [51], that AFCs originate from fetal kidney. This hypothesis is supported by a recent review describing that cells leave the fetal kidney during the transition from the pronephron to the metanephron, and reside within AF [37]. To confirm, we investigated AF-MSCs cultured in RCM, Chang C and Prime XV for the expression of typical renal markers such as SIX2, CITED1, PODXL, LHX1, BRN1 and PAX8. Irrespective of the used media, the third-trimester AF-MSCs expressed all of these markers (Fig. 4). In line with our results, nephron progenitor cells derived from the developing human kidney as well as from neonatal urine were previously reported to express the investigated marker [14, 15, 35, 55, 56].

We also investigated uptake of exogenous albumin as a key kidney function, which has been shown for human renal cells [57–59] as well neonatal urine cells [35]. Third-trimester AF-MSCs and HREpCs showed albumin endocytosis whereas fMSCs and HFF1 did not

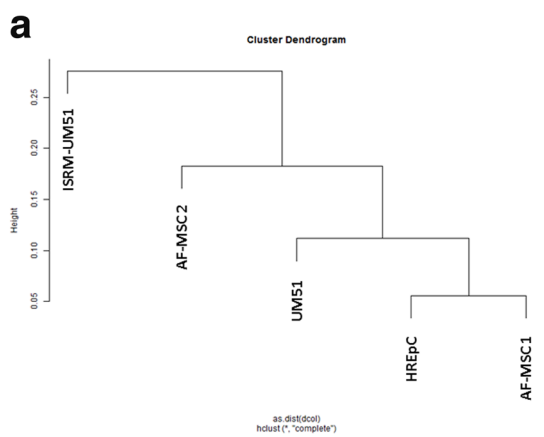

b

Sample	UM51	HREpC	AF-MSC 1	AF-MSC 2	ISRM-UM51
UM51	1,0000	0,9428	0,9095	0,8507	0,8259
HREpC	0,9428	1,0000	0,9550	0,8707	0,8366
AF-MSC 1	0,9095	0,9550	1,0000	0,8915	0,8018
AF-MSC 2	0,8507	0,8707	0,8915	1,0000	0,7772
ISRM-UM51	0,8259	0,8366	0,8018	0,7772	1,0000

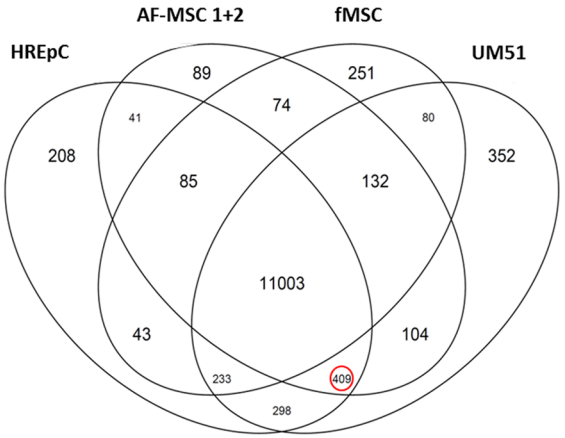

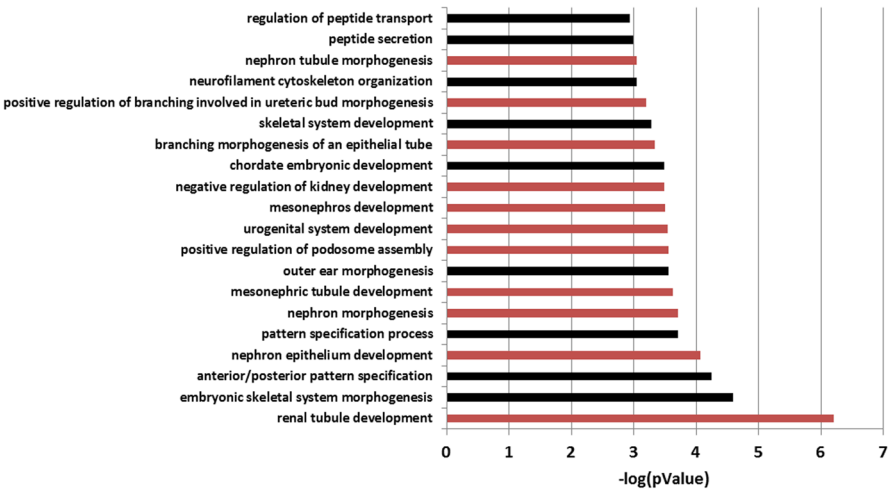

e

KEGG pathway	p_Value
Long-term potentiation	0,00087383
Gastric acid secretion	0,00117223
Hedgehog signaling pathway	0,00198962
Vascular smooth muscle contraction	0,00258798
Salivary secretion	0,00302843
Gap junction	0,0032031
Allograft rejection	0,00343478
Purine metabolism	0,0044932
Antigen processing and presentation	0,00832247
Oocyte meiosis	0,01007127
Basal cell carcinoma	0,0117044
TGF-beta signaling pathway	0,01183909
Asthma	0,0133057
Focal adhesion	0,01522146
Axon guidance	0,01834294
Toxoplasmosis	0,02029623
Pancreatic secretion	0,02338634
Melanogenesis	0,02338634
Long-term depression	0,02621439
Graft-versus-host disease	0,0318016
Type I diabetes mellitus	0,03573556
Phosphatidylinositol signaling system	0,03701893
Pathways in cancer	0,03773382
Type II diabetes mellitus	0,04208456
ECM-receptor interaction	0,0482962

Fig. 8 Third-trimester AF-MSCs express genes associated with renal-specific biological processes and have high overlap with kidney cells. Cluster dendrogram shows close relationship of AF-MSCs with UM51 and HREpCs (**a**), confirmed by Pearson correlation coefficients (**b**). Venn diagram analysis extracted 409 genes shared amongst AF-MSCs, UM51 and HREpCs (red circle) (**c**). Top 20 GO terms of the common 409 genes listed depending on their –log(*p* value), renal-related GOs indicated with red bars (**d**). Significant KEGG pathways for the 409 genes. Stem cell-related pathways shaded red (**e**). AF-MSC amniotic fluid mesenchymal stem cell, ECM extracellular matrix, fMSC fetal mesenchymal stem cell, HREpC human renal epithelial cell, KEGG Kyoto Encyclopedia of Genes and Genomes, TGF transforming growth factor

(Fig. 5a). Further, we analyzed the changes in morphology and protein/gene expression in the AF-MSCs upon differentiation by activation of WNT signaling as a consequence of inhibition of GSK3 using CHIR99201. Cell shapes became elongated and expression of renal progenitor markers C-KIT and SIX2 decreased, WT1 expression translocated from the nucleus to the cytoplasm and Nephrin expression remained cytoplasmic, which was also confirmed for cells isolated directly from a human kidney biopsy [37, 60]. The translocation of WT1 expression from the nucleus to cytoplasm has been described previously [61]. The cytoplasmic expression of WT1 will denote a loss of transcription factor activity.

Moreover, qRT-PCR revealed that the differentiated AF-MSCs acquired upregulated *BMP7* expression with

parallel decreased *SIX2*, *WT1* and *CD133* expression (Fig. 5d), as shown previously [62, 63]. One possible explanation for our observations could be that the antibody recognizes an epitope present on a variant of WT1 which we could not detect with our primers. Of course this is speculation and more studies are required to substantiate this observation.

Since nephrons are generated during the second and third trimesters [64], a synergistic relation between expression of kidney-associated genes in AF-MSCs and the gestational period can be postulated. To address this, we analyzed gene expression from previously published transcriptome data [32, 45] and performed a semiquantitative PCR of first, second and third-trimester samples to investigate any possible relationship between gradual expressions of renal genes with gestational time. The third-trimester AF-MSCs expressed increasing number of genes and GOs compared to second-trimester cells (Fig. 7a, b, d). For future research it would be of high value to have AF samples obtained from gestational week-wise time points to better understand the impact of the temporal developmental stage of the fetal kidney on the composition of the AF and likewise the identity of AF-MSCs. Cluster dendrogram analysis based on the transcriptome data showed that AF-MSCs cluster apart from pluripotent cells and cluster together with kidney-derived cells (Fig. 8a, b). In line with this, AF-MSCs shared more genes with human kidney cells UM51 and HREpCs than with fetal MSCs (Fig. 8c). Furthermore, GO analysis focusing on biological processes revealed the involvement of genes associated mostly with kidney development (Fig. 8d), which also can be observed in our previous analysis of AF specific genes [32].

Since the kidney is a complex organ and is composed of a multitude of different cell types, sorting and specification of distinct kidney cells from the amniotic fluid needs to be investigated.

Nevertheless, our results identify third-trimester human amniotic fluid-derived mesenchymal stem cells as of renal origin. As we have demonstrated before that these AF-MSCs also secrete immunomodulatory factors, they are highly suitable for transplantation, for example in chronic/acute kidney disease or graft versus host disease. These findings qualify these cells and the iPSCs derived from them as potent cells that can be used in the future for research on nephrogenesis, for modeling kidney-related diseases and for drug screening in combination with tissue engineering approaches such 3D organoid formation to further improve mimicking of kidney features in vitro.

Conclusions

We have demonstrated that third-trimester human AFCs originated from fetal kidney are mesenchymal stem cells (AF-MSCs) with retained renal cell gene expression and functionality. AFCs/AF-MSCs have been widely investigated; however, to date only a limited number of studies have attempted to reveal their enigmatic origin. Our results add an important milestone for the usefulness of these cells as a suitable source for future studies related to nephrogenesis, derivation of iPSCs, nephrotoxicity tests and kidney disease-related cell replacement therapies.

Additional files

Additional file 1: Table S1. Antibodies used in this study **Table S2.** Primers used for semiquantitative and quantitative real-time PCR. (DOCX 18 kb)

Additional file 2: Gene list of exclusive groups and shared genes of AF-MSCs, HREpCs and UM51. (XLS 995 kb)

Additional file 3: GOs of exclusive groups and shared genes of AF-MSCs, HREpCs and UM51. (XLS 331 kb)

Additional file 4: KEGG pathways of exclusive groups and shared genes of AF-MSCs, HREpCs and UM51. (XLSX 76 kb)

Abbreviations

AF: Amniotic fluid; AFC: Amniotic fluid cell; AF-MSC: Amniotic fluid mesenchymal stem cell; BM-MSC: Bone marrow-derived mesenchymal stem cell; BSA: Bovine serum albumin; CD: Cluster of differentiation; DAVID: Database for Annotation, Visualization and Integrated Discovery; ESC: Embryonic stem cell; FBS: Fetal bovine serum; fMSC: Fetal mesenchymal stem cell; GO: Gene ontology; HFF: Human foreskin fibroblast; HREpC: Human renal epithelial cell; iPSC: Induced pluripotent stem cell; KEGG: Kyoto Encyclopedia of Genes and Genomes; αMEM: Minimum essential medium alpha modification; MSC: Mesenchymal stem cell; PBS: Phosphate buffered saline; PCR: Polymerase chain reaction; RCM: Renal cell medium; REGM: Renal epithelial growth medium; RT: Room temperature; T1: First trimester; T2: Second trimester; T3: Third trimester

Acknowledgements

The authors thank Prof. Richard O. C. Oreffo, Centre for Human Development, Stem Cells and Regeneration, Faculty of Medicine, University of Southampton, UK for providing the fMSCs.

Funding

JA and TF acknowledge support from the Medical Faculty, Heinrich-Heine-University, Düsseldorf, Germany. In addition, JA and MSR acknowledge support from the German Academic Exchange Service (DAAD-91607303).

Availability of data and materials

The data and cells described in this manuscript can be made available upon request. The transcriptome data are available online at the National Center of Biotechnology Information (NCBI) Gene Expression Omnibus.

Authors' contributions

JA, TF, MSR and L-SS conceived the idea and designed the experiments. CH and PB collected third-trimester amniotic fluid samples. PVG collected first and second-trimester amniotic fluid samples and prepared the corresponding RNA. MB performed immunofluorescence staining of the HREpCs, and designed the renal specific primers. NG performed real-time PCR analysis. WW performed bioinformatic analysis. AN performed analysis of the CHIR99021-treated AF-MSCs and HREpCs. MSR and L-SS isolated the AFCs from third-trimester AF and characterized the AFCs/AF-MSCs. MSR and L-SS wrote the manuscript and JA edited it. All authors read and approved the manuscript.

Ethics approval and consent to participate

Full-term amniotic fluid samples from healthy donors were collected from the Department of Obstetrics and Gynaecology, Medical Faculty, Heinrich Heine University Düsseldorf, Germany, with informed patient consent as well as institutional ethical approval.

Consent for publication
All authors have agreed to submit this manuscript for publication.

Competing interests
The authors declare that they have no competing interests.

Publisher's Note

Author details
[1]Institute for Stem Cell Research and Regenerative Medicine, Medical Faculty, Heinrich Heine University, Moorenstraße 5, 40225 Düsseldorf, Germany. [2]Department of Obstetrics and Gynaecology, Medical Faculty, Heinrich Heine University Düsseldorf, Moorenstraße 5, 40225 Düsseldorf, Germany. [3]Institute for Women's Health, Maternal and Fetal Medicine Department, University College London, London WC1E 6HX, UK.

Received: 24 January 2018 Revised: 19 March 2018
Accepted: 10 April 2018 Published online: 25 April 2018

References

1. Kellum JA, Hoste EA. Acute kidney injury: epidemiology and assessment. Scand J Clin Lab Invest Suppl. 2008;241:6–11.
2. Hoste EA, Schurgers M. Epidemiology of acute kidney injury: how big is the problem? Crit Care Med. 2008;36(4 Suppl):S146–51.
3. Saidi RF, Kenari SKH. Challenges of organ shortage for transplantation: solutions and opportunities. Int J Organ Transplant Med. 2014;5(3):87–96.
4. Xia Y, Nivet E, Sancho-Martinez I, Gallegos T, Suzuki K, Okamura D, et al. Directed differentiation of human pluripotent cells to ureteric bud kidney progenitor-like cells. Nat Cell Biol. 2013;5(12):1507–15.
5. Taguchi A, Kaku Y, Ohmori T, Sharmin S, Ogawa M, Sasaki H, et al. Redefining the in vivo origin of metanephric nephron progenitors enables generation of complex kidney structures from pluripotent stem cells. Cell Stem Cell. 2014;14(1):53–67.
6. Freedman BS. Modeling kidney disease with iPS cells. Biomark Insights. 2015;10(Suppl 1):153–69.
7. Lam AQ, Freedman BS, Morizane R, Lerou PH, Valerius MT, Bonventre JV. Rapid and efficient differentiation of human pluripotent stem cells into intermediate mesoderm that forms tubules expressing kidney proximal tubular markers. J Am Soc Nephrol. 2014;25(6):1211–25.
8. Schutgens F, Verhaar MC, Rookmaaker MB. Pluripotent stem cell-derived kidney organoids: an in vivo-like in vitro technology. Eur J Pharmacol. 2016; 790:12–20.
9. Little MH. Generating kidney tissue from pluripotent stem cells. Cell Death Discovery. 2016;2:16053.
10. Al-Awqati Q, Oliver JA. Stem cells in the kidney. Kidney Int. 2002;61(2):387–95.
11. Kobayashi A, Mugford JW, Krautzberger AM, Naiman N, Liao J, McMahon AP. Identification of a multipotent self-renewing stromal progenitor population during mammalian kidney organogenesis. Stem Cell Reports. 2014;3(4):650–62.
12. Combes AN, Wilson S, Phipson B, Binnie BB, Ju A, Lawlor KT, et al. Haploinsufficiency for the Six2 gene increases nephron progenitor proliferation promoting branching and nephron number. Kidney Int. 2017; 17:30763–69.
13. Buzhor E, Omer D, Harari-Steinberg O, Dotan Z, Vax E, Pri-Chen S, et al. Reactivation of NCAM1 defines a subpopulation of human adult kidney epithelial cells with clonogenic and stem/progenitor properties. Am J Pathol. 2013;183(5):1621–33.
14. Metsuyanim S, Harari-Steinberg O, Buzhor E, Omer D, Pode-Shakked N, Ben-Hur H, et al. Expression of stem cell markers in the human fetal kidney. PLoS One. 2009;4(8):e6709.
15. Schedl A. Renal abnormalities and their developmental origin. Nat Rev Gen. 2007;8:791–802.
16. Higgins JP, Wang L, Kambham N, Montgomery K, Mason V, Vogelmann SU, et al. Gene expression in the normal adult human kidney assessed by complementary DNA microarray. Mol Biol Cell. 2004;15(2):649–56.
17. Georgas KM, Chiu HS, Lesieur E, Rumballe BA, Little MH. Expression of metanephric nephron-patterning genes in differentiating mesonephric tubules. Dev Dyn. 2011;240(6):1600–12.
18. Hendry C, Rumballe B, Moritz K, Little MH. Defining and redefining the nephron progenitor population. Pediatr Nephrol. 2011;26(9):1395–406.
19. Casiraghi F, Perico N, Cortinovis M, Remuzzi G. Mesenchymal stromal cells in renal transplantation: opportunities and challenges. Nat Rev Nephrol. 2016; 12(4):241–53.
20. Hamza AH, Al-Bishri WM, Damiati LA, Ahmed HH. Mesenchymal stem cells: a future experimental exploration for recession of diabetic nephropathy. Ren Fail. 2017;39(1):67–76.
21. Večerić-Haler Ž, Cerar A, Perše M. (Mesenchymal) Stem cell-based therapy in cisplatin induced acute kidney injury animal model: risk of immunogenicity and tumorigenicity. Stem Cells Int. 2017;2017:7304643.
22. Guillot PV, Gotherstrom C, Chan J, Kurata H, Fisk NM. Human first-trimester fetal MSC express pluripotency markers and grow faster and have longer telomeres than adult MSC. Stem Cells. 2007;25(3):646–54.
23. Romagnani P. Kidney regeneration: any prospects? Contrib Nephrol. 2011; 170:228–36.
24. Cananzi M, De Coppi P. CD117+ amniotic fluid stem cells: state of the art and future perspectives. Organ. 2012;8(3):77–88.
25. Perin L, Giuliani S, Jin D, Sedrakyan S, Carraro G, Habibian R, et al. Renal differentiation of amniotic fluid stem cells. Cell Prolif. 2007;40:936–48.
26. Perin L, Sedrakyan S, Giuliani S, Da Sacco S, Carraro G, Shiri L, et al. Protective effect of human amniotic fluid stem cells in an immunodeficient mouse model of acute tubular necrosis. PLoS One. 2010;5(2):e9357.
27. Sedrakyan S, Da Sacco S, Milanesi A, Shiri L, Petrosyan A, Varimezova R, et al. Injection of amniotic fluid stem cells delays progression of renal fibrosis. J Am Soc Nephrol. 2012;23(4):661–73.
28. Rosner M, Schipany K, Gundacker C, Shanmugasundaram B, Li K, Fuchs C, et al. Renal differentiation of amniotic fluid stem cells: perspectives for clinical application and for studies on specific human genetic diseases. Eur J Clin Investig. 2012;42:677–84.
29. Hauser PV, De Fazio R, Bruno S, Sdei S, Grange C, Bussolati B, Benedetto C, Camussi G. Stem cells derived from human amniotic fluid contribute to acute kidney injury recovery. Am J Pathol. 2010;177(4):2011–21.
30. Siegel N, Rosner M, Unbekandt M, Fuchs C, Slabina N, Dolznig H, et al. Contribution of human amniotic fluid stem cells to renal tissue formation depends on mTOR. Hum Mol Genet. 2010;19(17):3320–31.
31. De Coppi P, Bartsch G Jr, Siddiqui MM, Xu T, Santos CC, Perin L, et al. Isolation of amniotic stem cell lines with potential for therapy. Nat Biotechnol. 2007;25(1):100–6.
32. Spitzhorn LS, Rahman MS, Schwindt L, Ho HT, Wruck W, Bohndorf M, et al. Isolation and molecular characterization of amniotic fluid-derived mesenchymal stem cells obtained from caesarean sections. Stem Cells Int. 2017;2017:5932706.
33. Loukogeorgakis SP, De Coppi P. Amniotic fluid stem cells: the known, the unknown, and potential regenerative medicine applications. Stem Cells. 2017;35:1663–73.
34. Underwood MA, Gilbert WM, Sherman MP. Amniotic fluid: not just fetal urine anymore. J Perinatol. 2005;25:341–8.
35. Arcolino FO, Zia S, Held K, Papadimitriou E, Theunis K, Bussolati B, et al. Urine of preterm neonates as a novel source of kidney progenitor cells. J Am Soc Nephrol. 2016;27(9):2762–70.
36. Zhang D, Wei G, Li P, Zhou X, Zhang Y. Urine-derived stem cells: a novel and versatile progenitor source for cell-based therapy and regenerative medicine. Genes Dis. 2014;1(1):8–17.
37. Da Sacco S, Perin L, Sedrakyan S. Amniotic fluid cells: current progress and emerging challenges in renal regeneration. Pediatr Nephrol. 2017;1–11.
38. Siegel N, Valli A, Fuchs C, Rosner M, Hengstschläger M. Induction of mesenchymal/epithelial marker expression in human amniotic fluid stem cells. Reprod BioMed Online. 2009;19(6):838–46.
39. Zhou T, Benda C, Duzinger S, Huang Y, Li X, Li Y, et al. Generation of induced pluripotent stem cells from urine. J Am Soc Nephrol. 2011;22(7):1221–8.
40. Bohndorf M, Ncube A, Spitzhorn LS, Enczmann J, Wruck W, Adjaye J. Derivation and characterization of integration-free iPSC line ISRM-UM51 derived from SIX2-positive renal cells isolated from urine of an African male expressing the CYP2D6 *4/*17 variant which confers intermediate drug metabolizing activity. Stem Cell Res. 2017;25:18–21.
41. Gentleman C, Carey VJ, Bates DM, et al. Bioconductor: open software development for computational biology and bioinformatics. Genome Biol. 2004;5(10):R80.
42. Gautier L, Cope L, Bolstad BM, Irizarry RA. affy-analysis of Affymetrix GeneChip data at the probe level. Bioinformatics. 2004;20:307–15.
43. Huang DW, Sherman BT, Lempicki RA. Systematic and integrative analysis of large gene lists using DAVID bioinformatics resources. Nat Protoc. 2009;4(1):44–57.

44. Kanehisa M, Furumichi M, Tanabe M, et al. KEGG: new perspectives on genomes, pathways, diseases and drugs. Nucleic Acids Res. 2017;45(D1): D353–61.
45. Moschidou D, Drews K, Eddaoudi A, Adjaye J, De Coppi P, Guillot PV. Molecular signature of human amniotic fluid stem cells during fetal development. Curr Stem Cell Res Ther. 2013;8(1):73–81.
46. Zhang Y, McNeill E, Tian H, Soker S, Andersson KE, Yoo JJ, et al. Urine derived cells are a potential source for urological tissue reconstruction. J Urol. 2008;180:2226–33.
47. Lang R, Liu G, Shi Y, Bharadwaj S, Leng X, Zhou X, et al. Self-renewal and differentiation capacity of urine-derived stem cells after urine preservation for 24 hours. PLoS One. 2013;8(1):e53980.
48. Bharadwaj S, Liu G, Shi Y, Wu R, Yang B, He T, et al. Multipotential differentiation of human urine-derived stem cells: potential for therapeutic applications in urology. Stem Cells. 2013;31(9):1840–56.
49. Kim EY, Page P, Dellefave-Castillo LM, McNally EM, Wyatt EJ. Direct reprogramming of urine-derived cells with inducible MyoD for modeling human muscle disease. Skelet Muscle. 2016;6:32.
50. Qin D, Long T, Deng J, Zhang Y. Urine-derived stem cells for potential use in bladder repair. Stem Cell Res Ther. 2014;5(3):69.
51. Sutherland GR, Bain AD. Culture of cells from the urine of newborn children. Nature. 1972;239:231.
52. Zagoura DS, Trohatou O, Bitsika V, Makridakis M, Pappa KI, Vlahou A, et al. AF-MSCs fate can be regulated by culture conditions. Cell Death Dis. 2013;4:e571.
53. Bussolati B, Camussi G. Therapeutic use of human renal progenitor cells for kidney regeneration. Nat Rev Nephrol. 2015;11:695–706.
54. Wang H, Gomez JA, Klein S, Zhang Z, Seidler B, Yang Y, et al. Adult renal mesenchymal stem cell-like cells contribute to juxtaglomerular cell recruitment. J Am Soc Nephrol. 2013;24(8):1263–73.
55. Rosenblum ND. Developmental biology of the human kidney. Semin Fetal Neonatal Med. 2008;13(3):125–32.
56. Tong GX, Yu WM, Beaubier NT, Weeden EM, Hamele-Bena D, Mansukhani MM, et al. Expression of PAX8 in normal and neoplastic renal tissues: an immunohistochemical study. Mod Pathol. 2009;22(9):1218–27.
57. Tojo A, Kinugasa S. Mechanisms of glomerular albumin filtration and tubular reabsorption. Int J Nephrol. 2012;2012:481520.
58. Eyre J, Ioannou K, Grubb BD, Saleem MA, Mathieson PW, Brunskill NJ, et al. Statin-sensitive endocytosis of albumin by glomerular podocytes. Am J Physiol Renal Physiol. 2007;292:F674–81.
59. Xinaris C, Benedetti V, Novelli R, Abbate M, Rizzo P, Conti S, et al. Functional human podocytes generated in organoids from amniotic fluid stem cells. J Am Soc Nephrol. 2016;27(5):1400–11.
60. Musah S, Mammoto A, Ferrante TC, Jeanty SSF, Hirano-Kobayashi M, Mammoto T, et al. Mature induced-pluripotent-stem-cell-derived human podocytes reconstitute kidney glomerular-capillary-wall function on a chip. Nat Biomed Eng. 2017;1:0069.
61. Depping R, Schindler SG, Jacobi C, Kirschner KM, Scholz H. Nuclear transport of Wilms' tumour protein Wt1 involves importins α and β. Cell Physiol Biochem. 2012;29(1–2):223–32.
62. Park JS, Ma W, O'Brien LL, Chung E, Guo JJ, Cheng JG, et al. Six2 and Wnt regulate self-renewal and commitment of nephron progenitors through shared gene regulatory networks. Dev Cell. 2012;23(3):637–51.
63. Zeisberg M. Bone Morphogenic protein 7 and the kidney: current concepts and open questions. Nephrol Dial Transplant. 2006;21:568–73.
64. Little MH, McMahon AP. Mammalian kidney development: principles, progress, and projections. Cold Spring Harb Perspect Biol. 2012;4:4.

Part B: Non-invasive Sources of Mesenchymal Stem Cells and Their Characterization

3.3 Urine-derived Stem Cells as Innovative Platform for Drug Testing and Disease Modelling

Lucas-Sebastian Spitzhorn, Md Shaifur Rahman, Lisa Nguyen, Audrey Ncube, Martina Bohndorf, Wasco Wruck and James Adjaye

Abstract

Kidney-related diseases and associated health costs are on the rise. Due to the shortage of compatible organ donors, stem cell-based therapies are considered as alternative treatment options. To date, several adult stem cell sources have been established such as bone marrow, cord blood and amniotic fluid. Although these sources harbour stem cells with great regenerative potential, there are some limitations. Cord blood and amniotic fluid can only be accessed before and at birth, and bone marrow requires invasive procedures associated with risks and pain for the patient. So far, kidney biopsies are used to derive human kidney cells for research purposes. Recent investigations have shown that urine represents an alternative source of renal stem cells and differentiated cells originating from shed cells within the kidney. These include urine- derived mesenchymal stem cells (uMSCs) and renal epithelial tubular cells (uRETCs). These cells can be collected without the need of invasive or complex procedures. In this review, we describe the cellular and molecular features of these cells and emphasize possible future applications in drug screening and development, nephrotoxicity tests and disease modelling.

Publication Status: Published in Drug Target Review, Summer 2018, Issue 02

Impact Factor: NA

Approximated total share of contribution: 30%

Contribution on experimental design, realization and publication: JA, LSS, MSR and MB conceived the idea and designed the experiments. MB isolated urine derived stem cells. MB and AN generated iPSCs from the urine stem cells (uMSCs). LSS and MSR performed the staining for renal markers and the differentiation of uMSCs into bone, cartilage and fat. LN differentiated the uMSC-iPSCs into endothelial cells and generated kidney organoids. WW did the bioinformatic analysis. LSS designed the figures. LSS and MSR wrote the manuscript and JA edited it. All authors have read and approved the manuscript.

Journal link: https://www.drugtargetreview.com/article/32611/urine-derived-stem-cells/

Urine-derived stem cells as innovative platform for drug testing and disease modelling

Lucas-Sebastian Spitzhorn, Lisa Nguyen and Wasco Wruck

Institute for Stem Cell Research and Regenerative Medicine, Medical faculty, Heinrich Heine University Düsseldorf, Germany

Shaifur Rahman

Doctoral Student, Institute for Stem Cell Research and Regenerative Medicine, Medical faculty, Heinrich Heine University Düsseldorf, Germany

Audrey Ncube

Scientific Research Associate, Institute for Stem Cell Research and Regenerative Medicine, Medical faculty, Heinrich Heine University Düsseldorf, Germany

Martina Bohndorf

Qualified Medical Technical Assistant, Institute for Stem Cell Research and Regenerative Medicine, Medical faculty, Heinrich Heine University Düsseldorf, Germany

James Adjaye

Director Institute for Stem Cell Research and Regenerative Medicine, Medical faculty, Heinrich Heine University Düsseldorf, Germany

Kidneys are crucial for filtration of drugs and toxins and their proper function is essential for overall health. Unfortunately, due to disease and improper function, kidney transplantation or dialysis are necessary for millions of patients annually all over the world.[1,2]

BIOGRAPHY

SHAIFUR RAHMAN, Md, has a BSc and an MSc degree in Biotechnology and Genetic Engineering from Khulna University, Bangladesh. Additionally, he has an Erasmus Mundus Master degree in BioHealth Computing from University Joseph Fourier, France. He is now working as a doctoral student at the Institute for Stem Cell Research and Regenerative Medicine at Heinrich-Heine-University Düsseldorf, Germany and investigating therapeutic potentials of amniotic fluid cells.

RIGHT: The kidney metabolises drugs via cytochrome P450 and other protein systems

CLINICIANS face several hurdles, such as limited organ donors and high financial demands, during the course of administering the necessary treatment options.[3] The kidney metabolises drugs via cytochrome P450 and other protein systems.[4] The increasing prevalence of acute kidney injury (AKI) is associated with medical and economic burdens.[5] AKI, of which 19-26% are induced by drugs, can result in chronic kidney disease (CKD),[6,7] which increases the probability of developing renal cell carcinoma.[8] Nephrotoxicity caused by drugs is an important causative factor in the development of AKI and CKD.[9] It causes failure of about 7% of newly developed drugs, thus emphasising that pre-clinical models have to be improved.[10]

Several drugs are nephrotoxic per se. These side effects could be increased by prolonged medication and synergistic effects with other drugs, such as cephalosporins plus aminoglycosides, which are used in cancer treatment.[11] Although there are models such as cisplatin treatment[12] to investigate drug induced nephrotoxicity, more prospective studies and novel *in vitro* models are warranted to validate these approaches.

Embryonic and induced pluripotent stem cells (ESCs / iPSCs) have been differentiated into kidney-related cells, thus representing a potential alternative to native cells.[13-15]

The kidney is an organ of high complexity consisting of many cell types.[16] One key regulator

of nephrogenesis, SIX2, has been shown to be expressed in umbilical cord mesenchymal stem cells (uMSCs).[17] Bone marrow-derived mesenchymal stem cells (MSCs) have been successfully used to restore renal function deficits.[18] It has been shown that renal cells can be isolated from urine as well as from third trimester amniotic fluid, which mostly consists of foetal urine. Obtaining kidney biopsy-derived cells from patients is difficult; thus urine represents a substitution which enables personalised research approaches for kidney-related drug screening and toxicity tests. Building upon previous work showing that amniotic fluid mostly consist of foetal urine,[19] amniotic fluid-derived stem cells were recently also described as MSCs of renal origin[20] and have been used to generate podocytes.[21]

Urine is a source of stem cells

Derivation of patient-specific stem cells from urine has many advantages over other established stem cell sources. These autologous or human leukocyte antigens (HLA)-matched uMSCs are ideal for transplantation purposes. Additionally, it is possible to generate vast amounts of these cells because the source is nearly infinite and can be expanded *in vitro* on a large scale in a good manufacturing practice (GMP) setting. In case of infants and older patients with impaired wound healing, urine cells can be obtained non-invasively, without wounding, cost-effectively and easily cultured. uMSCs or uRETCs can be reprogrammed into iPSCs[17] also under GMP conditions.

Urine-derived stem cells have features of MSCs and kidney cells

Cellular and molecular characterisation of the uMSCs and uRETCs revealed similarities with amniotic fluid-derived MSCs.[20] Furthermore, they are able to differentiate into osteoblasts, adipocytes and chondrocytes and secreted cytokines capable of modulating the immune system and support healing processes. Besides their MSC marker expression, these cells express kidney-related

BIOGRAPHY

LUCAS-SEBASTIAN SPITZHORN has a BSc and an MSc degree in Biology from Heinrich-Heine University, Düsseldorf. Currently, he is finishing his PhD thesis, which includes work on bone-marrow-derived MSCs, amniotic fluid cells, urine-derived stem cells and liver cells at the Institute for Stem Cell Research and Regenerative Medicine at Heinrich-Heine-University Düsseldorf, Germany.

EXPERT VIEW

Liz Quinn
Associate Director, Stem Cell Marketing, Takara Bio USA

"This fundamental limitation restricts the utility of hpheps in multiple applications, including drug metabolism and metabolic disease research"

Overcoming the problems of working with human primary hepatocytes

Human primary hepatocytes (hpheps) are the gold standard for *in vitro* evaluation of drug metabolism, drug-drug interactions, and metabolic disease research. However, hpheps don't survive in standard 2D culture for very long – no longer than two or three days.

EXPERIMENTS are therefore limited due to their rapid loss of function when cultured *in vitro*, which is especially problematic for chronic toxicity studies that require longer usage windows to observe the effects of drugs.

This fundamental limitation restricts the utility of hpheps in multiple applications, including drug metabolism and metabolic disease research. To address this problem, 3D sandwich cultures with matrix overlays (Liu *et al.* 1999), bioreactors (Hoffman *et al.* 2012), and 3D spheroid cultures (Proctor *et al.* 2017) have been developed. Although these approaches can maintain some hepatocyte functions for several weeks *in vitro*, they do not entirely overcome the limitations of hpheps because these culture systems restrict the types of assays that can be performed. Further, they require advanced and expensive lab equipment, are not easy to use, or are not generally applicable to hpheps from different donors.

Another problem is the large variation between donors and a finite number of harvestable cells – normally from patient biopsies – from each donor. It is now possible to obtain batches of hpheps from commercial vendors. Though commercial vendors might provide a more convenient and reliable source of cells, each batch of isolated cells is donor-specific and, as such, needs to be pre-screened by the vendors and qualified for different functions (eg, transporter-mediated uptake, metabolic activity, CYP enzyme induction).

And to complicate things even further, each vendor provides their own culture medium to go with the cells, which can lead to variable results when comparing results from different vendors, donors and experiments. As a result, no matter what the source of hpheps, no universally accepted culture system currently exists and researchers need to pre-qualify each lot of cells prior to their experiments, which influences the ability to interpret their results.

BIOGRAPHY

LISA NGUYEN has a BSc in Biology from Heinrich-Heine University, Düsseldorf. She is currently working on her MSc thesis at the Institute for Stem Cell Research and Regenerative Medicine at Heinrich-Heine-University Düsseldorf, Germany. Her thesis is based on modelling nephrogenesis using urine-derived renal progenitor cells.

FIGURE 1

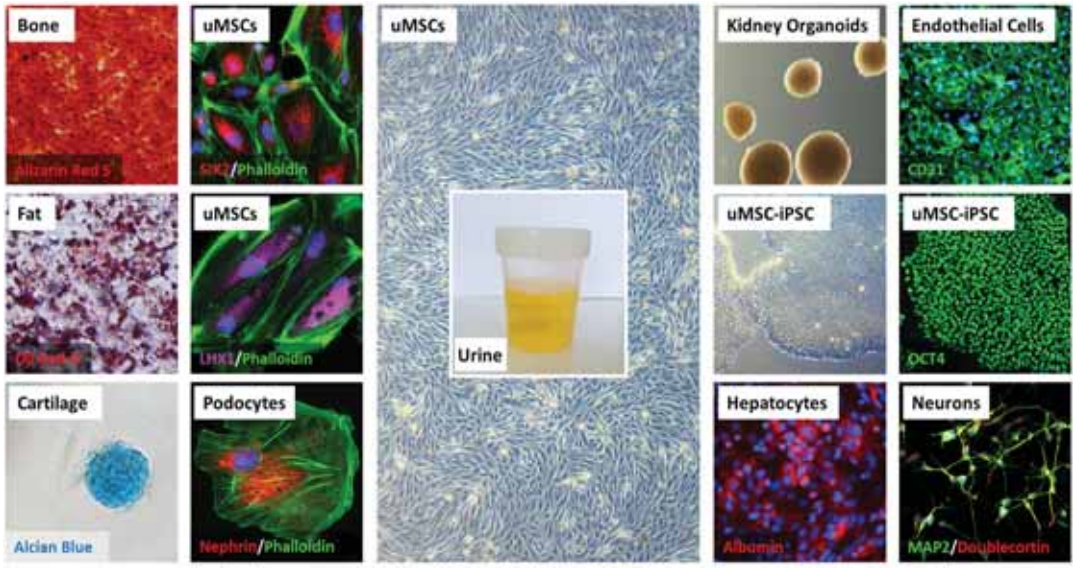

ABOVE: Molecular and cellular characteristics of uMSCs and uMSC-iPSCs. (Middle column) uMSCs with grain-like morphology were isolated from urine. (Left columns) They are able to differentiate into fat (Oil Red O), cartilage (Alcian Blue) and bone cells (Alizarin Red S) and additionally express renal markers SIX2, LHX1 and Nephrin and can be differentiated into podocyte-like cells. (Right columns) uMSC-iPSCs are positive for OCT4 and can be differentiated into endothelial cells (CD31), neuronal cells (MAP2 and Doublecortin), hepatocytes (Albumin) and form kidney organoids. Cell nuclei were stained using DAPI or Hoechst 33258

BIOGRAPHY

WASCO WRUCK has a diploma in computer science and a diploma in architecture from Technische Universität Berlin, Germany. He worked as a software developer with Siemens AG and BULL AG before joining the Max-Planck-Institute for Molecular Genetics in Berlin. There he worked as a Bioinformatician on microarray-based image analysis, application development and to evaluate various types of high-throughput genomics experiments. He then worked on a European Systems Biology research project at Charité Universitätsmedizin Berlin and was elected chair of the ERASysBio+ initiative's data management group. He currently works at the Institute for Stem Cell Research and Regenerative Medicine at Heinrich-Heine-University Düsseldorf, Germany.

markers such as SIX2, Nephrin and LHX1 and can be differentiated into podocyte-like cells (***Figure 1***). Furthermore, it was possible to efficiently generate iPSCs from these cells.[17] These uMSC-iPSCs can be differentiated into all cell types within the body including hepatocytes, neurons and endothelial cells (***Figure 1***).

Gene expression analysis confirms kidney origin of urine cells

Figure 2 shows a heatmap representation of genes associated with (A) pluri- and multipotency, (B) renal developmental processes, (C) encoding the core ADME (absorption, distribution, metabolism, and excretion) enzymes and (D) of the cytochrome P450 family. The heatmaps are based on uMSC transcriptome data sets described in the research[17,20] and also uRETCs obtained directly from urine using a selective medium for differentiated cells. Drugs up-regulate the enzyme systems responsible for their degradation or activation (Phase I) and conjugation (Phase II) to biochemical forms that can be excreted in bile or urine.[22-24] Genes coding Phase I and Phase II enzymes are included in the absorption, distribution, metabolism, and excretion (ADME) genes. The high similarity between both cell types is demonstrated by the predominantly consistent expression between both cell types. However, clustering of renal developmental genes shows a separation of uMSCs and uRETCs pointing to differences in these cells in nephrogenesis. These differences are shown in ***Figure 2E***. The subsets of genes exclusively expressed in uMSCs or uRETCs were further subjected to gene ontology (GO) analysis and revealed differences in kidney developmental processes, such as the GO-terms drug transmembrane transport, paramesonephric duct development, distal tubule morphogenesis for uRETCs and metanephric tubule development, glomerulus development for uMSCs (***Figure 2F***).

Improve disease modelling, drug screening and nephrotoxicity tests using 3D-based kidney organoids

Ethical concerns and the limited predictability of cross-species translation of research results increase the importance of *in vitro* models as an alternative to *in vivo* pre-clinical testing. Recent 3D approaches increase assay relevance but still need improvement.[25]

Moreover, uMSC-iPSCs are the basis for generating 3D kidney organoids. To resemble the complex kidney structure, it is useful to combine different cell types. We have generated 3D kidney organoids (***Figure 1***) by combining uMSCs as renal cells with uMSC-iPSCs differentiated endothelial cells (iECs) and mesenchymal stem cells (iMSCs) originating from the same individual.[17] This approach may enable researchers to better mimic human physiology in contrast to standard 2D cell culture systems. For future research and therapy, it is important to increase maturity, and thus functionality, in order to attain predictive

FIGURE 2

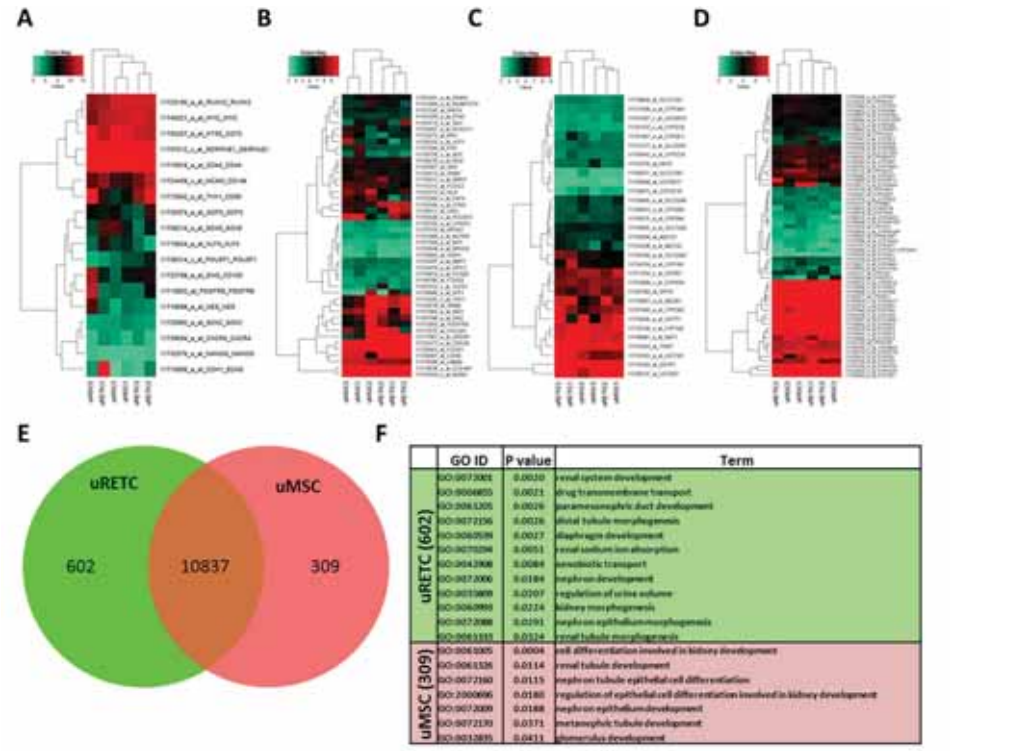

ABOVE: Gene expression profiles characterise renal developmental properties of uMSCs and uRETCs. Heatmap-based representations of co-regulated expression of distinct gene sets associated with (A) pluri- and multipotency, (B) renal developmental processes, (C) the core ADME genes (http://pharmaadme.org/joomla/index.php?option=com_content&task=view&id=14&Itemid=29) and (D) cytochrome P450 genes. uMSCs and uRETCs have high similarity. However, the clustering related to renal development demonstrates differences between both cell types (C). Values on the color key scales are logarithmic (base 2). (E) Venn diagram analysis of genes expressed in uMSCs and uRETCs identified 10837 genes expressed in common, 309 genes expressed in uMSCs and 602 genes expressed in uRETCs. (F) Genes exclusively expressed in uMSCs or uRETCs reveal many kidney-related terms which point to their distinct developmental potential.

value. Recent studies have shown bio-printing[26,27] and kidney-on-a-chip technology[28] as improved means of generating better *in vitro* models.

Perspectives

Urine is a source of stem cells that can be accessed non-invasively, with no pain and risk for the patient; has nearly unlimited availablity; and is cost-efficient. Urine should be considered as an alternative to established stem cell sources such as bone marrow and cord blood. Most importantly, uMSCs and uRETCs originate from the kidney and, thus, by-pass the need for donated kidneys. Combined with HLA analysis and analysis of the patient's CYP variants, the cells are perfectly suited for individualised drug screening, dose determination, disease modelling *in vitro* and eventually kidney-associated cell therapies.

ACKNOWLEDGEMENTS

James Adjaye acknowledges support from the medical faculty of the Heinrich Heine University- Düsseldorf, Germany. Md Shaifur Rahman acknowledges support from the German Academic Exchange Service (DAAD-91607303).

BIOGRAPHY

MARTINA BOHNDORF is a Qualified Medical Technical Assistant working at the Institute for Stem Cell Research and Regenerative Medicine- Heinrich-Heine-University Düsseldorf, Germany. She has extensive experience in culturing pluripotent stem cells and was instrumental in the development of the protocols for isolation and expansion of urine-derived stem cells.

BIOGRAPHY

AUDREY NOZITHELO NCUBE has a BSc in Applied Biology and MSc in Biomedical Sciences from Hochschule Bonn-Rhein-Sieg, Germany. The practical lab work for the two degrees was conducted at the Institute for Stem Cell Research and Regenerative Medicine at Heinrich-Heine-University Düsseldorf, Germany where she is now working as a Scientific Research Associate since 2016.

BIOGRAPHY

PROFESSOR DR JAMES AFFRAM ADJAYE has a BSc degree in Biochemistry from University College of Cardiff, Wales, and an MSc in Biochemistry from University of Sussex, Brighton. He has a PhD in Biochemistry from King's College, London. Professor Adjaye was head of the Molecular Embryology and Aging group at the Max Planck Institute for Molecular Genetics, Berlin, Germany. He is now Director of the Institute for Stem Cell Research and Regenerative Medicine within the Faculty of Medicine at the Heinrich-Heine-University, Düsseldorf, Germany. He is involved in systems biology-based projects, both at the national and international level where iPSCs are used to model Alzheimer's disease and Non-Alcoholic Fatty Liver Disease (NAFLD) and Nijmegen Breakage Syndrome.

> *"In case of infants and older patients with impaired wound healing, urine cells can be obtained non-invasively, without wounding, cost-effectively and easily cultured"*

REFERENCES

To view references, please visit:
drugtargetreview.com/2-18-Adjaye

3.4 The FGF, TGFβ and WNT axis Modulate Self-renewal of Human SIX2$^+$ Urine Derived Renal Progenitor Cells

Md Shaifur Rahman*, Wasco Wruck*, Lucas-Sebastian Spitzhorn, Lisa Nguyen, Martina Bohndorf, Soraia Martins, Fatima Asar, Audrey Ncube, Lars Erichsen, Nina Graffmann and James Adjaye

*These authors contributed equally.

Abstract

Human urine is a non-invasive source of renal stem cells with regeneration potential. Urine-derived renal progenitor cells were isolated from 10 individuals of both genders and distinct ages. These renal progenitors' express pluripotency-associated proteins- TRA-1-60, TRA-1-81, SSEA4, C-KIT and CD133, as well as the renal stem cell markers -SIX2, CITED1, WT1, CD24 and CD106. The transcriptomes of all SIX2$^+$ renal progenitors clustered together, and distinct from the human kidney biopsy-derived epithelial proximal cells (hREPCs). Stimulation of the urine-derived renal progenitor cells (UdRPCs) with the GSK3β-inhibitor (CHIR99021) induced differentiation. Transcriptome and KEGG pathway analysis revealed upregulation of WNT-associated genes- *AXIN2*, *JUN* and *NKD1*. Protein interaction network identified JUN- a downstream target of the WNT pathway in association with STAT3, ATF2 and MAPK1 as a putative negative regulator of self-renewal. Furthermore, like pluripotent stem cells, self-renewal is maintained by FGF2-driven TGFβ-SMAD2/3 pathway. The urine-derived renal progenitor cells and the data presented should lay the foundation for studying nephrogenesis in human.

Publication Status: Published in Sci Rep. 2020 Jan 20;10(1):739.

Impact Factor: 4.011

Approximated total share of contribution: 40%

Author contributions on experimental design, realization and publication: Conception: JA; Cell culture experiments: MSR, LSS, FA, MB and JA; Real Time PCR: FA, LE; Bisulphite sequencing: LE; Bioinformatics: WW and JA; Proliferation assays and Western blot analyses: SM; Derivation and characterisation of iPSCs: MB, NG and AN; Immunostaining and FACS analysis: MSR, MB, LSS, AN and L.N.; Writing of manuscript: MSR, WW, LSS, LN and JA; Final edits: JA. All authors approved the final version of the manuscript.

Pubmed link: https://www.ncbi.nlm.nih.gov/pubmed/31959818
Journal link: https://www.nature.com/articles/s41598-020-57723-2

www.nature.com/scientificreports

SCIENTIFIC REPORTS
nature research

OPEN

The FGF, TGFβ and WNT axis Modulate Self-renewal of Human SIX2$^+$ Urine Derived Renal Progenitor Cells

Md Shaifur Rahman[1,2], Wasco Wruck[1,2], Lucas-Sebastian Spitzhorn[1], Lisa Nguyen[1], Martina Bohndorf[1], Soraia Martins[1], Fatima Asar[1], Audrey Ncube[1], Lars Erichsen[1], Nina Graffmann[1] & James Adjaye[1*]

Human urine is a non-invasive source of renal stem cells with regeneration potential. Urine-derived renal progenitor cells were isolated from 10 individuals of both genders and distinct ages. These renal progenitors express pluripotency-associated proteins- TRA-1-60, TRA-1-81, SSEA4, C-KIT and CD133, as well as the renal stem cell markers -SIX2, CITED1, WT1, CD24 and CD106. The transcriptomes of all SIX2$^+$ renal progenitors clustered together, and distinct from the human kidney biopsy-derived epithelial proximal cells (hREPCs). Stimulation of the urine-derived renal progenitor cells (UdRPCs) with the GSK3β-inhibitor (CHIR99021) induced differentiation. Transcriptome and KEGG pathway analysis revealed upregulation of WNT-associated genes- *AXIN2*, *JUN* and *NKD1*. Protein interaction network identified JUN- a downstream target of the WNT pathway in association with STAT3, ATF2 and MAPK1 as a putative negative regulator of self-renewal. Furthermore, like pluripotent stem cells, self-renewal is maintained by FGF2-driven TGFβ-SMAD2/3 pathway. The urine-derived renal progenitor cells and the data presented should lay the foundation for studying nephrogenesis in human.

According to the International Society of Nephrology, more than 850 million people worldwide are afflicted with kidney diseases[1], which raises the quest for alternative therapies to overcome the limitations associated with current treatments including transplantation and dialysis. One of the most promising options is the utilization of renal stem cells for treating of kidney diseases, disease modelling, and drug development[2,3]. Renal stem/progenitor cells are self-renewing, multipotent cells with the ability to generate various cell types of the kidney to maintain renal function[4]. These progenitors are in abundance during fetal kidney development in which the renal progenitor surface marker CD24 and stem cell self-renewal marker CD133 cells are required for primordial nephrogenesis[5,6]. However, in adults, CD24, CD133 (Prominin-1) and vascular cell adhesion molecule 1 (CD106)-positive renal progenitors are present in renal tubules and capsules[7]. Two progenitor cell populations can be distinguished based on the expression of CD106. For instance, CD24$^+$CD133$^+$CD106$^-$ progenitors are present in proximal tubules whereas CD24$^+$CD133$^+$CD106$^+$ cells are localized in the Bowman's capsule. The latter can differentiate into a variety of cell types of renal tissue such as podocytes and tubular epithelial cells[4–7].

Several groups have identified urine as a non-invasive and repetitive source of renal progenitor cells[8,9]. It has been estimated that each day approximately 2,000 to 7,000 cells composed of differentiated epithelial cells, bi-potential epithelial cells (transitional cells), multipotent mesenchymal stem cells, and glomerular parietal cells are flushed out from the renal tubular network and the upper urinary tract into urine[10–12]. A subpopulation of these urine-derived cells are renal stem/progenitor cells which express master renal markers such as Sine Oculis Homeobox Homolog 2 (SIX2), Cbp/P300 Interacting Transactivator With Glu/Asp Rich Carboxy-Terminal Domain 1 (CITED1) and Wilms' Tumor 1 (WT1)[13–15] and CD24 and CD106[16]. Interestingly, these cells exhibit stem cell properties, i.e. expression of pluripotency-associated markers such as TRA-1-60, TRA-1-81, C-KIT (CD117), CD133 and SSEA4 and possess high proliferation capacity as they show telomerase activity. Further, they endow multi-differentiation potential and like bone marrow derived mesenchymal stem cells express

[1]Institute for Stem Cell Research and Regenerative Medicine, Medical Faculty, Heinrich Heine University Düsseldorf, 40225, Düsseldorf, Germany. [2]These authors contributed equally: Md Shaifur Rahman and Wasco Wruck. *email: james.adjaye@med.uni-duesseldorf.de

Vimentin, CD105, CD90, CD73 and not the hematopoietic stem cell markers- CD14, CD31, CD34 and CD45[17,18]. Although, research interest on urine derived renal stem cells is gradually increasing but the mechanistic role of genetic factors in these cells *in vitro* regarding progenitor/differentiated status maintenance is not clear.

Studies in mice have shown that Odd-skipped related 1 (Osr1), Six2, Wnt, Cited1 and Wt1 are required to maintain renal progenitor cells during kidney organogenesis[19–25]. Additionally, signalling pathways such as Fgf, Tgfβ and Notch play major roles in renal stem cell maintenance and differentiation[26–29]. The transcription factor Osr1 is an early marker specific for the intermediate mesenchyme (IM); *Osr1* knockout mice lack renal structures due to the failure to form the IM[30]. The homeodomain transcriptional regulator Six2 is expressed in the cap mesenchyme (CM) originating from metanephric mesenchyme. Six2 positive populations can generate all cell types of the main body of the nephron[31]. Inactivation of Six2 results in premature and ectopic renal vesicles, leading to a reduced number of nephrons and to renal hypoplasia[32]. Mechanistically, Osr1 plays a crucial role in Six2-dependent maintenance of mouse nephron progenitors by antagonizing Wnt-directed differentiation, whereas Wt1 maintains self-renewal by modulating Fgf signals[22,23]. Cited1 has been reported to be co-expressed with a fraction of $Six2^{+}$ cells undergoing self-renewal and these can be differentiated in response to activated WNT signaling during kidney development[25]. Furthermore, it has been demonstrated in mice that Bmp7 promotes proliferation of nephron progenitor cells via a Jnk-dependent mechanism involving phosphorylation of Jun and Atf2[33].

To date, research related to transcriptional regulatory control of mammalian nephrogenesis has been limited to the mouse[19,26] or to transcriptome "snapshots" in human[13]. A recent study demonstrated conserved and divergent genes associated with human and mouse kidney organogenesis[34], thus further highlighting the need for primary human renal stem cell models to better dissect nephrogenesis at the molecular level. Furthermore, species differences need to be considered, for example, mammalian nephrons arise from a limited nephron progenitor pool through a reiterative inductive process extending over days (mouse) or weeks (human) of kidney development[35]. Human kidney development initiates around 4 weeks of gestation and ends around 34–37 weeks of gestation. At the anatomical level, human and mouse kidney development differ in timing, scale, and global features such as lobe formation and progenitor niche organization[34–36]. These are all further evidence in support of the need of a reliable and robust human renal cell culture model.

Expression of pluripotency-associated proteins has enabled rapid reprogramming of urine derived mesenchymal and epithelial cells into induced pluripotent stem cells (iPSCs)[37–41]. Differentiation protocols for generating kidney-associated cell types from human pluripotent stem cells have mimicked normal kidney development[28,42–44]. For example, WNT activation using a GSK3β inhibitor (CHIR99021), FGF9, Activin A, Retinoic acid (RA) and BMP7 as instructive signals have been employed to derive functional podocytes, proximal renal tubules, and glomeruli[29,45–49]. Despite these efforts and achievements, there will always be variabilities between differentiation protocols, the maturation state of the differentiated renal cells and genes associated with temporal maturation during human kidney organoids formation from human iPSCs[50,51]. We propose that using native renal stem cells isolated directly from urine will circumvent most of the shortfalls and deficiencies associated with human pluripotent stem cell-based models.

Here we provide for the first time the full characterisation of renal progenitors at the transcriptome, secretome and cellular level, which has led to the identification of a gene regulatory network and associated signalling pathways that maintain their self-renewal. We anticipate that our data will enhance our meagre understanding of the properties of urine-derived renal stem cells, and enable the generation of renal disease models *in vitro* and eventually kidney-associated regenerative therapies.

Results

Urine-derived renal progenitors express a subset of pluripotent stem cell-associated markers and possess features typical of bone marrow-derived MSC. Urine samples were collected from 10 healthy adult donors (4 males-UM and 6 females-UF) with ages ranging from 21 to 61 years, and of mixed ethnicity (3 Africans and 7 Caucasians) (Supplemental Table S1). Attached cells emerged from processed urine as isolated clusters after 7 days, thereafter these acquired a "rice grain" fibroblast-like morphology resembling MSCs (Fig. 1A, Supplemental Fig. S1A). A selection of distinct urine-derived renal stem cells populations (n = 4) were used to assay cell proliferation and growth. After 3 days in culture, the cells exited the lag phase and growth began in an exponential phase. Cells attained stationary phase at day 7 of subculture (Fig. 1B). All four populations-UM27, UM16, UM51 and UF45 showed similar proliferation and growth patterns.

Flow cytometry analysis revealed that approximately 98.9% of the cells express SSEA4, TRA-1–60 (11.3%) and TRA-1-81 (16.5%) (Fig. 1C). These data were confirmed by immunofluorescent-based staining of SSEA4 which also express the proliferation-associated stem cell markers- C-KIT and CD133 (Fig. 1D). In order to reveal the detailed methylation pattern of the 5′-regulatory region of the OCT4 gene in the UM51, we employed standard bisulfite sequencing. In total 330 Cytosine-phosphatidyl-Guanine-dinucleotides (CpG) upstream of the transcription-starting site (TSS) of the OCT4 gene were analysed. Within this 469 bp long region, a dense methylation pattern was observed in the UM51 cells, with 92.4% (305) of the CpG dinucleotides identified were methylated (Fig. 1E). In contrast, iPSCs derived from UM51 had 72.12% (207) of analysed CpGs were unmethylated (Supplemental Fig. S1B).

Urine-derived renal progenitors express the mesenchymal marker- Vimentin and not the epithelial marker-E-Cadherin (Fig. 1D, Supplemental Fig. S1C). Flow cytometry analysis of critical MSC cell surface markers were negative for the hematopoietic markers CD14, CD20, CD34, and CD45 and positive for CD73, CD90 and CD105 albeit at variable levels (Supplemental Fig. S1D). Typical of MSCs, urine-derived renal progenitor cells can also differentiate into osteocytes, chondrocytes, and adipocytes when cultured in the respective differentiation medium for 3 weeks (Fig. 1F, Supplemental Fig. S1E). Furthermore, employing a cytokine array (n = 2), a plethora of trophic factors such as IL8, GDF-15, SERPINE-1, Angiogenin, VEGF, and Thrombospondin-1 were detected,

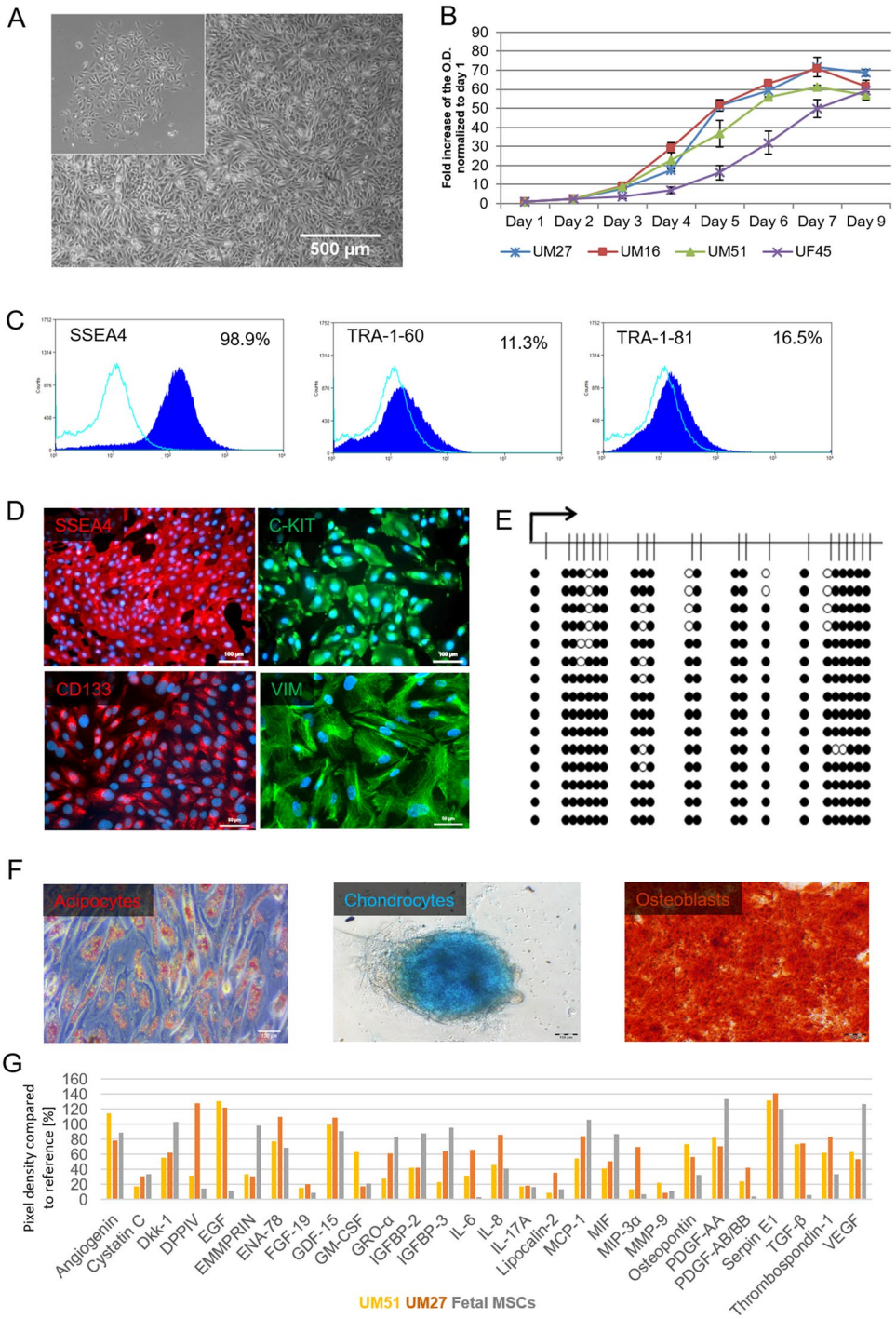

Figure 1. Propagation and characterisation of urine-derived renal progenitors. **(A)** Representative pictures of the "rice grain"-like appearance of the cells from the initial attachment to an elongated MSC-like morphology. **(B)** Growth curve analysis of selected urine-derived renal progenitors carried out using the Resazurin metabolic assay. Data are presented as means ± SEMs. **(C)** Immune-phenotyping for SSEA4, TRA-1-81 and TRA-1-60; and **(D)** immunofluorescence-based detection of the expression of pluripotency-associated stem cell- proteins SSEA4 (red), C-KIT (green), CD133 (red) and the mesenchymal-associated protein Vimentin (green); cell nuclei were stained using Hoechst/DAPI (scale bars: 100 µm and 50 µm). **(E)** Bisulfite sequencing of CpG island methylation patterns within the 5′- regulatory region of the OCT4 gene in UM51. Filled circles stand for methylated CpG dinucleotides. White circles stand for unmethylated CpGs. Arrows indicate the transcription start site. **(F)** *In vitro* Osteoblast, Chondrocyte and Adipocyte differentiation potential of urine-derived renal progenitors. **(G)** Cytokines secreted by urine-derived renal progenitors in culture media. Lists of significant GOs and KEGG pathways associated with the genes encoding the secreted cytokines are shown in Supplemental Fig. S1G.

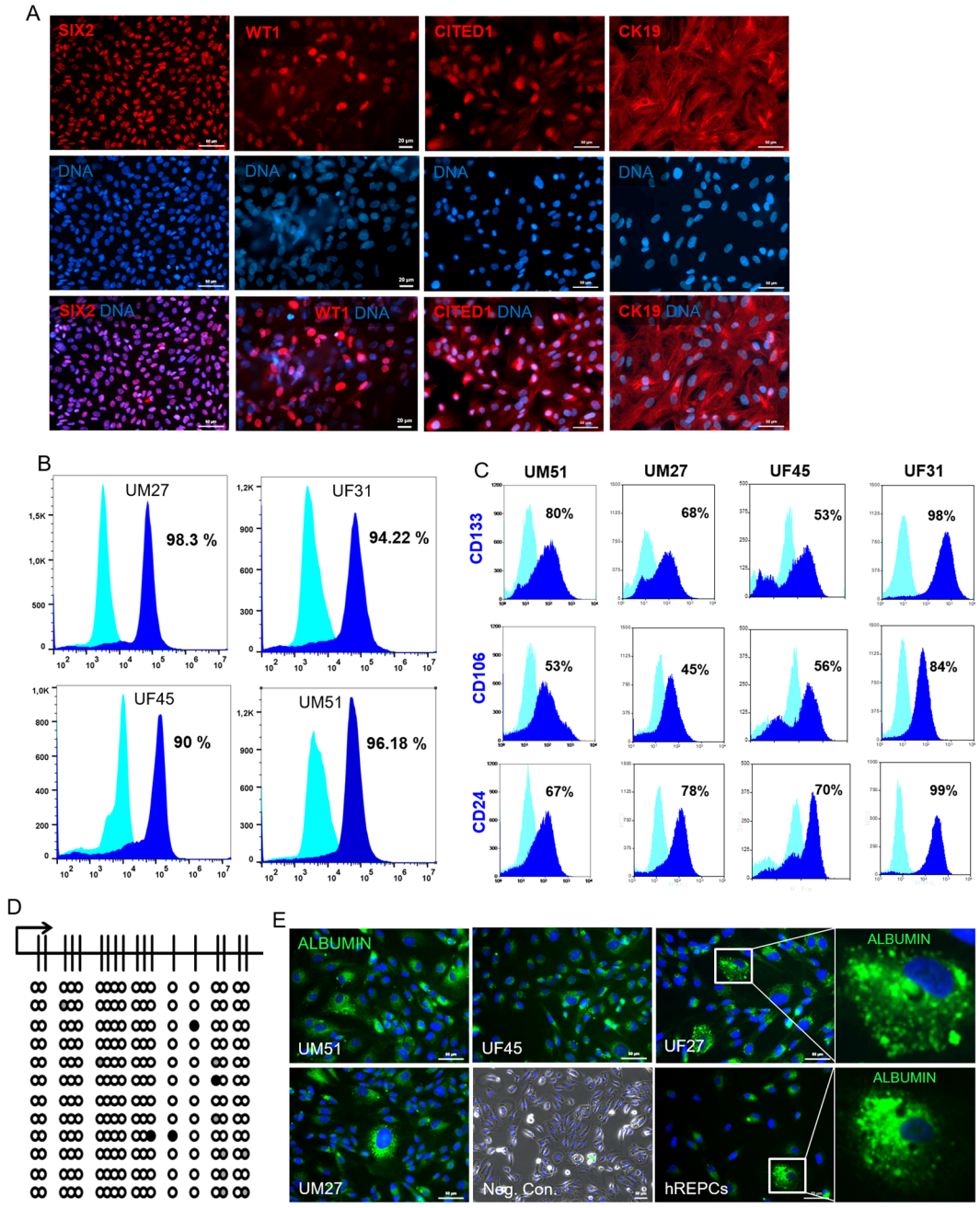

Figure 2. Expression of kidney-associated proteins in urine-derived renal progenitors and Albumin transport. **(A)** Urine-derived renal progenitors express the renal stem cell markers- SIX2, CITED1, WT1, and CK19. Renal markers (red) and cell nuclei were stained using DAPI/Hoechst (blue). **(B)** Flow cytometry analysis for the key renal stem cell transcription factor SIX2 and **(C)** Renal stem cell surface markers CD24, CD133, and CD106 of UM27, UF31, UF45 and UM51. **(D)** Detailed CpG methylation profiles of the SIX2 5′-regulatory region are documented as revealed by bisulfite sequencing. Filled circles represent methylated CpG dinucleotides and white circles unmethylated CpGs. Arrows indicate the transcription start site. 1.9% of CpG dinucleotides were found to be methylated. **(E)** Urine-derived renal progenitors (n = 4) like the human kidney biopsy-derived hREPCs also transport Albumin. Albumin was coupled to Alexa Fluor 488 (green) and cell nuclei stained with DAPI (blue). Scale bars indicate 50 µm.

and further analysis of their associated GOs and KEGG pathways revealed immune system related terms (Fig. 1G, Supplemental Fig. S1F-G).

Urine-derived renal progenitors express key renal progenitor cell markers and are able to endocytose Albumin. Immunofluorescence-based staining revealed expression of the key renal stem cell proteins such as CK19 and the transcription factors- SIX2, CITED1, WT1, as shown by representative images (Fig. 2A).

To determine the variability of SIX2$^+$cells between the progenitor cell preparations- UM27, UF31, UM51 and UF45 (n = 4) a flow cytometry analysis was performed. We observed approximately 95% SIX2$^+$ cells in UM27, UF31 and UM51 whereas UF45 had 90% SIX2$^+$ cells (Fig. 2B). In addition, to confirm the renal stemness status of the urine-derived progenitor cells a flow cytometry analysis was performed to evaluate expression of the renal progenitor markers CD24, CD106 and the self-renewal marker CD133 in the cell preparations- UM27, UF31, UM51 and UF45. CD24, CD133 and CD106 were variably expressed in the aforementioned cell preparations. For instance, 98% of the UF31 cell population was CD133$^+$, 99% of the cells were positive for CD24 and 84% of the cells were CD106$^+$. On the other hand, the UF45 sample displayed a different pattern for CD133 (68%), CD24 (70%) and CD106 (45%) positive cells, respectively (Fig. 2C). Bisulfite sequencing of a portion of the 5′-regulatory region of the SIX2 gene revealed methylation of only 1.9% of CpG dinucleotides (Fig. 2D). As, presence of albumin in urine is a mark of kidney cell functionality, and by the endo/exocytosis of albumin, kidney maintain the colloid osmotic pressure and transport biomolecules. We performed endocytosis assay and could show that urine-derived cells can transport Albumin (Fig. 2E). Furthermore, the CYP2D6 genotypes investigated were distinct between groups of individuals, thus reflecting potential diverse drug metabolizing activities. UM51 for example expresses the CYP2D6 *4/*17 genotype which confers an intermediate metabolizing activity whereas UF31 bears the CYP2D6*1/*41 genotype with an ultra-rapid metabolizing activity. The other three individuals (UF21, UF45 and UM27) are endowed with normal drug metabolizing activity (Supplemental Table S1).

Comparative transcriptome analysis of urine-derived renal progenitors and kidney-biopsy derived renal epithelial proximal cells (hREPCs). A hierarchical clustering analysis comparing the transcriptomes of urine derived renal progenitors with the kidney biopsy-derived renal epithelial proximal cells (hREPCs) revealed that all urine derived renal progenitors samples clustered together as a common cell type distinct from hREPCs (Fig. 3A). Additionally, expression of renal progenitor surface markers *CD24*, *CD106* and *CD133* were detected in urine-derived renal progenitors whilst *PODXL* was not expressed (Fig. 3B). These renal progenitors are of mesenchymal origin expressing *VIM*, however a scatter plot comparison between UM51 with hREPCs shows similarity with a high Pearson correlation of 0.9575 (Fig. 3C). The epithelial character of hREPCs is reflected by *CDH1* expression. The comparison of expressed genes (det-$p < 0.05$) in renal progenitors (UM51) and hREPCs in a venn diagram revealed a common 12281 gene-set, whereas 566 are expressed exclusively in UM51 and 438 exclusively in hREPCs (Fig. 3D). The 10 most over-represented GO BP terms (biological processes) in the UM51 exclusive gene-set include triglyceride homeostasis, kidney development and urogenital system development, whereas the hREPCs exclusive gene set includes chloride transmembrane transport, anion transport and response to lipopolysaccharides (Fig. 3E). The common gene set consists of 874 up-regulated genes (ratio > 2) in UM51 (e.g. renal tubule development, urogenital system development and anterior/posterior pattern specification) and 1042 down-regulated genes (ratio < 0.5) in UM51 (e.g. cell division and cholesterol biosynthetic process) (Fig. 3F).

Comparative gene expression analysis of urine-derived and kidney biopsies-derived renal progenitor cells. Gene expression of urine-derived renal progenitors was compared to public available datasets GSE23911 in which nephron progenitor cells were derived from adult human renal cortical tissue[52]. Additionally, the comparison was extended by two further datasets GSE74450 and GSE75949 which contain data from fetal kidney biopsy derived nephron progenitor cells[53,54]. We could show that urine-derived renal progenitors have a high level of similarity to other human nephron progenitors at the transcriptome level. The resulting number of expressed genes were comparable: 12112 genes in urine-derived renal progenitors, 8446 genes in GSE23911, 10597 genes in GSE74450 and 13895 genes in GSE75949. In the Venn diagram analysis most genes were found in the intersection of all genesets (4411), followed by the intersection of urine-derived renal progenitors with the fetal kidney genesets from GSE74450 and GSE75949. Among the intersection with single genesets urine-derived renal progenitors had the highest overlap with the GSE75949 pointing at the highest similarity with this geneset (Supplemental Fig. S2). A subset of genes expressed in common between urine-derived renal progenitors, GSE74450 and GSE75949, are associated with renal system development related GO's (BP) terms, thus confirming renal progenitor cell identity (Supplemental Table S5).

Confirmation of the renal origin of urine-derived progenitor cells and retention of renal-associated genes in urine-derived progenitors-iPSCs. A venn diagram-based comparison of gene expression (det-$p < 0.05$) in urine-derived renal progenitors and human foreskin fibroblasts (HFF) was carried out (Fig. 4A) in order to dissect common and distinct gene expression patterns. The majority of genes (11649) are expressed in common, 463 exclusively in urine-derived renal progenitors and 891 in fibroblasts. The 463 genes were further analysed for over-represented GOs and summarized as a GO network (Fig. 4B) with the tools REVIGO, and Cytoscape was used for the GO terms of the category BP. In addition to several developmental terms such as organ induction, regulation of embryonic development (high number of edges referring to similarity to many terms), specific renal-related terms including urogenital system development, mesenchymal cell proliferation involved in ureteric bud development and positive regulation of nephron tubule epithelial cell differentiation (marked with blue ellipse, intense red indicating higher significance) were identified. Interestingly, the non-canonical WNT signalling pathway, which plays a major role in kidney development, is also over-represented (orange ring-top left).

The dendrogram based on the global transcriptome analysis revealed a clear separation of urine-derived renal progenitors lines (n = 9) from the differentiated urine-derived renal progenitors (CHIR 99021 treated urine- derived renal progenitor cells, n = 3), urine derived renal progenitors-iPSCs (n = 4) and embryonic stem cells (H1 and H9) (Fig. 4C). Characterization of the derived urine derived renal progenitors-iPSCs is depicted in Supplemental Fig. S3. In the Venn diagram (Fig. 4D) we compared expressed genes (det-$p < 0.05$) in urine

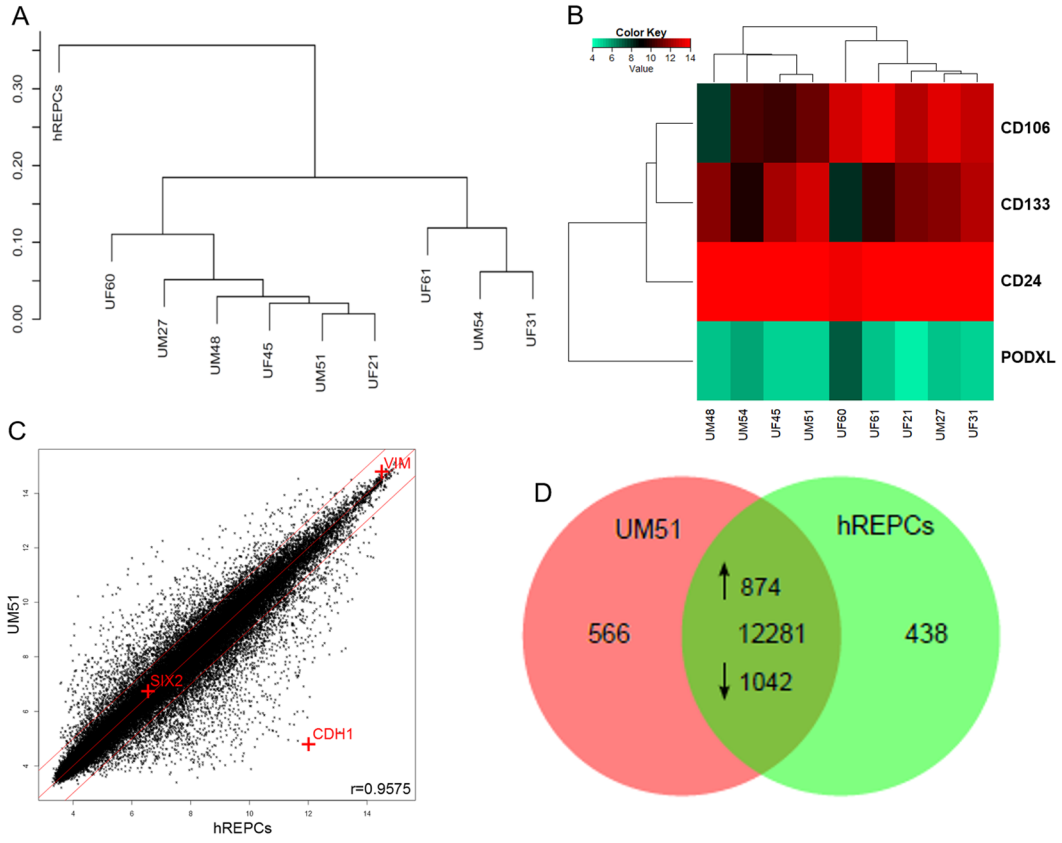

E

Term	Pvalue
triglyceride homeostasis	9,605E-06
kidney development	0,00042078
urogenital system development	0,00046036
collagen fibril organization	0,0004605
telencephalon development	0,000505
embryonic retina morphogenesis in camera-type eye	0,00051672
sensory organ development	0,00117891
neuronal stem cell population maintenance	0,00140151
cell morphogenesis involved in differentiation	0,00181875
generation of ovulation cycle rhythm	0,00187149

Term	Pvalue
chloride transmembrane transport	0,00014
prostate epithelial cord arborization involved in prostate glandular acinus morphogenesis	0,00031
regulation of branching involved in prostate gland morphogenesis	0,00031
response to lipopolysaccharide	0,00042
inorganic anion transport	0,00053
anion transport	0,00056
regulation of icosanoid secretion	0,00061
negative regulation of secretion	0,00072
prostate glandular acinus development	0,00102
positive regulation of cytosolic calcium ion concentration	0,00119

F

UM51 up (differentially expressed genes)	
Term	Pvalue
circulatory system development	4,102E-12
positive regulation of RNA biosynthetic process	4,4896E-09
urogenital system development	2,3935E-08
anterior/posterior pattern specification	2,6834E-08
positive regulation of nucleobase-containing compound metabolic process	4,7051E-08
positive regulation of biosynthetic process	2,6254E-07
muscle tissue development	9,4143E-07
renal tubule development	1,0127E-06
positive regulation of macromolecule metabolic process	1,5071E-06
tissue morphogenesis	2,9227E-06

UM51 down (differentially expressed genes)	
Term	Pvalue
localization of cell	5,3154E-15
organelle fission	8,1634E-14
cholesterol biosynthetic process	7,2679E-13
small molecule biosynthetic process	8,9168E-12
cell division	1,2264E-11
regulation of phosphorylation	5,8579E-11
regulation of phosphorus metabolic process	8,1264E-11
organic hydroxy compound biosynthetic process	8,8558E-10
negative regulation of molecular function	1,045E-09
secondary alcohol metabolic process	1,4932E-09

Figure 3. Transcriptome analysis of urine-derived renal progenitors in comparison to kidney biopsy-derived renal epithelial proximal cells- hREPCs. **(A)** A hierarchical cluster dendrogram based on transcriptomes of urine-derived renal progenitors with the kidney biopsy-derived renal epithelial proximal cells (hREPCs). **(B)** The heatmap of renal progenitor cell surface markers (*CD24, CD133, and CD106*) expressed in urine-derived renal progenitors. **(C)** Comparison of gene expression values of urine-derived renal progenitors (UM51) with hREPCs in a scatter plot confirms the mesenchymal phenotype of urine-derived renal progenitors, i.e. expression of Vimentin (*VIM*) and expression of E-cadherin (*CDH1*) in hREPCs. **(D)** Expressed genes (det-p < 0.05) in urine-derived renal progenitors (sample UM51) and hREPCs are compared in the Venn diagram. **(E)** The 10 most over-represented GO BP-terms in 566 UM51 genes include triglyceride homeostasis and kidney development and in 438 hREPCs genes include chloride transmembrane transport. **(F)** The 10 most over-represented GO BP-terms in the up- and down-regulated genes in UM51 in comparison to hREPCs are shown. The complete dataset is presented in Supplemental Table S4.

derived renal progenitors-iPSCs with ESCs and HFF-iPSCs. Most genes (12092) are expressed in common in all cell types while 150 genes are expressed exclusively in urine derived renal progenitors-iPSCs. The genes expressed exclusively in one cell type were further analysed for over-representation of GO terms. The treemap summarizing

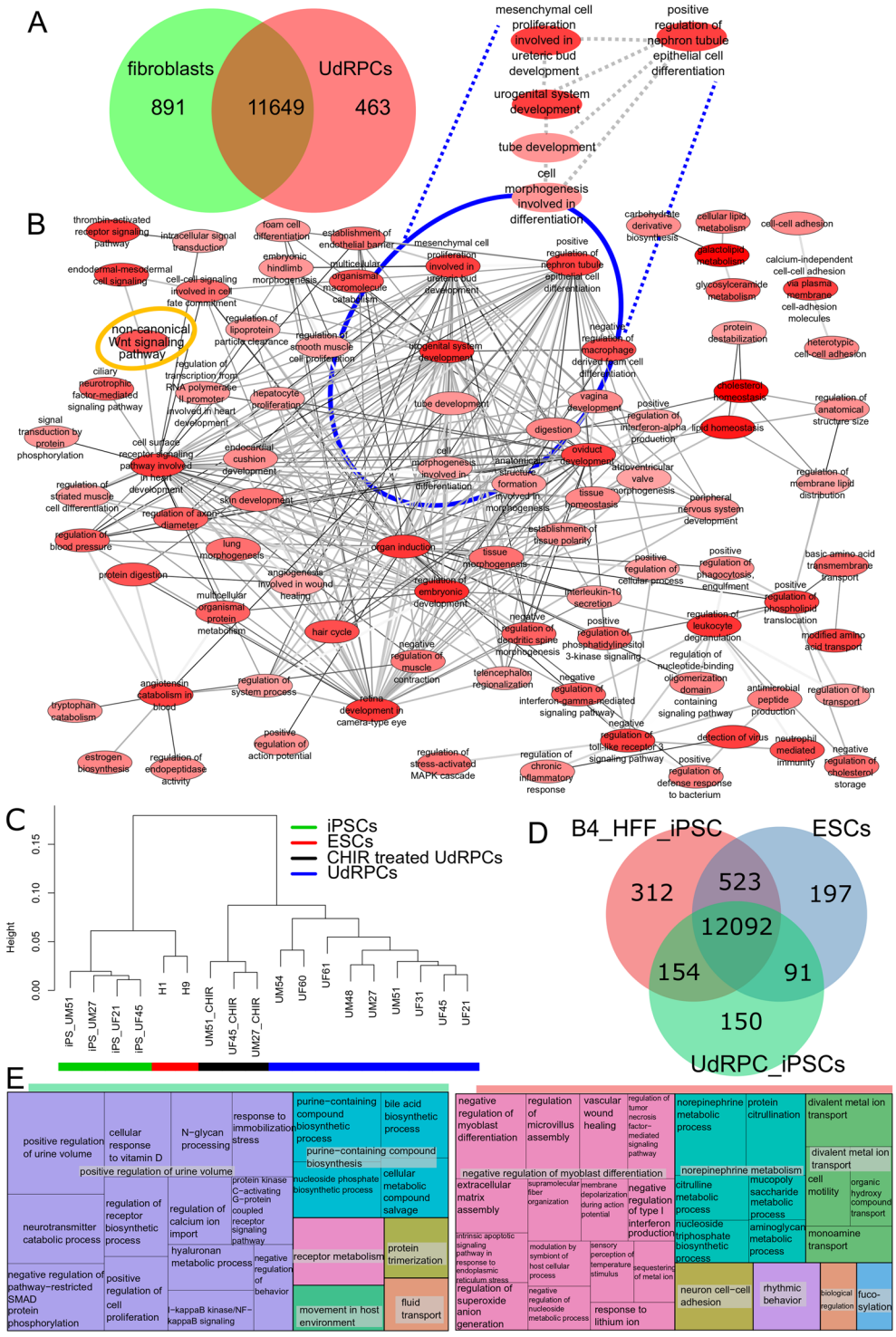

Figure 4. In-depth bioinformatic analysis of urine-derived renal progenitors and urine-derived renal progenitors derived-iPSCs. **(A)** Expressed genes (det-$p < 0.05$) in urine-derived renal progenitors (UdRPCs) and fibroblasts are compared in a venn diagram. Most genes are expressed in common (11649), 463 genes are expressed exclusively in urine-derived renal progenitors and 891 in fibroblasts. The subsets and urine-derived renal progenitors GOs are presented in supplemental_table_S4. **(B)** The gene ontology network was generated with the tools REVIGO and Cytoscape and summarizes the GO terms of category Biological Process (BP) over-represented in the 463 genes expressed exclusively in urine-derived renal progenitors. Several general developmental terms emerged, e.g. "organ induction". Specific renal-related terms including "urogenital system development" are marked with a blue ellipse. GOs are represented by the network nodes with the intensity of red indicating the significance of over-representation of a GO term. The edges refer to similarities between the GO terms. **(C)** The dendrogram shows a clear separation of urine-derived renal progenitors, differentiated urine-derived renal progenitors (CHIR treated UdRPCs of UM51, UM27, and UF45) (black bar), ESCs (H1 and

H9, red bar) and urine-derived renal progenitors-iPSCs (green bar). **(D)** Venn diagram of HFF-iPSCs, urine-derived renal progenitors-iPSCs (UdRPCs_iPScs) and ESCs. **(E)** GO terms of 150 genes expressed exclusively in urine-derived renal progenitors-iPSCs indicate that these iPSCs retain the memory of renal origin. In the treemap for the HFF-iPSCs the GO-BP terms of the 312 over-represented genes of the exclusive gene set are summarized. The most significant group is associated with negative regulation of myoblast differentiation including genes *DDIT3*, *MBNL3*, *TGFB1*, *ZFHX3* pointing at the fibroblast origin of these iPSCs. The entire dataset is presented in Supplemental Table S7.

the GO terms of category BP over-represented in the 150 genes expressed exclusively in urine derived renal progenitors-iPSCs (Fig. 4E) indicates that these iPSCs retain a memory of their kidney origin. In addition to the largest most significant group- positive regulation of urine volume, it consists of other renal-related GO terms (e.g. calcium transport, vitamin D). Stem-cell-related and developmental terms such as positive regulation of cell proliferation are due to their pluripotent nature. Within the treemap summarizing the GO-BP terms over-represented in the 312 genes expressed exclusively in HFF-iPSCs, the largest most significant group is associated with negative regulation of myoblast differentiation, thus pointing at the fibroblast origin of these iPSCs (Fig. 4E). Furthermore, within the treemap summarizing the GO-BP terms over-represented in the 197 genes expressed exclusively in ESCs, the largest most significant group is associated with negative regulation of astrocyte differentiation- hinting at their known propensity to differentiate into the ectodermal lineage (Supplemental Fig. S4).

WNT pathway activation by GSK3β inhibition induces differentiation of urine-derived renal progenitors into renal epithelial proximal tubular cells. To differentiate three independent renal progenitors preparations, the cells were treated with 10 μM CHIR99021 (WNT pathway activation by GSK3β inhibition) for 2 days and morphological changes from fibroblastic to elongated tubular shape were observed (Fig. 5A). In the Venn diagram, expressed genes (det-$p < 0.05$) in untreated urine-derived renal progenitors are compared to renal progenitors treated with CHIR99021. Genes expressed in common amounts to 11790, of these 2491 are upregulated in the CHIR99021 treatment ($p < 0.05$, ratio > 1.33) and 2043 are down-regulated ($p < 0.05$, ratio < 0.75) (Fig. 5B, Supplemental Table S8). Among the upregulated genes, 27 are considered "novel" (gene symbol starting with "LOC"), 21 among the down-regulated genes and 98 among the non-regulated genes (Supplemental Table S8). The heatmap based on the top 20 regulated genes shows a clear separation between untreated and treated cells (Fig. 5C). Amongst the up-regulated genes, the associated KEGG pathways include WNT-signaling (*AXIN2*, *JUN*, *NKD1*) (Supplemental Fig. S5). Over-representation analysis of the up-regulated genes and their associated KEGG pathways identified protein processing in endoplasmic reticulum as highly significant and several signalling pathways such as mTOR, Insulin, p53, AMPK and TNF. Over-representation analysis of the down-regulated genes and associated KEGG pathways revealed cell cycle, cellular senescence, focal adhesion, FoxO, ErbB and thyroid hormone signalling. Interestingly Hippo pathway was regulated in both undifferentiated and differentiated renal cells (Fig. 5D).

Regulation of self-renewal and differentiation in urine-derived renal progenitor cells. Further to the transcriptome analyses, a real-time PCR revealed downregulation of the stem cell self-renewal associated gene *CD133* and activated expression of the nephrogenesis-associated gene *BMP7* after CHIR99021 stimulation (Fig. 6A). Since FGF signaling is also crucial for maintaining self-renewal, we compared the transcriptome of differentiated cells (CHIR99021 treated) and progenitor cells to investigate the effect of CHIR99021 stimulation on FGF-signaling with respect to the genes from FGF and FGFR family; BMP7 and BMP4 from the BMP family. We detected an upregulation of FGF2 and FGF7 in undifferentiated renal progenitors (Fig. 6B). To validate this, we disrupted FGF signaling using fibroblast growth factor receptor (FGFR) inhibitor SU5402, and observed morphological changes (Supplemental Fig. S6). Interestingly, downregulation of the key renal transcription factor *SIX2* was detected in both the CHIR99021 and SU5402 treated cells (Fig. 6C). Furthermore, to identify the self-renewal regulators and pathways in urine-derived renal progenitor cells, a protein-protein-interaction network was generated. The network of the 40 proteins, encoded by the 20 most significantly up- and down-regulated genes between CHIR99021 treated and untreated urine-derived renal progeitors (Fig. 5C) indentified JUN as a major hub – in terms of having most connections to other proteins in the network. However, in the WNT-signaling pathway JUN is at the end of a downstream cascade from GSK3β, including further downstream targets- AXIN2 and CTNNB1. The genes encoding these proteins were differentially regulated by the CHIR99021 treatment (green nodes) (Fig. 6D). Several communities with more interactions within the community than to other communities can be detected in the network via community clustering of the network via edge-betweenness includes JUN (red), GSK3β / AXIN2 / CTNNB1 (green), LATS2 (yellow), EGFR (pink) (Fig. 6E). To analyze the effect of WNT activation on the TGFβ-SMAD pathway, Western blot analysis was performed to detect phosphorylation levels of SMAD 2/3 and SMAD 1/5/8 in UF45, UM51 and UM27. In the differentiated cells (urine-derived renal progenitors after CHIR treatment) a decreased level of phosphorylated SMAD 2/3 and increased levels of phosphorylated SMAD 1/5/8 were observed (Fig. 6F).

Discussion

Although relatively few renal cells are shed under healthy conditions compared to dysfunctional conditions[10,55], we were able to isolate, culture and expand urine cells from healthy donors. Here we describe urine as a reliable, non-invasive, robust and cheap source of renal stem cells, in contrast to amniotic fluid or kidney biopsies[56,57]. Urine derived stem cells can be expand from a single clone with high proliferation potency[37,58]. We

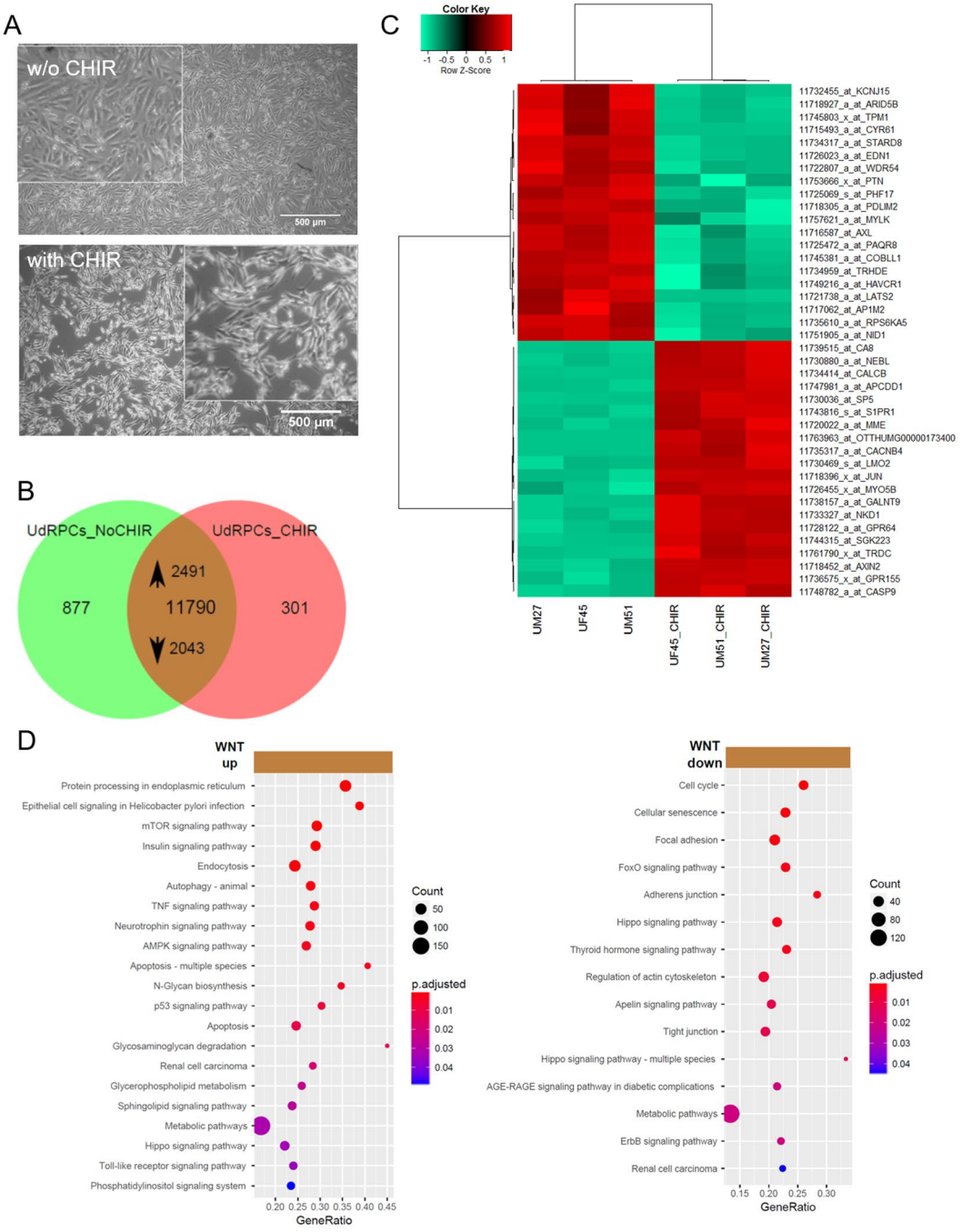

Figure 5. Supplementation of urine-derived renal progenitors with the GSK-3β inhibitor. **(A)** Activation of WNT signalling by supplementation with GSK-3β-inhibitor CHIR99021 led to differentiation into renal epithelial proximal tubular cells. **(B)** In the Venn diagram, expressed genes (det-$p < 0.05$) in untreated urine-derived renal progenitors (UdRPCs_NoCHIR) are compared to urine-derived renal progenitors treated with the GSK-3β-inhibitor CHIR99021 (UdRPCs_CHIR). Among the 11790 genes expressed in both conditions, 2491 are up-regulated in the CHIR99021 treatment ($p < 0.05$, ratio > 1.33) and 2043 down-regulated ($p < 0.05$, ratio < 0.75). **(C)** Heatmap of 3 independent urine-derived renal progenitor cell preparations with and without CHIR treatment. **(D)** Over-representation analysis of the up-regulated genes and associated KEGG pathways revealed protein processing in endoplasmic reticulum as highly significant and several signalling and metabolic pathways including mTOR, Insulin, p53 and TNF. Over-representation analysis of the down-regulated genes in KEGG pathways identified cell cycle, cellular senescence, focal adhesion, FoxO and adherens junction as most significant. Supplemental Table S8 provides the full list of regulated genes and associated pathways.

propose naming these cells as urine-derived renal progenitor cells, because they can be kept in culture for almost 12 passages whilst maintaining expression of the self-renewal associated proteins- SIX2, CITED1, CD133, C-KIT, TRA-1-60, TRA-1-81 and SSEA4 as has been shown by others[37,56]. Despite the expression of a subset of

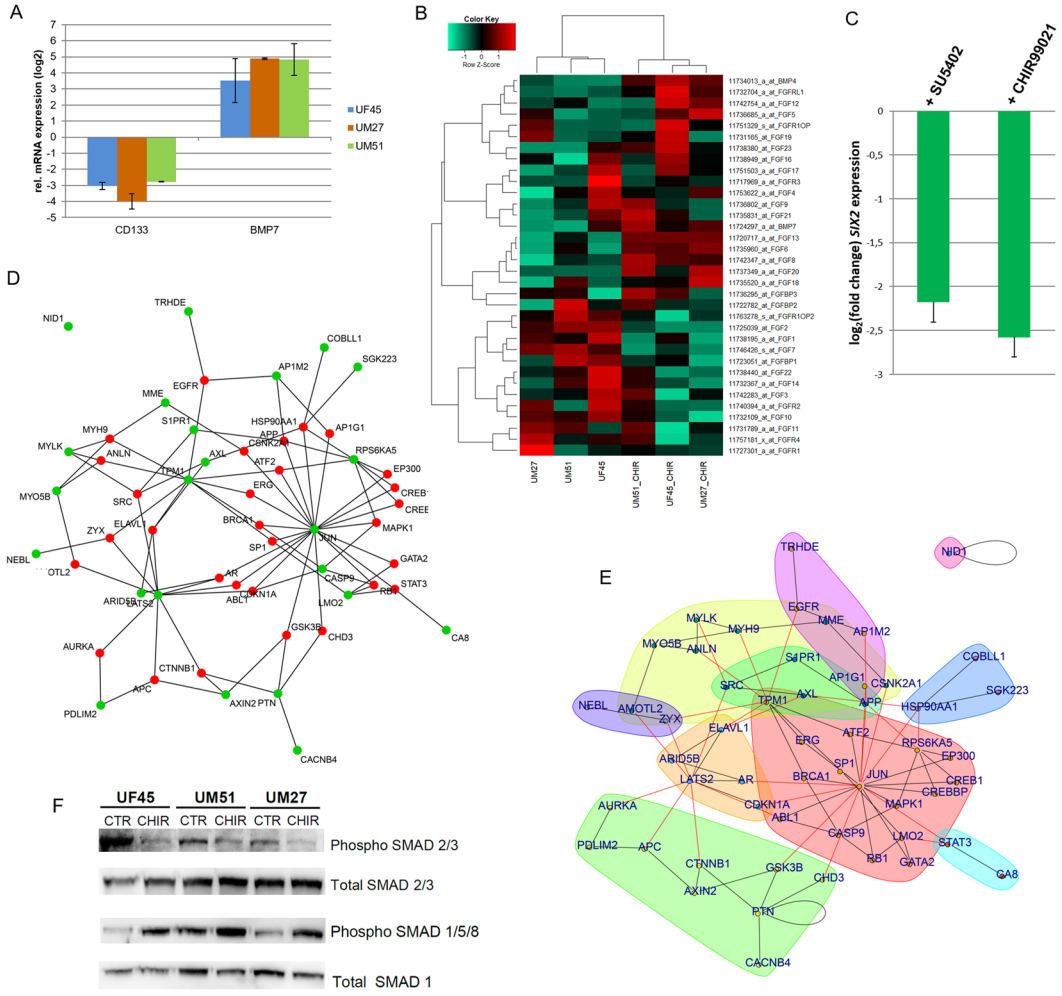

Figure 6. Regulation of self-renewal and differentiation in urine-derived renal progenitors. **(A)** Real-time PCR-based confirmation of down-regulation of *CD133* and activated expression of *BMP7* after CHIR stimulation. **(B)** Effect of CHIR99021 stimulation on FGF-signaling and BMP (BMP7 and BMP4) signaling. The heatmap depicts FGF signaling associated genes up and down regulated upon CHIR treatment of the urine-derived renal progenitors. **(C)** Downregulation of *SIX2* expression in differentiated urine-derived renal progenitors upon WNT stimulation using the GSK-3β-inhibitor CHIR99021 and blocking of FGF signaling using the FGF receptor inhibitor SU5402. **(D)** JUN is a major hub of protein interaction networks of urine-derived renal progenitors treated with CHIR. Based on the Biogrid database protein interaction networks were constructed from the set of the most highly regulated 40 genes either up- or down in the urine-derived renal progenitors treated with CHIR. The selected genes used to connect to the network with interactions from the Biogrid database are marked in green, genes added as Biogrid interactions are marked in red. Induction of WNT leading to GSK3B inhibition is reflected by the connection of GSK3B to JUN and to AXIN2 which is connected to CTNNB1 (β-catenin) – these all downstream targets of GSK3B in the WNT-signaling pathway. **(E)** Community clustering of the network identified several communities: JUN (red), GSK3B/AXIN2/CTNNB1 (green), LATS2 (yellow), EGFR (pink). Black lines refer to edges within a community, red lines to edges between different communities. **(F)** Western blot analysis of the phosphorylated levels of SMAD 2/3 and SMAD 1/5/8 in undifferentiated and differentiated UF45, UM51 and UM27.

pluripotency-associated factors, these renal progenitor cells do not express OCT4, SOX2 and NANOG- which are key pluripotency-regulating transcription factors[59,60]. Further evidence in support of the lack of OCT4 expression is our observed fully methylated CpG dinucleotides within the OCT4 promoter in the UM51 cells. Urine-derived renal progenitors are in fact bon-fide MSCs- i.e. they express VIM and not CDH1, adhere to plastic surfaces, express CD73, CD90 and CD105 and not the hematopoietic markers CD14, CD20, CD34, and CD45. Typical of MSCs, urine-derived renal progenitors can be differentiated into osteoblasts, chondrocytes and adipocytes[56,57,61]. They also secrete a plethora of cytokines and growth factors- such as EGF, GDF, PDGF and Serpin E1[62]. The multipotent features of urine-derived renal progenitors make these cells promising for studying nephrogenesis and in the future regenerative therapy of kidney-associated diseases.

Urine-derived renal progenitor cells express key renal progenitor-regulatory proteins SIX2, CITED1 and WT1 indicating they originate from the kidney as described from others[13,14,27,57,63]. Unmethylated CpG islands within

the 5′- regulatory region of the SIX2 gene confirm their progenitor status. Nuclear-localized SIX2 expression is critical for maintaining self-renewal of renal stem cell populations and has been described to co-localize with CITED1[25]. We observed CITED1 expression in both the nucleus and cytoplasm, this is supported by a subcellular fractionation study that demonstrated an abundant portion of CITED1 localized in the cytoplasm whereas only 5% were expressed in the nucleus[64]. As CITED1 is a cell cycle-dependent transcriptional co-factor and contains a nuclear export signal domain, the subcellular localization might be dependent on its phosphorylation status. We previously, showed CITED1 and WT1 expression in the nucleus and cytoplasm of amniotic fluid cells of renal origin[56]. Here, we observed that subpopulations of adult urine-derived progenitor cells express WT1 in the nucleus and in some cases, both nuclear and cytoplasmic localization was observed. Wt1 has nucleocytoplasmic shuttling activity, however, the shuttling of Wt1 between the nucleus and cytoplasm might regulate the activity as a transcription factor as a result of interaction with the cargo protein importins α1 and β[65,66].

In line with our study, urine-derived renal progenitor cells have been described to express the surface marker CD24, CD106, and CD133[16]. However, we observed variabilities in the numbers of cells expressing these markers between preparations. This variance might be due to the origin of the urine- shed cells in the adult[4,6,7,67]. For example, CD24 and CD133 positive cells have been found in renal tubules and the renal capsule, but $CD106^{+}$ cells are only present in the renal capsule.

Furthermore, urine-derived renal progenitors transport albumin[56,68]. The albumin filtration pathway partly takes place in the kidney and the presence of albumin in urine is used as a marker for cell functionality as described by the endo/exocytosis of albumin in kidney[69]. The GOs derived from the exclusively expressed genes in urine-derived renal progenitors (compared to HFF1) unveiled renal system development- related terms. To overcome the lack of reference human kidney biopsy-derived renal progenitors, we performed a meta-analysis comparing our data to nephron progenitor cell transcriptome datasets downloaded from NCBI GEO. The analyses revealed that our urine-derived renal progenitors share a high level of similarity with other human nephron progenitors at the transcriptome level[52–54]. Moreover, the GOs from the urine cell derived-iPSC exclusive genes-set, in contrast to pluripotent stem cells, identified terms related to renal function therefore implying the preservation of their kidney origin. As the conservation of tissue of origin in iPSCs might be linked to epigenetic memory[17,70], urine-derived renal progenitors as well as corresponding-iPSCs, especially with known CYP2D6 status, might be advantageous for differentiation into renal cells, modelling kidney-related diseases, nephrotoxicity studies and regenerative medicine[55].

Dissecting the gene regulatory mechanisms that drive human renal progenitor growth and differentiation *in vitro* represents the key step for translation but remains a challenge due to the absence of well-characterised primary urine derived stem cells. Here we have shown that urine-derived renal cells are a self-renewing stem cell population unlike the kidney biopsy-derived hREPCs which are differentiated renal epithelial cells. To demonstrate that urine-derived renal progenitors can maintain self-renewal when cultured under undifferentiation conditions but yet retain the potential for epithelial differentiation and nephrogenesis, we induced active WNT signalling, by treatment with the GSK-3β inhibitor- CHIR99021. The differentiated cells adopted an elongated tubular morphology and reduced proliferation as also shown for human ESC and iPSC derived renal epithelial cells[71–73]. Although WNT pathway activation induced an epithelial phenotype, we did not see a dramatic increase in *CDH1* expression at the time point and dose used but rather activation of *CDH-3* expression (8.86 fold). *Cdh-3*, a gene encoding a member of the cadherin superfamily, functions in epithelial cell morphogenesis in *Caenorhabditis elegans*[74] an event which is poorly understood in human nephrogenesis. Furthermore, the correlation co-efficient (0.941) of the WNT-induced differentiated UM51 with hREPCs is further evidence in support of the cellular identify of the UM51 differentiated cells.

In line with our previously published observations in amniotic fluidic-derived renal cells, the down-regulated expression of *SIX2*, *WT1*, *CD133* and upregulated expression of *BMP7* induced the loss of self-renewal[56]. Global transcriptome analyses also revealed the down-regulation of 2043 genes some of which are associated with pathways such as cell cycle, FoxO, Hippo and ErbB signalling. The Hippo pathway which is composed of WNT target genes such as *LATS2, AXIN2* and *CTNNB1* have been reported to regulate epithelialization of nephron progenitors[75,76].

We detected differential expression 40 genes in which 20 most significantly up- and down-regulated between WNT-induced differentiated and self-renewing urine-derived renal progenitors. Amongst the genes up regulated in the CHIR99021 treated cells are the WNT targets- *AXIN2*, *JUN* and *NKD1* known to be associated with WNT signalling. Interestingly, a protein interaction network identified JUN as a major hub connected to GSK3β and interlinked with ATF2, STAT3, GATA2 and MAPK1. In a mouse model, it has been reported that Bmp7 phosphorylates Jun and Atf2 via Jnk signalling which promote the proliferation of mouse nephron progenitors[33]. This indeed might be contradictory to our observed elevated expression of *BMP7* upon WNT induced differentiation of urine-derived renal progenitor cells- i.e. suppression of *BMP7* expression is needed to maintain self-renewal in urine-derived renal progenitor cells. However, in line with our results, during *in vitro* differentiation (mesenchymal to epithelial transition) of human renal cell line TK173, BMP7 is required for the activation of E-Cadherin and WNT4 expression[77]. Since, SMADs are a target of MAPK particularly of JNK, both BMPs and TGFβ can activate the SMAD circuit[78,79]. Both activation of the WNT pathway and inhibition of FGF signalling led to the down-regulation of the key renal progenitor self-renewal associated transcription factor SIX2 and the up-regulated expression of BMP7. This is in line with the reported interactions of BMP and FGF signalling during nephrogenesis[80–82]. Fibroblast growth factor signaling is essential for *in vivo* renal development as well as *in vitro* cultivation and maintenance of nephron progenitor cells as demonstrated by mouse model experiments where blocking of FGF receptors led to aberrant nephrogenesis[25,81].

Based on the present study and our previously published data in human amniotic fluid-derived renal cells[56], we propose that similar to self-renewal in human pluripotent stem cells[60,83], urine-derived renal progenitor cells maintain self-renewal by active FGF signalling leading to phosphorylated TGFβ- SMAD2/3. In contrast,

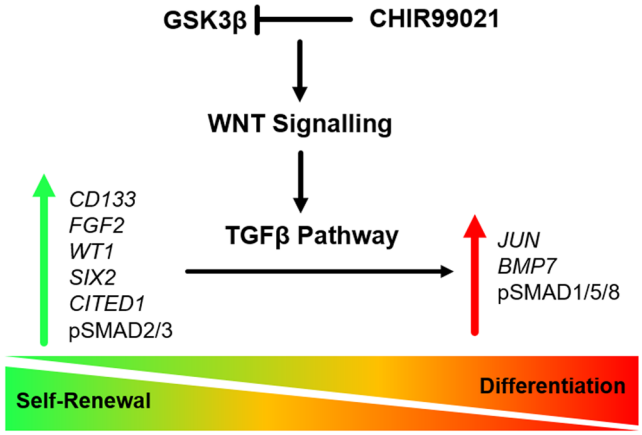

Figure 7. WNT/β-catenin and TGFβ pathway-mediated cell fate decisions in urine-derived renal progenitors. Self-renewal (inactive WNT/β-catenin signalling and active TGF-β/SMAD2/3 signalling) is maintained by elevated expression of the renal progenitor markers *SIX2*, *WT1*, *CITED1*, *CD133*, in addition to phospho-SMAD2/3 and FGF2 resulting in and down regulated expression of *BMP7*. In contrast, activation of WNT/β-catenin signalling induces upregulated expression of JUN and *BMP7* leading to activation of phospho-SMAD1/5/8, downregulated expression of *WT1, SIX2, CITED1, FGF2, CD133* and ultimately exit of self-renewal.

activation of WNT/β-catenin signalling leads to an upregulation of *JUN* and *BMP7* leading to activation of SMAD1/5/8 signalling and exit of self-renewal by downregulation of *WT1, SIX2*, *CITED1*, and *CD133* expression. To surmise, we derived a hypothetic scheme of the WNTβ catenin and TGFβ pathway-mediated cell fate decisions in urine-derived renal progenitor cells. This simplistic model is depicted in Fig. 7.

Comparing self-renewal of renal progenitor cells in both human (urine-derived renal progenitors) and mouse, it is clear that an intricate balance is needed between SIX2, WT1, CITED1 expression and Wnt/β-catenin activity in order to determine the cell fate of nephron progenitor cells[24,31,34,56]. Furthermore, it remains to be determined if indeed there exist subtle human and mouse differences in the gene regulatory network needed to maintain a self-renewing renal progenitor pool in both species and we believe that human urine-derived renal progenitor cells as described here will facilitate these studies.

Materials and methods

Ethics statement. In this study, urine samples were collected with the informed consent of the donors and the written approval (Ethical approval Number: 5704) of the ethical review board of the medical faculty of Heinrich Heine University, Düsseldorf, Germany. All methods were carried out in accordance with the approved guidelines. Medical faculty of Heinrich Heine University approved all experimental protocols.

Isolation, culture, and differentiation of urine-derived renal progenitor cells. Urine samples were collected from 10 healthy donors with diverse age, gender and ethnicity (Supplemental Table S1). Isolation and expansion of the urine-derived renal progenitors followed the previously established protocols[37,41]. For differentiation of the urine derived renal progenitors, 10 µM CHIR99021 was added to the cell culture medium for 2 days. Adult kidney biopsy derived primary human renal epithelial cells (hREPCs) (C-12665, Promo Cell, Germany) were used as control. To inhibit FGF signaling in urine derived renal progenitors, 15 µM SU5402 was added to the cell culture medium for 2 days.

Immunofluorescence staining. Immunofluorescence study was performed as described previously[84]. To analyse expression of specific markers, at 80% confluence, attached urine-derived renal progenitor cells of four individuals (Passages 4-5) were fixed with 4% PFA (Polysciences Inc., USA) for 15 min at room temperature (RT) and washed three times in PBS and permeability was increased using 1% Triton X-100 for 5 min. Next, for blocking we used: 10% normal goat serum (NGS; Sigma-Aldrich Chemie GmbH, Germany), 0.5% Triton X-100, 1% BSA (Sigma-Aldrich Chemie GmbH, Germany) and 0.05% Tween 20 (Sigma-Aldrich Chemie GmbH, Germany) in PBS for 2 h. The cells were incubated with primary antibodies (Supplemental Table S2) for 1 h at RT followed by three washes with PBS. Thereafter, the corresponding secondary Cy3-labeled, Alexa Fluor-555 or Alexa Fluor 488-labeled antibodies (Thermo Fisher Scientific, USA) and Hoechst 33,258 dye (Sigma-Aldrich Chemie GmbH, Germany) or DAPI (Southern Biotech, USA) were added. A fluorescence microscope (LSM700; Carl Zeiss Microscopy GmbH, Germany) was used for taking the pictures. All pictures were processed with the ZenBlue 2012 Software Version 1.1.2.0. (Carl Zeiss Microscopy GmbH, Germany).

CYP2D6 genotyping/phenotyping and Albumin endocytosis assay. CYP2D6 genotyping and phenotyping of five individuals (randomly selected) were carried out by CeGat GmbH Germany using genomic DNA. The CYP2D6 variant assay reveals the pharmacogenetics (PGx) profile of an individual's genotype and

phenotype based on tested pharmacogenetics markers. The assay identifies and discriminates individuals with poor, normal, intermediate and ultra-rapid metabolizing activity[85]. Albumin endocytosis assay was performed as described before[56]. For detailed description, see supplemental materials and methods.

Immunophenotyping by flow cytometry. At 90% confluence, adherent cells at passage 3–5 from UM27, UF31, UF45 and UM51 were detached from 6-well plates by incubation in TrypLE (Thermo Fisher Scientific, USA) at 37 °C. Then the cell samples were subjected to fluorescence-activated cell sorting (FACS) in order to specifically select for MSC cell surface markers, renal stem cell transcription factor $SIX2^+$ cells, and renal stem cell surface markers. Unstained cells and IgG isotype served as control for each cell sample. Dead cells and debris were gated on a two physical parameter dot plot followed by the exclusion of doublets by using pulse processing. Finally, the experimental cells positive subpopulation was gated. Sorting was done using CytoFLEX cell sorter (Beckman Coulter, USA), BD FACSCanto (BD Biosciences, Germany) and CyAn ADP (Beckman Coulter, USA). Histograms were generated using the Summit 4.3.02 software.

The analysis of MSC-associated cell surface marker expression of urine-derived renal progenitors was performed using MSC Phenotyping Kit (Miltenyi Biotec GmbH, Germany) according to the manufacturer's instructions and as described before[84]. For the pluripotency-associated markers, TRA-1-60, TRA-1-81, and SSEA4 dye-coupled antibodies were used (anti-TRA-1-60-PE, human (clone: REA157), number 130-100-347; anti-TRA-1-81-PE, human (clone: REA246), number 130-101-410, and anti-SSEA-4-PE, human (clone: REA101), number 130-098-369; Miltenyi Biotec GmbH, Germany). For $SIX2^+$ cell sorting, after blocking with Human TruStain blocking solution (Biolegend, USA) (5 µL each) for 10 min at RT, the cells (10^4 cells/condition) were stained with anti-m-SIX2 (Abnova, Taiwan) primary antibody overnight at 4 °C. After 3 times washing with the Permwash buffer (Invitrogen, Germany), mouse Alexa-Fluor 488 was conjugated by incubating 30 min at RT in the dark. For the renal stem cell surface markers anti-CD24-FITC (Sigma-Aldrich Chemie GmbH, Germany), VCAM-1/CD106-PE (R&D systems, USA) and CD133-APC (R&D systems, USA) were used according to manufacturer instructions for flow cytometry analysis. Briefly, after blocking and washing, cells were centrifuged at 300 x g for 10 min. 5 µl of antibody solution (1:50 dilution) were added to the cell suspension and the samples were incubated in the dark at 4 °C for 10 min. Cells were washed afterwards, and stored in 4% PFA at 4 °C until analysis.

Differentiation into adipocytes, chondrocytes and osteoblasts. Differentiation of urine-derived renal progenitors into adipocytes, chondrocytes and osteoblasts were tested using the StemPro Adipogenesis, Chondrogenesis, and Osteogenesis differentiation Kits (Gibco, Life Technologies, USA) as described before[56,84]. After the differentiation periods, cells were fixed using 4% PFA for 20 min at RT and stained with Oil Red-O for detecting adipocytes, Alcian Blue for chondrocytes, and Alizarin Red S for osteoblasts. A light microscope was used for imaging.

Western blot analysis. For protein extraction, cells were harvested and lysed in RIPA buffer (Sigma-Aldrich Chemie GmbH, Germany) supplemented with complete protease and phosphatase inhibitors cocktail (Roche, Switzerland). The lysates were separated on a 4–20% Bis-Tris gel and blotted onto a 0.45 µm nitrocellulose membrane (GE Healthcare Life Sciences, Germany). The membranes were then blocked with 5% skimmed milk in Tris-Buffered Saline Tween (TBS-T) and incubated overnight with the respective primary antibodies: Total Smad 1 (1:1000, TBS-T 5% BSA; CST, USA), phospho Smad 1/5/8 (1:1000, TBS-T 5% milk; CST, USA), Total Smad 2/3 (CST, 1:1000, TBS-T 5% BSA), and phospho Smad 2/3 (1:1000, TBS-T 5% milk; CST, USA). After incubation with the appropriate secondary antibodies, signals were acquired with a Fusion-FX7 imaging system.

Bisulfite genomic sequencing. Bisulfite sequencing was performed following bisulfite conversion with the EpiTec Kit (Qiagen, Germany). Primers were designed after excluding pseudogenes or other closely related genomic sequences which could interfere with specific amplification by amplicon and primer sequences comparison in BLAT sequence database (https://genome.ucsc.edu/FAQ/FAQblat.html). See supplemental materials and methods for full description.

Generation of iPSCs from urine-derived renal progenitors. Four urine-derived renal progenitor cell samples were reprogrammed into iPSCs (four lines) using an integration-free episomal based transfection system without pathway inhibition. Briefly, urine-derived renal progenitor cells were nucleofected with two plasmids pEP4 E02S ET2K (Addgene plasmid #20927) and pEP4 E02S CK2M EN2L (Addgene plasmid #20924) expressing a combination of pluripotency factors including OCT4, SOX2, LIN28, c-MYC, KLF4, and NANOG using the Amaxa 4D-Nucleofector Kit (Lonza, Swiss) according to the manufacturer's guidelines and as described previously[41]. Please see supplemental materials and methods for full description.

Quantitative RT-PCR analysis. RNA was isolated using the Direct-zol RNA MiniPrep Kit (Zymo Research, USA) according to provider guidelines. After checking the quality of mRNA, 500 ng of RNA were used for complementary DNA synthesized with the TaqMan Reverse Transcription Kit (Applied Biosystems, USA). Real-time quantitative PCR was performed in technical triplicates with Power SYBR Green Master Mix (Life Technologies, USA), 12.5 ng cDNA per sample and 0.6 µM primers on a VIIA7 (Life Technologies, USA) machine. Mean values were normalized to levels of the housekeeping gene ribosomal protein L37A calculated by the $2-\Delta\Delta Ct$ method. Primers used were purchased from MWG (Supplementary Table S3).

Microarray data analyses. Total RNA (1 µg) preparations were hybridized on the PrimeView Human Gene Expression Array (Affymetrix, Thermo Fisher Scientific, USA) at the core facility Biomedizinisches Forschungszentrum (BMFZ) of the Heinrich Heine University Düsseldorf. The raw data was imported into the

R/Bioconductor environment[86] and further processed with the package affy[87] using background-correction, logarithmic (base 2) transformation and normalization with the Robust Multi-array Average (RMA) method. For full details, please see supplemental materials and methods.

KEGG pathway, GO and network analysis. Gene ontology (GOs) terms were analysed within the Bioconductor environment employing the package GOstats[88]. GOs of category Biological Process (BP) were further summarized with the REVIGO tool[89] to generate treemaps populating the parameter for allowed similarity with tiny = 0.4. GO networks were generated from the REVIGO tool in xgmml format and imported into Cytoscape[90]. For full details, see supplemental materials and methods.

Activated WNT pathway associated protein interaction network. The network was constructed from the 20 most significantly up- and down down-regulated genes between CHIR99021 treatment and untreated controls. Genes were ranked by the limma-p-value and passed the criteria: detection p-value < 0.05 for the dedicated condition, ratio < 0.75 or ratio > 1.33, limma-p-value < 0.05. The resulting 40 genes were marked as green nodes in the network. Interacting proteins containing at least one protein coded by the 40 genes were retrieved from BioGrid version 3.4.161[91]. The plot of the interactions network was drawn employing the R package network[92]. See supplemental materials and methods for full description.

Additional materials and methods. For the materials and methods of the culture supernatant analysis, analysis of cell proliferation, meta-analysis for comparison of urine-derived renal progenitors to public nephron progenitor data sets and cell lines used in this study and culture conditions, please see supplemental materials and methods.

Statistics. All data are presented as arithmetic means ± standard error of mean. At least 3 independent experiments were used for the calculation of mean values. P values of < 0.05 were considered significant.

Data availability

All raw and processed data used in this study have been archived in NCBI gene expression omnibus under GEO accession number GSE128281. (https://www.ncbi.nlm.nih.gov/geo/query/acc.cgi?acc=GSE128281).

Received: 24 June 2019; Accepted: 31 December 2019;
Published online: 20 January 2020

References

1. https://ncdalliance.org/the-international-society-of-nephrology-isn (accessed: 23th October, 2019)
2. Rota, C., Morigi, M. & Imberti, B. Stem Cell Therapies in Kidney Diseases: Progress and Challenges. *Int. J. Mol. Sci.* **20**, 2790 (2019).
3. Marcheque, J., Bussolati, B., Csete, M. & Perin, L. Concise Reviews: Stem Cells and Kidney Regeneration: An Update. *Stem Cell Transl. Med.* **8**, 82–92 (2019).
4. Huling, J. & Yoo, J. J. Comparing adult renal stem cell identification, characterization and applications. *Journal of Biomedical Science*. **24**, Article number: 32 (2017).
5. Lazzeri, E. *et al*. Regenerative potential of embryonic renal multipotent progenitors in acute renal failure. *J. Am. Soc. Nephrol.* **18**, 3128–38 (2007).
6. Sagrinati, C. *et al*. Isolation and characterization of multipotent progenitor cells from the Bowman's capsule of adult human kidneys. *J. Am. Soc. Nephrol.* **17**, 2443–56 (2006).
7. Angelotti, M. L. *et al*. Characterization of Renal Progenitors Committed Toward Tubular Lineage and Their Regenerative Potential in Renal Tubular Injury. *Stem Cells.* **30**, 1714–1725 (2012).
8. Chen, C. Y. *et al*. Extracellular vesicles from human urine-derived stem cells prevent osteoporosis by transferring CTHRC1 and OPG. *Bone Res.* **7**, 18 (2019).
9. Choi, J. Y. *et al*. Potency of Human Urine-Derived Stem Cells for Renal Lineage Differentiation. *Tissue Eng. Regen. Med.* **14**, 775–785 (2017).
10. Ingelfinger, J. R. Nephrogenic adenomas as renal tubular outposts. *N. Engl. J. Med.* **29**, 684–686 (2002).
11. Zhang, D. *et al*. Urine-derived stem cells: A novel and versatile progenitor source for cell-based therapy and regenerative medicine. *Genes. Dis.* **1**, 8–17 (2014).
12. Ringsrud, K. M. Casts in the Urine Sediment. *Laboratory Med.* **32**, 191–193 (2001).
13. Da Sacco, S. *et al*. Direct Isolation and Characterization of Human Nephron Progenitors. *Stem Cell Transl. Med.* **6**, 419–433 (2017).
14. Harari-Steinberg, O. *et al*. Identification of human nephron progenitors capable of generation of kidney structures and functional repair of chronic renal disease. *EMBO Mol. Med.* **5**, 1556–1568 (2013).
15. Kreidberg, J. A. WT1 and kidney progenitor cells. *Organogenesis* **6**, 61–70 (2010).
16. Lazzeri, E. *et al*. Human Urine-Derived Renal Progenitors for Personalized Modeling of Genetic Kidney Disorders. *J. Am. Soc. Nephrol.* **26**, 1961–1974 (2015).
17. Manaph, N. P. A., Al-Hawwas, M., Bobrovskaya, L., Coates, P. T. & Zhou, X. F. Urine-derived cells for human cell therapy. *Stem Cell Res. Ther.* **9**, 189 (2018).
18. Bharadwaj, S. *et al*. Multipotential differentiation of human urine-derived stem cells: Potential for therapeutic applications in urology. *Stem Cell* **31**, 1840–1856 (2013).
19. O'Brien, L. L. *et al*. Transcriptional regulatory control of mammalian nephron progenitors revealed by multi-factor cistromic analysis and genetic studies. *PLoS Genet.* **14**, e1007181 (2018).
20. Ramalingam, H. *et al*. Disparate levels of beta-catenin activity determine nephron progenitor cell fate. *Dev. Biol.* **440**, 13–21 (2018).
21. Xu, J., Liu, H., Park, J. S., Lan, Y. & Jiang, R. Osr1 acts downstream of and interacts synergistically with Six2 to maintain nephron progenitor cells during kidney organogenesis. *Development* **141**, 1442–1452 (2014).
22. Kann, M. *et al*. WT1 targets Gas1 to maintain nephron progenitor cells by modulating FGF signals. *Development.* **142**, 1254–1266 (2015).
23. Motamedi, F. J. *et al*. WT1 controls antagonistic FGF and BMP-pSMAD pathways in early renal progenitors. *Nat. Commun.* **5**, 01–14 (2014).
24. Park, J. S. *et al*. Six2 and Wnt regulate self-renewal and commitment of nephron progenitors through shared gene regulatory networks. *Dev. Cell* **23**, 637–651 (2012).

25. Mari, C. & Winyard, P. Concise Review: Understanding the Renal Progenitor Cell Niche *In Vivo* to Recapitulate Nephrogenesis *In Vitro*. *Stem Cell Trans. Med.* **4**, 1463–1471 (2015).
26. Lawlor, K. T. *et al*. Nephron progenitor commitment is a stochastic process influenced by cell migration. *Elife.* **8pii**, e41156 (2019).
27. Murphy, A. J. *et al*. SIX2 and CITED1, markers of nephronic progenitor self-renewal, remain active in primitive elements of Wilms' tumor. *J. Pediatr. Surg.* **47**, 1239–1249 (2012).
28. Kobayashi, A. *et al*. Identification of a multipotent self-renewing stromal progenitor population during mammalian kidney organogenesis. *Stem Cell Reports.* **3**, 650–662 (2014).
29. Little, M. H. & Kairath, P. Does Renal Repair Recapitulate Kidney Development? *J. Am. Soc. Nephrol.* **28**, 34–46 (2017).
30. James, R. G., Kamei, C. N., Wang, Q., Jiang, R. & Schultheiss, T. M. Odd-skipped related 1 is required for development of the metanephric kidney and regulates formation and differentiation of kidney precursor cells. *Development.* **133**, 2995–3004 (2006).
31. Kobayashi, A. *et al*. Six2 defines and regulates a multipotent self-renewing nephron progenitor population throughout mammalian kidney development. *Cell Stem Cell.* **3**, 169–181 (2008).
32. Self, M. *et al*. Six2 is required for suppression of nephrogenesis and progenitor renewal in the developing kidney. *EMBO J.* **25**, 5214–5228 (2006).
33. Blank, U. *et al*. BMP7 promotes proliferation of nephron progenitor cells via a JNK-dependent mechanism. *Development.* **136**, 3557–3566 (2009).
34. Lindström, N. O. *et al*. Conserved and Divergent Features of Human and Mouse Kidney Organogenesis. *J. Am. Soc. Nephrol.* **3**, 785–805 (2018a).
35. Lindström, N. O. *et al*. Progressive Recruitment of Mes.enchymal Progenitors Reveals a Time-Dependent Process of Cell Fate Acquisition in Mouse and Human Nephrogenesis. *Dev. Cell.* **45**, 651–660 (2018b).
36. Thiagarajan, R. D. *et al*. Identification of anchor genes during kidney development defines ontological relationships, molecular sub-compartments and regulatory pathways. *PLoS One.* **6**, e17286 (2011).
37. Zhou, T. *et al*. Generation of induced pluripotent stem cells from urine. *J. Am. Soc. Nephrol.* **22**, 1221–1228 (2011).
38. Zhou, T. *et al*. Generation of human induced pluripotent stem cells from urine samples. *Nat. Protoc.* **7**, 2080–2089 (2012).
39. Uhm, K. O. *et al*. Generation of human induced pluripotent stem cells from urinary cells of a healthy donor using a non-integration system. *Stem Cell Res.* **21**, 44–46 (2017).
40. Sauer, V. *et al*. Human Urinary Epithelial Cells as a Source of Engraftable Hepatocyte-Like Cells Using Stem Cell Technology. *Cell Transplant.* **25**, 2221–2243 (2016).
41. Bohndorf, M. *et al*. Derivation and characterization of integration-free iPSC line ISRM-UM51 derived from SIX2-positive renal cells isolated from urine of an African male expressing the CYP2D6 *4/*17 variant which confers intermediate drug metabolizing activity. *Stem Cell Res.* **25**, 18–21 (2017).
42. Little, M. H., Combes, A. N. & Takasato, M. Understanding kidney morphogenesis to guide renal tissue regeneration. *Nat. Rev. Nephrol.* **12**, 624–635 (2016).
43. Chuah, J. K. C. & Zink, D. Stem cell-derived kidney cells and organoids: Recent breakthroughs and emerging applications. *Biotechnol. Adv.* **35**, 150–167 (2017).
44. van den Berg, C. W. *et al*. Renal Subcapsular Transplantation of PSC-Derived Kidney Organoids Induces Neo-vasculogenesis and Significant Glomerular and Tubular Maturation *In Vivo*. *Stem Cell Reports.* **10**, 751–765 (2018).
45. Rauch, C. *et al*. Differentiation of human iPSCs into functional podocytes. *PLoS One.* **13**, e0203869 (2018).
46. Tanigawa, S., Taguchi, A., Sharma, N., Perantoni, A. O. & Nishinakamura, R. Selective *In Vitro* Propagation of Nephron Progenitors Derived from Embryos and Pluripotent Stem Cells. *Cell Rep.* **15**, 801–813 (2016).
47. Morizane, R. *et al*. Nephron organoids derived from human pluripotent stem cells model kidney development and injury. *Nat. Biotechnol.* **33**, 1193–1200 (2015).
48. Morizane, R. & Bonventre, J. V. Generation of nephron progenitor cells and kidney organoids from human pluripotent stem cells. *Nat. Protoc.* **12**, 195–207 (2017).
49. Hariharan, K. *et al*. Parallel generation of easily selectable multiple nephronal cell types from human pluripotent stem cells. *Cell Mol. Life. Sci.* **76**, 179–192 (2019).
50. Phipson, B. *et al*. Evaluation of variability in human kidney organoids. *Nat. Methods* **16**, 79–87 (2019).
51. Wu, H. *et al*. Comparative Analysis and Refinement of Human PSC-Derived Kidney Organoid Differentiation with Single-Cell Transcriptomics. *Cell Stem Cell.* **23**, 869–881 (2018).
52. Lindgren, D. *et al*. Isolation and characterization of progenitor-like cells from human renal proximal tubules. *Am. J. Pathol.* **178**(2), 828–37 (2011).
53. Da Sacco, S. *et al*. Direct Isolation and Characterization of Human Nephron Progenitors. *Stem Cell Transl. Med.* **6**(2), 419–433 (2017).
54. https://www.ncbi.nlm.nih.gov/geo/query/acc.cgi?acc=GSE75949, (accessed on 23th October 2019)
55. Mulder, J. *et al*. Generation of infant- and pediatric-derived urinary induced pluripotent stem cells competent to form kidney organoids. *Pediatr Res*. (2019).
56. Rahman, M. S. *et al*. The presence of human mesenchymal stem cells of renal origin in amniotic fluid increases with gestational time. *Stem Cell Res. Ther.* **9**, 113 (2018).
57. Arcolino, F. O. *et al*. Urine of Preterm Neonates as a Novel Source of Kidney Progenitor Cells. *J. Am. Soc. Nephrol.* **27**, 2762–2770 (2016).
58. Romagnani, P. *et al*. Next generation sequencing and functional analysis of patient urine renal progenitor-derived podocytes to unravel the diagnosis underlying refractory lupus nephritis. *Nephrol. Dial. Transplant.* **31**, 1541–1545 (2016).
59. Babaie, Y. *et al*. Analysis of Oct4-dependent transcriptional networks regulating self-renewal and pluripotency in human embryonic stem cells. *Stem Cells.* **25**, 500–510 (2007).
60. Greber, B., Lehrach, H. & Adjaye, J. Silencing of core transcription factors in human EC cells highlights the importance of autocrine FGF signaling for self-renewal. *BMC Dev. Biol.* **7**, 46 (2007a).
61. Dominici, M. *et al*. Minimal criteria for defining multipotent mesenchymal stromal cells. The International Society for Cellular Therapy position statement. *Cytotherapy.* **8**, 315–317 (2006).
62. Zhang, D., Wei, G., Li, P., Zhou, X. & Zhang, Y. Urine-derived stem cells: A novel and versatile progenitor source for cell-based therapy and regenerative medicine. *Genes. Dis.* **1**, 08–17 (2014).
63. Combes, A. N. *et al*. Haploinsufficiency for the Six2 gene increases nephron progenitor proliferation promoting branching and nephron number. *Kidney Int.* **93**, 589–598 (2018).
64. Shi, G. *et al*. The Transcriptional Activity of CITED1 Is Regulated by Phosphorylation in a Cell Cycle-dependent Manner. *J. Biol. Chem.* **281**, 27426 (2006).
65. Vajjhala, P.R. *et al*. The Wilms' tumour suppressor protein, WT1, undergoes CRM1-independent nucleocytoplasmic shuttling. *FEBS Letters*. **554** (2003).
66. Depping, R. *et al*. Nuclear Transport of Wilms' Tumour Protein Wt1 Involves Importins α and β. *Cell Physiol. Biochem.* **29**, 223–232 (2012).
67. Shrestha, S. *et al*. Human renal tubular cells contain CD24/CD133 progenitor cell populations: Implications for tubular regeneration after toxicant induced damage using cadmium as a model. *Toxicol. Appl. Pharmacol.* **331**, 116–129 (2017).
68. Tojo, A. & Kinugasa, S. Mechanisms of glomerular albumin filtration and tubular reabsorption. *Int. J. Nephrol.* **2012**, 481–520 (2012).
69. Birn, H. & Christensen, E. I. Renal albumin absorption in physiology and pathology. *Kidney Int.* **69**, 440–9 (2006).
70. Kim, K. *et al*. Epigenetic memory in induced pluripotent stem cells. *Nature.* **467**, 285–290 (2010).

71. Takasato, M. *et al*. Directing human embryonic stem cell differentiation towards a renal lineage generates a self-organizing kidney. *Nat. Cell Biol.* **16**, 118–126 (2014).
72. Takasato, M. *et al*. Kidney organoids from human iPS cells contain multiple lineages and model human nephrogenesis. *Nature.* **526**, 564–568 (2015).
73. Brown, A. C., Muthukrishnan, S. D. & Oxburgh, L. A synthetic niche for nephron progenitor cells. *Dev. Cell.* **34**, 229–241 (2015).
74. Pettitt, J., Wood, W. B. & Plasterk, R. H. cdh-3, a gene encoding a member of the cadherin superfamily, functions in epithelial cell morphogenesis in Caenorhabditis elegans. *Development.* **122**, 4149–4157 (1996).
75. Reginensi, A. *et al*. A critical role for NF2 and the Hippo pathway in branching morphogenesis. *Nat. Commun.* **7**, 12309 (2016).
76. McNeill, H. & Reginensi, A. Lats1/2 Regulate Yap/Taz to Control Nephron Progenitor Epithelialization and Inhibit Myofibroblast Formation. *J. Am. Soc. Nephrol.* **28**, 852–861 (2017).
77. Zeisberg, M., Shah, A. A. & Kalluri, R. Bone morphogenic protein-7 induces mesenchymal to epithelial transition in adult renal fibroblasts and facilitates regeneration of injured kidney. *J. Biol. Chem.* **280**, 8094–100 (2005).
78. Derynck, R. & Zhang, Y. E. Smad-dependent and Smad-independent pathways in TGF-beta family signalling. *Nature* **425**, 577–584 (2003).
79. Yamaguchi, K. *et al*. Identification of a member of the MAPKKK family as a potential mediator of TGF-beta signal transduction. *Science.* **270**, 2008–2011 (1995).
80. Brown, A. C. *et al*. FGF/EGF signaling regulates the renewal of early nephron progenitors during embryonic development. *Development.* **138**, 5099–112 (2011).
81. Godin, R. E., Robertson, E. J. & Dudley, A. T. Role of BMP family members during kidney development. *Int. J. Dev. Biol.* **43**, 405–411 (1999).
82. Dudley, A. T., Godin, R. E. & Robertson, E. J. Interaction between FGF and BMP signaling pathways regulates development of metanephric mesenchyme. *Genes. Dev.* **13**, 1601–1613 (1999).
83. Greber, B., Lehrach, H. & Adjaye, J. Fibroblast growth factor 2 modulates transforming growth factor beta signaling in mouse embryonic fibroblasts and human ESCs (hESCs) to support hESC self-renewal. *Stem Cells.* **25**, 455–464 (2007b).
84. Spitzhorn, L. S. *et al*. Isolation and Molecular Characterization of Amniotic Fluid-Derived Mesenchymal Stem Cells Obtained from Caesarean Sections. *Stem Cell Int.* **2017**, 5932706 (2017).
85. Pinto, N. & Dolan, M. E. Clinically relevant genetic variations in drug metabolizing enzymes. *Curr. Drug. Metab.* **12**, 487–97 (2011).
86. Gentleman, R. C. *et al*. Bioconductor: open software development for computational biology and bioinformatics. *Genome Biol.* **5**, R80 (2004).
87. Gautier, L., Cope, L., Bolstad, B. M. & Irizarry, R. A. affy–analysis of Affymetrix GeneChip data at the probe level. *Bioinformatics.* **20**, 307–315 (2004).
88. Falcon, S. & Gentleman, R. Using GOstats to test gene lists for GO term association. *Bioinforma. Oxf. Engl.* **23**, 257–258 (2007).
89. Supek, F., Bošnjak, M., Škunca, N. & Šmuc, T. REVIGO Summarizes and Visualizes Long Lists of Gene Ontology Terms. *PLoS ONE.* **6**, e21800 (2011).
90. Shannon, P. *et al*. Cytoscape: A Software Environment for Integrated Models of Biomolecular Interaction Networks. *Genome Research.* **13**, 2498–2504 (2003).
91. Chatr-Aryamontri, A. *et al*. The BioGRID interaction database: 2017 update. *Nucleic Acids Res.* **45**, D369–D379 (2017).
92. Butts, C. network: A Package for Managing Relational Data in R. *J. Stat. Software.* **24**, 01–36 (2008).

Acknowledgements

James Adjaye acknowledges support from the medical faculty of the Heinrich Heine University- Düsseldorf, Germany. In addition, James Adjaye and Md Shaifur Rahman acknowledges support from the German Academic Exchange Service (DAAD-91607303). We acknowledge Dipl. Ing Katharina Raba, Institute of Transplantation Diagnostics and Cell Therapeutics, Heinrich Heine University, Germany for her kind assistance with the FACS analyses.

Author contributions

:Conception: J.A.; Cell culture experiments: M.S.R., L.S.S., F.A., M.B. and J.A.; Real Time PCR: F.A., L.E.; Bisulphite sequencing: L.E.; Bioinformatics: W.W. and J.A.; Proliferation assays and Western blot analyses: S.M.; Derivation and characterisation of iPSCs: M.B., N.G. and A.N.; Immunostaining and FACS analysis: M.B., L.S.S., A.N., M.S.R., L.N.; Writing of manuscript: M.S.R., W.W., L.S.S., L.N. and J.A.; Final edits: J.A. All authors approved the final version of the manuscript.

Competing interests

The authors declare no competing interests.

Additional information

Supplementary information is available for this paper at https://doi.org/10.1038/s41598-020-57723-2.

Correspondence and requests for materials should be addressed to J.A.

Reprints and permissions information is available at www.nature.com/reprints.

Publisher's note Springer Nature remains neutral with regard to jurisdictional claims in published maps and institutional affiliations.

Part C: Applications of Multipotent Stem Cells *in vitro* and *in vivo*

3.5 Human iPSC-derived MSCs (iMSCs) from Aged Individuals Acquire a Rejuvenation Signature

Lucas-Sebastian Spitzhorn, Matthias Megges, Wasco Wruck, Md Shaifur Rahman, Jörg Otte, Özer Degistirici, Roland Meisel, Rüdiger Volker Sorg, Richard O. C. Oreffo and James Adjaye

Abstract

Background: Primary mesenchymal stem cells (MSCs) are fraught with aging-related shortfalls. Human-induced pluripotent stem cell (iPSC)-derived MSCs (iMSCs) have been shown to be a useful clinically relevant source of MSCs that circumvent these aging-associated drawbacks. To date, the extent of the retention of aging-hallmarks in iMSCs differentiated from iPSCs derived from elderly donors remains unclear.

Methods: Fetal femur-derived MSCs (fMSCs) and adult bone marrow MSCs (aMSCs) were isolated, corresponding iPSCs were generated, and iMSCs were differentiated from fMSC-iPSCs, from aMSC-iPSCs, and from human embryonic stem cells (ESCs) H1. In addition, typical MSC characterization such as cell surface marker expression, differentiation capacity, secretome profile, and trancriptome analysis were conducted for the three distinct iMSC preparations - fMSC-iMSCs, aMSC-iMSCs, and ESC-iMSCs. To verify these results, previously published data sets were used, and also, additional aMSCs and iMSCs were analyzed.

Results: fMSCs and aMSCs both express the typical MSC cell surface markers and can be differentiated into osteogenic, adipogenic, and chondrogenic lineages in vitro. However, the transcriptome analysis revealed overlapping and distinct gene expression patterns and showed that fMSCs express more genes in common with ESCs than with aMSCs. fMSC-iMSCs, aMSC-iMSCs, and ESC-iMSCs met the criteria set out for MSCs. Dendrogram analyses confirmed that the transcriptomes of all iMSCs clustered together with the parental MSCs and separated from the MSC-iPSCs and ESCs. iMSCs irrespective of donor age and cell type acquired a rejuvenation-associated gene signature, specifically, the expression of *INHBE, DNMT3B, POU5F1P1, CDKN1C*, and *GCNT2* which are also expressed in pluripotent stem cells (iPSCs and ESC) but not in the parental aMSCs. iMSCs expressed more genes in common with fMSCs than with aMSCs. Independent real-time PCR comparing aMSCs, fMSCs, and iMSCs confirmed the differential expression of the rejuvenation (*COX7A, EZA2*, and *TMEM119*) and aging (*CXADR* and *IGSF3*)

signatures. Importantly, in terms of regenerative medicine, iMSCs acquired a secretome (e.g., angiogenin, DKK-1, IL-8, PDGF-AA, osteopontin, SERPINE1, and VEGF) similar to that of fMSCs and aMSCs, thus highlighting their ability to act via paracrine signaling.
Conclusions: iMSCs irrespective of donor age and cell source acquire a rejuvenation gene signature. The iMSC concept could allow circumventing the drawbacks associated with the use of adult MSCs und thus provide a promising tool for use in various clinical settings in the future.

Publication Status: Published in Stem Cell Res Ther. 2019 Mar 18;10(1):100.
Impact Factor: 4.62

Approximated total share of contribution: 15%

Author contributions on experimental design, realization and publication: JA, RO, MM, and LSS conceived the idea and designed the experiments. MM and LSS performed the characterization of primary MSCs and generation/characterization of iPSCs/iMSCs. MM, LSS, and MSR analyzed the results and wrote the draft manuscript. OD and RM provided RNA from MSCs of an aged individual (56 years), and JO performed the real-time PCR analysis. WW did the bioinformatical analysis. RVS provided aged MSCs for the cytokine array. JA edited and finally approved the manuscript. All authors reviewed and approved the submitted version.

Pubmed link: https://www.ncbi.nlm.nih.gov/pubmed/30885246
Journal link: https://stemcellres.biomedcentral.com/articles/10.1186/s13287-019-1209-x

Spitzhorn et al. Stem Cell Research & Therapy (2019) 10:100
https://doi.org/10.1186/s13287-019-1209-x

Stem Cell Research & Therapy

RESEARCH Open Access

Human iPSC-derived MSCs (iMSCs) from aged individuals acquire a rejuvenation signature

Lucas-Sebastian Spitzhorn[1†], Matthias Megges[1†], Wasco Wruck[1], Md Shaifur Rahman[1], Jörg Otte[1], Özer Degistirici[2], Roland Meisel[2], Rüdiger Volker Sorg[3], Richard O. C. Oreffo[4] and James Adjaye[1*]

Abstract

Background: Primary mesenchymal stem cells (MSCs) are fraught with aging-related shortfalls. Human-induced pluripotent stem cell (iPSC)-derived MSCs (iMSCs) have been shown to be a useful clinically relevant source of MSCs that circumvent these aging-associated drawbacks. To date, the extent of the retention of aging-hallmarks in iMSCs differentiated from iPSCs derived from elderly donors remains unclear.

Methods: Fetal femur-derived MSCs (fMSCs) and adult bone marrow MSCs (aMSCs) were isolated, corresponding iPSCs were generated, and iMSCs were differentiated from fMSC-iPSCs, from aMSC-iPSCs, and from human embryonic stem cells (ESCs) H1. In addition, typical MSC characterization such as cell surface marker expression, differentiation capacity, secretome profile, and trancriptome analysis were conducted for the three distinct iMSC preparations—fMSC-iMSCs, aMSC-iMSCs, and ESC-iMSCs. To verify these results, previously published data sets were used, and also, additional aMSCs and iMSCs were analyzed.

Results: fMSCs and aMSCs both express the typical MSC cell surface markers and can be differentiated into osteogenic, adipogenic, and chondrogenic lineages in vitro. However, the transcriptome analysis revealed overlapping and distinct gene expression patterns and showed that fMSCs express more genes in common with ESCs than with aMSCs. fMSC-iMSCs, aMSC-iMSCs, and ESC-iMSCs met the criteria set out for MSCs. Dendrogram analyses confirmed that the transcriptomes of all iMSCs clustered together with the parental MSCs and separated from the MSC-iPSCs and ESCs. iMSCs irrespective of donor age and cell type acquired a rejuvenation-associated gene signature, specifically, the expression of *INHBE*, *DNMT3B*, *POU5F1P1*, *CDKN1C*, and *GCNT2* which are also expressed in pluripotent stem cells (iPSCs and ESC) but not in the parental aMSCs. iMSCs expressed more genes in common with fMSCs than with aMSCs. Independent real-time PCR comparing aMSCs, fMSCs, and iMSCs confirmed the differential expression of the rejuvenation (*COX7A*, *EZA2*, and *TMEM119*) and aging (*CXADR* and *IGSF3*) signatures. Importantly, in terms of regenerative medicine, iMSCs acquired a secretome (e.g., angiogenin, DKK-1, IL-8, PDGF-AA, osteopontin, SERPINE1, and VEGF) similar to that of fMSCs and aMSCs, thus highlighting their ability to act via paracrine signaling.

Conclusions: iMSCs irrespective of donor age and cell source acquire a rejuvenation gene signature. The iMSC concept could allow circumventing the drawbacks associated with the use of adult MSCs und thus provide a promising tool for use in various clinical settings in the future.

Keywords: Aged MSC, Fetal MSCs, iPSCs, iMSCs, Transcriptome, Secretome, Rejuvenation, Aging

* Correspondence: james.adjaye@med.uni-duesseldorf.de
†Lucas-Sebastian Spitzhorn and Matthias Megges contributed equally to this work.
[1]Institute for Stem Cell Research and Regenerative Medicine, Medical Faculty, Heinrich Heine University, Düsseldorf, Moorenstr. 5, 40225 Düsseldorf, Germany
Full list of author information is available at the end of the article

Background

Primary human bone marrow-derived stem cells (MSCs) contain a sub-population of multipotent stem cells which retain osteogenic, chondrogenic, and adipogenic differentiation potential [1, 2]. Apart from the adult sources, these multipotent MSCs have been isolated from fetal femur [3]. Due to highly proliferative, immune-modulatory properties, and paracrine orchestration, MSCs offer significant therapeutic potential for an increasing aging demographic [4].

Although the bone marrow can be collected routinely to isolate MSCs, there are several drawbacks associated with the use of MSCs from aged individuals. Aging involves enhanced cellular senescence, instability of the genome, accumulation of DNA damage, changes in DNA repair pathways, oxidative stress, metabolic instability, and activated immune response [5–8]. In line with this, the expansion possibilities and application potential of primary MSCs are limited, in part, by changes in the differentiation/response potential and function of MSCs isolated from aged donors [9–11]. However, to date, it remains unclear whether there are any age-related differences in transcriptome and secretome signatures between human fetal MSCs and MSCs from elderly donors.

Recent studies have shown that the shortfalls associated with primary MSCs can be circumvented by reprogramming them to induced pluripotent stem cells (iPSCs) [12–14]. iPSCs have the potential to self-renew, bypass senescence and are similar to human embryonic stem cells (ESCs). However, the parental somatic aging signature and secretome properties and subsequent reflection in iPSC derivatives are unknown [15–17]. An iPSC-derived cell type that is of prime interest for circumventing shortfalls associated with primary MSCs are MSCs differentiated from iPSCs and ESCs (iMSCs). The similarity of iMSCs to primary MSCs and their regenerative potential in vivo has already been demonstrated [18, 19]. Moreover, the reflection of donor age in iMSCs was shown to be reverted into a younger state and at the same time reflected in iMSCs from patients with early onset aging syndromes [13, 20]. Although the paracrine effects of iMSCs have been indicated [21], relatively little is known about the potential to rejuvenate the paracrine features of MSCs from elderly patients via iMSC generation.

In view of this, there is a dire need to clarify in more detail whether age-related features inherent to primary MSCs isolated from elderly patients are retained in the corresponding iMSCs at the transcriptional, secretome, and functional level. In this study, we report the age-associated differences between fetal MSC (fMSC) populations and MSCs isolated from elderly donors with respect to their transcriptomes. We successfully reprogrammed fMSCs (55 days post conception) and adult MSC (aMSC; 60–74 years) to iPSCs and, subsequently, generated the corresponding iMSCs. In addition, iMSCs were also derived from ESCs. The iMSCs were similar although not identical to primary MSCs. We unraveled a putative rejuvenation and aging gene expression signature. We show that iMSCs irrespective of donor age and cell type re-acquired a similar secretome to that of their parental MSCs, thus re-enforcing their capabilities of context-dependent paracrine signaling relevant for tissue regeneration.

Methods

MSC preparations used in this study

Fetal femur-derived MSCs were obtained at 55 days post-conception as previously described [3] following informed, written patient consent. Approval was obtained by the Southampton and South West Hampshire Local Research Ethics Committee (LREC 296100). Mesenchymal stem cells, used for generation of iPSCs and iMSCs, were isolated from the bone marrow of a 74-year-old female donor as described before [22] after written informed consent. The corresponding protocol was approved by the research ethics board of the Charite-Universitätsmedizin, Berlin (IRB approval EA2/126/07). Aged MSCs (60 years, 62 years, and 70 years) were isolated as previously described [23]. Isolation of mesenchymal stem cells from 60 to 70-year-old individuals was approved under the Southampton and South West Hampshire Local Research Ethics Committee (LREC 194/99). Three primary fetal MSC preparations, fMSC1, fMSC2, and fMSC3, derived from different donors, were compared to MSCs isolated from elderly donors between 60 and 74 years of age; aMSC1, aMSC2, aMSC3, and aMSC4 (Additional file 1: Table S1). For meta-analyses, we included published transcriptome datasets of adult human MSCs which are referred to as MSC1, MSC2, and MSC3 [24] and adult MSCs from donors aged 29, 48, 60, and 76 years are referred to as MSC4, MSC5, MSC6, and MSC7 [25]. For the purpose of comparing the secretomes of iMSCs, fMSCs, and aMSCs, three additional MSC preparations from donors aged 62, 64, and 69 years were used, which had been generated and characterized (data not shown) at the Institute for Transplantation Diagnostics and Cell Therapeutics at Heinrich Heine University Hospital, Düsseldorf with patient consent and approval of the Ethics commission of the medical faculty Heinrich Heine University (Study number: 5013).

Cell culture

The culture of MSCs and iMSCs was carried out in αMEM, nucleosides, GlutaMAX with addition of 10% fetal bovine serum (Biochrom AG, Germany), penicillin/streptomycin, and nonessential amino acids (all from

Life Technologies, California, USA). MSCs and iMSCs were expanded with a seeding density of 1000 cells per cm^2. iMSCs were cultured in the same conditions starting from passage four [22].

Pluripotent stem cells (iPSCs and ESCs H1 and H9 (#WA01 and #WA09, respectively)) were cultured in unconditioned medium. The medium contained KO-DMEM, supplementation of 20% serum replacement, sodium pyruvate, nonessential amino acids, L-glutamine, penicillin/streptomycin, and 0.1mM β-mercaptoethanol (all from Life Technologies). Supplementation with basic fibroblast growth factor (bFGF) (Preprotech, USA) to a final concentration of 8 ng/ml was carried out before media change every day. Passaging of pluripotent stem cells was carried out with a splitting ratio of 1:3 to 1:10. Passaging was conducted manually using a syringe needle and a pipette under a binocular microscope or using a cell scraper and PBS (−). Mitomycin-C inactivated mouse embryonic fibroblasts were used as feeder cells seeded on cell culture dishes coated with Matrigel (BD) to culture iPSCs and ESCs. MSC culture was carried out at 37 °C and 5% CO_2 in a humidified atmosphere. Pluripotent stem cell culture was carried out under the same condition with additional hypoxic conditions in 5% O_2 [26].

In vitro differentiation of parental MSCs and iMSCs

Adipocyte differentiation was carried out using the StemPro Adipogenesis Differentiation Kit (Life technologies, USA). The MSCs were seeded at an initial density of 1×10^4 cells per cm^2 and induced to the adipogenic fate with differentiation medium and cultured for 21 days. Lipid filled vacuoles were visualized with Oil red O after adipogenic induction. Osteoblast differentiation was performed with the StemPro Osteogenesis Differentiation Kit (Life Technologies). Calcified matrix was visualized with Alizarin Red after osteogenic induction. The MSCs were seeded at a density of 5×10^3 cells per cm^2 in osteogenic induction media and cultured for 21 days. Chondrocyte differentiation was carried out using StemPro Chondrogenesis Differentiation Kit (Life Technologies). Acidic mucosubstances were visualized by Alcian Blue staining after chondrogenic induction.

Derivation of iPSCs from MSCs

fMSC-iPSC1, fMSC-iPSC2, and aMSC-iPSC1 were generated as previously described [22, 26]. Retroviral pluripotency induction in fetal femur-derived MSCs was carried out using pMX vector-based expression of *OCT4*, *SOX2*, *KLF4*, and *c-MYC*. Retrovirus generation was carried out in Phoenix cells using FuGENE HD Transfection Reagent (PROMEGA). Two hundred thousand MSCs were transduced. After transduction, MSCs were seeded onto Matrigel-coated cell culture plates with feeder cells (inactivated MEFs) at a density of 4000 cells per cm^2 for pluripotency induction. To reprogram them, the transduced MSCs were culture in N2B27-based medium with additions of 20% serum replacement, sodium pyruvate, nonessential amino acids, L-glutamine, penicillin/streptomycin, and 0.1mM β-mercaptoethanol (all from Life Technologies, USA) and bFGF (Preprotech, USA). After 14 days, the media was switched to mTeSR1 (Stem Cell Technologies, USA) as previously described [27]. The cells were cultured until ESC-like colonies became visible. The colonies were isolated manually and expanded for characterization. The resulting iPSCs were termed fMSC-iPSC3.

So termed, aMSC-iPSC2, were generated by using episomal plasmid-based reprogramming using the previously described combination of episomal plasmids 7F-2 [27]. The plasmids were delivered to aMSCs (62 years) by nucleofection using the Human MSC (Mesenchymal Stem Cell) Nucleofector Kit (Lonza, VPE-1001) and the Amaxa Nucleofector II (Lonza) following the manufacturer's instructions. aMSCs were cultured until passage two and the combination of 3 μg of pEP4 EO2S EN2K, 3.2 μg of pEP4 EO2S ET2K, and 2.4 μg of pCEP4-M2L was mixed with the 1×10^6 MSCs and nucleofected using the program U-23. Nucleofected aMSCs were expanded in MSC medium for 6 days and replated with a density of 6×10^4 cells per well of a six-well plate onto Matrigel and feeder cell-coated culture vessels. Further culture was carried out in N2B27-based medium as already described. Fifty micrograms per milliliter of L-ascorbic acid (Sigma-Aldrich) was added to the medium [28] with a media change every other day. After 14 days, the media was switched to mTeSR1 (Stem Cell Technologies) as previously described [27]. Further culture was carried out until ESC-like colonies could be isolated. ESC-like cell colonies were isolated manually with a syringe needle and pipette under a stereo microscope.

The isolated colonies were seeded onto freshly prepared feeder cell-coated plates as described previously [29, 30]. The characterization of the iPSC clones was initiated after six passages. The isolated iPSCs colonies were characterized as previously described [22]. The pluripotency of iPSCs generated from MSCs was tested in a similar fashion as previously described for the tool PluriTest (http://www.pluritest.org) [31] by cluster analysis within the R statistical programming environment [32] using function *hclust* to show similarity with embryonal stem cells within a dendrogram.

Embryoid body-based in vitro differentiation

iPSCs were seeded into low attachment culture dishes (Corning) and cultured in DMEM with additional 10% fetal bovine serum (Biochrom AG), sodium pyruvate,

L-glutamine, nonessential amino acids, and penicillin/streptomycin (all from Life Technologies) without bFGF for the generation of embryoid bodies (EBs). EBs were transferred onto gelatin-coated culture dishes after 10 days and cultured further for 10 days using the same conditions. Next, the cells were fixed in 4% paraformaldehyde (PFA) and stained using immunofluorescence-based detection of germ layer-specific markers.

Generation of iMSCs

iMSCs were generated from iPSCs and ESC line H1 as previously described [18]. In brief, iPSCs and ESCs were cultured without feeder cells on Matrigel. When confluency was reached, the medium was switched to unconditioned medium without bFGF supplementation or αMEM and with addition of 10 μM SB-431542 (Sigma-Aldrich) with a media change every day for 10 days. Next, the cells were trypsinized and seeded at a density of 4×10^4 cells per cm^2 onto uncoated culture dishes in MSC expansion medium. Subsequently, the cells were passaged and reseeded at a density of 2×10^4 cells per cm^2 under the same culture conditions. Finally, the cells were passaged and seeded at a density of 1×10^4 cells per cm^2. The seeding density was maintained in every further passage.

Flow cytometry

The surface marker expression of MSCs and iMSCs was analyzed using MSC Phenotyping Kit (Miltenyi). The cells were trypsinized, washed with PBS and stained with labeled antibodies as well as analyzed according to the manufacturer's instructions. For the analysis of the stained cells, fluorescence-activated cell sorting (FACS) calibur (BD) flow cytometer was used, the program CellQuestPro for data acquisition, and the softwares Cyflogic (http://www.cyflogic.com) and Microsoft Excel for data analysis.

Quantitative real-time polymerase chain reaction

The Power SYBR Green Master Mix (Life technologies) was used for quantitative real-time PCR analysis. Three hundred eighty-four-well format plates were used, and the reaction mixture had final volume of 10 μl as recommended in the manufacturer's protocol. An amount of 10 ng of cDNA was used for each reaction. The experiments were done in technical replicates. The ViiA7 (Life technologies) system was used to run the PCR with these conditions: 95°C for 10 min; 35 cycles of 95 °C, 60 °C, and 72 °C with 30 s each step. Melting curves were generated after all cycles were completed. The ^(−delta delta Ct) method was used to calculate relative gene expression levels using the CT mean values as an input. Normalization was done based on the housekeeping gene RPL37A. Table S2 shows primer sequences.

Immunofluorescence staining

Immunofluorescence staining was used to detect pluripotency markers in iPSCs and to detect expression of germ layer-specific marker in cells differentiated from iPSCs in an embryonic body-based in vitro pluripotency test. The cells were fixed at room temperature with 4% PFA for 20 min. Subsequently, the cells were washed three times in PBS and incubated in 1% Triton X-100 in PBS for 10 min at room temperature. Next, the cells were incubated in blocking solution: 10% FCS (Vector) and 0.1% Triton X-100 (Sigma-Aldrich) in PBS for 1 h. Then, the cells were incubated with the primary antibody at 4 °C in blocking solution overnight followed by three washes with PBS. Next, the cells were incubated with the secondary antibody at room temperature for 1 h followed by three more washes with PBS and a final incubation with DAPI (200 ng/ml, Invitrogen) in PBS for 20 min at room temperature. This was followed by image acquisition using a using the confocal microscope LSM510 (Carl Zeiss). A list of the used antibodies is provided in the supplement (Additional file 1: Table S3).

Gene expression analysis

The DNA+RNA+Protein Extraction Kit (Roboklon) was used to extract total RNA. The linear amplification kit (Ambion) was used to produce biotin-labeled cRNA form 500 ng of total RNA per sample. The samples were further processed using the Illumina BeadStation 500 platform (Illumina) following the manufacturer's protocol for hybridization and Cy3-streptavidin staining. HumanHT-12 v3.0 Gene Expression Bead Chips (Illumina) were used to hybridize the samples. Bead-level data was summarized to bead-summary data using the Gene Expression Module of the software GenomeStudio (Illumina) without normalization and background correction. Bead-summary data was imported into the R/Bioconductor [33] environment where it was background-corrected and normalized with quantile normalization from the package *lumi* [34]. The R_builtin function *cor* was used to compute the Pearson correlation values between the transcriptomes detected by microarray. Significant gene expression was calculated by determining the detection p value based on the difference to negative control beads. A gene with a detection p value ≤ 0.05 was considered to be expressed. Venn diagrams and heatmaps were generated employing the R/Bioconductor packages VennDiagram [35] and gplots [36]. Lists of human gene sets annotated to the Gene Ontology (GO)-terms cell cycle, senescence, response to oxidative stress, DNA damage repair, and aging were generated using AmiGO 2 version 2.3.1 (http://amigo2.berkeleybop.org/amigo) [37] and used to extract GO term-specific gene expression data sets which were analyzed by hierarchical clustering analysis. The data set of

the gene expression analysis will be accessible at the Gene Expression Omnibus (GEO) repository under the accession number GSE97311 (www.ncbi.nlm.nih.gov/geo/query/acc.cgi?acc=GSE97311).

Determination of differential expression

The linear models for microarrays from the R/Bioconductor *limma* package [38] were used to compute the differential p value to determine the significance of the difference between gene expression values. The computed differential p value was adjusted in R/Bioconductor with the *qvalue* false discovery rate (FDR) correction algorithm [39]. Genes with a FDR-corrected differential p value of ≤ 0.05 were considered significantly different. The up- or downregulation of these genes was calculated by determining the ratio of the average signals. A ratio higher than 1.33 was considered as upregulated, and a ratio lower than 0.75 was considered as downregulated.

Determination of the aged and rejuvenation gene signatures

Two gene signatures were determined which are characterizing the aging and rejuvenation processes. The gene signatures were identified based on combinations of gene expression of MSCs in differing age-related stages. The aged gene signature was defined by gene expression in the MSCs but not in the iMSCs and iPSCs, given by the combination of detection p values: $p\_{MSC} < 0.001 \Lambda$ $p\_{iMSC} > 0.1 \Lambda$ $p\_{iPSC} > 0.1$. The rejuvenation gene signature was defined by gene expression in the iMSCs and iPSCs but not in the MSCs, given by the combination of detection p values: $p\_{MSC} > 0.1 \Lambda$ $p\_{iMSC} < 0.001 \Lambda$ $p\_{iPSC} < 0.001$.

Functional annotation of gene sets

Database for Annotation, Visualization and Integrated Discovery (DAVID) Bioinformatics resources 6.7 (http://david.abcc.ncifcrf.gov) [40] was used for functional annotation analysis of gene sets. Lists of official gene symbols or Illumina IDs were used as input against human background. The default settings of DAVID Bioinformatics resources 6.7 were used. The option Kyoto Encyclopedia of Genes and Genomes (KEGG) terms was used for the annotation to pathways. The option GO_BP_Direct or GO_BP_Fat was used to for annotation to gene ontology terms of biological processes.

Protein association network

Based on the aged and rejuvenation gene signatures, two protein interaction networks were constructed. The interactions are based upon the Biogrid database version 3.4.161 [41] filtered for the taxonomy id 9606 (*Homo sapiens*). From the Biogrid dataset, all protein interactions containing at least one protein coded by the above mentioned aged and rejuvenation signatures were extracted separately for each signature. Both resulting networks were reduced by adding only the $n = 30$ interacting proteins with the most interactions to proteins coded by genes from the original sets. The R package *network* [42] was employed to visualize these interactions marking proteins from the original sets in green. Communities of related proteins within the networks were detected via an in-betweenness clustering analysis with the method *cluster_edge_betweenness* from the R package *igraph* [43].

Secretome analysis

The cell culture supernatants of three distinct fMSCs, three independent iMSCs, and three distinct aMSCs were collected, and 1 .5 ml each was used for subsequent analysis. The Proteome ProfilerTM Array Human (XL) Cytokine Array kit (R&D Systems, catalog number ARY022) was carried out according to the user's manual. Two reference spots showing successful performed analysis were located in three positions on the cytokine membrane (in upper left, lower left, and the lower right-corner). Horseradish peroxidase substrate and luminol enhancer solution (GE healthcare UK limited) were used to visualize protein distribution and amount on the membranes. The pictures were taken with Fusion-FX microscope (Fischer Biotec). The pixel density of the spots was measured using ImageJ, the background intensity was subtracted, and the values were finally calculated as percentage of the reference spots intensity. Values above 5% were classified as secreted. Cytokines with values above 20% of the reference were considered abundantly expressed.

Statistical analysis

The comparison of two groups was carried out using a two-tailed unpaired Student's t test. Significant difference was defined with p values ≤ 0.05. For microarray data analysis, a gene with an expression p value ≤ 0.01 was considered significantly expressed. A gene with a differential p value ≤ 0.01 was considered significantly different in terms of expression. Functional annotation was considered significant with a p value of ≤ 0.05.

Results

Mesenchymal stem cells of fetal and aged background differ in transcriptome level

Irrespective of donor age, fMSCs and aMSCs showed a typical MSC surface marker profile by expression of CD73, CD90, and CD105 and the absence of the hematopoietic markers CD14, CD20, CD34, and CD45 at the gene expression and protein level (Fig. 1a, b). ESCs H1 which were used as a negative control did not show expression of CD73 and CD105 at the gene

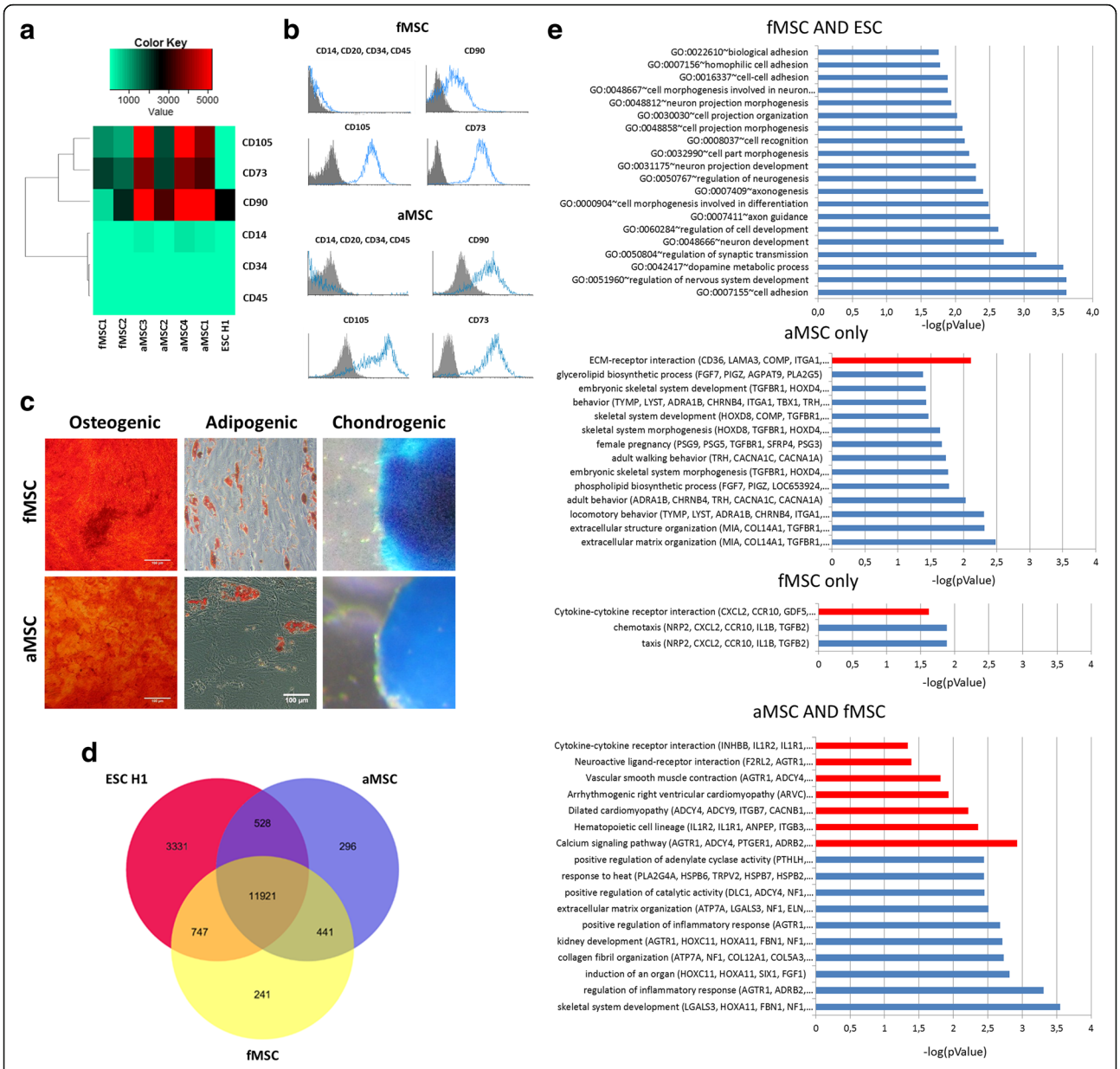

Fig. 1 Characterization of fMSCs and aMSCs. **a** fMSCs and aMSCs express typical MSC surface marker genes CD73, CD90, and CD105 but no hematopoietic marker genes. **b** fMSCs and aMSCs show MSC-typical surface marker expression detected by FACS. Blue: fluorophore-conjugated antibody against surface antigen. Gray: isotype control. **c** Confirmation of typical MSC lineage differentiation potential in fMSCs and aMSC. Alizarin Red staining visualized the calcified matrix in red. Adipogenic: Oil Red O staining was used to visualize fat vacuoles of adipocytes in red. Chondrogenic: Cells of pellet culture were stained with Alcian blue to visualize acidic mucosubstances in blue. Pictures were taken using a stereo microscope. **d** Overlapping and distinct gene expression between fMSCs, aMSCs, and ESCs with **e** related KEGG pathways and GO terms depicted as bar diagrams with –log(pValue). KEGG pathways are marked in red and GO terms in blue

expression level and had a lower expression of CD90 than the MSCs. Additionally, MSCs of both age groups could be differentiated into osteoblasts, adipocytes, and chondrocytes and stained positive for Alizarin Red S (bone), Oil Red O (fat), and Alcian Blue (cartilage), respectively (Fig. 1c).

Venn diagram-based analysis of the transcriptome data revealed a higher number of genes expressed in common between fMSCs and ESCs (747 genes) compared to the overlap of aMSCs and ESCs (Fig. 1d). The 747 genes were annotated to GO terms such as cell adhesion with a p value below 0.01. In addition, genes expressed in common between fMSCs and aMSCs (441) were annotated to KEGG pathways such as calcium signaling and GO terms such as skeletal system development with p values below 0.01. Genes exclusively expressed in fMSCs

(241) were annotated to the KEGG pathway cytokine-cytokine receptor interaction with a p value below 0.05, whereas the genes exclusively expressed in aMSCs (296) were annotated to ECM-receptor interaction and extracellular matrix organization with p values below 0.01 (Fig. 1e).

Derivation and characterization of iPSCs from fMSCs and aMSCs

We previously established two iPSC lines from fetal MSCs [26], named fMSC-iPSC1 and fMSC-iPSC2. Additionally, we have described an iPSC line from MSCs of a 74-year-old donor (aMSC-iPSC1) [22]. In the present study, MSCs isolated from a 62-year-old donor were successfully reprogrammed into iPSCs (aMSC-iPSC2) as well as a new iPSC line from fMSCs was created (fMSC-iPSC3).

Transcriptome analysis of the native MSCs, the corresponding iPSCs, and the ESC line H1 revealed two separated clusters. The first cluster included all MSC population irrespective of the donor age which was separated from the second cluster which includes the ESCs and all MSC-iPSCs (Fig. 2a). At the transcriptome level, there was a distinct level of heterogeneity in the results since MSCs and MSC-iPSCs did not show a separation by donor-cell age. All iPSC lines expressed pluripotency-associated markers (Additional file 1: Figure S1) and a transcriptome similar to ESCs (Fig. 2b). Moreover, both fMSC-iPSC3 and aMSC-iPSC2 expressed pluripotency marker at the protein level and formed embryoid bodies and differentiated into cell types representative of the three embryonic germ layers (Additional file 1: Figure S1).

iMSC from MSC-iPSCs of distinct age backgrounds and ESCs have MSC-typical marker expression and differentiation potential

fMSC-iPSC3, aMSC-iPSC2, and ESC line H1 were differentiated into MSCs and named fMSC-iMSCs, aMSC-iMSCs, and ESC-iMSCs. iMSCs displayed spindle-shaped morphologies comparable to primary MSCs (Fig. 3a). In addition, all iMSCs derived from primary MSCs expressed the MSC markers CD73, CD90, and CD105 but not the hematopoietic markers CD14, CD20, CD34, and CD45 (Fig. 3b). Oil Red O-positive fat droplets were detected in all iMSC preparations upon adipogenic induction. In addition, Alizarin Red-positive calcified matrix and Alcian Blue staining were detected following culture in osteogenic and chondrogenic medium, respectively (Fig. 3c). Although iMSCs were derived from pluripotent cells, they had a lower expression of pluripotency markers than the iPSC and ESCs they were derived from (Fig. 3d). Finally, comparison of the transcriptomes revealed a higher correlation co-efficient (R^2) between iMSCs and primary MSCs (0.917–0.964) than between iMSCs and iPSCs/ESCs (0.879–0.914). Moreover, we detected a higher similarity between the transcriptomes of fMSCs and ESCs (0.925–0.939) than between aMSCs and ESCs (0.855–0.885) (Additional file 1: Figure S2).

Primary MSCs and iMSCs have overlapping and distinct gene expression patterns revealing higher similarity between iMSCs and fMSCs

A Venn diagram-based representation of transcriptome data identified 12,487 genes commonly expressed between the fMSC-iMSCs, aMSC-iMSCs, and ESC-iMSCs. Within this shared gene set, numerous MSC-specific genes (CD73, CD90, CD105, and PDGFRβ), MSC-associated genes (VEGFA, Vimentin, SerpinE1, and MIF), and differentiation markers (RUNX2 and PPARγ) were present (Fig. 4a). Clustering analysis of the transcriptomes resulted in the formation of two similarity-based clusters separating iMSCs (irrespective of their source) together with primary MSCs from their corresponding iPSCs and ESC samples (Fig. 4b). Another Venn diagram-based analysis comparing iMSCs (combination of fMSC-iMSCs, aMSC-iMSCs, and ESC-iMSCs), fMSCs, and aMSCs revealed that more genes were expressed in common between iMSCs and fMSCs (534 genes) than between iMSCs and aMSCs (398 genes) with the majority of genes expressed in all three groups (11794). iMSCs proved the most distinct sample set with 923 exclusively expressed genes (Fig. 4c).

Importantly, a heatmap-based clustering analysis of expression of DNA damage repair (such as FEN1 and MSH6) and aging-associated genes (such as *FADS1* and *NOX4*) revealed that iMSCs irrespective of donor age or cell type of origin are more similar to fMSCs compared to aMSCs (Fig. 4d, e).

MSC-iMSCs acquired a rejuvenation signature

Genes expressed in iMSCs and pluripotent stem cells but not expressed in primary MSCs (fMSCs and aMSCs) were identified which we refer to as the rejuvenation signature. On a similar note, genes expressed in primary MSCs but not in pluripotent stem cells and iMSCs are referred to as the aging signature (Fig. 5a). Figure 5b shows a table based on the heatmap from Fig. 5a with the gene names within the rejuvenation and aging signature. To validate our rejuvenation and aging signatures, we carried out an additional analysis incorporating already published datasets of primary human MSCs of different ages [24, 25]. A hierarchical clustering analysis of gene expression including the new samples (MSC1–7) independently confirmed the validity of our rejuvenation signature (e.g., *PM20D2* and *HRASLS*) and aging

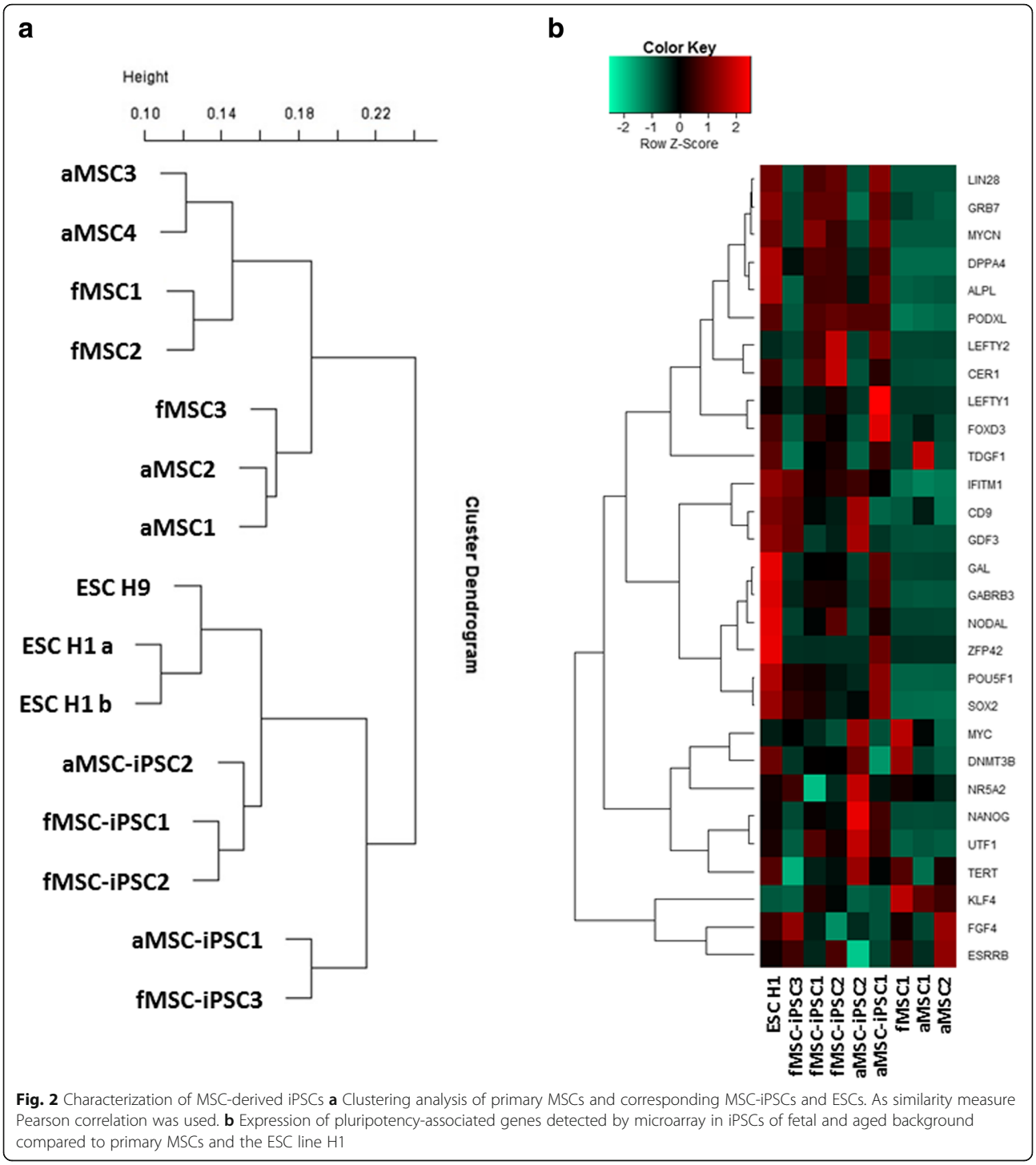

Fig. 2 Characterization of MSC-derived iPSCs **a** Clustering analysis of primary MSCs and corresponding MSC-iPSCs and ESCs. As similarity measure Pearson correlation was used. **b** Expression of pluripotency-associated genes detected by microarray in iPSCs of fetal and aged background compared to primary MSCs and the ESC line H1

signature (e.g. *FAM109B* and *EDIL3*) reflecting the respective expression levels (Fig. 5c).

For further verification of the rejuvenation signature, real-time PCR analysis was carried out using RNA from additional independent adult MSC (56 years) and iMSC samples from distinct age groups (urine-derived iPSC-derived iMSCs (51 years); ESC-iMSCs (prenatal), fMSC-iMSCs (prenatal), and HFF-iMSCs (human fetal foreskin-derived iPSC-derived iMSCs)) employing primers for genes of the rejuvenation (*IGSF3*, *CXADR*, *FAM84B*, *INHBE*, and *DNMT3B)* and aging signature (*COX7A*, *EZA2*, *EFEMP1*, *ENPP2*, and *TMEM119*) (Fig. 5d). For *IGSF3*, the mRNA expression level in all iMSC preparation was higher than that in the fMSCs

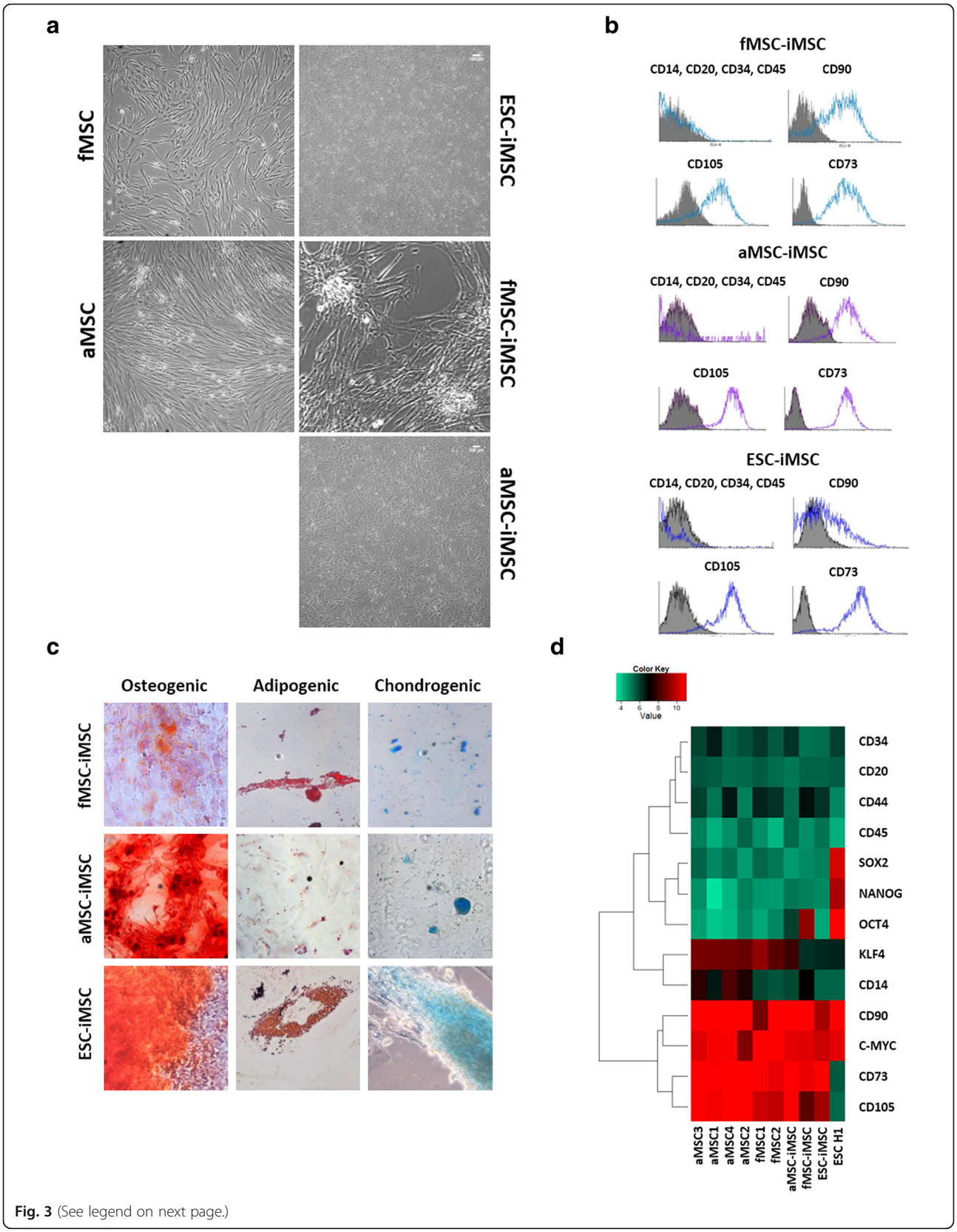

Fig. 3 (See legend on next page.)

(See figure on previous page.)
Fig. 3 Characterization of fMSC-iMSCs, aMSC- iMSCs, and ESC-iMSCs. **a** Morphology of iMSCs compared to native MSCs. **b** Flow cytometry-based analysis of MSC surface marker in iMSCs. Blue/Purple: iMSCs labeled with antibody specific to marker. Gray: isotype control. **c** Differentiation potential of iMSCs in vitro. Osteogenic: Alizarin Red S staining; adipogenic: Oil red O staining; chondrogenic: Alcian Blue staining. **d** Gene expression of MSC, hematopoietic, and pluripotency markers in iMSCs compared to primary MSCs and ESC H1. Representative images of $n = 3$ experiments

and aMSC samples whereas only three of the four iMSC samples showed increased *CXADR* expression levels. For *DNMT3B*, a rejuvenation signature, two of the four iMSC samples showed upregulation. The other two genes of the rejuvenation signature showed comparable levels in aMSCs and iMSCs. For the aging signature, *COX7A*, *EZA2*, *EFEMP1*, and *TMEM119* were expressed at lower levels in iMSCs than in aMSCs with the exception of *ENPP2* (Fig. 5d).

Protein association network analyses confirm rejuvenation and aging signature

Using the genes of the rejuvenation signature as input, a protein association network (PAN) was created adding the $n = 30$ interaction partners with the most interactions from the Biogrid database. We used community clustering to identify densely connected groups of proteins with fewer connections across groups. The rejuvenation signature PAN (Fig. 6a) includes communities characterized by INHBE (blue), TP53, CDKN1C, IL32 (light blue), CDK10 (petrol), ELAVL1 (purple), DNMT3B (yellow), and EEF1A2 (green).

Analogously, we generated a PAN based on the aging signature which revealed genes involved in the TGFβ and mTOR-signaling pathways as well as factors associated with oxidative stress including CAT (Fig. 6b). The aging signature PAN (Fig. 6b) includes communities characterized by HSPA5 (blue), GRB2 (light blue), CCDC8 (purple), CAT (petrol), EYA2 (yellow), APP (green), and TGFB1 (red).

iMSCs of different age backgrounds show overlapping secretomes with fetal MSCs

Based on a cytokine array, the secretomes of fMSC-iMSCs, aMSC-iMSCs, and ESC-iMSCs were found to be similar to the secretomes of primary fMSC1, fMSC2, and fMSC3 (Fig. 7a, b). iMSCs, independent from their origin, as well as fetal MSCs showed a large number overlap in the most abundantly secreted cytokines: angiogenin, BDNF, Chitinase 3-like 1, Dkk-1, EMMPRIN, ENA-78, endoglin, GDF-15, GROα, IGFBP-2, IGFBP-3, IL-6, IL-8, IL-11, LIF, MCP-1, MCP-3, MIF, osteopontin, PDGF-AA, pentraxin-3, serpin E1, thrombospondin-1, and VEGF (Fig. 7a, Additional file 1: Figure S3). KEGG pathway analysis of the common secreted cytokines showed their involvement in processes like cytokine-cytokine receptor interaction, TNF signaling pathway, chemokine signaling pathway, PI3K-Akt signaling pathway, HIF-1 signaling pathway, and Jak-STAT signaling pathway (Fig. 7b). Gene Ontology analysis of the common secreted cytokines showed involvement in processes such as regulation of growth factor activity, inflammatory response, positive regulation of ERK1 and ERK2 cascade, positive regulation of angiogenesis, and cell proliferation (Fig. 7c). In addition to this, the secretomes of fMSCs and iMSCs were compared to that of aMSCs (Fig. 7d, Additional file 1: Figure S3). In comparison to fMSCs and iMSCs (independent of the source), MSCs from aged individuals (aMSCs) secreted fewer cytokines and at lower levels except for IL6.

Discussion

Derivation and characterization of pluripotent stem cell-derived MSCs (iMSCs) are on the rise [18, 44–46]. iMSCs have been shown to enhance regeneration and healing when applied to a variety of animal models; multiple sclerosis, limb ischemia, arthritis, liver damage, bone defects, wound healing, and hypoxic-ischemia in the brain [46–53]. In this study, we comparatively and critically assessed the effect of donor age and cell type specificity on the iMSC "rejuvenated" signature based on transcriptome analysis and further studied their paracrine signaling potential by secretome analyses. We revealed that fMSCs share a higher transcriptome similarity with ESCs than with aMSCs. This age-related difference may be due to genes involved in cell adhesion (Fig. 1e), which is in agreement with the reported role of adhesion-related processes in pluripotent stem cells [54]. However, the iMSCs generated in this study met the criteria defined for primary MSCs to a certain extent in terms of morphology and surface marker expression (Fig. 3a,b), as previously shown for iMSC generation from fibroblast-derived iPSCs [18]. In agreement with the MSC criteria [2], the generated iMSCs were able to differentiate into bone, cartilage, and fat cells in vitro. In addition, we could successfully confirm a high level of similarity between primary MSCs and iMSCs on transcriptome level and could show that these iMSCs although originating from pluripotent cells are not pluripotent themselves (low similarity to iPSCs) which is important for potential use in future clinical applications.

The expression patterns of genes associated with aging and DNA damage repair in all iMSC populations

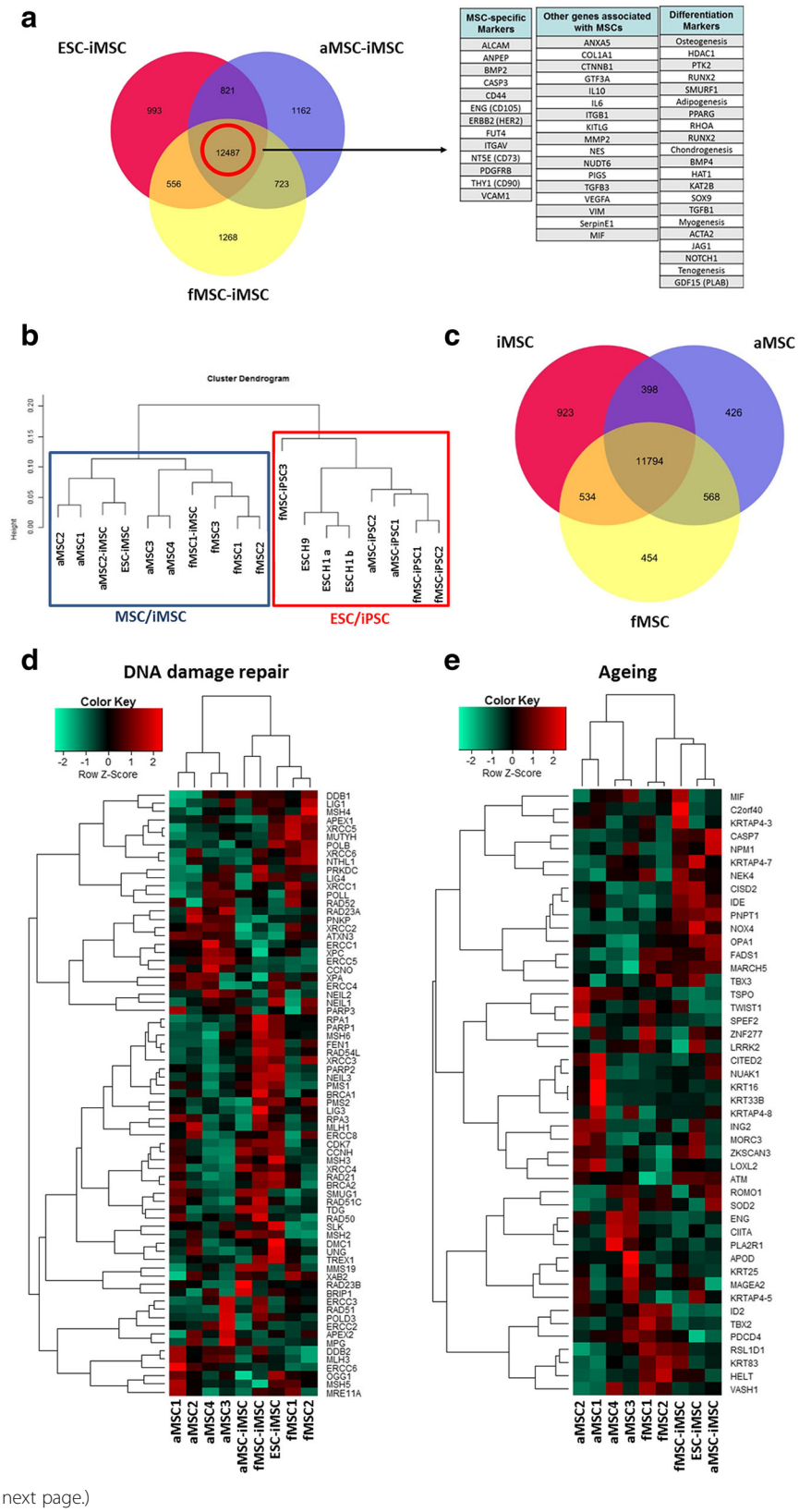

Fig. 4 (See legend on next page.)

(See figure on previous page.)
Fig. 4 Distinct and overlapping gene expression patterns between iMSCs and primary MSCs isolated from donors of distinct ages. **a** Venn diagram-based on expressed genes detected by microarrays of one sample each of fMSC-iMSCs, aMSC-iMSCs, and ESC-iMSCs. MSC-related genes were expressed in all three iMSC preparations. **b** Clustering dendrogram of Illumina gene expression experiments based on Pearson correlation. One cluster consists of iPSCs and ESCs (red box), and the other separated cluster contains primary MSCs as well as all three iMSC preparations (blue box). **c** Venn diagram of iMSCs and MSCs from fetal and aged donors based on expressed genes of one sample each **d** Heatmap showing clustering of primary MSCs and iMSCs for genes related to DNA damage repair. **e** Heatmap showing clustering of primary MSCs and iMSCs for aging-related genes

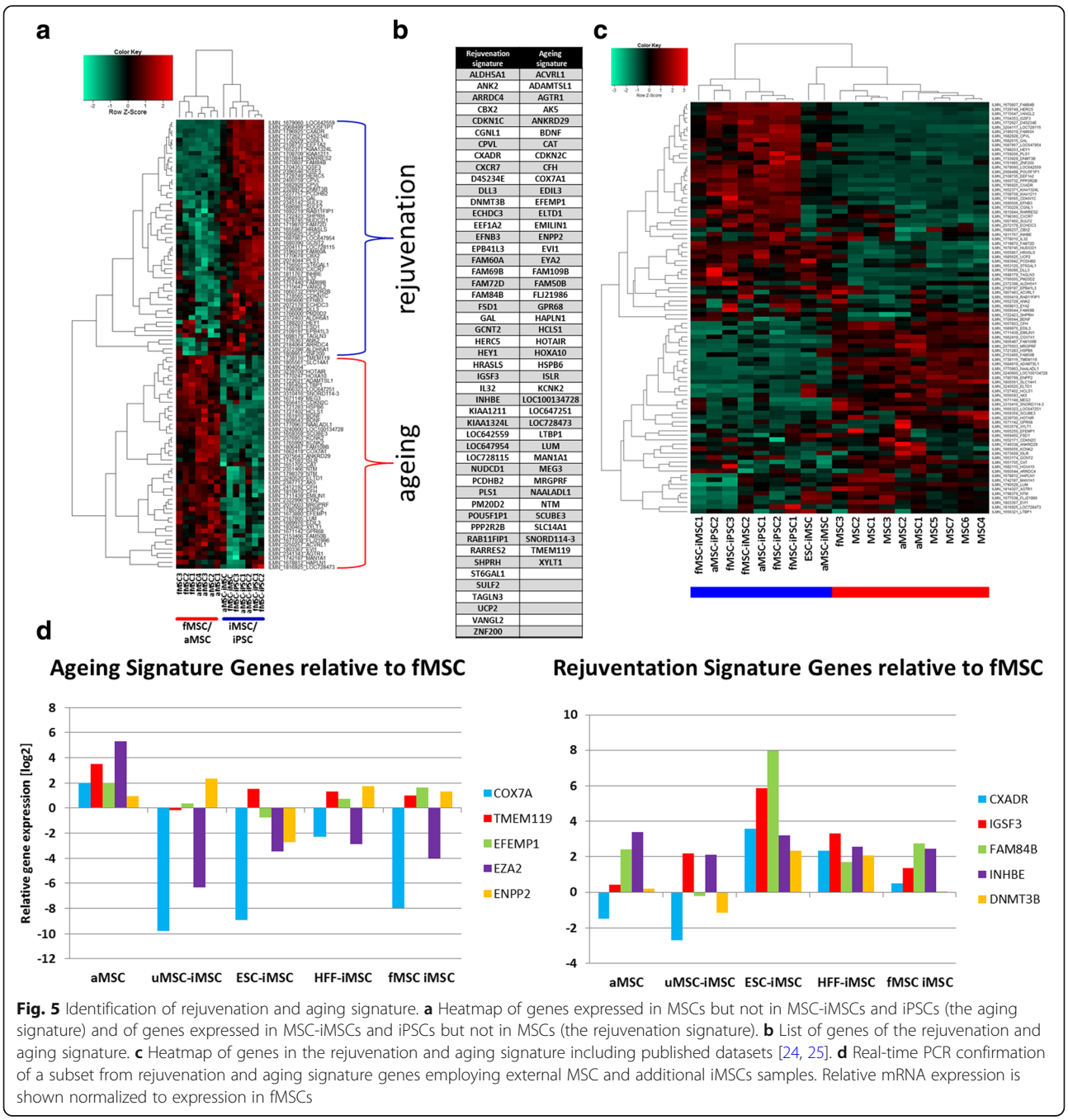

Fig. 5 Identification of rejuvenation and aging signature. **a** Heatmap of genes expressed in MSCs but not in MSC-iMSCs and iPSCs (the aging signature) and of genes expressed in MSC-iMSCs and iPSCs but not in MSCs (the rejuvenation signature). **b** List of genes of the rejuvenation and aging signature. **c** Heatmap of genes in the rejuvenation and aging signature including published datasets [24, 25]. **d** Real-time PCR confirmation of a subset from rejuvenation and aging signature genes employing external MSC and additional iMSCs samples. Relative mRNA expression is shown normalized to expression in fMSCs

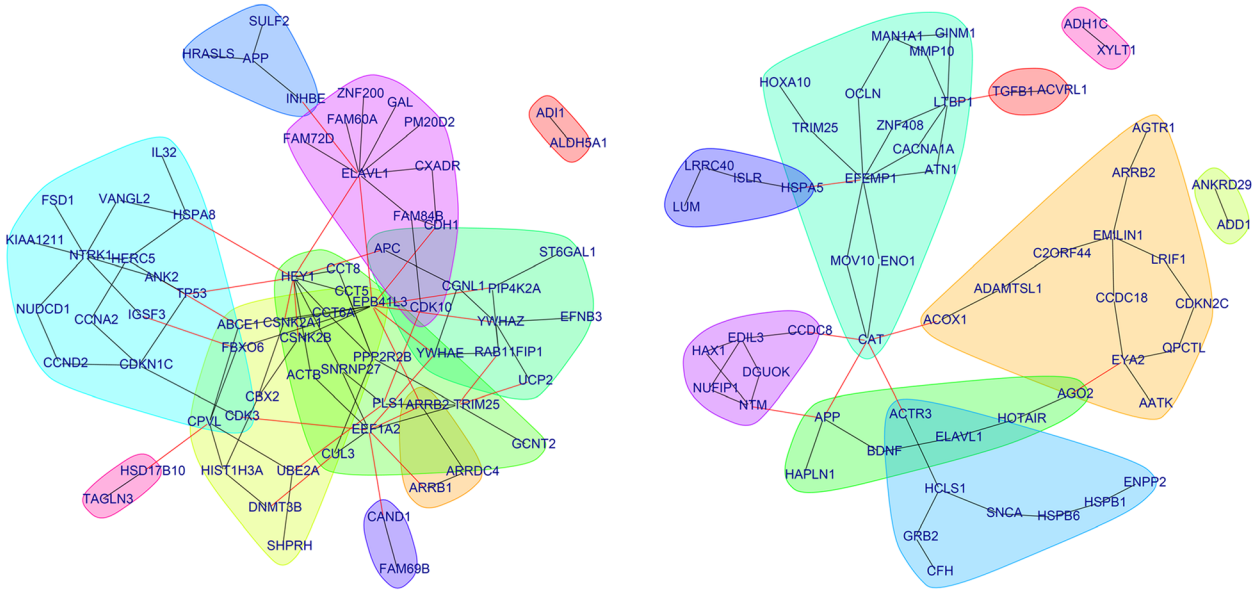

Fig. 6 Protein association network related to aging and rejuvenation signatures of gene expression in iMSCs and parental MSCs. Based on the Biogrid database protein interaction, networks have been constructed from the rejuvenation signature (**a**) and aging signature (**b**) listed in Fig. 5b. Most of the proteins coded by genes from both signatures can be connected to a network with interactions reported in the Biogrid database. Community clustering of the network via edge-betweenness reveals several communities with densely connected nodes and fewer connections across communities. Communities are indicated by dedicated color shading; edges between communities are colored red. **a** The rejuvenation signature PAN includes communities characterized by INHBE (blue), TP53, CDKN1C, IL32 (light blue), CDK10 (petrol), ELAVL1 (purple), DNMT3B (yellow), and EEF1A2 (green). **b** The aging signature PAN includes communities characterized by HSPA5 (blue), CCDC8 (purple), CAT (petrol), EYA2 (yellow), APP (green), and TGFB1 (red)

clustered closer to fMSCs than to aMSCs (Fig. 4d, e), thus indicating a rejuvenation. DNA damage has been shown to be associated with the complex process of aging before [55]. Irrespective of donor age and cell source, iMSCs acquired a rejuvenation gene signature also present in pluripotent stem cells but not in the parental MSCs (Fig. 5a, b). Conversely, we observed a gene set representing the aging signature comprising genes expressed in primary MSCs but not in pluripotent stem cells and iMSCs. We could independently confirm the extracted aging and rejuvenation signature by including already published datasets of adult MSCs [24, 25] in similarity analyses based on both gene sets (Fig. 5c). Further confirmation of the signatures was carried out at the mRNA level using additional MSC and iMSC samples (Fig. 5d). A large number of the genes within the rejuvenation signature play important roles in embryonic tissues and in development thus indicating the presence of features associated with early development in iMSCs, and therefore, it would appear, endowing iMSCs with enhanced regenerative properties. The rejuvenation signature PAN revealed communities characterized by INHBE, TP53, CDKN1C, IL32, CDK10, ELAVL1, DNMT3B, and EEF1A2. INHBE participates in the activin/nodal branch of the TGFB signaling pathway which is needed for maintenance of pluripotency [56, 57]. CDK10, CDKN1C, and TP53 are involved in cell cycle control which obviously plays an important role in stem cell self-renewal [58]. However, the detailed cell cycle coordination in order to determine cell fates is not fully uncovered. CDK10 like all members of the CDK family is responsible for cell cycle progression but is limited to the G2-M phase which Vallier et al. describe as necessary to block pluripotency upon induction of differentiation referring to Gonzalez et al. [59]. Gonzales et al. furthermore report that the ATM/ATR-CHEK2-TP53 axis enhances the TGFβ pathway to prevent pluripotent state dissolution. In a previous publication, we reported compromised induction of pluripotency in fibroblasts from a Nijmegen Breakage syndrome patient under conditions of impaired DNA damage repair and downregulated TP53 and cell cycle genes [60]. CDKN1C reduces cell proliferation by inhibiting cyclin/CdK complexes in the G1 phase [61] and is a major regulator of embryonic growth as has been reported by Andrews et al. for the imprinted domain on mouse distal chromosome 7 [62]. ELAVL1 (HuR) has been associated with regulation of growth and proliferation of vascular smooth muscle cells

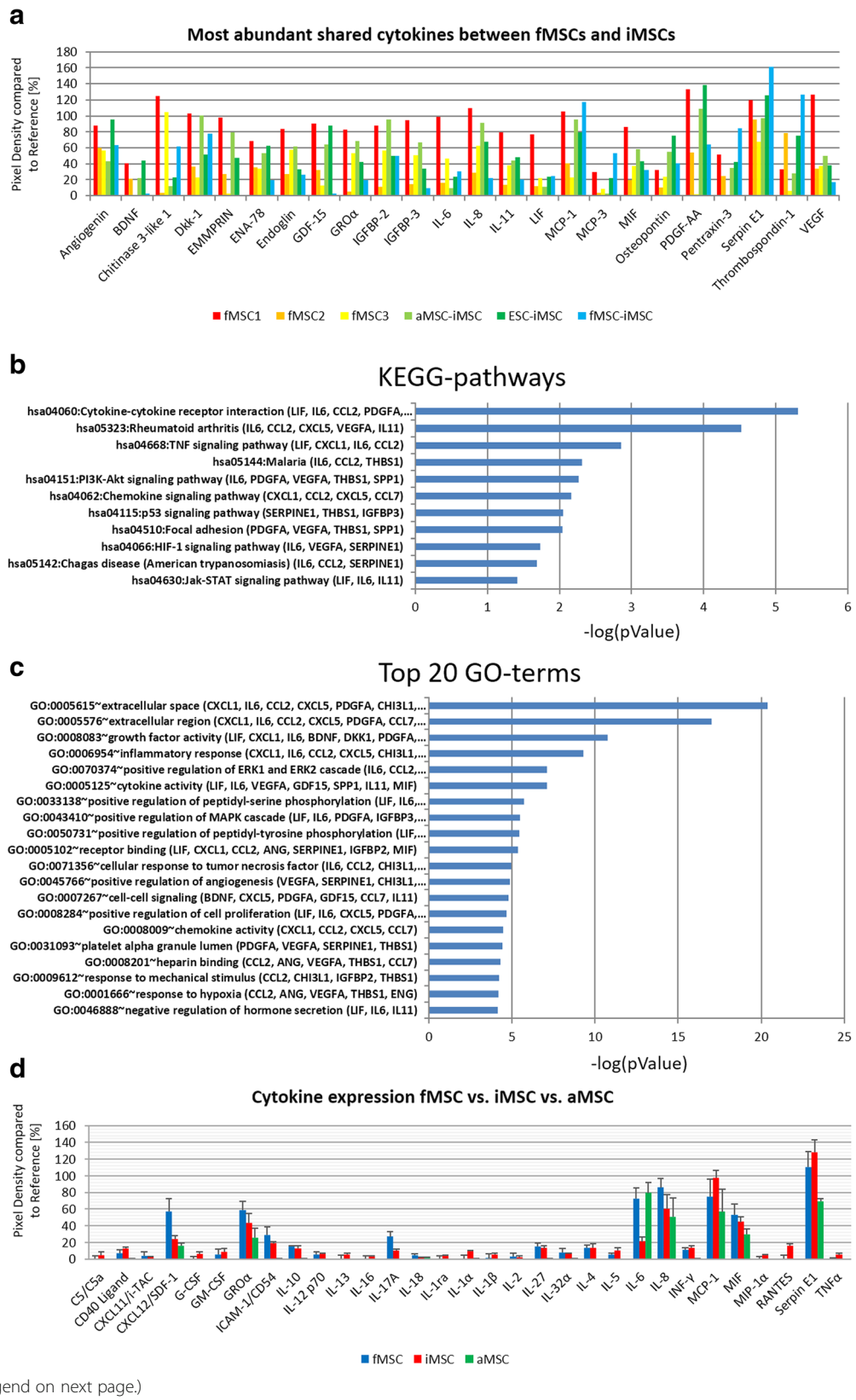

Fig. 7 (See legend on next page.)

(See figure on previous page.)
Fig. 7 Comparative analyses of the secretome of fMSCs, iMSCs, and aMSCs. **a** Cytokine expression of fMSC1, fMSC2, fMSC3, and iMSCs (fMSC-iMSCs, aMSC-iMSCs, and ESC-iMSCs) detected using membrane-based cytokine arrays. Expression plot of the most abundant cytokines shared between fMSCs and iMSCs; threshold of expression in comparison to reference spots was set to 20%. **b** KEGG pathway analysis of common cytokines between fMSCs and iMSCs–log(pValue). **c** GO terms associated with common secreted cytokines between fMSCs and iMSCs as –log(pValue). **d** Cytokine expression of fMSCs, iMSCs, and aMSCs (aMSC5, aMSC6, aMSC7)

[63]. DNMT3B has been reported to be essential for de novo methylation and mammalian development [64] and DMNT1 and DNMT3B were shown to decrease upon aging [65].

The aging signature PAN includes communities characterized by HSPA5, CCDC8, CAT, EYA2, APP, and TGFB1. Catalase (CAT) is an antioxidant which has been reported to have decreased activity upon aging in rats [66]. GRB2 is part of the mTOR-signaling pathway which coordinates eukaryotic cell growth and metabolism with environmental inputs [67]. TGFβ-signaling plays a major role in young and aging organisms but changes its functionality. Baugé et al. describe a shift of TGFβ-signaling from SMAD2/3 to SMAD1/5/8 as cause of a shift from chondrogenic differentiation and maturation in young joints to hypertrophic differentiation in aged or osteoarthritic joints [68]. BDNF has been reported to regulate the amyloid precursor protein APP [69] that is involved in activity-dependent synaptic plasticity and is upregulated after birth but then stays unchanged during aging in rat hippocampus [70].

Accordingly, the loss of the aging signature during iMSC derivation likely contributed to the advantageous features of iMSCs compared to primary MSCs. The observed fetal-like expression pattern of genes involved in DNA damage repair in iMSCs could be due to the involvement of this process in pluripotency induction. An alternative explanation could be that young or progenitor cells have a better capacity to repair DNA damage [71].

A rejuvenated state of processes involved in aging in iMSCs is furthermore likely as the epigenetic rejuvenation of MSCs through pluripotency induction has been described [13].

Of considerable potential significance, from a regenerative medicine perspective, iMSCs should have a similar secretome to that of the corresponding parental MSCs. In line with this, the secretion of GROα, IL-6, IL-8, MCP-1, MIF, SDF-1, and Serpin E1 in bone marrow-derived MSCs has been described [72]. A further study showed that MSCs derived from bone marrow secrete angiogenin, G-CSF, GM-CSF, GROα, IL-1α, IL-6, IL-8, INFγ, MCP-1, oncostatin M, RANTES, and TGFβ and do not secrete IL-2, IL-4, IL-10, IL-12, IL-13, MIP-1β, and SDF-1α [73], all in agreement with our iMSC secretome profile. Interestingly, we detected the secretion of anti-inflammatory and pro-inflammatory cytokines in iMSCs and fetal mesenchymal populations confirming findings in MSCs [74]. Gene Ontology analysis revealed overlapping capabilities to interact with the immune system and involvement in regeneration processes of fetal MSCs and iMSCs corroborating studies with MSCs derived from adult donors [75–77]. A KEGG pathway analysis revealed involvement of the overlapping secreted cytokines between fetal MSCs and iMSCs in TNF signaling pathway, Jak-STAT signaling pathway, and PI3K-Akt signaling pathway. Interestingly, we found SerpinE1, thrombospondin-1, IGFBP3, endoglin, and angiogenin to be abundantly secreted in fetal MSCs and iMSCs. The described role of SerpinE1, thrombospondin-1, and endoglin in wound healing [78–80] indicate a putative fetal-like feature of wound healing properties of iMSCs in vivo [81, 82]. Our analyses revealed that aMSCs compared to fMSCs and iMSC secrete a reduced repertoire of cytokines and at significantly lower levels. However, fMSCs, aMSCs, and iMSCs secrete comparable levels of IL6, IL8, SDF-1, MCP-1, MIF, Serpin E1, and GROα. This once again reinforces the notion that MSCs isolated from the elderly may not be as potent as fetal MSCs and pluripotent stem cell-derived MSCs.

Conclusions

In summary, the current study shows that MSCs of fetal and aged background are not identical and MSCs generated from iPSCs (iMSCs) bear typical characteristics of native MSCs but more in common with fetal MSCs. The key finding from our study is the identification of a rejuvenation gene signature in iMSCs (irrespective of donor age) which also is present in pluripotent stem cells but not in the parental MSCs. Most important for regenerative medicine, iMSCs irrespective of initial age re-acquire a more similar secretome to that of fetal MSCs than aged MSCs. In conclusion, our findings show that the acquisition of a rejuvenated phenotype in iMSCs re-enforces the utility of the "iMSC concept" in regenerative medicine and cell replacement therapy in an ever increasing aging population.

Additional file

Additional file 1: Table S1. List of primary MSC samples. Table S2. List of primers. **Table S3.** List of antibodies. Figure S1 Pluripotency marker staining of generated iPSC line from fMSCs and aMSCs as well as EB formation. **Figure S2.** Correlation coeficiency table. Figure S3 Cytokine membranes. (DOCX 2493 kb)

Abbreviations
aMSC: Adult MSC; CD: Cluster of differentiation; DAVID: Database for Annotation, Visualization and Integrated Discovery; EB: Embryoid body; ESCs: Embryonic stem cells; FACS: Fluorescence-activated cell sorting; fMSC: Fetal MSC; GEO: Gene Expression Omnibus; GO: Gene Ontology; iMSCs: iPSC-derived mesenchymal stromal cells; iPSCs: Induced pluripotent stem cells; KEGG: Kyoto Encyclopedia of Genes and Genomes; MSCs: Mesenchymal stem cells; PAN: Protein association network

Acknowledgements
We thank Prof. David Wilson, University of Southampton for access to fetal tissue and Dr. Kelvin Cheung, University of Southampton for derivation of fetal femur explant cultures. We thank Prof. G. Duda for providing MSCs from the 74-year-old.

Funding
Prof. Dr. James Adjaye acknowledges support from the Medical Faculty, Heinrich-Heine-University, Düsseldorf, Germany and support from the Federal Ministry of Education and Research-BMBF (01GN1005) and the Medical Faculty, Heinrich-Heine-University, Düsseldorf. Professor Dr. Richard Oreffo is supported by grants from the BBSRC (LO21072/1) and MRC (MR/K026682/1). In addition, Prof. Dr. James Adjaye and Mr. Md Shaifur Rahman acknowledge support from the German Academic Exchange Service (DAAD-91607303).

Availability of data and materials
The data and cells described in this manuscript can be made available upon request. The transcriptome data is available online at the National Center of Biotechnology Information (NCBI) Gene Expression Omnibus.

Authors contributions
JA, RO, MM, and LSS conceived the idea and designed the experiments. MM and LSS performed the characterization of primary MSCs and generation/characterization of iPSCs/iMSCs. MM, LSS, and MSR analyzed the results and wrote the draft manuscript. OD and RM provided RNA from MSCs of an aged individual (56 years), and JO performed the real-time PCR analysis. WW did the bioinformatical analysis. RVS provided aged MSCs for the cytokine array. JA edited and finally approved the manuscript. All authors reviewed and approved the submitted version.

Ethics approval and consent to participate
Fetal femur-derived MSCs were obtained following informed, written patient consent. Approval was obtained by the Southampton and South West Hampshire Local Research Ethics Committee (LREC 296100). Adult mesenchymal stem cells, used for generation of iPSCs and iMSCs, were isolated from the bone marrow after written informed consent. The corresponding protocol was approved by the research ethics board of the Charite-Universitätsmedizin, Berlin (IRB approval EA2/126/07). Isolation of mesenchymal stem cells from aged individuals was approved under the Southampton and South West Hampshire Local Research Ethics Committee (LREC 194/99). The Ethics commission of the medical faculty at Heinrich Heine University Düsseldorf also approved this study (Study number: 5013).

Consent for publication
Not applicable.

Competing interests
The authors declare that they have no competing interest.

Publisher's Note

Author details
[1]Institute for Stem Cell Research and Regenerative Medicine, Medical Faculty, Heinrich Heine University, Düsseldorf, Moorenstr. 5, 40225 Düsseldorf, Germany. [2]Division of Paediatric Stem Cell Therapy, Clinic for Pediatric Oncology, Hematology and Clinical Immunology, Medical Faculty, Heinrich Heine University, Düsseldorf, Moorenstr. 5, 40225 Düsseldorf, Germany. [3]Institute for Transplantation Diagnostics and Cell Therapeutics, Heinrich Heine University Hospital, Moorenstr, 5, 40225 Düsseldorf, Germany. [4]Bone and Joint Research Group, Centre for Human Development, Stem Cells and Regeneration, Institute of Developmental Sciences, University of Southampton, Southampton SO16 6YD, UK.

Received: 2 October 2018 Revised: 14 February 2019
Accepted: 6 March 2019 Published online: 18 March 2019

References
1. Bianco P, Robey PG. Skeletal stem cells. Development. 2015;142:1023–7.
2. Dominici M, Le Blanc K, Mueller I, Slaper-Cortenbach I, Marini F, Krause D, et al. Minimal criteria for defining multipotent mesenchymal stromal cells. The International Society for Cellular Therapy position statement. Cytotherapy. 2006;8:315–7.
3. Mirmalek-Sani SH, Tare RS, Morgan SM, Roach HI, Wilson DI, Hanley NA, et al. Characterization and multipotentiality of human fetal femur-derived cells: implications for skeletal tissue regeneration. Stem Cells. 2006;24:1042–53.
4. Ito H. Clinical considerations of regenerative medicine in osteoporosis. Curr Osteoporos Rep. 2014;12:230–4.
5. Zhou S, Greenberger JS, Epperly MW, Goff JP, Adler C, Leboff MS, et al. Age-related intrinsic changes in human bone-marrow-derived mesenchymal stem cells and their differentiation to osteoblasts. Aging Cell. 2008;7:335–43.
6. Moskalev AA, Shaposhnikov MV, Plyusnina EN, Zhavoronkov A, Budovsky A, Yanai H, et al. The role of DNA damage and repair in aging through the prism of Koch-like criteria. Ageing Res Rev. 2013;12:661–84.
7. Reuter S, Gupta SC, Chaturvedi MM, Aggarwal BB. Oxidative stress, inflammation, and cancer: how are they linked? Free Radic Biol Med. 2010;49:1603–16.
8. Brink TC, Demetrius L, Lehrach H, Adjaye J. Age-related transcriptional changes in gene expression in different organs of mice support the metabolic stability theory of aging. Biogerontology. 2009;10:549–64.
9. Oreffo RO, Bord S, Triffitt JT. Skeletal progenitor cells and ageing human populations. Clin Sci (Lond). 1998;94:549–55.
10. Stolzing A, Scutt A. Age-related impairment of mesenchymal progenitor cell function. Aging Cell. 2006;5:213–24.
11. Wagner W, Bork S, Horn P, Krunic D, Walenda T, Diehlmann A, et al. Aging and replicative senescence have related effects on human stem and progenitor cells. PLoS One. 2009;4:e5846.
12. Nasu A, Ikeya M, Yamamoto T, Watanabe A, Jin Y, Matsumoto Y, et al. Genetically matched human iPS cells reveal that propensity for cartilage and bone differentiation differs with clones, not cell type of origin. PLoS One. 2013;8:e53771.
13. Frobel J, Hemeda H, Lenz M, Abagnale G, Joussen S, Denecke B, et al. Epigenetic rejuvenation of mesenchymal stromal cells derived from induced pluripotent stem cells. Stem Cell Reports. 2014;3:414–22.
14. Zhao C, Ikeya M. Generation and applications of induced pluripotent stem cell-derived mesenchymal stem cells. Stem Cells Int. 2018:9601623.
15. Lapasset L, Milhavet O, Prieur A, Besnard E, Babled A, Aït-Hamou N, et al. Rejuvenating senescent and centenarian human cells by reprogramming through the pluripotent state. Genes Dev. 2011;25:2248–53.
16. Miller JD, Ganat YM, Kishinevsky S, Bowman RL, Liu B, Tu EY, et al. Human iPSC-based modeling of late-onset disease via progerin-induced aging. Cell Stem Cell. 2013;13:691–705.
17. Suhr ST, Chang EA, Tjong J, Alcasid N, Perkins GA, Goissis MD, et al. Mitochondrial rejuvenation after induced pluripotency. PLoS One. 2010;5:e14095.
18. Chen YS, Pelekanos RA, Ellis RL, Horne R, Wolvetang EJ, Fisk NM. Small molecule mesengenic induction of human induced pluripotent stem cells to generate mesenchymal stem/stromal cells. Stem Cells Transl Med. 2012;1:83–95.
19. Kimbrel EA, Kouris NA, Yavanian GJ, Chu J, Qin Y, Chan A, et al. Mesenchymal stem cell population derived from human pluripotent stem cells displays potent immunomodulatory and therapeutic properties. Stem Cells Dev. 2014;23:1611–24.
20. Cheung HH, Liu X, Canterel-Thouennon L, Li L, Edmonson C, Rennert OM. Telomerase protects werner syndrome lineage-specific stem cells from premature aging. Stem Cell Reports. 2014;2:534–46.
21. Hu GW, Li Q, Niu X, Hu B, Liu J, Zhou SM, et al. Exosomes secreted by human-induced pluripotent stem cell-derived mesenchymal stem cells attenuate limb ischemia by promoting angiogenesis in mice. Stem Cell Res Ther. 2015;6:10.
22. Megges M, Geissler S, Duda GN, Adjaye J. Generation of an iPS cell line from bone marrow derived mesenchymal stromal cells from an elderly patient. Stem Cell Res. 2015;15:565–8.

23. Yang X, Tare RS, Partridge KA, Roach HI, Clarke NM, Howdle SM, et al. Induction of human osteoprogenitor chemotaxis, proliferation, differentiation, and bone formation by osteoblast stimulating factor-1/pleiotrophin: osteoconductive biomimetic scaffolds for tissue engineering. J Bone Miner Res. 2003;18:47.
24. Leuning DG, Reinders ME, Li J, Peired AJ, Lievers E, de Boer HC, et al. Clinical-grade isolated human kidney perivascular stromal cells as an organotypic cell source for kidney regenerative medicine. Stem Cells Transl Med. 2017;6(2):405–18.
25. Park GC, Song JS, Park HY, Shin SC, Jang JY, Lee JC, et al. Role of fibroblast growth Factor-5 on the proliferation of human tonsil-derived mesenchymal stem cells. Stem Cells Dev. 2016;25:1149–60.
26. Megges M, Oreffo RO, Adjaye J. Episomal plasmid-based generation of induced pluripotent stem cells from fetal femur-derived human mesenchymal stromal cells. Stem Cell Res. 2016;16:128–32.
27. Yu J, Chau KF, Vodyanik MA, Jiang J, Jiang Y. Efficient feeder-free episomal reprogramming with small molecules. PLoS One. 2011;6:e17557.
28. Gao Y, Yang L, Chen L, Wang X, Wu H, Ai Z, et al. Vitamin C facilitates pluripotent stem cell maintenance by promoting pluripotency gene transcription. Biochimie. 2013;95:2107–13.
29. Hossini AM, Megges M, Prigione A, Lichtner B, Toliat MR, Wruck W, et al. Induced pluripotent stem cell-derived neuronal cells from a sporadic Alzheimer's disease donor as a model for investigating AD-associated gene regulatory networks. BMC Genomics. 2015;16:84.
30. Takahashi K, Tanabe K, Ohnuki M, Narita M, Ichisaka T, Tomoda K, et al. Induction of pluripotent stem cells from adult human fibroblasts by defined factors. Cell. 2007;131:861–72.
31. Müller FJ, Schuldt BM, Williams R, Mason D, Altun G, Papapetrou EP, et al. A bioinformatic assay for pluripotency in human cells. Nat Methods. 2011;8:315–7.
32. Ihaka R, Gentleman RR. A language for data analysis and graphics. J Comput Graph Stat. 1996;5:299–314.
33. Gentleman RC, Carey VJ, Bates DM, Bolstad B, Dettling M, Dudoit S, et al. Bioconductor: Open Software Development for Computational Biology and Bioinformatics. Genome Biol. 2004;5:R80.
34. Du P, Kibbe WA, Lin SM. Lumi: a pipeline for processing Illumina microarray. Bioinformatics. 2008;24:1547–8.
35. Chen H, Boutros PC. VennDiagram: a package for the generation of highly-customizable Venn and Euler diagrams in R. BMC Bioinformatics. 2011;12:35.
36. Warnes GR., Bolker B, Bonebakker L, Gentleman R, Huber W, Liaw A et al. Gplots: Various R Programming Tools for Plotting Data. http://CRAN.R-project.org/package=gplots. 2015. Accessed 13 Mar 2019.
37. Ashburner M, Ball CA, Blake JA, Botstein D, Butler H, Cherry JM, et al. Gene ontology: tool for the unification of biology. The Gene Ontology Consortium. Nat Genet. 2000;25:25–9.
38. Smyth GK. Linear models and empirical Bayes methods for assessing differential expression in microarray experiments. Stat Appl Genet Mol Biol. 2004;3:Article3.
39. Storey JD. A direct approach to false discovery rates. J R Stat Soc: Series B Stat Methodol. 2002;64:479–98.
40. Huang DW, Sherman BT, Lempicki RA. Systematic and integrative analysis of large gene lists using DAVID bioinformatics resources. Nat Protoc. 2009;4:44–57.
41. Chatr-Aryamontri A, Oughtred R, Boucher L, Rust J, Chang C, Nadine K, et al. The BioGRID Interaction Database: 2017 Update. Nucleic Acids Res. 2017;45:D369–79.
42. Butts CT. Network: a package for managing relational data in R. J Stat Softw. 2008;24:1–36
43. Csardi G, Nepusz Z. The Igraph Software Package for complex network research. Inter J Complex Syst. 2006;1695:1–9.
44. Liu Y, Goldberg AJ, Dennis JE, Gronowicz GA, Kuhn LT. One-step derivation of mesenchymal stem cell (MSC)-like cells from human pluripotent stem cells on a fibrillar collagen coating. PLoS One. 2012;7:e33225.
45. Diederichs S, Tuan RS. Functional comparison of human-induced pluripotent stem cell-derived mesenchymal cells and bone marrow-derived mesenchymal stromal cells from the same donor. Stem Cells Dev. 2014;23:1594–610.
46. Sheyn D, Ben-David S, Shapiro G, De Mel S, Bez M, Ornelas L, et al. Human induced pluripotent stem cells differentiate into functional mesenchymal stem cells and repair bone defects. Stem Cells Transl Med. 2016;5:1447–60.
47. Wang X, Kimbrel EA, Ijichi K, Paul D, Lazorchak AS, Chu J, et al. Human ESC-derived MSCs outperform bone marrow MSCs in the treatment of an EAE model of multiple sclerosis. Stem Cell Reports. 2014;3:115–30.
48. Lian Q, Zhang Y, Zhang J, Zhang HK, Wu X, Zhang Y, et al. Functional mesenchymal stem cells derived from human induced pluripotent stem cells attenuate limb ischemia in mice. Circulation. 2010;121:1113–23.
49. Gonzalo-Gil E, Pérez-Lorenzo MJ, Galindo M, Díaz de la Guardia R, López-Millán B, Bueno C, et al. Human embryonic stem cell-derived mesenchymal stromal cells ameliorate collagen-induced arthritis by inducing host-derived indoleamine 2,3 dioxygenase. Arthritis Res Ther. 2016;18:77.
50. Spitzhorn LS, Kordes C, Megges M, Sawitza I, Götze S, Reichert D, Schulze-Matz P, Graffmann N, Bohndorf M, Wruck W, Köhler JP, Herebian D, Mayatepek E, Oreffo RO, Häussinger D, Adjaye J. Transplanted human pluripotent stem cell-derived mesenchymal stem cells support liver regeneration in Gunn rats. Stem Cells Dev. 2018; https://doi.org/10.1089/scd.2018.0010. Epub ahead of print
51. Kuhn LT, Liu Y, Boyd NL, Dennis JE, Jiang X, Xin X, et al. Developmental-like bone regeneration by human embryonic stem cell-derived mesenchymal cells. Tissue Eng Part A. 2014;20:365–77.
52. Zhang J, Guan J, Niu X, Hu G, Guo S, Li Q, et al. Exosomes released from human induced pluripotent stem cells-derived MSCs facilitate cutaneous wound healing by promoting collagen synthesis and angiogenesis. J Transl Med. 2015;13:49.
53. Hawkins KE, Corcelli M, Dowding K, Ranzoni AM, Vlahova F, Hau KL, et al. Embryonic stem cell-derived mesenchymal stem cells (MSCs) have a superior neuroprotective capacity over fetal MSCs in the hypoxic-ischemic mouse brain. Stem Cells Transl Med. 2018;7:439–49.
54. Taleahmad S, Mirzaei M, Parker LM, Hassani SN, Mollamohammadi S, Sharifi-Zarchi A, et al. Proteome analysis of ground state pluripotency. Sci Rep. 2015;5:17985.
55. Freitas AA, Vasieva O, de Magalhães JP. A data mining approach for classifying DNA repair genes into ageing-related or non-ageing-related. BMC Genomics. 2011;12:27.
56. Greber B, Lehrach H, Adjaye J. Control of early fate decisions in human ES cells by distinct states of TGFbeta pathway activity. Stem Cells Dev. 2008;17:1065–77.
57. James D, Levine AJ, Besser D, Hemmati-Brivanlou A. TGFbeta/activin/nodal signaling is necessary for the maintenance of pluripotency in human embryonic stem cells. Development (Cambridge, England). 2005;132:1273–82.
58. Vallier L. Cell cycle rules pluripotency. Cell Stem Cell. 2015;17:131–2.
59. Gonzales KA, Liang H, Lim YS, Chan YS, Yeo JC, Tan CP, et al. Deterministic restriction on pluripotent state dissolution by cell-cycle pathways. Cell. 2015;162:564–79.
60. Mlody B, Wruck W, Martins S, Sperling K, Adjaye J. Nijmegen breakage syndrome fibroblasts and iPSCs: cellular models for uncovering disease-associated signaling pathways and establishing a screening platform for anti-oxidants. Sci Rep. 2017;7:Article 7516.
61. Eggermann T, Binder G, Brioude F, Maher ER, Lapunzina P, Cubellis MV, et al. CDKN1C mutations: two sides of the same coin. Trends Mol Med. 2014;20:614–22.
62. Andrews SC, Wood MD, Tunster SJ, Barton SC, Surani AM, John RM. Cdkn1c (p57Kip2) is the major regulator of embryonic growth within its imprinted domain on mouse distal chromosome 7. BMC Dev Biol. 2007;7:53.
63. Pullmann R, Juhaszova M, de Silanes IL, Kawai T, Mazan-Mamczarz K, Halushka MK, et al. Enhanced proliferation of cultured human vascular smooth muscle cells linked to increased function of RNA-binding protein HuR. J Biol Chem. 2005;280:22819–26.
64. Okano M, Bell DW, Haber DA, Li E. DNA methyltransferases Dnmt3a and Dnmt3b are essential for de novo methylation and mammalian development. Cell. 1999;99:247–57.
65. Ciccarone F, Malavolta M, Calabrese R, Guastafierro T, Bacalini MG, Reale A, et al. Age-dependent expression of DNMT1 and DNMT3B in PBMCs from a large European population enrolled in the MARK-AGE study. Aging Cell. 2016;15:755–65.
66. Tsay HJ, Wang P, Wang SL, Ku HH. Age-associated changes of superoxide dismutase and catalase activities in the rat brain. J Biomed Sci. 2000;7:466–74.
67. Saxton RA, Sabatini DM. mTOR signaling in growth, metabolism, and disease. Cell. 2017;168:960–76.
68. Baugé C, Girard N, Lhuissier E, Bazille C, Boumediene K. Regulation and role of TGFβ signaling pathway in aging and osteoarthritis joints. Aging and Disease. 2014;5:394–405.
69. Ruiz-León Y, Pascual A. Regulation of Beta-amyloid precursor protein expression by brain-derived neurotrophic factor involves activation of both the Ras and phosphatidylinositide 3-kinase signalling pathways. J Neurochem. 2004;88:1010–8.
70. Silhol M, Bonnichon V, Rage F, Tapia-Arancibia L. Age-related changes in brain-derived neurotrophic factor and tyrosine kinase receptor isoforms in the hippocampus and hypothalamus in male rats. Neuroscience. 2005;132:613–24.

71. Rocha CR, Lerner LK, Okamoto OK, Marchetto MC, Menck CF. The role of DNA repair in the pluripotency and differentiation of human stem cells. Mutat Res. 2013;752:25–35.
72. Hwang JH, Shim SS, Seok OS, Lee HY, Woo SK, Kim BH, et al. Comparison of cytokine expression in mesenchymal stem cells from human placenta, cord blood, and bone marrow. J Korean Med Sci. 2009;24:547–54.
73. Potian JA, Aviv H, Ponzio NM, Harrison JS, Rameshwar P. Veto-like activity of mesenchymal stem cells: functional discrimination between cellular responses to alloantigens and recall antigens. J Immunol. 2003;171:3426–34.
74. Aggarwal S, Pittenger MF. Human mesenchymal stem cells modulate allogeneic immune cell responses. Blood. 2005;105(4):1815–22.
75. Kalfalah F, Seggewiß S, Walter R, Tigges J, Moreno-Villanueva M, Bürkle A, et al. Structural chromosome abnormalities, increased DNA strand breaks and DNA strand break repair deficiency in dermal fibroblasts from old female human donors. Aging (Albany NY). 2015;7:110–22.
76. Katagiri W, Osugi M, Kawai T, Hibi H. First-in-human study and clinical case reports of the alveolar bone regeneration with the secretome from human mesenchymal stem cells. Head Face Med. 2016;12:5.
77. Kawai T, Katagiri W, Osugi M, Sugimura Y, Hibi H, Ueda M. Secretomes from bone marrow-derived mesenchymal stromal cells enhance periodontal tissue regeneration. Cytotherapy. 2015 Apr;17:369–81.
78. Jeansson M, Gawlik A, Anderson G, Li C, Kerjaschki D, Henkelman M, et al. Angiopoietin-1 is essential in mouse vasculature during development and in response to injury. J Clin Invest. 2011;121:2278–89.
79. Pérez-Gómez E, Jerkic M, Prieto M, Del Castillo G, Martín-Villar E, Letarte M, et al. Impaired wound repair in adult endoglin heterozygous mice associated with lower NO bioavailability. J Invest Dermatol. 2014;134:247–55.
80. Sun H, Mi X, Gao N, Yan C, Yu FS. Hyperglycemia-suppressed expression of Serpine1 contributes to delayed epithelial wound healing in diabetic mouse corneas. Invest Ophthalmol Vis Sci. 2015;56:3383–92.
81. Marzano F, Ventura A, Caratozzolo MF, Aiello I, Mastropasqua F, Brunetti G, et al. The p53 family member p73 modulates the proproliferative role of IGFBP3 in short children born small for gestational age. Mol Biol Cell. 2015; 26:2733–41.
82. Qu F, Wang J, Xu N, Liu C, Li S, Wang N, et al. WNT3A modulates chondrogenesis via canonical and non-canonical Wnt pathways in MSCs. Front Biosci (Landmark Ed). 2013;18:493–503.

3.6 Stem Cell Therapy

Nina Graffmann, Lucas-Sebastian Spitzhorn, Soraia Martins, Md Shaifur Rahman, Lisa Nguyen, James Adjaye

Abstract

Stem cell therapy and regenerative medicine have a tremendous potential for the treatment of a wide variety of currently fatal diseases. So far, routine stem cell-based therapies are limited to the treatment of hematologic and dermatologic malignancies, but the field is continuously evolving. One research focus lies on mesenchymal stem cells (MSCs) which have an immunomodulatory potential and support regenerative processes throughout the body. Pluripotent stem cells, on the other hand, can be differentiated into every cell type and might be able to replace damaged tissue in the future. Currently, stem cell based clinical trials are ongoing for a broad range of diseases affecting every organ, and the number of therapies that are obtaining approval, at least in certain countries, is continuously increasing. In this chapter we summarize the current state of research regarding stem cell-based therapies. We introduce stem cell sources along with selected indications for their use and relevant clinical trials. We discuss options as well as limitations and risks of these treatments.

Publication Status: Published In: Hock F., Gralinski M. (eds) Drug Discovery and Evaluation: Methods in Clinical Pharmacology. Springer, Cham. ISBN : 978-3-319-56637-5.
Impact Factor: NA
This article is reproduced with permission.
Approximated total share of contribution: 10%
Contribution on experimental design, realization and publication: MSR was responsible for the section “Skin defects”. All authors have read and approved the manuscript.

Publication link: https://link.springer.com/referenceworkentry/10.1007%2F978-3-319-56637-5_72-1

Stem Cell Therapy

Nina Graffmann, Lucas-Sebastian Spitzhorn, Soraia Martins, Md Shaifur Rahman, Lisa Nguyen, and James Adjaye

Contents

Abstract

Stem cell therapy and regenerative medicine have a tremendous potential for the treatment of a wide variety of currently fatal diseases. So far, routine stem cell based therapies are limited to the treatment of hematologic and dermatologic malignancies, but the field is continuously evolving. One research focus lies on mesenchymal stem cells (MSCs) which have an immunomodulatory potential and support regenerative processes throughout the body. Pluripotent stem cells, on the other hand, can be differentiated into every cell type and might be able to replace damaged tissue in the future. Currently, stem cell based clinical trials are ongoing for a broad range of diseases affecting every organ, and the number of therapies that are obtaining approval, at least in

N. Graffmann · L.-S. Spitzhorn · S. Martins · M. S. Rahman · L. Nguyen · J. Adjaye (✉)
Institute for Stem Cell Research and Regenerative Medicine, Heinrich Heine University, Düsseldorf, Germany
e-mail: Nina.Graffmann@med.uni-duesseldorf.de; Lucas-Sebastian.Spitzhorn@med.uni-duesseldorf.de; Soraia.Martins@med.uni-duesseldorf.de; Shaifur.Rahman@med.uni-duesseldorf.de; Lisa.Nguyen@med.uni-duesseldorf.de; James.Adjaye@med.uni-duesseldorf.de

F. J. Hock, M. R. Gralinski (eds.), *Drug Discovery and Evaluation: Methods in Clinical Pharmacology*,
https://doi.org/10.1007/978-3-319-56637-5_72-1

certain countries, is continuously increasing. In this chapter we summarize the current state of research regarding stem cell based therapies. We introduce stem cell sources along with selected indications for their use and relevant clinical trials. We discuss options as well as limitations and risks of these treatments.

Introduction

It is a long-standing goal of regenerative medicine to cure diseases by replacing defective cells/tissues with healthy ones. Nowadays, with increasing improvements in stem cell technology, this dream comes closer to reality, although there are still many obstacles to overcome.

Stem cell therapy was initiated as a treatment for blood malignancies over 50 years ago and is now an integral part of handling these conditions. Preparations containing skin stem cell have been used to treat severe burns since 1981. However, for all other diseases, stem cell therapy is still at a stage of intense research with many ongoing clinical trials. New techniques for genome editing as, for example, CRISPR/cas9 (clustered regularly interspaced short palindromic repeat) or TALEN (transcription activator-like effector nucleases) have also found their way into regenerative medicine and augment hopes that genetic defects can be efficiently and routinely corrected in the future.

Stem Cell Sources

Adult and Pluripotent Stem Cells

Stem cells are undifferentiated cells capable of dividing symmetrically to maintain a stem cell pool or asymmetrically to produce terminally differentiated cells. They can be separated into pluripotent and multipotent cells according to their differentiation potential(Table 1). Pluripotent stem cells can generate every cell type of the human body, while multipotent stem cells are restricted to a few, closely related cell types. Because of their ability to replace damaged cells and restore tissues, stem cells are of major interest for the field of regenerative medicine (Chagastelles and Nardi 2011).

Stem cells can be obtained from many different sources, each associated with specific advantages and disadvantages. Usually, the disease that should be treated defines which stem cell sources are suitable and if autologous or allogeneic transplantation is needed. In the case of autologous transplantation, stem cells are obtained directly from the patient which obviates the risk of immune rejection. Cells for allogeneic transplantation are derived from an independent donor who is not necessarily related to the patient. Therefore, it is always associated with varying intensities of immune reactions and usually necessitates, at least temporarily, an immunosuppressive treatment. Although autologous stem cells are safe from an immunological point of view, they often cannot be applied due to other shortcomings. If the disease is caused by a genetic defect, all cells of the patient carry this mutation and hence are not suitable for restoring the function of the affected organ. In addition, in some conditions, there is simply not enough time for the sometimes lengthy process of isolation, purification, and potential biotechnological modification of autologous stem cells (Champlin 2003).

Pluripotent Stem Cells (PSCs)

Embryonic stem cells (ESCs), which are pluripotent, are isolated from the inner cell mass of the blastocyst during preimplantation development (Thomson et al. 1998). High expectations are evoked by these cells as they renew themselves indefinitely, do not age in culture, and can be directed in vitro to differentiate into every cell type of the human body (Chagastelles and Nardi 2011). However, their use is limited by major ethical considerations, as they can only be obtained by destroying the embryo. Regulations on the use of ESCs vary from country to country and influence research as well as cell therapy (Chagastelles and Nardi 2011; Elstner et al. 2009).

In 2006/2007 these ethical limitations were overcome, when the group of Shinya Yamanaka in Kyoto, Japan, managed to reprogram terminally

Table 1 Definitions of stem cell-related terms

Term	Definition
Regenerative medicine	An area of medicine which uses cells or biological materials to treat diseases or improve organ/tissue functions
Advanced therapy medicinal product (ATMP)	Novel class of medicinal products comprising somatic cell therapeutics, gene therapeutics, and bioengineered tissue
Stem cells	Non-committed cells which have the ability to self-renew or generate higher differentiated daughter cells
Multipotent	Adult stem cells which differentiate only into a limited number of cell types, e.g., HSCs, MSCs, and NSCs
Pluripotent	Stem cells which can give rise to all cell types of the body. Naturally, only embryonic stem cells (ESCs), which reside in the inner cell mass of the blastocyst, are pluripotent. In culture, all cells can be coerced into pluripotency by overexpression of necessary factors (induced pluripotent stem cells, iPSCs)
Hematopoietic stem cells (HSCs)	Multipotent stem cells which reside in the bone marrow and form all cells of the blood
Mesenchymal stem cells (MSCs)	Multipotent stem cells which reside in almost all tissues and can differentiate into mesodermal cell types such as osteocytes, chondrocytes, and adipocytes. They secrete a variety of factors which reduce inflammation and promote regeneration
Neural stem cells (NSCs)	Multipotent stem cells which reside in the subventricular and the subgranular zone of the adult brain can differentiate into neurons, astrocytes, and oligodendrocytes. They secrete neurotrophic factors, cytokines, and growth factors
Holoclones	Subset of skin stem cells, with high proliferative and self-renewal potential
Gene editing	Molecular technique (e.g., zinc-finger nucleases, TALENs, and CRISPR/Cas9) for changing the DNA sequence in order to alter a gene's function or expression level
Autologous transplantation	Transplantation of cells that are taken from the patient
Allogeneic transplantation	Transplantation of cells which are taken from an independent donor
Good manufacturing practice (GMP)	(Inter)national rules to ensure high and consistent quality of medicinal products
Graft-versus-host disease (GvHD)	Potentially life-threatening conditions after HSC transplantation, where donor-derived immune cells attack cells from the patient

differentiated murine and later also human cells into pluripotent stem cells. These so-called induced pluripotent stem cells (iPSCs) can be generated by overexpressing a cocktail of pluripotency-associated transcription factors in somatic cells which eventually resets these cells into an undifferentiated state (Takahashi et al. 2007). This was a major breakthrough in the field of stem cell research and was honored in 2012 with the Nobel Prize in Physiology or Medicine for Yamanaka (shared with John B. Gurdon) (Fig. 1).

Today, almost every cell type has been successfully reprogrammed, and the technique itself has been optimized in order to increase efficiency as well as safety. In the earliest experiments, retroviruses were employed to overexpress the pluripotency factors. However, as retroviruses randomly integrate into the genome, they can potentially induce cancer formation if, for example, their integration destroys a tumor-suppressor gene or activates an oncogene. Nowadays, reprogramming is usually performed by using non-integrating episomal plasmids or Sendai viruses (Abu-Dawud et al. 2018). Nonetheless, undifferentiated PSCs still might elicit tumors in the recipient, simply because of their proliferative

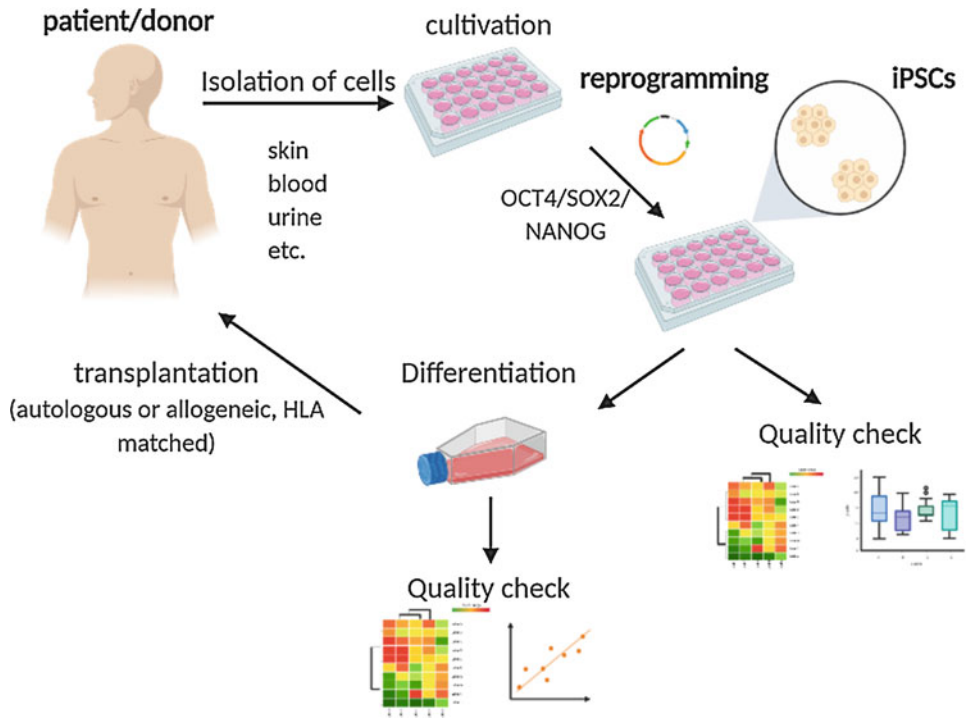

Fig. 1 Generation of iPSCs and their use as a potential cell therapeutics. Somatic cells are isolated from a donor, cultured, and reprogrammed into iPSCs. IPSCs are expanded and thoroughly checked, to ensure pluripotency and genomic integrity. Cells that pass the quality control are differentiated into the required cell type. After a quality assessment of the differentiated cells, ensuring successful differentiation and loss of pluripotent cells, the cells can be transplanted into the donor. Figure made in ©BioRender – biorender.com

potential. This is especially dangerous in the autologous setting where the transplanted cells are not recognized by the recipient's immune system. Therefore, sophisticated protocols have been established that allow efficient differentiation into all major cell types and include stringent quality controls to avoid transplantation of residual undifferentiated cells (Inoue et al. 2014).

iPSCs are associated with great anticipations for therapeutic employment as they can be generated from every patient; hence, their transplantation does not elicit immunological rejection. In addition, every given cell type can be reprogrammed which is especially interesting as it abolishes the need for invasive procedures, if, for instance, urine cells are taken as a source (Table 2). However, current data raise doubts regarding feasibility as reprogramming and all associated quality controls for excluding tumorigenic potential are not only very costly but, more importantly, time-intensive. Therefore, currently efforts are made to establish banks of iPSCs with homozygous HLA types in order to provide tolerable cells for a major part of the population. Japan with its very homogenous population is at the forefront of this and aims at having covered most of its population by 2030 (Kim et al. 2017).

Adult Multipotent Stem Cells

Hematopoietic Stem Cells (HSCs)

HSCs reside in specific niches in the bone marrow (BM) and can differentiate into all cells of the hematopoietic system. For transplantation, either they are isolated directly from BM aspirates, or they are collected by apheresis from peripheral blood after mobilization with granulocyte colony-stimulating factor (G-CSF). In both cases, the surface marker cluster of differentiation (CD)

Table 2 Ongoing clinical trials using PSCs listed at https://clinicaltrials.gov/ in August 2019

Disease	Therapy	Study ID	Sponsor	Country	Start
Spinal cord injury	ESC-derived OPCs	NCT01217008	Asterias Biotherapeutics	USA	2010
Stargardt macular dystrophy	hESC-derived RPE	NCT01345006	Astellas Institute for Regenerative Medicine	USA	2011
Dry AMD	hESC-derived RPE	NCT01344993	Astellas Institute for Regenerative Medicine	USA	2011
Stargardt macular dystrophy	hESC-derived RPE	NCT01469832	Astellas Institute for Regenerative Medicine	UK	2011
Dry AMD	hESC-derived RPE	NCT01674829	CHABiotech CO., Ltd	Korea	2012
Stargardt macular dystrophy	hESC-derived RPE	NCT01625559	CHABiotech CO., Ltd	Korea	2012
Exudative AMD	Autologous iPSC-derived RPE	UMIN000011929	RIKEN	Japan	2013
Spinal cord injury	ESC-derived OPCs	NCT02302157	Asterias Biotherapeutics	USA	2014
Ischemic heart disease	ESC derived $CD15^+$ $Isl\text{-}1^+$ progenitors	NCT02057900	Assistance Publique – Hôpitaux de Paris	France	2014
Type 1 diabetes mellitus	VC-01 combination product (device loaded with ESC-derived β-like cells)	NCT02239354	ViaCyte, California Institute for Regenerative Medicine (CIRM)	Canada, USA	2014
Dry AMD	hESC-derived RPE	NCT02286089	BioTime Inc.	Israel, USA	2015
Retinitis pigmentosa	hESC-derived RPE	ChiCTR-OCB-15007055	Institute of Zoology, Chinese Academy of Sciences	China	2015
Stargardt macular dystrophy, AMD, exudative AMD	hESC-derived RPE	NCT02903576	Federal University of São Paulo	Brazil	2015
AMD	hESC-derived RPE	NCT01691261	Pfizer	UK	2015
Dry AMD	hESC-derived RPE	NCT02590692	Regenerative Patch Technologies	USA	2015
AMD, Stargardt macular dystrophy	hESC-derived RPE	NCT02749734	Southwest Hospital, China	China	2015
PD	Human parthenogenetic neural stem cells	NCT02452723	Cyto Therapeutics Pty Limited	Australia	2016
Dry AMD	hESC-derived RPE	ChiCTR-OCB-15007054	Institute of Zoology, Chinese Academy of Sciences	China	2016
GvHD	CYP-001: iMSCs	NCT02923375	Cynata Therapeutics Ltd.	Australia, UK	2016
PD	ESC-derived NPC	NCT03119636	Chinese Academy of Sciences	China	2017
Dry AMD	hESC-derived RPE	NCT03046407	Chinese Academy of Sciences	China	2017
Neovascular AMD	Allogenic iPSC-derived RPE	UMIN000026003	Kobe City Medical Center General Hospital	Japan	2017

(*continued*)

Table 2 (continued)

Disease	Therapy	Study ID	Sponsor	Country	Start
Type 1 diabetes mellitus	VC-02 combination product (device loaded with ESC-derived β-like cells)	NCT03162926	ViaCyte	Canada	2017
Type 1 diabetes mellitus	VC-02 combination product (device loaded with ESC-derived β-like cells)	NCT03163511	ViaCyte, California Institute for Regenerative Medicine (CIRM)	Canada, USA	2017
PD	iPSC-derived dopaminergic progenitors	UMIN000033564	Kyoto University Hospital	Japan	2018
Dry AMD	hESC-derived RPE	NCT02755428	Chinese Academy of Sciences	China	2018
ALS	hESC-derived astrocytes	NCT03482050	Kadimastem	Israel	2018
Spinal cord injury	iPSC-derived NSCs	Approved	Keio University School of Medicine	Japan	2019
Retinitis pigmentosa	hESC-derived RPE	NCT03944239	Qi Zhou	China	2019
Retinitis pigmentosa due to monogenic mutation	hESC-derived RPE	NCT03963154	Centre d'Etude des Cellules Souches	France	2019
Heart failure	Allogenic iPSC-derived cardiomyocytes	NCT03763136	Help Therapeutics	China	2019
meniscus injury	hESC-derived MSC like cell	NCT03839238	Tongji Hospital	China	2019

34 can be used to separate HSCs from other cell types (Panch et al. 2017).

A third source of HSCs is the umbilical cord which contains stem cells in addition to very naïve immune cells. These cells can be collected directly after birth and are in contrast to HSCs from BM or apheresis frequently stored in liquid nitrogen for usage in the far future (Panch et al. 2017). Parents can choose to store the umbilical cord blood (UCB) either in public banks making it available for everyone or in private banks where it is kept exclusively for the donating family who also has to cover the costs. At the moment about six times more UCB units are stored in private banks than in public ones although the vast majority of UCB units used for transplantation are released by public banks (Ballen et al. 2015).

Routine allogeneic transplantation of HSCs only became possible after the human leukocyte antigen (HLA) system, which is fundamental for the function of the human immune system, was understood (Klein and Sato 2000; van Rood 1966). Nowadays, great efforts are undertaken to ensure that donor and recipient HLA type match in order to reduce the risk of graft-versus-host disease (GvHD) (Klein and Sato 2000). In this potentially life-threatening condition, donor-derived immune cells attack not only residual tumor cells in the recipient but also healthy tissue. Symptoms are ranging from rather mild skin reddening and itching toward massive damage of the gastrointestinal tract or the liver and always need special immunosuppressive treatments. If GvHD occurs in the first 100 days after transplantation, it is classified as acute and later as chronic. Over time, the new immune system is capable to adapt to the recipient's tissue surface antigens, and symptoms recede.

Mesenchymal Stem Cells (MSCs)

In 1924, Alexander A. Maximow identified cells residing within the bone marrow (BM) which had some similarities to fibroblasts. These cells were described to support hematopoiesis, the

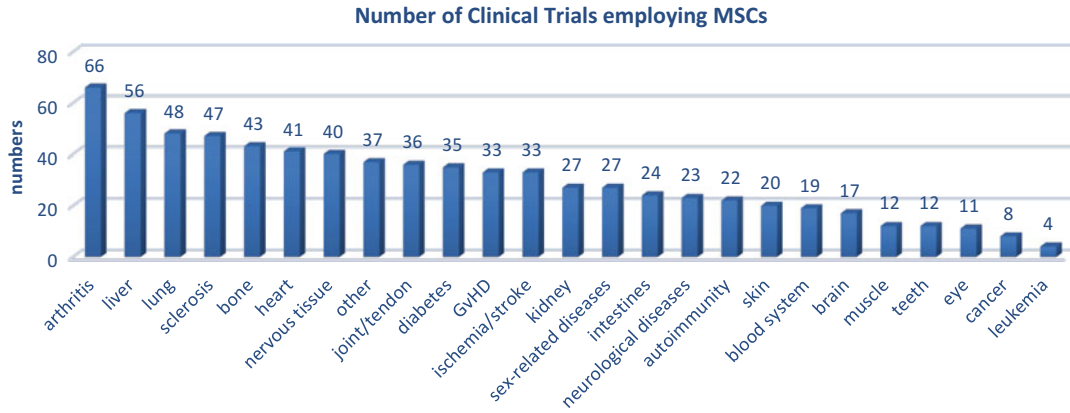

Fig. 2 Use of MSCs in clinical trials. Information on over 740 clinical trials using MSCs have been deposited at https://clinicaltrials.gov/ in March 2019

generation of blood cells (Maximow 1924). By exploiting their ability of plastic adherence, Friedenstein and colleagues isolated these cells from BM (Friedenstein et al. 1970). The term "mesenchymal stem cells" (MSCs) was established by Arnold I. Caplan in the 1990s (Caplan 1991). Although in the beginning MSCs were exclusively isolated from the perivascular region of the BM, several other sources for MSCs have been established in recent years: placenta, umbilical cord blood (UCB), heart, skin, pancreas, lung, brain, kidney, adipose tissue, cartilage, tendon, as well as amniotic fluid and urine (Wu et al. 2018; Fitzsimmons et al. 2018; Spitzhorn et al. 2017; Rahman et al. 2018).

In addition to their extensive in vitro proliferation potential, MSCs exhibit a multipotential differentiation capacity which manifests in their ability to form various cell types from the mesodermal lineage including the cartilage, bone, and fat (Fitzsimmons et al. 2018). In vitro, they can also differentiate in cell types from other lineages such as pancreatic β cells or cardiomyocytes, although it is controversially discussed if this happens in vivo, too (Segers and Lee 2008; Cho et al. 2018). The fate-determining decision is triggered by various factors such as cytokines and growth factors present in the stem cell niche – a distinct microenvironment in which the stem cells are located (Fitzsimmons et al. 2018).

MSCs exhibit a fibroblast-like, spindle-shaped morphology. They are characterized by the expression of specific cell surface markers (also referred to as immunophenotype) such as CD73, CD90, and CD105 and the of lack hematopoietic markers. Together with their differentiation capacity and their plastic adherence, these features were set as the minimal criteria to identify MSCs by the international society for cellular therapy (ISCT) (Dominici et al. 2006). MSCs also have the ability to secrete various cytokines and growth factors. Thus, they can support hematopoiesis in the BM and are able to suppress reactions of the immune system. They support regeneration processes by the release of distinct molecules, for example, vascular endothelial growth factor A (VEGF-A), hepatic growth factor (HGF), platelet-derived growth factor (PDGF), and various interleukins (Fitzsimmons et al. 2018). Furthermore, MSCs can react to factors released by the environment. They migrate to sites of inflammation or injury to support the regeneration process. As MSCs express only very low levels of HLA, they can be transplanted even without matching their HLA type to that of the patient (Fitzsimmons et al. 2018).

To investigate their therapeutic potential, MSCs have been employed in over 740 clinical trials (ongoing or completed) for a broad range of diseases and organs affected which underlines their versatility (Fig. 2).

In most clinical trials, MSCs from adult BM are used followed by the adipose tissue, umbilical cord tissue, and placenta (Galipeau and Sensebe

Table 3 Approved MSC-based therapies (aliancerm.org)

Product	Company	Indication	Treatment	Approval	Country
Queencell	Anterogen Co., Ltd.	Connective tissue disorders	Autologous adipose tissue MSCs	2010	South Korea
Cellgram-AMI	Pharmicell	AMI	Autologous BM-MSCs	2011	South Korea
Cupistem	Anterogen Co., Ltd.	Perianal fistula in Crohn's disease	Autologous adipose tissue MSCs	2012	South Korea
Cartistem	Medipost	Knee cartilage defects	Allogeneic UCB-MSC	2012	South Korea
Prochymal	Mesoblast Inc.	GvHD	Allogeneic BM-MSCs	2013	Canada, New Zealand
Neuronata-R	Corestem Inc.	ALS	Autologous BM-MSCs	2014	South Korea
Temcell HS	JCR Pharmaceuticals Co., Ltd.	GvHD	Allogeneic BM-MSCs	2015	Japan
Stempeucel	Stempeutics Research Pvt	Critical limb ischemia	Allogeneic BM-MSC	2017	India
Alofisel	TiGenix NV, Takeda Ltd.	Perianal fistulas in Crohn's disease	Allogeneic adipose tissue MSCs	2018	EU
Stemirac	Nipro Corp	Spinal cord injury	Autologous BM-MSC	2018	Japan
Neuronata-R	Corestem Inc.	ALS	Autologous BM-MSCs	2018	USA, orphan drug
Neuronata-R	Corestem Inc.	ALS	Autologous BM-MSCs	2019	EU, orphan drug

2018). The most prevalent way of administration is intravenously. This is very critical, because cell aggregation after infusion is one of the most prevalent adverse effects of MSC treatments (Caplan et al. 2019). MSCs are thawed immediately prior to transfusion. This is also a key step since it is well-known that the fitness of MSCs declines within the first 24 h after thawing which could impair their function (Caplan et al. 2019).

Despite the plethora of MSC-based clinical trials, so far worldwide only a few products based on MSCs have obtained clinical approval (Table 3).

MSC-Based Clinical Trials

In 1995 MSCs were the first cellular pharmaceutical tested in human. They were isolated from the BM of patients with hematologic malignancies in complete remission and reinfused intravenously (Lazarus et al. 1995). This study confirmed the safety of autologous MSC transplantation.

Later, MSCs were used in clinical trials to support hematopoietic recovery following high-dose myeloablative chemotherapy and accelerating hematopoiesis after BM transplantation (Fitzsimmons et al. 2018). The immunosuppressive capacity of MSCs is frequently used as a support in other transplantation settings, to reduce the risk of organ rejection or GvHD, especially if the HLA types of perfectly donor and recipient are not perfectly matching (Fitzsimmons et al. 2018).

In 2009, the first major industry-sponsored (Osiris Therapeutics (USA)) phase III trial of allogeneic MSCs for treatment of steroid-refractory GvHD (NCT00366145) was completed. Although it did not show an overall significant positive effect of the MSCs, it demonstrated that children with GvHD were responsive to this cellular treatment (Kurtzberg et al. 2014). In 2013, the therapeutic called Prochymal/remestemcel-L was conditionally approved in Canada and New Zealand for application in children with an obligation to prove its efficacy. Mesoblast Inc.

(Australia) took over the MSC therapeutic agents and focused on the prospective phase III trial (NCT00759018) (Kurtzberg et al. 2014). The overall response in the children 28 days after treatment was significantly improved in comparison to control patients. In Canada reimbursement issues prevented establishment as a common clinical treatment. In Japan on the other hand, the MSC therapy for GvHD and a proper reimbursement were approved and installed as Temcell in 2015 (JCR Pharmaceuticals Co. 2017).

For treating patients with complex perianal fistulas without inflammatory bowel disease, Cellerix S.A. sponsored a study of autologous adipose MSCs (NCT00475410). Forty-eight hours after thawing, the cells were injected in the area of the fistula. The outcome of the MSC group was not superior to the control group. After Cellerix S.A. was acquired by TiGenix NV in 2011, a new phase III clinical trial was initiated (NCT01541579), treating only Crohn's disease patients with an increased dose of allogeneic cells. The group receiving MSCs significantly improved their condition in comparison to the control group. The results disclosed in 2015 were reported to be the first completely successful outcome of MSCs in a clinical trial of an advanced state (Panés et al. 2016). The product, named Alofisel, was EMA approved first in 2009 as an orphan drug until it obtained full approval in 2018. A similar product, called Cupistem, got approval in South Korea.

The highest number of clinical trials with MSCs targets bone and cartilage diseases, for example, osteogenesis imperfecta, a genetic disorder which is characterized by mutations in the genes *collagen type I alpha 1 chain* (*COL1A)1* and *2*. This leads to osteopenia, multiple fractures, severe bone deformities, and considerably shortened stature. The first clinical trial to address this used allogeneic BM (containing MSCs) in children. It was shown that MSCs could migrate to the bone and improve bone structure (Horwitz et al. 1999). In a special case of such a treatment in 2005, allogeneic MSCs were transplanted in utero into a fetus with severe osteogenesis imperfecta. Within the first 2 years, only three fractures occurred, and correct growth tendencies as well as normal psychomotoric behavior were reported. At the age of 8 years, the same patient was treated again with MSCs of the same donor resulting in low-level beneficial outcome. This study has shown long-term safety, but still more work has to be done to unravel the effectiveness (Gotherstrom et al. 2014).

In patients suffering from osteoarthritis (OA), the articular cartilage is degenerated, and subchondral bone sclerosis and synovial inflammation lead to pain in the joints, local inflammations, and restricted movement. Intense research and many clinical trials are performed in this field, with limited positive outcome. In general, patients reported less pain and improved mobility after treatment, and improved cartilage quality could be observed, but due to study design, the evidence is not very reliable (Iijima et al. 2018). Nevertheless, South Korea approved Medipost's Cartistem in 2012, a product based on allogeneic UCB-MSCs which are plied to the joint during orthopedic surgery.

MSCs from Pluripotent Stem Cells (iMSCs)

The derivation of MSCs from BM or other sources is done routinely, but these invasive procedures are associated with certain risks (Sheyn et al. 2016). In the everyday clinical scenario with a high percentage of elderly people, the quality of MSCs is compromised due to cellular aging. This is manifested in higher levels of cellular senescence, DNA damage, oxidative stress, genomic instability, and immunogenicity which reduces their therapeutic potential (Yang 2018).

These hurdles can be bypassed by the generation of induced MSCs (iMSCs) from PSCs which have a rejuvenated phenotype (Frobel et al. 2014; Spitzhorn et al. 2019). Human iMSCs have been used in many preclinical studies for, e.g., liver and bone regeneration (Spitzhorn et al. 2018; Jungbluth et al. 2019, in press). A very important aspect for transplantation of iMSCs is the fact that although they are derived from PSCs, they are not tumorigenic and thus safe for transplantation. To date iMSCs have been successfully used in two clinical trials. Cynata Therapeutics Ltd. (Australia) is funding a phase I clinical study in which iMSCs coming from iPSCs are used for the treatment of steroid-resistant acute GvHD with preliminary

promising results (NCT02923375). The Tongji Hospital (China) in cooperation with the Chinese Academy of Sciences is running a phase I clinical trial for iMSCs generated from ESCs with the focus to evaluate the safety in treating meniscus injury patients (NCT03839238).

Neural Stem Cells (NSCs)

Neural stem cells (NSCs) are self-renewing multipotent cells with the potential to differentiate into neurons, astrocytes, and oligodendrocytes, the three main cell types in the central nervous system (CNS) (Seaberg and van der Kooy 2003). Additionally, NSCs are capable of secreting soluble molecules such as neurotrophic factors, cytokines, and growth factors. Due to these special characteristics, transplantation of NSCs is a promising treatment option for diseases associated with the CNS, for both regeneration of neural cells and restoration of the microenvironment at the injury site by providing trophic support.

First evidences of adult neurogenesis (the endogenous generation of new neurons) were described by Altman and Das in 1965 (Altman and Das 1965). In the adult brain, NSCs are confined primarily to two regions, the subventricular zone (SVZ) and the subgranular zone (SGZ). Adult neurogenesis is a dynamic but extremely coordinated process, where the proliferation, migration, and differentiation of the NSCs are controlled by microenvironmental stimuli. Although adult neurogenesis in the CNS is limited under normal physiological conditions, it can be induced after injury to recruit NSCs and reconstruct neural tissues. Unfortunately, in the case of severe injury, the response of activated NSCs is ineffective in keeping the balance between self-renewal and differentiation (Ming and Song 2011).

Cell therapy based on NSCs is now possible thanks to the comprehensive development of protocols based on growth factors to expand and differentiate these cells in vitro. NSCs can be derived from three major sources: directly extracted from primary CNS tissue (fetal and adult brain and spinal cord tissue), differentiated from pluripotent stem cells (PSCs), and through transdifferentiation from somatic cells (Tang et al. 2017).

NSCs derived from primary CNS: Human NSCs can be isolated directly from the ventricular zone of fetal brain tissue or from the SVZ of adult brain. After isolation, these cells can be propagated as single-cell suspensions that ultimately will form three-dimensional neurospheres in a medium supplemented with appropriate growth factors that allow proliferation, self-renewal, and expansion of NSCs in vitro (Gonzalez et al. 2016; Tang et al. 2017).

NSCs derived from PSCs: NSCs can be in vitro differentiated from ESCs and iPSCs via a process called neuroinduction. After this stage, NSCs can be maintained in culture in the same conditions as the NSCs directly isolated from the CNS. The use of iPSC-derived NSCs has advantages over ESC-derived NSCs since iPSCs can be generated from adult tissue, bypassing ethical issues. In addition, iPSC-derived NSCs can be obtained in a patient-specific manner, allowing autologous transplantation and thus overcoming the immune rejection (Tang et al. 2017; Gonzalez et al. 2016).

Transdifferentiation of somatic cells into NSCs: The generation of NSCs by transdifferentiation of somatic cells, a process that comprises the transformation of a somatic cell into another somatic cell type without undergoing the pluripotent stage, is a promising tool for therapeutic purposes. Although it was already shown that NPCs can be transdifferentiated from fibroblasts, urine cells, and MSCs, thus bypassing the tumorigenic potential of PSC-derived NSCs, it is a very recent field that needs further investigation (Tang et al. 2017).

Approval of Stem Cell Treatments

Stem cell therapy and regenerative medicine elicit high hopes – in patients who expect cures from a disease, as well as in industry that sees the great economic potential. This has led to the emergence of many clinics which perform unapproved stem cell treatments (Sipp et al. 2017).

The ethical and legal view on stem cells is highly divergent between countries. In the USA as well as in Europe, human cells and tissues are

mostly defined as advanced therapy technical medicinal products (ATMP). That means that they have to be approved by the US Food and Drug Administration (FDA) or the European Medicines Agency (EMA), respectively (Sakai et al. 2017). Usually this approval is only granted after thoroughly proving safety and efficacy of the treatment in controlled clinical trials. However, patients as well as industry express the need for a streamlined process which would reduce time and costs for approval. In 2014, Japan revised its law and introduced the Pharmaceuticals, Medical Devices, and Other Therapeutic Products (PMD) Act which provides conditional approval as long as the procedure has been proven to be safe. However, the new product has to prove its efficacy within 7 years. In the USA "the right to try" laws provide terminally ill patients the opportunity to test stem cell therapies before their final approval (Sakai et al. 2017). This provoked controversies as proper clinical trials are a highly valuable tool for determining safety and efficacy of novel treatments. On the other hand, many stem cell-based clinical trials (even in phase I/II) are only performed on terminally sick patients due to the high risks they are associated with, which decreases the likelihood of a positive outcome.

In parallel, a lot of unapproved stem cell therapies are on the market, many of them consisting in gaining MSCs, e.g., from liposuction and using these cells for a variety of treatments (Sipp et al. 2017; Goff et al. 2017). However, for these treatments neither safety nor efficacy has been studied in an accredited way, and in several cases there were dramatic outcomes such as severe infections or blinding (Marks et al. 2017). As clinics performing these unapproved treatments frequently advert them directly to patients with no independent physician explaining risks and benefits, they are very attractive for patients who are inclined to spend a lot of money and take incalculable risks (Sipp et al. 2017). Therefore, it is important to provide unbiased information to patients and educate the general population on risks and benefits of stem cell treatments.

Stem Cell-Based Regenerative Therapies

Hematopoietic System

From all areas of stem cell therapy, applications in the hematopoietic system have the longest history. The first allogeneic BM transplantation was performed in 1957 by E. Donnall Thomas, who paved the way for this kind of treatment and received the Nobel Prize in 1990 (Thomas et al. 1957). About 10 years after this first transplantation, techniques had developed that allowed for HLA typing, and the usage of stem cells from HLA-matched donors dramatically improved the outcomes of transplantations (Henig and Zuckerman 2014). As the HLA genotype limits the number of putative donors, international collaboration is mandatory. To this end the International Bone Marrow Transplant Registry (IBMTR) was established in 1972. The indications for HSC transplantation shifted with increasing knowledge about the diseases that are to be treated as well as with improved technologies that enable a broader spectrum of patients to be included (Little and Storb 2002).

In the beginning, predominantly hematopoietic cancers were treated with allogeneic stem cells. Later, also other blood malignancies were included, e.g., thalassemia or sickle cell anemia, and today also unrelated conditions as, e.g., solid tumors and autoimmune diseases are treated by HSC transplantation (Passweg et al. 2019).

Although therapy schemes have improved dramatically over time and the number of transplantations has increased immensely, HSC transplantation still is a very risky and stressful procedure for the patient. In a first step, the host's immune system and its stem cells have to be destroyed by irradiation and/or chemotherapy in order to remove the malignant cells. Nowadays there exist sophisticated protocols depending on the actual disease, which enable physicians to limit the destruction, especially of the stem cells, and thus allow also elder and fragile patients to undergo HSC transplantation (Gyurkocza et al. 2010). During the phase of engraftment, patients lack a functioning immune system and are very much at risk of developing

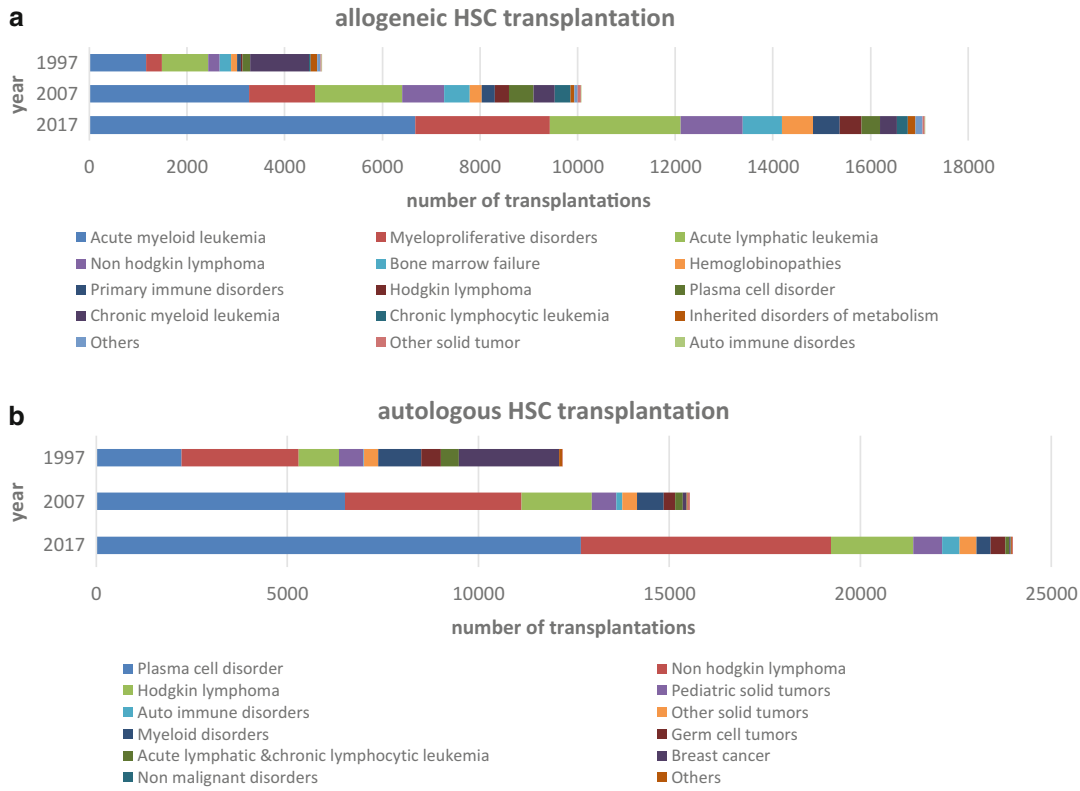

Fig. 3 Development of allogeneic (**a**) and autologous (**b**) HSC transplantation in Europe from 1997 to 2017. The number of HSC transplantations increased massively, with the frequency of distinct indications changing over time (Passweg et al. 2019)

infectious diseases. Only after the stem cells have homed into the BM niche, they efficiently produce new immune cells. However, in this phase the risk of GvHD is also augmented (Dowse and McLornan 2017) (Fig. 3).

Today, most HSCs for transplantation are collected via apheresis because this allows for a higher enrichment of stem cells, and the samples contain more T cells which are valuable for fighting the disease, called graft-versus-tumor/leukemia reaction. In addition, an increasing number of UCB transplants are performed. Although they contain less HSCs, which increases the risk of engraftment failure, their T cells are immature which reduces the risk of GvHD and allows for more HLA mismatches being present. Transplanting a combination of two independent UCB units seems to be the optimal solution in this case (Dowse and McLornan 2017; Panch et al. 2017).

Although HSC transplantation has been a routine treatment for many years, the mortality rates are still quite high. In acute leukemia it ranges between 7% and 27%, at 100 days post-allogeneic transplantation depending on disease severity. The leading causes are GvHD and infections. If patients survive for more than 2 years without relapse, their long-time survival rates are 80–92% (Henig and Zuckerman 2014).

Besides being a risky procedure, there are cases where allogeneic stem cell transplantation has additional benefits for the patients. Two patients who were infected with human immunodeficiency virus (HIV) reached remission for at least 20 and 18 months, respectively, after receiving allogeneic HSC transplants for treatment of leukemia or Hodgkin's lymphoma, respectively. Both patients were transplanted with HSCs from donors homozygous for a 32 base-pair deletion

within the *C-C chemokine receptor type 5 receptor* (*CCR5*) gene, which prevents expression of the receptor and thus precludes infection with HIV strains that need CCR5 as a co-receptor (Gupta et al. 2019).

Initial observations in the 1990s that HSC transplantation in cancer patients also improved coincidental autoimmune diseases (AD) developed this field as a new target for HSC transplantation. To date, several thousand patients have received HSC transplants (primarily autologous) to treat ADs, especially multiple sclerosis, Crohn's disease, and systemic sclerosis (Jessop et al. 2019). All ADs have in common that the patient's immune system attacks cells of its own body, leading to permanent inflammation followed by scar formation and impairment of the respective organ's function. HSC transplantation is capable of resetting the immune system, and it has been shown that after transplantation the amount of autoreactive immune cells can be reduced. However, HSC transplantation is still associated with many risks, and treatment outcome varies between patients and depends on disease severity. Nonetheless, many patients have long-term improvements, and for some ADs randomized controlled clinical trials have demonstrated the benefit of HSC transplantation compared to the best available conventional therapy (Jessop et al. 2019).

As HSC transplantation has been established a long time ago, it is also one of the fields where the most advanced techniques in terms of gene therapy are currently used. The first successful gene therapy trial was performed as early as 1990, although not targeting HSCs but T cells (Al-Saif 2019). Two patients who suffered from severe combined immune deficiency (SCID) caused by a mutation in the enzyme adenosine deaminase were included in this trial. The defective gene was exchanged for a functional copy in patients' T cells. Their blood values improved and they needed less medication after this treatment.

Current studies involve gene therapy directly in HSCs which can be performed in vivo as well as ex vivo. For in vivo gene therapy, genes are delivered to the HSCs by vectors or liposomes which can be injected into the bone or – after HSC mobilization – even intravenously. However, it has to be taken into account that these particles potentially can transfect also other cell types and frequently elicit strong immune reactions. On the other hand, they overcome transplantation-related issues as the need for chemotherapy in advance and the risk of poor engraftment. In ex vivo gene therapy, HSCs are collected from the patient and genes are modified in vitro. Besides simply overexpressing a healthy variant of the target genes, other possibilities include gene modification by applying, for example, TALENs or CRISPR/cas9. After the procedure, it is possible to selectively only transfer successfully modified cells back into the patient (Al-Saif 2019).

Currently, several clinical trials employing genetically engineered HSCs for transplantation are in progress. In sickle cell disease (SCD), a transversion of A to T within the coding region of the β-globin gene causes hemoglobin polymerization, which is associated with morphological changes of erythrocytes and impaired oxygen transport capacity. Standard treatment for SCD consists in applying hydroxyurea which increases the expression of the fetal y-globin, a molecule that prevents hemoglobin polymerization. Two gene therapies in clinical trials aim at increasing y-globin expression, either by overexpressing it directly (NCT02186418) or by inactivating a repressive factor (NCT03282656). In a different approach, a β-globin variant, which also prevents hemoglobin polymerization, is introduced into HSCs by a self-inactivating lentivirus (NCT02151526). Data from a first patient treated with this system indicate safety as well as efficacy (Al-Saif 2019).

In the future many therapy improvements are likely to be implied. One interesting novel approach concerns the field of chimeric antigen receptor (CAR) T-cell therapy. For this kind of therapy, until now, patient-derived T cells are genetically modified to express a chimeric antigen receptor specific for a tumor-related antigen. The engineered cells are then reinfused into the patient and supposed to eliminate the cancerous cells. As the whole procedure of engineering is very time-consuming, several groups are working on

protocols for differentiating iPSCs into T cells which can then be modified to express the chimeric receptor (Iriguchi and Kaneko 2019). A clinical trial with these cells has been already announced by a Japanese cooperation between the Center for iPS Cell Research and Application (CiRA) and Takeda (Kobayashi et al. 2019).

Skin Defects

The skin, the largest organ of the human body, is responsible for defending external stresses, regulating fluid retention and temperature, and mediating sensation. However, burns, infectious diseases, and inherited and acquired genetic defects of the skin affect about one billion people globally, leading to mortality and morbidity and requiring long-term hospitalization (Karimkhani et al. 2017). Keratinocyte cell-based autologous and allogeneic epithelial sheet transplantation is a clinically accepted technique, which has been used for more than 30 years to treat burned patients (Hernon et al. 2006). The clinical application of cultured epithelial allogeneic and autologous grafts to treat chronic ulcers, vitiligo, junctional epidermolysis bullosa (JEB)-non-Herlitz, JEB-Herlitz, recessive dystrophic epidermolysis bullosa (RDEB), epidermolysis bullosa (EB) simplex, and toxic epidermal necrolysis has also been reviewed (Petrof et al. 2014).

In 1975, for the first time, Rheinwald and Green isolated and cultivated human epidermal keratinocytes (the main basal cells of skin) obtained from a skin biopsy, which led to the development of cultured epithelial sheets (CEAs) (Rheinwald and Green 1975). Subsequently, in 1981 O'Connor et al. experimentally transplanted epidermal autografts to heal severe burn wounds using cultured keratinocyte clones (O'Connor and Mulliken 1981). These cells would nowadays be categorized – at least partly – as so-called holoclones, the undifferentiated colony-forming keratinocyte stem cells which have a higher growth and self-renewal potential compared to other colony-forming cell types (Barrandon and Green 1987). This type of skin equivalent graft is fabricated on a fibrin matrix where fibroblasts support the growth of an epithelial sheet containing basal and differentiated keratinocytes.

Beside the autologous keratinocyte-based therapy, promising findings were reported from a clinical trial (ten pediatric patients) using allogeneic BM-MSCs to manage second-degree burn wound healing (NCT02104713) and for the treatment of recessive dystrophic epidermolysis bullosa (RDEB) (EudraCT number 2012-001394-87, ISRCTN46615946). RDEB – a rare skin disease – results in the severe blistering of the skin, caused by a mutation in the *collagen type VII alpha 1 chain* (*COL7A1*) gene which impairs expression of the protein. In the RDEB clinical trial, patients were provided three infusions of allogeneic BM-MSCs. After 6 months of BM-MSC administration, improvement of wound healing, reduction of skin redness and blisters, and a decreased level of pain were noticed compared to the initial condition. Overall, the severity of the condition was reduced, and no substantial negative effects were reported (Petrof et al. 2015).

MSCs isolated from human UCB-MSCs are also widely studied and clinically accepted. They are in an early phase I clinical trial running until 2021 to evaluate the effect and safety for the treatment of psoriasis, a chronic and recurrent inflammatory skin disease (NCT03765957). In a case study published in 2018, injection of a MSC-containing cell preparation obtained from adipose tissue could significantly improve the condition. The mechanisms that are involved, particularly, whether and how these cells activate immune system associated growth factors and cytokines to support wound healing and reduce inflammation, are not well-understood (Comella et al. 2018).

Due to considerable progress in stem cell and genome editing technologies during the last decade, genetically engineered skin stem cell-based therapies for the treatment of fatal conditions such as Netherton syndrome (NS), junctional epidermolysis bullosa (JEB), and RDEB have found their way into experimental clinical treatments.

NS is a serious skin disorder caused by damage in the *serine peptidase inhibitor, kazal type 5* (*SPINK5*) gene that encodes a protein called

lymphoepithelial kazal-type inhibitor (LEKTI) that is responsible for the function of the skin barrier. The skin of *SPINK5*-mutated patients becomes red and scaly (ichthyosiform erythroderma). Functionally, the skin leaks fluid and loses the capacity to bind water which causes skin dryness and hypernatremic dehydration. This and other complications, e.g., bronchopneumonia or sepsis, lead to a high mortality rate in early life (Di et al. 2019).

Currently, there are no approved treatments to cure this lethal condition. Based on the principle of ex vivo gene modification in stem cells, a clinical phase I trial of grafting autologous epithelial sheets harboring intact *SPINK5* for NS has been conducted (Di et al. 2019) (NCT01545323). It proved successful in terms of gene modification and engraftment, but only transient functional correction was observed, possibly due to a limited number of stem cell holoclones within the graft.

A groundbreaking example of skin stem cell therapy is that of a child having recovered from a fatal form of JEB in Germany in 2017 after engraftment with epidermal sheets consisting of autologous skin stem cells which were genetically modified to contain healthy copies of the *Laminin Subunit Beta 3* (*LAMB3)* gene. Impressively, this *LAMB3* harboring epidermal autograft could restore dermal-epidermal adherence, and the long-lived skin stem cell holoclones could regenerate and renew the epidermis. Upon 1-month post-grafting, the new epidermis had formed without blisters, and the regenerated epidermis was strong and elastic alike healthy skin (Hirsch et al. 2017). Previously, in 2006, genetically engineered autologous keratinocyte grafts have been transplanted in a patient with laminin 332 deficiency (non-Herlitz junctional EB) (Mavilio et al. 2006). In a clinical study from Austria in 2014, genetically modified autologous epidermal sheets were grafted in an adult woman to cure from laminin 332-β3-dependent JEB with a large non-healing epidermal ulceration (Bauer et al. 2017). The transgenic epidermis expressed a normal amount of properly functional laminin 332 which is precisely located at the dermal-epidermal junction. These experimental results could benefit JEB patients with disrupted laminin 332.

The above-stated cases of JEB have demonstrated that it is possible to cure genetically damaged non-healing skin by using gene therapy in epidermal stem cells. However, for the EB simplex, which is not caused by the lack of the LAMB3 protein but by an active dysfunctional version of the protein, other approaches are necessary. Corrections with a gene-editing innovative tool like CRISPR/Cas9 might be possible. The feasibility of genome editing in skin stem cells using a self-inactivating (SIN) retroviral vector and CRISPR/Cas9 approach in a preclinical study in mice has already been reported (Hainzl et al. 2017; Izmiryan et al. 2018). Currently, this technique is also used in clinical trials in RDEB patients. The aim is to completely cure the disease using autologous skin grafts made of primary keratinocytes and fibroblasts with genetically edited type 7 collagen (NCT01263379, NCT02493816).

A special tissue composed of keratinocytes is the cornea of the eye. The integrity of this epithelial layer and the absence of blood vessels are crucial for proper vision. In a healthy setting, corneal cells are regenerated by limbal stem cells, located between the cornea and the bulbar conjunctiva. Thermal and chemical burns of the eye often destroy the limbal stem cells which results in vascularization of the cornea and ultimately vision loss (Pellegrini et al. 2009). Beginning in the late 1990s, the first patients were treated with transplants generated from limbal stem cells, and permanent restoration of the cornea was achieved in 76.6% of the cases. Importantly, a 10-year follow-up proved long-term stability of the regenerated tissue (Rama et al. 2010). The treatment relies on autologous cells which can be obtained if at least 1–2 mm intact limbal tissue is available. The cells are expanded and prepared for transplantation on a fibrin matrix. This product, marketed as Holoclar, was the first stem cell-based ATMP authorized by the European Medicines Agency in 2015.

Tremendous advancement of ESCs, iPSCs, and genome editing technology has been made during the last 10 years; now the major goal is to harness these technologies to generate unlimited amounts of genetically corrected keratinocytes not only from autologous but also from allogeneic donors.

Human PSCs can be differentiated into keratinocytes which are the basis for in vitro-generated functional epidermal sheets. These sheets could provide temporary skin substitutes for patients awaiting autografts (Guenou et al. 2009). Tolar and colleagues demonstrated that gene-corrected iPSCs could be generated from the skin of patients with a mosaic form of RDEB (Tolar et al. 2014). Compared to adult stem cells, iPSCs have a higher proliferation potential, allowing genetic manipulations and to overcome the autograft shortages. By generating iPSCs and, subsequently, iPSC-derived keratinocytes, they were able to provide proof of principle that iPSC technology can be used to generate essentially unlimited amounts of clinically normal epidermis from patients (Sebastiano et al. 2014; Wenzel et al. 2014).

Cardiac Diseases

The heart is the most important muscle in the human body. It pumps blood through the body and provides the essential oxygen and nutrient supply. Heart diseases can severely restrict the life of patients. Ischemic or coronary heart disease (CHD) is the most common form of heart diseases. It manifests in a reduced blood flow to the heart due to plaques which partially block its arteries. Complete blockage of the blood flow causes damage to the heart cells leading to myocardial infarction (MI) and even heart failure. Heart failure is defined as a syndrome that restricts the cardiac function of filling or ejecting blood in the ventricle, irrespective of cause. This condition has far-reaching consequences for the whole body and is not restricted to the heart only but can effect almost every other organ (Segers and Lee 2008).

Similar to other cases of organ failure, treatment of patients with end-stage heart failure includes organ transplantation, which greatly enhances the patients' quality of life as they regain physical endurance and are less hospitalized (Michler 2018). However, the demand of donor organs is much higher than the pool of available donors can manage. Many patients are also not eligible for transplantations depending on their conditions. They are particularly in the focus for the future use of stem cell therapy (Michler 2018).

The goal of stem cell treatment for heart diseases is the generation of cardiomyocytes and blood vessels, which support the regeneration of cardiac function (Michler 2018).

Some clinical trials already applied BM-MSCs. In an in vivo rodent model, differentiation of BM-MSCs to cardiomyocytes was reported when injected into the murine myocardium (Toma et al. 2002). However, it is debatable if these cells are able to generate cardiomyocytes in human patients, too. It is not proven that injected stem cells regenerate the heart tissue by differentiating into cardiomyocytes, but it is believed that secreted factors comprising growth factors, cytokines, and chemokines may improve the regeneration by activating reparative mechanisms and inhibiting apoptosis, fibrosis, and hypertrophy. Moreover, it seems that infused stem cells support the proliferation of cardiomyocytes and also recruit cardiac stem cells which regenerate the cardiac tissue (Segers and Lee 2008).

With regard to ischemic heart diseases, some clinical trials also showed that the injection of stem cells may lead to the formation of blood vessels which improved cardiac performance (Segers and Lee 2008).

In March 2019, more than 300 stem cell-based clinical studies for heart diseases were listed at https://clinicaltrials.gov/. Many of these are performed with BM-MSCs in various cell doses and varying infusion time points. Even though these cell therapies did not show significant improvements in the healing process of the heart diseases, there are some points which could be learned from these trials: (a) stem cell therapy is safe for patients, (b) therapy with cells is minimally effective, and (c) transdifferentiation of BM-MSCs does not occur in a frequency high enough to have an effect (Michler 2018).

In 2001/2002, the PERFECT phase II clinical trial, sponsored by Miltenyi Biotec GmbH, was initiated in order to study safety as well as efficiency of autologous $CD133^+$ BM-derived stem cells when injected into the myocardium during a coronary artery bypass graft (CABG). As primary

outcome, left ventricular contractility was measured and compared to CABG alone. Meanwhile, this study has developed into the first phase III clinical trial. Eighty-two patients with myocardial infarct were either injected with autologous $CD133^+$ BM-MSCs or placebo product while undergoing bypass surgery in a double-blinded and randomized fashion (Steinhoff et al. 2017). Analyses 180 days after the treatment showed that cardiac tissue repair and the improvement of left ventricular function were induced, possibly due to the presence of CD133 endothelial progenitor cells in the stem cell preparation (Steinhoff et al. 2017).

Between 2004 and 2005, 204 patients suffering from acute myocardial infarction (AMI) were treated in a phase III clinical trial called REPAIR-AMI (NCT00279175). The patients were randomly injected with autologous BM-MSCs or placebo medium into the infarct artery 3–7 days after infarct reperfusion therapy. The 12-month follow-up results showed a reduced number of patients who met the endpoint death, needed a revascularization, or had another MI in the BM-MSC-treated group than in the placebo group (Schachinger et al. 2006).

Another clinical trial combined the use of left ventricular assist devices (LVAD) with the injection of allogeneic MSCs (Ascheim et al. 2014) (NCT01442129). Thirty randomized patients suffering from end-stage heart failure were injected 25 million MSCs each during LVAD implantation. After 90 days, the functionality of the ventricle was checked while temporarily weaned from the LVAD. Even though an effect of MSCs was not clearly observed, the treated patients were able to wean of the LVAD more often and for longer periods.

Alternative to the injection of single cells, sphere-derived cells can be transplanted into the diseased tissue. Spheres are three-dimensional cell aggregates composed of cell types specific for one tissue or organ. In the clinical trial CADUCEUS (NCT00893360), patients with ischemic LV dysfunction were randomly injected with autologous cardiosphere-derived cells (CDC) generated from myocardial biopsies into the infarct-related artery 90 days after the myocardial infarct. The control group received standard treatment (Malliaras et al. 2014). Follow-up examination of the patients revealed no improvement of end-diastolic volume, end-systolic volume, and left ventricular ejection fraction. However, CDC treatment reduced scar mass and improved viable heart mass as well as regional contractility and systolic wall thickening (Malliaras et al. 2014).

Between 2013 and 2018, hESC-derived cardiovascular progenitors were transplanted into ten patients who suffered from ischemic heart failure in a clinical trial performed in France (NCT02057900). The generated cells were embedded into fibrin gel and were injected while the patients surgically received a coronary artery bypass grafting and/or a mitral valve procedure. A follow-up after 1 year revealed no adverse events during the recoveries and no tumor formation. None of the patients suffered from arrhythmias, and the patients' symptoms improved with increased systolic motion. Silent alloimmunization (immune response to antigens of an allogeneic donor) occurred in three patients. The conclusion was that the derivation of cardiovascular progenitor cells from hESCs was feasible, and transplantation of these cells was safe for short and medium term (Menasche et al. 2018).

All in all, many clinical trials with stem cell-based therapies for heart diseases were performed in the last 20 years. Especially, BM-MSCs were used extensively in these trials but with no or only minimal success. Nevertheless, there are, alone in the USA, more than 60 direct-to-costumer businesses cardiomyocytes promising to cure patients suffering from heart diseases with stem cells. These treatments are not authorized by the US FDA and expose the patients to incalculable risks (Goff et al. 2017). Until the mechanisms related to heart development and metabolism are better understood and risk factors are eliminated, stem cell therapy for heart diseases is still only at the very beginning.

Diabetes

Diabetes is one of the major health problems of our time. In 2017 about 425 million adults worldwide were affected with increasing tendencies. Ninety percent of the patients suffer from type 2 diabetes (T2D) which usually develops later in

life. Type 1 diabetes (T1D) can already start at a young age and currently affects more than 1.1 million children (Diabetes Facts & Figures 2019). T1D is an autoimmune disease where immune cells attack and destroy pancreatic β cells. These cells are responsible for the production of insulin in response to dietary glucose. Insulin enables cells, especially those of the muscles, to take up glucose for energy generation. If insulin is missing, blood glucose levels increase dangerously high which acutely can cause a diabetic coma. In the long term, elevated glucose levels can harm almost every organ, leading to cardiovascular problems, retinopathy, nephropathy, and neuropathy. In T2D the pancreas still produces insulin, but the peripheral tissues become resistant toward it, which means that insulin loses its ability to channel glucose into the cells. Other insulin-associated functions, especially its promoting effect on fat storage, remain intact. Over time, the pancreas becomes exhausted in T2D and stops producing insulin similar to T1D. While T1D always needs treatment with insulin injections, only later stages of T2D depend on injections (Kharroubi and Darwish 2015).

From the 145 stem cell-based clinical studies for diabetes listed in August 2019 at https://clinicaltrials.gov/, about one third deal with T2D, while the majority has been designed for T1D. Several approaches for stem cell therapy of diabetes have been tested. They are based either on the concept of replacing nonfunctional β cells by stem cell-derived ones or on exploiting the capacities of MSCs or HSCs to act as immunomodulators and improve the regeneration of lost cells. In view of this, MSCs are able to suppress T-cell responses and inhibit differentiation of dendritic cells as well as B-cell proliferation. They can stimulate the production of anti-inflammatory cytokines and suppress that of pro-inflammatory cytokines, as well as of reactive oxygen species. In addition, they can improve insulin signal transduction, while HSCs stimulate angiogenesis in the damaged islets as well as regeneration of endothelial progenitor cells (Sneddon et al. 2018).

Clinical trials for T1D and T2D usually employ MSCs from different sources or BM-derived mononuclear cells/HSCs either alone or in combination by intravenous injection or injection into the pancreatic artery. All clinical trials so far proved safety of the procedure and also showed limited therapeutic effects of the treatment. However, follow-up periods usually were no longer than 12 months, so we lack information on long-term success, and also no systematic study has been performed so far to determine which stem cell source and which mode of application are the best (Sneddon et al. 2018).

MSCs also have a capacity for in vitro differentiation into islet-like insulin-producing cells. These differentiated cells have been successfully used in clinical trials, although it is not yet clear whether they really replaced damaged β cells or if the positive effects were again due to immunomodulatory effects of MSCs (Cho et al. 2018).

In order to replace non-functioning β cells, novel techniques based on ESCs have been developed. To this end, ESCs are in vitro differentiated into insulin-producing β-like cells. Unfortunately, these cells are less efficient in insulin synthesis than primary β cells, which is probably due to the missing 3D structure of the organ, which provides a dedicated niche for β cells. Therefore, differentiation protocols are currently being developed which take also the 3D structure into account (Sneddon et al. 2018).

Besides cell maturation/function, cell therapy of the pancreas faces two main challenges which even hamper treatment with adult pancreatic cells. First, the transplanted cells home-in inefficiently into the pancreas, and second, they are frequently attacked by the host's immune system. To overcome both issues, several companies have developed encapsulation devices made of, e.g., alginate, polytetrafluoroethylene, silicone, or polycaprolactone. These devices can be transplanted either intraperitoneally or subcutaneously. Ideally, they provide sufficient blood and oxygen supply which ensures proper function of the encapsulated cells and allow the secreted insulin to exit the device. In addition, they protect the transplanted cells from the host's immune system and in the worst case prevent the escape of tumorigenic cells (Sneddon et al. 2018). One clinical phase I/II trial has been conducted by Sernova

Corp. employing isolated islet cells in a pouch (NCT01652911). The method proved to be safe. Six weeks after transplantation, the pouches were explanted, and histological analysis demonstrated that islets retained their macrostructure and were connected to new blood vessels. However, the end goal of long-term insulin independence of the patients could not be achieved. Another phase I/II clinical trial which is running until 2021 is currently conducted by ViaCyte to test safety and efficacy for a device loaded with ESC-derived insulin-producing β-like cells (NCT02239354). Preliminary results indicate that the devices are well-tolerated and that insulin-producing cells persist up to 2 years after transplantation (Pullen 2018).

Another stem cell-based technique tested for the treatment of diabetes is the so-called stem cell educator therapy. In this setting, mononuclear cells are separated from the patient's blood in a closed-loop cell separator. They are then educated to gain immune tolerance by briefly co-culturing them with adherent UCB stem cells. The educated mononuclear cells are reinfused into the patient (Zhao et al. 2013). A clinical phase I/II trial, performed by Tianhe Stem Cell Biotechnologies, demonstrated safety as well as efficacy of this treatment in T2D patients over up to 56 weeks (NCT01415726). Patients not only tolerated the treatment well but also had improved values for glycosylated hemoglobin (HbA1C), c-peptide, and homeostasis model assessment (HOMA) of insulin resistance. The company is now performing a phase II trial including T1D patients as well (NCT03390231) which is supposed to be completed by the end of 2020.

Liver Diseases

The liver is the central metabolic organ of the human body. It is involved in nutrient as well as in drug metabolism, and it produces a plethora of proteins which are secreted and have essential functions elsewhere in the body. The liver is a very complex organ. Eighty percent of its cells are hepatocytes which are responsible for the metabolic homeostasis. They store, release, and synthesize glucose and lipids according to the body's energy needs. They are involved in protein breakdown and detoxify ammonium ions in the urea cycle. The most important function of hepatocytes from a pharmacological point of view is the so-called first- and second-phase metabolism where drugs either get activated or detoxified by cytochrome P450 enzymes and afterward by conjugation with distinct cofactors (Stanger 2015).

There are mainly two indications for stem cell therapy in the liver. First, stem cells can be used to mitigate congenital metabolic defects. Second they are employed to restore liver tissue in the fibrotic/cirrhotic liver.

Several metabolic diseases are known where genetic defects of key enzymes either reduce the output of a specific pathway or impair this pathway completely. Usually, these are rare diseases, affecting less than 1 in 1500–2500 people, and they manifest early in childhood. Well-known examples are Crigler-Najjar syndrome or the various urea cycle defects. In Crigler-Najjar syndrome, patients lack the enzyme uridine diphosphate glucuronosyltransferase which is responsible for conjugating bilirubin – a degradation product of hemoglobin – and thus enabling its excretion. If unconjugated bilirubin accumulates in the body, it causes severe icterus which even affects the brain (kernicterus) leading to encephalopathy and thus triggering neurological damage and long-term cognitive defects. The current standard of care is a lifelong phototherapy for 10–12 h a day in order to convert unconjugated bilirubin with blue-light irradiation into a water-soluble form that can be excreted via the bile. Urea cycle defects result from mutations in any of the cycle's enzymes. This cycle is needed to detoxify ammonium ions which are generated during protein degradation and can, like unconjugated bilirubin, cause encephalopathy (Sokal 2014).

Two characteristics make metabolic diseases especially amenable for stem cell therapy. First, they are caused by an isolated mutation of one specific gene, and second, significant metabolic improvement can be obtained by replacing only 5% of total hepatocytes with healthy ones, while as few as 10% of healthy cells are expected to normalize liver function (Sokal 2014). From 2012

to 2014, a clinical phase I/II trial took place to evaluate the safety of a stem cell treatment in 6 pediatric Crigler-Najjar syndrome and 14 urea cycle disorder patients (NCT01765283) (Smets et al. 2019). Patients obtained transhepatic infusions with Heterologous Human Adult Liver-Derived Progenitor Cells (HepaStem), a product by the Belgian company Promethera. These stem cells are obtained by isolation and short-term cultivation of parenchymal liver cells which display a mesenchymal-like phenotype and preferentially differentiate into hepatocytes. They were administered in an immunosuppressive setting, and the safety could be proven in a 12-month follow-up period. In addition, a certain level of efficiency could also be shown. A proof-of-concept study in a 3-year-old girl suffering from a urea cycle disorder not only showed preliminary efficiency of the transplanted cells but also indicated that these cells were proliferating in the liver which means that maybe less cells are needed than initially expected (Sokal et al. 2014).

Currently, there are 20 clinical trials listed which employ stem cells to treat liver cirrhosis, while an additional 40 trials cover both cirrhosis and fibrosis (https://clinicaltrials.gov/, 5.8.2019). Most of these trials are conducted with autologous or allogeneic MSCs from various sources. All chronic liver diseases associated with inflammation (viral hepatitis, primary biliary cirrhosis, alcoholic and nonalcoholic fatty liver disease) can potentially progress via a fibrotic stage to the end stage of liver cirrhosis. In this condition, functional liver tissue is replaced by scars made of fibrotic material. The liver gets rigid and cannot perform its functional tasks properly anymore. In this phase, orthotopic liver transplantation is the only option to save the patient's life. However, there is a shortage of suitable donor organs, and researchers are working on cell therapies in order to temporarily improve the liver's function, enabling the patient to survive longer time periods before transplantation with the final goal to replace liver transplantation altogether. The first completed trials which all employed some kind of MSC obtained, e.g., from autologous fat tissue or BM indicate an overall safety of the procedure with limited success (Hu et al. 2019).

Kidney Diseases

The kidneys are a bean-shaped pair of organs, which are essential for removal of toxins and waste products from the blood, maintenance of fluid homoeostasis, secretion of hormones, and water reabsorption from urine. An adult kidney is composed of around one million nephrons, the functional units of the kidney.

Conditions such as diabetes and high blood pressure as well as genetic disorders are the main causes of chronic kidney disease (CKD). CKD is characterized by a gradual loss of renal functions which peaks in kidney failure at the worst outcome. In addition, acute kidney injury (AKI), which is defined as abrupt occurring kidney damage or failure, can cause renal diseases. Until now, kidney failure is only treatable with dialysis and finally organ transplantation. Transplantation is the only treatment which can recover kidney function, but it is accompanied with lifelong immunosuppression. Moreover, the organ demand is much higher than the available donor organs.

An alternative to organ transplantation and dialysis could be stem cell-based therapy. Researchers work on growing stem cell-derived organs in vitro, which may be used for transplantations and might cope with the high demand for donor organs. Another option may be injection of isolated stem cells into the affected region. It is proposed that these cells then differentiate into the required cell type within the organ.

One hereditary kidney disease is polycystic kidney disease (PKD). Characteristically, fluid-filled cysts form in the tubules of the kidney which increase the organ size and can spread to other organs. Damage in the kidney may result in end-stage renal disease and kidney failure. The autosomal dominant form of this disease (ADPKD) is caused by a mutation of the genes *polycystin* (*PKD*) *1* or *2*. The respective proteins are located in primary cilia and involved in calcium-dependent signalling pathways. Their dysfunction influences cell proliferation and structure

as well as fluid secretion (Igarashi and Somlo 2007). A clinical trial, performed in 2014, with a focus on ADPKD patients depended on the use of MSCs. It was hypothesized that an introduction of BM-MSCs can improve kidney function while acting anti-apoptotic, anti-fibrotic, and anti-inflammatory (NCT02166489). Six patients were chosen for this trial. 2×10^6 cells/kg autologous BM-MSCs were infused intravenously. The patients were observed afterward during a time span of 12 months. Overall, the procedure was safe for the patients, but the effects of the MSCs could not be evaluated due to the trial design (Makhlough et al. 2017).

Since the kidney contains a great variety of different cell types, this organ is especially challenging to model in vitro. Successful treatment of kidney diseases can only be obtained, when the affected or damaged cell types are recognized. Upon better understanding about the affected cell types in the different kinds of kidney diseases, more treatments and therapies will be established in the future.

Diseases of the Central Nervous System (CNS)

The central nervous system (CNS), composed of the brain, spinal cord, and retina, is one of the most complex and less understood systems in the human body. CNS disorders and injuries, among them neurodegenerative diseases, retinal degeneration, and spinal cord injury, not only cause devastating consequences for the patients and family members but are also a major economic burden.

Neurological disorders are complex and usually irreversible, partially due to the limited potential of endogenous regeneration of the CNS. With the lack of effective therapeutic approaches, stem cell-based therapy holds promising potential to treat CNS disorders.

Retinal Degradation

Retinal disorders were the first CNS conditions to be targeted with cell therapy. The retina comprises several neuronal layers, among them the photoreceptors (PRs) which convert the light inputs into signals that are then transmitted to the brain via the optic nerve. The PRs are in contact with a monolayer of retinal pigment epithelium (RPE), essential to maintain PR homeostasis. Degeneration of the PR due to their malfunction or due to degeneration of the RPE can lead to visual decline that ultimately ends up in blindness.

The leading causes of retina degeneration and blindness in Western countries are age-related macular degeneration (AMD) and retinitis pigmentosa. AMD can be subclassified into non-vascular AMD (dry form) and neovascular AMD (wet form). Another variant of this disease, which is not age-associated, is Stargardt macular degeneration. It is the most prevalent inherited macular dystrophy affecting both children and adults. While AMD is caused by the degeneration of the RPE, retinitis pigmentosa is caused by the degeneration of the PR and/or RPE. Retinitis pigmentosa is a group of heterogeneous inherited conditions with a prevalence of 1:4000. Since the PR and the RPE cannot be endogenously regenerated, stem cell therapy is a promising therapeutic alternative for treating these retinal degeneration conditions (Ben M'Barek and Monville 2019).

RPE and PR cells can be obtained from fetal and adult tissue, specifically from cadavers (allogeneic RPE) or from patients (autologous RPE) through a nasal surgery. The use of fetal tissue implies ethical concerns and showed variability related to the developmental state of the fetus, leading to the abandonment of this source. Adult RPE cells showed a huge limitation due to the low amount of cells that can be obtained, as well as the complications inherent to the surgery in case of autologous RPE isolation. With the development of efficient protocols to differentiate ESCs and iPSCs into specific retinal subtypes like RPE cells, retinal cell replacement is a promising target of CNS cell therapy, with multiple clinical trials ongoing (Goldman 2016).

The first clinical trials using ESC-derived RPEs to treat AMD and Stargardt disease were performed in 2012 (NCT01344993 and NCT013450060). The results of these studies provided evidence that ESC-derived RPEs were safe to treat these diseases. As a consequence, many other clinical trials emerged

placing retinal degeneration at the forefront of stem cell-based therapies. In 2014, the first clinical trial using autologous iPSC-derived RPEs was conducted at the RIKEN institute in Japan (UMIN000011929). However, it was aborted 1 year later due to safety concerns. There are currently three ongoing clinical trials using iPSC-derived RPEs, with more expected to be approved. The results from these trials will help to optimize the best formulation strategy to combat retinal degeneration (Ben M'Barek and Monville 2019; Schwartz et al. 2015).

Neurodegenerative Diseases

Neurodegenerative diseases are a heterogeneous group that can have a hereditary or a spontaneous origin, which all culminate in the loss of neurons or glia cells in the CNS. Stem cell-based therapy is emerging as a promising candidate to treat some of these diseases including Parkinson's disease (PD), Alzheimer's disease, Huntington's disease (HD), and amyotrophic lateral sclerosis (ALS), among others. Cell replacement therapy was already performed as a proof of concept in some of these conditions.

PD is the second most common degenerative disease of the CNS, affecting 1% of the population above 60 years (Tysnes and Storstein 2017). PD is characterized by the degeneration of the dopaminergic neurons (DAn) in the *substantia nigra pars compacta* (SNpc), causing the characteristic motor factors of PD like rigidity, bradykinesia, tremors, and postural instability, along with other non-motor symptoms. Another hallmark of PD is the presence of aggregated α-synuclein in the Lewy bodies and Lewy neurites in the substantia nigra. The loss of DAn is initially restricted to the SNpc, but it will progressively spread to other regions of the brain during the development of the disease. The exact etiology of PD remains unknown, and nowadays it is considered to be a multifactorial disease resulting from a complex interplay between genetic factors and environmental cues. Currently, the available pharmacological regiments for PD only treat the symptoms of the disease and not the underlying neurodegeneration process (Antony et al. 2013; Kalia and Lang 2015). Therefore, new therapeutic strategies are needed, with stem cell-based therapy being the most promising approach to slow or even stop the progression of this devastating disease. The first cell therapy trials for PD were performed more than 30 years ago, using fetal ventral mesencephalic cells (fVM), a source of DAn. These first trials showed long-term efficacy and survival. However, it has been reported that in some cases the transplanted cells exhibited disease-related pathology and there was a huge variability in the clinical response probably due to the variability of the cells transplanted (Barker et al. 2015). In order to standardize the approach of cell therapy for PD, TRANSEURO (NCT01898390), a European consortium conducting phase I clinical trials to investigate the benefits of transplantation of allogeneic dopaminergic neuroblasts derived from fVM into PD patients, was created.

High expectations for future PD treatments lie on emerging therapies based on hPSC-derived DAns. The preferential use of iPSCs over ESCs has been fostered by the systematic banking of HLA-matched iPSCs, avoiding the need for immunosuppression regime in the recipient. The development of good manufacturing practice (GMP)-grade protocols to obtain authentic and functional midbrain DAn cells from hPSCs lead to the creation of the global network initiative GForce-PD. This network encompasses different consortia like the European NeuroStemCellRepair and the NYSTEM-PD based on ESC-derived DAn and the Japanese Center for iPS Cell Research and Application (CiRA) based on allogeneic transplantation from HLA-matched iPSC-derived DAn cells. As part of the GForce-PD network, the first clinical trial using iPSC-derived DAns to treat PD started in August 2018 at Kyoto University by a team headed by Takahashi as part of the Japanese Haplobank CiRA (UMIN000033564). Furthermore, some clinical trials outside the GForce-PD have already started. The Chinese Academy of Sciences is using HLA-matched ESCs (NCT03119636), while an Australian Clinical trial (NCT02452723) sponsored by Cyto Therapeutics Pty Limited is based on human parthenogenetic stem cell-derived neural cells (Barker et al. 2019; Wenker and Pitossi 2019).

With more iPSC-derived cell therapies to treat PD already planned, the follow-up of these trials will likely be beneficial, not only for PD but also to develop new approaches for other neurodegenerative diseases.

ALS is a neurodegenerative disorder characterized by progressive degeneration of the upper and lower motor neurons. ALS has a devastating impact on the patient, and although the pathogenic basis is still unclear, stem cell-based therapy seems to have potential. The motor neuronal degeneration observed in ALS may arise from defective trophic support from astrocytes and microglia, whose replacement appears technically more feasible. Furthermore, the delivery of growth factors or extracellular vesicles might exert a neuroprotective effect.

Injection of human NSCs (NSI-566) originating from the spinal cord of an 8-week-old aborted fetus was performed in a phase I (NCT01348451) and phase II (NCT01730716) clinical trial. The results from these trials showed improved functional status scores of these patients, although survival did not differ from control groups. A phase 3 clinical trial is already planned (Goutman et al. 2018; Abati et al. 2019). Another trial using fetal tissue-derived NSCs in combination with gene therapy was approved in 2016. The human NSCs are engineered to produce Glial cell-derived neurotrophic factor (GDNF) (CNS10-NPC-GDNF) and injected in the spinal cord (NCT02943850). It is expected that these cells differentiate into neuroprotective astrocytes, increasing the survival of motor neuros in ALS patients. With more preclinical data suggesting that the malfunctioning of astrocytes is involved in ALS pathogenesis, a new clinical trial using ESC-derived astrocytes (NCT03482050) was approved in 2018. The results from these trials will give us insights about the safety and potential of PSCs in the treatment of ALS.

Beside these treatments, which are in the trial state, the Korean company Corestem has obtained approval for their product Neuronata-R in South Korea in 2014 after successful phase I and II clinical trials (NCT01363401). The treatment is based on repeated intrathecal injections of autologous BM-MSCs (Oh et al. 2015). In 2018 it also got permission as an orphan drug from the US FDA and EMA followed this classification in 2019.

Spinal Cord Injury (SCI)

SCI is one of the most devastating neurological injuries, including motor, sensory, and autonomic paralysis, with a prevalence (2016) of 27.04 million cases (GBD 2016 et al. 2019). SCI results from dislocation or fracture of the spine in the cervical of thoracic region and can be divided into two different phases, the acute and the chronic phases. In the acute phase, neurons and glia cells can undergo fast necrosis seconds to minutes after the injury (primary injury). The secondary injuries, depending on the extent of the primary injury, comprise the most critical phase. A cascade of destructive events occurs, including aberrant molecular signalling, inflammation, vascular changes, and secondary cellular dysfunctions. Weeks to months after the secondary injuries, the chronic phase takes place with scar formation as a consequence of the reactive gliolysis, formation of cysts, and gray matter demyelination (Cofano et al. 2019). Treatments for acute SCI are limited to the stabilization of the injured spine followed by rehabilitation in the chronic phase. Although some early medical treatments accounted for some significance recovery, there is no effective treatment.

The development of cell transplantation therapies to replace the damaged cells and to promote neural protection and regeneration of the injured spinal cord has shown great potential. A variety of different cell types have already been transplanted into injured spinal cord, in rodents and human, like olfactory ensheathing cells, oligodendrocyte precursor cells (OPCs), Schwann cells, NSCs derived from fetal tissue, and MSCs. In particular, from the 18 clinical trials conducted, 16 were based on MSCs. The big disadvantage of using MSCs for transplantation is their restricted differentiation potential. To overcome this, the first clinical trial using ESC-derived OPCs was approved in 2010 (NCT01217008). This study was terminated based on financial issues, and a second clinical trial was approved in 2015 (NCT02302157). This is the only PSCs-based clinical trial currently active, and the results are

expected to be published soon (Csobonyeiova et al. 2019; Pereira et al. 2019). Recently the beneficial effects of iPSC-derived NSCs transplantation for tissue recovery were shown. After transplantation these cells can differentiate into neurons and oligodendrocytes, myelinate the host axons, and secrete neurotrophic factors to prevent the secondary damage. In February 2019, the first clinical trial using allogenic iPSC-derived NSCs was approved. The study will be performed on four patients at the Keio University School of Medicine by a research team headed by Prof. Hideyuki Okano (Nagoshi et al. 2019; Tsuji et al. 2019)

Future Perspectives in Stem Cell-Based Therapy of the CNS

Although some neurodegenerative diseases share pathological mechanisms such as protein aggregation, misfolded proteins, and loss of local neurons, the underlying molecular mechanisms that lead to the CNS's progressive degeneration are unknown. There are still considerable problems in treating these diseases, and so far they do not make good targets for stem cell therapy, especially because the neurodegeneration is too widespread, diffuse, and currently irreversible. Alzheimer's disease, the most common and devastating form of dementia, is so far not a target for stem cell-based replacement therapy due to its high complexity, heterogeneity, and unclear pathogenesis. Other diseases are still not a target of stem cell-based clinical trials, but preclinical studies have shown the potential of such therapy. Huntington's disease(HD) is a fatal autosomal-dominant disease characterized by motor dysfunction, cognitive impairment, and psychiatric disturbances due to neurodegeneration. HD is caused by a mutation of the huntingtin (HTT) gene, and stem-cell based therapy is a potential strategy to restore neuronal function, replacing the lost neurons, and provide neurotrophic support. Several clinical trials using human fetal tissue to treat HD have been performed since 1990. The results from these very heterogeneous trials indicated that fetal transplantation in HD is safe but the clinical improvement did not last more than 4–6 years after transplantation. Finding an alternative to the fetal striatal graft transplantation is being a focus of research, with a set of preclinical studies based on PSCs ongoing based on PSCs. The results from these studies using PSC-based therapy are largely inconsistent. Thus, more preclinical work is necessary to confirm if PSCs have a therapeutic potential to treat HD.

Another disease where stem cell-based therapy is a potential target is ischemic stroke, an acute cerebrovascular disease caused by a decreased or interrupted blood supply in the brain. Ischemic stroke destroys a heterogeneous population of brain cells, making cell replacement therapy a difficult approach since neurons and glia cells that should be replaced are affected. Therefore, most clinical trials shifted to use MSCs in order to suppress the post-ischemic inflammatory response. The results from these clinical trials showed an improvement of the neurological symptoms in the patients. Although MSCs are an attractive and promising therapy, it is not a cell replacement therapy. The UK started a clinical trial already in phase II (NCT03629275) where an immortalized human NSC line (CTX0E03) is being used. Although (HLA-matched) iPSCs are still considered as a potential source for stem cell therapy to treat stroke, where the results from preclinical studies have been encouraging, additional studies and improvement in the strategies for cell replacement therapy are required.

Summary

A tremendous number of stem cell-based clinical trials (also for organs which we could not mention in this book chapter) are currently underway. Many of these focus on MSCs which can be applied in a wide variety of settings, to support regeneration, modulate the immune response, and maybe even restore damaged tissue (Fig. 4). As they do not have to be applied in an HLA-matched manner, allogeneic transplantation is facilitated. Cells differentiated from PSCs are currently emerging as treatment options for various diseases. Here, the hurdles for transplantation are higher because the

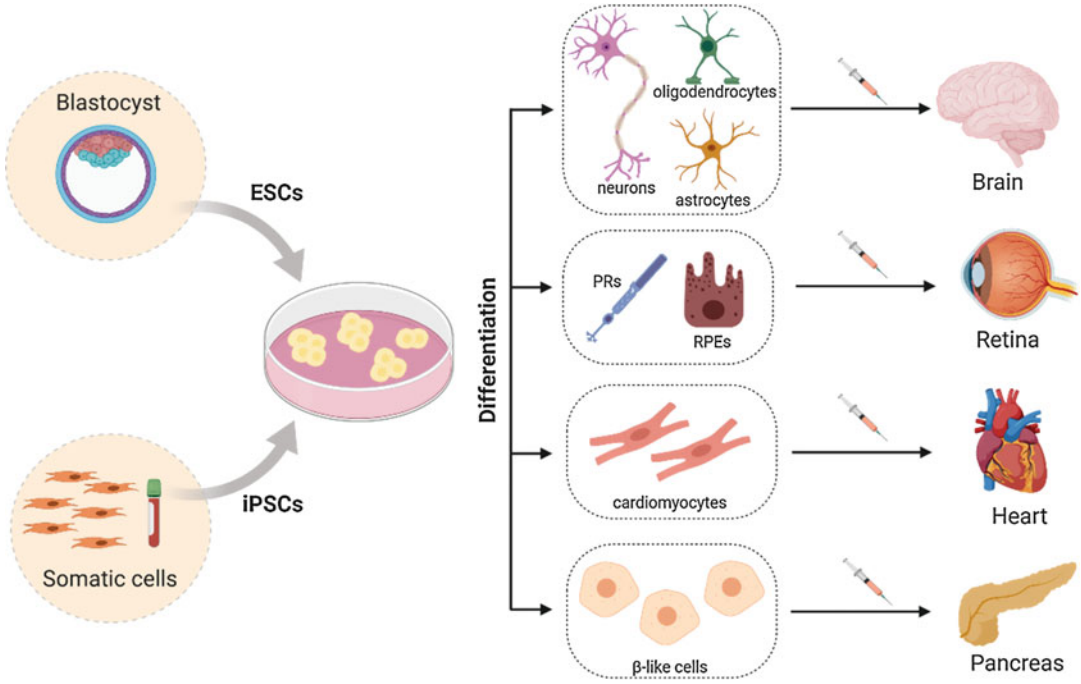

Fig. 4 Overview of the ongoing PSC-based clinical trials. PSCs isolated from the blastocyst (ESCs) or reprogrammed from somatic cells (iPSCs) are differentiated in vitro to generate neurons, oligodendrocytes, and astrocytes to treat central nervous system disorders, PRs and RPEs to treat retinal degenerative diseases, cardiomyocytes to treat heart diseases, and β-like cells to treat type 1 diabetes. After differentiation the cells are transplanted into the brain, retina, heart, or pancreas from the donor. Figure made in ©BioRender – biorender.com

possibility of immune rejection requires HLA matching and the tumorigenic potential of PSCs needs to be controlled.

While HSC and keratinocyte transplantation have been in the clinic for a long time, only selected MSC-based treatments have been approved in a limited number of countries. It will probably take much longer until PSC-based therapies will be available to a broad spectrum of patients. These novel treatments will need a close surveillance until we have fully understood their risks and benefits.

References and Further Reading

Abati E, Bresolin N, Comi GP, Corti S (2019) Preconditioning and cellular engineering to increase the survival of transplanted neural stem cells for motor neuron disease therapy. Mol Neurobiol 56(5):3356–3367. https://doi.org/10.1007/s12035-018-1305-4

Abu-Dawud R, Graffmann N, Ferber S, Wruck W, Adjaye J (2018) Pluripotent stem cells: induction and self-renewal. Philos Trans R Soc Lond Ser B Biol Sci 373 (1750). https://doi.org/10.1098/rstb.2017.0213

alliancerm.org. https://alliancerm.org/available-products/. Accessed 18 Sept 2019

Al-Saif AM (2019) Gene therapy of hematological disorders: current challenges. Gene Ther. https://doi.org/10.1038/s41434-019-0093-4

Altman J, Das GD (1965) Autoradiographic and histological evidence of postnatal hippocampal neurogenesis in rats. J Comp Neurol 124:319–335. https://doi.org/10.1002/cne.901240303

Antony PMA, Diederich NJ, Krüger R, Balling R (2013) The hallmarks of Parkinson's disease. FEBS J 280:5981–5993. https://doi.org/10.1111/febs.12335

Ascheim DD, Gelijns AC, Goldstein D, Moye LA, Smedira N, Lee S, Klodell CT, Szady A, Parides MK, Jeffries NO, Skerrett D, Taylor DA, Rame JE, Milano C, Rogers JG, Lynch J, Dewey T, Eichhorn E, Sun B, Feldman D, Simari R, O'Gara PT, Taddei-Peters WC, Miller MA, Naka Y, Bagiella E, Rose EA, Woo YJ (2014) Mesenchymal Precursor Cells as Adjunctive Therapy in Recipients of Contemporary Left Ventricular Assist Devices.

Circulation 129 (22):2287–2296. https://doi.org/10.1161/circulationaha.113.007412
Ballen KK, Verter F, Kurtzberg J (2015) Umbilical cord blood donation: public or private? Bone Marrow Transplant 50 (10):1271–1278. https://doi.org/10.1038/bmt.2015.124
Barker RA, Drouin-Ouellet J, Parmar M (2015) Cell-based therapies for Parkinson disease – past insights and future potential. Nat Rev Neurol 11:492–503. https://doi.org/10.1038/nrneurol.2015.123
Barker RA, Farrell K, Valle Guzman N, He X, Lazic SE, Moore S, Morris R, Tyers P, Wijeyekoon R, Daft D, Hewitt S, Dayal V, Foltynie T, Kefalopoulou Z, Mahlknecht P, Lao-Kaim NP, Piccini P, Bjartmarz H, Björklund A, Lindvall O, Nelander-Wahlestedt J, Parmar M, Paul G, Widner H, Church A, Dunnett S, Peall K, Rosser A, Marc Gurruchaga J, Palfi S, Piroth T, Winkler C (2019) Designing stem-cell-based dopamine cell replacement trials for Parkinson's disease. Nat Med 2:1045–1053. https://doi.org/10.1038/s41591-019-0507-2
Barrandon Y, Green H (1987) Three clonal types of keratinocyte with different capacities for multiplication. Proc Natl Acad Sci U S A 84(8):2302–2306. https://doi.org/10.1073/pnas.84.8.2302
Bauer JW, Koller J, Murauer EM, De Rosa L, Enzo E, Carulli S, Bondanza S, Recchia A, Muss W, Diem A, Mayr E, Schlager P, Gratz IK, Pellegrini G, De Luca M (2017) Closure of a large chronic wound through transplantation of gene-corrected epidermal stem cells. J Invest Dermatol 137(3):778–781. https://doi.org/10.1016/j.jid.2016.10.038
Ben M'Barek K, Monville C (2019) Cell therapy for retinal dystrophies: from cell suspension formulation to complex retinal tissue bioengineering. Stem Cells Int 2019:1–14. https://doi.org/10.1155/2019/4568979
Caplan AI (1991) Mesenchymal stem cells. J Orthop Res 9 (5):641–650. https://doi.org/10.1002/jor.1100090504
Caplan H, Olson SD, Kumar A, George M, Prabhakara KS, Wenzel P, Bedi S, Toledano-Furman NE, Triolo F, Kamhieh-Milz J, Moll G, Cox CS Jr (2019) Mesenchymal stromal cell therapeutic delivery: translational challenges to clinical application. Front Immunol 10:1645. https://doi.org/10.3389/fimmu.2019.01645
Chagastelles PC, Nardi NB (2011) Biology of stem cells: an overview. Kidney Int Suppl 1(3):63–67. https://doi.org/10.1038/kisup.2011.15
Champlin R (2003) Selection of autologous or allogeneic transplantation. In: Holland-Frei cancer medicine, vol 6. BC Decker, Hamilton
Cho J, D'Antuono M, Glicksman M, Wang J, Jonklaas J (2018) A review of clinical trials: mesenchymal stem cell transplant therapy in type 1 and type 2 diabetes mellitus. Am J Stem Cells 7(4):82–93
Cofano F, Boido M, Monticelli M, Zenga F, Ducati A, Vercelli A, Garbossa D (2019) Mesenchymal stem cells for spinal cord injury: current options, limitations, and future of cell therapy. Int J Mol Sci 20:2698. https://doi.org/10.3390/ijms20112698
Comella K, Parlo M, Daly R, Dominessy K (2018) First-in-man intravenous implantation of stromal vascular fraction in psoriasis: a case study. Int Med Case Rep J 11:59–64. https://doi.org/10.2147/IMCRJ.S163612
Connor B (2018) Concise review: the use of stem cells for understanding and treating Huntington's disease. Stem Cells 36:146–160. https://doi.org/10.1002/stem.2747
Csobonyeiova M, Polak S, Zamborsky R, Danisovic L (2019) Recent Progress in the regeneration of spinal cord injuries by induced pluripotent stem cells. Int J Mol Sci 20:3838. https://doi.org/10.3390/ijms20153838
Di WL, Lwin SM, Petrova A, Bernadis C, Syed F, Farzaneh F, Moulding D, Martinez AE, Sebire NJ, Rampling D, Virasami A, Zamiri M, Wang W, Hara H, Kadiyirire T, Abdul-Wahab A, Martinez-Queipo M, Harper JI, McGrath JA, Thrasher AJ, Mellerio JE, Qasim W (2019) Generation and clinical application of gene-modified autologous epidermal sheets in netherton syndrome: lessons learned from a phase 1 trial. Hum Gene Ther. https://doi.org/10.1089/hum.2019.049
Diabetes Facts & Figures (2019) International Diabetes Federation. https://www.idf.org/aboutdiabetes/what-is-diabetes/facts-figures.html. Accessed 5 Aust 2019
Dominici M, Le Blanc K, Mueller I, Slaper-Cortenbach I, Marini F, Krause D, Deans R, Keating A, Prockop D, Horwitz E (2006) Minimal criteria for defining multipotent mesenchymal stromal cells. The International Society for Cellular Therapy position statement. Cytotherapy 8(4):315–317. https://doi.org/10.1080/14653240600855905
Dowse R, McLornan DP (2017) Principles of haemopoietic stem cell transplantation. Medicine 45(5):322–326. https://doi.org/10.1016/j.mpmed.2017.02.009
Elstner A, Damaschun A, Kurtz A, Stacey G, Aran B, Veiga A, Borstlap J (2009) The changing landscape of European and international regulation on embryonic stem cell research. Stem Cell Res 2(2):101–107. https://doi.org/10.1016/j.scr.2008.10.003
Fitzsimmons REB, Mazurek MS, Soos A, Simmons CA (2018) Mesenchymal stromal/stem cells in regenerative medicine and tissue engineering. Stem Cells Int 2018:8031718. https://doi.org/10.1155/2018/8031718
Friedenstein AJ, Chailakhjan RK, Lalykina KS (1970) The development of fibroblast colonies in monolayer cultures of guinea-pig bone marrow and spleen cells. Cell Tissue Kinet 3(4)
Frobel J, Hemeda H, Lenz M, Abagnale G, Joussen S, Denecke B, Saric T, Zenke M, Wagner W (2014) Epigenetic rejuvenation of mesenchymal stromal cells derived from induced pluripotent stem cells. Stem Cell Rep 3(3):414–422. https://doi.org/10.1016/j.stemcr.2014.07.003
Galipeau J, Sensebe L (2018) Mesenchymal stromal cells: clinical challenges and therapeutic opportunities. Cell Stem Cell 22(6):824–833. https://doi.org/10.1016/j.stem.2018.05.004
GBD 2016, Traumatic Brain Injury and Spinal Cord Injury Collaborators SL, Theadom A, Ellenbogen RG,

Bannick MS, Montjoy-Venning W, Lucchesi LR, Abbasi N, Abdulkader R, Abraha HN, Adsuar JC, Afarideh M, Agrawal S, Ahmadi A, Ahmed MB, Aichour AN, Aichour I, Aichour MTE, Akinyemi RO, Akseer N, Alahdab F, Alebel A, Alghnam SA, Ali BA, Alsharif U, Altirkawi K, Andrei CL, Anjomshoa M, Ansari H, Ansha MG, Antonio CAT, Appiah SCY, Ariani F, Asefa NG, Asgedom SW, Atique S, Awasthi A, Quintanilla BPA, Ayuk TB, Azzopardi PS, Badali H, Badawi A, Balalla S, Banstola A, Barker-Collo SL, Bärnighausen TW, Bedi N, Behzadifar M, Behzadifar M, Bekele BB, Belachew AB, Belay YA, Bennett DA, Bensenor IM, Berhane A, Beuran M, Bhalla A, Bhaumik S, Bhutta ZA, Biadgo B, Biffino M, Bijani A, Bililign N, Birungi C, Boufous S, Brazinova A, Brown AW, Car M, Cárdenas R, Carrero JJ, Carvalho F, Castañeda-Orjuela CA, Catalá-López F, Chaiah Y, Champs AP, Chang J-C, Choi J-YJ, Christopher DJ, Cooper C, Crowe CS, Dandona L, Dandona R, Daryani A, Davitoiu DV, Degefa MG, Demoz GT, Deribe K, Djalalinia S, Do HP, Doku DT, Drake TM, Dubey M, Dubljanin E, El-Khatib Z, Ofori-Asenso R, Eskandarieh S, Esteghamati A, Esteghamati S, Faro A, Farzadfar F, Farzaei MH, Fereshtehnejad S-M, Fernandes E, Feyissa GT, Filip I, Fischer F, Fukumoto T, Ganji M, Gankpe FG, Gebre AK, Gebrehiwot TT, Gezae KE, Gopalkrishna G, Goulart AC, Haagsma JA, Haj-Mirzaian A, Haj-Mirzaian A, Hamadeh RR, Hamidi S, Haro JM, Hassankhani H, Hassen HY, Havmoeller R, Hawley C, Hay SI, Hegazy MI, Hendrie D, Henok A, Hibstu DT, Hoffman HJ, Hole MK, Rad EH, Hosseini SM, Hostiuc S, Hu G, Hussen MA, Ilesanmi OS, Irvani SSN, Jakovljevic M, Jayaraman S, Jha RP, Jonas JB, Jones KM, Shushtari ZJ, Jozwiak JJ, Jürisson M, Kabir A, Kahsay A, Kahssay M, Kalani R, Karch A, Kasaeian A, Kassa GM, Kassa TD, Kassa ZY, Kengne AP, Khader YS, Khafaie MA, Khalid N, Khalil I, Khan EA, Khan MS, Khang Y-H, Khazaie H, Khoja AT, Khubchandani J, Kiadaliri AA, Kim D, Kim Y-E, Kisa A, Koyanagi A, Krohn KJ, Defo BK, Bicer BK, Kumar GA, Kumar M, Lalloo R, Lami FH, Lansingh VC, Laryea DO, Latifi A, Leshargie CT, Levi M, Li S, Liben ML, Lotufo PA, Lunevicius R, Mahotra NB, Majdan M, Majeed A, Malekzadeh R, Manda A-L, Mansournia MA, Massenburg BB, Mate KKV, Mehndiratta MM, Mehta V, Meles H, Melese A, Memiah PTN, Mendoza W, Mengistu G, Meretoja A, Meretoja TJ, Mestrovic T, Miazgowski T, Miller TR, Mini G, Mirica A, Mirrakhimov EM, Moazen B, Mohammadi M, Molokhia M, Monasta L, Mondello S, Moosazadeh M, Moradi G, Moradi M, Moradi-Lakeh M, Moradinazar M, Morrison SD, Moschos MM, Mousavi SM, Murthy S, Musa KI, Mustafa G, Naghavi M, Naik G, Najafi F, Nangia V, Nascimento BR, Negoi I, Nguyen TH, Nichols E, Ningrum DNA, Nirayo YL, Nyasulu PS, Ogbo FA, Oh I-H, Okoro A, Olagunju AT, Olagunju TO, Olivares PR, Otstavnov SS, Owolabi MO, Mahesh PA, Pakhale S, Pandey AR, Pesudovs K, Pinilla-Monsalve GD, Polinder S, Poustchi H, Prakash S, Qorbani M, Radfar A, Rafay A, Rafiei A, Rahimi-Movaghar A, Rahimi-Movaghar V, Rahman M, Rahman MA, Rai RK, Rajati F, Ram U, Rawaf DL, Rawaf S, Reiner RC, Reis C, Renzaho AMN, Resnikoff S, Rezaei S, Rezaeian S, Roever L, Ronfani L, Roshandel G, Roy N, Ruhago GM, Saddik B, Safari H, Safiri S, Sahraian MA, Salamati P, Saldanha RF, Samy AM, Sanabria J, Santos JV, Milicevic MMMS, Sartorius B, Satpathy M, Savuon K, Schneider IJC, Schwebel DC, Sepanlou SG, Shabaninejad H, Shaikh MAA, Shams-Beyranvand M, Sharif M, Sharif-Alhoseini M, Islam SMS, She J, Sheikh A, Shen J, Sheth KN, Shibuya K, Shiferaw MS, Shigematsu M, Shiri R, Shiue I, Shoman H, Siabani S, Siddiqi TJ, Silva JP, Silveira DGA, Sinha DN, Smith M, Filho AMS, Sobhani S, Soofi M, Soriano JB, Soyiri IN, Stein DJ, Stokes MA, Sufiyan MB, Sunguya BF, Sunshine JE, Sykes BL, Szoeke CEI, Tabarés-Seisdedos R, Ao BJT, Tehrani-Banihashemi A, Tekle MG, Temsah M-H, Temsah O, Topor-Madry R, Tortajada-Girbés M, Tran BX, Tran KB, Car LT, Ukwaja KN, Ullah I, Usman MS, Uthman OA, Valdez PR, Vasankari TJ, Venketasubramanian N, Violante FS, Wagnew FWS, Waheed Y, Wang Y-P, Weldegwergs KG, Werdecker A, Wijeratne T, Winkler AS, Wyper GMA, Yano Y, Yaseri M, Yasin YJ, Ye P, Yimer EM, Yip P, Yisma E, Yonemoto N, Yoon S-J, Yost MG, Younis MZ, Yousefifard M, Yu C, Zaidi Z, Zaman SB, Zamani M, Zenebe ZM, Zodpey S, Feigin VL, Vos T, Murray CJL (2019) Global, regional, and national burden of traumatic brain injury and spinal cord injury, 1990–2016: a systematic analysis for the global burden of disease study 2016. Lancet Neurol 18:56–87. https://doi.org/10.1016/S1474-4422(18)30415-0

Goff ZD, Kichura AB, Chibnall JT, Hauptman PJ (2017) A survey of unregulated direct-to-consumer treatment centers providing stem cells for patients with heart failure. JAMA Intern Med 177(9). https://doi.org/10.1001/jamainternmed.2017.2988

Goldman SA (2016) Stem and progenitor cell-based therapy of the central nervous system: hopes, hype, and wishful thinking. Cell Stem Cell. https://doi.org/10.1016/j.stem.2016.01.012

Gonzalez R, Hamblin MH, Lee J-P (2016) Neural stem cell transplantation and CNS diseases. CNS Neurol Disord Drug Targets 15:881–886

Gotherstrom C, Westgren M, Shaw SW, Astrom E, Biswas A, Byers PH, Mattar CN, Graham GE, Taslimi J, Ewald U, Fisk NM, Yeoh AE, Lin JL, Cheng PJ, Choolani M, Le Blanc K, Chan JK (2014) Pre- and postnatal transplantation of fetal mesenchymal stem cells in osteogenesis imperfecta: a two-center experience. Stem Cells Transl Med 3(2):255–264. https://doi.org/10.5966/sctm.2013-0090

Goutman SA, Brown MB, Glass JD, Boulis NM, Johe K, Hazel T, Cudkowicz M, Atassi N, Borges L, Patil PG, Sakowski SA, Feldman EL (2018) Long-term phase 1/2 intraspinal stem cell transplantation outcomes in

ALS. Ann Clin Transl Neurol 5:730–740. https://doi.org/10.1002/acn3.567

Guenou H, Nissan X, Larcher F, Feteira J, Lemaitre G, Saidani M, Del Rio M, Barrault CC, Bernard FX, Peschanski M, Baldeschi C, Waksman G (2009) Human embryonic stem-cell derivatives for full reconstruction of the pluristratified epidermis: a preclinical study. Lancet 374(9703):1745–1753. https://doi.org/10.1016/S0140-6736(09)61496-3

Gupta RK, Abdul-Jawad S, McCoy LE, Mok HP, Peppa D, Salgado M, Martinez-Picado J, Nijhuis M, Wensing AMJ, Lee H, Grant P, Nastouli E, Lambert J, Pace M, Salasc F, Monit C, Innes AJ, Muir L, Waters L, Frater J, Lever AML, Edwards SG, Gabriel IH, Olavarria E (2019) HIV-1 remission following CCR5Delta32/Delta32 haematopoietic stem-cell transplantation. Nature 568(7751):244–248. https://doi.org/10.1038/s41586-019-1027-4

Gyurkocza B, Storb R, Storer BE, Chauncey TR, Lange T, Shizuru JA, Langston AA, Pulsipher MA, Bredeson CN, Maziarz RT, Bruno B, Petersen FB, Maris MB, Agura E, Yeager A, Bethge W, Sahebi F, Appelbaum FR, Maloney DG, Sandmaier BM (2010) Nonmyeloablative allogeneic hematopoietic cell transplantation in patients with acute myeloid leukemia. J Clin Oncol 28(17):2859–2867. https://doi.org/10.1200/JCO.2009.27.1460

Hainzl S, Peking P, Kocher T, Murauer EM, Larcher F, Del Rio M, Duarte B, Steiner M, Klausegger A, Bauer JW, Reichelt J, Koller U (2017) COL7A1 editing via CRISPR/Cas9 in recessive dystrophic epidermolysis bullosa. Mol Ther 25(11):2573–2584. https://doi.org/10.1016/j.ymthe.2017.07.005

Henig I, Zuckerman T (2014) Hematopoietic stem cell transplantation-50 years of evolution and future perspectives. Rambam Maimonides Med J 5(4):e0028. https://doi.org/10.5041/RMMJ.10162

Hernon CA, Dawson RA, Freedlander E, Short R, Haddow DB, Brotherston M, MacNeil S (2006) Clinical experience using cultured epithelial autografts leads to an alternative methodology for transferring skin cells from the laboratory to the patient. Regen Med 1(6):809–821. https://doi.org/10.2217/17460751.1.6.809

Hirsch T, Rothoeft T, Teig N, Bauer JW, Pellegrini G, De Rosa L, Scaglione D, Reichelt J, Klausegger A, Kneisz D, Romano O, Secone Seconetti A, Contin R, Enzo E, Jurman I, Carulli S, Jacobsen F, Luecke T, Lehnhardt M, Fischer M, Kueckelhaus M, Quaglino D, Morgante M, Bicciato S, Bondanza S, De Luca M (2017) Regeneration of the entire human epidermis using transgenic stem cells. Nature 551(7680):327–332. https://doi.org/10.1038/nature24487

Horwitz EM, Prockop DJ, Fitzpatrick LA, Koo WW, Gordon PL, Neel M, Sussman M, Orchard P, Marx JC, Pyeritz RE, Brenner MK (1999) Transplantability and therapeutic effects of bone marrow-derived mesenchymal cells in children with osteogenesis imperfecta. Nat Med 5(3):309–313. https://doi.org/10.1038/6529

Hu C, Zhao L, Li L (2019) Current understanding of adipose-derived mesenchymal stem cell-based therapies in liver diseases. Stem Cell Res Ther 10(1):199. https://doi.org/10.1186/s13287-019-1310-1

Igarashi P, Somlo S (2007) Polycystic kidney disease. J Am Soc Nephrol 18(5):1371–1373. https://doi.org/10.1681/ASN.2007030299

Iijima H, Isho T, Kuroki H, Takahashi M, Aoyama T (2018) Effectiveness of mesenchymal stem cells for treating patients with knee osteoarthritis: a meta-analysis toward the establishment of effective regenerative rehabilitation. NPJ Regen Med 3:15. https://doi.org/10.1038/s41536-018-0041-8

Inoue H, Nagata N, Kurokawa H, Yamanaka S (2014) iPS cells: a game changer for future medicine. EMBO J 33(5):409–417. https://doi.org/10.1002/embj.201387098

Iriguchi S, Kaneko S (2019) Toward the development of true "off-the-shelf" synthetic T-cell immunotherapy. Cancer Sci 110(1):16–22. https://doi.org/10.1111/cas.13892

Izmiryan A, Ganier C, Bovolenta M, Schmitt A, Mavilio F, Hovnanian A (2018) Ex vivo COL7A1 correction for recessive dystrophic epidermolysis bullosa using CRISPR/Cas9 and homology-directed repair. Mol Ther Nucleic Acids 12:554–567. https://doi.org/10.1016/j.omtn.2018.06.008

JCR Pharmaceuticals Co. L (2017) Annual Report. https://ssl4.eir-parts.net/doc/4552/ir_material_for_fiscal_ym4/63251/00.pdf

Jessop H, Farge D, Saccardi R, Alexander T, Rovira M, Sharrack B, Greco R, Wulffraat N, Moore J, Kazmi M, Badoglio M, Adams G, Verhoeven B, Murray J, Snowden JA (2019) General information for patients and carers considering haematopoietic stem cell transplantation (HSCT) for severe autoimmune diseases (ADs): a position statement from the EBMT Autoimmune Diseases Working Party (ADWP), the EBMT Nurses Group, the EBMT Patient, Family and Donor Committee and the Joint Accreditation Committee of ISCT and EBMT (JACIE). Bone Marrow Transplant 54(7):933–942. https://doi.org/10.1038/s41409-019-0430-7

Jungbluth P, Spitzhorn LS, Grassmann J, Tanner S, Latz D, Rahman MS, Bohndorf M, Wruck W, Sager M, Grotheer V, Kropil P, Hakimi M, Windolf J, Schneppendahl J, Adjaye J (2019) Human iPSC-derived iMSCs improve bone regeneration in minipigs. Bone Res 7 (1):32. https://doi.org/10.1038/s41413-019-0069-4

Kalia LV, Lang AE (2015) Parkinson's disease. Lancet (London, UK) 386:896–912. https://doi.org/10.1016/S0140-6736(14)61393-3

Karimkhani C, Dellavalle RP, Coffeng LE, Flohr C, Hay RJ, Langan SM, Nsoesie EO, Ferrari AJ, Erskine HE, Silverberg JI, Vos T, Naghavi M (2017) Global skin disease morbidity and mortality: an update from the global burden of disease study 2013. JAMA Dermatol 153(5):406–412. https://doi.org/10.1001/jamadermatol.2016.5538

Kharroubi AT, Darwish HM (2015) Diabetes mellitus: the epidemic of the century. World J Diabetes 6 (6):850–867. https://doi.org/10.4239/wjd.v6.i6.850

Kim JH, Kurtz A, Yuan BZ, Zeng F, Lomax G, Loring JF, Crook J, Ju JH, Clarke L, Inamdar MS, Pera M, Firpo MT, Sheldon M, Rahman N, O'Shea O, Pranke P, Zhou Q, Isasi R, Rungsiwiwut R, Kawamata S, Oh S, Ludwig T, Masui T, Novak TJ, Takahashi T, Fujibuchi W, Koo SK, Stacey GN (2017) Report of the international stem cell banking initiative workshop activity: current hurdles and progress in seed-stock banking of human pluripotent stem cells. Stem Cells Transl Med 6 (11):1956–1962. https://doi.org/10.1002/sctm.17-0144

Klein J, Sato A (2000) The HLA system. N Engl J Med 434 (10):702–709. https://doi.org/10.1056/NEJM200009073431006

Kobayashi K, Stamm C, Nakauchi A (2019) First iPSC-Derived CAR T-Cell Therapy Created by Kyoto University CiRA and Takeda Collaboration Enters Process Development Toward Clinical Testing. https://www.takeda.com/newsroom/newsreleases/2019/first-ipsc-derived-car-t-cell-therapy-created-by-kyoto-university-cira-and%2D%2Dtakeda-collaboration-enters-process-development-toward-clinical-testing/. Accessed 6 Sept 2019

Kurtzberg J, Prockop S, Teira P, Bittencourt H, Lewis V, Chan KW, Horn B, Yu L, Talano JA, Nemecek E, Mills CR, Chaudhury S (2014) Allogeneic human mesenchymal stem cell therapy (remestemcel-L, Prochymal) as a rescue agent for severe refractory acute graft-versus-host disease in pediatric patients. Biol Blood Marrow Transplant 20(2):229–235. https://doi.org/10.1016/j.bbmt.2013.11.001

Lazarus HM, Haynesworth SE, Gerson SL, Rosenthal NS, Caplan AI (1995) Ex vivo expansion and subsequent infusion of human bone marrow-derived stromal progenitor cells (mesenchymal progenitor cells): implications for therapeutic use. Bone Marrow Transplant 16 (4)

Little MT, Storb R (2002) History of haematopoietic stem-cell transplantation. Nat Rev Cancer 2(3):231–238. https://doi.org/10.1038/nrc748

Makhlough A, Shekarchian S, Moghadasali R, Einollahi B, Hosseini SE, Jaroughi N, Bolurieh T, Baharvand H, Aghdami N (2017) Safety and tolerability of autologous bone marrow mesenchymal stromal cells in ADPKD patients. Stem Cell Res Ther 8(1):116. https://doi.org/10.1186/s13287-017-0557-7

Malliaras K, Makkar RR, Smith RR, Cheng K, Wu E, Bonow RO, Marbán L, Mendizabal A, Cingolani E, Johnston PV, Gerstenblith G, Schuleri KH, Lardo AC, Marbán E (2014) Intracoronary cardiosphere-derived cells after myocardial infarction. J Am Coll Cardiol 63 (2):110–122. https://doi.org/10.1016/j.jacc.2013.08.724

Marks PW, Witten CM, Califf RM (2017) Clarifying stem-cell Therapy's benefits and risks. N Engl J Med 376 (11):1007–1009. https://doi.org/10.1056/NEJMp1613723

Mavilio F, Pellegrini G, Ferrari S, Di Nunzio F, Di Iorio E, Recchia A, Maruggi G, Ferrari G, Provasi E, Bonini C, Capurro S, Conti A, Magnoni C, Giannetti A, De Luca M (2006) Correction of junctional epidermolysis bullosa by transplantation of genetically modified epidermal stem cells. Nat Med 12(12):1397–1402. https://doi.org/10.1038/nm1504

Maximow AA (1924) Relation of blood cells to connective tissues and endothelium. Physiol Rev 4(4):533–563. https://doi.org/10.1152/physrev.1924.4.4.533

Menasche P, Vanneaux V, Hagege A, Bel A, Cholley B, Parouchev A, Cacciapuoti I, Al-Daccak R, Benhamouda N, Blons H, Agbulut O, Tosca L, Trouvin JH, Fabreguettes JR, Bellamy V, Charron D, Tartour E, Tachdjian G, Desnos M, Larghero J (2018) Transplantation of human embryonic stem cell-derived cardiovascular progenitors for severe ischemic left ventricular dysfunction. J Am Coll Cardiol 71(4):429–438. https://doi.org/10.1016/j.jacc.2017.11.047

Michler RE (2018) The current status of stem cell therapy in ischemic heart disease. J Card Surg 33(9):520–531. https://doi.org/10.1111/jocs.13789

Ming G, Song H (2011) Adult neurogenesis in the mammalian brain: significant answers and significant questions. Neuron. https://doi.org/10.1016/j.neuron.2011.05.001

Nagoshi N, Tsuji O, Nakamura M, Okano H (2019) Cell therapy for spinal cord injury using induced pluripotent stem cells. Regen Ther 11:75–80. https://doi.org/10.1016/J.RETH.2019.05.006

O'Connor NE, Mulliken JB (1981) Grafting of burns with cultured epithelium prepared from autologous epidermal cells. Lancet 1(8211):75–78

Oh KW, Moon C, Kim HY, Oh SI, Park J, Lee JH, Chang IY, Kim KS, Kim SH (2015) Phase I trial of repeated intrathecal autologous bone marrow-derived mesenchymal stromal cells in amyotrophic lateral sclerosis. Stem Cells Transl Med 4(6):590–597. https://doi.org/10.5966/sctm.2014-0212

Panch SR, Szymanski J, Savani BN, Stroncek DF (2017) Sources of hematopoietic stem and progenitor cells and methods to optimize yields for clinical cell therapy. Biol Blood Marrow Transplant 23(8):1241–1249. https://doi.org/10.1016/j.bbmt.2017.05.003

Panés J, García-Olmo D, Van Assche G, Colombel JF, Reinisch W, Baumgart DC, Dignass A, Nachury M, Ferrante M, Kazemi-Shirazi L, Grimaud JC, de la Portilla F, Goldin E, Richard MP, Leselbaum A, Danese S (2016) Expanded allogeneic adipose-derived mesenchymal stem cells (Cx601) for complex perianal fistulas in Crohn's disease: a phase 3 randomised, double-blind controlled trial. Lancet 388(10051):1281–1290. https://doi.org/10.1016/s0140-6736(16)31203-x

Passweg JR, Baldomero H, Basak GW, Chabannon C, Corbacioglu S, Duarte R, Kuball J, Lankester A, Montoto S, de Latour RP, Snowden JA, Styczynski J, Yakoub-Agha I, Arat M, Mohty M, Kroger N, European Society for B, Marrow T (2019) The EBMT activity survey report 2017: a focus on allogeneic HCT for nonmalignant indications and on the use of non-HCT cell therapies. Bone Marrow Transplant. https://doi.org/10.1038/s41409-019-0465-9

Pellegrini G, Rama P, Mavilio F, De Luca M (2009) Epithelial stem cells in corneal regeneration and epidermal gene therapy. J Pathol 217(2):217–228. https://doi.org/10.1002/path.2441

Pereira IM, Marote A, Salgado AJ, Silva NA (2019) Filling the gap: neural stem cells as a promising therapy for spinal cord injury. Pharmaceuticals (Basel, Switzerland) 12. https://doi.org/10.3390/ph12020065

Petrof G, Abdul-Wahab A, McGrath JA (2014) Cell therapy in dermatology. Cold Spring Harb Perspect Med 4 (6). https://doi.org/10.1101/cshperspect.a015156

Petrof G, Lwin SM, Martinez-Queipo M, Abdul-Wahab A, Tso S, Mellerio JE, Slaper-Cortenbach I, Boelens JJ, Tolar J, Veys P, Ofuya M, Peacock JL, Martinez AE, McGrath JA (2015) Potential of systemic allogeneic mesenchymal stromal cell therapy for children with recessive dystrophic epidermolysis bullosa. J Invest Dermatol 135(9):2319–2321. https://doi.org/10.1038/jid.2015.158

Pullen LC (2018) Stem cell-derived pancreatic progenitor cells have now been transplanted into patients: report from IPITA 2018. Am J Transplant 18(7):1581–1582. https://doi.org/10.1111/ajt.14954

Rahman MS, Spitzhorn L-S, Wruck W, Hagenbeck C, Balan P, Graffmann N, Bohndorf M, Ncube A, Guillot PV, Fehm T, Adjaye J (2018) The presence of human mesenchymal stem cells of renal origin in amniotic fluid increases with gestational time. Stem Cell Res Ther 9(1). https://doi.org/10.1186/s13287-018-0864-7

Rama P, Matuska S, Paganoni G, Spinelli A, De Luca M, Pellegrini G (2010) Limbal stem-cell therapy and long-term corneal regeneration. N Engl J Med 363 (2):147–155. https://doi.org/10.1056/NEJMoa0905955

Rheinwald JG, Green H (1975) Serial cultivation of strains of human epidermal keratinocytes: the formation of keratinizing colonies from single cells. Cell 6 (3):331–343. https://doi.org/10.1016/s0092-8674(75)80001-8

Sakai D, Schol J, Foldager CB, Sato M, Watanabe M (2017) Regenerative technologies to bed side: evolving the regulatory framework. J Orthop Translat 9:1–7. https://doi.org/10.1016/j.jot.2017.02.001

Schachinger V, Erbs S, Elsasser A, Haberbosch W, Hambrecht R, Holschermann H, Yu J, Corti R, Mathey DG, Hamm CW, Suselbeck T, Werner N, Haase J, Neuzner J, Germing A, Mark B, Assmus B, Tonn T, Dimmeler S, Zeiher AM (2006) Improved clinical outcome after intracoronary administration of bone-marrow-derived progenitor cells in acute myocardial infarction: final 1-year results of the REPAIR-AMI trial. Eur Heart J 27(23):2775–2783. https://doi.org/10.1093/eurheartj/ehl388

Schwartz SD, Regillo CD, Lam BL, Eliott D, Rosenfeld PJ, Gregori NZ, Hubschman J-P, Davis JL, Heilwell G, Spirn M, Maguire J, Gay R, Bateman J, Ostrick RM, Morris D, Vincent M, Anglade E, Del Priore LV, Lanza R (2015) Human embryonic stem cell-derived retinal pigment epithelium in patients with age-related macular degeneration and Stargardt's macular dystrophy: follow-up of two open-label phase 1/2 studies. Lancet 385:509–516. https://doi.org/10.1016/S0140-6736(14)61376-3

Seaberg RM, van der Kooy D (2003) Stem and progenitor cells: the premature desertion of rigorous definitions. Trends Neurosci 26:125–131. https://doi.org/10.1016/S0166-2236(03)00031-6

Sebastiano V, Zhen HH, Haddad B, Bashkirova E, Melo SP, Wang P, Leung TL, Siprashvili Z, Tichy A, Li J, Ameen M, Hawkins J, Lee S, Li L, Schwertschkow A, Bauer G, Lisowski L, Kay MA, Kim SK, Lane AT, Wernig M, Oro AE (2014) Human COL7A1-corrected induced pluripotent stem cells for the treatment of recessive dystrophic epidermolysis bullosa. Sci Transl Med 6(264):264ra163. https://doi.org/10.1126/scitranslmed.3009540

Segers VFM, Lee RT (2008) Stem-cell therapy for cardiac disease. Nature 451(7181):937–942. https://doi.org/10.1038/nature06800

Sheyn D, Ben-David S, Shapiro G, De Mel S, Bez M, Ornelas L, Sahabian A, Sareen D, Da X, Pelled G, Tawackoli W, Liu Z, Gazit D, Gazit Z (2016) Human induced pluripotent stem cells differentiate into functional mesenchymal stem cells and repair bone defects. Stem Cells Transl Med 5(11):1447–1460. https://doi.org/10.5966/sctm.2015-0311

Sipp D, Caulfield T, Kaye J, Barfoot J, Blackburn C, Chan S, De Luca M, Kent A, McCabe C, Munsie M, Sleeboom-Faulkner M, Sugarman J, van Zimmeren E, Zarzeczny A, Rasko JEJ (2017) Marketing of unproven stem cell-based interventions: a call to action. Sci Transl Med 9 (397). https://doi.org/10.1126/scitranslmed.aag0426

Smets F, Dobbelaere D, McKiernan P, Dionisi-Vici C, Broue P, Jacquemin E, Lopes AI, Goncalves I, Mandel H, Pawlowska J, Kaminska D, Shteyer E, Torre G, Shapiro R, Eyskens F, Clapuyt P, Gissen P, Pariente D, Grunewald S, Yudkoff M, Binda MM, Najimi M, Belmonte N, Vos B, Thonnard J, Sokal E (2019) Phase I/II trial of liver derived mesenchymal stem cells in pediatric liver based metabolic disorders: a prospective, open label, multicenter, partially randomized, safety study of one cycle of heterologous human adult liver-derived progenitor cells (HepaStem(R)) in urea cycle disorders and Crigler-Najjar Syndrome patients. Transplantation. https://doi.org/10.1097/TP.0000000000002605

Sneddon JB, Tang Q, Stock P, Bluestone JA, Roy S, Desai T, Hebrok M (2018) Stem cell therapies for treating diabetes: progress and remaining challenges. Cell Stem Cell 22(6):810–823. https://doi.org/10.1016/j.stem.2018.05.016

Sokal EM (2014) Treating inborn errors of liver metabolism with stem cells: current clinical development. J Inherit Metab Dis 37(4):535–539. https://doi.org/10.1007/s10545-014-9691-x

Sokal EM, Stephenne X, Ottolenghi C, Jazouli N, Clapuyt P, Lacaille F, Najimi M, de Lonlay P, Smets F (2014) Liver engraftment and repopulation by in vitro expanded adult derived human liver stem cells in a child with ornithine

carbamoyltransferase deficiency. JIMD Rep 13:65–72. https://doi.org/10.1007/8904_2013_257

Spitzhorn L-S, Rahman MS, Schwindt L, Ho H-T, Wruck W, Bohndorf M, Wehrmeyer S, Ncube A, Beyer I, Hagenbeck C, Balan P, Fehm T, Adjaye J (2017) Isolation and molecular characterization of amniotic fluid-derived mesenchymal stem cells obtained from caesarean sections. Stem Cells Int 2017:1–15. https://doi.org/10.1155/2017/5932706

Spitzhorn LS, Kordes C, Megges M, Sawitza I, Gotze S, Reichert D, Schulze-Matz P, Graffmann N, Bohndorf M, Wruck W, Kohler JP, Herebian D, Mayatepek E, Oreffo RO, Haussinger D, Adjaye J (2018) Transplanted human pluripotent stem cell-derived mesenchymal stem cells support liver regeneration in Gunn rats. Stem Cells Dev. https://doi.org/10.1089/scd.2018.0010

Spitzhorn LS, Megges M, Wruck W, Rahman MS, Otte J, Degistirici O, Meisel R, Sorg RV, Oreffo ROC, Adjaye J (2019) Human iPSC-derived MSCs (iMSCs) from aged individuals acquire a rejuvenation signature. Stem Cell Res Ther 10(1):100. https://doi.org/10.1186/s13287-019-1209-x

Stanger BZ (2015) Cellular homeostasis and repair in the mammalian liver. Annu Rev Physiol 77:179–200. https://doi.org/10.1146/annurev-physiol-021113-170255

Steinhoff G, Nesteruk J, Wolfien M, Kundt G, Börgermann J, David R, Garbade J, Große J, Haverich A, Hennig H, Kaminski A, Lotz J, Mohr F-W, Müller P, Oostendorp R, Ruch U, Sarikouch S, Skorska A, Stamm C, Tiedemann G, Wagner FM, Wolkenhauer O (2017) Cardiac function improvement and bone marrow response –. EBioMedicine 22:208–224. https://doi.org/10.1016/j.ebiom.2017.07.022

Takahashi K, Tanabe K, Ohnuki M, Narita M, Ichisaka T, Tomoda K, Yamanaka S (2007) Induction of pluripotent stem cells from adult human fibroblasts by defined factors. Cell 131(5):861–872. https://doi.org/10.1016/j.cell.2007.11.019

Tang Y, Yu P, Cheng L (2017) Current progress in the derivation and therapeutic application of neural stem cells. Nat Publ Group 8:3108. https://doi.org/10.1038/cddis.2017.504

Thomas ED, Lochte HL Jr, Lu WC, Ferrebee JW (1957) Intravenous infusion of bone marrow in patients receiving radiation and chemotherapy. N Engl J Med 257 (11):491–496. https://doi.org/10.1056/NEJM195709122571102

Thomson JA, Itskovitz-Eldor J, Shapiro SS, Waknitz MA, Swiergiel JJ, Marshall VS, Jones JM (1998) Embryonic stem cell lines derived from human blastocysts. Science 282(5391):1145–1147

Tolar J, McGrath JA, Xia L, Riddle MJ, Lees CJ, Eide C, Keene DR, Liu L, Osborn MJ, Lund TC, Blazar BR, Wagner JE (2014) Patient-specific naturally gene-reverted induced pluripotent stem cells in recessive dystrophic epidermolysis bullosa. J Invest Dermatol 134 (5):1246–1254. https://doi.org/10.1038/jid.2013.523

Toma C, Pittenger MF, Cahill KS, Byrne BJ, Kessler PD (2002) Human mesenchymal stem cells differentiate to a cardiomyocyte phenotype in the adult murine heart. Circulation 105(1):93–98. https://doi.org/10.1161/hc0102.101442

Tsuji O, Sugai K, Yamaguchi R, Tashiro S, Nagoshi N, Kohyama J, Iida T, Ohkubo T, Itakura G, Isoda M, Shinozaki M, Fujiyoshi K, Kanemura Y, Yamanaka S, Nakamura M, Okano H (2019) Concise review: laying the groundwork for a first-in-human study of an induced pluripotent stem cell-based intervention for spinal cord injury. Stem Cells 37:6–13. https://doi.org/10.1002/stem.2926

Tysnes O-B, Storstein A (2017) Epidemiology of Parkinson's disease. J Neural Transm 124:901–905. https://doi.org/10.1007/s00702-017-1686-y

van Rood JJ (1966) Leucocyte groups and histocompatibility. Vox Sang 11(3):276–292. https://doi.org/10.1111/j.1423-0410.1966.tb04603.x

Wenker SD, Pitossi FJ (2019) Cell therapy for Parkinson's disease is coming of age: current challenges and future prospects with a focus on immunomodulation. Gene Ther. https://doi.org/10.1038/s41434-019-0077-4

Wenzel D, Bayerl J, Nystrom A, Bruckner-Tuderman L, Meixner A, Penninger JM (2014) Genetically corrected iPSCs as cell therapy for recessive dystrophic epidermolysis bullosa. Sci Transl Med 6(264):264ra165. https://doi.org/10.1126/scitranslmed.3010083

Wu M, Zhang R, Zou Q, Chen Y, Zhou M, Li X, Ran R, Chen Q (2018) Comparison of the biological characteristics of mesenchymal stem cells derived from the human placenta and umbilical cord. Sci Rep 8(1):5014. https://doi.org/10.1038/s41598-018-23396-1

Yang YK (2018) Aging of mesenchymal stem cells: implication in regenerative medicine. Regen Ther 9:120–122. https://doi.org/10.1016/j.reth.2018.09.002

Zhao Y, Jiang Z, Zhao T, Ye M, Hu C, Zhou H, Yin Z, Chen Y, Zhang Y, Wang S, Shen J, Thaker H, Jain S, Li Y, Diao Y, Chen Y, Sun X, Fisk MB, Li H (2013) Targeting insulin resistance in type 2 diabetes via immune modulation of cord blood-derived multipotent stem cells (CB-SCs) in stem cell educator therapy: phase I/II clinical trial. BMC Med 11:160. https://doi.org/10.1186/1741-7015-11-160

3.7 Human iPSC-derived iMSCs Improve Bone Regeneration in Mini-pigs

Pascal Jungbluth, Lucas-Sebastian Spitzhorn, Jan Grassmann, Stephan Tanner, David Latz, Md Shaifur Rahman, Martina Bohndorf, Wasco Wruck, Martin Sager, Vera Grotheer, Patric Kröpil, Mohssen Hakimi, Joachim Windolf, Johannes Schneppendahl and James Adjaye

Abstract

Autologous bone marrow concentrate (BMC) and mesenchymal stem cells (MSCs) have beneficial effects on the healing of bone defects. To address the shortcomings associated with the use of primary MSCs, induced pluripotent stem cell (iPSC)-derived MSCs (iMSCs) have been proposed as an alternative. The aim of this study was to investigate the bone regeneration potential of human iMSCs combined with calcium phosphate granules (CPG) in critical-size defects in the proximal tibias of mini-pigs in the early phase of bone healing compared to that of a previously reported autograft treatment and treatment with a composite made of either a combination of autologous BMC and CPG or CPG alone. iMSCs were derived from iPSCs originating from human fetal foreskin fibroblasts (HFFs). They were able to differentiate into osteoblasts in vitro, express a plethora of bone morphogenic proteins (BMPs) and secrete paracrine signaling-associated cytokines such as PDGF-AA and osteopontin. Radiologically and histomorphometrically, HFF-iMSC + CPG transplantation resulted in significantly better osseous consolidation than the transplantation of CPG alone and produced no significantly different outcomes compared to the transplantation of autologous BMC + CPG after 6 weeks. The results of this translational study imply that iMSCs represent a valuable future treatment option for load-bearing bone defects in humans.

Publication Status: Published in Bone Res. 2019; 7: 32.
Impact Factor: 12.354

Approximated total share of contribution: 10%
Contribution on experimental design, realization and publication: JA, JS, JW, PJ and LSS conceived the ideas and designed the experiments. PJ, JS, JG, ST, M.H. and MS were responsible for the care of the animals, the operation procedure and the postoperative care. PJ, JS, JG, PK and ST performed the explantations, subsequent histomorphometrical, and radiological analyses. LSS, MSR and MB performed the characterization of the HFF-iPSCs and the generation and

characterization of the HFF-iMSCs. WW performed the transcriptome analyses. DL evaluated and processed the images of the histomorphometrical and radiological analyses. All authors contributed to the writing of the manuscript, and JA and JW approved the final version of the manuscript.

Pubmed link: https://www.ncbi.nlm.nih.gov/pmc/articles/PMC6813363/
Journal link: https://www.nature.com/articles/s41413-019-0069-4

ARTICLE OPEN

Human iPSC-derived iMSCs improve bone regeneration in mini-pigs

Pascal Jungbluth[1], Lucas-Sebastian Spitzhorn[2], Jan Grassmann[1], Stephan Tanner[1], David Latz[1], Md Shaifur Rahman[2], Martina Bohndorf[2], Wasco Wruck[2], Martin Sager[3], Vera Grotheer[1], Patric Kröpil[4], Mohssen Hakimi[5], Joachim Windolf[1], Johannes Schneppendahl[1] and James Adjaye[2]

Autologous bone marrow concentrate (BMC) and mesenchymal stem cells (MSCs) have beneficial effects on the healing of bone defects. To address the shortcomings associated with the use of primary MSCs, induced pluripotent stem cell (iPSC)-derived MSCs (iMSCs) have been proposed as an alternative. The aim of this study was to investigate the bone regeneration potential of human iMSCs combined with calcium phosphate granules (CPG) in critical-size defects in the proximal tibias of mini-pigs in the early phase of bone healing compared to that of a previously reported autograft treatment and treatment with a composite made of either a combination of autologous BMC and CPG or CPG alone. iMSCs were derived from iPSCs originating from human fetal foreskin fibroblasts (HFFs). They were able to differentiate into osteoblasts in vitro, express a plethora of bone morphogenic proteins (BMPs) and secrete paracrine signaling-associated cytokines such as PDGF-AA and osteopontin. Radiologically and histomorphometrically, HFF-iMSC + CPG transplantation resulted in significantly better osseous consolidation than the transplantation of CPG alone and produced no significantly different outcomes compared to the transplantation of autologous BMC + CPG after 6 weeks. The results of this translational study imply that iMSCs represent a valuable future treatment option for load-bearing bone defects in humans.

Bone Research (2019)7:32 ; https://doi.org/10.1038/s41413-019-0069-4

INTRODUCTION

The majority of bone fractures heal without complications. However, cases involving bone nonunion and large skeletal bone defects represent a challenge for orthopedic surgery. Despite its significant drawbacks, including donor site morbidity, limited availability, and poor bone quality, autologous bone grafting remains the gold standard for treatment.[1] The use of autologous bone marrow concentrate (BMC) or mesenchymal stem cells (MSCs) have been described as alternative treatment options for improving bone regeneration.[2,3]

BMC contains stem cells, growth factors, and immune cells and have been shown to improve bone regeneration.[4] MSCs are multipotent, which is manifested in their ability to differentiate into adipocytes, chondrocytes and osteoblasts in vitro.[5–8]

MSCs, as well as BMC, have been used in large animal studies for bone regeneration in weight-bearing and nonweight-bearing conditions.[4,9] However, the availability of MSCs is restricted and associated with complications such as donor site comorbidity related to the invasive isolation from bone marrow or other tissues such as fat.[10] Furthermore, it has been demonstrated that their differentiation and proliferation capacity decreases with donor age and the duration of culture.[11–13]

MSCs differentiated from embryonic or induced pluripotent stem cells (ESCs, iPSCs), termed iMSCs, represent an alternative to primary MSCs. As the use of ESCs is associated with ethical concerns, iPSC-derived iMSCs have been identified as a promising source of transplantable donor cells for regenerative therapies. The advantage of the use of iMSCs is that they can be generated from well-characterized and banked iPSCs with known HLA types. Another advantage of iMSCs over their native counterparts is that iMSCs have been characterized as rejuvenated MSCs.[14] Although they are derived from pluripotent cells (which are by definition tumorigenic), iMSCs themselves are free from the risk of tumor formation since they do not express oncogenic pluripotency-associated genes such as OCT4.[15] Moreover, iMSCs outperformed native MSCs in the treatment of multiple sclerosis in a rodent model.[16] More importantly, iMSCs have been successfully used in vivo to improve bone regeneration by their direct differentiation into bone cells and their recruitment of host cells in a radial defect model in mice.[10] The aim of this study was to evaluate the feasibility and impact of the use of a composite made of human iMSCs and calcium phosphate granules (CPG) for bone regeneration compared with that of a previously investigated autograft treatment, a composite made of autologous BMCs and CPG, and CPG alone in a critical-size long bone defect in mini-pigs under weight-bearing conditions in the early phase of bone healing. To the best of our knowledge, this investigation is the first to evaluate

[1]Department of Trauma and Hand Surgery, Heinrich Heine University Hospital Düsseldorf, Moorenstr. 5, 40225 Düsseldorf, Germany; [2]Institute for Stem Cell Research and Regenerative Medicine, Medical Faculty, Heinrich Heine University, Düsseldorf, Moorenstr. 5, 40225 Düsseldorf, Germany; [3]Animal Research Institute, Heinrich Heine University, Düsseldorf, Moorenstr. 5, 40225 Düsseldorf, Germany; [4]Department of Diagnostic and Interventional Radiology, Medical Faculty, Heinrich Heine University, Düsseldorf, Moorenstr. 5, 40225 Düsseldorf, Germany and [5]Vivantes Klinikum Am Urban, Dieffenbachstraße 1, 10967 Berlin, Germany
Correspondence: Johannes Schneppendahl (Johannes.Schneppendahl@med.uni-duesseldorf.de) or James Adjaye (james.adjaye@med.uni-duesseldorf.de)
These authors contributed equally: Pascal Jungbluth, Lucas-Sebastian Spitzhorn

Received: 22 October 2018 Revised: 4 June 2019 Accepted: 22 July 2019
Published online: 24 October 2019

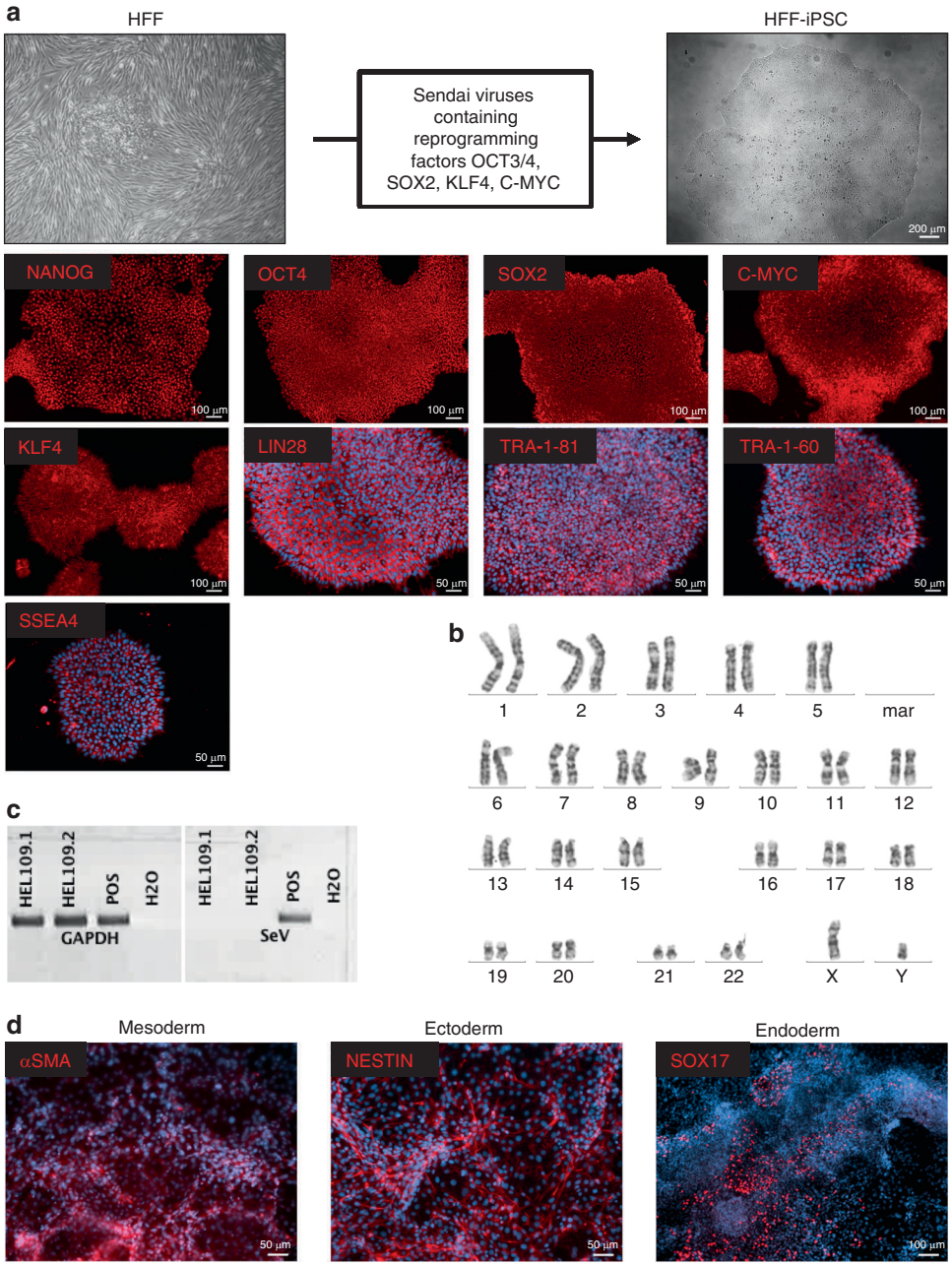

Fig. 1 Characterization of HFF-derived iPSCs. **a** Protocol used for the generation of HFF-iPSCs and the confirmation of pluripotency marker expression by immunofluorescence-based detection. **b** Karyotype of the HFF-iPSCs. **c** Viral vector dilution PCR. **d** Evaluation of embryoid body formation by using immunofluorescence-based staining. Cell nuclei are stained using Hoechst stain (blue)

the regenerative potential of human iMSCs in a large animal model under the aforementioned conditions.

RESULTS

Reprogramming of HFFs into iPSCs

Human fetal foreskin fibroblasts (HFFs) were used to generate iPSCs by employing Sendai viruses encoding the reprogramming factors OCT3/4, SOX2, KLF4, and C-MYC. The HFF-iPSCs grew as colonies and expressed the pluripotency-regulating transcription factors OCT4, SOX2, NANOG, C-MYC, and KLF4 in addition to LIN28, SSEA4, TRA-1-60, and TRA-1-81 (Fig. 1a). A normal human male karyotype (46, XY) with no chromosomal aberrations was observed (Fig. 1b), and the absence of viral DNA was confirmed by PCR (Fig. 1c). Embryoid body formation assays demonstrated the capability of the HFF-iPSCs to differentiate into mesoderm (αSMA), ectoderm (NESTIN) and endoderm (SOX17) (Fig. 1d).

Characterization of the HFF-iMSCs

The HFF-iPSCs were differentiated into HFF-iMSCs using a 14-day protocol that utilized the inhibition of the TGFβ pathway by SB431542.[17] HFF-iMSCs showed a typical fibroblast spindle-shaped morphology and expressed the MSC markers PDGFRβ and Vimentin. Importantly, in contrast to the HFF-iPSCs, they were devoid of OCT4 expression (Fig. 2a). Cell surface marker analysis revealed that they exhibited a typical MSC immunophenotype by expressing CD73, CD90, and CD105 versus the hematopoietic markers CD14, CD20, CD34, and CD45 (Fig. 2b). The HFF-iMSCs

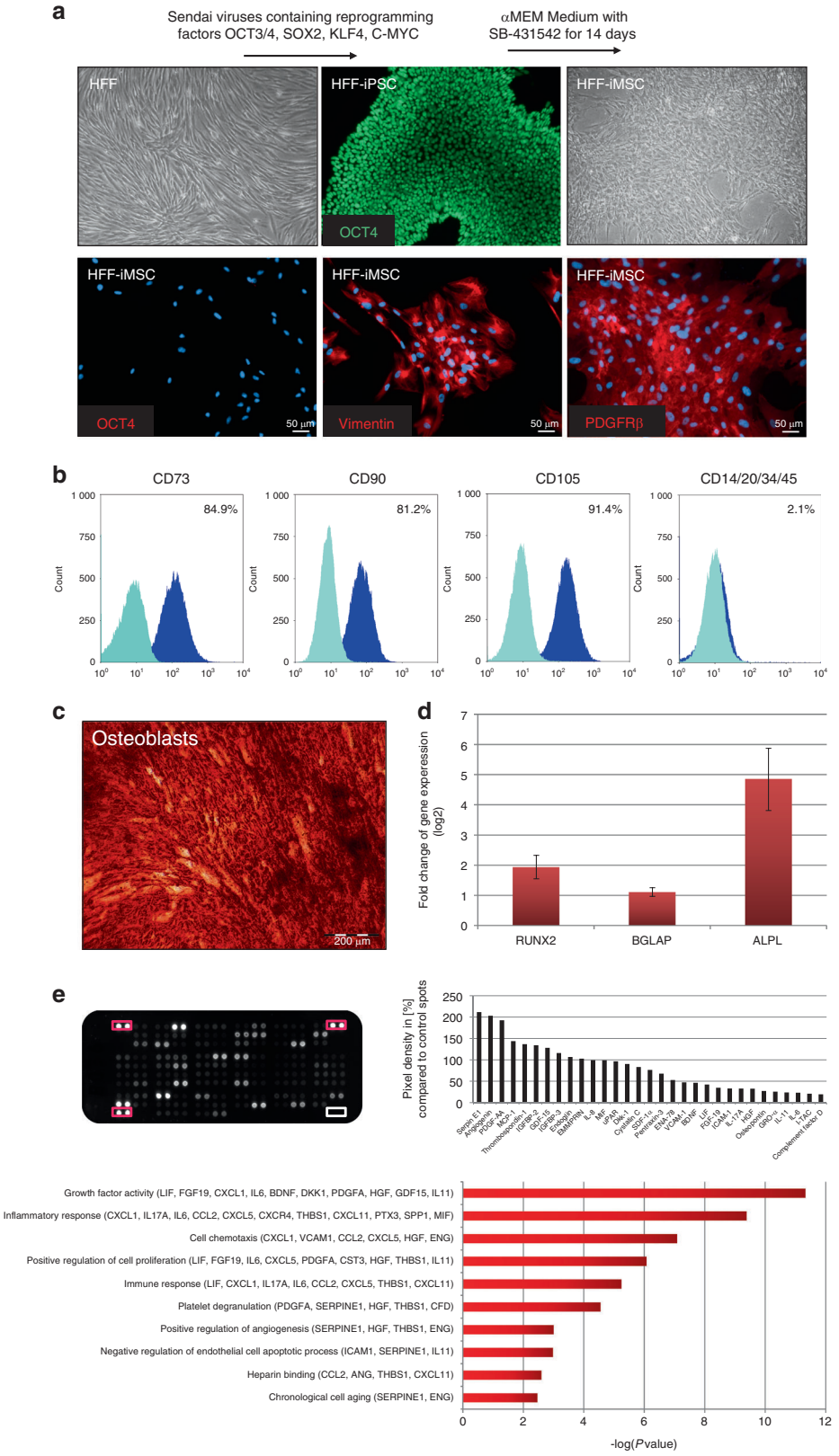

Fig. 2 Properties of HFF-iPSC-derived iMSCs. **a** HFF-iMCS were analyzed with respect to their morphology and protein expression. The cell nuclei were stained with Hoechst. **b** Flow cytometric analysis using MSC cell surface markers (dark blue: specific cell surface markers; light blue: antibody isotype controls). **c** Alizarin Red S staining after osteogenic differentiation for 3 weeks. **d** Quantitative real-time PCR results for bone-related genes (in triplicate, normalized to the levels in untreated cells). **e** Cytokine membrane incubated with HFF-iMSC-conditioned media (left) and the background-corrected top 31 detected cytokines representing each of the selected associated GO terms; *P*-value < 0.05 (right)

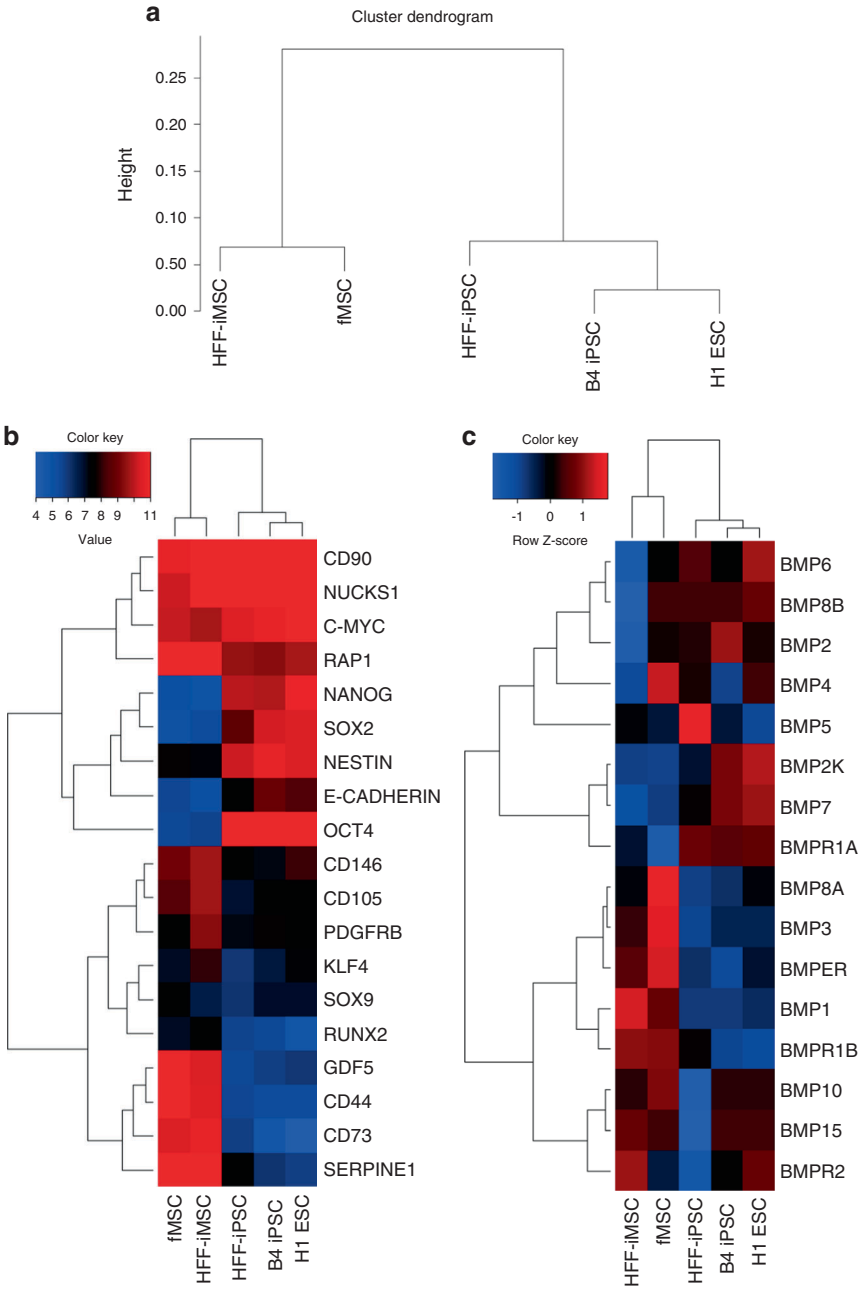

Fig. 3 Microarray analysis of the HFF-iMSCs. **a** Cluster dendrogram of the HFF-iMSCs, fMSCs and pluripotent stem cells. **b** Heatmap depicting differential gene expression in HFF-iMSCs, fMSCs and pluripotent stem cells (iPSCs and ESCs). **c** Heatmap displaying the differential expression of BMPs and their corresponding receptors

were able to differentiate into adipocytes and chondrocytes (Fig. S1). More importantly, osteoblast differentiation in vitro was confirmed by Alizarin Red S staining of the emerged calcium deposits (Fig. 2c) and also by the upregulated expression of the bone-related genes *RUNX2, BGLAP*, and *ALPL* (Fig. 2d). The secretome of the HFF-iMSCs was investigated using a cytokine membrane assay able to detect 103 distinct cytokines. The top 31 secreted cytokines included serpin E1, angiogenin, PDGF-AA, and osteopontin, which are known to play an important role in skeletal regeneration processes. The associated GO terms "growth factor activity", "cell chemotaxis" and "positive regulation of angiogenesis" imply the beneficial properties of these factors that are secreted by HFF-iMSCs (Fig. 2e).

Transcriptome and STR analysis of HFF-iMSCs

The transcriptomes of the HFF-iMSCs were compared with the transcriptomes of iPSCs, ESCs, and fMSCs by microarray analysis. Cluster analysis revealed two groups: one that included the pluripotent cells, including the HFF-iPSCs, B4-iPSCs, and H1-ESCs, and the other that included the MSCs, HFF-iMSCs and primary fetal MSCs (fMSCs) (Fig. 3a). The expression of the MSC marker genes *CD44, CD73, CD105, CD146*, and *PDGFRβ* was confirmed. Notably, the expression of the key pluripotency-associated transcription factors, *OCT4, NANOG*, and *SOX2* was downregulated in HFF-iMSCs compared to iPSCs and ESCs (Fig. 3b). Furthermore, transcriptome analysis revealed the expression of several BMPs and their corresponding receptors (Fig. 3c). Pearson correlation

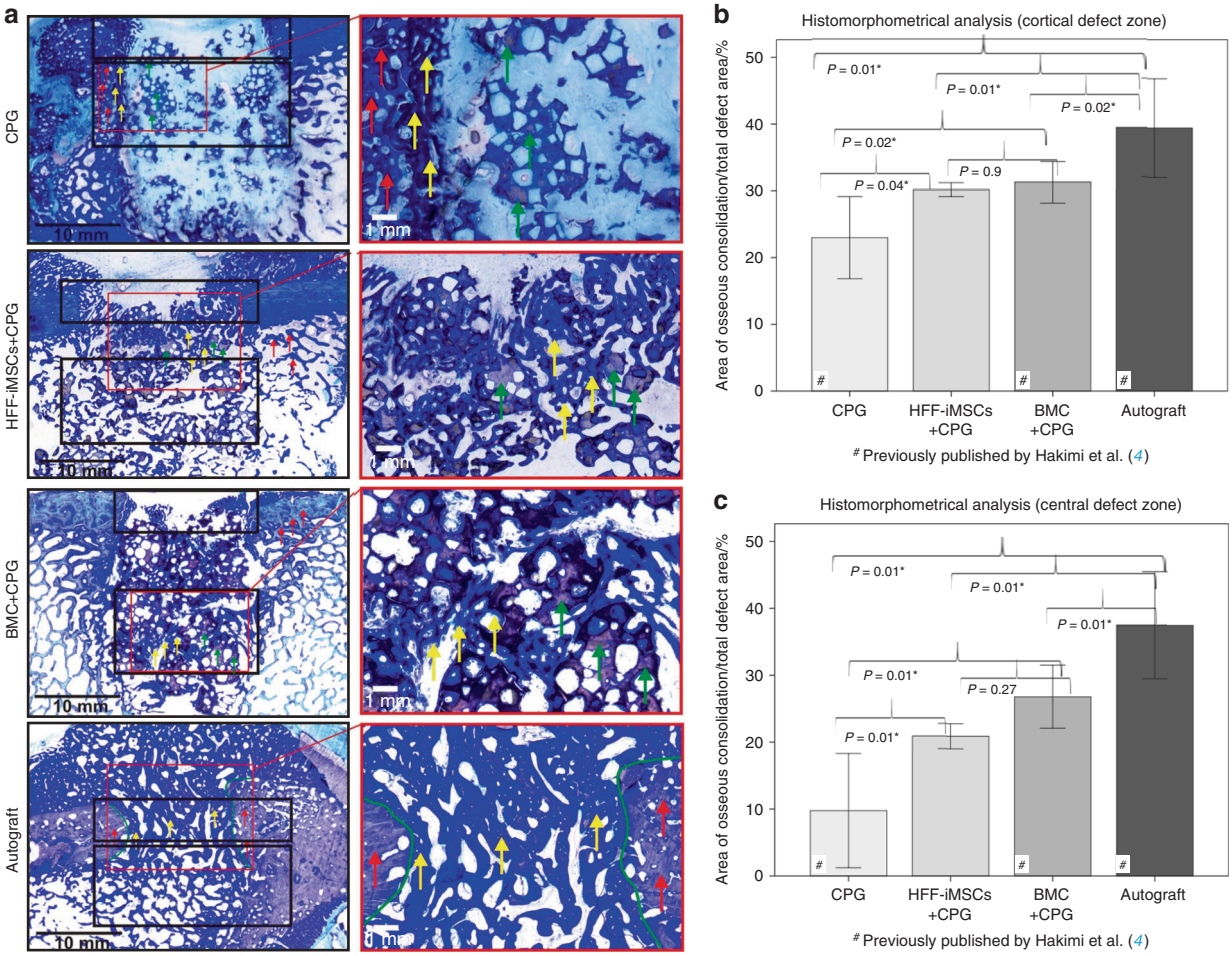

Fig. 4 Histomorphometrical and radiological analysis of regenerated bone defects after 6 weeks. **a** Representative histological bone sections from all experimental groups after a regeneration period of six weeks (left: overview image depicting the cortical (upper black box) and central defect zones (lower black box); right: detailed image); yellow arrows: newly formed bone (royal blue); red arrows: former cortical bone (purple); green arrows: nonresorbed remnants of the CPG. **b** Histomorphometrical evaluation of the cortical defect zone. **c** Histomorphometrical evaluation of the central defect zone. The results for the CPG, BMC + CPG and Autograft groups were previously published by our group.[4] $n = 8$ for each group; values are presented with the standard deviation)

analysis of the transcriptome data showed a high correlation of HFF-iMSCs with fMSCs (R^2 value 0.947) and a low correlation with pluripotent stem cells (Fig. S2). Short-tandem-repeat (STR) analysis of the parental HFFs, HFF-iPSCs, and HFF-iMSCs verified their common genetic background (Fig. S3).

Multilevel analysis of bone defect regeneration

CPG loaded with HFF-iMSCs were transplanted into a critical-size bone defect in the proximal tibia (see Fig. S5) in 8 mini-pigs. The results of the multilevel analysis were compared to those of the analysis of the three previously described standardized experimental groups, CPG, BMC + CPG and Autograft,[4] which were used as controls within the present study to reduce the unnecessary sacrifice of mini-pigs.

Histological evaluation

Defect closure in all 4 experimental groups was confirmed by radiographic analysis after 6 weeks of regeneration (Fig. 4a). According to the histomorphometrical analysis of the cortical area, new bone formation was significantly lower in the CPG group compared to that in the CPG + HFF-iMSC ($P < 0.04$), CPG + BMC ($P < 0.02$), and Autograft groups ($P < 0.01$). The area of new bone formation was 23% ± 6.2% in the CPG group and 31.2% ± 3.1% in the BMC + CPG group, and in the HFF-iMSCs + CPG group, the defect filling area was 30.1% ± 1%. This, however, was significantly inferior (vs. HFF-iMSCs + CPG $P < 0.01$, vs. BMC + CPG $P < 0.02$) compared to the mean osseous consolidation of 39.4% ± 7.4% observed in the Autograft group. No significant differences were observed between the HFF-iMSCs + CPG and BMC + CPG groups ($P = 0.9$).

Similar results were observed in the central defect area. A mean osseous consolidation of 9.8% ± 8.5% was observed when using CPG alone. This was significantly lower than that in all other groups ($P < 0.01$). The area of new bone formation in the central defect area of the HFF-iMSC + CPG group was 20.9% ± 1.9%, and it was 26.8% ± 4.7% in the BMC + CPG group and 37.4% ± 8% in the Autograft group. The values observed in the Autograft group were significantly greater than those observed in all other groups ($P < 0.01$). No significant differences were observed between the HFF-iMSCs + CPG and the BMC + CPG group ($P = 0.27$). Relevant histological signs of inflammation caused by the grafting materials/cells were not found in any of the specimens (Fig. 4a–c).

Multidetector computed tomography (MDCT) volumetry

The mean extent of bone defect consolidation was 46% ± 10.1% in the CPG + HFF-iMSCs group, 53.5% ± 19.1% in the BMC + CPG group, and 81.1% ± 5.1% in the Autograft group. The volume of new bone formation within the defect was 26.1% ± 5.1% in the CPG group, which was significantly inferior compared to that in all

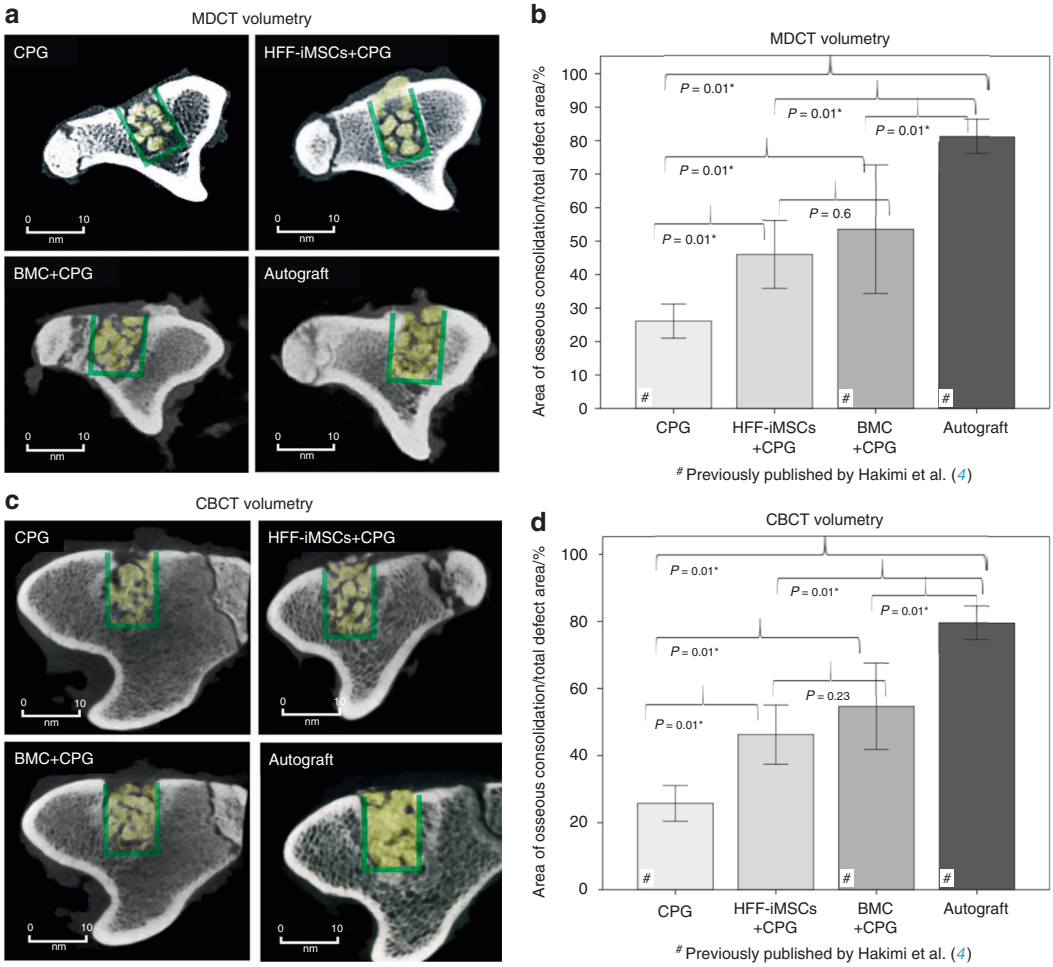

Fig. 5 Radiological analysis of regenerated bone defects after 6 weeks. **a** Axial MDCT volumetry images of the tibial defect; only areas with a density >500 HU are indicated (yellow area). The green circled area represents the defect zone. **b** MDCT volumetry evaluation of bone defect consolidation. **c** Axial CBCT volumetry images of the tibial defect; only areas with a density >2 350 HU are indicated (yellow area). The green circled area represents the defect zone. **d** CBCT volumetry evaluation of bone defect consolidation. The results for the CPG, BMC + CPG and Autograft groups were previously published by our group.[4] $n = 8$ for each group; values are presented with the standard deviation

other groups ($P < 0.01$). Concerning the volume of new bone formation, the HFF-iMSCs + CPG group was similar to the BMC + CPG group ($P = 0.6$), and the volume in both groups was significantly lower compared to that of the Autograft group ($P < 0.01$) (Fig. 5a, b)

Cone-beam computed tomography (CBCT) volumetry

CBCT volumetry analysis of the mean osseous consolidation in the HFF-iMSCs + CPG group, the BMC + CPG group, and the Autograft group found a volume of new bone formation of 46.3% ± 8.8%, 54.7% ± 12.8%, and 79.5% ± 5%, respectively, in the defect area. The volume of new bone formation was significantly greater in the Autograft group compared to the HFF-iMSCs + CPG and BMC + CPG groups ($P < 0.01$). There were no significant differences between the HFF-iMSCs + CPG and BMC + CPG groups ($P = 0.23$). The reconstructed area in the CPG group was 25.8% ± 5.3% and was significantly lower compared to that in all other groups ($P < 0.01$) (Fig. 5c, d).

DISCUSSION

Within the limitations of this translational study, it could be demonstrated that a composite containing human HFF-iMSCs and CPG was potent in inducing bone regeneration in the early phase of bone healing during the first six weeks. This in vivo model approximates the preclinical setting, as the species-specific (mini-pig) bone regeneration capacity (1.2–1.5 mm per day) mimics that found in humans under normal anatomical and physiological conditions.[18] In current clinical practice, the treatment of large bone defects and bone nonunion in humans relies on bone grafting.[19] Bone marrow-derived MSC (BM-MSC) transplantation has been proposed as a possible alternative.[20–22] However, the scarcity of bone grafts, donor-associated disorders, the invasiveness of BM-MSC collection and immune rejection are possible drawbacks. Recently, the craniofacial bone regeneration potential of autologous MSCs was reported in small-animal models.[9] For long bone reconstruction in sheep and for human facial remodeling, the utility of BM-MSCs has also been demonstrated in combination with scaffolds and BMP7.[21,23] However, to date, only a limited number of studies have implemented preclinical animal models for weight-bearing long bone defect regeneration.

In this study, human iMSCs were used, as it has been reported that the differentiation and proliferation potential of primary MSCs in vitro diminish upon aging.[12] In contrast, iMSCs generated from iPSCs or ESCs, when compared to BM-MSCs, show a similar phenotype but have a longer life span.[24] Human iMSCs are characterized by a superior molecular signature in terms of rejuvenation compared to adult MSCs.[14] Furthermore, iMSCs are currently in use in a human phase 1 clinical trial of GvHD [NCT02923375].

In this investigation, HFFs were used for iPSC generation by employing nonintegrating Sendai viruses; thus, the resulting HFF-iPSC line was devoid of transgenes. The HFF-iPSCs were positive for the Yamanaka factors[25] and were chromosomally normal. The HFF-iMSCs that differentiated from the HFF-iPSCs expressed typical MSC markers, such as CD105 and Vimentin, and were devoid of the pluripotency-associated markers OCT4 and NANOG; subsequently, they did not result in tumor formation, as also observed in our earlier study.[15] However, to ensure patient safety, long-term studies need to be conducted to evaluate the probability of tumor formation.

Upon osteogenic differentiation in vitro, the HFF-iMSCs showed a high rate of calcification and expressed high levels of the key transcription factor *RUNX2*[26] and other important bone-related genes, including *BGLAP* and *ALPL*. Furthermore, they secreted immune-modulatory and osteo-regenerative cytokines such as PDGF-AA and osteopontin, thus avoiding the necessity for additional supplementation in cell culture. It was previously reported that BM-MSC supernatants induce the expression of bone-related genes, such as *BGLAP* and *ALPL*,[27] and iPSC-MSCs have been shown to inhibit caspase activity in T-cells by producing TGF-β.[28]

To attain significance and clinical impact, we used 32 skeletally mature mini-pigs that were split into four groups of eight. Of these four groups, three groups were previously described by our group[4] and were used as references in the present study: the autologous spongiosa group was used as the gold standard autograft control, the autologous BMC (bone marrow concentrate) combined with CPG group served as the positive control and the CPG alone group was used as the negative control. For the present study, HFF-iMSCs loaded on calcium phosphate granules were transplanted into a surgically induced bone defect in 8 mini-pigs. In all cases, even though no immunosuppression was administered to the pigs, obvious postoperative events, such as inflammatory reactions were not observed histologically. By applying histomorphometric, MDCT and CBCT analyses, we observed the successful reconstruction of bone mass. To mimic the surgical procedures used in humans, the implantation and explantation were performed by an expert group of orthopedic surgeons according to standard clinical protocols used for human patients.

In the current study, a minimal number of cells (1×10^6) was transplanted to simulate the conditions typical to clinical settings, where the feasibility of long-term in vitro cell expansion is limited due to the amount of restricted time available for the treatment of the patient. Radiologically and histomorphometrically, the transplantation of the HFF-iMSCs loaded on CPG led to significantly better osseous consolidation in the central and cortical defect zones compared to that obtained with the use of CPG alone. Furthermore, in comparison with the composite of autologous BMC + CPG, no significant differences could be found in the cortical and central defect areas. These results are noteworthy since BMCs contain platelets and growth factors in addition to bone marrow MSCs,[4,29] whereas the iMSCs were transplanted without the addition of exogenous factors. Furthermore, autologous BMC was used when the iMSCs were of human origin, and no administration of immune suppression was necessary. As expected, both radiologically and histomorphometrically, autologous bone transplantation resulted in the highest rate of new bone formation, which was significantly higher compared to that observed in all other groups. In a rat model of critical-size cranial defects, human iMSCs performed comparably to human MSCs (bone marrow and umbilical cord) and showed 2.8-fold improved regeneration compared to calcium phosphate cement alone after 12 weeks.[30] Another study demonstrated that human iMSCs contributed to substantial bone formation and produced a significantly better outcome than primary human BM-MSCs in a mouse radial defect model.[10] In addition to the use of iMSC in in vivo studies, a protocol has been described for generating bone substitutes by the incubation of iMSC-loaded scaffolds in a perfusion bioreactor system with the aim of using these in personalized bone tissue engineering in the near future.[31] In addition to the use of different scaffold materials, the supplementation of BM-MSCs with growth factors such as BMP-7 has been used to stimulate osteogenic reconstruction.[23]

Moreover, the transplantation of primed or osteogenic-differentiated MSCs into bone defect models has also been reported.[9,32] In the current study, human iMSCs were transplanted without the addition of growth factors and at their full multipotent capacity to enable HFF-iMSCs to function as immunosuppressors and inducers of regeneration (paracrine effects) and to directly contribute to bone formation. The successful outcome of the transplantation of the composite of HFF-iMSCs and micro- and macroporous calcium phosphate granules (CPG) may have been due to the characteristics of the specific scaffold material used. An in vitro compatibility test of HFF-iMSCs and CPG (see Fig. S4) showed that HFF-iMSCs can be absorbed by CPG and remain alive and functional within the scaffold material. The CPGs that were utilized are composed of carbonated, calcium-deficient apatite calcium phosphate. They mimic human bone material more closely than HA or TCP cement.[33] Another advantage of CPG is the presence of both small and large pores, which enable the three-dimensional ingrowth of newly formed bone mass into the scaffold material.[34] Furthermore, the use of granules leads to a faster resorption rate in vivo when compared to the use of compact blocks of identical material.[35] The reported high wicking capability of CPG[33] enabled the transplantation of iMSCs into bone defects after absorption into the scaffold material. CPG was used as a scaffold material because it has been shown to have beneficial effects on bone reconstruction.[36] Furthermore, CPG have been used successfully as a scaffold material in combination with other fluid osteoinductive substances, such as platelet-rich plasma (PRP), BMC and a combination of both in the animal model used by our group.

One limitation of our study is the use of CT to evaluate the newly formed bone; this method cannot discriminate between the bone substitute material CPG and newly formed bone mass because both structures have comparable densities. However, the radiological and histomorphometrical analyses used in this study represent well-established evaluation methods that have been used by our group in previous studies with this type of animal model.[4,37–39] Under these circumstances, a high correlation between the results of the histomorphometrical analysis and the two independent CT analyses confirmed the reliability of our system for evaluating osseous consolidation noninvasively, as previously shown.[4] Furthermore, this investigation did not make an exact determination of the molecular mechanism(s) associated with bone regeneration and did not evaluate whether neo-bone formation was a direct effect of the implanted cells or the effects of secreted factors, such as immune modulation and pro-angiogenic signaling factors. Since the factors secreted from MSCs and iMSCs have been described as significantly influencing the therapeutic effect via interaction with immune cells,[40,41] immune modulation and paracrine signaling might have played a pivotal role, as indicated by the analysis of the secretome of the HFF-iMSCs that revealed the presence of serpin E1, angiogenin, PDGF-AA and osteopontin; in addition, the transcriptome analysis showed the expression of several BMPs associated with bone regeneration.[23,42] Furthermore, it must be taken into account that the BMP2/4 and NF-κb signaling pathways play important roles in the paracrine pathways involved in the bone regeneration process by regulating the secretory profile of MSCs.[43,44] Key components of these pathways, RAP1 and NUCKS1, were shown to be expressed by HFF-iMSCs (see Fig. 3b). We postulate that there are potential mechanisms whereby HFF-iMSCs might contribute to the

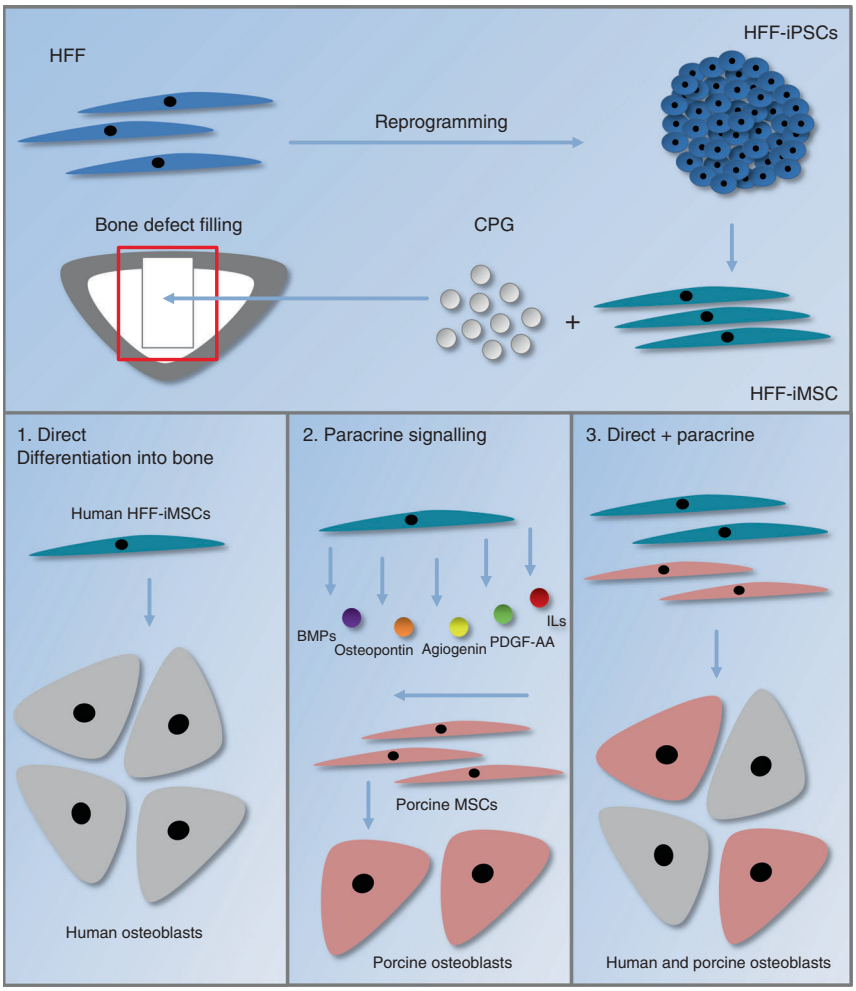

Fig. 6 Possible modes of action of the HFF-iMSCs. We propose three potential mechanisms whereby HFF-iMSCs contribute to the regeneration of critical-size bone defects. 1: Niche-induced differentiation into human osteoblasts; 2: paracrine signaling-induced regeneration by the activation and recruitment of resident stem cells; 3: a combination of niche-induced differentiation and paracrine signaling

regeneration of critical-size bone defects, including (i) their niche-induced differentiation into human osteoblasts, (ii) their paracrine signaling-induced regeneration via the activation and recruitment of resident porcine stem cells, and (iii) a combination of differentiation and paracrine signaling (Fig. 6). Ultimately, iMSC tracing experiments will be required to investigate the homing/chemotactic effects of iMSCs and the efficiency of their expansion in vivo in subsequent studies.

The positive effects of the human HFF-iMSC composite in the early phase of bone healing could possibly lead to follow-up experiments that would be conducted for longer than 6 weeks. Additionally, the monitoring of defect healing, biomechanical evaluation and an increase in the numbers of transplanted cells could be of use in future studies.

Using the iPSC approach, it is possible to generate HLA-matched iMSCs for treating distinct bone defects, thus reducing the need for patient-derived BMCs as well as BM-MSCs. Human HFF-iMSC engrafting was shown in vivo to lead to the formation of new bone six weeks posttransplantation, thus demonstrating the usefulness of iMSCs for the future treatment of large bone defects. However, clinical applications will require significant improvements to optimize applicability, ensure patient safety and increase the in-depth understanding of the basic biomolecular processes involved in regeneration and the long-term posttransplantation effects.

MATERIALS AND METHODS

Generation of HFF-iPSCs

Human fetal foreskin fibroblasts were reprogrammed at the Biomedicum Stem Cell Center (Helsinki, Finland) using Sendai virus vectors encoding the reprogramming factors OCT3/4, SOX2, KLF4, and C-MYC. The reprogramming and culture of the iPSCs were carried out under feeder-free conditions using Matrigel (Becton Dickinson, Heidelberg, Germany) and E8 medium (Thermo Fisher Scientific, Darmstadt, Germany) or StemMACS IPS BREW medium (Miltenyi Biotec, Bergisch Gladbach, Germany). The clearance of the Sendai virus was confirmed by PCR; we referred to the HFF-derived iPSCs as HFF-iPSCs.

Embryoid body formation

The pluripotency of the iPSCs was confirmed by an embryoid body assay demonstrating the ability of the iPSCs to spontaneously differentiate into cell types representative of the three germ layers (ectoderm, mesoderm, and endoderm) as described previously.[45] Please refer to Table S1 for a list of the antibodies used. Further details are provided in the Supplementary Methods.

Karyotyping of the HFF-iPSCs

The karyotype analysis was carried out by the Institute of Human Genetics and Anthropology, Heinrich-Heine-University, Düsseldorf, Germany.

Generation of HFF-iMSCs

iMSCs were generated from HFF-iPSCs by using a modified version of an already published protocol[17] that utilized the TGFβ pathway inhibitor SB 431542 to facilitate epithelial to mesenchymal transition. The iPSCs were cultured under feeder-free conditions on Matrigel (Becton Dickinson, New Jersey, USA) using human StemMACS iPS BREW XF medium (Miltenyi Biotec). When the cell layer covered ~50% of the well, the medium was switched to α-MEM (alpha-modified minimum essential medium; Sigma-Aldrich, Taufkirchen, Germany) supplemented with 10% FBS, 1% GlutaMAX and 1% $P{\cdot}S^{-1}$ without basic fibroblast growth factor. This medium was supplemented with 10 $\mu mol{\cdot}L^{-1}$ SB 431542 (Miltenyi Biotec). For 14 days, the cell culture medium was changed daily. The cells were harvested using TrypLE Express and were reseeded onto uncoated culture dishes in α-MEM without SB 431542 supplementation. After several passaging steps, the cells were characterized as iMSCs. The general cell culture reagents were obtained from Gibco (Thermo Fisher Scientific, Darmstadt, Germany).

Transcriptome analysis

The microarray analysis was performed by using the PrimeView Human Gene Expression Array platform (Affymetrix, Thermo Fisher Scientific). The data are accessible online via the National Center of Biotechnology Information (NCBI) Gene Expression Omnibus. Further processing of the nonnormalized bead summary data was performed using R/Bioconductor software[46] with the affy package (http://bioconductor.org/packages/release/bioc/html/ affy.html).[47] After background correction, the values were converted to a logarithmic scale (to base 2), and normalization was performed using the robust multi-array average method. Ethically approved fetal MSCs (kindly provided by Prof. Richard O.C. Oreffo, University of Southampton-UK) were used as the reference cells.

Flow cytometry

The MSC Phenotyping Kit Human (# 130-095-198) from Miltenyi Biotec was used to identify the cell surface profile of the HFF-iMSCs according to the manufacturer's instructions. The labeled cells were analyzed using a FACSCanto from BD Biosciences (Heidelberg, Germany). The histograms were generated using Summit 4.3.02 software. The protocol used for cell preparation can be found in the Supplementary Methods.

Demonstration of the multipotency of HFF-iMSCs

The differentiation of HFF-iMSCs into adipocytes, chondrocytes, and osteoblasts was performed with the STEMPRO Adipogenesis, Chondrogenesis and Osteogenesis Differentiation Kit (Thermo Fisher Scientific). The differentiation was carried out for 3 weeks with media changes every 2–3 days. After this period, the cells were fixed with PFA and stained as described previously.[48] The staining procedures are described in the Supplementary Methods.

Secretome analysis of the HFF-iMSC-conditioned media

The molecules secreted from the HFF-iMSCs were identified using the Proteome Profiler Human Cytokine Array Panel A (R&D Systems), which consists of a membrane with 103 different spotted antibodies, according to the user manual. For the detection of cytokines, 1.5 mL of conditioned medium from HFF-iMSCs was incubated on the cytokine membrane. The membrane was analyzed by detecting the emitted chemiluminescence. The pixel density of each spot, representing the amount of bound cytokine, was analyzed using ImageJ software. The value of the negative control was subtracted from all other values. Then, every value was divided by the mean of the values of the reference spots and multiplied by 100 to determine the percentage value in comparison to the reference spots.

Immunofluorescence staining

The cells were stained as described previously.[48] Please refer to the Supplementary Methods for a detailed description. The list of primary antibodies used can be found in the Supplementary Material (Table S1).

Real-time reverse transcriptase-polymerase chain reaction (qRT-PCR)

Real-time quantitative PCR was performed for each technical triplicate using the Power SYBR Green Master Mix (Life Technologies) with a VIIA7 instrument (Life Technologies). The program used consisted of the denaturation of the samples at 95 °C for 2 min, followed by 40 cycles of amplification (30 s of denaturation at 95 °C, annealing at the primer-specific temperature (57 °C–63 °C) for 30 s, and extension at 72 °C for 30 s). The primers were purchased from MWG, and the specific sequences, as well as the amplicon sizes, are provided in the Supplementary Material (Table S2). For the analysis of the qRT-PCR data, the housekeeping gene encoding ribosomal protein L37A was used to normalize the values of the tested genes. The expression levels were calculated using the ΔΔCT method and are shown as the mean value with the standard error of mean. The procedures used for RNA isolation and cDNA synthesis are described in the Supplementary Methods.

Bone defect model and cell transplantation

All animals were handled in compliance with the guidelines for the care and use of animals at our institution and in accordance with the EU Directive 2010/63/EU for animal experiments. Approval from the regional ethics committee for animal experiments (LANUV NRW, Recklinghausen, Germany) was obtained (Permit Number: 84-02.04.2015.A042). In this study, 8 female Goettingen mini-pigs (aged 20–28 months, weight 24 kg–35 kg) were used. Based on previous studies performed by our group utilizing a similar animal model and an a priori power analysis, a sample size of 8 was determined to have a power of 80%, and a *P*-value of 0.05 denoted significance.[49]

The animals were randomly assigned to one of the study groups (each group consisted of eight Goettingen mini-pigs). All defects were filled entirely using a volume of 2.4 cm^3. In the CPG group, the defects were filled with calcium granules alone, and in the BMC + CPG group, the defects were filled with autologous BMCs in combination with CPG. In the autograft group, the defects were filled with autologous bone harvested from the iliac crest. For this, the iliac crest was exposed, and a Kirschner guide wire (K-wire) was inserted. Using a cannulated reamer placed on the guide wire, cancellous bone was harvested. The results from these 3 groups have been reported by our group[4] and were used as controls in the present study to avoid the loss of additional animals and for ethical reasons. Preliminary experiments were carried out by our group in which the same defect was created in the proximal tibia of four mini-pigs without the addition of any filling material. Because of a proximal tibia fracture that occurred within 3 days after operation, all of these animals had to be sacrificed prematurely.[50] Therefore, the defect model used in the current study fulfills the criteria of a critical-size defect model. To prevent the unnecessary sacrifice of additional animals and for ethical reasons, the present study was carried out without a no treatment control.

In accordance with the animal model developed by our group,[49] a cylindrical defect of 11 mm diameter and 25 mm depth was created in the right proximal tibia medially using a cannulated reamer (Aesculap AG & Co. KG, Tuttlingen, Germany). In the CPG, BMC + CPG and HFF-iMSCs + CPG groups spherical, micro- and macroporous (micro: 2 µm–10 µm; macro: 150 µm–550 µm), carbonated, and apatite calcium phosphate granules 2 mm–4 mm in size (Calcibon® Granules, Biomet Deutschland GmbH, Berlin, Germany) were used.

All surgical procedures were performed with single anesthesia by the same experienced surgeon under strict aseptic conditions. Further methodological details are described in the Supplementary Methods. Using a medial approach in the right proximal tibia, the defect was created 10 mm distal to the joint line and 12 mm anterior to the most posterior aspect of the tibia. In the BMC group, bone marrow was harvested from the iliac crest, and mononuclear cells were concentrated to generate bone marrow concentrate (BMC) using a point-of-care device (MarrowStim® mini concentration system, Biomet Biologics, Inc., Warsaw, Indiana, USA) as described previously.[4] In the HFF-iMSCs + CPG group, the CPG were soaked with a mixture of 1×10^6 HFF-iMSCs (passage numbers 5, 7, and 9) for five minutes prior to implantation. The soft tissues were closed in layers.

Postoperatively, all animals were allowed to bear their full weight. At 42 days after the procedure, the animals were sacrificed using 3% sodium pentobarbital (Eutha 77, Essex Pharma GmbH, München, Germany). The proximal tibia was harvested by a sharp dissection tool and fixed in 10% neutral buffered formalin solution for 14 days. Figure S5 shows a schematic of the bone defect.

Statistical analysis

The statistical analysis was performed using SPSS software (version 21.0, SPSS Inc., Chicago, IL, USA). The mean values and standard deviations were calculated. The outcome measures of the radiological and histomorphometrical evaluations were examined by one-way analysis of variance (ANOVA). Differences between the independent variables were checked with post hoc tests [Tukey's HSD (honestly significant difference) test]. Significance was defined at a P-value < 0.05.

Multidetector computed tomography (MDCT)

Using a 64-detector row CT scanner (SOMATOM Sensation Cardiac 64, Siemens Medical Solutions, Germany), radiographic analysis was performed as described previously.[39] In brief, volumetric measurements were performed with respect to density in Hounsfield units (HU) according to axial images. A threshold value of 500 HU was defined for osseous consolidation, and the defect volume was measured three times at different HU ranges:

(i) Overall size of the defect: measured by including all pixels with an density between −100 and +3 000 HU.
(ii) Areas of consolidation: measurement of pixels with densities between 500 and 3 000 HU.
(iii) Nonconsolidated areas: measurement of all pixels with densities between −100 and 500 HU.

Quantitative cone-beam CT (CBCT) volumetry

Using a CBCT scanner with a flat panel detector (PaX-Duo3D, Vatech, Korea), images were obtained as described previously.[38] The bone defect volume and extent of new bone formation were evaluated quantitatively using DICOM viewer (Osirix Imaging Software, 64-Bit extended version, Pixmeo, Geneva, Switzerland). With respect to the density values, the volumetric measurements were performed after semiautomatic selection and by marking pixels with predefined density values on the axial images. Based on the mean density values of cortical and trabecular bone, a threshold value of 2 350 was defined for bone consolidation, and volumetric measurements of the defect were performed three times with three different settings:

(i) Overall size of defect: measured by including all pixels in the outlined defect
(ii) Areas of consolidation: measurement of pixels with densities >2 350
(iii) Nonmineralized areas: measurement of all pixels with densities <2 350.

The relative extent of bone regeneration and the absolute volumes of bone consolidation were determined.

Histological preparation of the bone segments

For nondecalcified sectioning, all specimens were dehydrated using an ascending series of graded alcohol and xylene prior to infiltration and embedding in methylmethacrylate. Serial sections were cut in the axial direction using a diamond wire saw (Exakt®, Apparatebau, Norderstedt, Germany). Before staining, the toluidine blue-stained sections were ground to a final thickness of approximately 50 µm.

Histomorphometrical analysis

Two experienced investigators who were blinded to the experimental groups performed all histomorphometric analyses and microscopic observations as described previously.[49] In brief, the areas of new bone formation (μm^2) and the percentage of total new bone formation were measured in the cortical and central defect areas (see Fig. S5). After visual identification, the tissue type was determined manually and assigned a color on three sections from each specimen. Based on this, the areas of newly formed bone, connective tissue, and CPG were calculated according to the total bone defect area.

DATA AVAILABILITY

The HFF, HFF-iPSC and HFF-iMSC transcriptome data are accessible online via the National Center of Biotechnology Information (NCBI) Gene Expression Omnibus.

ACKNOWLEDGEMENTS

Prof. Dr. James Adjaye and Prof. Dr. Joachim Windolf acknowledge support from the medical faculty at Heinrich-Heine-University, Düsseldorf, Germany. In addition, Prof. Dr. James Adjaye and Mr. Md Shaifur Rahman, acknowledge support from the German Academic Exchange Service (DAAD-91607303). We thank Prof. Richard O.C. Oreffo at the Center for Human Development, Stem Cells and Regeneration, Faculty of Medicine, University of Southampton, United Kingdom, for providing the fMSCs. We acknowledge Dr. Claus Kordes at the Clinic of Gastroenterology, Hepatology and Infectious Diseases, Heinrich Heine University, Düsseldorf, Germany, for his assistance with the osteogenic differentiation imaging and Katharina Raba at the Institute of Transplantation Diagnostics and Cell Therapeutics, Heinrich Heine University, for her assistance with the FACS analyses.

AUTHOR CONTRIBUTIONS

J.A., J.S., J.W., P.J. and L.S.S. conceived the ideas and designed the experiments. P.J., J. S., J.G., S.T., M.H. and M.S. were responsible for the care of the animals, the operation procedure and the postoperative care. P.J., J.S., J.G., P.K. and S.T. performed the explantations and subsequent histomorphometrical and radiological analyses. L.S.S., M.S.R. and M.B. performed the characterization of the HFF-iPSCs and the generation and characterization of the HFF-iMSCs. W.W. performed the transcriptome analyses. D.L. evaluated and processed the images of the histomorphometrical and radiological analyses. All authors contributed to the writing of the manuscript, and J.A. and J.W. approved the final version of the manuscript.

ADDITIONAL INFORMATION

The online version of this article (https://doi.org/10.1038/s41413-019-0069-4) contains supplementary material, which is available to authorized users.

Competing interests: The authors declare no competing interests.

REFERENCES

1. Faour, O., Dimitriou, R., Cousins, C. A. & Giannoudis, P. V. The use of bone graft substitutes in large cancellous voids: any specific needs? *Injury* **42**, 87–90 (2011).

2. Herten, M. et al. Bone marrow concentrate for autologous transplantation in minipigs. Characterization and osteogenic potential of mesenchymal stem cells. *Vet. Comp. Orthop. Traumatol.* **26**, 34–41 (2013).
3. Grayson, W. L. et al. Stromal cells and stem cells in clinical bone regeneration. *Nat. Rev. Endocrinol.* **11**, 140–150 (2015).
4. Hakimi, M. et al. The composite of bone marrow concentrate and PRP as an alternative to autologous bone grafting. *PLoS ONE* **9**, e100143 (2014).
5. Friedenstein, A. J., Chailakhyan, R. K. & Gerasimov, U. V. Bone marrow osteogenic stem cells: in vitro cultivation and transplantation in diffusion chambers. *Cell Tissue Kinet.* **20**, 263–272 (1987).
6. Pittenger, M. F. et al. Multilineage potential of adult human mesenchymal stem cells. *Science* **284**, 143–147 (1999).
7. Bianco, P., Riminucci, M., Gronthos, S. & Robey, P. G. Bone marrow stromal stem cells: nature, biology, and potential applications. *Stem Cells* **19**, 180–192 (2001).
8. Dominici, M. et al. Minimal criteria for defining multipotent mesenchymal stromal cells. The International Society for Cellular Therapy position statement. *Cytotherapy* **8**, 315–317 (2006).
9. Bhumiratana, S. et al. Tissue-engineered autologous grafts for facial bone reconstruction. *Sci. Transl. Med.* **8**, 343ra83 (2016).
10. Sheyn, D. et al. Human induced pluripotent stem cells differentiate into functional mesenchymal stem cells and repair bone defects. *Stem Cells Transl. Med.* **5**, 1447–1460 (2016).
11. Duscher, D. et al. Aging disrupts cell subpopulation dynamics and diminishes the function of mesenchymal stem cells. *Sci. Rep.* **4**, 7144 (2014).
12. Yang, Y. K., Ogando, C. R., Wang See, C., Chang, T. Y. & Barabino, G. A. Changes in phenotype and differentiation potential of human mesenchymal stem cells aging in vitro. *Stem Cell Res Ther.* **9**, 131 (2018).
13. Palumbo, S., Tsai, T. L. & Li, W. J. Macrophage migration inhibitory factor regulates AKT signaling in hypoxic culture to modulate senescence of human mesenchymal stem cells. *Stem Cells Dev.* **23**, 852–865 (2014).
14. Frobel, J. et al. Epigenetic rejuvenation of mesenchymal stromal cells derived from induced pluripotent stem cells. *Stem Cell Rep.* **3**, 414–422 (2014).
15. Spitzhorn, L. S. et al. Transplanted human pluripotent stem cell-derived mesenchymal stem cells support liver regeneration in gunn rats. *Stem Cells Dev.* **27**, 1702–1714 (2018).
16. Wang, X. et al. Human ESC-derived MSCs outperform bone marrow MSCs in the treatment of an EAE model of multiple sclerosis. *Stem Cell Rep.* **3**, 115–130 (2014).
17. Chen, Y. S. et al. Small molecule mesengenic induction of human induced pluripotent stem cells to generate mesenchymal stem/stromal cells. *Stem Cells Transl. Med.* **1**, 83–95 (2012).
18. Schlegel, K. A., Lang, F. J., Donath, K., Kulow, J. T. & Wiltfang, J. The monocortical critical size bone defect as an alternative experimental model in testing bone substitute materials. *Oral. Surg. Oral. Med Oral. Pathol. Oral. Radio. Endod.* **102**, 7–13 (2006).
19. Li, Y. et al. Bone defect animal models for testing efficacy of bone substitute biomaterials. *J. Orthop. Transl.* **3**, 95–104 (2015).
20. Quarto, R. et al. Repair of large bone defects with the use of autologous bone marrow stromal cells. *N. Engl. J. Med.* **344**, 385–386 (2001).
21. Warnke, P. H. et al. Growth and transplantation of a custom vascularised bone graft in a man. *Lancet* **364**, 766–770 (2004).
22. Ismail et al. Mesenchymal stem cell implantation in atrophic nonunion of the long bones: a translational study. *Bone Jt. Res.* **5**, 287–293 (2016).
23. Reichert, J. C. et al. A tissue engineering solution for segmental defect regeneration in load-bearing long bones. *Sci. Transl. Med.* **4**, 141ra93 (2012).
24. Lian, Q. et al. Functional mesenchymal stem cells derived from human induced pluripotent stem cells attenuate limb ischemia in mice. *Circulation* **121**, 1113–1123 (2010).
25. Takahashi, K. et al. Induction of pluripotent stem cells from adult human fibroblasts by defined factors. *Cell* **131**, 861–872 (2007).
26. Komori, T. Requisite roles of Runx2 and Cbfb in skeletal development. *J. Bone Min. Metab.* **21**, 193–197 (2003).
27. Zhou, W., Liu, Q. & Xu, B. Improvement of bone defect healing in rats via mesenchymal stem cell supernatant. *Exp. Ther. Med.* **15**, 1500–1504 (2018).
28. Li, C. L. et al. Human iPSC-MSC-derived xenografts modulate immune responses by inhibiting the cleavage of caspases. *Stem Cells* **35**, 1719–1732 (2017).
29. Jungbluth, P. et al. Concentration of platelets and growth factors in platelet-rich plasma from Goettingen minipigs. *GMS Inter. Plast. Reconstr. Surg. Dgpw.* **3**, Doc11 (2014).
30. Wang, P. et al. Bone tissue engineering via nanostructured calcium phosphate biomaterials and stem cells. *Bone Res.* **2**, 14017 (2014).
31. de Peppo, G. M., Vunjak-Novakovic, G. & Marolt, D. Cultivation of human bone-like tissue from pluripotent stem cell-derived osteogenic progenitors in perfusion bioreactors. *Methods Mol. Biol.* **1202**, 173–184 (2014).
32. Schubert, T. et al. The enhanced performance of bone allografts using osteogenic-differentiated adipose-derived mesenchymal stem cells. *Biomaterials* **32**, 8880–8891 (2011).
33. Tas, A. C. Preparation of porous apatite granules from calcium phosphate cement. *J. Mater. Sci. Mater. Med* **19**, 2231–2239 (2008).
34. Weiss, P. et al. Synchrotron X-ray microtomography (on a micron scale) provides three-dimensional imaging representation of bone ingrowth in calcium phosphate biomaterials. *Biomaterials* **24**, 4591–4601 (2003).
35. Bohner, M. & Baumgart, F. Theoretical model to determine the effects of geometrical factors on the resorption of calcium phosphate bone substitutes. *Biomaterials* **25**, 3569–3582 (2004).
36. Zhang, J., Liu, W., Schnitzler, V., Tancret, F. & Bouler, J. M. Calcium phosphate cements for bone substitution: chemistry, handling and mechanical properties. *Acta Biomater.* **10**, 1035–1049 (2014).
37. Jungbluth, P. et al. The early phase influence of bone marrow concentrate on metaphyseal bone healing. *Injury* **44**(Oct), 1285–1294 (2013).
38. Kröpil, P. et al. Cone beam CT in assessment of tibial bone defect healing: an animal study. *Acad. Radiol.* **19**, 320–325 (2012).
39. Riegger, C. et al. Quantitative assessment of bone defect healing by multidetector CT in a pig model. *Skelet. Radiol.* **41**, 531–537 (2012).
40. Li, X. et al. iPSC-derived mesenchymal stem cells exert SCF-dependent recovery of cigarette smoke-induced apoptosis/proliferation imbalance in airway cells. *J. Cell Mol. Med.* **21**, 265–277 (2017).
41. Li, X. et al. Mesenchymal stem cells alleviate oxidative stress-induced mitochondrial dysfunction in the airways. *J. Allergy Clin. Immunol.* **141**, 1634–1645 (2018).
42. Schmidt-Bleek, K., Willie, B. M., Schwabe, P., Seemann, P. & Duda, G. N. BMPs in bone regeneration: Less is more effective, a paradigm-shift. *Cytokine Growth Factor Rev.* **27**, 141–148 (2016).
43. Ding, Y. et al. Rap1 deficiency-provoked paracrine dysfunction impairs immunosuppressive potency of mesenchymal stem cells in allograft rejection of heart transplantation. *Cell Death Dis.* **9**, 386 (2018).
44. Zhang, Y. et al. Absence of NUCKS augments paracrine effects of mesenchymal stem cells-mediated cardiac protection. *Exp. Cell Res.* **356**, 74–84 (2017).
45. Bohndorf, M. et al. Derivation and characterization of integration-free iPSC line ISRM-UM51 derived from SIX2-positive renal cells isolated from urine of an African male expressing the CYP2D6 *4/*17 variant which confers intermediate drug metabolizing activity. *Stem Cell Res.* **25**, 18–21 (2017).
46. Gentleman, R. C. et al. Bioconductor: open software development for computational biology and bioinformatics. *Genome Biol.* **5**, R80 (2004).
47. Gautier, L., Cope, L., Bolstad, B. M. & Irizarry, R. A. affy-analysis of Affymetrix GeneChip data at the probe level. *Bioinformatics* **20**, 307–315 (2004).
48. Rahman, M. S. et al. The presence of human mesenchymal stem cells of renal origin in amniotic fluid increases with gestational time. *Stem Cell Res Ther.* **9**, 113 (2018).
49. Hakimi, M. et al. Combined use of platelet-rich plasma and autologous bone grafts in the treatment of long bone defects in mini-pigs. *Injury* **41**, 717–723 (2010).
50. Jungbluth, P. et al. Platelet-rich plasma on calcium phosphate granules promotes metaphyseal bone healing in mini-pigs. *J. Orthop. Res.* **28**, 1448–1455 (2010).

Part D: Fabrication of Scaffolds and Gels for Bone Defect Restoration and Burn Wound Healing as a Component of Combined ATMPs

3.8 Fabrication of Biocompatible Porous Scaffolds based on Hydroxyapatite/Collagen/ Chitosan Composite for Restoration of Defected Maxillofacial Mandible Bone

Md Shaifur Rahman, Md Masud Rana, Lucas-Sebastian Spitzhorn, Naznin Akhtar, Md Zahid Hasan, Naiyyum Choudhury, Tanja Fehm, Jan T. Czernuszka, James Adjaye, and Sikder M. Asaduzzaman

Abstract

Fabrication of scaffolds from biomaterials for restoration of defected mandible bone has attained increased attention due to limited accessibility of natural bone for grafting. Hydroxyapatite (Ha), collagen type 1 (Col1) and chitosan (Cs) are widely used biomaterials which could be fabricated as a scaffold to overcome the paucity of bone substitutes. Here, rabbit Col1, shrimp Cs and bovine Ha were extracted and characterized with respect to physicochemical properties. Following the biocompatibility, degradability and cytotoxicity tests for Ha, Col1 and Cs a hydroxyapatite/ collagen/ chitosan (Ha·Col1·Cs) scaffold was fabricated using thermally induced phase separation technique. This scaffold was cross-linked with (1) either glutaraldehyde (GTA), (2) de-hydrothermal treatment (DTH), (3) irradiation (IR) and (4) 2-hydroxyethyl methacrylate (HEMA), resulting in four independent types (Ha·Col1·Cs-GTA, Ha·Col1·Cs-IR, Ha·Col1·Cs-DTH and Ha·Col1·Cs-HEMA). The developed composite scaffolds were porous with 3D interconnected fiber microstructure. However, Ha·Col1·Cs-IR and Ha·Col1·Cs-GTA showed better hydrophilicity and biodegradability. All four scaffolds showed desirable blood biocompatibility without cytotoxicity for brine shrimp. In vitro studies in the presence of human amniotic fluid-derived mesenchymal stem cells revealed that Ha·Col1·Cs-IR and Ha·Col1·Cs-DHT scaffolds were non-cytotoxic and compatible for cell attachment, growth and mineralization. Further, grafting of Ha·Col1·Cs-IR and Ha·Col1·Cs-DHT was performed in a surgically created non-load-bearing rabbit maxillofacial mandible defect model. Histological and radiological observations indicated the restoration of defected bone. Ha·Col1·Cs-IR and Ha·Col1·Cs-DHT could be used as an alternative treatment in bone defects and may contribute to further development of scaffolds for bone tissue engineering.

Publication Status: Published in Prog Biomater. 2019 Sep;8(3):137-154.
Impact Factor: NA

This article is reproduced with permission.
Approximated total share of contribution: 50%

Contribution on experimental design, realization and publication: MSR, MMR, LSS, NA, SMA, NC, JTC and JA conceived the idea. MMR, MSR, NA, and LSS designed and performed the experimental work and analyses the data. JTC analysed the physical characterization of the scaffold and scaffold constituent's data. MZH performed the in vitro brine shrimp cytotoxicity and RBC haemolysis assay. MMR, MSR, MZH and LSS wrote the manuscript. NC, SMA, JTC and JA edited the manuscript. NC, SMA and JA supervised the work. All the authors read and approved the final manuscript.

Pubmed link: https://www.ncbi.nlm.nih.gov/pmc/articles/PMC6825626/
Journal link: https://link.springer.com/article/10.1007/s40204-019-0113-x

Progress in Biomaterials (2019) 8:137–154
https://doi.org/10.1007/s40204-019-0113-x

ORIGINAL RESEARCH

Fabrication of biocompatible porous scaffolds based on hydroxyapatite/collagen/chitosan composite for restoration of defected maxillofacial mandible bone

Md Shaifur Rahman[1] · Md Masud Rana[2] · Lucas-Sebastian Spitzhorn[1] · Naznin Akhtar[3] · Md Zahid Hasan[2] · Naiyyum Choudhury[4] · Tanja Fehm[5] · Jan T. Czernuszka[6] · James Adjaye[1] · Sikder M. Asaduzzaman[2]

Received: 23 January 2019 / Accepted: 29 April 2019 / Published online: 29 May 2019

Abstract

Fabrication of scaffolds from biomaterials for restoration of defected mandible bone has attained increased attention due to limited accessibility of natural bone for grafting. Hydroxyapatite (Ha), collagen type 1 (Col1) and chitosan (Cs) are widely used biomaterials which could be fabricated as a scaffold to overcome the paucity of bone substitutes. Here, rabbit Col1, shrimp Cs and bovine Ha were extracted and characterized with respect to physicochemical properties. Following the biocompatibility, degradability and cytotoxicity tests for Ha, Col1 and Cs a hydroxyapatite/collagen/chitosan (Ha·Col1·Cs) scaffold was fabricated using thermally induced phase separation technique. This scaffold was cross-linked with (1) either glutaraldehyde (GTA), (2) de-hydrothermal treatment (DTH), (3) irradiation (IR) and (4) 2-hydroxyethyl methacrylate (HEMA), resulting in four independent types (Ha·Col1·Cs-GTA, Ha·Col1·Cs-IR, Ha·Col1·Cs-DTH and Ha·Col1·Cs-HEMA). The developed composite scaffolds were porous with 3D interconnected fiber microstructure. However, Ha·Col1·Cs-IR and Ha·Col1·Cs-GTA showed better hydrophilicity and biodegradability. All four scaffolds showed desirable blood biocompatibility without cytotoxicity for brine shrimp. In vitro studies in the presence of human amniotic fluid-derived mesenchymal stem cells revealed that Ha·Col1·Cs-IR and Ha·Col1·Cs-DHT scaffolds were non-cytotoxic and compatible for cell attachment, growth and mineralization. Further, grafting of Ha·Col1·Cs-IR and Ha·Col1·Cs-DHT was performed in a surgically created non-load-bearing rabbit maxillofacial mandible defect model. Histological and radiological observations indicated the restoration of defected bone. Ha·Col1·Cs-IR and Ha·Col1·Cs-DHT could be used as an alternative treatment in bone defects and may contribute to further development of scaffolds for bone tissue engineering.

Keywords Hydroxyapatite · Collagen · Chitosan · Scaffold · Biocompatibility · AF-MSCs · Mandible bone defect · Bone tissue engineering

Abbreviations

Ha	Hydroxyapatite
Col1	Collagen type 1
Cs	Chitosan
SEM	Scanning electron microscopy

Electronic supplementary material The online version of this article (https://doi.org/10.1007/s40204-019-0113-x) contains supplementary material, which is available to authorized users.

✉ Sikder M. Asaduzzaman
sikderasad@yahoo.com

[1] Institute for Stem Cell Research and Regenerative Medicine, Medical Faculty, Heinrich-Heine-Universität Düsseldorf, 40225 Düsseldorf, Germany

[2] Institute of Tissue Banking and Biomaterial Research, Atomic Energy Research Establishment, 1349 Dhaka, Bangladesh

[3] School of Medicine, Geelong Waurn Ponds Campus, Deakin University, Waurn Ponds, Victoria 3217, Australia

[4] Bangladesh Atomic Energy Regulatory Authority, Dhaka, Bangladesh

[5] Department of Obstetrics and Gynaecology, Medical Faculty, Heinrich-Heine-Universität Düsseldorf, 40225 Düsseldorf, Germany

[6] Department of Materials, University of Oxford, Oxford OX1 3PH, UK

HaCol1Cs	Hydroxyapatite-collagen type 1-chitosan
XRD	X-ray diffraction
XRF	X-ray fluorescence spectroscopy
HPLC	High-performance liquid chromatography
SDS-PAGE	Sodium dodecyl sulfate polyacrylamide gel electrophoresis
FTIR	Fourier-transform infrared spectroscopy
GTA	Glutaraldehyde
DHT	De-hydrothermal treatment
IR	Irradiation
TIPS	Thermally induced phase separation
kGy	Kilo gray
DT	Denaturation temperature
HEMA	2-Hydroxyethyl Methacrylate
Co60γ	Cobalt sixty gamma
LDT	Liquid displacement technique
TGA	Thermal gravimetric analyzer
PBS	Phosphate buffer saline
TFA	Trifluoroacetic acid
n-β-TCP	Nano-β-tricalcium phosphate/collagen
DW	Distilled water
RT	Room temperature
PSC	Pepsin soluble collagen
ASC	Acid soluble collagen
PLGA	Poly lactic-co-glycolic acid
AF-MSCs	Amniotic fluid-derived mesenchymal stem cells
ARS	Alizarin red staining

Introduction

Bone fractures remain a challenge in reconstructive and rehabilitation surgery. For instance, periodontal bone defects are very common in developing world and require a large amount of medical resources (Wang et al. 2016; Gaihre et al. 2017). Currently, implantable biomaterials such as demineralized bone granules, auto- and allografts are available and clinically used. However, these approaches involve several drawbacks such as post-operative pain, increased blood loss, and secondary surgical wounds (Kumar et al. 2016; Oryan et al. 2014). Allografting could overcome these limitations, but it is associated with the risk of infectious diseases, an insufficient number of donors and high costs (Greenwald et al. 2012). Recombinant growth factors, cell-based engineered bone substitutes and commercial scaffolds are sophisticated alternatives which are widely accepted in the developed world but are too expensive for patients in the low-income countries (Mao and Mooney 2015; Tollemar et al. 2016; Tong et al. 2016a, b). Recently, the interest in the development of scaffolds from naturally available and low-cost bioactive materials has increased significantly (Baino et al. 2015; Yi et al. 2016). These materials could improve bone function by providing a suitable microenvironment for tissue growth and regeneration (Yu et al. 2013; Polo-Corrales et al. 2014; Maisani et al. 2017).

Since hydroxyapatite (Ha) and collagen type 1 (Col1) are the major constituents of human bone, they are widely studied as promising materials for scaffold preparation. For example, the usefulness of porous nano-Ha/Col scaffolds for restoration of critical-size bone defect was reported (Wang et al. 2017). Beside commercial available synthetic Ha, many laboratories have extracted Ha from bio-waste such as bovine bones (Wua et al. 2016; Kim et al. 2014; Sofronia et al. 2014). Bioactive molecules such as Col1 and chitosan (Cs) are also used as components for bone composite engineering (Wang et al. 2016; Croisier and Jérôme 2013; Maji et al. 2016; Tong et al. 2016a, b) which can be extracted from animal skins (Kukhareva et al. 2010; Pacak et al. 2014) and brine shrimp, respectively (Khan et al. 2005; Maji et al. 2016). For instance, human mandible bone defects were restored by grafting of Col1 in combination with dental pulp progenitor cells (d'Aquino et al. 2009; Chamieh et al. 2016). Cs has reactive amine and hydroxyl groups which promote osteoblast growth and in vivo bone formation (Levengood and Zhang 2014) and has structural similarities with glycosaminoglycans, a major component of bone and cartilage (Nagahama et al. 2009; Gravel et al. 2006). In an advanced study, Cs and Cs-hydrogel were used as a bio-printable ink for bone tissue engineering (Demirtaş et al. 2017).

Ha, Col1 and Cs were described to have desired properties such as tissue compatibility, antibacterial activity, non-toxicity, non-immunogenicity, non-carcinogenicity and solubility (Pallela et al. 2012). These components can form a direct chemical bond with living cells/tissues and promote tissue growth, which makes them interesting for the use in orthopedic and dental applications (Rodríguez-Vázquez et al. 2015; Echazú et al. 2016). For example, the applicability of collagen-hydroxyapatite scaffolds for restoration of the mandible in the rabbit has been demonstrated (Zhang et al. 2013). Additionally, human adipose-derived MSCs seeded into a Col-Ha scaffold-promoted ectopic bone formation after implantation in the mouse (Calabrese et al. 2017). Cs in combination with silk-fibroin was observed to be biocompatible with osteogenic potentials when transplanted in a rabbit mandible defects model, including TGF-β1 supplementation (Tong et al. 2016a, b).

Ha, Col1 and Cs are usually animal originated and easy to obtain. So far, composites out of Ha, Cs and Col1 for non-load-bearing mandible bone restoration have not been widely studied. We fabricated Ha·Col1·Cs scaffolds from in-house rabbit skin (Col1), bovine bones (Ha) and prawn shell (Cs) and modified them using different cross-linking methods. The resulting scaffolds were characterized for cytotoxicity, biodegradability, in vivo biocompatibility and physical, chemical, and morphological properties.

Materials and methods

Fabrication procedures of Ha·Col1·Cs scaffolds

The in-house extraction methods of Ha, Col1 and Cs from naturally available sources have been described in Supplementary Materials and Methods. Scaffolds were fabricated according to a previous described thermally induced phase separation method with some modifications (Chen et al. 2010). In brief, 3 g Ha was weighed into a flask and deionized water was added. The mixture was stirred at room temperature (RT) for 5 h and was ultrasonicated until the Ha powder was thoroughly dispersed. At the same time, 70 mL of collagen solution (5 mg/mL) was transferred into another flask and stirred at RT. Then, 1.67 g of chitosan was added slowly to the collagen solution and stirred at RT to form a chitosan–collagen mixture. After that, the Ha solution was added to the collagen–chitosan mixture and stirred for 2 h to disperse thoroughly. Afterwards, the mixture was transferred to a mold and pre-frozen at − 40 °C for 24 h, followed by freeze-drying at − 55 °C using a constant cooling freeze-drying protocol.

The resulting freeze-dried scaffold was modified using four different methods: chemical cross-linking with (1) HEMA and (2) GTA solution and physical crosslinking by (3) DHT and (4) IR. Cross-linkings were accomplished by immersing the freeze-dried scaffold in a cross-linker solution containing 2.5% HEMA or 2.5% GTA solution, respectively, for 4 h at RT. The scaffolds were washed with deionized water for 1 h. After that, scaffolds were frozen and lyophilized as described above. For the DHT method, lyophilized scaffolds were put under a vacuum at a temperature of 110 °C for 24 h. For IR, fabricated scaffolds were irradiated at 5–30 kGy using Co60γ sources. The resulting scaffolds were named according to the methods used for modification: Ha·Col1·Cs-GTA, Ha·Col1·Cs-IR, Ha·Col1·Cs-DTH and Ha·Col1·Cs-HEMA.

X-ray diffraction (XRD) analysis

The phase and crystallinity of Ha nano-powder were evaluated using XRD (X'Pert PRO PW 3040, PANalytical, Netherlands). The parameter was CuKα radiation with a wavelength of 1.78896 Å and over a range of 2θ from 10° to 70° angle, step size 0.02/s with 40 kV voltages and 30 mA current. The XRD pattern was analyzed and compared with "X"pert high score and "X'Pert plus" software ["Xpert Highscore" File No. 01-086-0740 (ICDD 2005)] to identify the phase (Degen et al. 2014; Markvardsen et al. 2008).

Fourier-transform infrared spectroscopy (FTIR) analysis

The stretching frequencies of Ha were examined by FTIR analysis (FTIR 8400S, Shimadzu spectrophotometer, Japan) in the range of 4000–400 cm^{-1}. For Col1, samples were directly placed in the sample holder (IRprestige21, Shimadzu, Japan). FTIR spectra were recorded with FTIR 8400S Shimadzu Spectrophotometer in the range of 4000–700 cm^{-1}, at a resolution 4 cm^{-1}, number of scan: 20 times. For identifying organic, polymeric and inorganic materials within the four distinct Ha·Col1·Cs scaffolds, infrared light was used.

Scanning electron microscopy (SEM) imaging

The morphology of Ha crystals as well as the pore structure morphology of the Ha·Col1·Cs scaffolds was obtained by SEM (JSM 6490LA, Jeol, Japan). The surface of the scaffolds was platinum coated to make it conductive and then the samples were placed inside the SEM chamber.

Determination of porosity and density of Ha·Col1·Cs scaffold

The density and porosity of the fabricated scaffolds were measured by liquid displacement test (LDT) using ethanol as the liquid. A sample with a known weight (W) was immersed in a graduated cylinder in a known volume of ethanol (V_1) for 5 min. The total volume of ethanol in the cylinder and ethanol impregnated scaffold was V_2. The ethanol impregnated scaffold was removed from the cylinder and the residual ethanol volume was recorded (V_3). For each scaffold, five independent measurements were done ($n = 5$). The density (d) and the porosity (ϵ) of the scaffolds are calculated using these formulas:

$$d = {}^{W}/_{(V_2 - V_3)}, \tag{1}$$

$$\varepsilon = {}^{(V_1 - V_3)}/_{(V_2 - V_3)}. \tag{2}$$

Determination of swelling ability of Ha·Col1·Cs scaffold

The swelling ability was determined by the percentage of water absorption. Dry weight of the scaffold was denoted as Wd.

In brief, the scaffolds were immersed in PBS buffer solution with pH 7.4 at 37 °C for 2, 24, 48 and 72 h. Afterward, the scaffolds were taken out and their wet weight (W_{w1}) was

measured. In this case, we assessed the swelling ability of the scaffold structure employing its porous structure. In the second measurement, the same swollen samples were pressed between filter paper to remove the fluid remaining in the pores and then weighed (W_{w2}). In this way, the intrinsic water absorbance ability of the scaffold material was assessed. For each scaffold, five independent measurements were done ($n=5$). The swelling ratio of the scaffold was defined as the ratio of the weight increase ($W_w - W_d$) to the initial weight (W_d) according to following equation:

$$\text{Swelling ability}(\%) = (W_W - W_d)/W_d \times 100, \quad (3)$$

where W_W represents W_{w1} or W_{w2}.

Stability test for Ha·Col1·Cs scaffolds

Dried scaffolds were immersed into two different aqueous solutions (pH 4 and 7) at RT for intervals from 1 day up to 5 days. Scaffolds were then removed and dried for 48 h in a vacuum oven at 50 °C. A second weighing was conducted to determine the stabilities of the scaffolds by determining their weight loss. The stability of the scaffolds in the aqueous solution was calculated with the following equation:

$$S = (W_2/W_1) \times 100, \quad (4)$$

where S is the percentage of the weights of the scaffolds remaining after the test, W_1 and W_2 are, respectively, the weights of dried scaffolds before and after the test.

Assessment of mechanical strength

Samples with a diameter of 15 mm and a height of 14 mm were prepared for mechanical strength testing. The test was carried out using a mechanical testing machine (Z.05, Zwick/Roell, Germany) at RT. The cross-head speed was set at 2 mm/min. The compressive modulus was calculated from the slope of the stress–strain curve in the linear region (strain from 2 to 5%). Each measurement was repeated five times and the average value was calculated.

Biodegradability study of Ha·Col1·Cs scaffolds

To study the biodegradability, scaffolds were immersed in PBS-containing lysozyme (10,000 U/ml) at 37 °C for up to 21 days. At specific time points, the scaffolds were washed in deionized water to remove ions absorbed on the surface. Consecutively, the samples were lyophilized.

The degradation of the scaffold was calculated using following equation:

$$\text{Biodegradability}(\%) = \frac{W_o - W_t}{W_o} \times 100, \quad (5)$$

where W_0 is the initial and W_t is the dry weight of the scaffold.

In vitro cytotoxicity and biocompatibility assay for Ha, Col1, Cs and Ha·Col1·Cs scaffolds

Cytotoxicity tests of the extracted Col1, Ha, Cs and scaffolds on brine shrimp (*Artemia salina*) were performed as described (Khan et al. 2012).

For in vitro blood biocompatibility assay, heparinized human blood was used. Ha, Col1 and Cs and Ha·Col1·Cs scaffolds powder were diluted with different ratios of blood. Blood sample diluted at the same ratios with deionized water and PBS served as controls. These mixtures were spread on glass slides after 2 h incubation at RT and observed under a light microscope.

In vitro cell culture, attachment and growth in the presence of scaffold

Amniotic fluid-derived mesenchymal stem cells (AF-MSCs) were isolated and cultured in Chang C media containing 88% αMEM (Minimum Essential Medium Eagle Alpha Modification; Sigma) with 10% FBS, 1% GlutaMAX, 1% penicillin/streptomycin (all Gibco), 10% Chang B Basal Medium, and 2% Chang C supplement (Irvine Scientific) as described earlier (Spitzhorn et al. 2017). For observing the attachment, compatibility and growth of AF-MSCs in the presence of the Ha·Col1·Cs scaffolds, equal numbers of cells were seeded in 12-well plates with equal amounts scaffold nano-powder. Wells without any scaffold powder served as negative controls. Light microscopy images of the cells were taken on days 2, 5 and 10.

In vitro degradability and mineralization study

To test the degradability of the scaffolds by AF-MSCs, we continued the cell attachment and growth assay for 21 days and the size-reduction of scaffold nano-powder particles was observed microscopically. After 21 days, upon degradation of the nano-powder, mineralized nodules were formed at the site of clustered AF-MSCs which were confirmed using alizarin red staining. The respective wells were washed three times with PBS and stained as described previously (Rahman et al. 2018).

Histological and radiological analysis of in vivo grafted Ha·Col1·Cs scaffolds

The experimental model used in this study was a surgically created mandible critical-sized defect in rabbits (*Oryctolagus cuniculus*). Prior to the study, ethical approval was obtained from the institutional animal ethics committee of atomic

energy research establishment. The surgery protocol was conducted in accordance with the regulations on animal welfare and complied with the guidelines.

During the experimental period, the rabbits were held in cages with pelleted food, hay and water at RT in a humidity controlled room. All animals were subjected to 12 h day/night cycles. Importantly, the animals were acclimatized for 15 days prior to surgery. Total 16 adult male rabbits (1.5–2.0 kg) were recruited for the study and assigned in 4 groups: mandibular defects were implanted with (1) Ha·Col1·Cs-IR, (2) Ha·Col1·Cs-DHT, and (3) human bone graft/chips as a positive control, or (4) empty defect as a negative control. Under aseptic conditions, the rabbits were first intravenously anesthetized with 2% pentobarbital sodium (30 mg/kg). The hair on the site of the mandible was then trimmed. Then a 20 mm longitudinal skin incision was made and subcutaneous tissues were separated gently along the upper edge of the rabbit mandible. An appropriate defect size of 15 mm height × 3 mm width × 2 mm depth was made, using an orthopedic hand drill machine with a drill bit size of 1.5 mm, under saline irrigation to avoid thermal necrosis. To make the scaffolds compliant and resilient, the scaffolds were soaked in blood that oozed out from the incision during surgery. The scaffold constructs were then implanted into the defect. Subsequently, the skin incision was then sutured with nylon, using horizontal mattress sutures. The surgical wound was cleaned with povidone iodine (5%) and dressed with nitro-furazone ointment. Animals were housed in individual pens for 7 days post-surgery to restrict activity during the initial stages of healing and then transferred to group pens for the remainder of the study. Analgesia and antibiotics were administered after surgery. Inj. Ceftriaxone 250 mg (TRIZON VET, ACME Laboratories Ltd, Bangladesh) was administered twice for 7 days Intra-muscular (I/M) and Inj. ketoprofen (K-Pain Vet, ACI Limited, Bangladesh) 0.5 mL was administered once daily (I/M). Sutures were removed on day 8. After 4 months, the experimental animals were killed, the skin was excised and the mandible bone samples of the scaffold-treated site were surgically collected for histological examinations. Excised bone fragments were fixed, dehydrated, and embedded in paraffin and cut into 5 mm sections with a microtome. Tissue sections were subjected to hematoxylin and eosin (H&E) staining and were viewed with a light microscope (Olympus BX51, Japan). X-ray radiological images were taken to observe in vivo bone formation at several time points during the progression of recovery.

Results

Fabrication of Ha·Col1·Cs scaffolds from hydroxyapatite, collagen, and chitosan

The manufacturing process of Ha·Col1·Cs scaffold as described in the method section led to a stable co-precipitated Ha·Col1·Cs composite consisting of Ha, Col1 and Cs. To optimize the molecular links between the constituents, the composite material was chemically and physically cross-linked. Four types of scaffolds Ha·Col1·Cs-IR, Ha·Col1·Cs-GTA, Ha·Col1·Cs-DHT, and Ha·Col1·Cs-HEMA were prepared using physical cross-linkers DHT and IR; and chemical method cross-linking with HEMA and GTA solution (Fig. 1). The characterization of in-house-extracted hydroxyapatite and collagen type 1 has been provided in supplementary results (Figures S1, S2).

Fourier-transform infrared spectroscopy (FTIR) analysis of the scaffolds

FTIR analysis revealed the usefulness of chemical and physical cross-linker in the scaffold to form better network (Fig. 2). The FTIR spectra of native Ha clearly exhibit peaks at 602, 962, and 1035 cm^{-1}, corresponding to PO_4^{-3} ion. A small and sharp band was detected at 3572 cm^{-1}, corresponding to the stretching mode of the –OH group, which results from hydrated calcium phosphate such as Ha. A weak peak was observed at 876 cm^{-1} and strong peak at 1450 cm^{-1} which correspond to the stretching vibration of CO_3^{2-} ions confirming that Ha crystals containing CO_3^{2-}. The characteristic bands for HPO_4^{2-} were shown at 1133 cm^{-1}, 1064 cm^{-1}, 989 cm^{-1}, 577 cm^{-1} and 527 cm^{-1}. Similarly, the broad bands at about 3200 and 2800 cm^{-1} corresponded to the absorbed hydrate ion and short peaks in the range 3570–3670 cm^{-1} belong to the stretching vibrations of lattice OH– ions of hydroxyapatite (Fig. 2a).

For chitosan, the spectrum around 3430 cm^{-1} attributed to the pooled stretching vibration of OH and N–H groups. The band at 2845 cm^{-1} corresponded to the CH bond stretching. The comprehensive bands at 1637 and 1543 cm^{-1} were assigned to the existence of amide I and amide II groups. The sharp band at 1408 cm^{-1} was attributed to the stretching of carbonyl from the COO^- group. The low intense bands at 1382 and 1321 cm^{-1} were attributed to the CH bending vibrations of the ring. The featured peaks of C–O–C glycosidic linkage were shown at the region of 1153–1021 cm^{-1} (Fig. 2a). FTIR of collagen type 1 detected bands of amide A (3299 cm^{-1}), amide B (2950–2919 cm^{-1}), amide I (1632–1664 cm^{-1}), amide II (1500–1585 cm^{-1}) and amide III (1200–1300 cm^{-1}) (Fig. 2a).

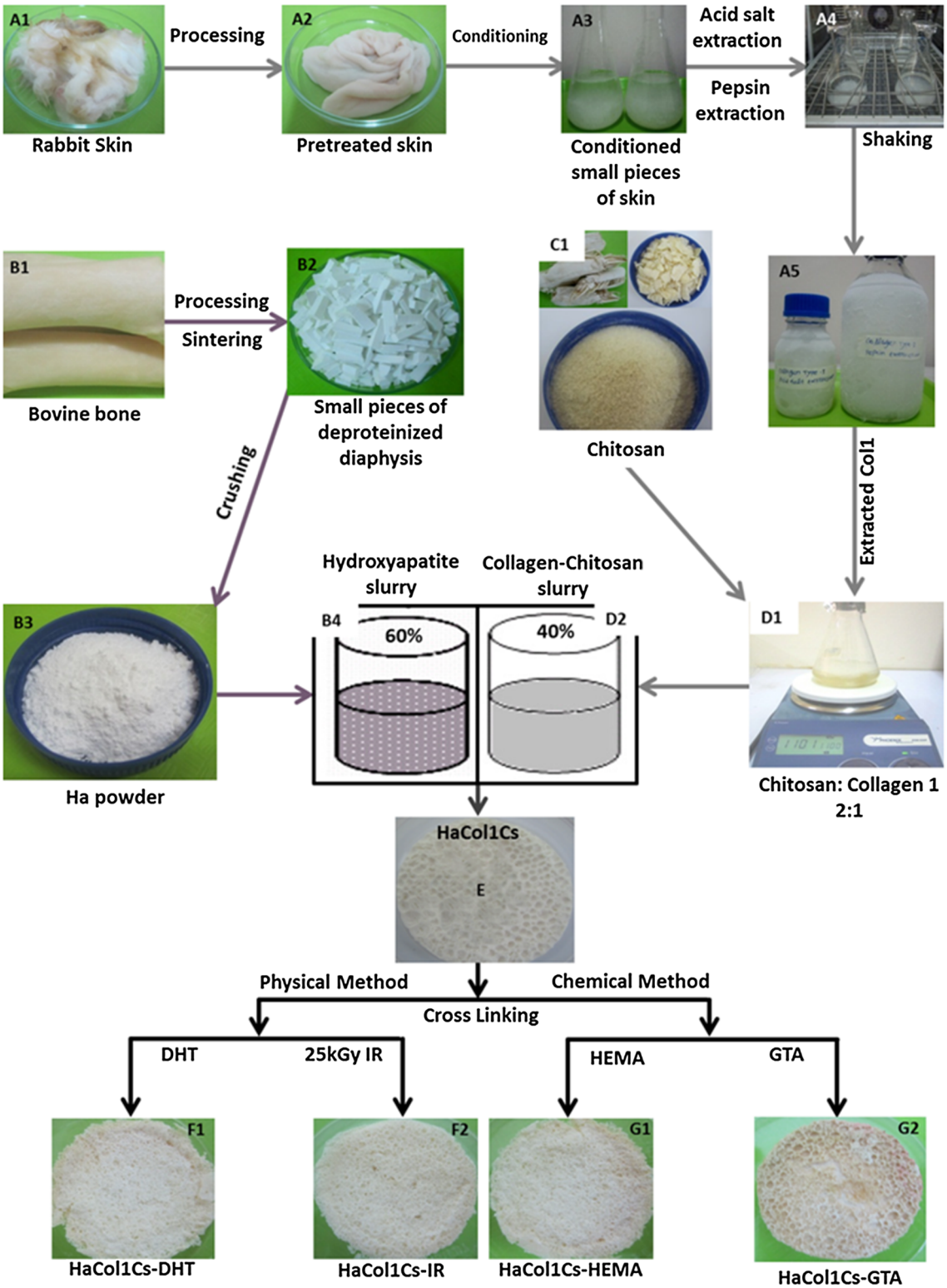

Fig. 1 Schematic representation for the fabrication of porous Ha·Col1·Cs scaffold. (A1–A5) Isolation steps of Col1. (B1–B3) Extraction and processing of Ha. (B4) Dispersion of HA powders in the water. (C1) Extracted brine shrimp derived Cs. (D1) Mixing of Cs in the Col1 solution at 2:1 ratio. (B4 and D2) Mixture of Ha slurry, and Cs-Col1 solution at 60:40 ratio and homogenization. (E) Freeze-dried Ha·Col1·Cs scaffold without cross-linkers. Cross-linked fabricated scaffold with physical method (DHT and IR) (F1-F2) and chemical method (HEMA and GTA) (G1-G2)

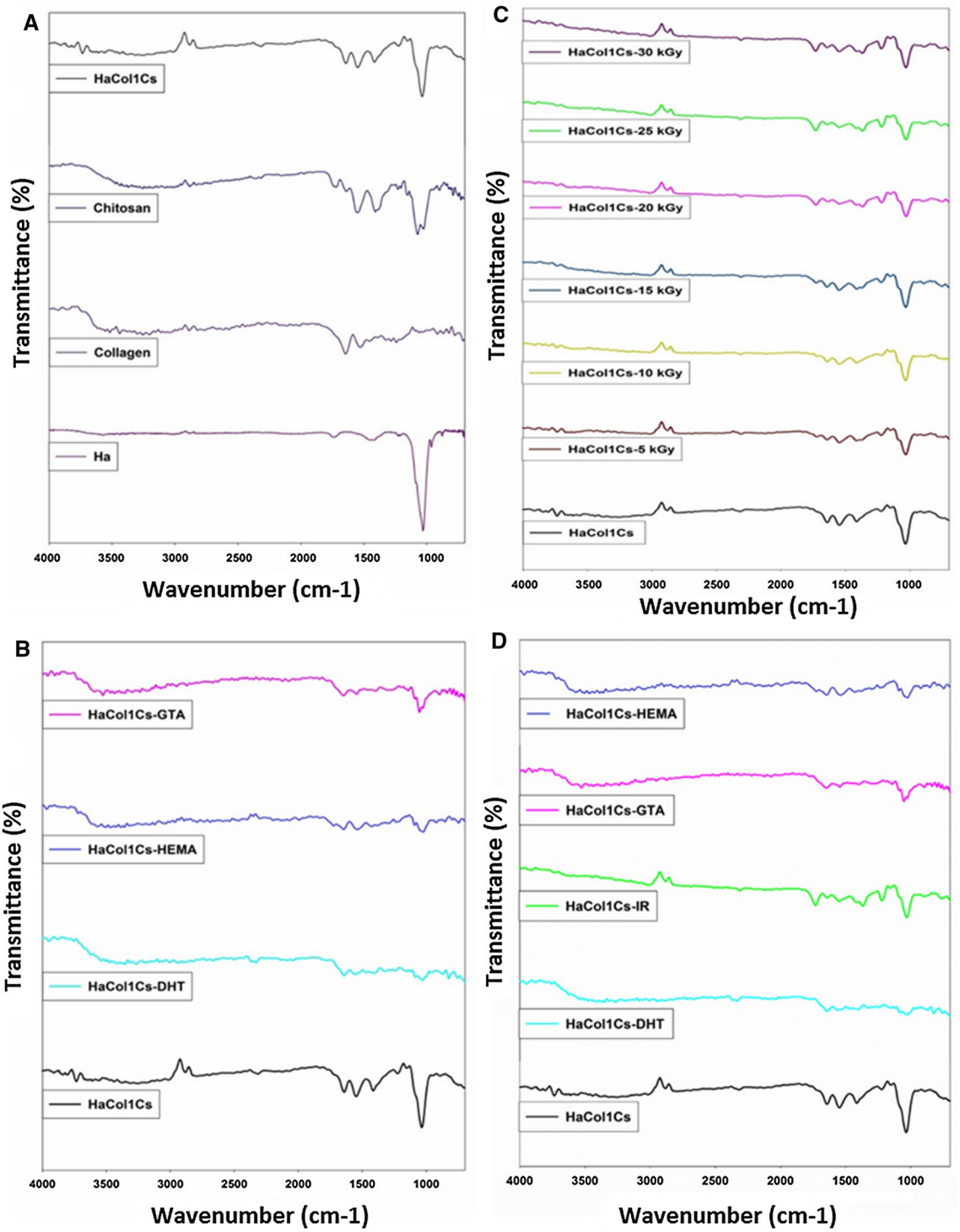

Fig. 2 FTIR spectra of Ha·Col1·Cs scaffolds with and without cross linkers. **a** Ha·Col1·Cs (without cross-linkers) spectra with corresponding individual constituents namely Ha, Cs and Col1. **b** FTIR analysis for Ha·Col1·Cs-DHT, Ha·Col1·Cs-HEMA, and Ha·Col1·Cs-GTA where Ha·Col1·Cs (without cross-linkers) served as reference. **c** Effects of various radiation doses on Ha·Col1·Cs scaffold as a cross-linker. **d** Comparative analysis of FTIR spectra between Ha·Col1·Cs (without cross-linkers), Ha·Col1·Cs-DHT, Ha·Col1·Cs-IR (25 kGy), Ha·Col1·Cs-HEMA and Ha·Col1·Cs-GTA

The main absorption bands of Ha·Col1·Cs scaffolds (without cross-links) are amide A (3299 cm^{-1}), amide B (2950–2919 cm^{-1}) and amide I (1632–1664 cm^{-1}) with N–H stretching signature. Amide II (1500–1585 cm^{-1}) and amide III (1200–1300 cm^{-1}) were also detected in the composite. A free N–H stretching vibration is present between 3400 and 3440 cm^{-1}. When the NH group of a peptide is evolved in a hydrogen bond, this position is moved to around 3300 cm^{-1}. The characteristic bands for OH– appeared at 3452–3782 cm^{-1}. Other functional groups such as amide III, PO_4^{3-} V_3, and asymmetric HPO_4^{2-} were detected (Fig. 2a).

In this study, carbonate V_2 was identified in sample Ha·Col1·Cs-DHT, Ha·Col1·Cs-IR and Ha·Col1·Cs-GTA at 824–870 cm^{-1}, 898 cm^{-1} and 897 cm^{-1} sequentially. CO_3 V_3 was detected in the samples Ha·Col1·Cs (1412, 1543 cm^{-1}), Ha·Col1·Cs-DHT (1402, 1560 cm^{-1}), Ha·Col1·Cs-IR (1415, 1549 cm^{-1}) and Ha·Col1·Cs-GTA (1397, 1545 cm^{-1}). Amide I was found for samples Ha·Col1·Cs, Ha·Col1·Cs-DHT, Ha·Col1·Cs-IR and Ha·Col1·Cs-GTA at 1639, 1643 cm^{-1}; 1641 and 1645 cm^{-1} correspondingly. The N–H stretching was also shown for sample Ha·Col1·Cs, Ha·Col1·Cs-DHT, Ha·Col1·Cs-IR and Ha·Col1·Cs-GTA at 3213, 3398 cm^{-1}; 3266 cm^{-1}; 3123, 3572 cm^{-1}; and 3185, 3526 cm^{-1}, respectively. Besides this, other functional groups such as amide III, PO_4 V_3 and asymmetric HPO_4^{2-} were found (Fig. 2b).

In case of various irradiated samples (Fig. 2c), FTIR spectra showed a band of amide I stretching at ~ 1635 $cm^{-1}$for Ha·Col1·Cs without cross-linking and for the irradiated scaffolds (5–20 kGy). However, a high radiation dose (25 and 30 kGy) shifted the band to 1643 cm^{-1}. The amide II stretch at 1543 cm^{-1} was stable in all of the scaffolds, which indicated that radiation has no impact on amide II bond.

When HEMA was cross-linked to Ha·Col1·Cs, C=O stretching vibration was observed to shift from 1720 to 1608 cm^{-1} due to amide II of collagen. The interaction of the alkane group with the –OH group of HEMA shifted the –OH group. The C–O stretching of HEMA was visible due to its shift from 1153 to 1091 cm^{-1} because of cross-linking with amide III of collagen (Fig. 2d).

Morphology analysis of the scaffolds from scanning electron microscopy (SEM) image

SEM images showed that all scaffolds exhibited irregular porous structures with moderate interconnections among the pores (Fig. 3). The wall of the macro-pores was detected to contain micro-pores. The pore diameter was 111.8–212.6 µm (mean 156.77 µm ± 37) for the Ha·Col1·Cs composite (Fig. 3a). On the other hand, the pore diameter of Ha·Col1·Cs-IR, Ha·Col1·Cs-DHT, Ha·Col1·Cs-GTA and Ha·Col1·Cs-HEMA were 74.43–341.12 µm (mean 164.3 µm ± 86) (Fig. 3b), 87.86–125.68 µm (mean 101.69 µm ± 17) (Fig. 3c), 212.6–376.09 µm (mean 273.43 µm ± 49) (Fig. 3d) and 98–204 µm (mean 142 µm ± 40) (Fig. 3e), respectively.

Porosity, density, stability, mechanical strength and degradation study

The porosity and density of the fabricated scaffolds were measured by liquid displacement test (LDT) using ethanol as a fluid. Ha·Col1·Cs-DHT, Ha·Col1·Cs-IR and Ha·Col1·Cs-GTA scaffolds showed porosities of 94.24, 95.29 and 90.64%, in the order given. The highest porosity (96.21%) was found in Ha·Col1·Cs without any cross-linker (Fig. 4a). Among the samples, the highest density was found for Ha·Col1·Cs-GTA (0.38 g/cm^3) and the lowest was found for Ha·Col1·Cs without any cross-linker (0.28 g/cm^3) (Fig. 4b). The highest swelling ratio was observed for the scaffold of without cross-linking (~ 306.24%) and the lowest was detected for Ha·Col1·Cs-GTA (~ 106.24%) after 72 h (Fig. 4c).

The biodegradation rate also varied between the different scaffolds. The lowest degradation rate was found in Ha·Col1·Cs-GTA which was 10% (day 1) and 16% (day 21). On the other hand, scaffold without cross-linker (Ha·Col1·Cs) showed a faster degradation rate of 39% (day 1) and 55% (day 21) (Fig. 4d).

Mechanical strength test revealed that all cross-linked scaffolds had a higher mechanical strength than the initial Ha·Col1·Cs indicating that, mechanical properties of the scaffold were affected by cross-linking. Among the cross-linked scaffold, Ha·Col1·Cs-DHT showed the highest strength (1.4 N/mm^2) whereas Ha·Col1·Cs-GTA and Ha·Col1·Cs-IR had values around 1.2 N/mm^2 (Fig. 4e).

Stability test of the fabricated scaffolds illustrated that scaffolds with cross-linker were more stable than Ha.Col.Cs without linker. In general, samples more stable were lower stable in neutral pH (pH 7.0) than on mild acidic conditions (pH 4.0). In both cases, Ha·Col1·Cs-GTA showed the highest stability (Fig. 4f).

In vitro cytotoxicity and human blood biocompatibility analysis

Brine shrimp lethality bioassay revealed that the composite biomaterials constituents (Ha, Cs and Col1) individually and the scaffold Ha·Col1·Cs as well as the physical cross-linked Ha·Col1·Cs-DHT, Ha·Col1·Cs-IR did not have a cytotoxic effect at a concentration of < 1 mg/mL. However, chemical cross-linked scaffold Ha·Col1·Cs-HEMA and Ha·Col1·Cs-GTA were observed to be more lethal than others. In general, the mortality rate was increasing above 1 mg/mL concentration of the scaffolds (Fig. 5a). Biocompatibility was assessed by incubation of individual materials with human

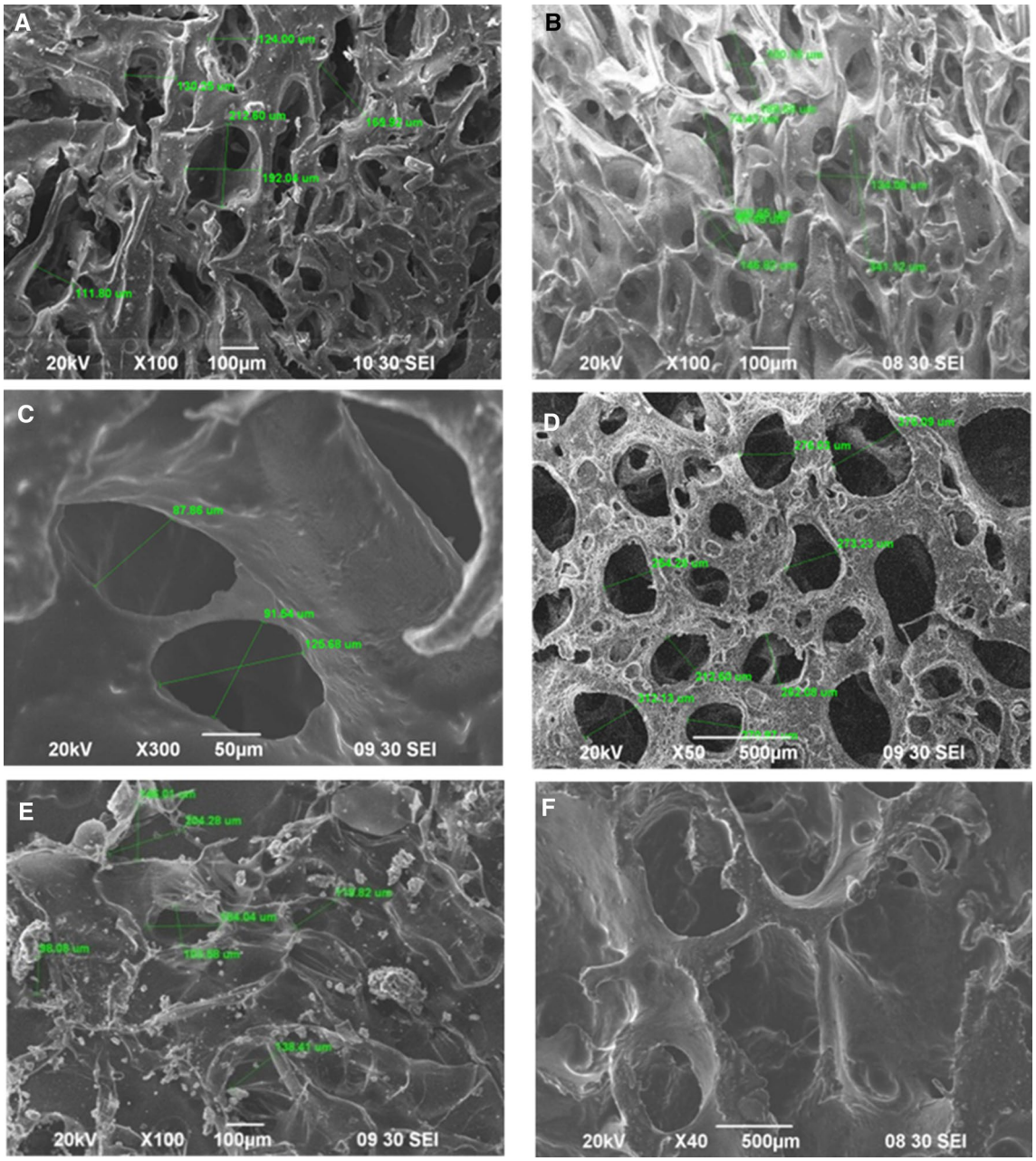

Fig. 3 SEM micrographs of different Ha·Col1·Cs scaffolds and human bone graft (HBG) from horizontal cross-sections at the middle region of the scaffold. **a** Ha·Col1·Cs scaffold without cross-linked. **b** Ha·Col1·Cs-IR scaffold cross-linked with 25 kGy gamma irradiation. **c** Ha·Col1·Cs-DHT scaffold cross-linked with DHT method. **d** Ha·Col1·Cs-GTA scaffold cross-linked with GTA solution. **e** Ha·Col1·Cs-HEMA scaffold cross-linked with HEMA. **f** Human bone graft served as positive control

red blood cells (RBCs) and showed no adverse effect on RBCs (Fig. 5b).

AF-MSCs attachment, growth and mineralization observation

We demonstrated human AF-MSCs attachment, viability and growth in the presence of the respective scaffolds nano-powder (Fig. 6a). In the presence of Ha·Col1·Cs-IR and Ha·Col1·Cs-DHT, normal cell behavior was observed (Fig. 6A1, A4). In case of Ha·Col1·Cs-HEMA, a lower number of cells attached and the morphology of the cells was changed (Fig. 6A3, A8). However, Ha·Col1·Cs-GTA was observed to be lethal for AF-MSCs leaving almost no living cells after 2 days (Fig. 6A2). These results exhibit the compatibility of the Ha·Col1·Cs-IR and Ha·Col1·Cs-DHT

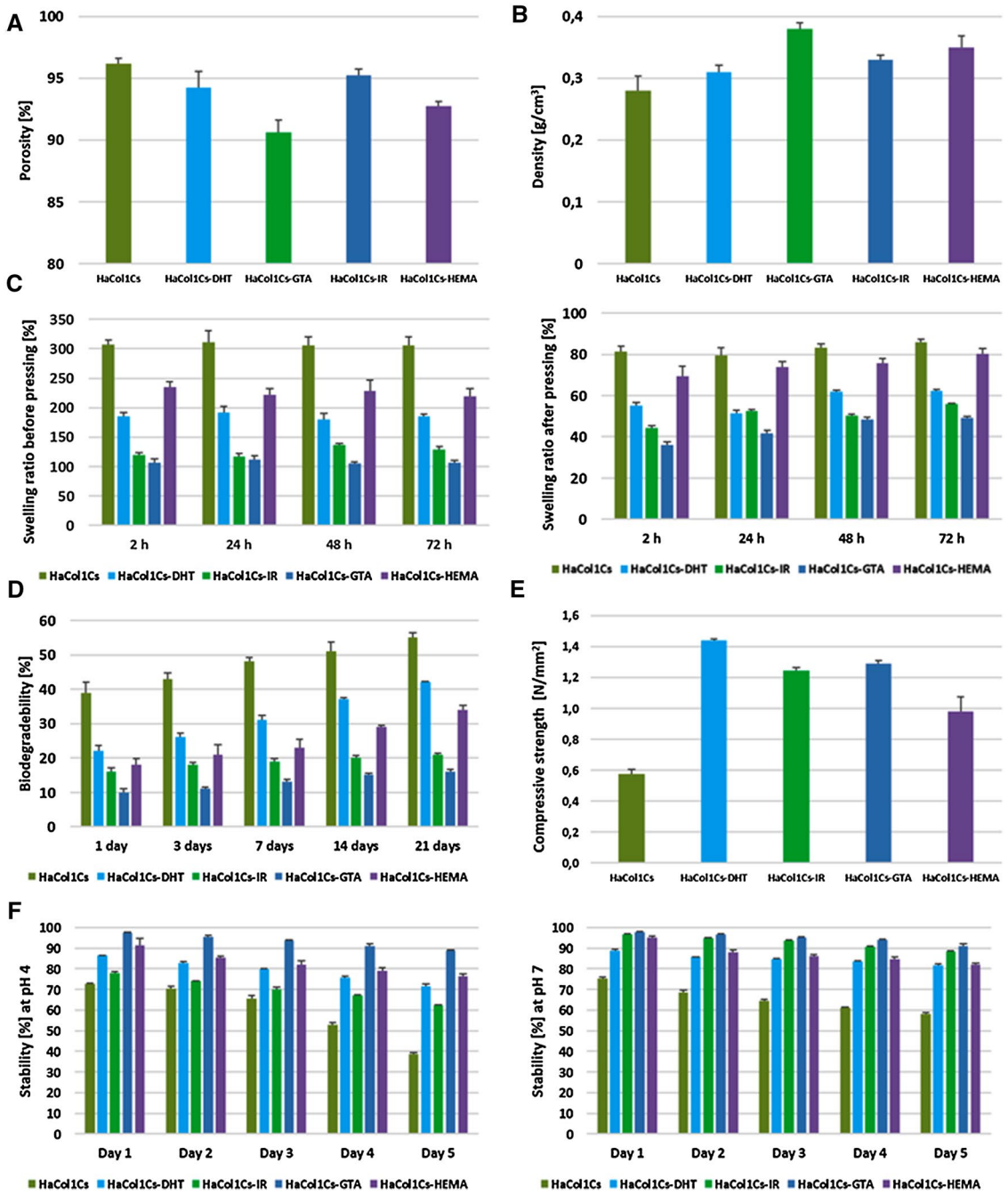

Fig. 4 Physicochemical characterization of the fabricated scaffolds. **a** Porosity range of the scaffolds. **b** Density of the fabricated scaffolds. **c** Swelling percentage of Ha·Col1·Cs (non-cross-linked and cross-linked) scaffolds at different soaking time: (left) swelling percentage of scaffold composition on the overall water uptake and (right) swelling percentage of scaffold material itself. **d** Enzymatic degradation studies of Ha·Col1·Cs (non-cross-linked and cross-linked) scaffolds. **e** Mechanical strength. **f** Stabilities of Ha·Col1·Cs scaffolds (non-cross-linked and cross-linked) in aqueous solution: (left) stability test at pH 4.0 and (right) stability test at pH 7.0

for AF-MSCs. After 5 days a uniform interconnection of MSC network on the scaffolds as well as multiple cell–cell contacts were visualized (Figs. 5A9, 6A6). At day 10, we observed the AF-MSC confluency was more than 90% in the presence of Ha·Col1·Cs-IR (Fig. 6A11), Ha·Col1·Cs-DHT (Fig. 6A14) and Ha·Col1·Cs-HEMA (Fig. 6A13) indicating no negative effect on proliferation. We also noticed that cells adapted to Ha·Col1·Cs-GTA with time, allowing growth of the surviving cells (Fig. 6A12).

Regarding in vitro mineralization in the presence of MSCs, we observed that clusters of MSCs aggregated together around the scaffolds particles and formed boney-like

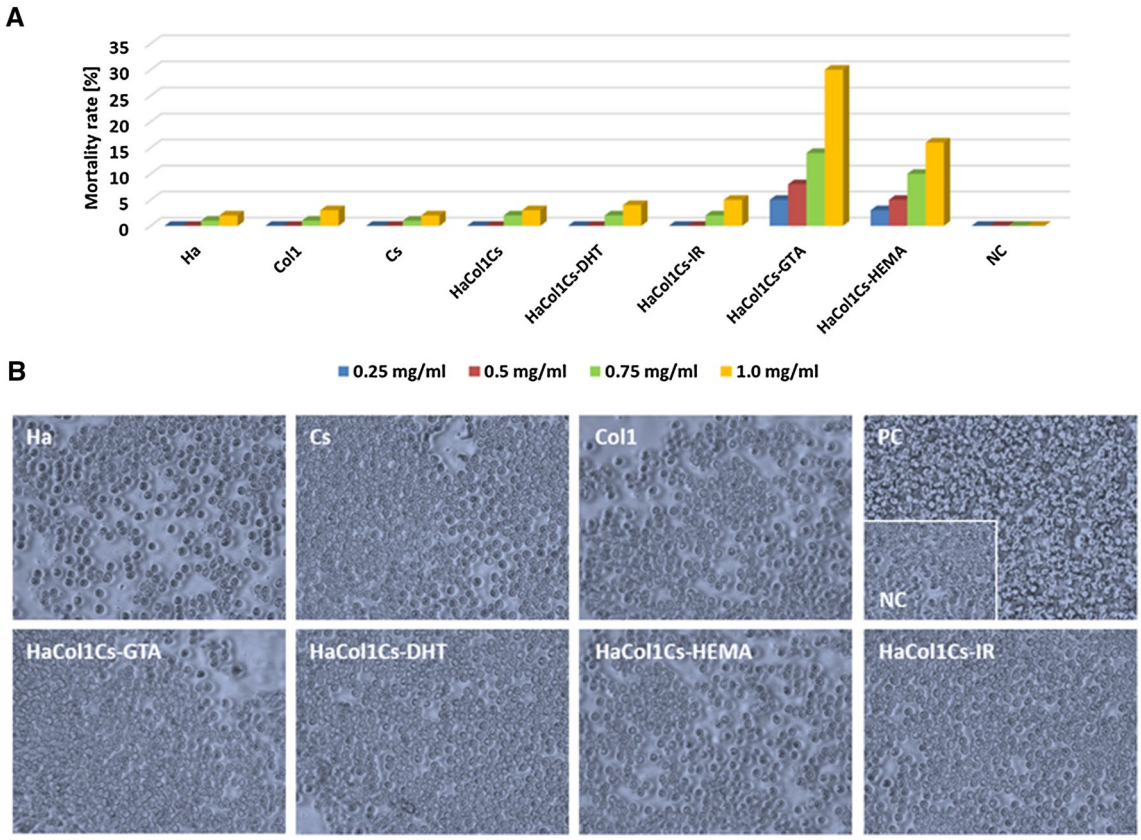

Fig. 5 In vitro cytotoxicity and human blood biocompatibility of Ha·Col1·Cs scaffolds and its constituents. **a** Brine shrimp lethality assay. **b** RBC hemolysis biocompatibility assay. PC positive control, and distilled water served as NC negative control

structure (Fig. 6B1–B5). Calcium phosphate deposition by the AF-MSCs was also evidenced by Alizarin Red staining (ARS) in the presence of scaffolds at day 21(Fig. 6B6–B10). An enhanced mineral deposition was found for the composite of Ha·Col1·Cs-IR and Ha·Col1·Cs-DHT compared to Ha·Col1·Cs-HEMA (Fig. 6B6, B9).

In vivo grafting of Ha·Col1·Cs-IR and Ha·Col1·Cs-DHT into a rabbit mandible defect model

Based on the physicochemical and in vitro biological tests, Ha·Col1·Cs-IR and Ha·Col1·Cs-DHT were qualified as good candidates to be transplanted in a rabbit maxillofacial mandible defect model (Fig. 7a). By 2 h post-operation, the rabbits appeared to be normal with regards to their eating habits and movements. Furthermore, we did not observe any adverse reactions or post-operative complications such as abnormal bleeding or infection at surgical sites. Further, we did not notice any signs of inflammation such as swelling, and the grafted materials were confirmed to be intact within the defects. However, after 4 weeks, the surgical area of each rabbit was healed with minor scar marks and covered with new hair (Fig. 7B13–B16).

Post-operative histological and radiological analysis

Hematoxylin and eosin (H&E) staining was done to access the comparative histology of the experimented mandible bones which were implanted with Ha·Col1·Cs–IR, Ha·Col1·Cs-DHT, human bone graft (gold standard positive control), and defects without transplantations served as a negative control. No significant differences were observed between Ha·Col1·Cs-DHT and Ha·Col1·Cs-IR concerning the formation of new blood vessels, and new bone structures (Fig. 8a). However, the human bone graft was superior whereas empty controls were inferior when compared to Ha·Col1·Cs-DHT and Ha·Col1·Cs-IR regarding bone regeneration 4 weeks after transplantation. Representative radiological images of the Ha·Col1·Cs-IR transplanted group revealed the gradual regeneration and filling of the defected rabbit mandible (Fig. 8B1–B4).

Discussion

All biomaterials used in this study were obtained from bio-waste which would have been discarded. As such we have extracted Ha from bovine cortical bone, Col1 from

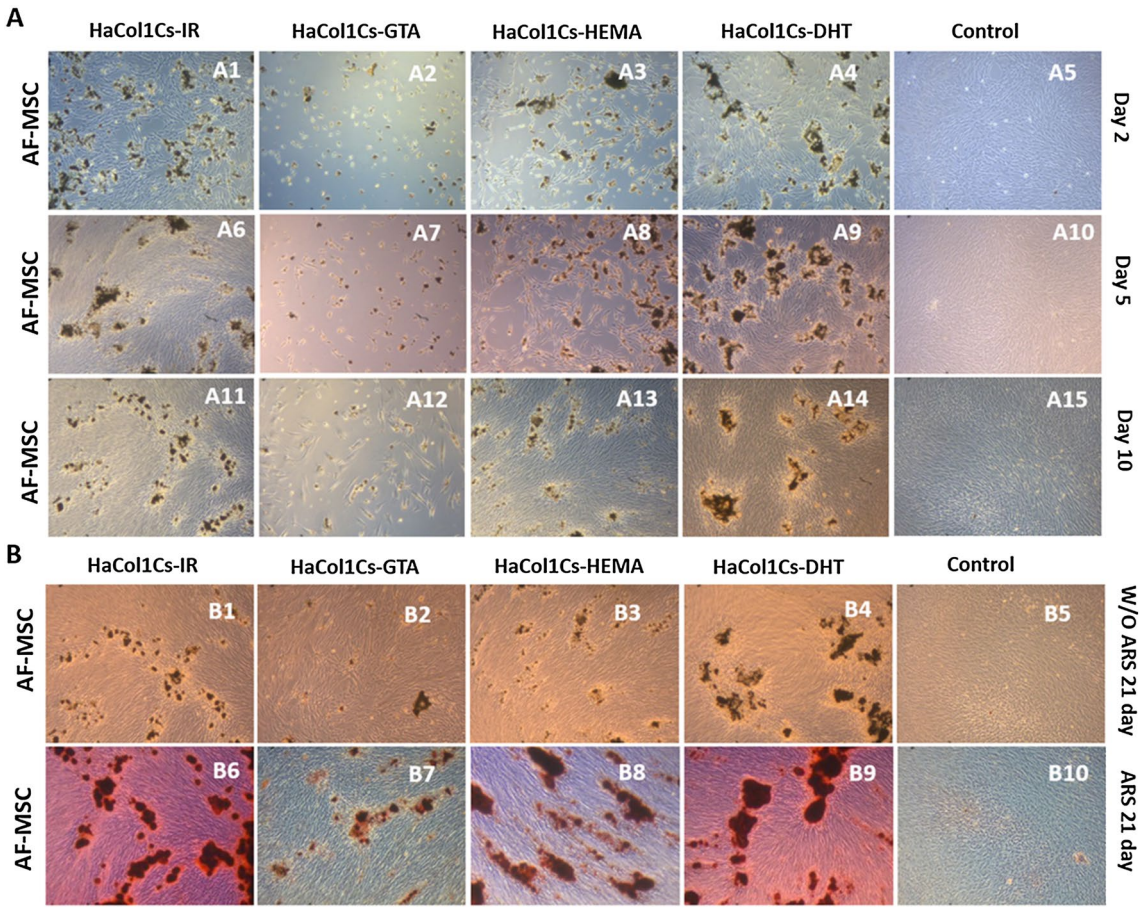

Fig. 6 AF-MSC attachment, growth and mineralization analysis in presence of various Ha·Col1·Cs scaffolds. **a** AF-MSC attachment and growth in presence of the formulated scaffolds powder. **b** In vitro mineralization of AF-MSCs in presence of distinct scaffolds. Calcification was evidenced by Alizarin Red (ARS) staining

slaughtered rabbit skin and Cs from prawn shell (Fig. 1A1, B1, C1). Thus, we have used materials and procedures which are a biologically safe and economically desirable (Rincón-López et al. 2018; Pachence 1996; El-Jawhari et al. 2016; Khan et al. 2005, 2012). Recently, these constituents for the fabrication of scaffold gained attention encompassing tunable chemical (molding ability into various geometries and formation of porous structures) and biological (suitable for cell growth and osteo-conduction) properties (Wang et al. 2017; Dan et al. 2016; Qasim et al. 2017; Zhang et al. 2013; Demirtaş et al. 2017; Chamieh et al. 2016; Balagangadharan et al. 2017).

In line with our FTIR analysis (Fig. 2a), the major band of the amide I in cross-linked Ha-Col1 sample was focused at 1653 cm^{-1} and minor bands at 1636 and 1663 cm^{-1} (Boskey et al. 1999; Epaschalis et al. 2001). In general, no significant changes were observed in the mineral phase of the scaffold due to radiation; however, new bonds (C–N triple bond and C–C triple bond) were formed in the polymer phase (Fig. 2c). Due to the irradiation, bonds could be formed between the polypeptide chains without utilizing the acidic and basic side chains which control the pore structure. Since, cellular attachment and infiltration are significantly affected by the scaffolds' mean pore size (Murphy et al. 2010); we have measured this parameter by SEM. The mean pore diameter for all scaffolds was found to range from 98 to 204 µm (Fig. 3), which is similar to pore sizes reported for other microparticle-based scaffolds (100–800 µm) (Reves et al. 2009) and above the required minimum size (50 µm) as needed for osteogenesis (Cheung et al. 2015).

In this study, Ha·Col1·Cs scaffolds were fabricated by thermally induced phase separation technique (Fig. 1e) with good porosity (90.64–96.21%) and water absorption capacity (Fig. 4a, c). The measured porosity reached the recommended porosity of ≥ 90% for bone substitute materials to accommodate osteoblasts or osteoprogenitor cells (Sabir et al. 2002). Therefore, this scaffold was qualified to be good penetrable by cell suspensions, required nutrient, metabolites, and soluble signals. The density of the fabricated scaffold ranged from 0.28 to 0.38 g/cm^3 (Fig. 4b), whereas the

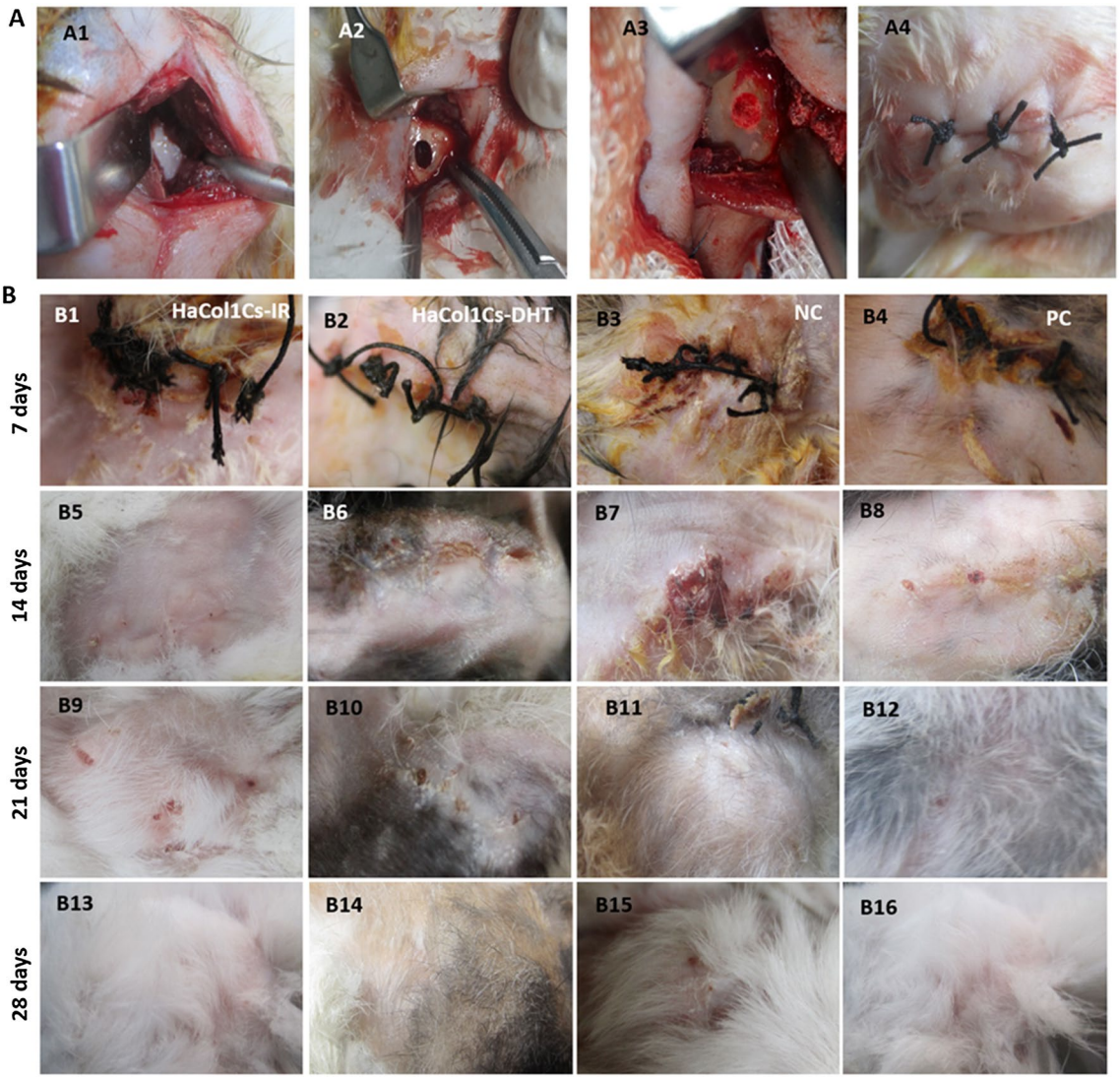

Fig. 7 In vivo grafting of scaffold in the surgically created rabbit maxillofacial mandible defect (non-load bearing) model. **a** Surgical and implantation procedures. (A1) Surgical incision showed the site of mandible to be drilled. (A2) Drilled defect chamber in the mandible of rabbits. (A3) Defect filled with scaffold. (A4) Sutured incision. **b** Post-grafting recovery observation from day 7 to day 28

apparent density of trabecular bone was reported to range from 0.14 to 1.10 g/cm^3 (Evans et al. 1992).

The swelling ability depends on the microstructure and hydrophilic nature of the scaffold (Yan et al. 2010). Since Col1 and Cs are both hydrophilic materials, the fabricated scaffolds were shown to have a relevant swelling ability which is in favor of maintaining the porous structure (Chen et al. 2016). The scaffolds without cross-linker showed relatively lower stability than the cross-linked Ha·Col1·Cs scaffolds (Fig. 4f). It was also revealed that the stability of the Ha·Col1·Cs scaffolds was reduced in acidic condition which has been shown before (Khan et al. 2012). We could show that cross-linking had a profound effect on the mechanical stability of the scaffold. Ha·Col1·Cs-DHT showed the best strength amongst the cross-linked scaffolds (Fig. 4e). Different studies also presented similar compressive strength in the hydroxyapatite-collagen scaffold and showed that the compressive strength of the collagen scaffold was increased by de-hydrothermal treatment (Kozlowska and Sionkowska 2015; Nitzsche et al. 2010).

One feature of a good bone scaffold is that the scaffold and its degradation products should not provoke an inflammatory response (Velasco et al. 2015; Alaribe et al. 2016). The degradation rate of porous scaffold influences cell vitality, cell growth, and even host response (She et al. 2008; Tan et al. 2007). In our study, the biodegradation was best for Ha·Col1·Cs without cross-linking and varied between the different cross-linker methods (Fig. 2e) whereas Ha·Col1·Cs-DHT was better degradable than the others. Aqueous mixtures of collagen and chitosan form

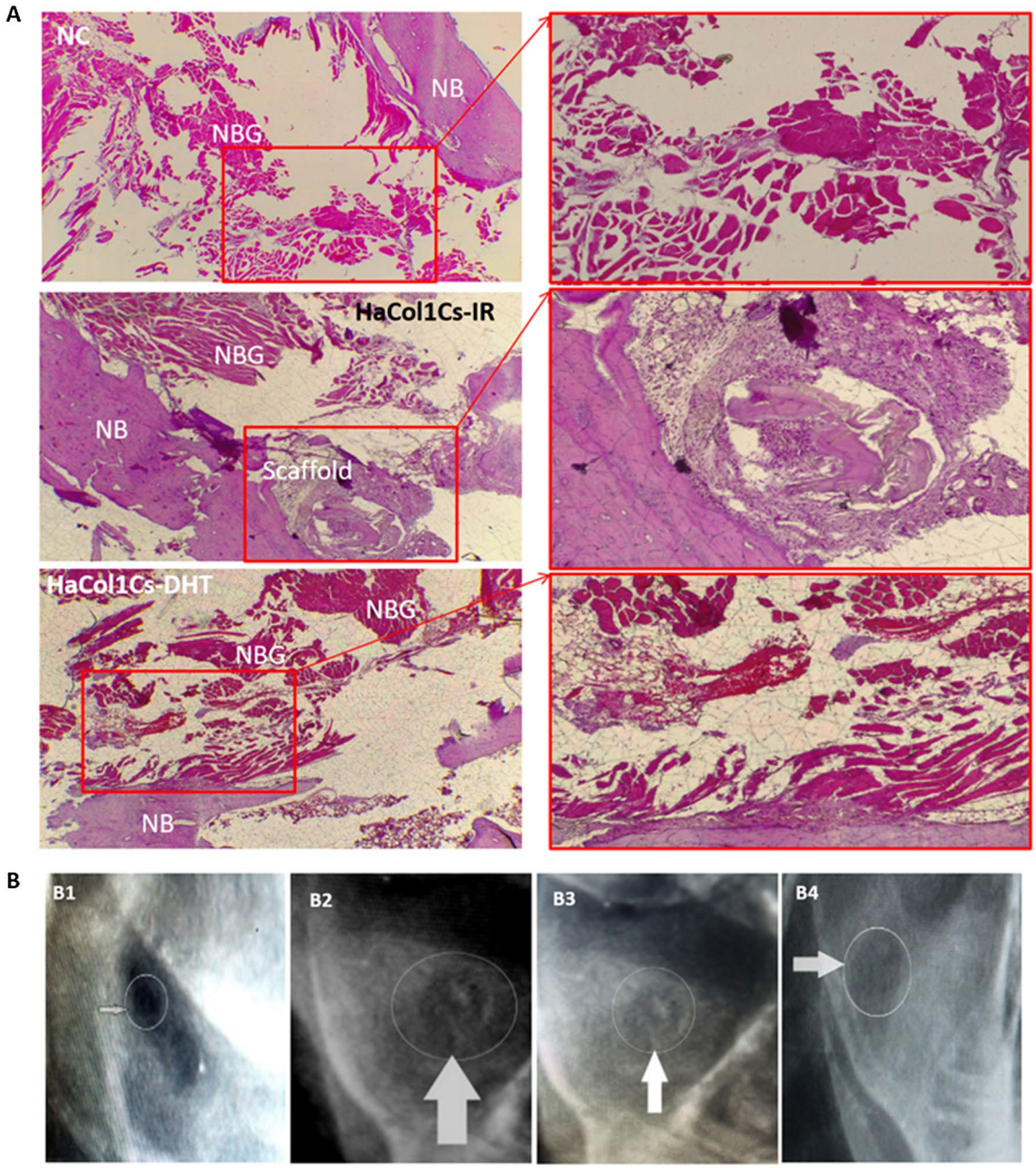

Fig. 8 Post-operative histological and radiological analysis. **a** Histological analyses of the treated defects after 4 months. Defected mandible without any implant/graft (first lane), Ha·Col1·Cs-IR (second lane), and Ha·Col1·Cs-DHT (third lane) whereas native bone (NB) and newly bone growth (NBG) are distinguished. **b** Representative radiological images during the recovery period in the Ha·Col1·Cs-IR group from (B1) day 1 to (B4) 4 months

electrostatic interactions between positively charged amino groups and negatively charged carboxyl groups leading to a complex structure (Taravel and Domard 1996; Khan et al. 2012). Cross-linking with DHT is supposed to cause the formation of new amide bonds in protein-based materials (Geiger et al. 2003). For this reason, it seems evident that DHT makes collagen more resistant to enzymatic degradation (Wahl and Czernuszka 2006).

The Ha·Col1·Cs-IR exhibited a lower biodegradability than Ha·Col1·Cs-DHT which may be due to the cross-linking method in which high-energy ionizing radiation or photoinitiator molecules are used. This method eventually influences the mechanical properties and degradation behavior of irradiated collagen-based scaffolds (Davidenko et al. 2015; Hovakimyan et al. 2012; Lew et al. 2007).

Our extracted Ha, Col1 and Cs were RBC biocompatible and non-toxic to brine shrimp larvae, which qualify these as biomaterial precursors for scaffold preparation (Khan et al. 2012; Levengood and Zhang 2014). Furthermore, we observed Ha·Col1·Cs-IR and Ha·Col1·Cs-DHT were compatible for AF-MSCs attachment and growth (Fig. 6A1, A4) which may be due to Col1 which is widely used as a coating material and constituent of scaffolds supporting cell attachment (Cooke et al. 2008; Wang et al. 2017; Zhang et al. 2013).

Ha·Col1·Cs-GTA inhibited cell attachment and growth of AF-MSCs (Fig. 6A2, A12). Previously it has been reported that adipose-derived stem cells attached and grew slowly in presence of a GTA–sponge (Yang et al. 2018). Although GTA is a widely used chemical cross-linker, it was reported that the functional aldehyde groups of GTA are toxic for cells (Oryan et al. 2014) and may cause significant biohazard problems, which has limited its application in commercial products (Yoo et al. 2011).

Alizarin red staining provided a proof that the AF-MSCs formed calcium-based mineral deposits around the scaffolds at day 21(Fig. 6b). Mineralization was reported to be induced by the osteoconductive nano-Ha powder present in the composites (Zhang et al. 2014; O'Brien 2011). In line with our work, chitosan–gelatin/nanohydroxyapatite scaffolds have been shown to support MC3T3-E1 cell attachment, proliferation, and mineralization (Dan et al. 2016).

At cellular level, the composite scaffold acts as an impermanent matrix for cell proliferation until new bone tissue is completely regenerated (Wattanutchariya and Changkowchai 2014). In vivo compatibility and utility of Ha·Col1·Cs-IR and Ha·Col1·Cs-DHT were evaluated (Fig. 7). We observed that both compatible contributed to mandible bone restoration. This regeneration capacity was superior to non-treatment of the defect but was inferior to the gold standard bone graft (Fig. 8). In line with our study, it was previously demonstrated that the nHAC/PLGA scaffolds implanted rabbit critical-size mandible defect possessed tissue compatibility and higher bone restoration capacity compared to empty controls (Wang et al. 2017).

Here, we did not add any growth factors, or cells to the scaffolds. By addition of bone-marrow MSCs to nanohydroxyapatite/collagen/poly L-lactide scaffolds total bone formation in a rabbit critical-size mandibular bone defect model was significantly higher than without the addition of stem cells (Wang et al. 2016). Therefore, for optimal bone healing, a combination of stem cells and biomaterials was reported to be needed to treat periodontal bone defects (Wang et al. 2017), suggesting the necessities of additional studies including mesenchymal cells. Additionally, more studies should aim to reveal the regulatory mechanisms involved in the complex process of biomineralization in vivo.

Conclusion

We have successfully fabricated Ha·Col1·Cs scaffolds from low cost and locally available polymeric bioactive materials using thermally induced phase separation technique with the cross-linkers such as GTA, DTH, IR and HEMA. All four formulated scaffolds showed substantial physicochemical and morphological features. Preliminary in vitro tests on AF-MSCs identified Ha·Col1·Cs-DHT and Ha·Col1·Cs-IR scaffolds as the most competent materials. In vivo, Ha·Col1·Cs-IR and Ha·Col1·Cs-DHT scaffolds significantly supported new bone formation in a maxillofacial mandible defect model making these scaffolds promising for the use in treatment of bone defects. However, 3D porous scaffold design, in vivo transplantation and clinical applications are still requiring significant improvement to harness optimum applicability. In-depth understanding of the basic fabrication processes involved and the post-transplantation mechanisms may help to achieve clinical relevance.

Acknowledgements The authors acknowledge the support from CRP (IAEA Research Contract no. 18343/R1), International Atomic Energy Agency, Austria. Prof. Dr. James Adjaye acknowledges support from the Medical Faculty, Heinrich Heine University Düsseldorf and Mr. Md. Shaifur Rahman acknowledges support from the German Academic Exchange Service (DAAD-91607303).

Author contributions MSR, MMR, LSS,NA, SMA, NC, JTC and JA conceived the idea. MMR, MSR, NA, and LSS designed and performed the experimental work and analyses the data. JTC analyzed the physical characterization of the scaffold and scaffold constituents data. MZH performed the in vitro brine shrimp cytotoxicity and RBC hemolysis assay. MMR, MSR, MZH and LSS wrote the manuscript. NC, SMA, JTC and JA edited the manuscript. NC, SMA and JA supervised the work. All the authors read and approved the final manuscript.

Funding For the purchasing of lab instruments and reagents, funds had been provided by the International Atomic Energy Agency, Austria (CRP Contract no. 18343/R1). No funding has been obtained for publication charge. The funding agency did not have any contribution on experimental idea, design, work, manuscript writing, and publication.

Compliance with ethical standards

Conflict of interests The authors declare that they have no competing interest.

Ethics approval The study was conducted according to the protocol approved by ethical committee of the Atomic Energy Research Establishment, Bangladesh and ethical committee of the Jahangirnagar University, Bangladesh. Post-slaughter bovine bone and rabbit skin were collected for research purpose from the healthy animals. AF-MSC samples from healthy human donors were collected during full-term C-sections from the Obstetrics and Gynaecology faculty, Heinrich Heine University Düsseldorf, Germany, with the patient informed consent as well as institutional ethical approval.

Consent for publication All the authors have agreed to publish the data in your esteemed Journal.

Availability of data and materials The data and materials have been presented in the main manuscript and can be given upon request.

References

Alaribe FN, Manoto SL, Motaung SCKM (2016) Scaffolds from biomaterials: advantages and limitations in bone and tissue engineering. Biologia 71(4):353–366. https://doi.org/10.1515/biolog-2016-0056

Baino F, Novajra G, Vitale-Brovarone C (2015) Bioceramics and scaffolds: a winning combination for tissue engineering. Front Bioeng Biotechnol 3:202. https://doi.org/10.3389/fbioe.2015.00202

Balagangadharan K, Dhivya S, Selvamurugan N (2017) Chitosan based nanofibers in bone tissue engineering. Int J Biol Macromol 104(Pt-B):1372–1382. https://doi.org/10.1016/j.ijbiomac.2016.12.046

Boskey AL, Wright TM, Blank RD (1999) Collagen and bone strength. J Bone Miner Res 14:330–335

Calabrese G, Giuffrida R, Forte S, Fabbi C, Figallo E, Salvatorelli L, Memeo L, Parenti R, Gulisano M, Gulino R (2017) Human adipose-derived mesenchymal stem cells seeded into a collagen-hydroxyapatite scaffold promote bone augmentation after implantation in the mouse. Sci Rep 7:7110. https://doi.org/10.1038/s41598-017-07672-0

Chamieh F, Collignon AM, Coyac BR, Lesieur J, Ribes S, Sadoine J, Llorens A, Nicoletti A, Letourneur D, Colombier ML, Nazhat SN, Bouchard P, Chaussain C, Rochefort GY (2016) Accelerated craniofacial bone regeneration through dense collagen gel scaffolds seeded with dental pulp stem cells. Sci Rep 6:38814. https://doi.org/10.1038/srep38814

Chen JS, Tu SL, Tsay RY (2010) A morphological study of porous polylactide scaffolds prepared by thermally induced phase separation. J Taiwan Inst Chem Eng 41(2):229–238

Chen Z, Du T, Tang X, Liu C, Li R, Xu C, Tian F, Du Z, Wu J (2016) Comparison of the properties of collagen–chitosan scaffolds after γ-ray irradiation and carbodiimide cross-linking. J Biomater Sci Polym Ed 27(10):937–953. https://doi.org/10.1080/09205063.2016.1169478

Cheung RCF, Ng TB, Wong JH, Chan WY (2015) Chitosan: an update on potential biomedical and pharmaceutical applications. Laurienzo P, ed. Mar Drugs 3(8):5156–5186. https://doi.org/10.3390/md13085156

Cooke MJ, Phillips SR, Shah DS, Athey D, Lakey JH, Przyborski SA (2008) Enhanced cell attachment using a novel cell culture surface presenting functional domains from extracellular matrix proteins. Cytotechnology 56(2):71–79. https://doi.org/10.1007/s10616-007-9119-7

Croisier F, Jérôme C (2013) Chitosan-based biomaterials for tissue engineering. Eur Polym J 49(4):780–792. https://doi.org/10.1016/j.eurpolymj.2012.12.009

d'Aquino R, De Rosa A, Lanza V, Tirino V, Laino L, Graziano A, Desiderio V, Laino G, Papaccio G (2009) Human mandible bone defect repair by the grafting of dental pulp stem/progenitor cells and collagen sponge biocomplexes. Eur Cell Mater 12(18):75–83

Dan Y, Liu O, Liu Y, Zhang YY, Li S, Feng XB, Shao ZW, Yang C, Yang SH, Hong JB (2016) Development of novel biocomposite scaffold of chitosan-gelatin/nanohydroxyapatite for potential bone tissue engineering applications. Nanoscale Res Lett 11:487. https://doi.org/10.1186/s11671-016-1669-1

Davidenko N, Bax DB, Schuster CF, Farndale RW, Hamaia SW, Best SM, Cameron RE (2015) Optimization of UV irradiation as a binding site conserving method for crosslinking collagen-based scaffolds. J Mater Sci Mater Med 27:14. https://doi.org/10.1007/s10856-015-5627-8

Degen T, Sadki M, Bron E, König U, Nénert G (2014) The high score suite. Powder Diffr 29(S2):S13–S14

Demirtaş TT, Irmak G, Gümüşderelioğlu M (2017) A bioprintable form of chitosan hydrogel for bone tissue engineering. Biofabrication 9(3):035003. https://doi.org/10.1088/1758-5090/aa7b1d

Echazú MIA, Tuttolomondo MV, Foglia ML, Mebert AM, Alvarez GS, Desimone MF (2016) Advances in collagen, chitosan and silica biomaterials for oral tissue regeneration: from basics to clinical trials. J Mater Chem B 4:6913–6929. https://doi.org/10.1039/C6TB02108E

El-Jawhari JJ, Sanjurjo-Rodríguez C, Jones E, Giannoudis PV (2016) Collagen-containing scaffolds enhance attachment and proliferation of non-cultured bone marrow multipotential stromal cells. J Orthop Res 34(4):597–606. https://doi.org/10.1002/jor.23070

Epaschalis EP, Verdelis K, Dotty SB, Boskey AL, Mendelsohn R, Yamauchi M (2001) Spectroscopic characterization of collagen crosslinks in bone. J Bone Miner Res 16(10):1821–1828

Evans LA, Macey DJ, Webb J (1992) Calcium biomineralization in the regular teeth of the chiton, acanthopleura hirtosa. Calcif Tissue Int 51:78–82

Gaihre B, Uswatta S, Jayasuriya AC (2017) Reconstruction of craniomaxillofacial bone defects using tissue-engineering strategies with injectable and non-injectable scaffolds. J Funct Biomater 8(4):49. https://doi.org/10.3390/jfb8040049

Geiger M, Li RH, Friess W (2003) Collagen sponges for bone regeneration with rhBMP-2. Adv Drug Deliv Rev 55:1613–1629

Gravel M, Gross T, Vago R, Tabrizian M (2006) Responses of mesenchymal stem cell to chitosan–coralline composites microstructured using coralline as gas forming agent. Biomaterials 27(9):1899–1906. https://doi.org/10.1016/j.biomaterials.2005.10.020

Greenwald MA, Kuehnert MJ, Fishman JA (2012) Infectious disease transmission during organ and tissue transplantation. Emerg Infect Dis 18(8):e1. https://doi.org/10.3201/eid1808.120277

Hovakimyan M, Guthoff RF, Stachs O (2012) Collagen cross-linking: current status and future directions. J Ophthalmol 2012:406850. https://doi.org/10.1155/2012/406850

Khan MA, Ferdous S, Mustafa AI (2005) Improvement of physico-mechanical properties of chitosan films by photo-curing with acrylic monomers. J Polym Environ 13(2):193–201

Khan MN, Islam JMM, Khan MA (2012) Fabrication and characterization of gelatin-based biocompatible porous composite scaffold for bone tissue engineering. J Biomed Mater Res, Part A 100(11):3020–3028. https://doi.org/10.1002/jbm.a.34248

Kim BS, Kang HJ, Yang SS, Lee J (2014) Comparison of in vitro and in vivo bioactivity: cuttlefish-bone-derived hydroxyapatite and synthetic hydroxyapatite granules as a bone graft substitute. Biomed Mater 9(2):025004. https://doi.org/10.1088/1748-6041/9/2/025004

Kozłowska J, Sionkowska A (2015) Effects of different crosslinking methods on the properties of collagen–calcium phosphate composite materials. Int J Biol Macromol 74:397–403

Kukhareva LV, Shamolina II, Polevaia EV (2010) Method of preparation of tissue engineering and cell cultivation collagen by acid extraction of calf skin. Tsitologiia 52(7):597–602

Kumar A, Nune KC, Misra RD (2016) Biological functionality of extracellular matrix-ornamented three-dimensional printed

hydroxyapatite scaffolds. J Biomed Mater Res A 104(6):1343–1351. https://doi.org/10.1002/jbm.a.35664
Levengood SL, Zhang M (2014) Chitosan-based scaffolds for bone tissue engineering. J Mater Chem B Mater Biol Med 2(21):3161–3184. https://doi.org/10.1039/C4TB00027G
Lew DH, Liu PH, Orgill DP (2007) Optimization of UV cross-linking density for durable and nontoxic collagen GAG dermal substitute. J Biomed Mater Res B Appl Biomater 82(1):51–56
Maisani M, Pezzoli D, Chassande O, Mantovani D (2017) Cellularizing hydrogel-based scaffolds to repair bone tissue: how to create a physiologically relevant micro-environment? J Tissue Eng 8:1–26
Maji K, Dasgupta S, Pramanik K, Bissoyi A (2016) Preparation and evaluation of gelatin-chitosan-nanobioglass 3D porous scaffold for bone tissue engineering. Int J Biomater 2016:9825659. https://doi.org/10.1155/2016/9825659
Mao AS, Mooney DJ (2015) Regenerative medicine: current therapies and future directions. Proc Natl Acad Sci USA 112(47):14452–14459. https://doi.org/10.1073/pnas.1508520112
Markvardsen AJ, Shankland K, David WIF, Johnston JC, Ibberson RM, Tucker M, Nowell H, Griffin T (2008) ExtSym: a program to aid space-group determination from powder diffraction data. J Appl Crystallogr J Appl Cryst 41(6):1177–1181
Murphy CM, Haugh MG, O'Brien FJ (2010) The effect of mean pore size on cell attachment, proliferation and migration in collagen glycosaminoglycan scaffolds for tissue engineering. Biomaterials 31:461–466
Nagahama H, Rani VV, Shalumon KT, Jayakumar R, Nair SV, Koiwa S, Furuike T, Tamura H (2009) Preparation, characterization, bioactive and cell attachment studies of alpha-chitin/gelatin composite membranes. Int J Biol Macromol 44(4):333–337. https://doi.org/10.1016/j.ijbiomac.2009.01.006
Nitzsche H, Lochmann A, Metz H, Hauser A, Syrowatka F, Hempel E, Müller T, Thurn-Albrecht T, Mäder K (2010) Fabrication and characterization of a biomimetic composite scaffold for bone defect repair. J Biomed Mater Res A 94(1):298–307
O'Brien FJ (2011) Biomaterials and scaffolds for tissue engineering. Mater Today 14:88–95
Oryan A, Alidadi S, Moshiri A, Maffulli N (2014) Bone regenerative medicine: classic options, novel strategies, and future directions. J Orthop Surg Res 9(1):18. https://doi.org/10.1186/1749-799X-9-18
Pacak CA, MacKay AA, Cowan DB (2014) An improved method for the preparation of type I collagen from skin. J Vis Exp 83:51011. https://doi.org/10.3791/51011
Pachence JM (1996) Collagen-based devices for soft tissue repair. J Biomed Mater Res 33(1):35–40
Pallela R, Venkatesan J, Janapala VR, Kim SK (2012) Biophysicochemical evaluation of chitosan hydroxyapatite-marine sponge collagen composite for bone tissue engineering. J Biomed Mater Res, Part A 100(2):486–495. https://doi.org/10.1002/jbm.a.33292
Polo-Corrales L, Latorre-Esteves M, Ramirez-Vick JE (2014) Scaffold design for bone regeneration. J Nanosci Nanotechnol 14(1):15–56
Qasim SB, Najeeb S, Delaine-Smith RM, Rawlinson A, Ur Rehman I (2017) Potential of electrospun chitosan fibers as a surface layer in functionally graded GTR membrane for periodontal regeneration. Dent Mater 33(1):71–83. https://doi.org/10.1016/j.dental.2016.10.003
Rahman MS, Spitzhorn LS, Wruck W, Hagenbeck C, Balan P, Graffmann N, Bohndorf M, Ncube A, Guillot PV, Fehm T, Adjaye J (2018) The presence of human mesenchymal stem cells of renal origin in amniotic fluid increases with gestational time. Stem Cell Res Ther 9:113. https://doi.org/10.1186/s13287-018-0864-7
Reves BT, Bumgardner JD, Cole JA, Yang Y, Haggard WO (2009) Lyophilization to improve drug delivery for chitosan-calcium phosphate bone scaffold construct: a preliminary investigation. J Biomed Mater Res B Appl Biomater 90(1):1–10. https://doi.org/10.1002/jbm.b.31390
Rincón-López JA, Hermann-Muñoz JA, Giraldo-Betancur AL, De Vizcaya-Ruiz A, Alvarado-Orozco JM, Muñoz-Saldaña J (2018) Synthesis, characterization and in vitro study of synthetic and bovine-derived hydroxyapatite ceramics: a comparison. Materials 11(3):333. https://doi.org/10.3390/ma11030333
Rodríguez-Vázquez M, Vega-Ruiz B, Ramos-Zúñiga R, Saldaña-Koppel DA, Quiñones-Olvera LF (2015) Chitosan and its potential use as a scaffold for tissue engineering in regenerative medicine. Biomed Res Int. https://doi.org/10.1155/2015/821279 **(Article ID 821279)**
Sabir MI, Xu X, Li L (2002) A review on biodegradable polymeric materials for bone tissue engineering applications. J Mater Sci 44(21):5713–5724
She Z, Zhang B, Jin C, Feng Q, Xu Y (2008) Preparation and in vitro degradation of porous three-dimensional silk fibroin/chitosan scaffold. Polym Degrad Stab 93(7):1316–1322
Sofronia AM, Baies R, Anghel EM, Marinescu CA, Tanasescu S (2014) Thermal and structural characterization of synthetic and natural nanocrystalline hydroxyapatite. Mater Sci Eng C Biol Appl 43:153–163. https://doi.org/10.1016/j.msec.2014.07.023
Spitzhorn LS, Rahman MS, Schwindt L, Ho HT, Wruck W, Bohndorf M, Wehrmeyer S, Ncube A, Beyer I, Hagenbeck C, Balan P, Fehm T, Adjaye J (2017) Isolation and molecular characterization of amniotic fluid-derived mesenchymal stem cells obtained from caesarean sections. Stem Cells Int 2017:5932706. https://doi.org/10.1155/2017/5932706
Tan H, Gong Y, Lao L, Mao Z, Gao C (2007) Gelatin/chitosan/hyaluronan ternary complex scaffold containing basic fibroblast growth factor for cartilage tissue engineering. J Mater Sci Mater Med 18(10):1961–1968
Taravel MN, Domard A (1996) Collagen and its interactions with chitosan III. Some biological and mechanical properties. Biomaterials 17(4):451–455
Tollemar V, Collier ZJ, Mohammed MK, Lee MJ, Ameerde GA, Reid RR (2016) Stem cells, growth factors and scaffolds in craniofacial regenerative medicine. Genes Diseases 3(1):56–71. https://doi.org/10.1016/j.gendis.2015.09.004
Tong S, Xu DP, Liu ZM, Du Y, Wang XK (2016a) Synthesis and in vitro and in vivo evaluation of a novel TGF-β1-SF-CS three-dimensional scaffold for bone tissue engineering. Int J Mol Med 38(2):367–380. https://doi.org/10.3892/ijmm.2016.2651
Tong S, Xu DP, Liu ZM, Du Y, Wang XK (2016b) Synthesis of the new-type vascular endothelial growth factor-silk fibroin-chitosan three-dimensional scaffolds for bone tissue engineering and in vitro evaluation. J Craniofac Surg 27(2):509–515. https://doi.org/10.1097/SCS.0000000000002296
Velasco MA, Narváez-Tovar CA, Garzón-Alvarado DA (2015) Design, materials, and mechanobiology of biodegradable scaffolds for bone tissue engineering. Biomed Res Int 2015:729076. https://doi.org/10.1155/2015/729076
Wahl DA, Czernuszka JT (2006) Collagen—hydroxyapatite composites for hard tissue repair. Eur Cell Mater 11:43–56
Wang X, Xing H, Zhang G, Wu X, Zou X, Feng L, Wang D, Li M, Zhao J, Du J, Lv Y, Lingling E, Liu H (2016) Restoration of a critical mandibular bone defect using human alveolar bone-derived stem cells and porous nano-HA/collagen/PLA scaffold. Stem Cells Int 2016:8741641. https://doi.org/10.1155/2016/8741641
Wang X, Wu X, Xing H, Zhang G, Shi Q, Lingling E, Liu N, Yang T, Wang D, Qi F, Wang L, Liu H (2017) Porous nanohydroxyapatite/collagen scaffolds loading insulin PLGA particles for restoration of critical size bone defect. ACS Appl Mater Interfaces 9(13):11380–11391. https://doi.org/10.1021/acsami.6b13566
Wattanutchariya W, Changkowchai W (2014) Characterization of porous scaffold from chitosan-gelatin/hydroxyapatite for bone grafting. proceedings of the international multi conference of

engineers and computer scientists, vol 2, IMECS March 12–14, 2014, Hong Kong

Wua SC, Hsua HC, Hsua SK, Changb YC, Ho WF (2016) Synthesis of hydroxyapatite from egg shell powders through ball milling and heat treatment. J Asian Ceram Soc 4(1):85–90

Yan LP, Wang YJ, Ren L, Wu G, Caridade SG, Fan JB, Wang LY, Ji PH, Oliveira JM, Oliveira JT, Mano JF, Reis RL (2010) Genipin-cross-linked collagen/chitosan biomimetic scaffolds for articular cartilage tissue engineering applications. J Biomed Mater Res A 96a:465–475

Yang X, Lu Z, Wu H, Li W, Zheng L, Zhao J (2018) Collagen-alginate as bioink for three-dimensional (3D) cell printing based cartilage tissue engineering. Mater Sci Eng C Mater Biol Appl 83:195–201. https://doi.org/10.1016/j.msec.2017.09.002

Yi H, Rehman FU, Zhao C, Liu B, He N (2016) Recent advances in nano scaffolds for bone repair. Bone Res 4:16050

Yoo JS, Kim YJ, Kim SH, Choi SH (2011) Study on genipin: a new alternative natural crosslinking agent for fixing heterograft tissue. Korean J Thorac Cardiovasc Surg 44(3):197–207

Yu B, Zhang Y, Li X, Wang Q, Ouyang Y, Xia Y, Yu B, Lin B, Li S, Fan Y, Chen Y (2013) The use of injectable chitosan/nano-hydroxyapatite/collagen composites with bone marrow mesenchymal stem cells to promote ectopic bone formation in vivo. J Nanomater 2013:506593

Zhang X, Xu M, Liu X, Zhang F, Wei Y, Meng S, Dai X, Duan A, Deng X (2013) Restoration of critical-sized defects in the rabbit mandible using autologous bone marrow stromal cells hybridized with nano-β-tricalcium phosphate/collagen scaffolds. J Nanomater 2013:913438. https://doi.org/10.1155/2013/913438

Zhang X, Li XW, Li JG, Sun XD (2014) Preparation and mechanical property of a novel 3D porous magnesium scaffold for bone tissue engineering. Mater Sci Eng C Mater Biol Appl 42:362–367

3.9 Characterization of Burn Wound Healing Gel Prepared from Human Amniotic Membrane and *Aloe vera* Extract

Md Shaifur Rahman, Rashedul Islam, Md Masud Rana, Lucas-Sebastian Spitzhorn, Mohammad Shahedur Rahman, James Adjaye and Sikder M. Asaduzzaman

Abstract

Background: Skin burn wound is a notable medical burden worldwide. Rapid and effective treatment of burnt skin is vital to fasten wound closure and healing properly. Amniotic graft and Aloe vera are widely used as wound managing biomaterials. Sophisticated processing, high cost, availability, and the requirement of medics for transplantation limit the application of amnion grafts. We aim to prepare a novel gel from amnion combined with the Aloe vera extract for burn wound healing which overcome the limitations of graft.

Methods: Two percent human amniotic membrane (AM), Aloe vera (AV) and AM+AV gels were prepared. In vitro cytotoxicity, biocompatibility, cell attachment, proliferation, wound healing scratch assays were performed in presence of the distinct gels. After skin irritation study, second-degree burns were induced on dorsal region of Wistar rats; and gels were applied to observe the healing potential in vivo. Besides, macroscopical measurement of wound contraction and re-epithelialization; gel treated skin was histologically investigated by Hematoxylin and eosin (H&E) staining. Finally, quantitative assessment of angiogenesis, inflammation, and epithelialization was done.

Results: The gels were tested to be non-cytotoxic to nauplii and compatible with human blood and skin cells. Media containing 500 μg/mL AM+AV gel were observed to promote HaCaT and HFF1 cells attachment and proliferation. In vitro scratch assay demonstrated that AM+AV significantly accelerated wound closure through migration of HaCaT cells. No erythema and edema were observed in skin irritation experiments confirming the applicability of the gels. AV and AM+AV groups showed significantly accelerated wound closure through re-epithelialization and wound contraction with $P < 0.01$. Macroscopically, AM and AM+AV treated wound recovery rates were 87 and 90% respectively with $P < 0.05$. Histology analysis revealed significant epitheliazation and angiogenesis in AM+AV treated rats compared to control ($P < 0.05$). AM+AV treated wounds had thicker regenerated epidermis, increased number of blood vessels, and greater number of proliferating keratinocytes within the epidermis.

Conclusion: We demonstrated that a gel consisting of a combination of amnion and Aloe vera extract has high efficacy as a burn wound healing product. Amniotic membrane combined with the carrier Aloe vera in gel format is easy to produce and to apply.

Publication Status: Published in BMC Complement Altern Med. 2019; 19: 115.
Impact Factor: 2.479

Approximated total share of contribution: 50%

Contribution on experimental design, realization and publication: MSR (1) and MSR (2) conceived the idea. MSR (1), RI, and MSR (2) designed the experiment. MSR1, MMR, LSS and RI performed the experimental work and analysis the data. MSR (1) and RI wrote the initial draft and SMA, MSR2, LSS, JA edited the manuscript. SMA and MSR (2) supervised the work from start to end. JA supervised the in vitro study. All authors read and approved the final manuscript.

Pubmed link: https://www.ncbi.nlm.nih.gov/pubmed/31159783

Journal link:
https://bmccomplementmedtherapies.biomedcentral.com/articles/10.1186/s12906-019-2525-5

BMC Complementary and Alternative Medicine

RESEARCH ARTICLE Open Access

Characterization of burn wound healing gel prepared from human amniotic membrane and *Aloe vera* extract

Md Shaifur Rahman[1,3], Rashedul Islam[2], Md Masud Rana[3], Lucas-Sebastian Spitzhorn[1], Mohammad Shahedur Rahman[2], James Adjaye[1] and Sikder M. Asaduzzaman[3*]

Abstract

Background: Skin burn wound is a notable medical burden worldwide. Rapid and effective treatment of burnt skin is vital to fasten wound closure and healing properly. Amniotic graft and *Aloe vera* are widely used as wound managing biomaterials. Sophisticated processing, high cost, availability, and the requirement of medics for transplantation limit the application of amnion grafts. We aim to prepare a novel gel from amnion combined with the *Aloe vera* extract for burn wound healing which overcome the limitations of graft.

Methods: Two percent human amniotic membrane (AM), *Aloe vera* (AV) and AM+AV gels were prepared. In vitro cytotoxicity, biocompatibility, cell attachment, proliferation, wound healing scratch assays were performed in presence of the distinct gels. After skin irritation study, second-degree burns were induced on dorsal region of Wistar rats; and gels were applied to observe the healing potential in vivo. Besides, macroscopical measurement of wound contraction and re-epithelialization; gel treated skin was histologically investigated by Hematoxylin and eosin (H&E) staining. Finally, quantitative assessment of angiogenesis, inflammation, and epithelialization was done.

Results: The gels were tested to be non-cytotoxic to nauplii and compatible with human blood and skin cells. Media containing 500 μg/mL AM+AV gel were observed to promote HaCaT and HFF1 cells attachment and proliferation. In vitro scratch assay demonstrated that AM+AV significantly accelerated wound closure through migration of HaCaT cells. No erythema and edema were observed in skin irritation experiments confirming the applicability of the gels. AV and AM+AV groups showed significantly accelerated wound closure through re-epithelialization and wound contraction with $P < 0.01$. Macroscopically, AM and AM+AV treated wound recovery rates were 87 and 90% respectively with $P < 0.05$. Histology analysis revealed significant epitheliazation and angiogenesis in AM+AV treated rats compared to control ($P < 0.05$). AM+AV treated wounds had thicker regenerated epidermis, increased number of blood vessels, and greater number of proliferating keratinocytes within the epidermis.

Conclusion: We demonstrated that a gel consisting of a combination of amnion and *Aloe vera* extract has high efficacy as a burn wound healing product. Amniotic membrane combined with the carrier *Aloe vera* in gel format is easy to produce and to apply.

Keywords: Amniotic membrane, *Aloe vera*, Angiogenesis, Burn, Epithelialization, Gel, Healing, Inflammation, Wound

* Correspondence: sikderasad@yahoo.com
[3]Institute of Tissue Banking and Biomaterial Research, Atomic Energy Research Establishment, Dhaka 1349, Bangladesh
Full list of author information is available at the end of the article

Background

Globally, burn injury is rated as the fourth frequent out of all injuries. Approximately 500,000 burn patients have to be treated in the USA each year [1]. Despite recent advances in burn wound skin management, the death rates remain high throughout the world [2] with a vast majority (eleven fold higher) in low-income countries [3]. For instance, in 2003, about 173,000 children were burned in Bangladesh where burn is the fifth leading cause of childhood illness [4]. However, in particular, peoples of rural areas are more prone to the burden of burn related mortalities and morbidities. Fast aid and swift treatment for burn patients are vital to increase the survivability by closuring and protecting the burn wounds as immediately as possible to mitigate disabilities and fatalities. In most of the developing countries, peoples would like to treat burn injuries immediately at home before going to a clinic [3]. Nevertheless, there are still lacking of a low cost and effective fast aid product to manage of burn injuries in an efficient and rapid manner [5].

Pathophysiologically, burn is considered one of the most severe types of wound as it is easily susceptible to infection due to vascular necrotic tissue and loosening of epidermal integrity [6]. Healing of wounds is a dynamic process including various overlapping phases [7] such as 'early inflammatory phase' that inhibits infection during healing as well as destroys necrotic tissue and triggers signals essential for wound repair [8], the 'proliferative phase' involves wound closure and restoration of vascular network [9] and finally the wound scar matures during the 'wound remodeling phase' [10]. Nonetheless, burn wound healing is often interrupted by excess inflammation leading to delayed healing and increased pain. Furthermore, scar tissue formation, incomplete re-epithelialization and absence of complete collagen remodeling are also hindering issues of burn healing [11, 12]. During skin wound healing two cell types, namely keratinocytes and fibroblasts, interact in the proliferative phase [9]. By a feedback loop keratinocytes and fibroblasts increase cell proliferation rate and wound contraction vigorously [13]. The immune cell- macrophages that stimulate keratinocytes and fibroblasts to release the factors for increasing angiogenesis, collagen production, and epithelialization [7]. Due to having these features, keratinocytes based burn wound healing products such as single cell keratinocyte spray solution and keratinocyte cell sheet are available in the developed world [13, 14]. In 2013, the possibility of amniotic fluid derived mesenchymal cells (AF-MSCs) as a source for cell based wound healing therapy has been reported [15, 16]. But the usefulness of these highly sophisticated and costly therapeutic products remains out of affordability for third world people.

Human amniotic membrane graft is one of the most medically accepted and widely used biomaterials in burn wound healing treatment from 1910 on [17, 18]. It acts as a scaffold for proliferation and differentiation of new epithelial cells due to presence of factors such as fibronectin, elastin, nidogen, collagen types I, III, IV, V, VI, and hyaluronic acid [19–21]. Alongside lacking of histocompatibility antigens HLA-A, B and DR [22], it possesses an anti-inflammatory effect [23]. However, the processing, transportation and storage of intact thin sheet of amniotic membrane has limited clinical applications due to associated cost. In 2017, the Atala group reported that dissolved amniotic membrane with hyaluronic acid gel can speed up the skin wound healing process [24]. Besides the human materials, plants extract are also experimented to have burn healing properties. For instance, *Aloe vera* (AV) has been used in treating burn associated wound and observed to be effective in burn wound management [25, 26]. Because of anti-inflammatory effects, AV is of high usefulness in the treatment of skin wounds and first to second degree burns [27]. Additionally, AV treatment significantly increased the collagen synthesis and remodels collagen composition (type III) to promote wound healing, contraction and the breaking strength of resulting scar tissue [28, 29]. Importantly, it has been demonstrated that AV has greater efficacy over silver sulfadiazine cream in the treatment of second-degree burns [30, 31]. In the developed world, recombinant growth factors and cellular tissue-engineered skin substitutes-based wound treatments are available and clinically practiced [32]. However, this sophisticated approach is associated with high costs for patients in the low-income countries [33]. Some reported commercial skin grafts such as integra and biobrane are available which have been shown to improve wound healing but they are also expensive and sometimes do not deliver optimal outcomes [34, 35]. Thus, there is a need for a wound healing product with high clinical efficiency, which can be used rapidly, but retains the activity of a biological treatment.

Clinically, amnion has been applied as a wound covering bioactive material to heal split thickness skin burn wounds as well as for children with partial-thickness facial burns [36, 37]. From our experience, amniotic membrane as a graft for burn wounds enclosure in Bangladesh appears to be advantageous [38]. But the limited number of membrane donors and the lack of trained personnel in amniotic graft processing are major challenges. Further, amniotic membrane grafting service is available only in city areas at a very limited scale. Other limitations including instant requirement of physicians to do the transplantation of the graft and the sheet of amnion is generally held in place with sutures or additional bandaging [24]. Considering the described

treatment limitations on the one side and the advantages of wound healing properties of human amnion and *Aloe vera* on the other side; this study aimed to develop a novel cost efficient product which in fact should be easy to produce and to store, physiologically effective and which application does not require a medic. Thus, we prepared three novel gel products from the extract of amniotic membrane (AM), *Aloe vera* (AV) and the combination (AM+AV) which were later characterized both in vitro and in vivo. We have demonstrated the usefulness of AM, AV and AM+AV gels as wound healing biomaterials which can accelerate burn wound closure through contraction, re-epithelialization, reduced inflammation and increasing angiogenesis in an animal model for skin burn.

Methods

Ethical approval

The collection and use of cesarean sections derived amniotic membrane for research and grafting purpose was approved by the ethical committee of Atomic Energy Research Establishment, and permitted by the "Human Organ / Tissue Donation and Transplantation Act, 1999" Govt. of Bangladesh. Written consent from the amniotic membrane donor was taken for amniotic membrane collection for use in research purpose. The ethics committee of Jahangirnagar University recommended and approved the animal model (Wistar Rats) for this study of skin irritation, burn induction following ARRIVE guidelines. All efforts were made to prevent any unnecessary and harmful animal handling.

Collection of placenta and preparation of human amniotic membrane

Human placenta/amniotic sacs were collected during cesarean sections and kept in 4 °C. Within 24 h we processed and prepared the membrane as described before [24, 38]. Amniotic membranes were separated carefully from chorionic membrane manually and washed with PBS (Gibco) repeatedly until a complete elimination of blood clots was achieved. After that, the whitish membranes were transferred into sterile petri dishes and frozen at subzero temperature overnight and freeze-dried (Alpha1-4LD, CHRIST, Germany) at − 55 °C for 24 h. Dried amniotic membranes were sterilized using gamma radiation at 10KGy with cobalt-60γ radiation sources. The membranes were then aseptically processed into powder form which was later used for gel preparation.

Preparation of *Aloe vera* extract

Fresh *Aloe vera* leaves were collected from the medicinal plant garden of NIB (National Institute of Biotechnology), Bangladesh by Rashedul Islam and Md Masud Rana. The plant *Aloe vera* were identified and collection of leaves kindly permitted by Md Moniruzzaman, Scientific Officer, NIB, Bangladesh. First of all, the leaves were washed with distilled water (DW) and wiped with 70% ethanol. The lower part of the leaves was cut to allow *Aloe* latex to be removed. After removal of latex, the leaves were taken into a laminar chamber and cut in equal pieces of about $4cm^2$. The leaves were merged in absolute alcohol for 5 min to further sterilize. Leaves were then peeled off and the juice was collected by scraping. Afterwards, the juice was poured into dishes and allowed to freeze; and finally freeze dried at − 55 °C for 48 h to obtain powder form. It was possible to extract 635 g juice from 1 kg of leaves which finally led to 8 g of powder.

Formulation and evaluation of physico-chemical properties of gel

From the dried amniotic membrane powder and *Aloe vera* powder, 2 gram of each sample was used for gel preparation. In total three types of gel formulations were prepared (i) AM (6% CMC-Na (Loba Chemie), 2% AM (2 g of amniotic membrane powder), 0.02% methyl paraben (SUPELCO-Sigma Aldrich), 5% glycerine (CP, China), 0.05% triethanol-amine (Merck), and DW up to 100 ml), (ii) AV (6% CMC-Na, 2% AV (2 g of *Aloe vera* powder), 0.02% methyl paraben, 5% glycerine, 0.05% triethanol-amine, and DW up to 100 ml), and (iii) AM+AV (6% CMC-Na, 1% AM (1 g of amniotic membrane powder), 1% AV (1 g of *Aloe vera* powder), 0.02% methyl paraben, 5% glycerine, 0.05% triethanol-amine, and DW up to 100 ml). The homogeneity of all formulated gels was confirmed by visual analysis. For assessing the pH of the different gel preparations, 2.5 g of each gel was dissolved in 25 ml of DW and incubated for 2 h. The measurements were done in triplicates and the average values were taken into consideration. The pH of these gels ranged from 6.5 to 6.9.

In vitro biocompatibility and cytotoxicity assay

In vitro biocompatibility and cytotoxicity test were done as described by Khan et al., (2012) [39]. To do the heparinized human blood biocompatibility assay, AM, AV and AM+AV gels were diluted with different ratios of blood. A blood sample of the same donor diluted with DW and saline water (SW) at the same ratios as done for the gels was used as a control. After an incubation time of 2 h at room temperature, the blood/gel mixtures were spread on glass slides, and observed under a light microscope for possible morphological changes in the blood cells.

In vitro cytotoxicity tests of the AM, AV and AM+AV gels were performed using the brine shrimp (*Artemia salina*) lethality bioassay method. *Artemia salina* eggs were hatched in a 1 L conical flask, filled with sterile artificial sea water (pH = 8.5) and constant aeration for

48 h. After hatching, active nauplii free from egg shells were collected and used for the assay. All three gels were dissolved in artificial seawater at 2.0, 1.0, 0.75, 0.50, and 0.25 mg/mL concentration in petri dishes in which the active nauplii were inoculated. After overnight incubation, the viability of the nauplii was counted. Artificial sea water without additions served as negative control and 0.50 mg/mL of vincristine sulfate (Sigma) was considered as positive control.

Human skin cell biocompatibility tests were performed by exposing HaCaT cells (CLS Heidelberg, Germany) for 48 h in the specific culture medium containing the formulated gels at distinct concentrations. Cells were cultured in DMEM (Gibco/Life Technologies) with 10% Fetal Bovine Serum (FBS) (Gibco/Life Technologies) and 1% Penicillin/Streptomycin (Gibco) at 37 °C in 5%CO_2. These tests resulted in an optimal gel concentration of 500 μg/mL.

In vitro cell attachment and proliferating assay

For cell attachment study, 50 thousand of human keratinocytes (HaCaT) and human fibroblast (HFF1 cell line (ATCC; SCRC-1041)) cells were seeded in 2 ml media containing the previously prepared gels at a concentration of 500 μg/mL. The cells were allowed to attach to the culture dish undisturbed for 2, 4, 6, and 8 h in case of HFF1; for 3, 6, 9 and 12 h in case of HaCaT, respectively. At each time interval microscopic images were taken to evaluate the attachment rate of the cells in the different conditions. To assess the proliferation of HaCaT and HFF1, equal numbers of cells were expanded on plates in the media containing AM, AV and AM+AV gels. The images were taken from day 2 to day 6 to visualize the proliferation of the cells. Media were replaced every other day.

In vitro wound healing scratch assay

The scratch assay was performed as described by D'Agostino and co-workers to study cell migration and to determine the time period required for wound closure in vitro [40] in presence of the three gel formulations (500 mg/mL). When cells attained 95–100% confluency, HaCaT and HFF1 were serum starved for 24 h before initiation of the scratch wound. Scratch wounds were created in confluent cell monolayers using a sterile p200 pipette tip ensuring that each wound had the same dimensions. After that, the cells which were detached by this process were removed from the culture dish by three times washing with PBS. Cell migration and wound closure were observed at 0 h, 18 h and 30 h and images were taken by light microscopy.

In vivo irritability study

To assess in vivo irritability and applicability of the gels, the dorsal skin hairs of female Wistar rats were shaved on the date of experiment [41]. Total 12 animals were experimented and randomly were assigned to three groups (AM, AV and AM+AV). The animals were treated with 1 ml gel daily up to 7 days and finally the treated skin was visually examined for erythema and edema.

Rat model for artificial burn induction, re-epithelization and wound contraction

In total 40 healthy female Wistar rats of 180–200 g body weight were used in this study and randomly assigned into four experimental groups (control/no gel, treated with AV, treated with AM and treated with AM+AV). All animals received human care according to the guideline for the care and use of laboratory animals published by NIH. Rats were fed a standard rat chow and tap water ad libitum. The rats were kept in the animal quarter at a temperature of 25 ± 2 °C, humidity 50–55% and with 14 h light/10 h dark cycles. Each rat was anesthetized with Ketamine HCl solution (Gonoshasthaya Pharmaceuticals Ltd., Bangladesh) of 100 mg/Kg body weight by intra peritoneal injection. Subsequently, the hair at dorsal region was trimmed using electric hair clipper and then shaved with sharp blade. The shaved areas were cleansed with alcohol swab.

Burns were created using a piece of aluminum (981.875mm^2) heated to 100 °C for 5mins which was applied for 15 s on the shaved area of rats [42]. The animals were treated with 1 ml of the distinct gel on daily basis, topically, for a period of 30 days. Re-epithelization was monitored by recording the number of days required for crust to fall away, leaving no raw wound behind [43]. To monitor wound contraction, progressive changes in wound area were measured. Using the formula [42] below, the percentage of wound contraction was calculated on the respective day.

$$\%\ Wound\ Contraction = ((Initial\ Wound\ Size – Final\ Wound\ Size)/Initial\ Wound\ Size) \times 100$$

At the specific days, the gel treated and non-treated animals were anesthetized by intraperitoneally administration of 100 mg/kg ketamine, skin tissue/biopsy were taken and finally rats were sacrificed by cervical dislocation. Skin tissues were collected for histopathological analysis.

Histology of skin: hematoxylin and eosin (H&E) staining

Skin specimens from each group were collected on the 6th, 12th, 18th, 24th, and 30th day after burn induction.

Skin biopsies were embedded in paraffin blocks after overnight fixation in 10% formal saline solution. Embedded skin tissues were cut into sections of 5 μm thickness using a microtome (Leica, RM 2125 RTS, USA) and collected on glass slides. Afterwards, the sections were deparaffinized and stained with H&E. The stained histological sections were examined and evaluated in random order. Images were taken with Optika B-350 light microscope. A score of 0–3 was given to each section according to presence of inflammatory cells and levels of angiogenesis and epithelialization as previously described by Sedighi et al., 2016 [44] and Kulac et al., 2013 [45] with minimal modifications (Table 1).

Statistical analysis

All statistical analyses were calculated by one way independent test using SPSS (SPSS version 22.0, SPSS Inc., Chicago, IL, USA). All quantitative data were presented in this study including mean (±) standard deviations (SD). $P < 0.05$ was considered as statistically significant.

Results

Preparation and physico-chemical properties of gel

Donated full term human placentas were collected during cesarean sections, the erythrocytes were depleted and the amnion was separated (Fig. 1a1-a6) for further processing. Afterwards, amniotic membranes were lyophilized, gamma irradiated, blended and finally freeze-dried to obtain powder (Fig. 1a7-a9). The juice of fresh *Aloe vera* leaves was collected and freeze-dried to extract powder for further use (Fig. 1b1-b2).

The obtained amnion (AM) and *Aloe vera* (AV) powders were used to formulate the 2% gels (AM, AV and AM+AV) as described in methods section. The pH of all three gel formulations was measured and ranged from 6.5 to 6.9 (AM 6.7, AV 6.5 and AM+AV 6.9). All formulated gels were found to be semi-solid and homogeneous in nature. The color of the AV gel was off-white while the AM and AM+AV gels were yellowish white whereas all gels were semi-transparent (Fig. 1a10, b3, c).

In vitro biocompatibility and cytotoxicity analysis

Upon incubation of human blood with gel samples (2:1 ratio), red blood cells (RBCs) were observed to be intact (Fig. 2a1-a3). Normal saline (SW) also showed similar results (Fig. 2a5) whereas DW caused RBC lysis (Fig. 2a4).

Brine shrimp lethality bioassay method was used to evaluate the in vitro cytotoxic effect of the formulated AM, AV and AM+AV gels (Fig. 2a6). A concentration of 0.25 mg/ml did not affect the viability. At a concentration of 0.5 mg/ml and 0.75 mg/ml, the mortality rate of the nauplii was 1%. Increasing the concentration (2 mg/ml) of gels led to an increase in mortality rate to 3–4% (Fig. 2a6).

Keratinocytes (HaCaT) and fibroblasts (HFF1) play important roles in the skin tissue during wound healing processes. Therefore, we tested biocompatibility of AM+AV gels on HaCaT cells at concentrations of 50-500 μg/mL (Fig. 2b1-b4) and could not observe any difference in cell viability. The concentration of 500 μg/mL was also observed to be compatible for human fetal foreskin derived fibroblast (HFF1) cells when cultured in presence of AM+AV (Fig. 2b5). Together with the previous results we observed 500 μg /mL concentration (Fig. 2b4) as an optimum gel concentration for in vitro use which was further confirmed for the compatibility of AV as well as AM gels (Fig. 2c1-c3).

Attachment and proliferation of HaCaT and HFF1 cells in vitro

The time required for the attachment of HaCaT and HFF1 in presence of the three different types of gel (AM, AV, AM+AV) was evaluated. No effects on HFF1 cell attachment within the first 2 h were noted in presence of AV and AM gels compared to control media (Fig. 3a1-a3). But HFF1 in AM+AV gel containing media showed a better attachment rate within the first 2 h (Fig. 3a4). At six to 8 hours of culture duration, it was visually observed that the HFF1 attachment rate in the AM+AV condition was approximately 1.5 fold higher (Fig. 3a12, a16) than in the other conditions.

Table 1 Histological scoring parameter of epithelialization, angiogenesis, granulation tissue formation, and inflammatory cells

Parameter/Score	0	1	2	3
Inflammatory cells	1–5 inflammatory cells per histological field	5–8 inflammatory cells per histological field	8–11 inflammatory cells per histological field	11–15 inflammatory cells per histological field
Epithelialization	Absence of epithelial proliferation in ≥70% of tissue	Incomplete epidermal organization in ≥50% of tissue	Moderate epithelial proliferation in ≥60% of tissue	Complete epidermal remodeling in ≥80% of tissue
Angiogenesis	Absence of angiogenesis including congestion and hemorrhage	2–4 vessel per site, congestion and hemorrhage	4–6 vessel per site, slight congestion	7–8 vessel per site vertically disposed towards the epithelial surface
Granulation Tissue	None, completely disorganized and distorted	Minimal/immature thin	Mild/moderately mature granule layer	Evident/ Thick, ≥80% organized

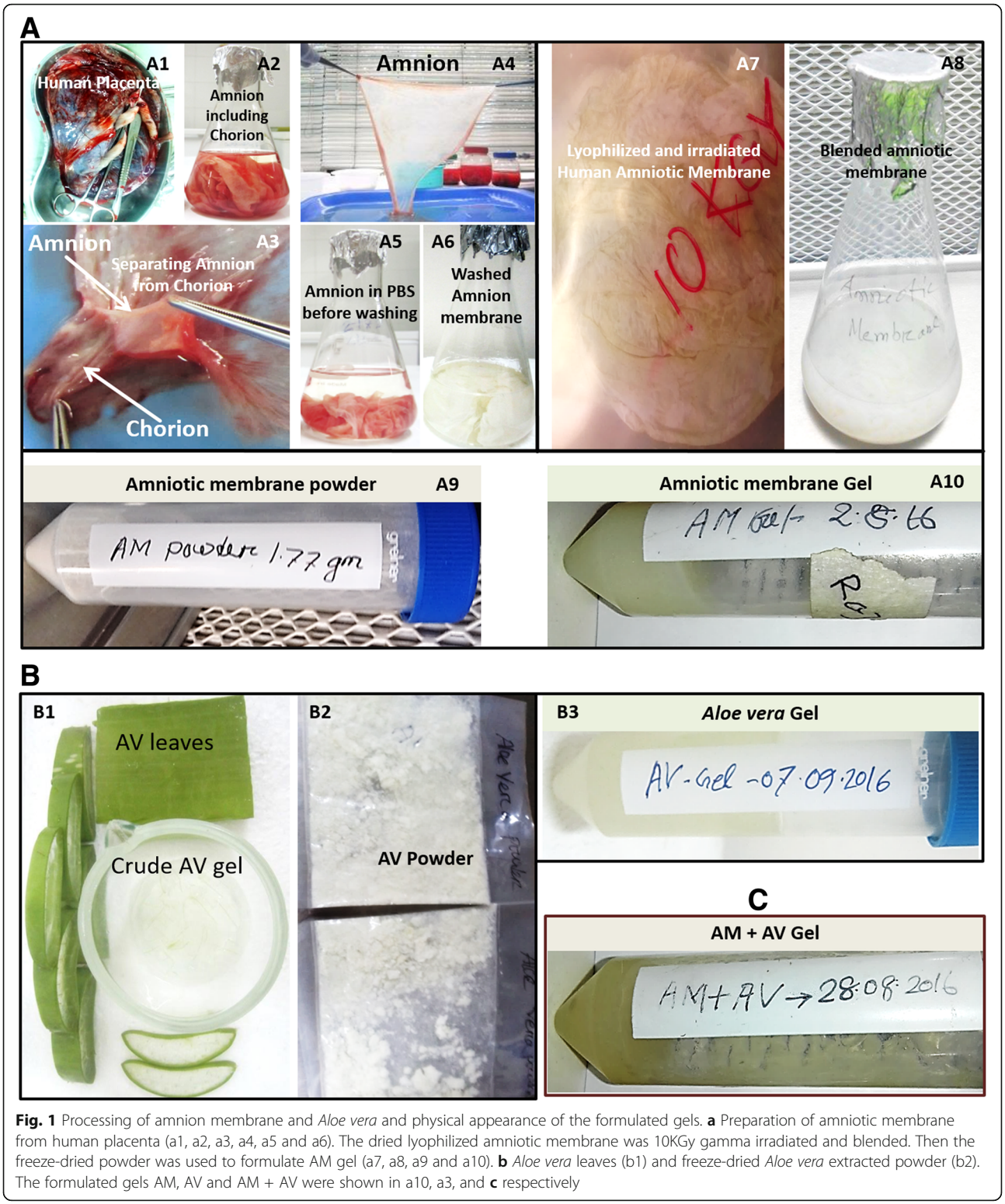

Fig. 1 Processing of amnion membrane and *Aloe vera* and physical appearance of the formulated gels. **a** Preparation of amniotic membrane from human placenta (a1, a2, a3, a4, a5 and a6). The dried lyophilized amniotic membrane was 10KGy gamma irradiated and blended. Then the freeze-dried powder was used to formulate AM gel (a7, a8, a9 and a10). **b** *Aloe vera* leaves (b1) and freeze-dried *Aloe vera* extracted powder (b2). The formulated gels AM, AV and AM + AV were shown in a10, a3, and **c** respectively

However, HaCaT cells took at least 3 h to attach on culture dish in presence of the gels (AM, AV, AM+AV) in media at the concentration of 500 μg/mL (Fig. 3b1-b4). The HaCaT cell attachment rates were significantly higher when we applied AM and AM+AV gel in the culture media (Fig. 3b2, b6, b10; Fig. 3b4, b8, b12). In case of AV, we did not observe any difference between media alone and media with AV at various time points (Fig. 3b1, b3;

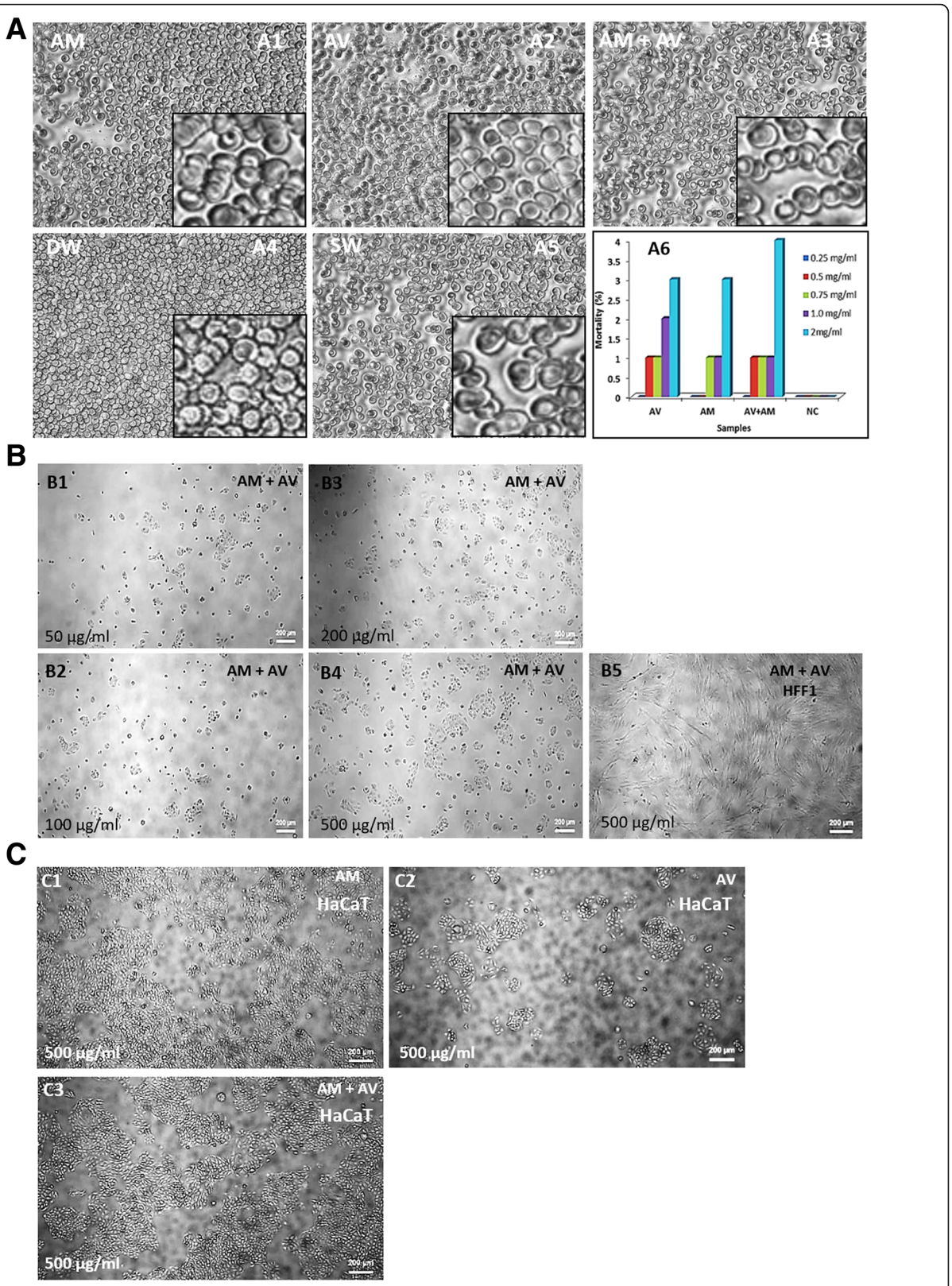

Fig. 2 Heparinized human blood biocompatibility (**a**), brine shrimp lethality bioassay (a6); HaCaT and HFF1 cells compatibility with gels (**b** and **c**). RBC morphology of heparinized blood incubated with AM (a1), AV (a2), AM+AV (a3), DW (a4) and SW (a5). a6 diagram shows the mortality percentages of brine shrimp (*A. salina*). 500 µg/mL was shown to be suitable for HaCaT and HFF1 cells in vitro (**b** and **c**)

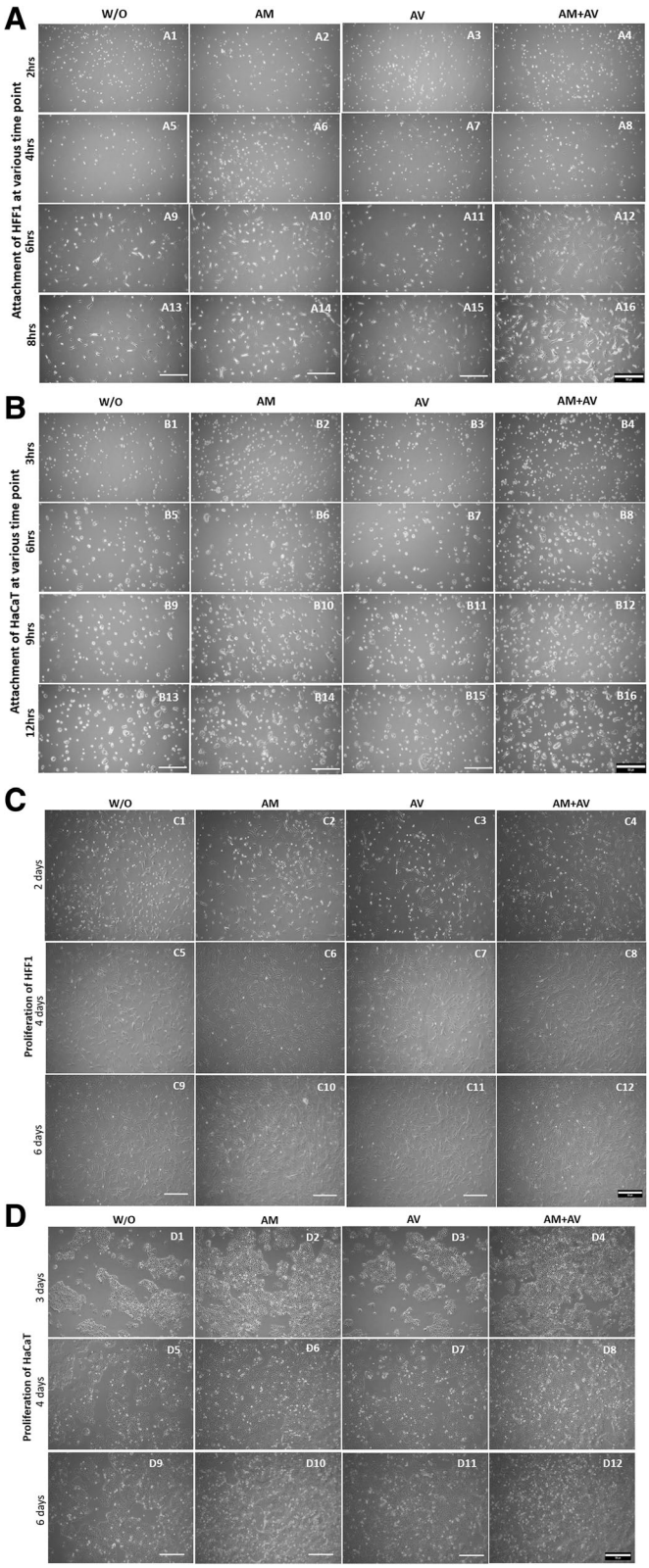

Fig. 3 Representative microscopic images for HFF1 and HaCaT cell attachment and proliferation. **a** HFF1 cells (2 h to 8 h) and (**b**) HaCaT cells (3 h to 12 h) attachment test. **c** Proliferation tests of HFF1 for 2, 4, and 6 days. **d** The proliferation of HaCaT from day 3 to day 6 in media with and without gels

Fig. 3b5, b7; Fig. 3b9, b11; Fig. 3b13, b15). Beside the cell attachment study, we also qualitatively examined the proliferation of HFF1 and HaCaT when incubated with the gels from day two to day six. We did not observe any significant effect of the gels on the proliferation of HFF1 cells during the examination periods (Fig. 3c1-c12). However, media with AM and AV + AM gels were noticed to increase the proliferation rate of HaCaT cells two fold (Fig. 3d1-d12).

In vitro wound healing and in vivo irritability study of the gels

The in vitro scratch assay was performed to measure cell migration in the scratching zone. Consequently, we wanted to detect whether these formulated gels (concentration 500 μg/mL) can promote the rate of wound healing in human keratinocytes (HaCaT) and fibroblasts (HFF1) via scratch assays. The cells were serum starved for at least 24 h before producing the scratch wound. Thus, the cells' ability to proliferate was inhibited, and it was assured that wound closure was only due to cell migration. Our result showed that the healing velocity of HaCaT and HFF1 with AM and AM+AV gel treatment was higher than for untreated cells and AV treated (Fig. 4a, b). HaCaT cells filled the scratch area faster when compared to HFF1 after 30 h.

To analyze the applicability and irritability of the prepared gel, skin irritation assay were performed applying a rat model. After topical application of all gels for a period of 7 days, it was observed that the gel did not induce any edema or erythema (Fig. 4c). This result indicated the safety of gels to be applied topically. We also observed that the hair formation was also normal compared to non-treated rats.

Macroscopic evaluation of wound closure and quantitative measurement of wound contraction and re-epithelialization

After few hours of the second degree burn induction, the rats were restless indicating the pain. No bubbles were observed on the burn area, however, it was noticed that white color burn damaged the skin barrier. Subsequently, hyperemia occurred into the damaged tissue area. After treating the rats with gels at day one, within few hours, white color burn turned into a fully hyperemic zone in each group which indicated the presence of red blood cells undergoing extravasation (Fig. 5a, day 0 panel). At day six, all groups showed the presence of thick dry crusts but the group treated with AM+AV gel had a slightly wet crust (Fig. 5a day 6 panel). Edges of crust were found to be partially detached. At 12 days after burn induction, control group showed discrete detachment of crust while other treatment groups showed continuous detachment of edges. In this stage of injury staining of crusts were almost same. As the full burn wound was covered with crust scar tissue was not observed until the 12th day (Fig. 5a, day 12 panel). On day 18, scar tissue became clearly visible in the edges of the wounds in each group and contractions were clearly visible (Fig. 5a, day 18 panel). At day 24, crusts disappeared from all groups and scar tissue became clearly visible. The AV treated group showed faster healing but this group left more scar tissue than AM and control groups (Fig. 5a, day 24 panel). Re-epithelialization had been completed in all treatment groups leaving scar tissues after 4 weeks (Fig. 5a, day 30 panel). Macroscopically, the AV group showed a better healing rate but included more scar tissue while other groups showed less healing rate than the AV group with minimal scar formation.

However, a variation in wound contraction rates were noticed from group to group (Fig. 5b1, b2). At day 6, the AV treated group showed significantly ($P < 0.001$) better healing rate which was two folds higher than in the other groups. The healing rate of the AM treated group was also found to be significantly increased ($P < 0.01$) when compared to AM+AV ($P > 0.05$). Twelve days post burning, the control group had the lowest healing rate (34.93%) whereas AV treated group wound healing was about 50% ($P < 0.01$). At the same time point, the healing rate of the AM treated group was 47.22% ($P < 0.01$) and of the AM+AV 48.08% of the wound were found to be healed ($P < 0.05$) (Fig. 5b1, b2). On the 18th day, AV treated group reached a healing rate of 76.6% ($P < 0.001$) . It was observed that the wound healing rate of the AM+AV group (73%) was better than in the AM treated group (67%). But, statistical evaluation showed a higher significance in the AM treated group ($P < 0.01$) in comparison with AM+AV ($P < 0.05$). At day 24, the percent of wound contraction in the AV group also showed better results compared with the other two groups. Interestingly, wounds from the AV group were demonstrated to be healed about 95% ($P < 0.001$) whereas the control group showed a healing of 80%. Nevertheless, AM treated and AM+AV treated wound recovery rate were 87 and 90% respectively with $P < 0.05$ (Fig. 5b1, b2).

Average re-epithelialization period in all groups were observed (Fig. 5c). In AV treated animals mean epithelialization was visualized within 27 days of post burning, control group required at least 32.5 days. The re-epithelialization period of AM and AM+AV treated rats took 30 and 29 days, respectively. However, both AV and AM+AV groups were statistically significant ($P < 0.001$) (Fig. 5c).

Histological analysis in terms of skin tissue organization, angiogenesis, and re-epithelialization

Figure 6a shows representative photomicrograph of skin sections stained with H&E from all groups. The comparison of angiogenesis, inflammation score and

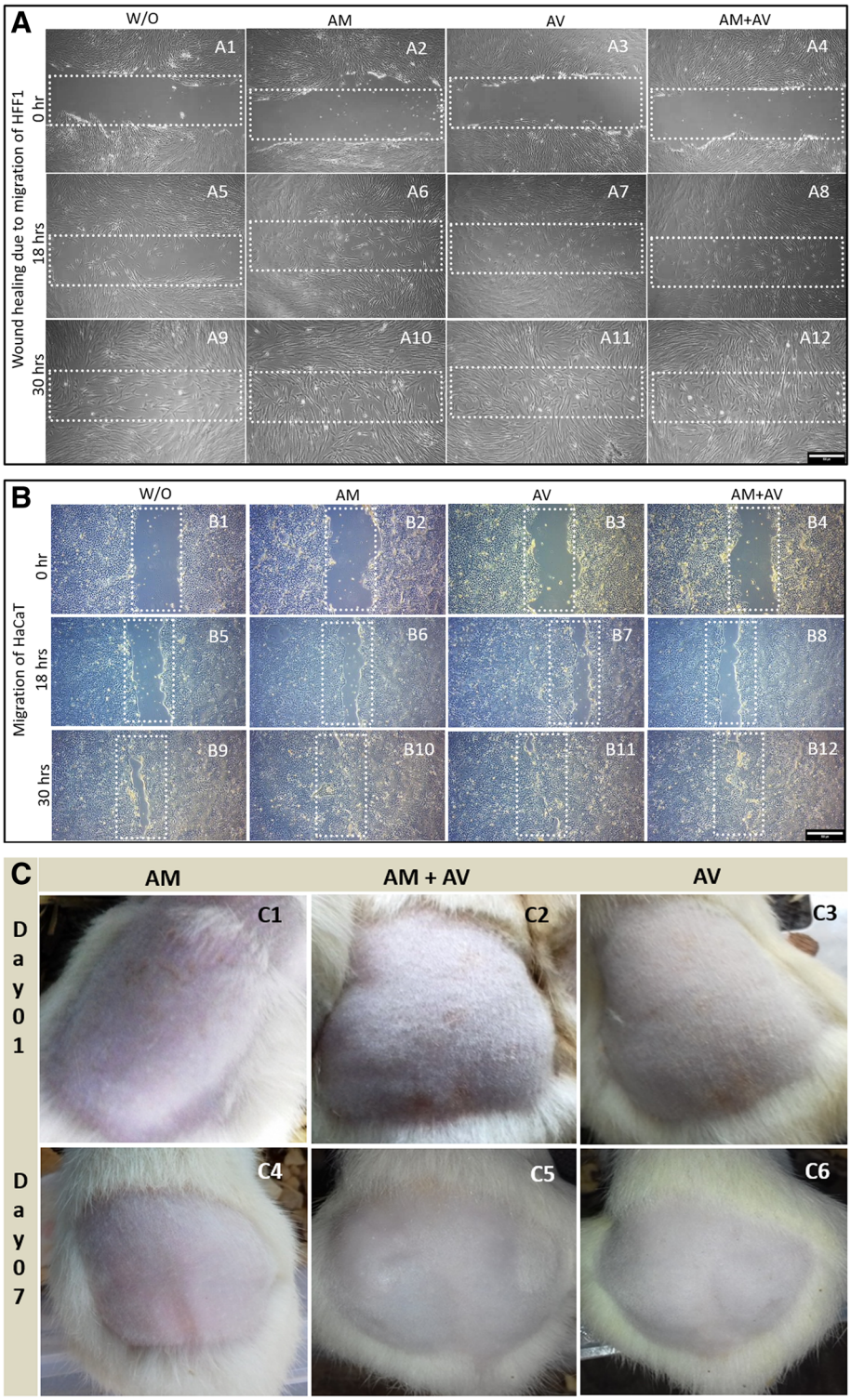

Fig. 4 In vitro wound healing and in vivo skin irritation study. **a** Migration of HFF1 cells to close the wound area. **b** The HaCaT cell migration to fill the scratch zone in presence of the three different gels in the cell culture media whereas cell culture medium without gels served as the negative control. **c** Topical application of the gels for irritation assay on shaved rats, which were observed from day 0 to day 7

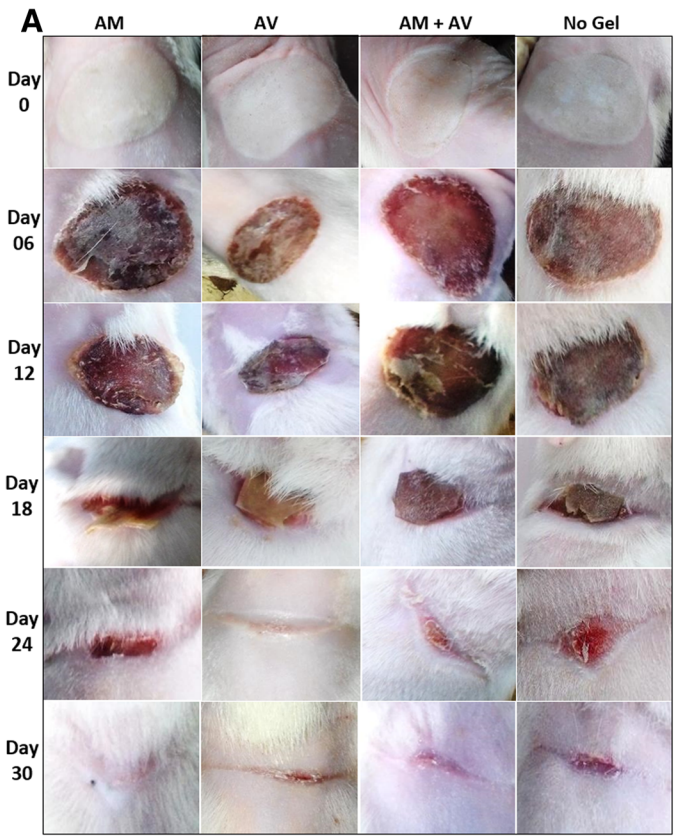

B

B1

Percentage of wound contraction at respective day ± Standard deviation				
Group	Day 6	Day 12	Day 18	Day 24
control	14.8±.0.77	34.93±4.48	59.8±2.4	80.15±2.80
AM	16.37±1.04	47.22±6.6	67.36±4.83	87.52±5.40
AV	34.37±5.31	52.95±12.06	76.6±5.61	95.64±1.99
AM+AV	15.78±1.77	48.08.±13.76	73.02±10.92	90.912±7.30

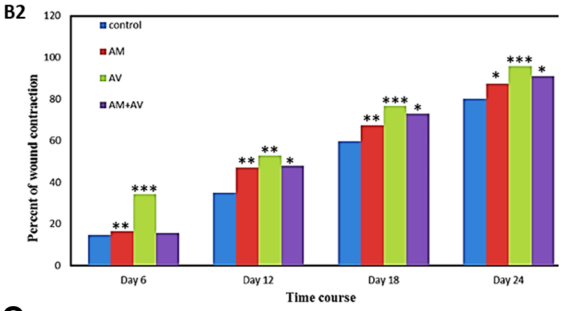

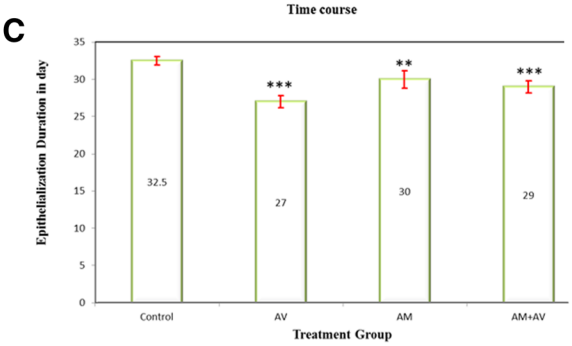

Fig. 5 Evaluation of wound closure, measurement of wound contraction and re-epithelialization. **a** Macroscopic wound healing images of Wistar rats at day 0, 6, 12, 18, 24 and 30 which were treated with AM, AV, AM+AV gel or without any gel (control). **b** Clinical evaluation of wound healing regarding wound contraction in rats at day 6, 12, 18, 24 (b1) and (b2) (level of significant was set * $P < 0.05$, ** $P < 0.01$ and *** $P < 0.001$). **c** Epithelialization period in different groups (*$P < 0.05$, ** $P < 0.01$ and *** $P < 0.001$)

re-epithelialization along with treatment duration between all experimental groups are presented in Fig. 6b, c and d. At day 6, coagulative necrosis was identified including damage of dermal and epidermal layer (Fig. 6a1-a4). Remarkably, inflammatory cells in the wound area were increased in all groups. Highest infiltrations of inflammatory cells were detected in non-treated rats, and AM treated animals showed the lowest infiltration (Fig. 6c). In the AV and AM+AV group moderate numbers of inflammatory cells were observed (Fig. 6a3, a4).

Within the first few days no significant difference in angiogenesis score was observed amongst the groups (Fig. 6a1-a4, 6d). However, AM and AM+AV gel treated skin were shown to have appearance of more neovascularization (Fig. 6a5-a20) with time. On the 12th day post burning, all treated groups appeared to have induced neo-epithelialization, in contrast to the control (Fig. 6a5-a8, 6b). At day 18, neo-epithelization was clearly visible with incomplete epidermal and dermal layer (Fig. 6a9-a12, 6b).

After 18 days, the number of inflammatory cells was also reduced significantly in AM and AV treated groups. But, in AM+AV treated group the inflammatory score was increased in a significant amount ($P < 0.05$); even higher than in the control group (Fig. 6c). Angiogenesis was significantly increased in each group ($P < 0.05$) at day 18 post burning (Fig. 6d) compared to control.

The H&E stained skin section of day 24 showed an increase in epithelialization level (Fig. 6a13-a16). Epithelialization score was found to be significantly increased in each treatment group compared to the control group. Among treated groups, AM+AV had a higher epithelialization ($P < 0.05$) rate than AV (Fig. 6b). However, at this stage inflammation in AM+AV treated group increased again, while other treatment groups showed reduced inflammation (Fig. 6c). At day 24, angiogenesis in the AV group ($P < 0.05$), was higher than in the AM and the AM+AV group (Fig. 6d) but all groups showed elevated levels than the control.

H&E stained skin biopsies on the 30th day of treatment displayed maximum epithelialization in the AM+AV group including more inflammatory cells (Fig. 6a17-a20, 6b, 6c). Moreover, angiogenesis was also increased in AM and AM+AV group compared to control (Fig. 6d).

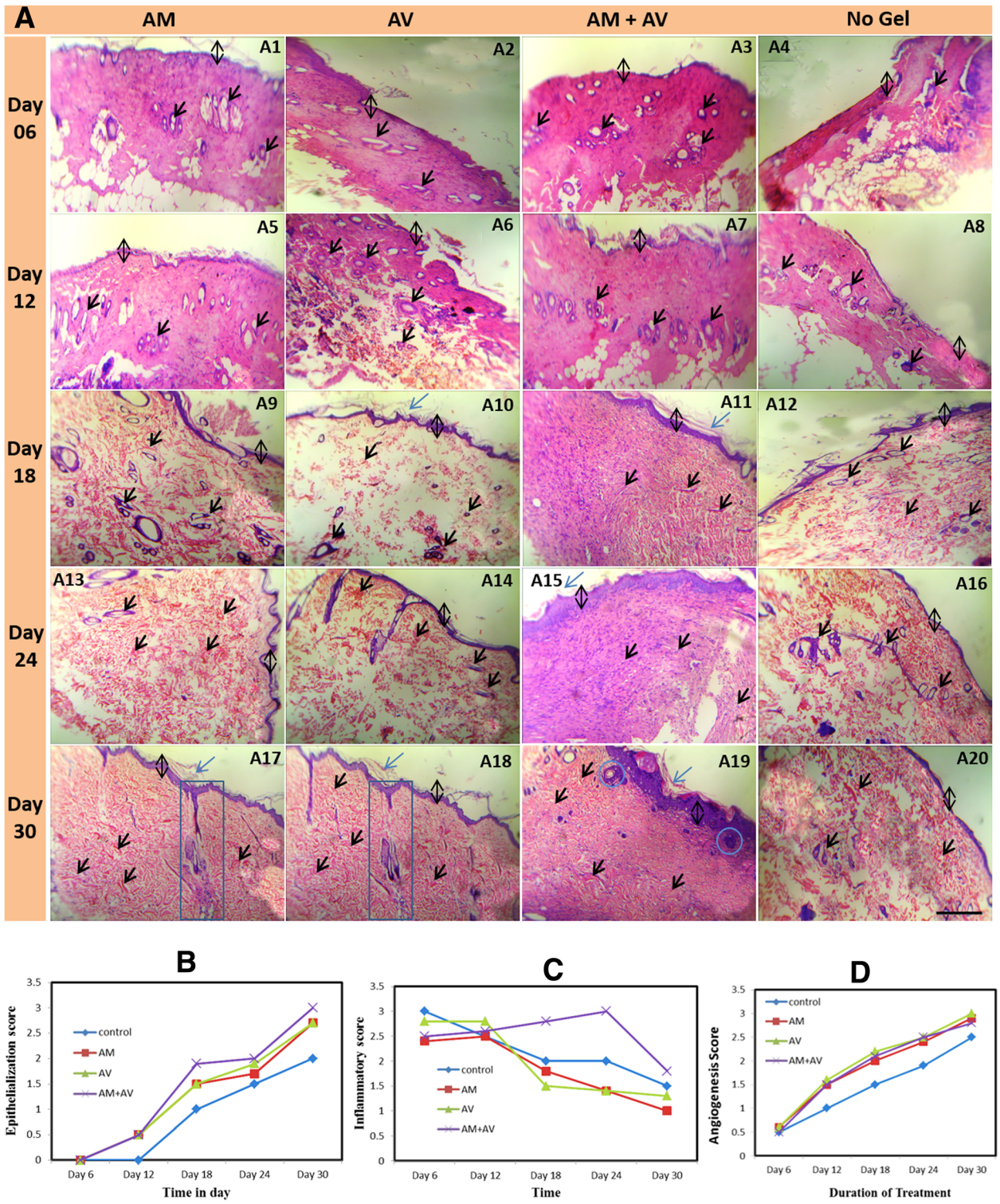

Fig. 6 Haematoxylin and Eosin (H&E) staining of skin at different time points during the gel-based treatment (**a**). Stained images (100x magnification) were shown for all four groups (AM, AV, AM+AV, and non-treated control) at day 6 (a1-a4), 12 (a5-a8), 18 (a9-a12), 24 (a13-a16) and 30 (a17-a20). Re-epithelialization (**b**), inflammatory (**c**), and angiogenesis (**d**) scoring from the images represents a qualitative and quantitative assessment of healing. Black double headed arrow represents the thickness of epidermis; single headed blue arrow shows the keratinized zone of skin, single headed black arrow projects the blood vessel, formation of new glands beneath the epidermis is shown in blue box (a17, a18), and inside the blue round box (a19) some basal keratinocytes were shown

Discussion

Beside active ingredients, the applicability of burn wound healing gel is dependent on the properties such as pH, appearance, homogeneity, and viscosity. Carbopol is a widely used gelling agent for producing burn-healing gels for skin application. CMC-Na salt is another agent used alongside with carbopol [46]. However, in this study the gel was prepared from human amniotic membrane extract (AM), *Aloe vera* extracts (AV), and a combination of both AM+AV using 6% CMC-Na salt as a gelling agent. Extensive studies confirm the effectiveness and safety of lyophilized amnion as a wound dressing and grafting materials for promoting the healing process and preventing infections [47]. Khorasani et al., (2009) reported that AV cream or gel could be more effective than silver sulfadiazine cream in treating burn wound healing [30]. The end products (gels) in all three conditions evaluated in this study were homogenous, granule less and of a whitish creamy color (Fig. 1a10, 1b3, 1c). In addition, pH of all formulations ranged between 6.5–6.9, and this pH does not interfere with skin physiology [48]. Erythema and edema are the common symptoms of skin irritation which lasts for three to 7 days [49]. Our formulated gels did not induce any irritation including no erythema or edema on rat skin upon topical application for a period of 7 days (Fig. 4c). Thus, CMC-Na salt, AM and AV extract formulated gel could be useful as wound healing gel as the gels have good spreadability and consistency. In vitro and in vivo studies clearly and collectively demonstrated the potentials of the formulated gels from amnion when combined with *Aloe vera*. In this preliminary research, we found that the formulated gels can induce and accelerate the proliferation and attachment of HaCaT and HFF1 cells (Fig. 3), and promote wound healing in vitro (Fig. 4a, b) [50]. Amnion has been reported to facilitate the migration of epithelial cells, reinforces attachment, and promotes proliferation [51].

Macroscopic morphological analysis demonstrated the gel-based acceleration of re-epithelialization and wound contraction in vivo (Fig. 5a, b, c). Microscopic observation of AM+AV gel treated tissue sections allowed us to appreciate the effectiveness of the formulated gel in regard to epidermis and dermis formation and the thickness of epidermis (Fig. 6a). In present study, we observed that upon completion of wound healing few scar tissues remained in all treated rats. Scar formation in all kinds of wound healing are normal [52] and exist even after complete healing. However, the AM treated experimental group had the lowest scar formation. Regardless of the variation in treatment procedures, second degree burn required 25–35 days to heal completely [53]. Due to presence of anti-inflammatory characteristics [23, 44], amniotic gel treated rats had lower inflammation than AV and AM+AV (Fig. 6c). Inflammation is an early stage event for burn healing which should be decreased within a certain healing period [54]. During wound healing, at early phases inflammatory cells increased but in later stages decreased gradually due to granulation, the formation of new capillaries, and deposition of collagen [2]. Excluding collagen level determination, other incidences are similar to our study [55]. Histological analysis revealed that the AM+AV group had a higher epithelialization rate apart from inflammation (Fig. 6a19, 6b). Wound healing is related to wound contraction and wound re-epithelialization [56] which has been shown for gel treatment in a mouse model [50].

Angiogenesis is another important event in burn healing where endothelial cells' proliferation rate in the wound area is rapidly increased after burning to form blood vessels. Hamid and Soliman (2015) reported that AV can increase angiogenesis [2] for a better supply with nutrients and oxygen because of acemannan in AV [57]. Histologically, AM, AV and AM+AV treated wounds had increased numbers of blood vessels, particularly small and newly formed (Fig. 6a17-a19, 6d). Besides supporting in vitro keratinocyte proliferation, we also observed some proliferating basal keratinocytes in vivo residing in the intermediate zone of the epidermis and dermis (Fig. 6a19). These properties of the tested gels could be explained by the presence of stimulatory factors in amniotic membrane which also been supported from the results of Murphy et al. (2017) [24].

Amniotic membrane has been reported to provide a niche for the cells to adhere, grow, proliferate, migrate and differentiate, and could possibly contribute to the production of angiogenic micro-environment indirectly which allows AM to improve burn healing [58]. We found that a combination of both AM and AV synergistically improved epithelialization. On day 30, epithelialization profile was significantly higher in the AM+AV group. Amniotic membrane is composed of collagen type IV, V and VII which promotes growth of epithelial cells, facilitates epithelial cell migration, strengthens basal epithelial cell adhesion, promotes differentiation of epithelial cell, and prevents apoptotic cell death [59]. In principal, we have prepared gels from medically discarded materials, at low cost that provides excellent burn wound coverage. These formulated gels showed potential to be used as fast aid ointment in burn wound management. Although we demonstrated significant improvement of burn wound healing in rats treated with AM+AV gel, however, some limitations are associated with this animal model such as the remarkable native regeneration potential of the rat skin. For future application, it would be crucial to identify the key factors in the amnion that are responsible for the acceleration of the wound healing process.

Conclusion

Taken together the in vitro and in vivo data, our findings clearly demonstrate that amniotic membrane combined with *Aloe vera* extract significantly enhances burn wound healing, thus indicating that the amniotic membrane and *Aloe vera* possesses potent wound healing activities. Amniotic membrane is a globally accepted biological biomaterial for second and third degree burn. *Aloe vera* gel has been reported to have burn healing capacity as well. The combination of both AM and AV has been shown to have promising effect in internal epithelialization with less scar formation. Gels containing AM extract individually and in combination with AV could be used alternatively in the treatment of burn. However, further investigation is required to assess optimal concentration of the used extracts and key factors present in AM and AV to find out the best combination for burn healing. Moreover, it is also of great importance to unfold the underlying molecular mechanisms. As a further investigation step, cell based therapies using skin progenitor cells in combination with the tested gels, could be another way to accelerate wound healing.

Abbreviations

AM: Amniotic membrane; AV: *Aloe vera*; CMC-Na: Sodium carboxymethyl cellulose; C-sections: Caesarean sections; H&E: Hematoxylin and eosin; HaCaT: (Ha = human adult, Ca = calcium, T = temperature); HCl: Hydrogen chloride; HFF1: Human foreskin fibroblast 1; HLA: Human leukocyte antigens; HLA-DR: Human leukocyte antigen – antigen D related; KGy: Kilo gray; PBS: Phosphate buffer saline; SD: Standard deviations

Acknowledgements

The authors acknowledge the technical support from Institute of Tissue Banking and Biomaterial Research (ITBBR), Atomic Energy Research Establishment (AERE) and Animal facilities from Dept. of Pharmacy, Jahangirnagar University, Bangladesh. Dr. SM Asaduzzaman acknowledges the support from Govt. of Bangladesh, International Atomic Energy Agency (IAEA) and the technical supports from Prof. Dr. Shahadath and Dr. Matin throughout the work. Prof. Dr. Adjaye acknowledges the support from the Medical Faculty, Heinrich-Heine-University, Düsseldorf, Germany. In addition, Prof. Dr. Adjaye and Md Shaifur Rahman acknowledge support from the German Academic Exchange Service (DAAD-91607303).

Authors' contributions

MSR^1 and MSR^2 conceived the idea. MSR^1, RI, and MSR^2 designed the experiment. MSR^1, MMR, LSS and RI performed the experimental work and analysis the data. MSR^1 and RI wrote the initial draft and SMA, MSR^2, LSS, JA edited the manuscript. SMA and MSR^2 supervised the work from start to end. JA supervised the in vitro study. All authors read and approved the final manuscript.

Funding

For the purchasing of lab instruments and reagents, funds had been provided by ADP Govt. of Bangladesh and International Atomic Energy Agency. RI was supported from the NSICT Fellowship, MoST, Govt. of Bangladesh. MSR^1 was supported by DAAD-91607303, Germany. No funding has been provided for publication charge. Funding agency did not have any contribution on experimental idea, design, work, manuscript writing, and publication.

Availability of data and materials

The data and materials have been presented in the main manuscript and can be given upon request.

Ethics approval and consent to participate

The study was conducted according to the protocol approved by the ethical committee of the Atomic Energy Research Establishment and Jahangirnagar University, Bangladesh. The research work on/with human organ, tissue, and cell has been permitted in Institute of Tissue Banking and Biomaterial Research under the Human Organ / Tissue Donation and Transplantation Act, 1999, Govt. of Bangladesh. Post delivered amniotic membrane was collected for research purpose with the written consent from the healthy donor.

Consent for publication

Not Applicable.

Competing interests

The authors declare that they have no competing interest.

Author details

[1]Institute for Stem Cell Research and Regenerative Medicine, Medical Faculty, Heinrich Heine University, 40225 Düsseldorf, Germany. [2]Bio-resource Technology and Industrial Biotechnology Laboratory, Department of Biotechnology and Genetic Engineering, Jahangirnagar University, Dhaka 1342, Bangladesh. [3]Institute of Tissue Banking and Biomaterial Research, Atomic Energy Research Establishment, Dhaka 1349, Bangladesh.

Received: 1 September 2017 Accepted: 17 May 2019
Published online: 03 June 2019

References

1. Miller SF, Bessey P, Lentz CW, Jeng JC, Schurr M, Browning S. ABA NBR committee. National burn repository 2007 report: a synopsis of the 2007 call for data. J Burn Care Res. 2008;29:862–70.
2. Hamid AAA, Soliman MF. Effect of topical *Aloe vera* on the process of healing of full-thickness skin burn: a histological and immunohistochemical study. J of Histology and Histopathology. 2015;2:3.
3. He S, Alonge O, Agrawal P, et al. Epidemiology of burns in rural Bangladesh: an update. tchounwou PB edt. Int. J. Environ. Res. Public Health. 2017;14:381.
4. Mashreky SR, Rahman A, Chowdhury SM, Giashuddin S, SvanstrOm L, Linnan M, Shafinaz S, Uhaa IJ, Rahman F. Epidemiology of childhood burn: yield of largest community based injury survey in Bangladesh. Burns. 2008;34:856–62.
5. Atiyeh B, Masellis A, Conte C. Optimizing burn treatment in developing low- and middle-income countries with limited health care resources (part 1). Ann Burns Fire Disasters. 2009;22:121–5.
6. Tehrani S, Lotfi P, Tehrani S, et al. Healing effect of sesame ointment on second-degree burn wound in rats. Galen Medical J. 2016;5:56–62.
7. Gurtner GC, Werner S, Barrandon Y, Longaker MT. Wound repair and regeneration. Nature. 2008;453:314–21.
8. Tiwari VK. Burn wound: how it differs from other wounds? Indian J of Plastic Surgery. 2012;45:364.
9. Werner S, Krieg T, Smola H. Keratinocyte–fibroblast interactions in wound healing. J of Invest Dermatol. 2007;127(5):998–1008.
10. Pastar I, Stojadinovic O, Yin NC, Ramirez H, Nusbaum AG, Sawaya A, Tomic-Canic M. Epithelialization in wound healing: a comprehensive review. Adv in Wound Care. 2014;3:445–64.
11. Guo S, Dipietro LA. Factors affecting wound healing. J Dent Res. 2010;89:219–29.
12. Xue M, Jackson CJ. Extracellular matrix reorganization during wound healing and its impact on abnormal scarring. Adv Wound Care (New Rochelle). 2015;4:119–36.
13. Ter Horst B, Chouhan G, Moiemen NS, Grover LM. Advances in keratinocyte delivery in burn wound care. Adv Drug Deliv Rev. 2017;S0169-409X(17):30096–0.
14. Lootens L, Brusselaers N, Beele H, Monstrey S. Keratinocytes in the treatment of severe burn injury: an update. Int Wound J. 2013;10:6–12.
15. Yang JD, Choi DS, Cho YK, Kim TK, Lee JW, Choi KY, Chung HY, Cho BC, Byun JS. Effect of amniotic fluid stem cells and amniotic fluid cells on the wound healing process in a white rat model. Arch Plast Surg. 2013;40:496–504.
16. Skardal A, Mack D, Kapetanovic E, et al. Bioprinted amniotic fluid-derived stem cells accelerate healing of large skin wounds. Stem Cells Transl Med. 2012;1:792–802.

17. Davis JW. Skin transplantation with a review of 550 cases at the Johns Hopkins Hospital. Johns Hopkins Med J. 1910;15:307.
18. Bujang-Safawi E, Halim AS, et al. Dried irradiated human amniotic membrane as a biological dressing for facial burns-a 7-year case series. Burns. 2010;36:876–82.
19. Tehrani FA, Ahmadiani A, et al. The effects of preservation procedures on antibacterial property of amniotic membrane. Cryobiology. 2013;67:293–8.
20. Riau AK, Beuerman RW, Lim LS, et al. Preservation, sterilization and de-epithelialization of human amniotic membrane for use in ocular surface reconstruction. Biomaterials. 2010;31:216–25.
21. Higa K, Shimmura S, et al. Hyaluronic acid-CD44 interaction mediates the adhesion of lymphocytes by amniotic membrane stroma. Cornea. 2005;24:206–12.
22. Shimazaki J, Shinozaki N, Tsubota K. Transplantation of amniotic membrane and limbal autograft for patients with recurrent pterygium associated with symblepharon. Br J Ophthalmology. 1998;82:235–40.
23. Solomon A, Rosenblatt M, Monroy D. Suppression of interleukin 1 alpha and interleukin 1 beta in the human limbal epithelial cells cultured on the amniotic membrane stromal matrix. Br J Ophthalmol. 2001;85:444–9.
24. Murphy SV, Skardal A, Song L, et al. Solubilized amnion membrane hyaluronic acid hydrogel accelerates full-thickness wound healing. Stem Cells Transl Med. 2017;6:2020–32.
25. Biswas TK, Mukherjee B. Plant medicines of Indian origin for wound healing activity: a review. The Int J of Lower Extremity Wounds. 2003;2:25–39.
26. Khan AW, Kotta S, Ansari SH, et al. Formulation development, optimization and evaluation of *Aloe vera* gel for wound healing. Pharmacogn Mag. 2013;9:S6–S10.
27. Ajmera N, Chatterjee A, Goyal V. *Aloe vera*: It's effect on gingivitis. J of Ind Society of Periodontology. 2013;17:435–8.
28. Chithra R, Sajithlal GB, Chandrakasan G. Influence of *Aloe vera* on collagen characteristics in healing dermal wounds in rats. Mol Cell Biochem. 1998;181:71–6.
29. Heggers JP, Kucukcelebi A, Listengarten D, Stabenau J, Ko F, Broemeling LD, Robson MC, Winters WD. Beneficial effect of aloe on wound healing in an excisional wound model. J Altern Complement Med. 1996;2:271–7.
30. Khorasani G, Hosseinimehr SJ, Azadbakht M, Zamani A, Mahdavi MR. *Aloe* versus silver sulfadiazine creams for second-degree burns: a randomized controlled study. Surg Today. 2009;39(7):587–91.
31. Akhoondinasab MR, Akhoondinasab M, Saberi M. Comparison of healing effect of *Aloe vera* extract and silver sulfadiazine in burn injuries in experimental rat model. World J of Plastic Surgery. 2014;3:29–34.
32. Hirsch T, Rothoeft T, Teig N, Bauer JW, Pellegrini G, De Rosa L, Scaglione D, Reichelt J, et al. Regeneration of the entire human epidermis using transgenic stem cells. Nature. 2017;551:327–32.
33. Pereira RF, Bártolo PJ. Traditional therapies for skin wound healing. Adv in Wound Care. 2016;5:208–29.
34. Lesher AP, Curry RH, Evans J, Smith VA, Fitzgerald MT, Cina RA, Streck CJ, Hebra AV. Effectiveness of biobrane for treatment of partial-thickness burns in children. J Pediatr Surg. 2011;46:1759–63.
35. Rahmanian-Schwarz A, Beiderwieden A, Willkomm L-M, et al. A clinical evaluation of biobrane® and suprathel® in acute burns and reconstructive surgery. Burns. 2011;37:1343–8.
36. Mohammadi AA, Seyed Jafari SM, Kiasat M, Tavakkolian AR, Imani MT, Ayaz M, Tolide-ie HR. Effect of fresh human amniotic membrane dressing on graft take in patients with chronic burn wounds compared with conventional methods. Burns. 2013;39:349–53.
37. Branski LK, Herndon DN, Celis MM, Norbury WB, Masters OE, Jeschke MG. Amnion in the treatment of pediatric partial-thickness facial burns. Burns. 2008;34:393–9.
38. Akhtar N, Rahman MS, Jamil HM, Arifuzzaman M, Miah MM, Asaduzzaman SM. Tissue banking in Bangladesh: 12 years of experience (2003-2014). Cell Tissue Bank. 2016;17:189–97.
39. Khan MN, Islam JM, Khan MA. Fabrication and characterization of gelatin-based biocompatible porous composite scaffold for bone tissue engineering. J Biomed Mater Res A. 2012;100:3020–8.
40. D'Agostino A, Stellavato A, Busico T, Papa A, Tirino V, Papaccio G, La Gatta A, De Rosa M, Schiraldi C. In vitro analysis of the effects on wound healing of high- and low-molecular weight chains of hyaluronan and their hybrid H-HA/L-HA complexes. BMC Cell Biol. 2015;16:19.
41. Choi J, Kim H, Choi J, Oh SM, Park J, Park K. Skin corrosion and irritation test of sunscreen nanoparticles using reconstructed 3D human skin model. Environmental Health and Toxicology. 2014;29:e2014004.
42. Guo H-F, Ali RM, Hamid RA, Zaini AA, Khaza'ai H. A new model for studying deep partial-thickness burns in rats. Int J Burns Trauma. 2017;7:107–14.
43. Babu B, Ravi M, Kumar BN, Sudheendra VH, Ravishankar B. Burn wound healing potential of plain ghrita and Sahasradhauta ghrita on wistar albino rats. Indian J Tradit Knowl. 2015;14:273–8.
44. Sedighi A, Mehrabani D, Shirazi R. Histopathological evaluation of the healing effects of human amniotic membrane transplantation in third-degree burn wound injuries. Comp Clin Pathol. 2016;25:381–5.
45. Kulac M, Aktas C, Tulubas F, et al. The effects of topical treatment with curcumin on burn wound healing in rats. J of Mol Histology. 2013;44:83–90.
46. Amit S, Saraswati B, Kamalesh U, Kumud U. Formulation and evaluation of a novel herbal gel of *Equisetum arvense* extract. J of Pharmacognosy and Phytochemistry. 2013;1:80–6.
47. John T. Human amniotic membrane transplantation. Ophthalmol Clin. 2003;16:43–65.
48. Ramane SB, Syed VN, Biyani KR. Evaluation of wound healing activity of polyherbal gel–a novel herbal formulation. Int J of Res in Pharmaceutical and Biomedical Sciences. 2013;4:788–94.
49. Das T, Debnath J, Nath B, Dash S. Formulation and evaluation of an herbal cream for wound healing activity. Int J Pharm Pharm Sci. 2014;6:693–7.
50. Lien LT, Tho NT, Ha DM, Hang PL, Nghia PT, Thang ND. Influence of phytochemicals in piper betle Linn leaf extract on wound healing. Burns and Trauma. 2015;3:1–8.
51. Gupta A, Keshri GK, Yadav A, et al. Superpulsed (Ga-as, 904 nm) low-level laser therapy (LLLT) attenuates inflammatory response and enhances healing of burn wounds. J Biophotonics. 2014;8:489–501.
52. Pereira Ddos S, Lima-Ribeiro MH, Santos-Oliveira R, Cavalcanti Cde L, de Pontes-Filho NT, Coelho LC, Carneiro-Leão AM, Correia MT. Topical application effect of the isolectin hydrogel (Cramoll 1,4) on second-degree burns: experimental model. J Biomed Biotechnol. 2012;2012:184538.
53. Ramli NA, Wong TW. Sodium carboxymethylcellulose scaffolds and their physicochemical effects on partial thickness wound healing. Int J Pharm. 2011;403:73–82.
54. Broughton G, Jeffrey EJ, Attinger CE. The basic science of wound healing. Plast Reconstr Surg. 2006;117(7):12S–34S.
55. Busuioc CJ, Popescu FC, Mogoşanu GD, et al. Angiogenesis assessment in experimental third degree skin burns: a histological and immunohistochemical study. Romanian J of Morphology and Embryology. 2010;52:887–95.
56. Zielins ER, Atashroo DA, Maan ZN, Duscher D, Walmsley GG, Hu M, et al. Wound healing: an update. Regen Med. 2014;9:817–30.
57. Yagi A, Egusa T, Arase M, Tanabe M, Tsuji H. Isolation and characterization of the glycoprotein fraction with a proliferation-promoting activity on human and hamster cells in vitro from *Aloe vera* gel. Planta Med. 1997;63:18–21.
58. Hashim SNM, Yusof MFH, Zahari W, Noordin KBAA, Kannan TP, Hamid SSA, Mokhtar KI, Ahmad A. Angiogenic potential of extracellular matrix of human amniotic membrane. Tissue Eng Regen Med. 2016;13:211–7.
59. Malhotra C, Jain AK. Human amniotic membrane transplantation: different modalities of its use in ophthalmology. World J Transplant. 2014;4:111–21.

Publisher's Note

3.10 Amnion and Collagen-based Blended Hydrogel Improves Burn Healing Efficacy on a Rat Skin Wound Model in the Presence of Wound Dressing Biomembrane

Md Masud Rana, Md Shaifur Rahman, Md Akib Ullah, Ayesha Siddika, Md Liakat Hossain, Md Shamim Akhter, Md Zahid Hasan, Sikder M Asaduzzaman

Abstract

Background: A burn wound is one of the most frequent and devastating injuries for patients which requires extensive care. Early treatment of burn wounds improves healing significantly.

Objective: This study was designed to investigate the efficacy of amnion and collagen-based hydrogels on cutaneous burn wound healing in rats with covering membrane.

Methods: We prepared a novel cell free hydrogel comprising human amnion, rabbit collagen, carboxymethyl cellulose sodium salt, citric acid, methyl paraben, propyl paraben, glycerin and triethanol amine. The wound covering membrane was developed from rabbit collagen and prawn shell chitosan. Beside swelling ratio, water absorption, equilibrium water content, gel fraction and spreadability analysis, in vitro cytotoxicity and biocompatibility tests were performed for the formulated hydrogels. Following the skin irritation study, second-degree burns were created on the dorsal region of the rats and the gels were applied with/without covering membrane to study the wound contraction and re-epithelialization period.

Results: The formulated hydrogels were observed non-cytotoxic and compatible with human blood cells. No erythema and edema were found in skin irritation assay confirming the safety and applicability. Hydrogel consisting in a combination of amnion and collagen demonstrated significantly rapid wound healing, driven by complete re-epithelialization (16.75 ± 0.96 days) and closure by wound contraction (72 ± 3.27%, $P < 0.0000009$) when wound dressing membrane was used, whereas this gel alone healed about 62.5 ± 4.43% ($P < 0.00001$) and required 18.75 ± 0.50 days to complete re-epithelialization. Additionally, the gel with covering membrane treated group had maximum average body weight, food and water intake.

Conclusion: The amnion and collagen-based blended gel offers alternative possibilities to treat skin wounds when covered with film, which could overcome the limitations associated with modern therapeutic products such as high costs, long manufacturing times, complexities, storing, and presence of living biomaterials.

Publication Status: Published in Biomed Mater Eng. 2020;31(1):1-17.

Impact Factor: 0.993

This article is reproduced with permission.

Approximated total share of contribution: 30%

Contribution on experimental design, realization and publication: MMR and MSR conceived the idea. MMR, MSR and MAU designed the experiment. MMR, MAU, AS and MLH performed the experimental work. MSR, MMR, MSA and MZH analysed the data. MSR and MMR, MAU wrote the initial draft and MSA, MZH and SMA edited the manuscript. MSR and SMA supervised the work from start to end. All authors read and approved the final manuscript.

Pubmed link: https://pubmed.ncbi.nlm.nih.gov/32144968/
Journal link:
https://content.iospress.com/articles/bio-medical-materials-and-engineering/bme201076

Bio-Medical Materials and Engineering 31 (2020) 1–17
DOI 10.3233/BME-201076
IOS Press

Amnion and collagen-based blended hydrogel improves burn healing efficacy on a rat skin wound model in the presence of wound dressing biomembrane

Md Masud Rana[a,†], Md Shaifur Rahman[a,b,*†], Md Akib Ullah[c], Ayesha Siddika[a], Md Liakat Hossain[a], Md Shamim Akhter[c], Md Zahid Hasan[a] and Sikder M. Asaduzzaman[a]
[a]*Institute of Tissue Banking and Biomaterial Research, Atomic Energy Research Establishment, Dhaka, Bangladesh*
[b]*Institute for Stem Cell Research and Regenerative Medicine, Medical Faculty, Heinrich Heine University, Düsseldorf, Germany*
[c]*Biotechnology and Genetic Engineering Discipline, Khulna University, Khulna, Bangladesh*

Received 19 November 2019
Accepted 9 January 2020

Abstract.
BACKGROUND: A burn wound is one of the most frequent and devastating injuries for patients which requires extensive care. Early treatment of burn wounds improves healing significantly.
OBJECTIVE: This study was designed to investigate the efficacy of amnion and collagen-based hydrogels on cutaneous burn wound healing in rats with covering membrane.
METHODS: We prepared a novel cell free hydrogel comprising human amnion, rabbit collagen, carboxymethyl cellulose sodium salt, citric acid, methyl paraben, propyl paraben, glycerin and triethanol amine. The wound covering membrane was developed from rabbit collagen and prawn shell chitosan. Beside swelling ratio, water absorption, equilibrium water content, gel fraction and spreadability analysis, *in vitro* cytotoxicity and biocompatibility tests were performed for the formulated hydrogels. Following the skin irritation study, second-degree burns were created on the dorsal region of the rats and the gels were applied with/without covering membrane to study the wound contraction and re-epithelialization period.
RESULTS: The formulated hydrogels were observed non-cytotoxic and compatible with human blood cells. No erythema and edema were found in skin irritation assay confirming the safety and applicability. Hydrogel consisting in a combination of amnion and collagen demonstrated significantly rapid wound healing, driven by complete re-epithelialization (16.75 ± 0.96 days) and closure by wound contraction (72 ± 3.27%, $P < 0.0000009$) when wound dressing membrane was used, whereas this gel alone healed about 62.5 ± 4.43% ($P < 0.00001$) and required 18.75 ± 0.50 days to complete re-epithelialization. Additionally, the gel with covering membrane treated group had maximum average body weight, food and water intake.
CONCLUSION: The amnion and collagen-based blended gel offers alternative possibilities to treat skin wounds when covered with film, which could overcome the limitations associated with modern therapeutic products such as high costs, long manufacturing times, complexities, storing, and presence of living biomaterials.

Keywords: Amnion, collagen, hydrogel, chitosan, biomembrane, burns, wound healing, epithelialization

*Corresponding author: Md Shaifur Rahman. E-mail: mdshaifur@gmail.com.
†These authors contributed equally to this work.

1. Introduction

Burn injury is considered one of the most common and devastating medical burdens worldwide since the ancient period of human history. Globally, 265,000 individuals die every year because of burns [1]. The vast majority of the burn incidents occur in low- and middle-income countries and almost half happens in the South-East Asia region. For instance, according to WHO, nearly 173,000 children are moderately or severely burned every year in Bangladesh [2]. The standard burn wound treatment, currently clinically practised, is the engrafting of an autologous split thickness skin graft and amniotic mebrane allograft which results in a clearly advantageous outcome [3–5]. However, the limited availability of healthy donor skin, amniotic graft, high cost, complex manufacturing, and complex storage are the difficulties which hinder the incorporation of these grafts into routine clinical use. In addition, the requirement of tissue banking facilities, patients' need to come to the clinic, and lack of expertise of the medical personnel in graft transplantation are the limitations. Furthermore, human amniotic membrane dressings perform better if replaced every other day [6]. Despite recent tremendous advances in wound care products such as stem cells, Integra, AlloDerm and Biobrane, recombinant growth factors and cellular tissue-engineered skin substitutes-based wound treatments [7–9], these commercial advanced treatments are associated with high costs for patients in low-income countries. Traditional therapies based on discarded biomaterials such as amniotic membrane extracts, collagen, chitosan, blended hydrogel, are considered to be an interesting and promising alternative [10–16].

Amnion is widely used as a burn wound healing material and known as an ideal biological burn wound dressing material [17]. It acts as a scaffold for proliferation and differentiation of native skin cells due to the presence of fibronectin, elastin, nidogen, collagen types I, III, IV, V and VI and hyaluronic acid which finally lead to the promotion of neo-epithelialization [18]. The structural protein-collagen is involved in all three phases of the wound-healing cascade [19]. Collagen stimulates cellular migration and contributes to form new healthy granulation tissue very quickly over the burn, helping to heal rapidly. Collagen-based biomaterials have been reported to stimulate and recruit specific cells, such as macrophages and fibroblasts, along the healing cascade to enhance and influence wound healing [19]. A cationic biopolymer chitosan was reported to disrupt the outer membrane of bacteria and hamper the growth of infectious substances [20] which is a beneficial biological property for wound healing by protecting the wound from microbial infection. These chitosan and collagen are eco-friendly biomaterials as they do not produce any harmful residues. These biomaterials can provide moisture or absorption, depending on the mode of preparation and delivery system [13]. In developing countries, people would like to treat burn injuries at home unless the complications increase to a certain level. However, patients respond best when rapid treatments are available for fast closureing and protecting wounds. There is a need of a low cost and effective fast aid product to manage burn injuries [4] that is easy to produce and store, is physiologically effective and its application does not require medication. The limitations related to modern therapeutics, increasing numbers of burn injuries, and the advantages of naturally available biomaterials rationalize to formulate the hydrogels consisting of amnion and collagen. Here, we have demonstrated the usefulness of amnion and collagen blended hydrogel which can significantly accelerate wound closure through contraction and re-epithelialization in an animal model for skin burns in the presence of biomembrane.

2. Materials and methods

2.1. Preparation of amnion powder

Amniotic sacs were collected from a sero-negative donor (HIV, Syphilis, Hepatitis B and C viruses) after caesarean deliveries with the written consent of the donor. After collection, the amnion extracts were prepared as described previously [12]. In short, the amnion membranes were carefully separated from chorionic by forceps and the separated amnion membranes were washed with PBS containing streptomycin and penicillin. After washing, the membranes were freeze dried at −55 °C overnight. The freeze dried membranes were then minced into small pieces and sealed into plastic bags for radiation sterilization at 10kGy using cobalt 60γ source. The small pieces of membrane were then aseptically processed into powder form which was later used for gel preparation.

2.2. Isolation of collagen from rabbit skin

Rabbit skin collagen was isolated according to the method as described before [21]. Pretreated rabbit skins were cut into small pieces (approx. 1 cm^2 each) and suspended in 0.5 M acetic acid solution at a solid-to-solvent ratio of 1:10 (w/v). After shaking at 200 rpm for 24 hrs at RT, the sample was filtered and the liquid soluble portion was called acetic acid soluble collagen. The non-dissolved residue was used for pepsin soluble collagen extraction as follows: the residues were re-suspended in a new solution of 0.5 M acetic acid at a concentration of 1:10 (w/v) and pepsin at a concentration of 2 mg/ml. All samples were filtered and stored at 4 °C at the end of every single extraction. Both collagens were precipitated with a solution of 2.6 M NaCl. After being centrifuged at 10,000 rpm for 30 min, the samples were re-suspended in five volumes of 0.5 M acetic acid and were dialysed for 48 hrs in DW and dialysis membrane tubing with 6–8 kDa Mw cut-off. Finally, the resulted dialyzed collagen was freeze dried at −55 °C for further use.

2.3. Extraction of chitosan from shrimp shells

Chitosan was extracted from shrimp shells according to the method established by Khan et al., 2005 [22]. In short, waste prawn shells were washed with hot DW and were dried in an oven at 105 °C for 72 hrs. Dried shells were ground using a blender and deproteinized with 3% NaOH and demineralized with 3% HCl. The deproteinized and demineralized chitin was then neutralized and dried in oven at 105 °C for 24 hrs. Chitosan was obtained by deacetylation of chitin with 50% NaOH where the ratio of chitin: NaOH $\frac{1}{4}$ was 1:20 (w/w) at 100 °C for 3 hrs. After this process, solids separated from the alkali layer were extensively washed with distilled water to remove traces of alkali. The resultant solid was dried in a vacuum oven at 50 °C for 24 hrs.

2.4. Formulation of hydrogel

Amnion and collagen powder was dissolved in 1% citric acid. When these amnion and collagen powders were completely homogenized, other ingredients (i.e. antibacterial ingredients such as methyl paraben and propyl paraben, and moisturizing agent glycerin) were added. Subsequently, triethanolamine was added dropwise to neutralize pH 7. In one glass tube, all the components were added under continuous stirring except carboxymethyl cellulose sodium (CMC-Na). In another tube, different concentrations of gelling

Table 1
The composition of the nine types of formulated gels (HG1-HG9)

Sample no.	CMC-Na	Amnion powder	Collagen powder	Citric acid	Methyl paraben	Propyl paraben	Glycerin	Triethanol amine
HG1	4%	2%	0	1%	0.02%	0.002%	5%	70 µl
HG2	4%	1%	1%	1%	0.02%	0.002%	5%	60 µl
HG3	4%	0	2%	1%	0.02%	0.002%	5%	65 µl
HG4	5%	2%	0	1%	0.02%	0.002%	5%	60 µl
HG5	5%	1%	1%	1%	0.02%	0.002%	5%	65 µl
HG6	5%	0	2%	1%	0.02%	0.002%	5%	70 µl
HG7	6%	2%	0	1%	0.02%	0.002%	5%	60 µl
HG8	6%	1%	1%	1%	0.02%	0.002%	5%	65 µl
HG9	6%	0	2%	1%	0.02%	0.002%	5%	65 µl

Table 2
The concentration of collagen and chitosan for developing the blended biomembranes

Sample no.	Collagen	Chitosan
BM1	10 mg/ml	10 mg/ml
BM2	12 mg/ml	8 mg/ml
BM3	8 mg/ml	12 mg/ml
BM4	14 mg/ml	6 mg/ml
BM5	6 mg/ml	14 mg/ml
BM6	15 mg/ml	5 mg/ml
BM7	5 mg/ml	15 mg/ml
BM8	16 mg/ml	4 mg/ml
BM9	4 mg/ml	16 mg/ml
BM10	18 mg/ml	2 mg/ml
BM11	2 mg/ml	18 mg/ml

agent- CMC-Na were prepared at 60 °C which formed a transparent solution. Finally, both solutions were mixed gently at 40 °C under aseptic condition. The formulated hydrogels (HG) were then placed to cool down to 30 °C. The ingredients and concentrations are listed in Table 1.

2.5. *Development of collagen-chitosan blended biomembranes*

Collagen-chitosan blended membranes were prepared using the solvent evaporation method as described by Indrani et al. 2017 [13]. Chitosan was dissolved in 100 mL of 1% acetic acid by stirring at RT for 6h and neutralized with 1 M NaOH. Separately, collagen was dissolved in 0.5 M acetic acid by stirring for 12h at RT. These two polymeric solutions were then mixed in a ratio as listed in Table 2 and stirred for 24–48 h at RT. From the resultant polymer blend 5 mL of each blend was poured into a petri dish and freeze dried. The freeze dried membrane was washed several times with DW, and freeze dried again at least for 12 h. Finally, the dried membranes were subjected to gamma-ray irradiation.

2.6. Determination of swelling ratio and water absorption

Measurements of the swelling capacity of the hydrogels were performed as described by Abdallah, 2019 [23]. The swelling ratio was calculated according to the following equation: Swelling ratio = [Ws − W*d*]/Wd, where Ws is the weight of sweollen gel and Wd is the weight of the dry gel.

The percentage of the water absorption was estimated according to the methods of Bhuiyan et al., 2015 [24]. Water absorption % was calculated according to the following equation: Water absorption [%] = [Wt − Wi] × 100, where Wt is the weight of swollen gel sample at time 't' and Wi is the initial weight of dry gel samples.

2.7. Determination of gel fraction and equilibrium water content

The percentage of the gel fraction was determined according to the method as described previously [25]. The gel fractions of the samples were calculated gravimetrically according to the following equation: Gel fraction (%) = [Wd/Wi] × 100, where Wd is the weight of dried gel after extraction and Wi is the initial weight of dried gel.

Equilibrium water content (EWC) was estimated as described by Kim et al., 2003 [26]. EWC was calculated using the following formula: EWC [%] = [(Weq − Wi)/Weq] × 100. Where, Weq is the weight of swollen gel at equilibrium and Wi is the initial weight of dry gel.

2.8. Spreadability assesment

Spreadability assesment was performed according to method of Abdul et al., 2013 [27]. In short, 1 gm of gel was placed within a circle of 2.3 cm diameter pre-marked on a glass plate of 20 × 20 cm, over which a second glass plate was placed. A weight of 500 gm in the form of water-filled beaker was allowed to rest on the upper glass plate for 5 min. The increase in the diameter due to gel spreading was noted.

2.9. In vitro cytotoxicity and red blood cell compatibility test

In vitro cytotoxicity test was performed on brine shrimp as described by Bundela and Bajpai, 2008 [28]. The final gel samples were dissolved in artificial seawater at different concentrations and the active nauplii were inoculated. After overnight incubation, the nauplii were counted. Here, 0.5 mg/ml of Vincristine PCH (Pharmachemie BV, the Netherlands) was used as positive control and sea water was served as negative control.

Heparinized human blood was used to test the biocompatibility of the selected gel samples as described by Bhowmik et al., 2017 [29]. Tested samples were prepared using blood and selected gel at 3:1 ratio. Blood sample of the same donor was also diluted at the same ratio with distilled water and normal saline which served as positive and negative control, respectively. After mixing, the mixtures were kept in an incubator for 2 h at 37 °C. The samples were then spread on glass slides and observed under an inverted microscope (20× magnification).

2.10. Skin irritation studies

To assess *in vivo* irritability and applicability of the gels, the dorsal skin-hairs of the selected female Wistar rats were shaved on the date of experiment [30]. In total eight animals were examined and were

randomly assigned to four groups (i. amnion gel, ii. gel consisting of amnion and collagen, iii. without dressing membrane, and iv. collagen gel). The animals were treated with 1 ml gel daily up to four days and finally the treated skin was visually examined for erythema and edema.

2.11. Artificial burn induction, wound contraction and re-epithelialization

In total, 24 healthy female Wistar rats of 100–150 g body weight were randomly assigned into six experimental groups: i. 1% silver sulfadiazine (Burnsil, Beximco Pharmaceuticals Ltd, Bangladesh) as positive control, ii. without gel served as negative control, iii. treated with collagen gel, iv. treated with amnion gel, v. treated with amnion and collagen blended gel with and vi. without covering membrane. Each rat was anesthetized with Ketamine HCl solution 100 mg/kg (Gonoshasthaya Pharmaceuticals Ltd, Bangladesh) body weight by intraperitonial injection. Subsequently, the hair at dorsal region was trimmed and properly shaved with a sharp blade and cleansed with an alcohol swab.

Burns were created using a piece of aluminum (2.5 cm diameter) heated to 100 °C for 5 min. The hot aluminum was gently applied for 15 seconds on the shaved area [31]. The animals were treated with 1 ml of gels on a daily basis, topically, for a period of 16 days. Gross changes in the wounds were evaluated from day 0 to 16 post burn. Images were taken regularly using a Canon IXUS 130 camera, and the morphological evaluation such as appearance of the wound was recorded. Re-epithelization was monitored by recording the number of days required for crust to fall away, leaving no raw wound behind [12]. To monitor wound contraction, progressive changes in the wound area were measured. The wound margin was traced at 4 days intervals by millimeter measuring scale and measurements were continued up to 16 days. After every four days, the healed area was calculated by subtracting initial wound area to the unhealed area [11]. Using the formula below, the percentage of wound contraction was calculated on the respective day. The percentage of wound contraction was calculated taking the initial area of wound (625 mm^2) as 100%.

$$\%\text{Wound contraction} = \frac{\text{Initial Wound Area} - \text{Final Wound Area}}{\text{Initial Wound Area}} \times 100.$$

2.12. Statistical analysis

All statistical analyses were calculated by one way independent test using SPSS version 22.0 (SPSS Inc., Chicago, IL, USA) on a Microsoft Excel 2010 platform. All quantitative data presented in this study include mean (±) standard deviations (SD). $P < 0.05$ was considered statistically significant.

3. Results

3.1. General observations of the formulated hydrogels and biomembrane

Full-term human placentas were collected during cesarean sections. The erythrocytes were depleted and the amnion was separated from chorion membrane for further processing. Afterwards, amniotic membranes were lyophilized, freeze dried, blended and finally gamma irradiated to obtain powder and make amnion solution (Fig. 1A). Collagen was isolated from rabbit skin and freeze dried to extract powder for further use (Fig. 1B). With the addition of several ingradients including distinct concentrations of amnion solutions, collagen solutions, and CMC-Na solutions, in total nine types of hydrogels were prepared (the composition of hydrogels is shown in Table 1). The gels were presereved in frozen

conditions (Fig. 1C). All of the formulated hydrogels were found to be semi-solid and homogeneous in nature with good consistency (Fig. 1D). The pH of all nine gel formulations was measured and ranged from 6.56 to 7.3. The color of gels containing only amnion extracts were off-white while the gels containing both amnion and collagen were light white. In case of gel containing collagen alone, the color was found to be deep white (Fig. 1E). However, all gels formulations were semi-transparent, viscous and flexible visually (Fig. 1F). The chitosan-collagen blended biomembrane were prepared from the rabbit skin derived collagen and prawn shell derived chitosan (Fig. 1G–J). We observed that a mixture of collagen concentration (10 mg/ml) and chitosan concentration (10 mg/ml) formed a transparent biomembrane (Fig. 1K).

3.2. Physical characterization of the formulated hydrogels and biomembrane

One of the crucial ingredients of the formulation of hydrogel is the gelling agent. Different percentages of gel formulations were tried in order to select the best gelling agent. Gels containing 4.0% of Na-CMC formed a very thin gel. With 5.0% gelling agent somewhat better gel was obtained but gel containing 6.0% of Na-CMC formed uniform and smooth gel. Thus, 6.0% of Na-CMC was selected as the optimized concentration of gelling agent. However, we have prepared nine types (HG1–HG9) of hydrogel gels contained 1–2% of amnion powder, collagen powder and amnion-collagen together with 4–6% of Na-CMC (Table 1). The swelling ratio of the gels ranged from ~1.26 to ~2.59 (Fig. 2A). The water absorption and equilibrium water content of these formulated gels were observed to increase from ~19.23% to ~25.85% and ~55.7% to ~72.1%, respectively with the incraesing percentage of Na-CMC (Fig. 2B, 2C). The gel fraction of hydrogel was denoted to vary from ~70.83% to ~87.30% (Fig. 2D). The value of gel spreadability of the formulated gels was measured which ranged from ~3.9 to ~6.3 cm (Fig. 2E). Spreadability of 6% gels was found lower because high concentration gels tend to be thicker and spread less. Although three distinct concentrations of CMC-Na were added to form the hydrogels, but 6% of CMC-Na gels possed better physical properties in terms of swelling ratio, water absorption, equilibrium water content, gel fraction and spreadability. The chitosan-collagen blended biomembrane (Table 2) were evaluated based on physical properties such as swelling ratio, water absorption (%) and equilibrium water content (%). We observed that the membrane (BM1) composed of the equal concentrations of chitosan (10 mg/ml) and collagen (10 mg/ml) possed highest water absorption, equilibrium water content and swelling ratio whereas BM8 (Collagen 16 mg/ml: Chotosan 4 mg/ml) were lowest (Fig. 2F, 2G, 2H).

3.3. In vitro biocompatibility, cytotoxicity and in vivo skin irritation studies

Upon incubation of human blood with gel samples *in vitro*, less than 2% hemolysis was observed and the red blood cells remained intact in 3:1 ratio which indicated biocompatibility of the gel samples. On the other hand, cell damage observed when distilled water (positive control) incubated with the same ratio (Fig. 3A). The brine shrimp lethality assay was performed to observe the *in vitro* cytotoxic effect of the final formulated gel samples. We did not observ any death of the nauplii, not even at the higher doses of gel samples apart from amnion-collagen blended hydrogels and amnion-collagen blended gel in presence of biomembrane. Similar results were found in the case of saline water incubation (negative control). However, in these cases, no death of the nauplii was noticed when the doses limited to 0.25 and 0.75 mg/ml. At a concentration of 1 mg/ml about 15% deaths of the nauplii were observed (Fig. 3B). To analyze the applicability of the prepared gel, skin irritation assay were performed in vivo using a rat model. After topical application of all nine types of hydrogels for a period of 48 hrs, it was observed that

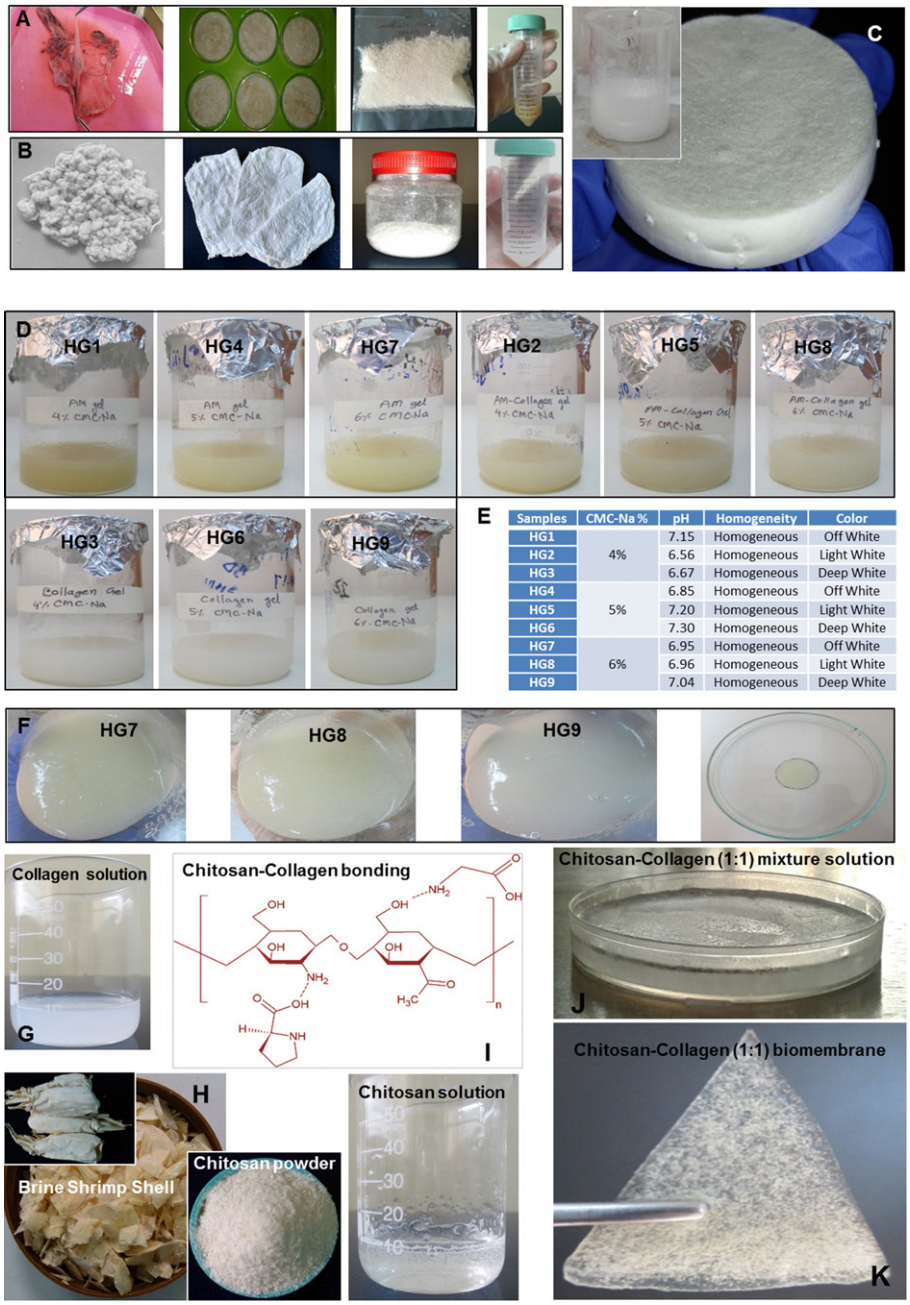

Samples	CMC-Na %	pH	Homogeneity	Color
HG1	4%	7.15	Homogeneous	Off White
HG2		6.56	Homogeneous	Light White
HG3		6.67	Homogeneous	Deep White
HG4	5%	6.85	Homogeneous	Off White
HG5		7.20	Homogeneous	Light White
HG6		7.30	Homogeneous	Deep White
HG7	6%	6.95	Homogeneous	Off White
HG8		6.96	Homogeneous	Light White
HG9		7.04	Homogeneous	Deep White

Fig. 1. Preparation amnion, collagen and chitosan; and the physical appearance of the formulated hydrogels and biomembrane. (A) Seperation of amnion from chorion. The dried lyophilized amniotic membrane was 10 kGy gamma irradiated and amnion solution. (B) Rabbit skin derived freeze dried powder was used to formulate collagen solution. (C) Representative picture of frozen hydrogel. (D) Physical appearance of all nine types of the gels. (E) pH, color and homogenecities of the formulated gels. (F) Six percent CMC-Na hydrogels appeared as semi-solid like flexible lubricants, viscus, and semitransparent. Gel sample placed within circle of petridish. (G) The preparation of chitosan and collagen blended bio-polymer, bonding between chitosan and collagen, membrane solution before freeze drying and the representative image of prepared biomembrane sheet.

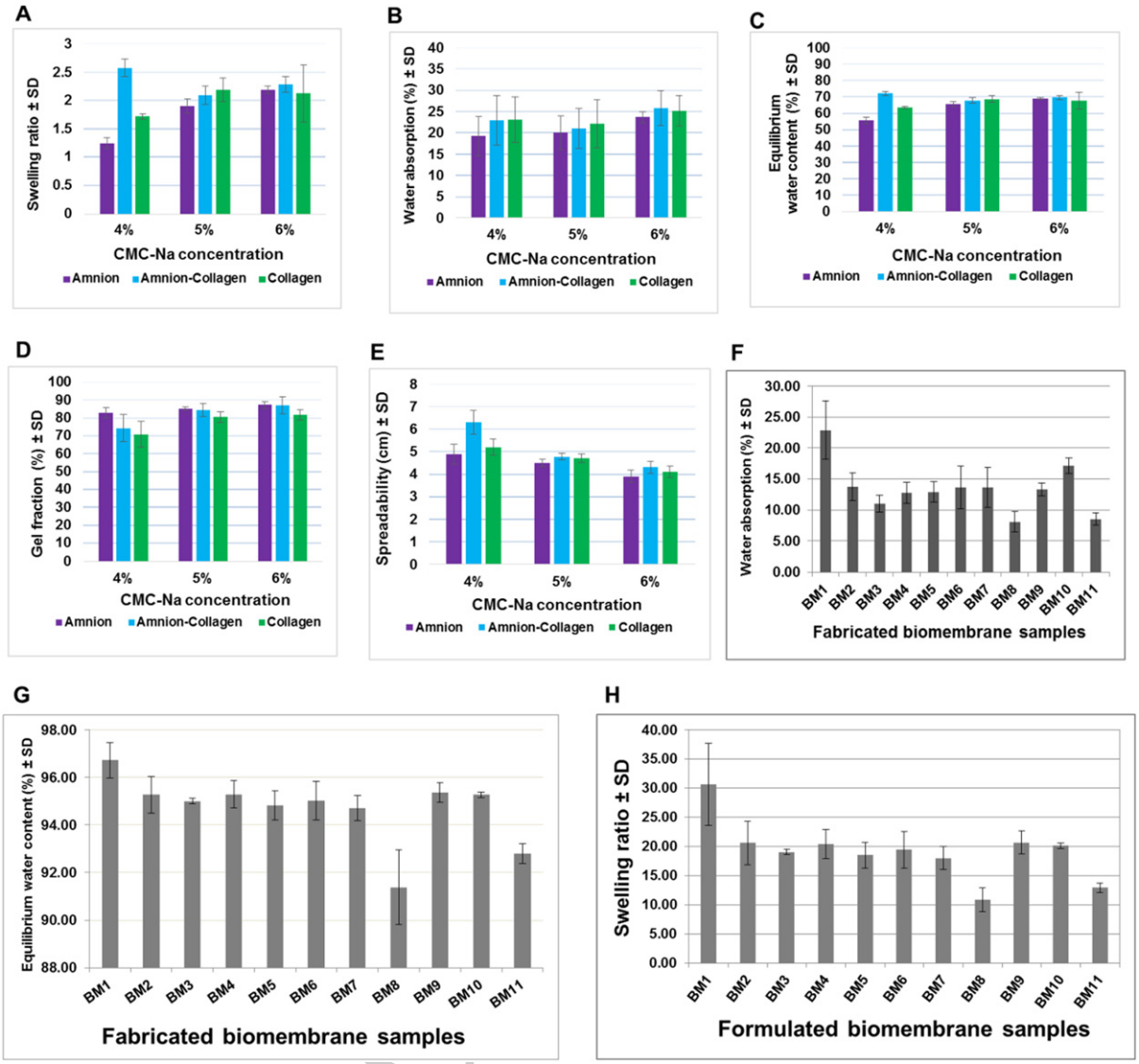

Fig. 2. Physical properties of the hydrogels and biomembranes in terms of swelling ratio, water absorption, equilibrium water content, gel fraction and spreadability. Distinct hydrogel samples at different CMC-Na concentrations (A) swelling ratio, (B) water absorption (%), (C) equilibrium water content (%), (D) gel fraction (%), and (E) spreadability in cm. Fabricated biomembrane samples (F) water absorption (%), (G) equilibrium water content (%) and (H) swelling ratio at various chitosan: collagen ratio.

the gel did not induce any edema or erythema (Fig. 3C). To test the biotic and abiotic stress tolerability, at least for few days, we expose the experimental gel and membrane samples to normal environmental conditions in a room. We did not observed any shrinkage, deterioration or any macroscopically visible microbial growth on it (Fig. 3D). This result indicated the safety of gels to be applied topically. We also observed that the hair formation was normal compared to non-treated rats.

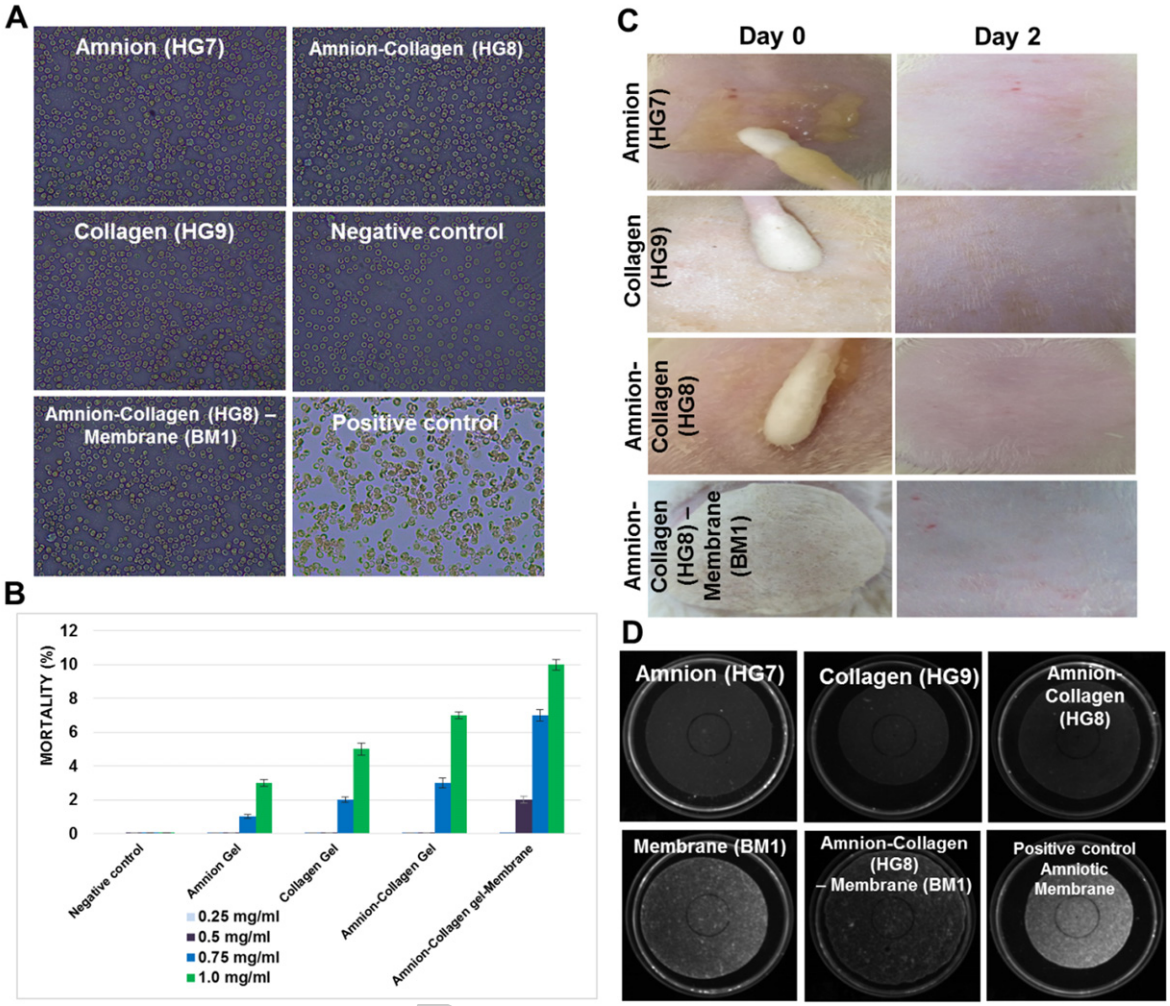

Fig. 3. Biocompatibity, cytoxicity and irritability analyis. (A) Human blood biocompatibility were shown by RBC morphology of heparinized blood incubated with distinct hydrogels with 6% CMC-Na and biomembrane. Microscopic view of blood cells at 20× magnification. (B) Brine shrimp lethality bioassay shows the mortality percentages of brine shrimp. (C) Topical application of the gels for *in vivo* skin irritation assay on shaved rats. (D) To observed the samples self-deterioration when expose to environmental stress for 4 days. Amniotic membrane graft served as positive control.

3.4. Wound contraction, re-epithelialization, and behaviour analysis

Initially on day 0, using a 2.5 cm diameter piece of aluminum, a second-degree burn was created in all experimental anesthetized rats (Fig. 4A) which produced a painful injury, with no bubbles, white color and subsequently hyperemia occurred into the damaged tissue area. After 30 minutes of burn injury, respective gel was applied in each group of rats except negative control. On day 4, negative control and collagen group showed wet crust where amnion, amnion-collagen blended with/without biomembrane and positive control group showed slight dry and thick dry crust, respectively. On day 8, negative control and collagen group were observed with less detachment of crust edge rather than all treated rat groups. On day 12, scar

tissue and contraction became clearly visible in each group. On day 16, crusts were all disappeared and re-epithelialization was completed in amnion-collagen blended with/without biomembrane group showed better healing rate with no scar tissue while other groups showed moderate healing with scar tissue and a minor wound (Fig. 4B).

The rate of wound contractions varied from group to group. From the begining of topical gel treatment, for instance on day 4, amnion-collagen blended treated group was noticed with maximum healing rate in presence of biomembrane, which was four folds to control group and statistically most significant ($P < 0.0002$). However, amnion-collagen in absence of biomembrane and amnion gel treated groups were also statistically significant (amnion-collagen $P < 0.0004$, amnion $P < 0.0006$). After 8 days of post burning, amnion-collagen blended gel when covered with biomembrane contracted about 34 ± 2.31% ($P < 0.000006$). Negative control group had least wound contraction rate of 9.33 ± 2.31% while amnion and amnion-collagen without biomembrane treated groups were 25.33 ± 2.31% ($P < 0.0007$) and 32 ± 3.27% ($P < 0.00007$), respectively. Similar pattern of wound contraction were visualized also on day 12 and 16. On 12th day of treatment, amnion-collagen blended gel with biomembrane group the contraction were reached to 52 ± 3.27% ($P < 0.000003$). Healing rate of amnion-collagen and amnion treated groups were 46 ± 2.31% ($P < 0.000007$) and 40 ± 3.27% ($P < 0.00007$), respectively. On day 16, amnion-collagen blended gel including biomembrane treated group showed superiority 72 ± 3.27% ($P < 0.0000009$) while negative control group healed only 22.67 ± 2.31%. Amnion-collagen, amnion, positive control and collagen treated groups were healed 62.5 ± 4.43% ($P < 0.00001$), 52 ± 3.27% ($P < 0.00004$), 41 ± 3.83% ($P < 0.0004$) and 36 ± 4% ($P < 0.001$), respectively (Fig. 4C).

In cases of average re-epithelialization period in all experimented groups, biomembrane covered amnion-collagen blended gel treated group required only about 16 days while amnion collagen, amnion, positive control, collagen and negative control groups needed 19, 20, 22, 24 and 28 days, respectively. The amnion-collagen in presence of biomembrane ($P < 0.000002$) and amnion-collagen without membrane ($P < 0.000007$) treated groups were statistically more significant than amnion treated group ($P < 0.0001$) and positive control group ($P < 0.0002$) (Fig. 4D). During wound healing process the behaviours factors such as body weight, water and food intake have been influced. We observed that body weight gaining was highest when applying the amnion-collagen blended gel with dressing membrane. For the cases of food and water intake, we also noticed better food and water intake in amnion-collagen blended gel when covered by membrane (Fig. 4E–G).

4. Discussion

Traditional therapies based on discarded biomaterials are interesting alternatives for dressing burn and skin wounds, which improves healing, is readily available, easily applicable, economical, prevents infection and desiccation, and facilitates healing [32]. Previously, we studied burn wound healing gel products consisting of a combination of amnion and Aloe vera extract [12]. The application of collagen over the injured burn improved the healthy granulation tissue which enabled rapid healing [33,34]. Here, we described that a gel consisting of a combination of amnion and collagen extract has the potential as a burn wound healing product in hydrogel format which is easy to produce and apply. Again, chitosan has been reported as an antimicrobial biomaterial which could prevent penetration of bacteria into the wound [35]. The blend of chitosan and collagen could form a membrane which prevents bacterial infection and maintains the moister around the wound as well [13,36]. So, we believe that covering the wounded area

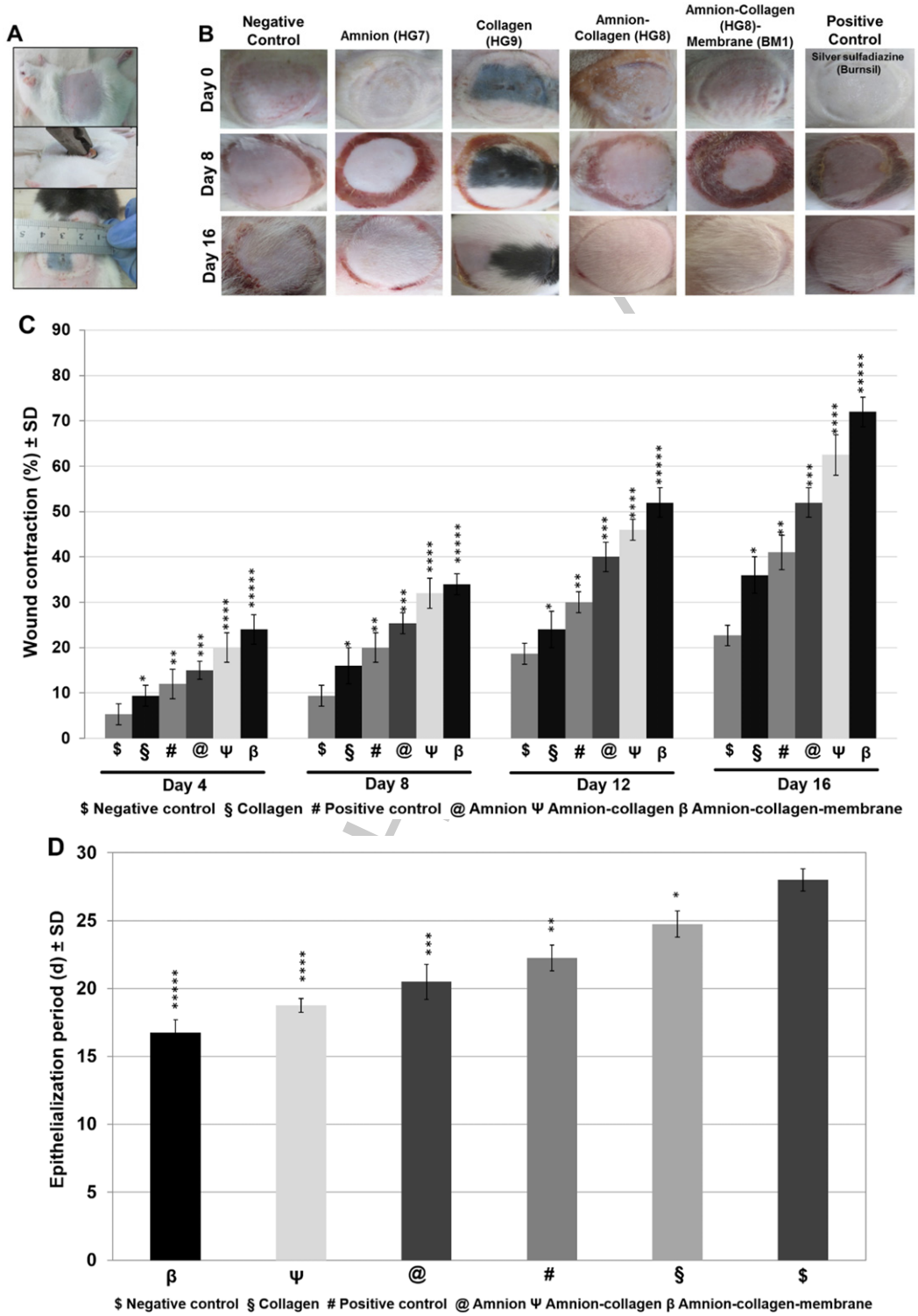

Fig. 4. For caption see next page.

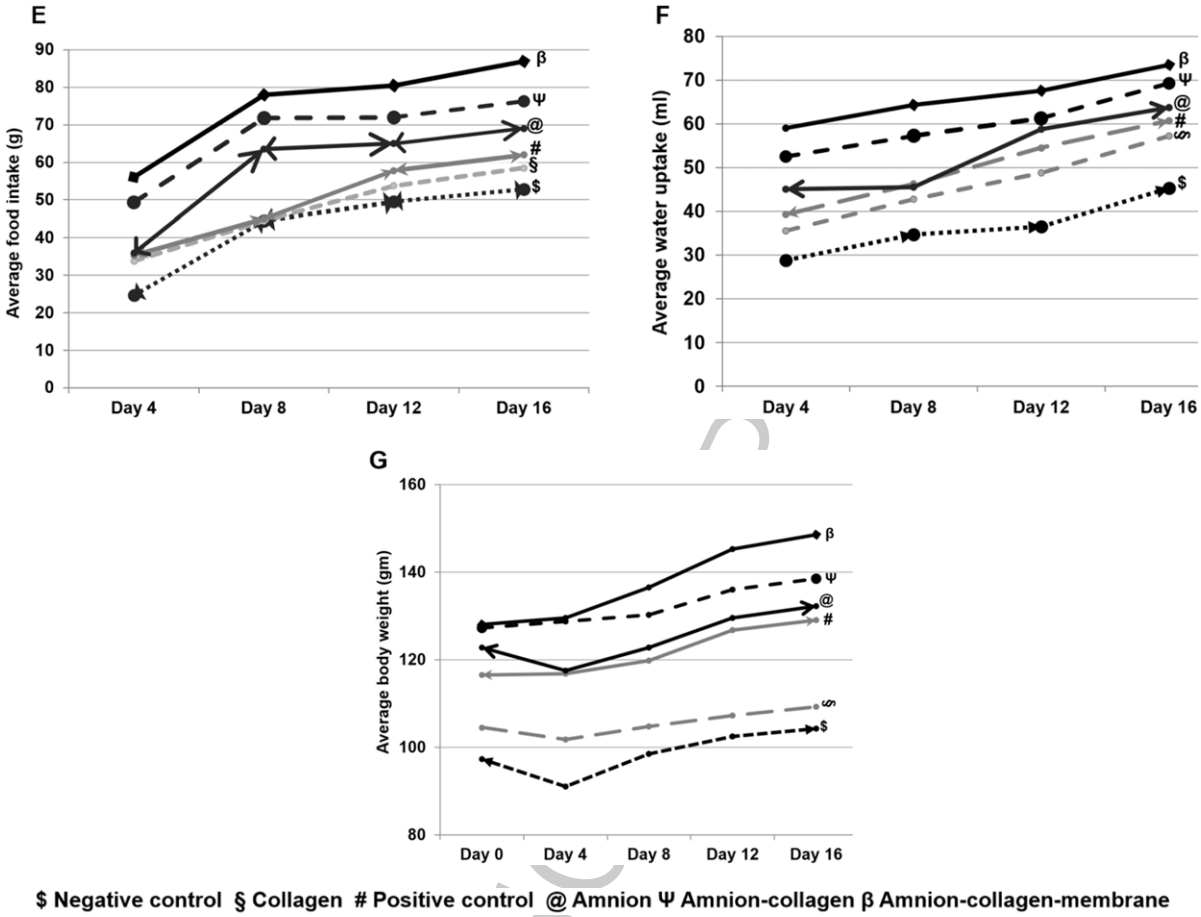

Fig. 4 (Continued). Macroscopic evaluation of wound closure and quantitative measurement of wound contraction, re-epithelialization and behaviour. (A) Burn induction process and initial wound area measurement. (B) Macroscopic wound healing representative images of Wistar rats on day 0, 8, and 16 which were treated with amnion, collagen, amnion-collagen blened gel with or without covering films, and controls. (C) Clinical evaluation of wound healing regarding wound contraction in rats at day 4, 8, 12, and 16. (D) Complete re-epithelialization period required for different groups of treated animals. * indicates the level of significance against negative control group. The changes in behaviours factors such as average (E) food intake, (F) water uptake and (G) body weight over the courses of wound healing treatment.

with the chitosan-collagen biomembrane onto the amnion-collagen hydrogel may speed up the healing process by serving as a synergistic function and protecting the wound area from the external environment.

One of the crucial ingredients of the formulation of hydrogel is the gelling agent. Thus 6% Na-CMC was selected as the optimized concentration of gelling agent. Another study also showed that gel containing 6.0% of Na-CMC formulated uniform gel that was effective for wound healing [12]. Considering all the formulated gel types, the gels consisting of amnion and collagen in CMC-Na (6%) has been observed with promising physical properties in most instances. These three formulations were found to be homogeneous, viscous and flexible in nature with good consistency. Additionally, lower values of spreadability indicating that they spread less and possed the tendency to stick to the wound area over a longer period of time which is eventually expected for topical application [37,38]. The spreadibility could easily be increased by a small amount of shear [39]. Furthermore, we experienced that it was hard to maintain the gel texture

above 6% of CMC-Na. the outer surface of our body acts as a defense barrier where pH level increase from epidermis to dermis requires to formulate a gel with a pH range of 6.5–7.3 which is desirable for the skin [38]. The pH of the finally selected formulations ($n = 3$) was found to be between 6.95 and 7.04 which implies that gels were suitable for skin wound healing therapy and the formulation can thus be used without the risk of irritation to the skin.

Regarding the fabricated biomembrane, the equal concentrations of chitosan (10 mg/ml) and collagen (10 mg/ml) could formed a dressing film which possess better biophysical properties as a protective barrier [13]. The biocompatibility, safety and applicability of the blended gel and biomembrane were confirmed by *in vitro* cytotoxicity, human red blood cell compatibility, and skin irraitation assay [12]. *In vivo* no nauplii death was observed in presence of gel samples at lower concentrations. However, with increasing concentrations the lethality of the gels attributed due to formation of viscous layer on the gills of nauplii and the reduction of dissolved oxygen in water as the high amount of the gel samples led to high viscosity [40]. *In vitro* RBC did not undergo lysis or coagulation in contact with gels indicating its biocompatibility and ansence of osmotic shock [12,40]. After applying the amnion-collagen gels with and without covering membrane on a shaved rat, no edema or erythemas were found [12].

Wound contraction and re-epithelialization are an integral part of the healing process, which closes wounds and keeps it safe from the external environment and shrinkage of the wounded area by repairing the tissues [41]. However, we observed that the rate of wound contraction and re-epithelialization varied from group to group but maintained a similar pattern. The wound contraction on day 16 for the amnion-collagen group with biomembrane showed a statistically more significant ($72 \pm 3.27\%$ with $P < 0.0000009$) contarction rate in comparison to the other groups. Furthermore, the amnion-collagen treated group showed faster re-epithelialization (16.75 ± 0.96 days) in comparison to other rat groups when the wound was covered by membrane. Our results indicate that the combination of amnion and collagen imparted exclusive wound healing properties of both biomaterials [10,11,42], and the addition of membrane top served as an excellent wound covering material which protected the wound area from external stress and maintained moisture as well when the membrane was composed of chitosan and collagen [43]. We did not notice any negative effects on rats' behaviour during the treatment period. The amnion-collagen blended gels with or without dressing membrane rats group were observed with significant average body weight, food intake and water uptake. The protective barrier of biomembrane [13] in combination with hydrogels may help the rats to be healthier and maintain their body weight and eating behaviour. We did not add any growth factors or cells to the gels and membranes. The addition of skin progenitor cells could significantly increase the healing rate. For optimal wound healing, a combination of skin stem cells and biomaterials therefore need to be tested.

5. Conclusion

All biomaterials used in this study were obtained from naturally available bio-waste. The procedures used for the preparation of hydrogels and biomembrane are biologically safe and economically desirable. For instance, we have extracted amnion from C-section derived placenta, collagen from slaughtered rabbit skin, and chitosan from prawn shell. We developed a biocompatible wound healing gel with a combination of amnion and collagen which significantly enhances the efficacy of burn wound healing in the presence of chitosan-collagen wound dressing biomembrane. However, further investigation is required to study the underlying molecular mechanisms of wound healing, in particular which factors are responsible for the healing.

Acknowledgements

The authors acknowledge the technical support and animal facilities from the Institute of Tissue Banking and Biomaterial Research, Atomic Energy Research Establishment, Bangladesh. SM Asaduzzaman acknowledges the support from the Government of Bangladesh, and the International Atomic Energy Agency, Austria. In addition, Md Shaifur Rahman acknowledges support from the German Academic Exchange Service (DAAD-91607303).

Conflict of interest

None to report.

Contribution

MMR and MSR conceived the idea and designed the experiments. MMR and MAU performed the experiment. MMR, MSR and MAU analysed the data. MSR and MMR wrote the manuscript. AS and MLH provided and nurished the animals. MSA, MZH and SMA supervised the works and finally edited the manuscrpt. All authors approved the final version.

References

[1] S. Tripathee and S.J. Basnet, Epidemiology of burn injuries in Nepal: a systemic review, *Burns Trauma* **5** (2017), 10.
[2] S.J. Chong, Abstracts from the 12th Asia Pacific Burn Congress: Singapore. 14–17 August 2019, *Burns Trauma* **7**(Suppl 1) (2019), 27.
[3] H. Debels, M. Hamdi, K. Abberton and W. Morrison, Dermal matrices and bioengineered skin substitutes: a critical review of current options, *Plast Reconstr Surg Glob Open* **3**(1) (2015), e284.
[4] M.S. Rahman, N. Akhtar, M.Z. Hasan and S.M. Asaduzzaman, Human tissue banking in Bangladesh: hope for the patients of massive burns, surgical wound and bone associated complications, *Int J Burns Trauma* **9**(2) (2019), 23–27.
[5] T. John, Human amniotic membrane transplantation: Past, present, and future, *Ophthalmol Clin North Am* **16** (2003), 43–65.
[6] J.T. Shores, A. Gabriel and S. Gupta, Skin substitutes and alternatives: a review, *Adv Skin Wound Care* **20**(9, Part 1) (2007), 493–508.
[7] T. Hirsch, T. Rothoeft, N. Teig, J.W. Bauer, G. Pellegrini, L. De Rosa et al., Regeneration of the entire human epidermis using transgenic stem cells, *Nature* **551**(7680) (2017), 327–332.
[8] A.P. Lesher, R.H. Curry, J. Evans et al., Effectiveness of Biobrane for treatment of partial thickness burns in children, *J Pediatr Surg* **46** (2011), 1759–1763.
[9] A. Rahmanian Schwarz, A. Beiderwieden, L.M. Willkomm et al., A clinical evaluation of Biobrane® and Suprathel® in acute burns and reconstructive surgery, *Burns* **37** (2011), 1343–1348.
[10] S.V. Murphy, A. Skardal, R.A. Nelson Jr, K. Sunnon, T. Reid, C. Clouse, N.D. Kock, J. Jackson, S. Soker and A. Atala, Amnion membrane hydrogel and amnion membrane powder accelerate wound healing in a full thickness porcine skin wound model, *Stem Cells Transl Med* **00** (2019), 1–12.
[11] S.V. Murphy, A. Skardal, L. Song, K. Sutton, R. Haug, D.L. Mack et al., Solubilized amnion membrane hyaluronic acid hydrogel accelerates full-thickness wound healing, *Stem Cells Transl Med* **6**(11) (2017), 2020–2032.
[12] M.S. Rahman, R. Islam, M.M. Rana et al., Characterization of burn wound healing gel prepared from human amniotic membrane and Aloe vera extract, *BMC Complement Altern Med* **19**(1) (2019), 115.
[13] D.J. Indrani, F. Lukitowati and Y. Yulizar, Preparation of chitosan/collagen blend membranes for wound dressing: a study on FTIR spectroscopy and mechanical properties, *IOP Conf. Ser.: Mater. Sci. Eng.* **202** (2017), 012020.

[14] K. Dhaliwal and N. Lopez, Hydrogel dressings and their application in burn wound care, *Br J Community Nurs* **23** (2018), S24–S27.
[15] A. Oryan, M. Jalili, A. Kamali and B. Nikahval, The concurrent use of probiotic microorganism and collagen hydrogel/scaffold enhances burn wound healing: An in vivo evaluation, *Burns* **44**(7) (2018), 1775–1786.
[16] A.T. Iacob, M. Drăgan, N. Gheţu et al., Preparation, characterization and wound healing effects of new membranes based on chitosan, hyaluronic acid and arginine derivatives, *Polymers (Basel)* **10**(6) (2018), 607.
[17] T. Dinh and C. Lewis, Amnion applications in the foot and ankle, *Clin Podiatr Med Surg* **36**(4) (2019), 563–576.
[18] R. Mohan, A. Bajaj and M. Gundappa, Human amnion membrane: potential applications in oral and periodontal field, *J Int Soc Prev Community Dent* **7**(1) (2017), 15–21.
[19] P. Krzyszczyk, R. Schloss, A. Palmer and F. Berthiaume, The role of macrophages in acute and chronic wound healing and interventions to promote pro-wound healing phenotypes, *Front Physiol* **9** (2018), 419.
[20] T. Dai, M. Tanaka, Y.Y. Huang and M.R. Hamblin, Chitosan preparations for wounds and burns: antimicrobial and wound-healing effects, *Expert Rev Anti Infect Ther* **9**(7) (2011), 857–879.
[21] M.S. Rahman, M.M. Rana, L.S. Spitzhorn, N. Akhtar, M.Z. Hasan et al., Fabrication of biocompatible porous scaffolds based on hydroxyapatite/collagen/chitosan composite for restoration of defected maxillofacial mandible bone, *Prog Biomater* **8**(3) (2019), 137–154.
[22] M.A. Khan, S. Ferdous and A.I. Mustafa, Improvement of physico-mechanical properties of chitosan films by photo-curing with acrylic monomers, *J Polym Environ* **13** (2005), 193.
[23] A.M. Abdallah, The effect of hydrogel particle size on water retention properties and availability under water stress, *International Soil and Water Conservation Research* **7**(3) (2019), 275–285.
[24] M.A.Q. Bhuiyan, M.S. Rahman, M.S. Rahaman, M. Shajahan and N.C. Dafader, Improvement of swelling behaviour of poly (vinyl pyrrolidone) and acrylic acid blend hydrogel prepared by the application of gamma radiation, *Organic Chem Curr Res* **4** (2015), 138.
[25] M.M. Bhuyan, N.C. Dafader, K. Hara et al., Synthesis of potato starch-acrylic-acid hydrogels by gamma radiation and their application in dye adsorption, *Int. J. Polym. Sci.* **2016** (2016), 9867859.
[26] S.J. Kim, S.J. Park and S.I. Kim, Synthesis and characteristics of interpenetrating polymer network hydrogels composed of poly(vinyl alcohol) and poly(N-isopropylacrylamide), *React. Funct. Polym.* **55**(1) (2003), 61–67.
[27] W.K. Abdul, K. Sabna, H.A. Shahid, K.S. Rakesh, K. Amit and A. Javed, Formulation development, optimization and evaluation of aloe vera gel for wound healing, *Pharmacog. Magaz.* **9**(1) (2013), 6–10.
[28] H. Bundela and A.K. Bajpai, Designing of hydroxyapatite-gelatin based porous matrix as bone substitute: correlation with biocompatibility aspects, *Pol. Lett.* **2**(3) (2008), 201–213.
[29] S. Bhowmik, J.M.M. Islam, T. Debnath, M.Y. Miah, S. Bhattacharjee and M.A. Khan, Reinforcement of gelatin-based nanofilled polymer biocomposite by crystalline cellulose from cotton for advanced wound dressing applications, *Polymers* **9**(4) (2017), 222.
[30] J. Choi, H. Kim, J. Choi, S.M. Oh, J. Park and K. Park, Skin corrosion and irritation test of sunscreen nanoparticles using reconstructed 3D human skin model, *Environ Health Toxicol* **29** (2014), e2014004.
[31] H.F. Guo, R.M. Ali, R.A. Hamid, A.A. Zaini and H. Khaza'ai, A new model for studying deep partial-thickness burns in rats, *Int J Burns Trauma* **7**(6) (2017), 107–114.
[32] A.A. Mohammadi, B. Sabet and H. Riazi, Human amniotic membrane dressing: an excellent method for outpatient management of burn wounds, *Ira. Jour. of Med. Sci.* **34**(1) (2009), 61–64.
[33] O. Singh, S.S. Gupta, M. Soni, S. Moses, S. Shukla and R.K. Mathur, Collagen dressing versus conventional dressings in burn and chronic wounds: a retrospective study, *J Cutan Aesthet Surg* **4**(1) (2011), 12–16.
[34] M. Jridi, S. Bardaa, D. Moalla, T. Rebaii, N. Souissi, Z. Sahnoun and M. Nasri, Microstructure, rheological and wound healing properties of collagen-based gel from cuttlefish skin, *Int J Biol Macromol* **77** (2015), 369–374.
[35] G. Kravanja, M. Primožič, Ž. Knez and M. Leitgeb, Chitosan-based (Nano) materials for novel biomedical applications, *Molecules* **24**(10) (2019), pii: E1960.
[36] T. Dai, E. Yang, Y. Sun, L. Zhang, L. Zhang, N. Shen, S. Li, L. Liu, Y. Xie, S. Wu and Z. Gao, Preparation and drug release mechanism of CTS-TAX-NP-MSCs drug delivery system, *Int J Pharm* **456**(1) (2013), 186–194.
[37] R.F. El-Kased, R.I. Amer, D. Attia and M.M. Elmazar, Honey-based hydrogel: in vitro and comparative in vivo evaluation for burn wound healing, *Sci Rep* **7**(1) (2017), 9692.
[38] A.W. Khan, S. Kotta, S.H. Ansari, R.K. Sharma, A. Kumar and J. Ali, Formulation development, optimization and evaluation of aloe vera gel for wound healing, *Pharmacogn Mag* **9**(Suppl 1) (2013), S6–S10.
[39] M.X. Chen, K.S. Alexander and G. Baki, Formulation and evaluation of antibacterial creams and gels containing metal ions for topical application, *J Pharm (Cairo)* **2016** (2016), 5754349.

[40] M.N. Khan, J.M.M. Islam and M.A. Khan, Fabrication and characterization of gelatin-based biocompatible porous composite scaffold for bone tissue engineering, *J Biomed Mater Res. Part A.* **100**(11) (2012), 3020–3028.
[41] C.J. Yeh, C.C. Chen, Y.L. Leu, M.W. Lin, M.M. Chiu and S.H. Wang, The effects of artocarpin on wound healing: in vitro and in vivo studies, *Sci Rep* **7**(1) (2017), 15599.
[42] L.E. Dickinson and S. Gerecht, Engineered biopolymeric scaffolds for chronic wound healing, *Front Physiol* **7** (2016), 341.
[43] C. Tangsadthakun, S. Kanokpanont, N. Sanchavanakit, T. Banaprasert and S. Damrongsakkul, Properties of collagen/chitosan scaffolds for skin tissue engineering, *J. Met. Mater. Miner.* **16**(1) (2006), 37–44.

Results - Unpublished

Part E: Generation of iPSCs from Third Trimester AF-MSCs and Differentiation Potential of AF-MSCs into Keratinocyte Like Cells

3.11 Spontaneous Chromosome Loss-gain-loss During iPSCs Generation from Full-term Human AF-MSCs with Chromosomes 18T

Md Shaifur Rahman, Lucas-Sebastian Spitzhorn, Martina Bohndorf, Tanja Fehm, James Adjaye

Abstract

Amniotic fluid mesenchymal cells (AF-MSCs) of female foetus were isolated from early third trimester (29 weeks of gestation) amniotic fluid bearing the trisomy in chromosome 18 (18T-AF-MSCs). These cells were reprogrammed into AF-iPSCs by nucleofection of a combination of two episomal-based plasmids omitting TGFβ, MEK and GSK3β pathway inhibition. The expression of pluripotency-associated markers-OCT4, SOX2, NANOG, KLF4, SSEA4, TRA-1-60, TRA-1-81, and LIN28 were shown by immunostaining and flow cytometry for OCT4. Furthermore, embryoid body (EB) formation and their differentiation ability into the three germ layers-ectoderm, mesoderm and endoderm confirmed the iPSCs status of AF-iPSCs. Karyotype analysis revealed AF-iPSCs with extra 20 chromosomes (20T-AF-iPSCs) but not with chromosome 18 at passage 7. After several more passaging (>P15), we found that the trisomy 20 were lost and converted to normal diploid AF-iPSCs spontaneously. These findings indicate the genomic instability of AF-iPSCs generation from AF-MSCs with trisomy 18. The loss-gain-loss of chromosome during AF-iPSCs generation may be a random event that remain to be clear.

Publication Status: Unpublished work, manuscript in preparation.

This manuscript is reproduced with the permission of all contributors.

Approximated total share of contribution: 70%

Contribution on experimental design, and lab work and realization: JA and MSR conceived the idea. MSR, MB and LSS designed the experiment. MSR and MB performed the experimental work. MSR analysed the data. MSR wrote the initial draft and JA edited the manuscript. All authors read and approved the enclosed version (Please find in the results section).

Brief Reports

Spontaneous chromosome loss-gain-loss during iPSCs generation from full-term human AF-MSCs with chromosome 18T

Md Shaifur Rahman[1], Lucas-Sebastian Spitzhorn[1], Martina Bohndorf[1], Tanja Fehm[2], James Adjaye[1#]

1. Institute for Stem Cell Research and Regenerative Medicine, Medical Faculty, Heinrich-Heine-University Düsseldorf, 40225 Düsseldorf, Germany

2. Department of Obstetrics and Gynaecology, Medical Faculty, Heinrich Heine University Düsseldorf, 40225 Düsseldorf, Germany

[#]Correspondence: james.adjaye@med.uni-duesseldorf.de

Abstract

Amniotic fluid mesenchymal cells (AF-MSCs) of female foetus were isolated from early third trimester (29 weeks of gestation) amniotic fluid bearing the trisomy in chromosome 18 (18T-AF-MSCs). These cells were reprogrammed into AF-iPSCs by nucleofection of a combination of two episomal-based plasmids omitting TGFβ, MEK and GSK3β pathway inhibition. The expression of pluripotency-associated markers-OCT4, SOX2, NANOG, KLF4, SSEA4, TRA-1-60, TRA-1-81, and LIN28 were shown by immunostaining and flow cytometry for OCT4. Furthermore, embryoid body (EB) formation and their differentiation ability into the three germ layers- ectoderm, mesoderm and endoderm confirmed the iPSCs status of AF-iPSCs. Karyotype analysis revealed AF-iPSCs with extra 20 chromosomes (20T-AF-iPSCs) but not with chromosome 18 at passage 7. After several more passaging (>P15), we found that the trisomy 20 were lost and converted to normal diploid AF-iPSCs spontaneously. These findings indicate the genomic instability of AF-iPSCs generation from AF-MSCs with trisomy 18. The loss-gain-loss of chromosome during AF-iPSCs generation may be a random event that remain to be clear.

Background

The trisomy 18 syndrome, also known as Edwards syndrome, is a common chromosomal disorder due to the presence of an extra chromosome 18. Chromosome 18T phenotypes as abnormal development of several tissues and organ of foetus including cardiac malformation, limb anomalies, dolichocephaly and mental disability (Xing *et al*., 2018; Li *et al*., 2017; van Praagh *et al*., 1989). Although chromosome 18 encompass lowest gene density, but 18T has been reported as one of the leading cause of miscarriage and immature birth, and even reported to die within first few months of life. After discovery of iPSCs technology, significant work has undertaken on various genetic disease modelling using iPSCs. However, the pathologic and molecular mechanisms of 18T remain limited. Previously, several workers tried to reprogrammed amniotic fluid cells with 18T (AFCs-18T) into iPSCs (Xing *et al*., 2018; Li *et al*., 2017). Xing et al. (2018) successfully developed one AF-iPSCs-18T line whereas in other

AF-iPSCs-T8 line generated from same AF cells were observed with a gain of extra chromosome 8. In the case of Li *et al*. (2017) attempts, the first few passages of AF-iPSCs maintained 18T, but after 10 passages 18T loss and AF-iPSCs line appeared to be normal. This type of autonomous rescue from chromosome 21T have also been reported (Inoue *et al*., 2019).

It is well evident that iPSCs are prone to genetic and epigenetic instability. Random accumulation of genomic and epigenetic alterations hampers the properties and quality or use of iPSCs in clinical and disease modelling research (Lund *et al*., 2012). These instabilities have been described to be associated with cancers, so such autonomous instability is not desirable in iPSCs preparations. One of the frequent chromosomal aberration is PSCs with 20T, which was reported to increase cell survival with the excessive expression of Bcl-xL (Nguyen *et al*., 2014; Avery *et al*., 2013). Here this study shows an autonomous chromosome loss-gain-loss during iPSCs generation from full-term human AF-MSCs with chromosomes 18T. Nevertheless, how this abnormalities arise, how to get to read out of this unexpected instability during culture and reprogramming is yet to solve.

Materials and Methods

Amniotic fluid cell isolation and culture

Human amniotic fluid were obtained from Department of Obstetrics and Gynaecology, Heinrich Heine University Düsseldorf, Germany with the Institutional ethical approval as well as the informed consent was obtained at time of sample collection to help ensure donor's privacy. Amniotic fluid sample was collected during C-sections (29 weeks of gestation) and processed as described previously (Spitzhorn *et al*., 2017). The cells were cultured in Chang C Medium (Irvine Scientific, USA) containing 88% αMEM (Sigma) with 10% FBS, 1% GlutaMAX, 1% penicillin/streptomycin (all Gibco), 10% Chang B Basal Medium, and 2% Chang C supplement (Irvine Scientific, USA) at 37°C and 5% CO_2. Once attached, the cells were visible after 4–7 days and the medium was changed. Upon attainment of 90% confluency, the cells were detached using TrypLE Express (Thermo Fisher Scientific) and seeded into other plate formats or frozen.

Reprogramming of AF-MSC into induced pluripotent cells (AF-iPSCs)

AF-MSCs were reprogrammed as described previously using a combination of the two episomal based plasmids pEP4EO2SCK2MEN2L and pEP4EO2SET2K (7F1) coding for OCT4, SOX2, NANOG, LIN28, c-MYC and KLF-4 (Bohndorf et al., 2017). Once nucleofected, after 24 hours the culture medium was replaced with N2B27 medium containing DMEM-F12, 1% N-2 Supplement, 2% B27® Supplement without vitamin A, 1% P/S, 0.5% GlutaMAX™, 0.18% 2-Mercaptoethanol, 1% NEAA (all Gibco) and 100 ng/mL FGF2 (Peprotech). This

medium continued for 14 days changed daily. Afterwards N2B27 medium were replaced with StemMACS iPS-Brew XF Medium (Miltenyi, Germany) for rest of days. IPSCs like colonies emerged at two weeks post-nucleofection. However, after three weeks, well-defined distinct iPSC colonies were manually picked, and passaged for expansion on Matrigel®-coated plates in StemMACS iPS-Brew XF Medium.

PCR for vector dilution and sex (*AMEL*) determination

Genomic DNA was extracted from the parental AF-MSCs, AF-iPSCs and the hESCs H1 employing the DNeasy Blood and Tissue Kit (Qiagen). PCRs to confirm vector dilution and *AMEL* analysis were performed using GoTaq® DNA Polymerase (Promega). Primer sequences are exo-*OCT4* (AGTGAGAGGCAACCTGGAGA/ AGGAACTGCTTCCTTCACGA), endo-*OCT4* (GTGGAGGAAGCTGACAACAA/ ATTCTCCAGGTTGCCTCTCA), and *Amel* (ACCTCATCCTGGGCACCCTGGTT/ AGGCTTGAGGCCAACCATCAG).

Immunofluorescence staining

AF-iPSCs and cells of the three germ layers (after EB differentiation) were fixed with 4% paraformaldehyde (PFA) for 15 minutes at room temperature (RT) on a rocking platform. To block for intracellular staining, the buffer contained 10% normal goat serum (NGS; Sigma, Germany), 0.5% Triton X-100, 1% BSA (Sigma, Germany), and 0.05% Tween 20 (Sigma, Germany), all dissolved in PBS. If extracellular structures were to be stained, Triton and Tween were omitted. After blocking for 2 hours at RT, primary antibodies- OCT-4A (C30A3) rabbit mAb number 2840, Rabbit anti-NANOG (4903S), rabbit anti-SOX2 (3579S), LIN28, SSEA4 (MC813) mouse mAb number 4755, TRA-1-60 mouse mAb number 4746, TRA-1-81 mouse mAb number 4745 (CST, USA), rabbit anti-Nestin (Sigma Aldrich; N5413), anti-aSMA (Dako; # M0851) and Rabbit anti-AFP (Cell Signaling Technology, Cat# 2137S) were diluted in blocking buffer/PBS and added to the cells with an incubation time of 1 hour at RT. After washing for three times with 0.05% Tween 20 in PBS, the appropriate secondary Cy3- or Alexa Fluor 488-labelled antibodies (Thermo Fisher Scientific, USA) and Hoechst 33258 dye (Sigma-Aldrich Chemie GmbH, Germany, 1 : 5000 in blocking buffer) were applied for visualization of the primary antibodies and cell nuclei, respectively. Images were taken with a fluorescence microscope (LSM700; Zeiss, Oberkochen, Germany).

Embryoid body (EB) formation

Embryoid body (EB)-based differentiation was performed to confirm pluripotency. Sub-confluent AF-iPSCs were transferred into a T25 flask and were cultured in an upright position for one week in high glucose DMEM, containing 1% NEAA. Afterwards, EBs were transferred onto gelatin coated 12-well plates and allowed to differentiate for 10 to 14 additional days and then fixed and stained for immunofluorescence-based protein detection.

Flow cytometry for OCT4

AF-iPSCs were stained with an APC-coupled OCT4 antibody (Miltenyi, Germany) for 10 minutes at 4°C. Cells were washed with PBS and fixed with 4% PFA for 15 minutes at RT. Fluorescence was measured using the CyAn ADP Flow Cytometer (Dako, USA). Analysis was performed with the Summit4.3 software (Beckman Coulter, USA). Cells stained with an APC isotype control were served as negative control.

Karyotype (G-banding) analysis

Karyotype analysis was performed and evaluated at the Institute of Human Genetics, Heinrich-Heine-University, Düsseldorf.

Results and Discussion

Here we represent the generation of a karyotypically normal AF-iPSCs line from AF-MSCs with trisomy at chromosomes 18 (Li *et al*., 2017). To omit the genomic integration of transgenes by conventional retrovirus-based reprogramming methods, the non-integrating episomal plasmid-based reprogramming was performed by nucleofection of vectors expressing *OCT4*, *SOX2*, *NANOG*, *KLF4*, *c-MYC* and *LIN28* (Bohndorf *et al*., 2017; Slamecka *et al*., 2015; Drews *et al*., 2015). After 14 days, the iPSCs like colony were appeared. Upon several passaging of the picked colony, AF-iPSCs had attained the typical iPSCs morphology (Figure 1). At passage 6 to know whether episomal vectors persisted in iPSCs, the vector dilution of AF-iPSCs was confirmed by analysing expression of exogenous *OCT4* (vector) whereas the endogenous *OCT4* was served as control. At P6, *OCT4* expression from plasmid vectors in iPSCs were not detected indicating that at this stage the loss of vectors. The PCR of AMEL confirmed the sexual identity of AF-iPSCs with the parental AF-MSCs line (Figure 1). Expression of the key pluripotency related transcription factors were observed by immunostaining of OCT4, SOX2, NANOG and KLF4; and the flow cytometry detected more than 90% AF-iPSCs were positive for OCT4 (Li *et al*., 2017; Slamecka *et al*., 2015; Xing *et al*., 2018; Drews *et al*., 2015). In addition, these iPSCs line showed positivity for the pluripotency associated cell surface markers LIN28, SSEA-4, TRA-1-60 and TRA-1-81 (Drews *et al*., 2015) (Figure 1).

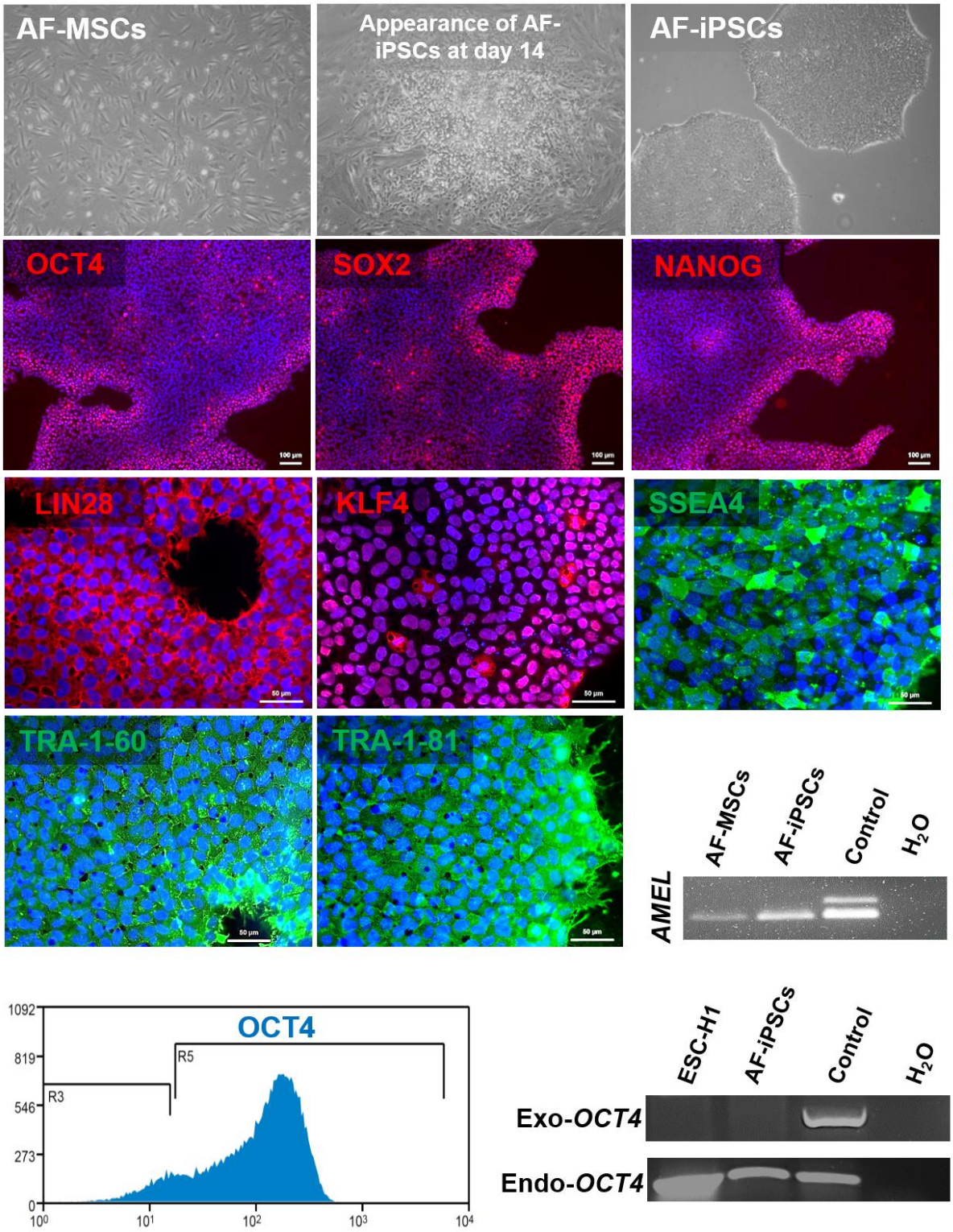

Figure 1: Characterization of AF-iPSCs generated from 18T AF-MSCs. At day 14, iPSCs like cell cluster appeared. Manually picked and subsequent sub-cultured AF-iPSCs observed with the typical iPSC morphology. AF-iPSCs express the pluripotency associated transcription factors OCT4, NANOG, SOX2 and KLF4 as well as the characteristic surface markers LIN28, SSEA-4, TRA-1-60 and TRA-1-81. More than 90% cells were detected positive for OCT4 as shown by flow cytometry analysis. *AMEL* gene PCR represents the same sex background of AF-MSCs and AF-iPSCs. RT-PCR of exo-OCT4 and endo-OCT4 confirms the loss of the reprogramming plasmids.

Tri-lineage differentiation potential had been investigated using the embryoid body (EB)-based spontaneous differentiation *in vitro.* The EB of AF-iPSCs were capable to differentiate into the cell type's representative of the three germ layers- ectoderm (NESTIN), -mesoderm (SMA – smooth muscle actin) and -endoderm (AFP) (Drews *et al*., 2015) (Figure 2).

The karyotype analysis showed that the parental cells (AF-MSCs at P4) contained 18T with the karyotype of 47, XX, +18 [20]/46, XX [4]. Cytogenetic and FISH analysis of the AF-iPSCs (at P6) revealed a karyotype of 47, XX, +18[2]/47, XX, + 20[2]/46, XX [21] with trisomy of 18T (3.4%) and 20T (5.1%). The FISH analysis performed by Leica and Kreatech (Germany) using the probe of BCL2-IGH and ON 20q//SE20 at the location of 18q21//14q32 and 20q12//q11. FISH ISCN is (BCL2x3, IGHx2) [9/231], (D20Z1, S20S108) x [11/215]. Xing *et al*. (2018) established a stable amniotic fluid iPSC line with trisomy 18 successfully. However, in our case, at passage 7, the trisomy AF-iPSCs line were observed with loss of 18T and gain of 20T (47, XX, +20 [18]/46, XX [6]). An interpretation of this AF-iPSCs-T20 that during reprogramming normal AF-MSCs might gain T20 spontaneously instead of translocation of chromosome from T18. Like ours, Xing *et al*. (2018) also described instability of T18 in AF-iPSCs line obtained from same AF cells. After 10 passaging, their iPSCs line gained an extra chromosome 8. In agreement with previously described, we also noticed the spontaneous differentiation of AF-iPSCs line with trisomy that prone to differentiate into neural rosette structure (Xing *et al*., 2018; Li *et al*., 2017). Trisomy 20 mosaicism is one of the most common forms of autosomal mosaicism diagnosed prenatally after amniocentesis (Wallerstein *et al*., 2002). T20 manifests relatively mild clinical features such as growth delay and renal anomalies (Velissariou *et al*., 2002; Ensenauer *et al*., 2005; Djalali *et al*., 1985). The clinical significance of T20 remains unknown. T20 in AF-iPSCs has not previously been described. Therefore, beside stable T18-AF-iPSCs line, establishing stable AF-iPSCs-T20 may aid in a better understanding of the molecular mechanisms underlying T20. Figure 2 shows the representative karyogramm of parental cells (AF-MSCs-T18), AF-iPSCs-T20 (P7) and AF-iPSCs (P15).

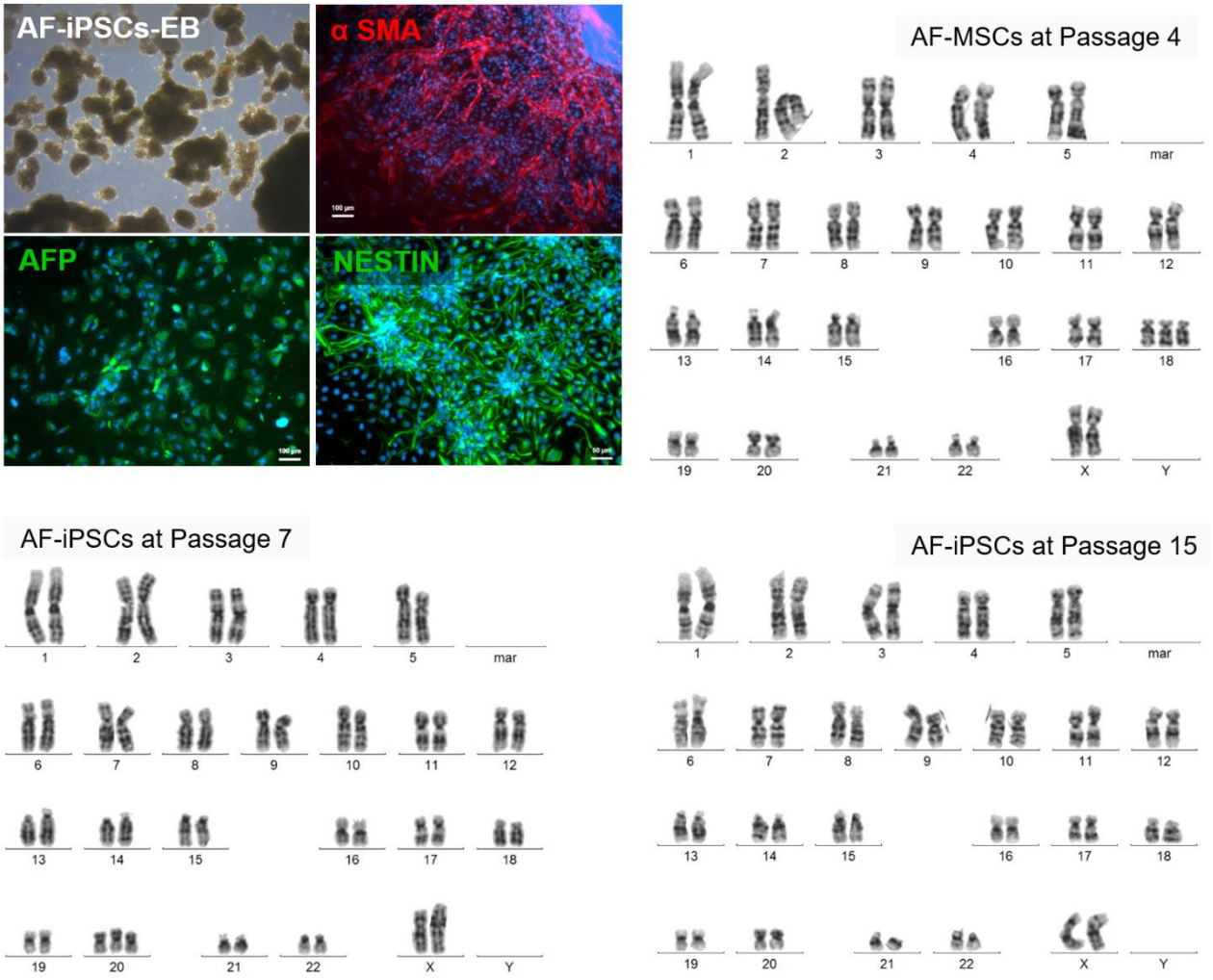

Figure 2: After formation of embryoid bodies (EBs), the cells differentiated spontaneously into all three germ layers *in vitro* and express germ layer specific proteins such as ectoderm (NESTIN), endoderm (AFP) and mesoderm (Alfa-SMA). Karyogramm of parental cells (AF-MSCs-T18), AF-iPSCs-T20 (P7) and AF-iPSCs (P15).

Interestingly, the AF-iPSCs line were observed with a normal karyotype at passage 15 indicating gradual loss-gain-loss of chromosomal instability. Previously Li et al. (2017) tried to generate 18T-iPSCs from amniotic fluid cells, however, after several passages the trisomy lost spontaneously. Another study described about spontaneous rescue from T21 to normal chromosomal arrangement without any genetic manipulation or exposure to irradiation/ chemical (Inoue et al., 2019). *In vitro,* anaphase lagging and chromosome non-disjunction can be the explanation for the gain and loss of full chromosome during mitosis (Nguyen et al., 2013). Cculture condition and culture duration might have effect on the genetic/ epigenetic instability of PSCs (Garitaonandia et al., 2015) indicating the importance of well-defined culture conditions to minimize acquisition of chromosomal abnormalities.

The current findings confirms that AF-18T cells prone to loss/gain/loss trisomy mutation during iPSCs derivation. Establishment of efficient and reproducible method to reprogram AF-MSCs-T18 into stable AF-iPSCs-T18 still need. Nevertheless, how the AF-iPSCs line we established,

exhibiting or switching their genomic instability (chromosomal loss-gain-loss) during passaging is a question to study further.

Acknowledgements

JA acknowledges financial support from the Medical Faculty, Heinrich-Heine-University, Düsseldorf. MSR acknowledge support from the German Academic Exchange Service (DAAD-91607303).

References

Drews K, Matz P, Adjaye J. Generation of iPSC lines from primary human amniotic fluid cells. Stem Cell Res. 2015;15(3):712-714.

Spitzhorn LS, Rahman MS, Schwindt L, *et al*. Isolation and Molecular Characterization of Amniotic Fluid-Derived Mesenchymal Stem Cells Obtained from Caesarean Sections. Stem Cells Int. 2017;2017:5932706.

Slamecka J, Salimova L, McClellan S, *et al*. Non-integrating episomal plasmid-based reprogramming of human amniotic fluid stem cells into induced pluripotent stem cells in chemically defined conditions. Cell Cycle. 2016;15(2):234-249.

Bohndorf M, Ncube A, Spitzhorn LS, Enczmann J, Wruck W, Adjaye J. Derivation and characterization of integration-free iPSC line ISRM-UM51 derived from SIX2-positive renal cells isolated from urine of an African male expressing the CYP2D6 *4/*17 variant which confers intermediate drug metabolizing activity. Stem Cell Res. 2017;25:18-21.

Li T, Zhao H, Han X, *et al*. The spontaneous differentiation and chromosome loss in iPSCs of human trisomy 18 syndrome. Cell Death Dis. 2017;8(10):e3149.

Xing K, Cui Y, Luan J, Zhou X, Shi L, Han J. Establishment of a human trisomy 18 induced pluripotent stem cell line from amniotic fluid cells. Intractable Rare Dis Res. 2018;7(2):94-99.

Van Praagh S, Truman T, Firpo A, *et al*. Cardiac malformations in trisomy-18: a study of 41 postmortem cases. J Am Coll Cardiol. 1989;13(7):1586-1597.

Velissariou V, Antoniadi T, Gyftodimou J, *et al*. Maternal uniparental isodisomy 20 in a foetus with trisomy 20 mosaicism: clinical, cytogenetic and molecular analysis. Eur J Hum Genet. 2002;10(11):694-698.

Ensenauer RE, Shaughnessy WJ, Jalal SM, Dawson DB, Courteau LK, Ellison JW. Trisomy 20 mosaicism caused by a maternal meiosis II error is associated with normal intellect but multiple congenital anomalies. Am J Med Genet A. 2005;134A(2):202-206.

Djalali M, Steinbach P, Schwinger E. *et al*. On the significance of true trisomy 20 mosaicism in amniotic fluid culture. Hum Genet. 1985; 69, 321–326.

Inoue M, Kajiwara K, Yamaguchi A *et al*. Autonomous trisomic rescue of Down syndrome cells. Lab Invest. 2019; 99, 885–897.

Nguyen HT, Geens M, Spits C. Genetic and epigenetic instability in human pluripotent stem cells. Hum Reprod Update. 2013;19(2):187-205. doi:10.1093/humupd/dms048

Lund R, Närvä E. Lahesmaa R. Genetic and epigenetic stability of human pluripotent stem cells. Nat Rev Genet. 2012; 13, 732–744.

Avery S, Hirst AJ, Baker D, Lim CY, Alagaratnam S, Skotheim RI, *et al*. BCL-XL Mediates the Strong Selective Advantage of a 20q11.21 Amplification Commonly Found in Human Embryonic Stem Cell Cultures. Stem Cell Reports. 2013;1: 379–386. pmid:24286026

Nguyen HT, Geens M, Mertzanidou A, Jacobs K, Heirman C, Breckpot K, *et al*. Gain of 20q11.21 in human embryonic stem cells improves cell survival by increased expression of Bcl-xL. Mol Hum Reprod. 2014;20: 168–177. pmid:24217388.

Garitaonandia I, Amir H, Boscolo FS, *et al*. Increased risk of genetic and epigenetic instability in human embryonic stem cells associated with specific culture conditions. PLoS One. 2015;10(2):e0118307.

3.12 Derivation of CK14+/CK5+ Keratinocyte Like Cells from Third Trimester Amniotic Fluid Cells

Md Shaifur Rahman, Lucas Sebastian-Spitzhorn, Tanja Fehm, James Adjaye

Abstract

Primary keratinocyte's invasive collection procedures, finite life span and proliferative capacity in vitro limit clinical use. Amniotic fluid contains heterogeneous mixtures of mesenchymal and epithelial cells. We hypothesized that keratinocyte cells could be derived from amniotic fluid directly or amniotic fluid stem cell can also be differentiated into keratinocyte like status. During culturing of AF cells, at passage zero, a sub-population of AF cells were positive for the basal keratinocyte marker CK14, CK5 and suprabasal CK10, indicating presence of epithelial cells. However, after several passaging (above 3) these cells did not express any keratinocyte markers but mesenchymal marker-Vimentin. These two sub-populations commonly expressed CK19 and CK18. Using a keratinocyte induction media (KIM) containing hrBMP4, we are able to re-induce the basal keratinocyte markers CK14 and CK5 in these cells. These AFSC derived keratinocytes are morphologically as well as in terms of keratinocyte marker expression resembles with the keratinocyte line-HaCat. These keratinocyte-like cells could offer an option to bioengineered epidermis usable for autologous foetal spina bifida repair and other skin wound healing management in future.

Publication Status: Unpublished work, manuscript in preparation.

This manuscript is reproduced with the permission of all contributors.

Approximated total share of contribution: 80%

Contribution on experimental design, and lab work and realization: JA and MSR conceived the idea. MSR and LSS designed the experiment. MSR performed the experimental work. MSR analysed the data. MSR wrote the initial draft and JA edited the manuscript. All authors read and approved the enclosed version (Please find in the results section).

Short Communications

Derivation of CK14$^+$/CK5$^+$ keratinocyte like cells from third trimester amniotic fluid cells

Md Shaifur Rahman[1], **Lucas Sebastian-Spitzhorn**[1], **Tanja Fehm**[2], **James Adjaye**[1, #]

1. Institute for Stem Cell Research and Regenerative Medicine, Heinrich Heine University Düsseldorf, 40225 Düsseldorf, Germany
2. Department of Obstetrics and Gynaecology, Heinrich Heine University Düsseldorf, 40225 Düsseldorf, Germany

[#]Corresponding author: James.Adjaye@med.uni-duesseldorf.de

Abstract

Primary keratinocyte's invasive collection procedures, finite life span and proliferative capacity *in vitro* limit clinical use. Amniotic fluid contains heterogeneous mixtures of mesenchymal and epithelial cells. We hypothesized that keratinocyte cells could be derived from amniotic fluid directly or amniotic fluid stem cell can also be differentiated into keratinocyte like status. During culturing of AF cells, at passage zero, a sub-population of AF cells were positive for the basal keratinocyte marker CK14, CK5 and suprabasal CK10, indicating presence of epithelial cells. However, after several passaging (above 3) these cells did not express any keratinocyte markers but mesenchymal marker-Vimentin. These two sub-populations commonly expressed CK19 and CK18. Using a keratinocyte induction media (KIM) containing hrBMP4, we are able to re-induce the basal keratinocyte markers CK14 and CK5 in these cells. These AFSC derived keratinocytes are morphologically as well as in terms of keratinocyte marker expression resembles with the keratinocyte line-HaCat. These keratinocyte like cells could offer an option to bioengineered epidermis usable for autologous foetal spina bifida repair and other skin wound healing management in future.

Keyword: Amniotic fluid, Amniotic fluid stem cells, Keratinocyte, Cytokeratin14, CK10, CK5.

Introduction

Primary keratinocyte shows characteristics of ageing associated replicative senescence *in vivo* due to short telomere. There are many additional shortcomings such as immune rejection, shortage of donor skin tissue and the spread of skin diseases from skin grafting. Alternatives to skin grafting reported from iPSC and ESC derived-keratinocyte based regenerated epidermis, but there also have ethical challenges, immunological problems, chance of tumorigenicity, and short telomere *in vitro* as well. Therefore, there is an urge of novel cells to regenerate epidermis, which will overcome the current pitfalls.

Human amniotic cells represent immune-privileged cells with characteristics between embryonic and adult stem cells. Extensive research with cell-based therapy suggests that amniotic stem cells harbour enormous therapeutic potentials. It grows easily in culture in absence of senescence, has high expansion potential and retained genomic stability. Initial passages of these cells contains a heterogeneous population of various cell types- such as epithelial and mesenchymal. In 1982, Chen examined the presence of cytokeratin filament of amniotic cells. He observed the presence of cytokeratin in primary culture of AF predominantly in contrast to subcultured fibroblast like AF cells. Previously we described that after several passaging third trimester amniotic fluid stem cells simultaneously expressed both epithelial markers (K19 and K18) and mesenchymal one (Vimentin). These Vimentin positive cells express CD29, CD44, CD73, CD90 and CD105 but not haematopoietic markers. Recently, we observed that AF stem cell express pluripotency-associated markers CD133, c-KIT, SSEA-4, TRA-1-60, and TRA-1-81, indicating their greater differentiation and clinical potentials.

The role of amniotic stem cells conditioned media were tested *in vitro* wound healing and photo aged skin model. For example, a facilitated cell proliferation in the dermal fibroblast, skin epidermal cell, and an accelerated cell migration were noticed in presence of the human amniotic fluid stem cells derived

factors. Additionally, these condition media has observed with the potential to improve damage skin regeneration. Basler and his colleagues differentiated amniotic cells into keratinocyte like cells, which were positive CK8 but not the typical keratinocyte marker 14 (Basler *et al*., 2019). Bone marrow derived mesenchymal cells were differentiated into CK19+/CK18+ epithelial cells using EGF, KGF, HGF and insulin-like growth factor-II (Păunescu *et al*., 2007). In the contexts we hypothesized that the subpopulation of amniotic fluid cells expressing epithelial stem cell marker genes are advantageous as an attractive and novel source of keratinocyte cells for skin regeneration in the long-term culture. In addition, subcultured AF cells can also be possible to differentiate into keratinocyte which yet to be established.

Given the limited success of iPSC and ESC-derived keratinocyte with low proliferative capacity and shortage of skin draft, in near future it will be difficult to provide personalized therapies to patients with varied skin disorders. Therefore, sustained keratinocyte like epithelial cells from amniotic fluid and the differentiated ASC-K could be a novel alternative for regenerative medicine and skin tissue engineering *in vivo* in allo, auto or xenografting and wound healing treatment.

Materials and Methods

Isolation and culture of amniotic fluid-derived cells

Full-term amniotic fluid samples were collected during C-sections of healthy donor from the department of Obstetrics and Gynaecology, Heinrich Heine University Düsseldorf, Germany and kept at 4°C until processed. In general, within 4 hours amniotic fluid were processed and AF cells were isolated as described previously (Spitzhorn et al., 2018, Rahman et al., 2019). Afterwards, the cells were cultured in Chang C Medium (Irvine Scientific, CA, USA) containing 88% αMEM (Sigma, Germanz) with 10% FBS, 1% GlutaMAX, 1% penicillin/streptomycin (all Gibco), 10% Chang B medium, and 2% Chang C supplement (Irvine Scientific, CA, USA) at 37°C and 5% CO_2. After the appearance of initially attached cells (days 3–5), the medium was replaced with fresh media. This heterogenous cell clusters kept in culture to grow until reaching almost 90 % confluency. The AF cells were then detached using TrypLE Express (Thermo Fisher Scientific, USA) and sub-cultured for expansion, experiment or frozen. Immortalized keratinocyte cell line- HaCat (Cell lines service, Germany) were served as positive control. HaCat cells were cultured in MG30 media for expansion (Cell lines service, Germany).

Differentiation of AF cells into keratinocyte like cells

Amniotic fluid cells (AF-MSCs) of passage 3 were differentiated into AF keratinocyte like cells (AF-KC) using the method as described by Sun et al. (2015) and Basler et al. (2019) with modification. We did use unselected cells as after passage 3, the cell compositions in Chang-C media are almost homogenous. First of all, we plated the cells in 12-well plates at a density of 1× 104 cells per well. To convert AF cells into AF-KC, AF cells were cultured in keratinocyte induction media (KIM) for 1 months. KIM composed of 50% keratinocyte basal medium-2 (KBM2) and 50% HaCat cultured condition medium of Keratinocyte growth medium 2 (KGM2) (both medium purchased from Promocell). KBM2 supplemented with 10% FBS, 10 ng/ml rhEGF (R&D Systems, USA), 5 µg/ml insulin (Sigma-Aldrich), 0.5 µg/ml hydrocortisone (Sigma-Aldrich), 1 µg/ml isoproterenol (Sigma-Aldrich), 1.37 ng/ml triiodothyronine (Sigma-Aldrich), 24 µg/ml adenine (Sigma-Aldrich), 0.5 nM hrBMP4 (R&D Systems) and 50 µg/ml ascorbic acid (Sigma-Aldrich). After four weeks, the cells were cultured in KGM2 medium.

Immunofluorescent staining for keratinocyte markers

To analyse the cytokeratin filaments, AF cells (P0 and P3) and AFSC-K were cultured in 12 well plates. At 40–60% confluency, media were aspirated and the cells were washed with PBS (Gibco) and subsequently fixed using 4% PFA (Polysciences Inc., PA, USA) for 15 minutes at RT on a rocking

platform. Then blocking buffer (10% normal goat serum (NGS), 1% BSA, and 0.05% Tween 20 (all Sigma) in PBS) was added to the cells. After blocking for 2 hours at RT, the primary antibodies such as Vimentin (5G3F10) mouse mAb number 3390 (CST, USA, dilution 1:200), Mouse anti-CK18 (Acris Antibodies GmbH, Herford, dilution 1:200), mouse anti-CK14 (Abcam, dilution 1:1000), rabbit anti-CK5 (Abcam, dilution 1:150), mouse anti-CK10 (Novus biologicals, dilution 1:150), rabbit anti-Nestin (Sigma Aldrich Chemie GmbH, Steinheim, dilution 1:1000), Rabbit anti-CK19, NB100-687 (Novus Biologicals, USA, dilution 1:100) were added with an incubation period of 1 hour at RT or overnight at 4°C. Then the cells were washed three times using 0.05% Tween 20 in PBS and followed by addition of the corresponding secondary Cy3-labeled or Alexa Fluor 488-labeled antibodies (Thermo Fisher Scientific, USA) and Hoechst 33258 dye (Sigma-Aldrich Chemie GmbH, Germany) or DAPI (Southern Biotech). The incubation period for secondary antibody and DNA staining were 1 hour at RT under dark condition. Finally, the cell plates were washed three times each five minutes with PBS, and images were taken with a fluorescence microscope (LSM700; Zeiss, Oberkochen, Germany). All pictures were processed with the ZenBlue 2012 Software Version 1.1.2.0. (Carl Zeiss Microscopy GmbH, Jena, Germany). By using same method HaCat cells were also stained as positive control.

Results and Discussion

Primary Culture of Amniotic Fluid Cells

Within four hours upon drawing of full-term C-section derived amniotic fluid; we isolated and cultured the cells in Chang-C media (Spitzhorn *et al*., 2017; Rahman *et al*., 2018). After three days, attached cells were observed and we replaced new media. Albeit this passage zero cells were heterogeneous in terms of morphologies as the cells supposed to be exfoliated from amniotic epithelium membrane, foetal skin, and foetal renal system (Siegel *et al*., 2009; Rosner *et al*., 2012; Rahman *et al*., 2018; Miki *et al*., 2005) (Figure 1). As described by Chen *et al*., (1982), we stained the cells at P0 for the cytokeratin CK14, CK18, CK5, CK19, CK10 and Nestin (Figure 1). We observed a sub-population of these were positive for these keratin filament indicating the presence of epithelial cell types. This is usual, interpreting that these epithelial cells belonging to the amniotic epithelium and/or foetal skin (Murphy *et al*., 2014; Siegel *et al*., 2009). The presence of EGF in amniotic fluid probably help to sustain for keeping the features of differentiated epithelial cell.

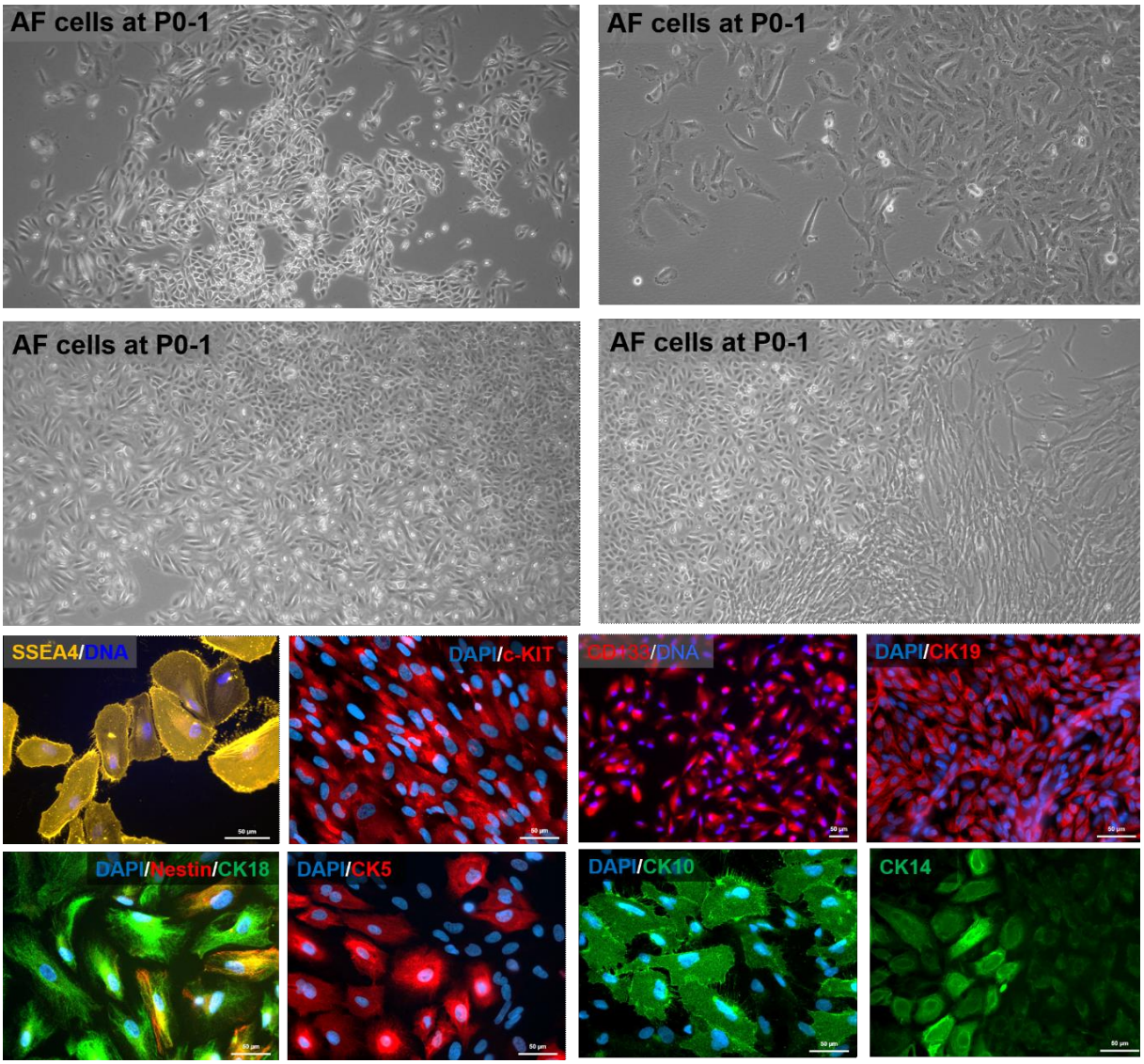

Figure 1: Morphological heterogeneities present in initial attached (passage 0-1) AF cells. A sub-population of these cells express cytokeratin markers CK19, CK10, CK14, CK5, CK18 and Nestin, beside stem cell protein SSEA4, CD133 and c-KIT.

However, after several passaging, these epithelial cells were disappeared and the fibroblastic like cells were leftover, which were relatively homogeneous (Chen *et al*., 1982; Spitzhorn *et al*., 2017; Rahman *et al*., 2019) (Figure 2). Surprisingly, we noticed that the sub cultured (P>3) cells endows MSCs properties-Vim (+) and negative for the typical keratinocyte markers such as CK14, CK5 and CK10 but positive for CK18 and CK19 (Sun *et al*., 2015; Rahman *et al*., 2019). The expression of CK8, CK19, Z01, CD51 and CK18 indicating the instinct nature of human amniotic cells for ectodermal fate (Siegel *et al*., 2009; Sun *et al*., 2015; Basler *et al*., 2019; Rahman *et al*., 2019; Păunescu *et al*., 2007). The methodology including specific culture conditions are yet to be established for maintaining these epithelial cells long-term culture and expansion. Indeed, these cells can be served as a primary source of keratinocyte like linages as it expressed CK14 and CK5 during initial culture.

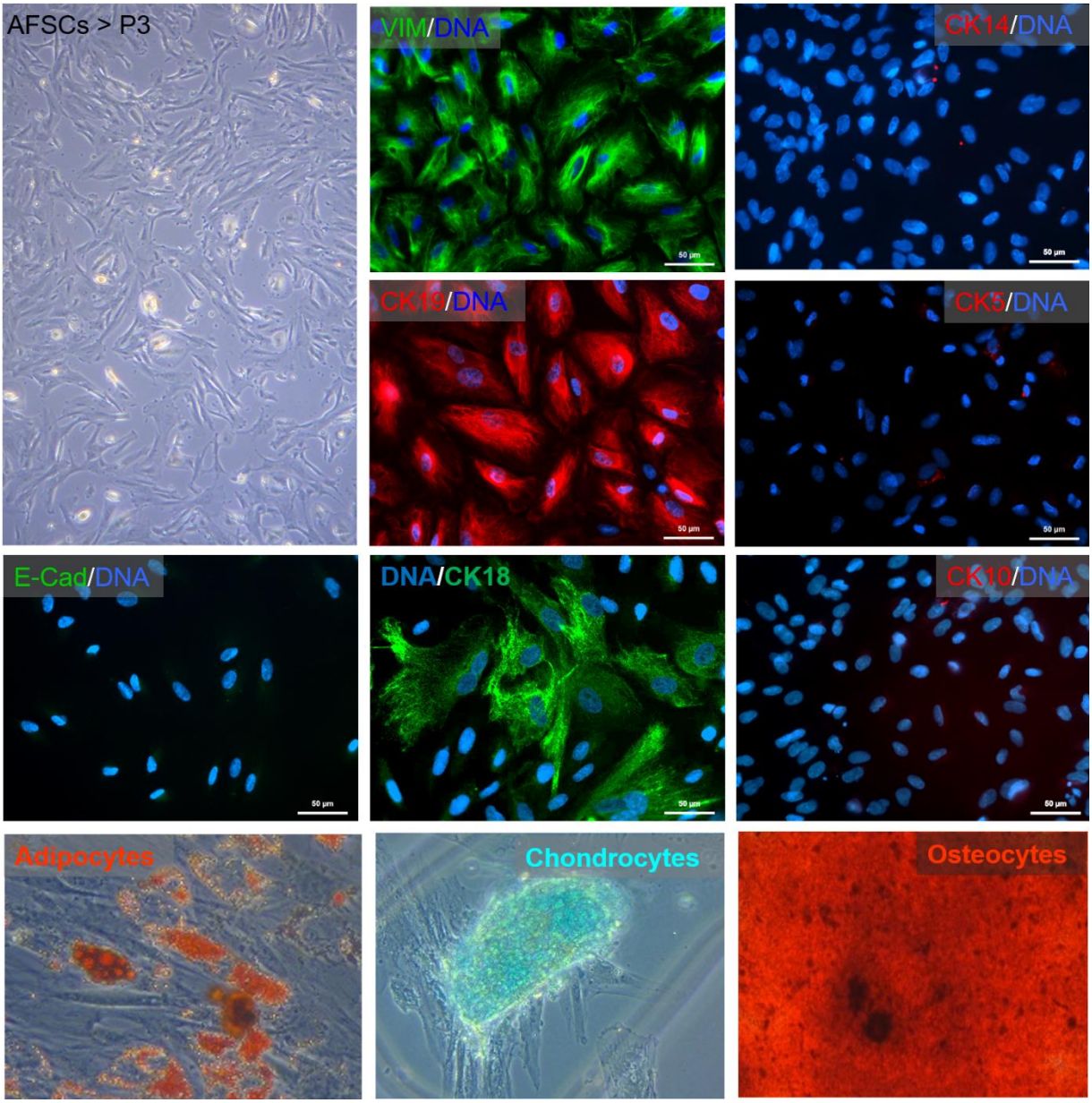

Figure 2: Characteristics of AF cells after several sub-culture (> passage 3, P3) in terms of epithelial marker expressions. Bright field image shows a homogeneous cell type with fibroblast like MSC morphology. They express MSC marker Vimentin and negative for typical epithelial protein E-Cadherin. Although they express cytokeratin filament CK18, CK19 but no expression of the typical epidermal keratinocyte filamentous protein CK14, CK5 and CK10. MSC features of AF cells further confirmed by their differentiation potency towards fat cells, cartilage cells and bone cells.

Differentiation of amniotic fluid cells into keratinocyte like status

The preliminary results of our study indicating that the acquisition of an epithelial phenotype was possible from human AFCs using a specific differentiation protocol described by Sun *et al*., (2015) with modification. After four weeks of AF cells culture in KIM, we observed 60-70% of the cells able to differentiate into keratinocyte like status as evidenced by their rounded polygonal shape and by the expression of CK14, CK5 and CK10 (Figure 3). In our protocol, we used BMP4 and Vitamin C to induce AF cells into keratinocyte like cells (AF-KC), which suppress neural fate and activate ectodermal fate. The role of BMP4 for the derivation of keratinocyte from pluripotent stem cells were already been reported (Kogut *et al*., and Petrova *et al*., 2014). BMP4 supplementation is critical for keratinocyte induction. When we omited BMP4 in induction media, AF cells did not differentiate into epithelial cell like status (Figure 4). One important modification of KIM media formulation was that we replaced

cAMP inducer cholera toxin (CT) with isoproterenol (ISO). ISO a clinically approved pharmaceutical grade synthetic chemical compound and the effects of ISO on human are well studied as replacer of hazardous CT (Ghio *et al*., 2018). Generally, within three weeks in differentiation media the AFCs started to get epithelial morphologies. The fibroblastic morphology of AF cells gradually turned into the rounded or polygonal shape of keratinocyte-like cells indicating time-dependency. However, after 30 days we subcultured the differentiated cells. We noticed that first two passages of AF-KC grown and proliferated well. Afterwards the differentiated cells started to detached and dying out. The morphological analysis of the AF-KC showed that most of the cobblestone-pattern cells were present in the middle of the clusters, indicating that the paracrine effects of the growth factors might play import role during differentiation. Culturing the cells on collagen, gelatin or fibronectin need to be tested which might support to the cells to sustain longer period.

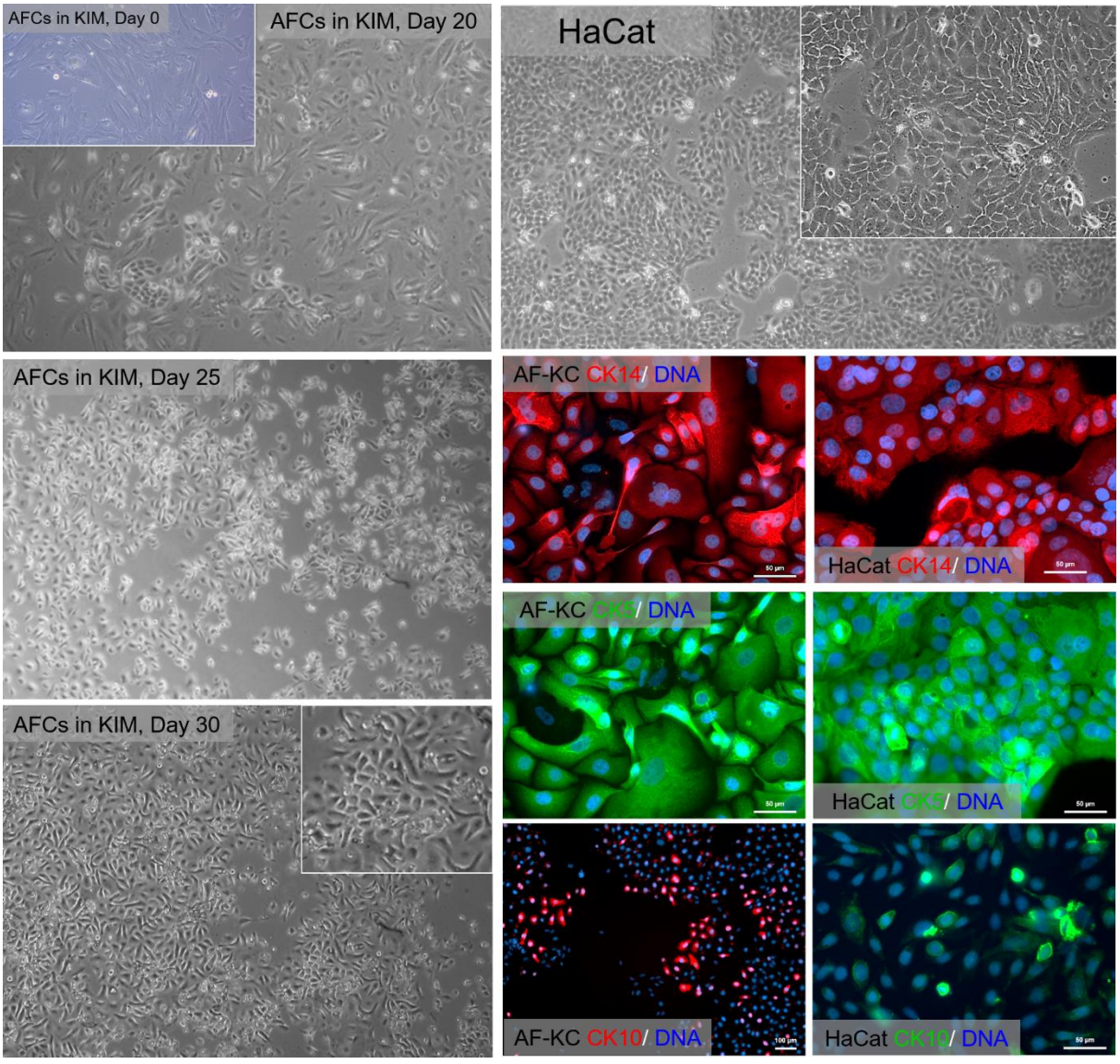

Figure 3: Derivation of keratinocyte like cells from AFCs. Upon culturing of AF cells (>P3) in KIM media, polygonal cobblestone like morphologies were appeared gradually. After 30 days, these KIM induced AF-KC were stained positive for the epidermal keratinocyte filamentous marker CK14, CK5, and CK10. HaCat cells served as positive control.

Since in the starter AF sample contains a subpopulation of epithelial like cells, we cultured passage 0 cells in ready-made keratinocyte growth media (KGM2). We noticed some cluster of epithelial like cells

which indicating media based selection of the cells (Figure 4). Nevertheless, after sub culturing, these cells did not sustain further for proliferation.

Apart from these, when we included SB-431542 (a TGF-ß inhibitor) in KIM, it took two weeks to switch the morphology of AFCs (P3) from mesenchymal to epithelial (Figure 4). In compared to KIM alone, large number of the cells in the plates were attained cobblestone like morphology. The functional analysis of these differentiated cells yet to do. Additionally, we tried to differentiate AFCs (P3) in KIM in presence of A83-01 (an inhibitor of epithelial-to-mesenchymal transition) which apparently seemed does not work (Figure 4).

During the differentiation period, we observed epithelial like morphology in some lines within two weeks in KIM alone. These cells detached from plate in the following week indicating their terminal differentiation. As KGF were described to have proliferation stimulatory effects on AF epithelial cells (Fatimah *et al*., 2012), we added KGF (10ng/ml) in KIM. These KGF treated cells sustained few more days until day 25 but not prolong the proliferation longer period (Figure 4). The results indicated that KGF stimulates the differentiation at early stage towards epithelial cells (Fatimah *et al*., 2012). KGF has been reported as a factor for mesenchymal to epithelial differentiation (Păunescu *et al*., 2007). The paracrine action of KGF might have positive effect on maintenance of epithelial cells in culture, as the differentiated cells are lacking of KGF (Casey and MacDonald, 1997).

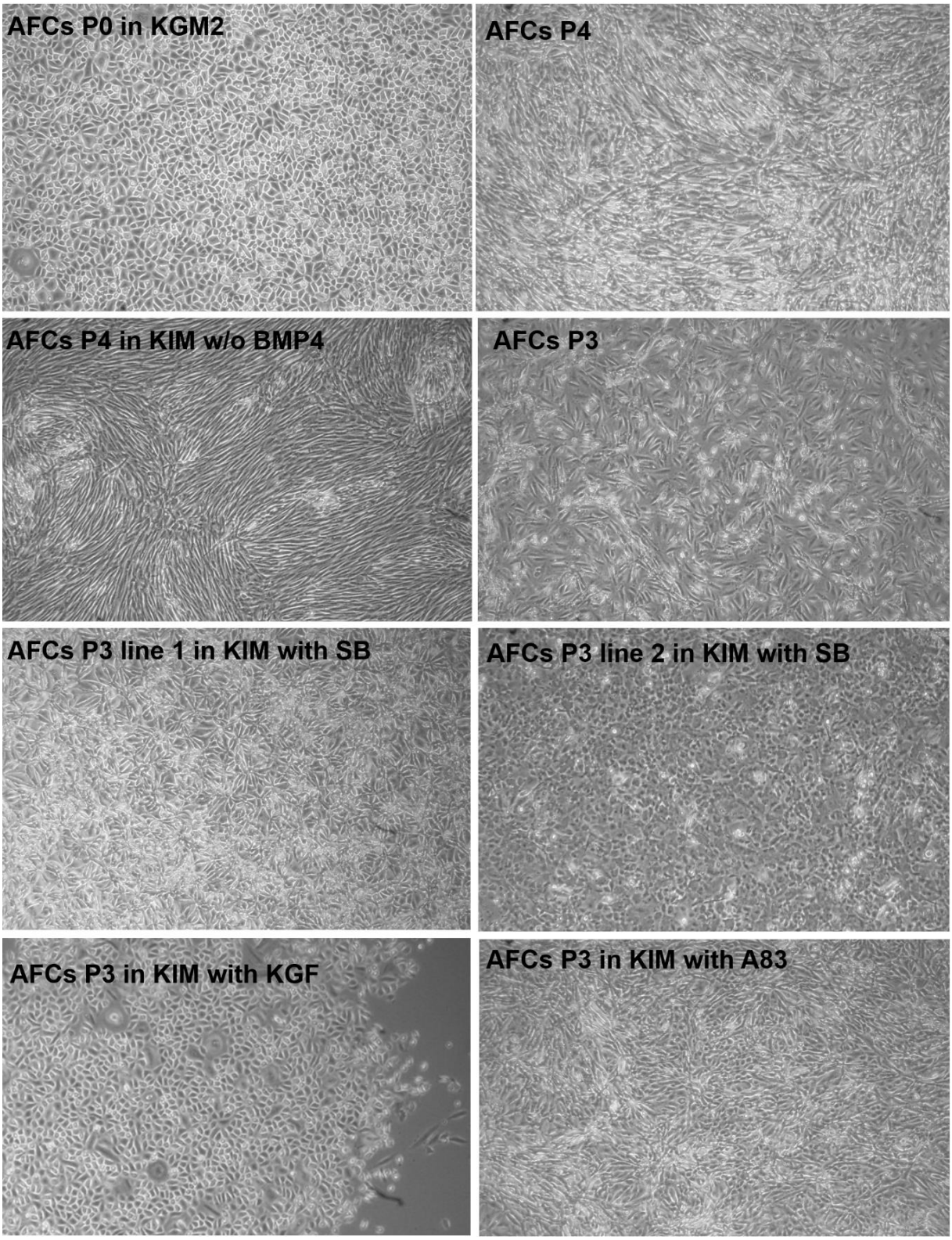

Figure 4: Morphological changes observed during the differentiation when applied various conditions. Culture of AF cells at P0 in KGM2 media. Morphological appearance of AFCs in KIM in absence of BMP4. Effects of the small molecules SB and A83 (epithelial-to-mesenchymal transition inhibitors) on phenotype of AFCs (P3). Effects of epidermal growth factor 7 (KGF) on the proliferation of KIM induced AF-KC differentiatiated cells.

The protocol established by Păunescu et al. (2007) might be an option to derivation of keratinocyte from amniotic cells which yet to examine. The biological characteristics and origin of AF cells suggesting their potential for epidermal regeneration. It could be possible to convert AF cells into keratinocytes, still there is lacking of efficient protocol. The robustness of the methodology for differentiation of AF

cells toward a keratinocyte lineage relies primarily on the ability to maintain long-term keratinocyte cultures.

Acknowledgements
JA and TF acknowledge support from the Medical Faculty, Heinrich-Heine-University, Düsseldorf, Germany. In addition, MSR acknowledge support from the German Academic Exchange Service (DAAD-91607303).

Ethics approval and consent to participate
Full-term amniotic fluid samples from healthy donors were collected from the Department of Obstetrics and Gynaecology, Medical Faculty, Heinrich Heine University Düsseldorf, Germany, with informed patient consent as well as institutional ethical approval.

Authors' contributions
JA and MSR conceived the idea and designed the experiments. TF provided the third-trimester amniotic fluid samples. MSR and LSS isolated the AFCs from third-trimester AF and cultured the AFCs/AF-MSCs. MSR and LSS performed the differentiation experiments and stained the cells. MSR and LSS wrote the manuscript and JA edited it. All authors read and approved the manuscript.

Consent for publication
All authors have agreed to submit this manuscript for publication.

Competing interests
The authors declare that they have no competing interests.

Contributor Information
Md Shaifur Rahman, Email: Shaifur.Rahman@med.uni-duesseldorf.de
Lucas-Sebastian Spitzhorn, Email: Lucas-Sebastian.Spitzhorn@med.uni-duesseldorf.de
Tanja Fehm, Email: Tanja.Fehm@med.uni-duesseldorf.de
James Adjaye, Email: James.Adjaye@med.uni-duesseldorf.de

References
Siegel N, Valli A, Fuchs C, Rosner M, Hengstschläger M. Induction of mesenchymal/epithelial marker expression in human amniotic fluid stem cells. *Reprod Biomed Online*. 2009;19(6):838-846. doi:10.1016/j.rbmo.2009.09.015

Rosner M, Schipany K, Shanmugasundaram B, Lubec G, Hengstschläger M. Amniotic fluid stem cells: future perspectives. *Stem Cells Int*. 2012;2012:741810. doi:10.1155/2012/741810

Miki T, Lehmann T, Cai H, Stolz DB, Strom SC. Stem cell characteristics of amniotic epithelial cells. *Stem Cells* (Dayton, Ohio). 2005;23(10):1549-1559. DOI: 10.1634/stemcells.2004-0357.

Basler M, Pontiggia L, Biedermann T, *et al*. Bioengineering of Fetal Skin: Differentiation of Amniotic Fluid Stem Cells into Keratinocytes. *Fetal Diagnosis and Therapy*. 2020 ;47(3):198-204. DOI: 10.1159/000502181.

Sun Q, Li F, Li H, *et al*. Amniotic fluid stem cells provide considerable advantages in epidermal regeneration: B7H4 creates a moderate inflammation microenvironment to promote wound repair. *Sci Rep*. 2015;5:11560.

Spitzhorn LS, Rahman MS, Schwindt L, *et al*. Isolation and Molecular Characterization of Amniotic Fluid-Derived Mesenchymal Stem Cells Obtained from Caesarean Sections. *Stem Cells Int*. 2017;2017:5932706.

Rahman MS, Spitzhorn LS, Wruck W, *et al*. The presence of human mesenchymal stem cells of renal origin in amniotic fluid increases with gestational time. *Stem Cell Res Ther*. 2018;9(1):113. doi:10.1186/s13287-018-0864-7

Păunescu V, Deak E, Herman D, *et al*. In vitro differentiation of human mesenchymal stem cells to epithelial lineage. *J Cell Mol Med*. 2007;11(3):502-508. doi:10.1111/j.1582-4934.2007.00041.x

Murphy SV, Kidyoor A, Reid T, Atala A, Wallace EM, Lim R. Isolation, cryopreservation and culture of human amnion epithelial cells for clinical applications. *J Vis Exp*. 2014;(94):52085. doi:10.3791/52085.

Ghio SC, Cantin-Warren L, Guignard R, Larouche D, Germain L. Are the Effects of the Cholera Toxin and Isoproterenol on Human Keratinocytes' Proliferative Potential Dependent on Whether They Are Co-Cultured with Human or Murine Fibroblast Feeder Layers?. *Int J Mol Sci*. 2018;19(8):2174. doi:10.3390/ijms19082174.

Casey ML, MacDonald PC. Keratinocyte Growth Factor Expression in the Mesenchymal Cells of Human Amnion. *The Journal of Clinical Endocrinology & Metabolism*. 1997; 82(10): 3319–3323. https://doi.org/10.1210/jcem.82.10.4294.

Fatimah SS, Tan GC, Chua KH, Tan AE, Hayati AR. Effects of epidermal growth factor on the proliferation and cell cycle regulation of cultured human amnion epithelial cells. *Journal of Bioscience and Bioengineering.* 2012;114(2):220-227. DOI: 10.1016/j.jbiosc.2012.03.021.

Kogut I, Roop DR, Bilousova G. Differentiation of human induced pluripotent stem cells into a keratinocyte lineage. *Methods Mol Biol*. 2014;1195:1-12. doi:10.1007/7651_2013_64

Petrova A, Celli A, Jacquet L, *et al*. 3D In vitro model of a functional epidermal permeability barrier from human embryonic stem cells and induced pluripotent stem cells. *Stem Cell Reports*. 2014;2(5):675-689. Published 2014 Apr 24. doi:10.1016/j.stemcr.2014.03.009

4. Discussion

4.1 Third Trimester Amniotic Fluid is a non-invasive Source of Mesenchymal Stem Cells

MSCs in studies today are mostly isolated from the bone marrow, first and second trimester amniotic fluid, and adipose tissues using invasive collection techniques. For instance, BM-MSCs are isolated from the bone marrow using needle apheresis or bone marrow aspiration, and liposuction procedure for obtaining AD-MSCs [Kraft *et al*., 2020; Hequet, 2015; Schneider *et al*., 2017; Savoia *et al*., 2017]. Early trimester amniotic fluid is routinely collected through amniocentesis [Alfirevic *et al*., 2017; Ogilvie and Akolekar, 2014]. There are several limitations and risks associated with the use of these invasive collection procedures, which in turn affect the easiness to obtain the starter material for isolation of MSCs.

Exceptionally, the collection of full-term AF during C-section deliveries could serve as an alternative source of MSCs, which does not require additional invasive or harmful procedures since AF is a clinical side product which routinely discarded in the clinical everyday life. For the purpose of this research, amniotic fluid was collected from the women hospital during C-sections, and processed to isolate the cells. It was observed that BM-MSCs, AD-MSCs and UC-MSCs attached to the cell culture plate within 24 hours [Kern *et al*., 2006] but AF-MSCs took at least three days to attach after plating. The culture conditions, heterogeneous mixture of various cell types, and the presence of a limited number of stem cells could be the reason behind prolonged adherence time to the plastic plate for passage zero. In agreement with Hoehn *et al.,* where he demonstrated a second trimester AF [Hoehn *et al*., 1974; Hoehn and Salk, 1982], we also observed floating cells, and morphologically different types of attached cells- such as fibroblast, epithelial, and mesenchymal like cells. However, all other cell types were diluted out within time by serial passaging except mesenchymal cells. For instance, epithelial-like AF cells were reported to go into senescence with prolonged culture [Wolfrum *et al*., 2010]. In line with these studies, we experienced that after passage three, these cells were homogenous in morphology, and expressed mesenchymal marker-Vimentin and were negative for the typical epithelial marker E-Cadherin.

In conformity to the ISCT criteria [Dominici *et al*., 2006], these third trimester AF derived mesenchymal stem cells did not show the expression of the hematopoietic markers but did express CD73, CD90, and CD105. Of note, the level of expression of this cluster of differentiation could

vary among individuals, sources of cells, and the gestation time, also for AF-MSCs [Tsai *et al*., 2007; Kitala *et al*., 2019]. Similar to BM-MSCs and first trimester AF-MSCs, 3rd term AF-MSCs can readily differentiate into osteogenic, adipogenic and chondrogenic lineages under standard *in vitro* differentiation inducing conditions [Pipino and Pandolfi, 2015; Preitschopf *et al*., 2012; Pievani *et al*., 2014]. Upon the satisfaction of full-term C-section derived AF-MSCs to the ISCT minimal criteria, we analyzed the secreted cytokines using cytokine profiling membrane array. We quantified the presence of cytokines; CCL2, CXCL1, CXCL12, CSF2, ICAM, IL-6, IL-8, IL-21, MIF, and SERPINE1 in the conditioned media from the AF-MSCs culture. This result complied with the secreted cytokines of BM-MSCs, CB-MSCs, kPMSC and placental MSCs as reported from others [Hwang *et al*., 2009; Park *et al*., 2009; Leuning *et al*., 2019]. In agreement to our results, Mirabella and her colleagues also identified proangiogenic and antiangiogenic factors such as VEGF, CXCL12, IL-8, CCL2, IFNγ and IP-10 in AF cells conditioned media [Mirabella *et al*., 2013]. It is well described that these trophic factors secreted by AF-MSCs play an important role in immunomodulation and regeneration during the healing process at the site of impaired tissues either directly or indirectly [Ranzoni *et al*., 2016; Zagoura *et al*., 2012]. The typical MSC features, and trophic factors released by AF-MSCs hold a great therapeutic benefit for MSC based cellular therapies to treat various clinical conditions for different organs such as the heart, skeletal, liver, lung, and the kidneys.

Regarding the pluripotency status of the AFSCs, several publications have reported that, full term AF cells expresses OCT4, NANOG and SOX2 [Moschidou *et al*., 2013; Prusa *et al*., 2003; Moschidou *et al*., 2012]. These results were only demonstrated by immunostaining and real time PCR assays with no further studies addressing their functionality. In contrast, we did not observe these protein expressions in AF-MSCs. Moreover, AF cells do not express the key pluripotency transcription factor OCT4A [Vlahova *et al*., 2019]. The AF cells obtained from first and second trimester of gestation period were also found to be positive for OCT4, NANOG, SOX2, c-MYC, and KLF4 as reported by others [Antonucci *et al*., 2014; Rodrigues *et al*., 2019]. The number of passages, culture methods, media, and the gestational period of cells could influence the expression of pluripotency factors and functionality variabilities. However, we could show that a subpopulation of AF-MSCs express several pluripotency associated proteins such as SSEA4, C-KIT, TRA-1-60, and TRA-1-81. These results relate to the studies on BM-MSCs and mid trimester

AF-MSCs [Moschidou *et al*., 2013; Gang *et al*., 2007; Moschidou *et al*., 2012; Blazquez-Martinez *et al*., 2014]. Based on the variance in the pluripotency associated protein expression in AF-MSC at distinct gestational stages, we interpreted that 1st and 2nd term AFSCs could be more susceptible for reprogramming events.

4.2 Kidney is the Origin of the Full-term Amniotic Fluid-derived Mesenchymal Stem Cells

It is well described that amniotic fluid is composed of fetal urine, which contains a heterogeneous mixture of various cell types [Underwood *et al*., 2005; Sutherland and Bain, 1972; Loukogeorgakis and Coppi, 2017]. After several passaging, a subpopulation of cells known as mesenchymal stem cells grow in the culture dish. [Spitzhorn *et al*., 2017]. There are conflicting results, concerning the origin of the AF cells from the tissue [Da Sacco *et al*., 2018]. Our group reported previously that, germ cells is the origin of the first trimester AFCs [Moschidou *et al*., 2013]. When we analyzed gene ontology term (GO terms) from globally expressed genes in full term AF-MSCs, it was revealed that most of the biological processes related to skeletal and renal system development [Spitzhorn *et al*., 2017]. Additionally, we observed similar morphology among AF-MSCs and kidney biopsy derived renal cells [Zhang *et al*., 2008; Lang *et al*., 2013; Kim *et al*., 2016]. In recent times, renal systems has been identified as the tissue of origin for urine cells [Arcolino *et al*., 2016; Da Sacco *et al*., 2018; Bohndorf *et al*., 2017]. Based on this supporting information, we investigated third trimester AF-MSCs to unravel their origin and the possibility of their kidney origin.

In line with our results, a subpopulation of urine-derived cells was shown to express pluripotency-associated proteins such as C-KIT, SSEA4, TRA-1-60 and TRA-1-81 [Zhang *et al*., 2008; Bharadwaj *et al*., 2013]. We did not observe the expression of OCT4 in full term AF-MSCs, but an elevated level of OCT4 and NANOG were reported in 2nd trimester fetal nephron progenitors by other [Metsuyanim *et al*., 2009]. This finding indicated the declining of expression of stemness associated proteins of renal cells with gestational time. Like a sub-population of renal cells, third trimester AF-MSCs were positive for Vimentin, CK19, CD73, CD90, CD105 and CD133 [Buzhor *et al*., 2013]. In accordance to our studies, preterm neonatal urine cells and fetal renal cells were found to express Vimentin and CD133 but not hematopoietic markers [Arcolino *et al*., 2016]. In addition, a similar multipotent differentiation potential into adipocytes, osteocytes and

chondrocytes were reported for human kidney cells and AF-MSCs [Bharadwaj *et al*., 2013; Nguyen *et al*., 2019]. Moreover, the overlapping cytokine profiles between kPMSCs and AF-MSCs is a supportive evidence for the renal identity of AF-MSCs [Leuning *et al*., 2019; Spitzhorn *et al*., 2017].

In 1972, Sutherland and Bain were able to culture the cells from amniotic fluid (fetal urine). Later on, Da Sacco *et al.* [2017] they reported that these cells can exfoliate from the fetal kidney during the pro-nephron to the meta-nephron transition, and deposit within AF. A subpopulation of these renal cells possessed MSC properties and were reported to be positive for metanephric mesenchyme markers such as SIX2, CITED1, CK19 and PAX2 [Bussolati and Camussi, 2015; Da Sacco *et al*., 2018; Wang *et al*., 2013]. Similar to other previous studies on renal progenitors obtained from developing kidney and neonatal urine [Arcolino *et al*., 2016; Metsuyanim *et al*., 2009; Schedl, 2007; Tong *et al*., 2009; Rosenblum, 2008], AF-MSCs expressed the typical renal markers- SIX2, CITED1, PODXL, LHX1, BRN1 and PAX8. To confirm functionality, we detected that AF-MSCs endocytosed albumin as shown for kidney biopsy-derived and neonatal urine cells [Arcolino *et al*., 2016; Tojo and Kinugasa; 2012; Xinaris *et al*., 2016; Eyre *et al*., 2007]. At transcriptome level, we noticed a similar pattern of gene expression among AF-MSCs, human urine-derived kidney cells-UM51 and kidney biopsy-derived commercially available renal cells HREpCs. The multipotent features similar to MSCs and the renal identity of AF-MSCs, indicate the potentialities of these cells for studying nephrogenesis and regenerative therapy of renal dysfunctionalities.

Of note, the developmental stage formation of nephrons starts at 2nd term and ends up during 3rd trimester of gestation [Little and McMahon, 2012]. Therefore, in principle, there is a synergistic association among the renal developmental regulatory gene expression and the time of gestation. Using a semi quantitative PCR analysis of mRNA samples from distinct trimesters and previously published transcriptome data [Spitzhorn *et al*., 2017; Moschidou *et al*., 2013], we observed a gradual increase in the numbers of renal associated gene expression with gestational time. This result hints towards the increasing expression of genes related to differentiation to form diverse functional cell types and compartmentalization [Little *et al*., 2016; Khoshdel *et al*., 2020]. To identify the basic gene regulatory network involved in the differentiation of AF-MSCs, we stimulated WNT signaling by inhibiting GSK3β using CHIR99201. Like kidney biopsy derived

cells, the expression of renal progenitor protein such as C-KIT and SIX2 decreased upon CHIR99201 treatment. Interestingly, a translocation from nucleus to cytoplasm was found for the renal progenitor associated transcription factor-WT1 as reported previously [Depping *et al*., 2012]. Indeed, the shuttling of WT1 into cytoplasm means the inactivation of transcriptional factor functionality. At genomic level, we observed in line with another study, an upregulation of *BMP7* and downregulation of *SIX2, WT1*, and *CD133* we quantified them in CHIR99201 treated AF-MSCs after differentiation [Musah *et al*., 2017; Park *et al*., 2012; Zeisberg, 2006]. This subset of genes represents putative regulators of self-renewal in renal progenitors, which needs to be confirmed at protein levels. Understanding the molecular mechanisms underlying the maintenance of stemness in renal progenitor cells and their specific differentiation into mature functional cells is important for their application in functional *in vitro* models and for the use in future therapeutically applications.

4.3 Urine is a Non-invasive, Robust and Repetitive Source of Renal Mesenchymal Stem Cells

Around the globe, millions of people are facing kidney-associated diseases such as acute renal injury or a chronic kidney disease [GBD Chronic Kidney Disease Collaboration, 2020]. Current treatment options- dialysis and kidney transplantations faces the challenge of shortage of altruistic kidney donors, high cost, and co-morbidity [Chawla *et al*., 2017]. Indeed, management of kidney patients cripple down health care economy and deteriorate life quality of the post transplanted/regular dialysis patients [Schütte-Nütgen *et al*., 2019; Rodrigue *et al*., 2013; Mannon, 2019]. Due to promising clinical potentials of stem cell-based therapies, scientist awe currently investigating various cells types for transplantation as an alternative treatment option of kidney injuries. These cell types include biopsy derived renal cells, ESC/iPSCs derived kidney cells, BM-MSCs, and AF-MSCs [Rota *et al*., 2019; George *et al*., 2019; Sivanathan and Coates, 2020; Liu *et al*., 2020; Bochon *et al*., 2019, Marcheque *et al*., 2019]. Aforementioned sources could have several shortfalls such as invasive collection methods, high cost, probabilities to form cancer, and robustness of source. Based on these contexts and our previous works on the renal identity of full-term AF-MSCs [Rahman *et al*., 2018], we have explored urine as a non-invasive, repetitive and inexpensive source of renal progenitor cells, in disparity to amniotic fluid or kidney biopsies. We isolated, cultured, and expanded renal progenitors sourced from the urine of healthy adult donors. In contrast to diseased/injured kidney, very limited number of renal progenitor cells are exfoliated

from a healthy kidney [Ingelfinger, 2002; Mulder *et al*., 2020]. However, it was possible to expand urine progenitors up to 12 passages from a single clone of initially attached cells signifying their high proliferation capacity [Romagnani *et al*., 2016; Zhou *et al*., 2011].

In accordance with our findings, renal progenitor cells were shown to express only a subset of pluripotent stem cell related proteins such as CD133, C-KIT, TRA-1-60, TRA-1-81 and SSEA4 [Lazzeri *et al*., 2015; Rahman *et al*., 2018; Zhou *et al*., 2011]. In fact, urine progenitors are bon-fide MSCs as these cells fulfil the ISCT criteria of MSCs [Dominici *et al*., 2006]. Like multipotent MSCs, urine-derived renal cells can give rise to osteoblasts, chondrocytes and adipocytes under appropriate differentiation conditions [Arcolino *et al*., 2016; Rahman *et al*., 2018]. Essentially, these cells lack the key pluripotency-regulating transcription factors-OCT4, SOX2 and NANOG [Babaie *et al*., 2007; Greber *et al*., 2007]. Using a bisulfite sequencing of CpG dinucleotides within the vicinity of the OCT4 promoter of urine progenitors, we observed full methylation within the 5′- regulatory region of the *OCT4* gene showing its inactivated state. Urine-derived cells were observed to secrete molecular factors- such as EGF, GDF, PDGF and Serpin E1 as observed in AF-MSCs and kPMSCs [Leuning *et al*., 2018; Spitzhorn *et al*., 2017; Zhang *et al*., 2014]. The multipotent MSC characteristics of urine stem cells and the cytokines released by these cells are very promising for regenerative therapy of kidney-associated diseases.

For the most important evidence of renal identity of urine-derived cells, we revealed the expression of renal progenitor-regulatory proteins SIX2, CITED1 and WT1 as previously reported [Da Sacco *et al*., 2017; Harari-Steinberg *et al*., 2013; Murphy *et al*., 2012; Combes *et al*., 2018]. The master renal stem cell transcription factor SIX2 maintains self-renewal in association with CITED1 [Mari *et al*., 2015]. However, as reported previously we observed that, only a few percentage of cells expressed CITED1 in the nucleus and mostly cytoplasmic regions [Shi *et al*., 2006]. The shuttling of CITED1 might depend on the phosphorylation condition. Like our studies on AF-MSCs, WT1 were expressed in both the nucleus and the cytoplasm, but more prominently in nucleus [Rahman *et al*., 2018]. It has been described that WT1 interacting cargo Importin regulate the nucleocytoplasmic shuttling, in turn, control the activity of WT1 as a transcription factor [Vajjhala *et al*., 2003; Depping *et al.,* 2012]. In addition to CD133/C-KIT/SIX2 positivity, the progenitor status of urine cells was evidenced by the unmethylated 5′- regulatory region of the *SIX2* gene.

Furthermore, we observed a high similarity between human renal stem cells and urine-derived renal cells on genomic level. Since, we do not have access to kidney biopsy-derived renal progenitors, we did this comparative in silico meta-analysis among publicly available human renal cells transcriptomes [https://www.ncbi.nlm.nih.gov/geo/query/acc.cgi?acc=GSE75949; Lindgren *et al*., 2011] and urine derived renal progenitors. In diagnosis, quantification of Albumin in urine is considered as a proof for renal functionality [Birn and Christensen, 2006]. The albumin filtration (exo/endocytosis) takes place in the nephrons, we performed exogenous Albumin infiltration assay, and revealed that urine-derived renal cells are able to endocytose Albumin as shown by others [Rahman *et al*., 2018; Tojo and Kinugasa, 2012]. Taken all the evidences together, we could say that urine-derived progenitors are multipotent MSCs and originated from kidney.

Kidney is one of the most complex organ systems where at least 26 types of cell orchestrate together to function properly [Quaggin, 2016; Hammerman, 2003]. Therefore, the exact location from where the urine cells are exfoliated still needs to be confirmed. To address this issue, we did FACS analysis of distinct cell preparations, and detected variabilities between the cell samples in terms of the number of cells positive for CD24, CD106, and CD133 expression [Lazzeri *et al*., 2015; Huling and Yoo, 2017; Sagrinati *et al*., 2006; Shrestha *et al*., 2017; Romagnani and Remuzzi, 2014]. We found out that, urine progenitors did not express *PODXL* as analyzed from the urine derived renal cells transcriptome. By definition, CD24+CD106+CD133+*PODXL*- cells are bipotent renal stem cells that have the potential to differentiate into podocyte progenitors CD24+CD106+CD133+PODXL+ or tubular progenitors CD24+CD106-CD133+PODXL-. More specifically as described by others, we could say that CD24+CD133+CD106- urine cells extends from renal tubules and CD24+CD106+CD133+ cells shed from renal capsule [Angelotti *et al*., 2012; Huling and Yoo, 2017].

4.4 Molecular Mechanisms of Self-renewal and Differentiation of Renal Progenitors *in vitro*

Due to the lack of human primary renal progenitor cells in the research environment, the molecular mechanisms of self-renewal and differentiation has not been well-studied using human renal progenitors *in vitro*. Taking the advantages of the non-invasive sources like full term amniotic fluid and adult urine into consideration, we could show that full term AF-MSCs and adult human urine-derived stem cells are renal progenitors [Rahman *et al*., 2018]. Remarkably, these cells are multipotent MSCs, which can maintain self-renewal unlike the biopsy derived differentiated renal

epithelial cells (hREpCs). In an experiment, we stimulated WNT signaling by supplementing the GSK-3β inhibitor- CHIR99021 in urine cell culture media. Upon 2-3 days of treatment, the progenitor cells attained elongated tubular (epithelial) phenotype beside cessation of proliferation. Previous studies have shown similar types of changes for human pluripotent stem cells (ESCs and iPSCs) derived renal epithelial cells [Takasato *et al*., 2014; Brown *et al*., 2015]. The higher correlation co-efficient among the expressed genes of CHIR99021 treated cells and hREpCs further supports the loss of self-renewal.

Upon CHIR99021 induced inhibition of GSK-3β in urine progenitors, we observed a decrease in *SIX2, WT1, CD133* expression and upregulation of *BMP7* as previously identified in AF derived renal progenitors [Rahman *et al*., 2018]. Elevated levels of BMP7 upon differentiation had previously been shown for human renal cell line TK173 with BMP7 being essential for the stimulation of WNT4 during the MET process [Zeisberg *et al*., 2005]. It is well described that FGF signaling is critical for *in vivo* renal development and *in vitro* self-renewal maintenance of renal progenitor cells [Mari *et al*., 2015]. Likewise, we observed a down-regulation of *SIX2* in differentiated renal cells when blocking the FGF signaling using SU5402. Additionally, CHIR treated cells' transcriptome also revealed the suppression of *FGF1*, *FGF2* and *FGF7* beside over expression of *BMP7*. In agreement with other studies, we could show that, activation of WNT signaling and inhibition of FGF signaling led to cessation of self-renewal during nephrogenesis [Brown *et al*., 2011; Dudley *et al*., 1999]. However, we did not analysis which member of the WNT is activated during urine renal progenitor differentiation. Amongst the most significant differentially expressed genes in differentiated-WNT stimulated cells, we identified up-regulation of the WNT targets- *AXIN2, JUN* and *NKD1*. Previously, WNT target genes such as *LATS2*, *AXIN2* and *CTNNB1* were shown to regulate epithelialization of renal stem cells [Reginensi *et al*., 2016; McNeill and Reginensi, 2017]. *In silico* string-based PPI network community cluster analysis detected a hub of regulatory proteins interacted with GSK3β where JUN was positioned as central protein in association with ATF2, STAT3, GATA2 and MAPK1.

In principal, MAPK such as JNK targets SMADs whereas TGFβ/BMPs can also trigger SMADs [Yamaguchi *et al*., 1995; Derynck and Zhang, 2003]. We detected a higher SMAD2/3 and lower SMAD1/5/8 phosphorylation levels in undifferentiated renal progenitors in contrast to

differentiated cells. Based on this work and previously published data in PSCs and AF-MSCs [Rahman *et al*., 2018; Greber *et al*., 2007a; Greber *et al*., 2007b], we could demonstrate that activated FGF signaling maintain self-renewal in urine progenitors by phosphorylation of TGFβ-SMAD2/3 whereas in differentiated cells stimulated WNT/β-Cat signaling activated SMAD1/5/8 phosphorylation, and up-regulate JUN, BMP7 expression. In contrast to mouse renal cells, we understood that a finely tuned balance among the expression of SIX2, WT1, CITED1 and Wnt/β-catenin activity dictates the renal stem cells fate [Park *et al*., 2012; Kobayashi *et al*., 2008; Lindström *et al*., 2018]. There is a substantial difference in the renal development in mouse and human, for example, they differ in timing of kidney formation initiation, scale, lobe formation and progenitor niche organization [Lindström *et al*., 2018; Thiagarajan *et al.,* 2011]. Due to this restricted knowledge transfer from mouse to human, the research on human renal cell material has to be emphasized. Therefore, human urine derived renal cell culture models could be used to investigate the gene regulatory network of self-renewing renal progenitors.

4.5 Reprogramming of AF-MSCs and uMSCs into iPSCs Without Pathways Perturbation

After the seminal discovery by Yamanaka [Takahashi *et al*., 2007], it was well established that forced expression of the key pluripotency factors- OCT4, SOX2, C-MYC and KLF4 is sufficient to convert any cell type into pluripotent embryonic stem cell-like state. First trimester AF cells were reported to express the pluripotency related proteins C-KIT, OCT4, NANOG, and SOX2 at certain level although functionally, they were not pluripotent stem cells. Interestingly, it was possible to induce the c-KIT+ first trimester AF cells into pluripotent state when the culture media and matrix supplemented with valproic acid [Moschidou *et al*., 2012]. Microarray analysis of these valproic acid treated cells contradicted their pluripotency status as they differed from ESCs in terms of global gene expression [Moschidou *et al*., 2013]. In the cases of third trimester AF cells, previously we observed the expression of pluripotency-associated proteins such as C-KIT, SSEA4, TRA-1-60 and TRA-1-81 but not OCT4, SOX2 or NANOG [Spitzhorn *et al*., 2017]. In line with other studies, it could be interpreted that the pluripotency potentials of AF cells inversely proportionally relate with pregnancy period [Rahman *et al*., 2018]. This explanation has further been shown on transcriptome cluster analysis. Based on the above context, we speculated that AF-MSCs are not true pluripotent but are likely to be easily induced into iPSC.

Following our previous reprogramming method, early third trimester AF-MSCs of female fetus bearing the trisomy in chromosomes 18 was reprogrammed by nucleofection using a combination of two episomal-based plasmids omitting TGFβ, MEK and GSK3β pathway inhibition. The trisomy 18 syndrome, also known as Edwards syndrome, is a common chromosomal disorder due to the presence of an extra chromosome 18, either full, mosaic trisomy, or partial trisomy 18q [Cereda and Carey, 2012]. These AF-iPSCs were positive for pluripotent-associated markers- OCT4, SOX2, NANOG, KLF4, SSEA4, TRA-1-60, TRA-1-81, and LIN28 [Li *et al*., 2017; Slamecka *et al*., 2016]. Furthermore, embryoid body (EB) formation and differentiation of the EB into the three germ layers- ectoderm, mesoderm and endoderm were investigated [Li *et al*., 2017]. Interestingly, during the karyotype analysis of AF-iPSCs at passages 7, we found a trisomy in chromosome 20 whereas chromosome 18 was normal. Trisomy 20 mosaicism is one of the most common forms of autosomal mosaicism diagnosed prenatally after amniocentesis [Velissariou *et al*., 2002; Chen et al., 2020]. How a translocation from chromosome 18 to 20 could have happened in early passages of AF-iPSCs culture and therefore calls for further investigations. Since reprogramming is technically sensitive and highly sophisticated, the culture condition or spontaneous translocation could be the reason. However, at passage 15, we observed a normal karyotype in this AF-iPSCs line. Previously, the loss of an extra 18^{th} chromosome and attainment of normal karyotype after 10 passaging were shown in AF-iPSCs with chromosome 18 trisomy [Li *et al*., 2017]. As the chromosomal trisomy including T18 and T20 in corresponding AF-iPSCs lines has not previously been described and the clinical significance remains unknown, the AF-iPSCs line could aid in a better understanding of the molecular mechanisms underlying T18 and T20.

Like the full-term AF-MSCs, adult human UdRPCs' express pluripotency-associated proteins- TRA-1-60, TRA-1-81, SSEA4, C-KIT and CD133 but not the key pluripotency factors such as OCT4 [Rahman *et al*., 2017; Vlahova *et al*., 2019]. Using same protocol as described before [Bonhdorf *et al*., 2017], uMSCs and full-term AF-MSCs were reprogrammed into iPSCs. The pluripotency-associated proteins- TRA-1-60, TRA-1-81, SSEA4, C-KIT and CD133 might facilitate swift converting of these mesenchymal cells into iPSCs. Interestingly, based on the gene expression analysis, GOs of uMSCs-iPSCs in comparison to ESCs detected terms of renal functionality, which denotes kidney as the origin of the uMSCs-iPSCs. The reservation of tissue

of origin identity in iPSCs could be explained by the epigenetic memory [Kim *et al*., 2010; Pavathuparambil Abdul Manaph *et al*., 2018] and could be an advantage in differentiating these iPSCs back into renal cell types.

4.6 Generation of Mesenchymal Stem Cells (iMSCs) from iPSCs and Their Application

Although a large number of MSC based clinical trials are ongoing, there are several issues related to MSCs still under scrutiny. The main issues for scrutiny still remain; the invasive collection procedures, limited autologous cells, donor site morbidity, patients' age of autologous cells as well the *in vitro* properties which could influence the safety and quality from donor to recipient [Wang *et al*., 2014; Spitzhorn *et al*., 2018]. We have shown that iPSCs derived MSCs (iMSCs) is an alternative of native MSCs. As reported before, iPSCs or ESCs can be differentiated into iMSCs and possess all the criteria of a bon-fide MSCs [Chen *et al*., 2012; Hu *et al*., 2015]. Even, like BM-MSCs, iMSCs were observed to release anti-inflammatory, pro-angiogenic and pro-inflammatory factors [Kimbrel *et al*., 2014]. Most importantly, iMSCs were observed to overcome ageing shortfalls and regained rejuvenation properties [Sabapathy and Kumar, 2016]. We compared the transcriptome of iMSCs (derived from aged donor MSCs via iPSCs), fMSCs (young donors) and the MSCs from aged donors. When we considered DNA damage repair and ageing related gene expression amongst the samples, iMSCs differed from aged MSCs but showed similarities with fMSCs. This result indicated the rejuvenation of the iMSCs as it was derived through iPSCs. During the reprogramming of iPSCs from aged MSCs, the reversion of DNA damage and the changes in patterns of epigenetic material could lay behind the gain of fMSC-like the gene expression for DNA damage repair in the iMSCs [Frobel *et al*., 2014]. We also identified a group of genes such as *INHBE*, *DNMT3B*, *POU5F1P1*, *CDKN1C* and *GCNT2* as rejuvenation markers as they were expressed commonly between iMSCs and PSCs but absent in the aged MSCs. The gain of young state and loss of aging signature makes iMSCs a starter cell type with versatile potential for research and applications in contrast to adult MSCs.

Because iMSCs harbor the typical MSC features, iMSCs has undergone preclinical experiments to treat multiple sclerosis, limb ischemia, arthritis, liver damage, bone defects, and wound healing [Sheyn *et al*., 2016; Wang *et al*., 2014; Sabapathy and Kumar, 2016]. Our group previously projected that, iMSCs contribute liver regeneration in a Gunn rats model [Spitzhorn *et al*., 2018]. Although the preclinical outcomes of the iMSCs based therapy are praiseworthy most studies are

employing small animal models with limited prediction value for humans. For instance, iMSCs has been used successfully to reconstruct critical size cranial defect in rats and radial defect in mice in contrast to native MSCs [Sheyn *et al*., 2016].

Preclinical studies of bone regeneration in human-scale larger animal model such as sheep or pigs are limited but most appreciable and accepted as shown for BM-MSCs [Warnke *et al*., 2004; Reichert *et al*., 2012a; Reichert *et al*., 2012b]. For the first time, we transplanted iMSCs loaded on CPG in mini-pig as an *in vivo* weight bearing bone reconstruction model. We differentiated human skin cell derived iPSCs into iMSCs, which had typical MSC features and they expressed the osteogenic transcription factor-*RUNX2 in vitro* [Loebel *et al*., 2015; Jungbluth *et al*., 2019, Komori, 2003]. Without addition of any growth factors, we observed significant bone healing which is comparable to autologous BM concentrate. However, we did not investigate how this cell improve bone regeneration and their long-term effect.

4.7 Fabrication of Biodegradable Gel and Scaffold for Wound Healing and Bone Defect Management

In preclinical stages, AF-MSCs were showed to have promising outcome when used as somatic-cell therapeutics. Recently, cells embedded in bioengineered scaffolds or biodegradable matrices developed from naturally available materials as combined ATMPs (Advance therapeutic medicinal products) are increasing significantly. Since the combined ATMPs consist of cells and *in vitro* prepared matrices, logically this therapeutic could have better effect on tissue regeneration compared to individual application. Concerning skin wound healing gel or matrices preparation as part of combined ATMPs, the applicability of amniotic membrane [Murphy *et al*., 2017], collagen [Singh *et al*., 2011] and *Aloe vera* gel [Khorasani *et al*., 2009] are well reported. We developed a gel from amniotic membrane (AM) and *Aloe vera* (AV) leaves extract, which was compatible for HaCaT and HFF1 *in vitro*. Using a mouse burn wound healing model, we noticed that AM+AV accelerated wound closure through re-epithelialization, wound contraction and angiogenesis. Another example of this type of gel product is AM and Collagen blended hydrogel, which was also found promising for skin wound healing as experimented on rat skin burn healing [Rana *et al*., 2020]. For cell component, first we tried to differentiate AF-MSCs into keratinocyte-like cells following the protocol described previously with minor modification [Sun *et al*., 2015]. However, in our hands the protocol worked only one time out of three trials. We supplemented the

keratinocyte induction media with Isoproterinol instead of Choleratoxin. The differentiated AFSCs (AFSC-K) expressed epidermal markers- K5, K14 and K10. Interestingly, AFSCs were reported to initiate and contribute in skin wound healing process of burn wound mice model [Sun *et al*., 2015]. Thus, the transplantation of AF-MSCs or AFSC-K in combination with the above-described gels need to be tested for wound healing.

Bone fractures for instance; periodontal or load bearing long bone defects are very common in the developing world. The applicability of biomaterial based engineered scaffold are found promising for the use in orthopedic and dental applications, as the living cells can bind with the scaffold and promote tissue regeneration [Rodríguez-Vázquez *et al*. 2015; Echazú *et al*. 2016]. Collagen (Col)-hydroxyapatite (Ha) scaffold is one example, which is investigated for the restoration of the rabbit mandible bone defect [Zhang *et al*. 2013]. As combined ATMPs, human AD- MSCs loaded Col-Ha scaffold were reported to stimulate ectopic bone development upon implantation in the mouse [Calabrese *et al*. 2017]. We have developed a scaffold (Ha-Col1-Cs) from Ha, Col, and Chitosan (Cs), which was compatible for AF-MSCs attachment and growth *in vitro*. Upon transplantation, we observed the restoration of artificially induced maxillofacial defected bone. However, Wang et al. reported that combination of stem cells and scaffold have better bone healing potency than individual applications [Wang et al., 2017a and 2016]. Rat AFSCs premixed with platelet rich plasma (PRP) for restoration of bone defect in a modified rat maxillary alveolar defect model were superior in comparison to the controls [Wang *et al*., 2017b]. For the development of 3D bioengineered matrices, AFSCs were suggested as an effective cell types for repair of large bone defects [Peister *et al*., 2011]. Therefore, for optimal bone healing, a combination of AF-MSCs or uMSCs and scaffolds could represent an alternative.

5. Conclusion and Future Outline

In these studies, we have reported that AF cells can be collected non-invasively from full-term amniotic fluid. A subpopulation out of these cells are MSCs (AF-MSCs). Additionally, AF-MSCs are able to secrete distinct numbers of cytokines and growth factors. Furthermore, these cells could undergo osteogenic differentiation. The trophic factors released by AF-MSCs and the osteogenic potential have great importance for future bone defect related therapies. It is also possible to differentiate AF-MSCs into keratinocyte like cells, which may be useful to generate epidermal sheet near future. The biocompatibility of AF-MSCs with various scaffold have also been demonstrated, thereby as a component of combined tissue-engineered therapeutics, AF-MSCs can be trialed in preclinical settings.

Secondly, we have demonstrated that third trimester AF-MSCs are originally fetal renal cells which exfoliated from the kidney. *In vitro,* we could show that these cells retained self-renewal, express renal markers and endow renal functionality. Therefore, renal originated AF-MSCs might be more appreciable for transplantation, for instance in chronic/acute kidney illness or graft versus host disease. Logically, as these AF-MSCs are renal progenitor cells, they have enormous potentials for renal disease modeling, renal developmental studies, renal repair, and drug screening. Since the kidney is composed of various cells and initial AF samples contains heterogeneous mixture of these cell types, sorting and detection of specific renal cells from AF are still to do.

Thirdly, we described urine as a reliable, non-invasive, repetitive and economical source of renal progenitor cells, in contrast to amniotic fluid or kidney biopsies derived cells. Like AF-MSCs, urine derived renal progenitors are also MSCs, and are able to secrete immunomodulatory and other factors. Urine derived cells express a group of pluripotency related proteins, which make them easy to reprogram them into iPSCs. These renal progenitors and corresponding-iPSCs, with known CYP2D6, might have immense potential for differentiation into renal cells, modelling kidney-related diseases, and nephrotoxicity studies. The beauty of the urine derived renal progenitors is the fact that it can be collected without any invasive procedures. Drug-induced nephrotoxicity is one of the prominent risks associated with the modeling of *in vivo* kidney disease, and possess the risk of toxicity for new drugs awaiting approval as this could compromise the renal system. Here urine derived renal cells could be used *in vitro* to recognize the effect of the novel

drug as soon as possible during drug development. Urine-derived renal progenitors and the corresponding iPSCs may serve as an innovative platform for modeling kidney-related diseases and for drug screening, eventually in combination with tissue engineering approaches. It is therefore possible to generate 3D kidney organoid to mimic the renal system *in vitro*.

Finally, we identified the gene regulatory network for the maintenance of self-renewal in urine-derived renal progenitor cell *in vitro*. Similar to AF-MSCs and PSCs, urine derived renal stem cells maintained self-renewal through active FGF signaling, leading to phosphorylation of TGFβ-SMAD2/3. On the other hand, cessation of self-renewal was observed upon activation of the WNT/β-catenin signaling which upregulated JUN and *BMP7* expression and suppressed *WT1, SIX2, CITED1,* and *CD133* expression. This result unfolded an important understanding related to nephrogenesis *in vitro*. Compared to mouse renal cells, we observed a contradictory that, sustained expression of *Bmp7* is required to maintain self-renewal in mouse renal progenitor cells. Further experimentations are needed to explore the existing human and mouse differences in gene regulatory network in the renal developmental context. This could contribute to a better understanding of the renal development and furthermore to innovative clinical therapies for treating renal diseases.

The research and preclinical applications using AF-MSCs, uMSCs, iMSCs and various cell types differentiated from iPSCs are booming currently. Beside cell-based therapies alone, cells combined with scaffolds (combined Advanced therapy medicinal products (ATMPs)) could be more promising to treat various clinical conditions for different organs including the heart, the skeletal, the liver, the lung, and the kidneys.

6. Conference Talks and Poster Presentation

6.1 Conference Talk/Abstract:

- The FGF, TGFβ and WNT axis modulate self-renewal of human $SIX2^+$ urine derived renal progenitor cells. NRW stem cell network-retreat, Bonn, 2019.

6.2 Conference Abstract/Posters:

- Dissecting the Complexity in Amniotic Fluid-Derived Cells Obtained from Caesarean Sections. 9th International Meeting Stem Cell Network NRW, Münster, 2017.

- Third trimester amniotic fluid harbours mesenchymal stem cells of renal origin. 6th International Meetings of GSCN, Heidelberg, 2018.

- Human fetal foreskin iPSC-derived iMSCs support regeneration in a Goettingen mini-pig bone defect model. Stem Cell Community Day, Düsseldorf, 2018.

- Human urine as a non-invasive source of kidney progenitor cells amenable for nephrotoxicity studies. The European Society for Alternatives to Animal Testing-EUSAAT 2019, Linz, 2019.

- Human fetal foreskin iPSC-derived iMSCs support regeneration in a Goettingen mini-pig bone defect model. 6th International Meetings of GSCN, Heidelberg, 2018.

7. Bibliography

Alcayaga-Miranda F, Cuenca J, Khoury M (2017) Antimicrobial Activity of Mesenchymal Stem Cells: Current Status and New Perspectives of Antimicrobial Peptide-Based Therapies. *Front Immunol.* 8:339. doi:10.3389/fimmu.2017.00339

Alfirevic Z, Navaratnam K, Mujezinovic F (2017) Amniocentesis and chorionic villus sampling for prenatal diagnosis. *Cochrane Database Syst Rev*. 9(9):CD003252. doi:10.1002/14651858.CD003252.pub2

Angelotti ML, Ronconi E, Ballerini L, *et al.* (2012) Characterization of renal progenitors committed toward tubular lineage and their regenerative potential in renal tubular injury. *Stem Cells*. 30(8):1714-1725. doi:10.1002/stem.1130.

Ankrum JA, Ong JF, Karp JM (2014) Mesenchymal stem cells: immune evasive, not immune privileged. *Nat Biotechnol.* 32(3):252-260. doi:10.1038/nbt.2816

Antonucci I, Di Pietro R, Alfonsi M, *et al.* (2014) Human second trimester amniotic fluid cells are able to create embryoid body-like structures in vitro and to show typical expression profiles of embryonic and primordial germ cells. *Cell Transplant.* 23(12):1501-1515. doi:10.3727/096368914X678553

Arcolino FO, Zia S, Held K, Papadimitriou E, Theunis K, Bussolati B, *et al.* (2016) Urine of preterm neonates as a novel source of kidney progenitor cells. *J Am Soc Nephrol*. 27(9):2762–2770. doi:10.1681/ASN.2015060664.

Atala A, Lanza R (2012) Handbook of Stem Cells. Academic Press. ISBN 978-0-12-385943-3.

Babaie Y, Herwig R, Greber B, *et al.* (2007) Analysis of Oct4-dependent transcriptional networks regulating self-renewal and pluripotency in human embryonic stem cells. *Stem Cells*. 25(2):500-510. doi:10.1634/stemcells.2006-0426.

Barboni B, Mangano C, Valbonetti L, Marruchella G, Berardinelli P, Martelli A, *et al.* (2013) Synthetic Bone Substitute Engineered with Amniotic Epithelial Cells Enhances Bone Regeneration after Maxillary Sinus Augmentation. *PLoS One.* 8(5): e63256. https://doi.org/10.1371/journal.pone.0063256.

Barker RA, Parmar M, Studer L, Takahashi J (2017) Human Trials of Stem Cell-Derived Dopamine Neurons for Parkinson's Disease: Dawn of a New Era. *Cell Stem Cell*. 21(5):569-573. doi:10.1016/j.stem.2017.09.014.

Barui A, Datta P (2019) Biophysical factors in the regulation of asymmetric division of stem cells. *Biol Rev Camb Philos Soc*. 94(3):810-827. doi:10.1111/brv.12479.

Behnke J, Kremer S, Shahzad T, *et al.* (2020) MSC Based Therapies-New Perspectives for the Injured Lung. *J Clin Med.* 9(3):682. doi:10.3390/jcm9030682.

Bento G, Shafigullina AK, Rizvanov AA, Sardão VA, Macedo MP, Oliveira PJ (2020) Urine-Derived Stem Cells: Applications in Regenerative and Predictive Medicine. *Cells.* 9(3):573. doi:10.3390/cells9030573.

Berebichez-Fridman R, Montero-Olvera PR (2018) Sources and Clinical Applications of Mesenchymal Stem Cells: State-of-the-art review. *Sultan Qaboos Univ Med J.* 18(3):e264-e277. doi:10.18295/squmj.2018.18.03.002.

Berebichez-Fridman R, Montero-Olvera PR (2018) Sources and Clinical Applications of Mesenchymal Stem Cells: State-of-the-art review. *Sultan Qaboos Univ Med J.* 18(3):e264-e277. doi:10.18295/squmj.2018.18.03.002.

Bharadwaj S, Liu G, Shi Y, *et al.* (2013) Multipotential differentiation of human urine-derived stem cells: potential for therapeutic applications in urology. *Stem Cells*. 31(9):1840-1856. doi:10.1002/stem.1424.

Bianconi E, Piovesan A, Facchin F, *et al.* (2013) An estimation of the number of cells in the human body. *Ann Hum Biol*. 40(6):463-471. doi:10.3109/03014460.2013.807878.

Birn H, Christensen EI (2006) Renal albumin absorption in physiology and pathology. *Kidney Int* . 69(3):440-449. doi:10.1038/sj.ki.5000141.

Blazquez-Martinez A, Chiesa M, Arnalich F, Fernandez-Delgado J, Nistal M, De Miguel MP (2014) c-Kit identifies a subpopulation of mesenchymal stem cells in adipose tissue with higher telomerase expression and differentiation potential. *Differentiation*. 87(3-4):147-160. doi:10.1016/j.diff.2014.02.007.

Bochon B, Kozubska M, Surygała G, *et al.* (2019) Mesenchymal Stem Cells-Potential Applications in Kidney Diseases. *Int J Mol Sci.* 20(10):2462. doi:10.3390/ijms20102462.

Bohndorf M, Ncube A, Spitzhorn LS, Enczmann J, Wruck W, Adjaye J (2017) Derivation and characterization of integration-free iPSC line ISRM-UM51 derived from SIX2-positive renal cells isolated from urine of an African male expressing the CYP2D6 *4/*17 variant which confers intermediate drug metabolizing activity. *Stem Cell Res.* 25:18-21. doi:10.1016/j.scr.2017.10.004.

Brink TC, Demetrius L, Lehrach H, Adjaye J (2009) Age-related transcriptional changes in gene expression in different organs of mice support the metabolic stability theory of aging. *Biogerontology.* 10:549-564.

Brown AC, Adams D, de Caestecker M, Yang X, Friesel R, Oxburgh L (2011) FGF/EGF signaling regulates the renewal of early nephron progenitors during embryonic development. *Development*. 138(23):5099-5112. doi:10.1242/dev.065995.

Brown AC, Muthukrishnan SD, Oxburgh L (2015) A synthetic niche for nephron progenitor cells. *Dev Cell.* 34(2):229-241. doi:10.1016/j.devcel.2015.06.021.

Bukowiecki R, Adjaye J, Prigione A (2014) Mitochondrial function in pluripotent stem cells and cellular reprogramming. *Gerontology.* 60(2):174-182. doi:10.1159/000355050.

Bulut Ö, GÜrsel İ (2020) Mesenchymal stem cell derived extracellular vesicles: promising immunomodulators against autoimmune, autoinflammatory disorders and SARS-CoV-2 infection. *Turk J Biol.* 44(3):273-282. doi:10.3906/biy-2002-79.

Bussolati B, Camussi G (2015) Therapeutic use of human renal progenitor cells for kidney regeneration. *Nat Rev Nephrol*.11(12):695-706. doi:10.1038/nrneph.2015.126.

Buzhor E, Omer D, Harari-Steinberg O, *et al.* (2013) Reactivation of NCAM1 defines a subpopulation of human adult kidney epithelial cells with clonogenic and stem/progenitor properties. *Am J Pathol*.;183(5):1621-1633. doi:10.1016/j.ajpath.2013.07.034.

Calabrese G, Giuffrida R, Forte S, Fabbi C, Figallo E, Salvatorelli L, Memeo L, Parenti R, Gulisano M, Gulino R (2017) Human adipose-derived mesenchymal stem cells seeded into a collagen-hydroxyapatite scaffold promote bone augmentation after implantation in the mouse. *Sci Rep.* 7:7110. https://doi.org/10.1038/s41598-017-07672-0

Caplan AI (1991) Mesenchymal stem cells. *J Orthop Res*. 9(5):641-650. doi:10.1002/jor.1100090504.

Cargnoni A, Romele P, Bonassi Signoroni P, *et al.* (2020) Amniotic MSCs reduce pulmonary fibrosis by hampering lung B-cell recruitment, retention, and maturation. *Stem Cells Transl Med.* 10.1002/sctm.20-0068. doi:10.1002/sctm.20-0068.

Carlos Andrés Chacón-Martínez, Janis Koester, Sara A (2018) Signaling in the stem cell niche: regulating cell fate, function and plasticity. *Development.* 145:dev165399.

Cereda A, Carey JC (2012) The trisomy 18 syndrome. *Orphanet J Rare Dis.* 7:81. doi:10.1186/1750-1172-7-81.

Chawla, L., Bellomo, R., Bihorac, A *et al.* (2017) Acute kidney disease and renal recovery: consensus report of the Acute Disease Quality Initiative (ADQI) 16 Workgroup. *Nat Rev Nephrol*. 13:241–257. https://doi.org/10.1038/nrneph.2017.2.

Chen CP, Kuo YL, Chern SR, *et al.* (2020) Prenatal diagnosis of low-level mosaic trisomy 20 by amniocentesis in a pregnancy with a favorable outcome. *Taiwan J Obstet Gynecol.* 59(2):327-330. doi:10.1016/j.tjog.2020.01.026.

Chen CY, Rao SS, Tan YJ, *et al*. (2019) Extracellular vesicles from human urine-derived stem cells prevent osteoporosis by transferring CTHRC1 and OPG. *Bone Res*. 7:18. doi:10.1038/s41413-019-0056-9.

Chen YS, Pelekanos RA, Ellis RL, Horne R, Wolvetang EJ, Fisk NM (2012) Small molecule mesengenic induction of human induced pluripotent stem cells to generate mesenchymal stem/stromal cells. *Stem Cells Transl Med*. 1(2):83-95. doi:10.5966/sctm.2011-0022.

Cheung TH, Rando TA (2013) Molecular regulation of stem cell quiescence. *Nat Rev Mol Cell Biol.* 14(6):329-340. doi:10.1038/nrm3591.

Chrzanowski W, Kim SY, McClements L (2020) Can Stem Cells Beat COVID-19: Advancing Stem Cells and Extracellular Vesicles Toward Mainstream Medicine for Lung Injuries Associated With SARS-CoV-2 Infections. *Front Bioeng Biotechnol.* 8:554. doi:10.3389/fbioe.2020.00554.

Combes AN, Wilson S, Phipson B, *et al.* (2018) Haploinsufficiency for the Six2 gene increases nephron progenitor proliferation promoting branching and nephron number. *Kidney Int.* 93(3):589-598. doi:10.1016/j.kint.2017.09.015.

Cooper K, Viswanathan C (2011) Establishment of a mesenchymal stem cell bank. *Stem Cells Int.* 2011;2011:905621.

Da Sacco S, Perin L, Sedrakyan S (2018) Amniotic fluid cells: current progress and emerging challenges in renal regeneration. *Pediatr Nephrol*. 33(6):935-945. doi:10.1007/s00467-017-3711-7.

Da Sacco S, Thornton ME, Petrosyan A, *et al.* (2017) Direct Isolation and Characterization of Human Nephron Progenitors. *Stem Cells Transl Med*. 6(2):419-433. doi:10.5966/sctm.2015-0429.

De Coppi P, Bartsch G Jr, Siddiqui MM, *et al*. (2007) Isolation of amniotic stem cell lines with potential for therapy. *Nat Biotechnol*. 25(1):100-106. doi:10.1038/nbt1274

de Witte SF, Franquesa M, Baan CC, Hoogduijn MJ (2016) Toward Development of iMesenchymal Stem Cells for Immunomodulatory Therapy. *Front Immunol.* 6:648. doi:10.3389/fimmu.2015.00648.

Depping R, Schindler SG, Jacobi C, Kirschner KM, Scholz H (2012) Nuclear transport of Wilms' tumour protein Wt1 involves importins α and β. *Cell Physiol Biochem*. 29(1-2):223-232. doi:10.1159/000337603.

Derynck R, Zhang YE (2003) Smad-dependent and Smad-independent pathways in TGF-beta family signalling. *Nature*. 425(6958):577-584. doi:10.1038/nature02006.

Dominici M, Le Blanc K, Mueller I, *et al*. (2006) Minimal criteria for defining multipotent mesenchymal stromal cells. The International Society for Cellular Therapy position statement. *Cytotherapy.* 8(4):315-317. doi:10.1080/14653240600855905.

Donnelly H, Salmeron-Sanchez M, Dalby MJ (2018) Designing stem cell niches for differentiation and self-renewal. *J R Soc Interface.* 15: 20180388. http://dx.doi.org/10.1098/rsif.2018.0388.

Drews K, Matz P, Adjaye J (2015) Generation of iPSC lines from primary human amniotic fluid cells. *Stem Cell Res.*15(3):712-714. doi:10.1016/j.scr.2015.11.003.

Dubich T, Wirth D (2018) Function or Expansion: How to Investigate Cells of Human Blood Vessels. *Front. Young Minds*. 6:25. doi: 10.3389/frym.2018.00025.

Dudley AT, Godin RE, Robertson EJ (1999) Interaction between FGF and BMP signaling pathways regulates development of metanephric mesenchyme. *Genes Dev*. 13(12):1601-1613. doi:10.1101/gad.13.12.1601.

Duscher D, Rennert RC, Januszyk M, Anghel E, *et al.* (2014) Aging disrupts cell subpopulation dynamics and diminishes the function of mesenchymal stem cells. *Sci Rep.* 4:7144.

Echazú MIA, Tuttolomondo MV, Foglia ML, Mebert AM, Alvarez GS, Desimone MF (2016) Advances in collagen, chitosan and silica biomaterials for oral tissue regeneration: from basics to clinical trials. *J Mater Chem B.* 4:6913–6929. https://doi.org/10.1039/C6TB02108E

Evans M, Kaufman M (1981) Establishment in culture of pluripotential cells from mouse embryos. *Nature.* 292:154–156. https://doi.org/10.1038/292154a0.

Eyre J, Ioannou K, Grubb BD, *et al.* (2007) Statin-sensitive endocytosis of albumin by glomerular podocytes. *Am J Physiol Renal Physiol*. 292(2):F674-F681. doi:10.1152/ajprenal.00272.2006.

Fan Y, Chong YS, Choolani MA, Cregan MD, Chan JK (2010) Unravelling the mystery of stem/progenitor cells in human breast milk. *PLoS One.* 5(12):e14421. doi:10.1371/journal.pone.0014421.

Friedenstein AJ, Gorskaja JF, Kulagina NN (1976) Fibroblast precursors in normal and irradiated mouse hematopoietic organs. *Experimental Hematology.* 4 (5): 267–74.

Frobel J, Hemeda H, Lenz M, Abagnale G, Joussen S, Denecke B, Sarić T, Zenke M, Wagner W (2014) Epigenetic rejuvenation of mesenchymal stromal cells derived from induced pluripotent stem cells. *Stem Cell Reports.* 3(3):414-22. doi:10.1016/j.stemcr.2014.07.003.

Galipeau J, Sensébé L (2018) Mesenchymal Stromal Cells: Clinical Challenges and Therapeutic Opportunities. *Cell Stem Cell.* 22(6):824-833. doi:10.1016/j.stem.2018.05.004.

Gang EJ, Bosnakovski D, Figueiredo CA, Visser JW, Perlingeiro RC (2007) SSEA-4 identifies mesenchymal stem cells from bone marrow. *Blood*. 109(4):1743-1751. doi:10.1182/blood-2005-11-010504.

GBD Chronic Kidney Disease Collaboration (2020) Global, regional, and national burden of chronic kidney disease, 1990-2017: a systematic analysis for the Global Burden of Disease Study 2017. *Lancet*. 395(10225):709-733. doi:10.1016/S0140-6736(20)30045-3.

George SK, Abolbashari M, Kim TH, *et al.* (2019) Effect of Human Amniotic Fluid Stem Cells on Kidney Function in a Model of Chronic Kidney Disease. *Tissue Eng Part A*. 25(21-22):1493-1503. doi:10.1089/ten.TEA.2018.0371.

Graffmann N, Spitzhorn LS, Martins S, Rahman MS, Nguyen L, Adjaye J (2020) Stem Cell Therapy. In: Hock F, Gralinski M (eds) *Drug Discovery and Evaluation: Methods in Clinical Pharmacology*. Springer, Cham.

Greber B, Lehrach H, Adjaye J (2007a) Silencing of core transcription factors in human EC cells highlights the importance of autocrine FGF signaling for self-renewal. *BMC Dev Biol.* 7:46. doi:10.1186/1471-213X-7-46.

Greber B, Lehrach H, Adjaye J (2007b) Fibroblast growth factor 2 modulates transforming growth factor beta signaling in mouse embryonic fibroblasts and human ESCs (hESCs) to support hESC self-renewal. *Stem Cells*. 25(2):455-464. doi:10.1634/stemcells.2006-0476.

Greenberg BE (2015) Reprogramming to Pluripotency Using Small Molecule Compounds. *Theses and Dissertations (ETD)*. Paper 97. http://dx.doi.org/10.21007/etd.cghs.2015.0117.

Guan J, Zhang J, Li H, *et al.* (2015) Human Urine Derived Stem Cells in Combination with β-TCP Can Be Applied for Bone Regeneration. *PLoS One*. 10(5):e0125253. doi:10.1371/journal.pone.0125253.

Hammerman MR (2003) Tissue engineering the kidney. *Kidney Int*. 63(4):1195-1204. doi:10.1046/j.1523-1755.2003.00890.x.

Harari-Steinberg O, Metsuyanim S, Omer D, *et al.* (2013) Identification of human nephron progenitors capable of generation of kidney structures and functional repair of chronic renal disease. *EMBO Mol Med.* 5(10):1556-1568. doi:10.1002/emmm.201201584.

Hariharan K, Stachelscheid H, Rossbach B, *et al.* (2019) Parallel generation of easily selectable multiple nephronal cell types from human pluripotent stem cells. *Cell Mol Life Sci.* 76(1):179-192. doi:10.1007/s00018-018-2929-2.

Hauser PV, De Fazio R, Bruno S, *et al.* (2010) Stem cells derived from human amniotic fluid contribute to acute kidney injury recovery. *Am J Pathol.* 177(4):2011-2021. doi:10.2353/ajpath.2010.091245

Hequet O (2015) Hematopoietic stem and progenitor cell harvesting: technical advances and clinical utility. *J Blood Med*. 6:55-67. doi:10.2147/JBM.S52783.

Herz F, Schermer A, Koss LG (1979) Short-term culture of epithelial cells from urine of adults. *Proc Soc Exp Biol Med.* 161:153–157.

Hoehn H, Bryant EM, Karp LE, Martin GM (1974) Cultivated cells from diagnostic amniocentesis in second trimester pregnancies. I. Clonal morphology and growth potential. *Pediatr Res.* 8(8):746-754. doi:10.1203/00006450-197408000-00003.

Hoehn H, Salk D (1982) Morphological and biochemical heterogeneity of amniotic fluid cells in culture. *Methods Cell Biol*. 26:11-34. doi:10.1016/s0091-679x(08)61362-x.

https://www.ncbi.nlm.nih.gov/geo/query/acc.cgi?acc=GSE75949

Hu G, Li Q, Niu X, *et al.* (2015) Exosomes secreted by human-induced pluripotent stem cell-derived mesenchymal stem cells attenuate limb ischemia by promoting angiogenesis in mice. *Stem Cell Res Ther.* 6:10. https://doi.org/10.1186/scrt546.

Hu K (2014) Vectorology and factor delivery in induced pluripotent stem cell reprogramming. *Stem Cells Dev.* 23(12):1301-1315. doi:10.1089/scd.2013.0621.

Huling J, Yoo JJ (2017) Comparing adult renal stem cell identification, characterization and applications. *J Biomed Sci.* 24(1):32. doi:10.1186/s12929-017-0339-7.

Hwang JH, Shim SS, Seok OS, *et al.* (2009) Comparison of cytokine expression in mesenchymal stem cells from human placenta, cord blood, and bone marrow. *J Korean Med Sci.* 24(4):547-554. doi:10.3346/jkms.2009.24.4.547.

Ingelfinger JR (2002) Nephrogenic adenomas as renal tubular outposts. *N Engl J Med*. 347(9):684-686. doi:10.1056/NEJMe020084.

Jungbluth P, Spitzhorn L, Grassmann J. *et al*. (2019) Human iPSC-derived iMSCs improve bone regeneration in mini-pigs. *Bone Res.* 7:32. https://doi.org/10.1038/s41413-019-0069-4.

Kern S, Eichler H, Stoeve J, Klüter H, Bieback K (2006) Comparative analysis of mesenchymal stem cells from bone marrow, umbilical cord blood, or adipose tissue. *Stem Cells*. 24(5):1294-1301. doi:10.1634/stemcells.2005-0342.

Khoshdel Rad N, Aghdami N, Moghadasali R (2020) Cellular and Molecular Mechanisms of Kidney Development: From the Embryo to the Kidney Organoid. *Front Cell Dev Biol*. 8:183. doi:10.3389/fcell.2020.00183.

Khoury M, Cuenca J, Cruz FF, Figueroa FE, Rocco PRM, Weiss DJ (2020)Current status of cell-based therapies for respiratory virus infections: applicability to COVID-19. *Eur Respir J*. 55(6):2000858. doi:10.1183/13993003.00858-2020.

Kim EY, Page P, Dellefave-Castillo LM, McNally EM, Wyatt EJ (2016) Direct reprogramming of urine-derived cells with inducible MyoD for modeling human muscle disease. *Skelet Muscle*. 6:32. doi:10.1186/s13395-016-0103-9.

Kim K, Doi A, Wen B, *et al.* (2010) Epigenetic memory in induced pluripotent stem cells. *Nature*. 467(7313):285-290. doi:10.1038/nature09342.

Kimbrel EA, Kouris NA, Yavanian GJ, *et al.* (2014) Mesenchymal stem cell population derived from human pluripotent stem cells displays potent immunomodulatory and therapeutic properties. *Stem Cells Dev*. 23(14):1611-1624. doi:10.1089/scd.2013.0554.

King NM, Perrin J (2014) Ethical issues in stem cell research and therapy. *Stem Cell Res Ther.* 5(4):85. doi:10.1186/scrt474.

Kitala D, Klama-Baryła A, Misiuga M, *et al.* (2019) Heterogeneous Mixture of Amniotic Cells is Likely a Better Source of Stem Cells than Adipose Tissue. *Arch. Immunol. Ther. Exp.* 67:189–196. https://doi.org/10.1007/s00005-019-00538-5.

Knoepfler PS (2009) Deconstructing stem cell tumorigenicity: a roadmap to safe regenerative medicine. *Stem Cells.* 27(5):1050-1056. doi:10.1002/stem.37.

Kobayashi A, Valerius MT, Mugford JW, *et al.* (2008) Six2 defines and regulates a multipotent self-renewing nephron progenitor population throughout mammalian kidney development. *Cell Stem Cell*. 3(2):169-181. doi:10.1016/j.stem.2008.05.020.

Koike C, Zhou K, Takeda Y, *et al.* (2014) Characterization of amniotic stem cells. *Cellular Reprogramming.* 16(4):298–305. doi: 10.1089/cell.2013.0090.

Komori, T (2003) Requisite roles of Runx2 and Cbfb in skeletal development. *J. Bone Min. Metab.* 21:193–197.

Khorasani G, Hosseinimehr SJ, Azadbakht M, Zamani A, Mahdavi MR (2009) Aloe versus silver sulfadiazine creams for second-degree burns: a randomized controlled study. *Surg Today.* 39(7):587–91.

Kot M, Baj-Krzyworzeka M, Szatanek R, Musiał-Wysocka A, Suda-Szczurek M, Majka M (2019) The Importance of HLA Assessment in "Off-the-Shelf" Allogeneic Mesenchymal Stem Cells Based-Therapies. *Int J Mol Sci.* 20(22):5680. doi:10.3390/ijms20225680.

Kraft DL, Walck ER, Carrasco A, *et al.* (2020) The MarrowMiner: A Novel Minimally Invasive and Effective Device for the Harvest of Bone Marrow. *Biol Blood Marrow Transplant*. 26(2):219-229. doi:10.1016/j.bbmt.2019.08.027.

Lang R, Liu G, Shi Y, *et al.* (2013) Self-renewal and differentiation capacity of urine-derived stem cells after urine preservation for 24 hours. *PLoS One*. 8(1):e53980. doi:10.1371/journal.pone.0053980.

Lawlor KT, Zappia L, Lefevre J, *et al.* (2019) Nephron progenitor commitment is a stochastic process influenced by cell migration. *Elife*. 8:e41156. doi:10.7554/eLife.41156.

Lazarus HM, Haynesworth SE, Gerson SL, Rosenthal NS, Caplan AI (1995) Ex vivo expansion and subsequent infusion of human bone marrow-derived stromal progenitor cells (mesenchymal progenitor cells): implications for therapeutic use. *Bone Marrow Transplant*. 16(4):557-564.

Lazzeri E, *et al.* (2007) Regenerative potential of embryonic renal multipotent progenitors in acute renal failure. *J. Am. Soc. Nephrol.* 18:3128–38. doi: 10.1681/ASN.2007020210.

Lazzeri E, Ronconi E, Angelotti ML*, et al.* (2015) Human Urine-Derived Renal Progenitors for Personalized Modeling of Genetic Kidney Disorders. *J Am Soc Nephrol.* 26(8):1961-1974. doi:10.1681/ASN.2014010057.

Leuning, D.G., Beijer, N.R.M., du Fossé, N.A. *et al.* (2018) The cytokine secretion profile of mesenchymal stromal cells is determined by surface structure of the microenvironment. *Sci Rep.* 8:7716. https://doi.org/10.1038/s41598-018-25700-5.

Li T, Zhao H, Han X, *et al.* (2017) The spontaneous differentiation and chromosome loss in iPSCs of human trisomy 18 syndrome. *Cell Death Dis.* 8(10):e3149. doi:10.1038/cddis.2017.565.

Lian Q, Zhang Y, Zhang J, *et al.* (2010) Functional mesenchymal stem cells derived from human induced pluripotent stem cells attenuate limb ischemia in mice. *Circulation.* 121(9):1113-1123. doi:10.1161/CIRCULATIONAHA.109.898312.

Liang CC, Shaw SW, Huang YH, Lin YH, Lee TH (2017) Bladder Transplantation of Amniotic Fluid Stem Cell may Ameliorate Bladder Dysfunction After Focal Cerebral Ischemia in Rat. *Stem Cells Transl Med.* 6(4):1227-1236. doi:10.1002/sctm.16-0212.

Lin T, Wu S (2015) Reprogramming with Small Molecules instead of Exogenous Transcription Factors. *Stem Cells Int.* 2015:794632. doi:10.1155/2015/794632.

Linder D (1976) Culture of cells from the urine and bladder washings of adults. *Somatic Cell Genet.* 2:281–283.

Lindgren D, Boström AK, Nilsson K, *et al.* (2011) Isolation and characterization of progenitor-like cells from human renal proximal tubules. *Am J Pathol*. 178(2):828-837. doi:10.1016/j.ajpath.2010.10.026.

Lindström NO, McMahon JA, Guo J, *et al*. (2018) Conserved and Divergent Features of Human and Mouse Kidney Organogenesis. *J Am Soc Nephrol.* 29(3):785-805. doi:10.1681/ASN.2017080887

Little M, Combes A, Takasato M (2016) Understanding kidney morphogenesis to guide renal tissue regeneration. *Nat Rev Nephrol.* 12**:** 624–635. https://doi.org/10.1038/nrneph.2016.126.

Little MH, Kairath P (2017) Does Renal Repair Recapitulate Kidney Development?. *J Am Soc Nephrol.* 28(1):34-46. doi:10.1681/ASN.2016070748.

Little MH, McMahon AP (2012) Mammalian kidney development: principles, progress, and projections. *Cold Spring Harb Perspect Biol*. 4(5):a008300. doi:10.1101/cshperspect.a008300.

Liu X, Rui T, Zhang S, Ding Z (2019) Heterogeneity of MSC: Origin, Molecular Identities, and Functionality. *Stem Cells Int*. 2019:9281520. doi:10.1155/2019/9281520.

Liu Y, Ma W, Liu B. *et al.* (2017) Urethral reconstruction with autologous urine-derived stem cells seeded in three-dimensional porous small intestinal submucosa in a rabbit model. *Stem Cell Res Ther.* 8:63. https://doi.org/10.1186/s13287-017-0500-y.

Liu, D., Cheng, F., Pan, S. *et al.* (2020) Stem cells: a potential treatment option for kidney diseases. *Stem Cell Res Ther.* 11:249. https://doi.org/10.1186/s13287-020-01751-2.

Loebel C, Czekanska EM, Bruderer M, Salzmann G, Alini M Stoddart MJ (2015) *In vitro* osteogenic potential of human mesenchymal stem cells is predicted by Runx2/Sox9 ratio. *Tissue Engineering Part A.* 21(1-2):115-123.

Loukogeorgakis SP, De Coppi P (2017) Concise Review: Amniotic Fluid Stem Cells: The Known, the Unknown, and Potential Regenerative Medicine Applications. *Stem Cells.* 35(7):1663-1673. doi:10.1002/stem.2553

Lukomska B, Stanaszek L, Zuba-Surma E, Legosz P, Sarzynska S, Drela K (2019) Challenges and Controversies in Human Mesenchymal Stem Cell Therapy. *Stem Cells Int*. 2019:9628536. doi:10.1155/2019/9628536.

Manaph NPA, Al-Hawwas M, Bobrovskaya L, Coates PT, Zhou XF (2018) Urine-derived cells for human cell therapy. *Stem Cell Res. Ther.* 9:189. doi: 10.1186/s13287-018-0974-2.

Mannon RB (2019) Acute Kidney Injury in Kidney Transplants: New Insights. *Nephron*. 143(3):193-196. doi:10.1159/000500550.

Marcheque J, Bussolati B, Csete M, Perin L (2019) Concise Reviews: Stem Cells and Kidney Regeneration: An Update. *Stem Cells Transl Med.* 8(1):82-92. doi:10.1002/sctm.18-0115.

Mari C, Winyard P (2015) Concise Review: Understanding the Renal Progenitor Cell Niche In Vivo to Recapitulate Nephrogenesis In Vitro. *Stem Cells Transl Med.* 4(12):1463-1471. doi:10.5966/sctm.2015-0104

Martin GR (1981) Isolation of a pluripotent cell line from early mouse embryos cultured in medium conditioned by teratocarcinoma stem cells. *Proc Natl Acad Sci.* 78(12):7634-7638. doi:10.1073/pnas.78.12.7634.

Matz P, Adjaye J (2016) Episomal-based generation of an iPS cell line from human fetal foreskin fibroblasts. *Stem Cell Res.* 16(1):67-69. doi:10.1016/j.scr.2015.12.009.

McNeill H, Reginensi A (2017) Lats1/2 Regulate Yap/Taz to Control Nephron Progenitor Epithelialization and Inhibit Myofibroblast Formation. *J Am Soc Nephrol*. 28(3):852-861. doi:10.1681/ASN.2016060611.

Megges M, Oreffo RO, Adjaye J (2016) Episomal plasmid-based generation of induced pluripotent stem cells from fetal femur-derived human mesenchymal stromal cells. *Stem Cell Res.* 16(1):128-132. doi:10.1016/j.scr.2015.12.013

Metsuyanim S, Harari-Steinberg O, Buzhor E, *et al.* (2009) Expression of stem cell markers in the human fetal kidney. *PLoS One.* 4(8):e6709. doi:10.1371/journal.pone.0006709.

Mirabella T, Gentili C, Daga A, Cancedda R (2013) Amniotic fluid stem cells in a bone microenvironment: driving host angiogenic response. *Stem Cell Res*. 11(1):540-551. doi:10.1016/j.scr.2013.02.006.

Mitalipov S, Wolf D (2009) Totipotency, pluripotency and nuclear reprogramming. *Adv Biochem Eng Biotechnol.*114:185-199. doi:10.1007/10_2008_45.

Morigi M, De Coppi P (2014) Cell therapy for kidney injury: different options and mechanisms--mesenchymal and amniotic fluid stem cells. *Nephron Exp Nephrol.* 126(2):59. doi:10.1159/000360667.

Morrison SJ, Kimble J (2006) Asymmetric and symmetric stem-cell divisions in development and cancer. *Nature*. 441(7097):1068-1074. doi:10.1038/nature04956

Morrison SJ, Spradling AC (2008) Stem cells and niches: mechanisms that promote stem cell maintenance throughout life. *Cell.* 132(4):598-611. doi:10.1016/j.cell.2008.01.038.

Moschidou D, Drews K, Eddaoudi A, Adjaye J, de Coppi P, Guillot PV (2013a) Molecular signature of human amniotic fluid stem cells during fetal development. *Current Stem Cell Research & Therapy.* 8(1):73–81. doi: 10.2174/1574888X11308010009.

Moschidou D, Mukherjee S, Blundell MP, *et al.* (2012) Valproic acid confers functional pluripotency to human amniotic fluid stem cells in a transgene-free approach. *Mol Ther*. 20(10):1953-1967. doi:10.1038/mt.2012.117.

Moschidou D, Mukherjee S, Blundell MP, *et al.* (2013b) Human mid-trimester amniotic fluid stem cells cultured under embryonic stem cell conditions with valproic acid acquire pluripotent characteristics. *Stem Cells Dev*. 22(3):444-458. doi:10.1089/scd.2012.0267.

Moskalev AA, Shaposhnikov MV, Plyusnina EN, Zhavoronkov A, Budovsky A, Yanai H, Fraifeld VE (2013) The role of DNA damage and repair in aging through the prism of Koch-like criteria. *Ageing Res Rev.* 12(2):661-84.

Motamedi FJ, Badro DA, Clarkson M, *et al.* (2014) WT1 controls antagonistic FGF and BMP-pSMAD pathways in early renal progenitors. *Nat Commun*. 5:4444. doi:10.1038/ncomms5444

Mulder J, Sharmin S, Chow T, *et al.* (2020) Generation of infant- and pediatric-derived urinary induced pluripotent stem cells competent to form kidney organoids. *Pediatr Res.* 87(4):647-655. doi:10.1038/s41390-019-0618-y.

Murphy AJ, Pierce J, de Caestecker C, *et al.* (2012) SIX2 and CITED1, markers of nephronic progenitor self-renewal, remain active in primitive elements of Wilms' tumor. *J Pediatr Surg.* 47(6):1239-1249. doi:10.1016/j.jpedsurg.2012.03.034.

Murphy SV, Skardal A, Song L, et al. (2017) Solubilized Amnion Membrane Hyaluronic Acid Hydrogel Accelerates Full-Thickness Wound Healing. *Stem Cells Transl Med.* 6(11):2020-2032. doi:10.1002/sctm.17-0053

Musah S, Mammoto A, Ferrante TC, *et al.* (2017) Mature induced-pluripotent-stem-cell-derived human podocytes reconstitute kidney glomerular-capillary-wall function on a chip. *Nat Biomed Eng*. 1:0069. doi:10.1038/s41551-017-0069.

Nguyen L, Spitzhorn LS, Adjaye J (2019) Constructing an Isogenic 3D Human Nephrogenic Progenitor Cell Model Composed of Endothelial, Mesenchymal, and SIX2-Positive Renal Progenitor Cells. *Stem Cells Int*. 2019:3298432. doi:10.1155/2019/3298432.

Noronha IL, Cavaglieri RC, Janz FL, *et al*. (2011) The potential use of stem cells derived from human amniotic fluid in renal diseases. *Kidney Int Suppl*. 1(3):77-82. doi:10.1038/kisup.2011.18

Noronha NC, Mizukami A, Caliári-Oliveira C, *et al.* (2019) Priming approaches to improve the efficacy of mesenchymal stromal cell-based therapies. *Stem Cell Res Ther.* 10(1):131. doi:10.1186/s13287-019-1224-y

O'Brien LL, Guo Q, Bahrami-Samani E, *et al.* (2018) Transcriptional regulatory control of mammalian nephron progenitors revealed by multi-factor cistromic analysis and genetic studies. *PLoS Genet.*14(1):e1007181. doi:10.1371/journal.pgen.1007181

Ogilvie C, Akolekar R (2014) Pregnancy Loss Following Amniocentesis or CVS Sampling-Time for a Reassessment of Risk. *J Clin Med*. 3(3):741-746. doi:10.3390/jcm3030741

Ouyang B, Sun X, Han D, Chen S, Yao B, Gao Y, *et al.* (2014) Human Urine-Derived Stem Cells Alone or Genetically-Modified with FGF2 Improve Type 2 Diabetic Erectile Dysfunction in a Rat Model. *PLoS One*. 9(3): e92825. https://doi.org/10.1371/journal.pone.0092825

Ouyang B, Xie Y, Zhang C, *et al.* (2019) Extracellular Vesicles From Human Urine-Derived Stem Cells Ameliorate Erectile Dysfunction in a Diabetic Rat Model by Delivering Proangiogenic MicroRNA. *Sex Med.* 7(2):241-250. doi:10.1016/j.esxm.2019.02.001.

Park CW, Kim KS, Bae S, *et al.* (2009) Cytokine secretion profiling of human mesenchymal stem cells by antibody array. *Int J Stem Cells.* 2(1):59-68. doi:10.15283/ijsc.2009.2.1.59.

Park JS, Ma W, O'Brien LL, *et al.* (2012) Six2 and Wnt regulate self-renewal and commitment of nephron progenitors through shared gene regulatory networks. *Dev Cell*. 23(3):637-651. doi:10.1016/j.devcel.2012.07.008.

Patki S, Kadam S, Chandra V, *et al.* (2010) Human breast milk is a rich source of multipotent mesenchymal stem cells. *Hum Cell.* 23:35–40. https://doi.org/10.1111/j.1749-0774.2010.00083.x

Pavathuparambil Abdul Manaph N, Al-Hawwas M, Bobrovskaya L, Coates PT, Zhou XF (2018) Urine-derived cells for human cell therapy. *Stem Cell Res Ther*. 9(1):189. doi:10.1186/s13287-018-0932-z.

Perin L, Giuliani S, Jin D, *et al.* (2007) Renal differentiation of amniotic fluid stem cells. *Cell Prolif*. 40(6):936-948. doi:10.1111/j.1365-2184.2007.00478.x

Perrier AL, Tabar V, Barberi T, *et al.* (2004) Derivation of midbrain dopamine neurons from human embryonic stem cells. *Proc Natl Acad Sci.* 101(34):12543-12548. doi:10.1073/pnas.0404700101.

Petrenko Y, Vackova I, Kekulova K *et al.* (2020) A Comparative Analysis of Multipotent Mesenchymal Stromal Cells derived from Different Sources, with a Focus on Neuroregenerative Potential. *Sci Rep.* 10: 4290. https://doi.org/10.1038/s41598-020-61167-z.

Phipson B, Er PX, Combes AN, *et al.* (2019) Evaluation of variability in human kidney organoids. *Nat Methods*. 16(1):79-87. doi:10.1038/s41592-018-0253-2.

Pievani A, Scagliotti V, Russo FM, *et al.* (2014) Comparative analysis of multilineage properties of mesenchymal stromal cells derived from fetal sources shows an advantage of mesenchymal stromal cells isolated from cord blood in chondrogenic differentiation potential. *Cytotherapy*.16(7):893-905. doi:10.1016/j.jcyt.2014.02.008.

Pipino C, Pandolfi A (2015) Osteogenic differentiation of amniotic fluid mesenchymal stromal cells and their bone regeneration potential. *World J Stem Cells*. 7(4):681-690. doi:10.4252/wjsc.v7.i4.681.

Peister A, Woodruff MA, Prince JJ, Gray DP, Hutmacher DW, Guldberg RE (2011) Cell sourcing for bone tissue engineering: amniotic fluid stem cells have a delayed, robust differentiation compared to mesenchymal stem cells. *Stem Cell Res*. 7(1):17-27. doi:10.1016/j.scr.2011.03.001

Pittenger MF, Discher DE, Péault BM, Phinney DG, Hare JM, Caplan AI (2019) Mesenchymal stem cell perspective: cell biology to clinical progress. *NPJ Regen Med*. 4:22. doi:10.1038/s41536-019-0083-6.

Preitschopf A, Zwickl H, Li K, *et al.* (2012) Chondrogenic differentiation of amniotic fluid stem cells and their potential for regenerative therapy. *Stem Cell Rev Rep*. 8(4):1267-1274. doi:10.1007/s12015-012-9405-4.

Prigione A, Adjaye J (2014) A mitochondrial strategy for safeguarding the reprogrammed genome. *Cell Regen (Lond).* 3(1):5. doi:10.1186/2045-9769-3-5.

Prigione A, Fauler B, Lurz R, Lehrach H, Adjaye J (2010) The senescence-related mitochondrial/oxidative stress pathway is repressed in human induced pluripotent stem cells. *Stem Cells.* 28(4):721-733. doi:10.1002/stem.404.

Prigione A, Ruiz-Pérez MV, Bukowiecki R, Adjaye J (2015) Metabolic restructuring and cell fate conversion. *Cell Mol Life Sci.* 72(9):1759-1777. doi:10.1007/s00018-015-1834-1.

Prusa AR, Marton E, Rosner M, Bernaschek G, Hengstschläger M (2003) Oct-4-expressing cells in human amniotic fluid: a new source for stem cell research?. *Hum Reprod*. 18(7):1489-1493. doi:10.1093/humrep/deg279

Quaggin SE (2016) Kindling the Kidney. *N Engl J Med.* 374(3):281-283. doi:10.1056/NEJMcibr1514351.

Rahman MS, Spitzhorn LS, Wruck W, *et al.* (2018) The presence of human mesenchymal stem cells of renal origin in amniotic fluid increases with gestational time. *Stem Cell Res Ther*. 9(1):113. doi:10.1186/s13287-018-0864-7.

Rahman MS, Rana MM, Spitzhorn LS, *et al.* (2019) Fabrication of biocompatible porous scaffolds based on hydroxyapatite/collagen/chitosan composite for restoration of defected maxillofacial mandible bone. *Prog Biomater.* 8(3):137-154. doi:10.1007/s40204-019-0113-x

Rana MM, Rahman MS, Ullah MA, et al. (2020) Amnion and collagen-based blended hydrogel improves burn healing efficacy on a rat skin wound model in the presence of wound dressing biomembrane. *Biomed Mater Eng.* 31(1):1-17. doi:10.3233/BME-201076

Ranzoni A, Corcelli M, Hau K. *et al.* (2016) Counteracting bone fragility with human amniotic mesenchymal stem cells. *Sci Rep.* 6:39656. https://doi.org/10.1038/srep39656.

Ranzoni AM, Corcelli M, Hau KL, *et al.* (2016) Counteracting bone fragility with human amniotic mesenchymal stem cells. *Sci Rep*. 6:39656. doi:10.1038/srep39656

Rauch C, Feifel E, Kern G, *et al.* (2018) Differentiation of human iPSCs into functional podocytes. *PLoS One*. 13(9):e0203869. doi:10.1371/journal.pone.0203869

Reginensi A, Enderle L, Gregorieff A, Johnson RL, Wrana JL, McNeill H (2016) A critical role for NF2 and the Hippo pathway in branching morphogenesis. *Nat Commun*. 7:12309. doi:10.1038/ncomms12309.

Reichert JC, Cipitria A, Epari DR, *et al.* (2012a) A tissue engineering solution for segmental defect regeneration in load-bearing long bones. *Sci Transl Med*. 4(141):141ra93. doi:10.1126/scitranslmed.3003720.

Reichert JC, Epari DR, Wullschleger ME, *et al.* (2012b) Knochen-Tissue-Engineering. Rekonstruktion segmentaler Knochendefekte kritischer Größe in der Schafstibia [Bone tissue engineering. Reconstruction of critical sized segmental bone defects in the ovine tibia]. *Orthopade*. 41(4):280-287. doi:10.1007/s00132-011-1855-x.

Reuter S, Gupta SC, Chaturvedi MM, Aggarwal BB (2010) Oxidative stress, inflammation, and cancer: how are they linked? *Free Radic Biol Med.* 49:1603-1616.

Rodrigue JR, Schold JD, Mandelbrot DA (2013) The decline in living kidney donation in the United States: random variation or cause for concern?. *Transplantation*. 96(9):767-773. doi:10.1097/TP.0b013e318298fa61.

Rodrigues M, Blattner C, Stuppia L (2019) Amniotic Fluid Cells, Stem Cells, and p53: Can We Stereotype p53 Functions?. *Int J Mol Sci.* 20(9):2236. doi:10.3390/ijms20092236.

Rodríguez-Vázquez M, Vega-Ruiz B, Ramos-Zúñiga R, Saldaña-Koppel DA, Quiñones-Olvera LF (2015) Chitosan and Its Potential Use as a Scaffold for Tissue Engineering in Regenerative Medicine. *Biomed Res Int*. 2015:821279. doi:10.1155/2015/821279

Romagnani P, Giglio S, Angelotti ML, *et al.* (2016) Next generation sequencing and functional analysis of patient urine renal progenitor-derived podocytes to unravel the diagnosis underlying refractory lupus nephritis. *Nephrol Dial Transplant.* 31(9):1541-1545. doi:10.1093/ndt/gfw234.

Romagnani P, Remuzzi G (2014) CD133+ renal stem cells always co-express CD24 in adult human kidney tissue. *Stem Cell Res*. 12(3):828-829. doi:10.1016/j.scr.2013.12.011.

Rosenblum ND (2008) Developmental biology of the human kidney. *Semin Fetal Neonatal Med*. 13(3):125-132. doi:10.1016/j.siny. 10.005.

Rota C, Morigi M, Imberti B (2019) Stem Cell Therapies in Kidney Diseases: Progress and Challenges. *Int J Mol Sci*. 20(11):2790. doi:10.3390/ijms20112790.

Sabapathy V, Kumar S (2016) hiPSC-derived iMSCs: NextGen MSCs as an advanced therapeutically active cell resource for regenerative medicine. *J Cell Mol Med.* 20(8):1571-1588. doi:10.1111/jcmm.12839.

Sagrinati C, Netti GS, Mazzinghi B, *et al.* (2006) Isolation and characterization of multipotent progenitor cells from the Bowman's capsule of adult human kidneys. *J Am Soc Nephrol.* 17(9):2443-2456. doi:10.1681/ASN.2006010089.

Sánchez-Romero N, Schophuizen CM, Giménez I, and Masereeuw R (2016) *In vitro* systems to study nephropharmacology: 2D versus 3D models. *Eur J Pharmacol.* 790:36–45.

Savoia A, Perna A, Di Pasquale B, *et al.* (2017) Characterization of adipose-derived stem cells freshly isolated from liposuction aspirates performed with Prolipostem®. *biomed dermatol.* 1: 1. https://doi.org/10.1186/s41702-017-0003-6

Schedl A (2007) Renal abnormalities and their developmental origin. *Nat Rev Genet*. 8(10):791-802. doi:10.1038/nrg2205.

Schneider S, Unger M, van Griensven M, Balmayor ER (2017) Adipose-derived mesenchymal stem cells from liposuction and resected fat are feasible sources for regenerative medicine. *Eur J Med Res.* 22(1):17. doi:10.1186/s40001-017-0258-9.

Schütte-Nütgen K, Finke M, Ehlert S, *et al.* (2019) Expanding the donor pool in kidney transplantation: Should organs with acute kidney injury be accepted? -A retrospective study. *PLoS One*. 14(3):e0213608. doi:10.1371/journal.pone.0213608.

Sedrakyan S, Da Sacco S, Milanesi A, *et al.* (2012) Injection of amniotic fluid stem cells delays progression of renal fibrosis. *J Am Soc Nephrol.* 23(4):661-673. doi:10.1681/ASN.2011030243.

Sell S (2013) Stem Cells Handbook. Springer Science & Business Media. New York, p. 143. ISBN 978-1-4614-7696-2. https://doi.org/10.1007/978-1-4614-7696-2

Sheyn D, Ben-David S, Shapiro G, De Mel S, Bez M, Ornelas L, Sahabian A, Sareen D, Da X, Pelled G, Tawackoli W, Liu Z, Gazit D, Gazit Z (2016) Human Induced Pluripotent Stem Cells Differentiate Into Functional Mesenchymal Stem Cells and Repair Bone Defects. *Stem Cells Transl Med.* (11):1447-1460.

Shi G, Boyle SC, Sparrow DB, Dunwoodie SL, Shioda T, de Caestecker MP (2006) The transcriptional activity of CITED1 is regulated by phosphorylation in a cell cycle-dependent manner. *J Biol Chem.* 281(37):27426-27435. doi:10.1074/jbc.M602631200.

Shrestha S, Somji S, Sens DA, *et al.* (2017) Human renal tubular cells contain CD24/CD133 progenitor cell populations: Implications for tubular regeneration after toxicant induced damage using cadmium as a model. *Toxicol Appl Pharmacol.* 331:116-129. doi:10.1016/j.taap.2017.05.038.

Shukuya K, Ogura S, Tokuhara Y, et al. (2016) Novel round cells in urine sediment and their clinical implications. *Clin Chim Acta.* 457:142-149. doi:10.1016/j.cca.2016.04.017.

Siegel N, Rosner M, Unbekandt M, *et al*. (2010) Contribution of human amniotic fluid stem cells to renal tissue formation depends on mTOR. *Hum Mol Genet.* 19(17):3320-3331. doi:10.1093/hmg/ddq236

Singh O, Gupta SS, Soni M, Moses S, Shukla S, Mathur RK (2011) Collagen dressing versus conventional dressings in burn and chronic wounds: a retrospective study. *J Cutan Aesthet Surg*. 4(1):12-16. doi:10.4103/0974-2077.79180

Siegel N, Valli A, Fuchs C, Rosner M, Hengstschläger M (2009) Induction of mesenchymal/epithelial marker expression in human amniotic fluid stem cells. *Reprod BioMed Online*.19(6):838–846. doi: 10.1016/j.rbmo.2009.09.015.

Simoni G, Colognato R (2009) The amniotic fluid-derived cells: the biomedical challenge for the third millennium. *Journal of Prenatal Medicine*. 3(3):34–36.

Sipp D, Robey PG, Turner L (2018) Clear up this stem-cell mess. *Nature.* 561(7724):455-457. doi:10.1038/d41586-018-06756-9

Sivanathan KN, Coates PT (2020) Improving human kidney function in renovascular disease with mesenchymal stem cell therapy. *Kidney Int*. 97(4):655-656. doi:10.1016/j.kint.2019.12.020.

Slamecka J, Salimova L, McClellan S, *et al.* (2016) Non-integrating episomal plasmid-based reprogramming of human amniotic fluid stem cells into induced pluripotent stem cells in chemically defined conditions. *Cell Cycle*. 15(2):234-249. doi:10.1080/15384101.2015.1121332.

Sobhani A, Khanlarkhani N, Baazm M, *et al.* (2017) Multipotent Stem Cell and Current Application. *Acta Med Iran*. 55(1):6-23.

Spitzhorn L, Megges M, Wruck W, *et al.* (2019) Human iPSC-derived MSCs (iMSCs) from aged individuals acquire a rejuvenation signature. *Stem Cell Res Ther.* 10:100.

Spitzhorn LS, Kordes C, Megges M, *et al.* (2018) Transplanted Human Pluripotent Stem Cell-Derived Mesenchymal Stem Cells Support Liver Regeneration in Gunn Rats. *Stem Cells Dev.* 27(24):1702-1714. doi:10.1089/scd.2018.0010.

Spitzhorn LS, Rahman MS, Schwindt L, *et al.* (2017) Isolation and Molecular Characterization of Amniotic Fluid-Derived Mesenchymal Stem Cells Obtained from Caesarean Sections. *Stem Cells Int*. 2017:5932706. doi:10.1155/2017/5932706

Steens J, Klein D (2018) Current Strategies to Generate Human Mesenchymal Stem Cells In Vitro. *Stem Cells Int*. 2018:6726185. doi:10.1155/2018/6726185.

Steinle H, Weber M, Behring A, *et al.* (2019) Reprogramming of Urine-Derived Renal Epithelial Cells into iPSCs Using srRNA and Consecutive Differentiation into Beating Cardiomyocytes. *Mol Ther Nucleic Acids.* 17:907-921. doi:10.1016/j.omtn.2019.07.016.

Sun YQ, Deng MX, He J, *et al.* (2012) Human pluripotent stem cell-derived mesenchymal stem cells prevent allergic airway inflammation in mice. *Stem Cells*. 30(12):2692-2699. doi:10.1002/stem.1241.

Sun YQ, Zhang Y, Li X, *et al.* (2015) Insensitivity of Human iPS Cells-Derived Mesenchymal Stem Cells to Interferon-γ-induced HLA Expression Potentiates Repair Efficiency of Hind Limb Ischemia in Immune Humanized NOD Scid Gamma Mice. *Stem Cells.* 33(12):3452-3467. doi:10.1002/stem.2094.

Sun Q, Li F, Li H, et al. (2015) Amniotic fluid stem cells provide considerable advantages in epidermal regeneration: B7H4 creates a moderate inflammation microenvironment to promote wound repair. *Sci Rep.* 5:11560. doi:10.1038/srep11560

Sutherland GR, Bain AD (1972) Culture of cells from the urine of newborn children. *Nature*. 239(5369):231. doi:10.1038/239231a0.

Takahashi K, Tanabe K, Ohnuki M, *et al.* (2007) Induction of pluripotent stem cells from adult human fibroblasts by defined factors. *Cell.* 131(5):861-872. doi:10.1016/j.cell.2007.11.019.

Takahashi K; Yamanaka S (2006) Induction of Pluripotent Stem Cells from Mouse Embryonic and Adult Fibroblast Cultures by Defined Factors. *Cell.* 126 (4): 663–676. doi:10.1016/j.cell.2006.07.024.

Takasato M, Er PX, Becroft M, *et al.* (2014) Directing human embryonic stem cell differentiation towards a renal lineage generates a self-organizing kidney. *Nat Cell Biol*. 16(1):118-126. doi:10.1038/ncb2894.

Tara F, Lotfalizadeh M, Moeindarbari S (2016) The effect of diagnostic amniocentesis and its complications on early spontaneous abortion. *Electron Physician.* 8(8):2787-2792. doi:10.19082/2787

Teodelinda M, Michele C, Sebastiano C, Ranieri C, Chiara G (2011) Amniotic liquid derived stem cells as reservoir of secreted angiogenic factors capable of stimulating neo-arteriogenesis in an ischemic model. *Biomaterials*. 32(15):3689–3699. doi: 10.1016/j.biomaterials.2011.01.071.

Thiagarajan RD, Georgas KM, Rumballe BA, *et al.* (2011) Identification of anchor genes during kidney development defines ontological relationships, molecular subcompartments and regulatory pathways. *PLoS One.* 6(2):e17286. doi:10.1371/journal.pone.0017286.

Thieme CJ, Weist BJD, Mueskes A, *et al.* (2019) The TreaT-Assay: A Novel Urine-Derived Donor Kidney Cell-Based Assay for Prediction of Kidney Transplantation Outcome. *Sci Rep*. 9(1):19037. doi:10.1038/s41598-019-55442-x.

Thomson JA, Itskovitz-Eldor J, Shapiro SS, *et al.* (1998) Embryonic stem cell lines derived from human blastocysts. *Science.* 282(5391):1145-1147. doi:10.1126/science.282.5391.1145.
Tojo A, Kinugasa S (2012) Mechanisms of glomerular albumin filtration and tubular reabsorption. *Int J Nephrol*. 2012:481520. doi:10.1155/2012/481520.

Tojo A, Kinugasa S (2012) Mechanisms of glomerular albumin filtration and tubular reabsorption. *Int J Nephrol.* 481520. doi:10.1155/2012/481520.

Tong GX, Yu WM, Beaubier NT, *et al.* (2009) Expression of PAX8 in normal and neoplastic renal tissues: an immunohistochemical study. *Mod Pathol*. 22(9):1218-1227. doi:10.1038/modpathol.2009.88.

Torricelli F, Brizzi L, Bernabei PA, *et al.* (1993) Identification of hematopoietic progenitor cells in human amniotic fluid before the 12th week of gestation. *Italian Journal of Anatomy and Embryology.* 98(2):119–126.

Tran C, Damaser MS (2015) The potential role of stem cells in the treatment of urinary incontinence. *Ther Adv Urol.* 7(1):22-40. doi:10.1177/1756287214553968.

Tsai MS, Hwang SM, Chen KD, *et al.* (2007) Functional network analysis of the transcriptomes of mesenchymal stem cells derived from amniotic fluid, amniotic membrane, cord blood, and bone marrow. *Stem Cells*. 25(10):2511-2523. doi:10.1634/stemcells. 2007-0023.

Ullah I, Subbarao RB, Rho GJ (2015) Human mesenchymal stem cells - current trends and future prospective. *Biosci Rep*. 35(2):e00191. doi:10.1042/BSR20150025

Ullah M, Liu DD, Thakor AS (2019) Mesenchymal Stromal Cell Homing: Mechanisms and Strategies for Improvement. *iScience.* 15:421-438. doi:10.1016/j.isci.2019.05.004

Umrath F, Weber M, Reinert S, Wendel HP, Avci-Adali M, Alexander D (2020) iPSC-Derived MSCs Versus Originating Jaw Periosteal Cells: Comparison of Resulting Phenotype and Stem Cell Potential. *Int J Mol Sci*. 21(2):587. doi:10.3390/ijms21020587.

Underwood MA, Gilbert WM, Sherman MP (2005) Amniotic fluid: not just fetal urine anymore. *J Perinatol*. 25(5):341-348. doi:10.1038/sj.jp.7211290.

Vajjhala PR, Macmillan E, Gonda T, Little M (2003) The Wilms' tumour suppressor protein, WT1, undergoes CRM1-independent nucleocytoplasmic shuttling. *FEBS Lett*. 554(1-2):143-148. doi:10.1016/s0014-5793(03)01144-x.

Velissariou V, Antoniadi T, Gyftodimou J, *et al.* (2002) Maternal uniparental isodisomy 20 in a foetus with trisomy 20 mosaicism: clinical, cytogenetic and molecular analysis. *Eur J Hum Genet.* 10(11):694-698. doi:10.1038/sj.ejhg.5200867.

Vlahova F, Hawkins KE, Ranzoni AM, *et al.* (2019) Human mid-trimester amniotic fluid (stem) cells lack expression of the pluripotency marker OCT4A. *Sci Rep*. 9(1):8126. doi:10.1038/s41598-019-44572-x.

Wagner W, Bork S, Horn P, Krunic D, Walenda T, Diehlmann A, Benes V, Blake J, Huber FX, Eckstein V, Boukamp P, Ho AD (2009) Aging and replicative senescence have related effects on human stem and progenitor cells. *PLoS One.* 4(6):e5846.

Wagner W, Ho AD, Zenke M (2010) Different facets of aging in human mesenchymal stem cells. *Tissue Eng Part B Rev.* 16(4):445-53.

Wagner W, Horn P, Castoldi M, Diehlmann A, Bork S, Saffrich R, Benes V, Blake J, Pfister S, Eckstein V, Ho AD (2008) Replicative senescence of mesenchymal stem cells: a continuous and organized process. *PLoS One*. 3(5):e2213.

Wang H, Gomez JA, Klein S, *et al.* (2013) Adult renal mesenchymal stem cell-like cells contribute to juxtaglomerular cell recruitment. *J Am Soc Nephrol*. 24(8):1263-1273. doi:10.1681/ASN.2012060596.

Wang X, Kimbrel EA, Ijichi K, *et al.* (2014) Human ESC-derived MSCs outperform bone marrow MSCs in the treatment of an EAE model of multiple sclerosis. *Stem Cell Reports.* 3(1):115-130. doi:10.1016/j.stemcr.2014.04.020.

Wang X, Xing H, Zhang G, Wu X, Zou X, Feng L, Wang D, Li M, Zhao J, Du J, Lv Y, Lingling E, Liu H (2016) Restoration of a critical mandibular bone defect using human alveolar bone-derived stem cells and porous nano-HA/collagen/PLA scaffold. *Stem Cells Int.* 2016:8741641. https://doi.org/10.1155/2016/8741641

Wang X, Wu X, Xing H, Zhang G, Shi Q, Lingling E, Liu N, Yang T, Wang D, Qi F, Wang L, Liu H (2017a) Porous nanohydroxyapatite/collagen scaffolds loading insulin PLGA particles for restoration of critical size bone defect. *ACS Appl Mater Interfaces*. 9(13):11380–11391. https://doi.org/10.1021/acsami.6b13566

Wang M, Li H, Si J, *et al.* (2017b) Amniotic fluid-derived stem cells mixed with platelet rich plasma for restoration of rat alveolar bone defect. *Acta Biochim Biophys Sin (Shanghai)*. 49(3):197-207. doi:10.1093/abbs/gmw133

Warnke PH, Springer IN, Wiltfang J, *et al.* (2004) Growth and transplantation of a custom vascularised bone graft in a man. *Lancet*. 364(9436):766-770. doi:10.1016/S0140-6736(04)16935-3.

Wolfrum K, Wang Y, Prigione A, Sperling K, Lehrach H, Adjaye J (2010) The LARGE principle of cellular reprogramming: lost, acquired and retained gene expression in foreskin and

amniotic fluid-derived human iPS cells. *PLoS One*. 5(10):e13703. doi:10.1371/journal.pone.0013703.

Wu H, Uchimura K, Donnelly EL, Kirita Y, Morris SA, Humphreys BD (2018) Comparative Analysis and Refinement of Human PSC-Derived Kidney Organoid Differentiation with Single-Cell Transcriptomics. *Cell Stem Cell.* 23(6):869-881.e8. doi:10.1016/j.stem.2018.10.010.

Wu R, Huang C, Wu Q, *et al.* (2019) Exosomes secreted by urine-derived stem cells improve stress urinary incontinence by promoting repair of pubococcygeus muscle injury in rats. *Stem Cell Res Ther.* 10:80. https://doi.org/10.1186/s13287-019-1182-4.

Xinaris C, Benedetti V, Novelli R, *et al.* (2016) Functional Human Podocytes Generated in Organoids from Amniotic Fluid Stem Cells. *J Am Soc Nephrol*. 27(5):1400-1411. doi:10.1681/ASN.2015030316.

Yamaguchi K, Shirakabe K, Shibuya H, *et al.* (1995) Identification of a member of the MAPKKK family as a potential mediator of TGF-beta signal transduction. *Science*. 270(5244):2008-2011. doi:10.1126/science.270.5244.2008.

Yamahara K, Hamada A, Soma T, *et al.* (2019) Safety and efficacy of amnion-derived mesenchymal stem cells (AM01) in patients with steroid-refractory acute graft-versus-host disease after allogeneic haematopoietic stem cell transplantation: a study protocol for a phase I/II Japanese trial. *BMJ Open.* 9(7):e026403. doi:10.1136/bmjopen-2018-026403.

Yuki K, Fujiogi M, Koutsogiannaki S (2020) COVID-19 pathophysiology: A review. *Clin Immunol.* 215:108427. doi:10.1016/j.clim.2020.108427.

Zagoura DS, Roubelakis MG, Bitsika V, *et al.* (2012) Therapeutic potential of a distinct population of human amniotic fluid mesenchymal stem cells and their secreted molecules in mice with acute hepatic failure. *Gut*. 61(6):894-906. doi:10.1136/gutjnl-2011-300908.

Zavatti M, Bertoni L, Maraldi T, *et al.* (2015) Critical-size bone defect repair using amniotic fluid stem cell/collagen constructs: effect of oral ferutinin treatment in rats. *Life Sci.* 121:174-183. doi:10.1016/j.lfs.2014.10.020.

Zeisberg M (2006) Bone Morphogenic protein 7 and the kidney: current concepts and open questions. *Nephrol Dial Transplant.* 21:568–573. doi: 10.1093/ndt/gfk010.

Zeisberg M, Shah AA, Kalluri R (2005) Bone morphogenic protein-7 induces mesenchymal to epithelial transition in adult renal fibroblasts and facilitates regeneration of injured kidney. *J Biol Chem*. 280(9):8094-8100. doi:10.1074/jbc.M413102200.

Zhang D, Wei G, Li P, Zhou X, Zhang Y (2014) Urine-derived stem cells: A novel and versatile progenitor source for cell-based therapy and regenerative medicine. *Genes Dis*. 1(1):8-17. doi:10.1016/j.gendis.2014.07.001

Zhang X, Xu M, Liu X, Zhang F, Wei Y, Meng S, Dai X, Duan A, Deng X (2013) Restoration of critical-sized defects in the rabbit mandible using autologous bone marrow stromal cells hybridized with nano-β-tricalcium phosphate/collagen scaffolds. *J Nanomater.* 2013:913438. https://doi.org/10.1155/2013/913438

Zhang Y, McNeill E, Tian H, *et al.* (2008) Urine derived cells are a potential source for urological tissue reconstruction. *J Urol*. 180(5):2226-2233. doi:10.1016/j.juro.2008.07.023.

Zhou T, Benda C, Duzinger S, *et al.* (2011) Generation of induced pluripotent stem cells from urine. *J Am Soc Nephrol*. 22(7):1221-1228. doi:10.1681/ASN.2011010106.

Zhu Q, Li Q, Niu X, *et al.* (2018) Extracellular Vesicles Secreted by Human Urine-Derived Stem Cells Promote Ischemia Repair in a Mouse Model of Hind-Limb Ischemia. *Cell Physiol Biochem*. 47(3):1181-1192. doi:10.1159/000490214.

8. Acknowledgements

First and foremost, I would like to express my outermost gratitude to the Almighty who kept me healthy during the Covid 19 pandemic and reached the end point of my PhD thesis. Entirely during my doctoral journey, the person who guided me from start to end was Prof. Dr. James Adjaye, my supervisor. I would like to acknowledge him greatest level. He created the environment very easy going and stress free from the beginning as I came as an overseas student. At the scientific level, he always forwarded his hands and advised instantly like a father figure when I felt any difficulties during the four years of the trip. I learned a lot from him not only about scientific aspects but also for personal development as a human being. It would have been impossible without his direct guidance, inspiration and assistance. He is a great teacher and more importantly, he is a wonderful human being. It was a great honour to be a member of Prof. Adjaye's group.

Regarding my colleagues, I must have to mention first none other than Dr. Lucas-Sebastian Spitzhorn to whom I am grateful who constantly provided me proper suggestions like a brother and taught me immensely in every way. Secondly, I would like to thank, the most humble man I have ever seen, Dipl.-Ing. Wasco Wruck who helped to carry the bioinformatics analysis throughout the doctoral research. On the ground of laboratory work, I should have to express special gratitude to Martina Bohndorf for her extended expert hands to overcome experimental problems and to learn new experimental procedures whenever I need. Of course, I am grateful to Dr. Nina Graffmann, Dr. Jörg Otte, Dr. Lars Erickshen, Soraia Martins, Audrey Ncube, Silke Wehrmeyer, Osmond Adjei and Thien Dieu Lisa Nguyen for their friendly support, encourage and amazing help. I am glad that I get to know great people like you all. I hope my relationship with Adjaye's lab and the friendship with you people will continue coming decades.

Out of my working station, I would like to thank Prof. Dr. Tanja Fehm, Department of Obstetrics and Gynaecology for providing the amniotic fluid. I also appreciate the collaboration from Dr. Pascale V. Guillot, Institute for Women's Health, Maternal and Fetal Medicine Department, University College London, and Prof. Dr. Richard O. C. Oreffo, Bone and Joint Research Group, Centre for Human Development, Stem Cells and Regeneration, Institute of Developmental Sciences, University of Southampton, UK. I am also grateful to Dr. SM Asaduzzaman (CSO), Institute for Tissue Banking and Biomaterial Research, Atomic Energy Research Establishment, Bangladesh for his collaboration. I also express very special thanks to Prof. Dr. Constantin Czekelius for being my co-supervisor and helped for the continuation of funding. I would like to express my gratitude to my examination committee members for their

valuable time to review my thesis. A special appreciation goes to Deutscher Akademischer Austauschdienst (DAAD) for providing fund and generous help in administrative things.

Apart from academia, it was great to have Ms. Rita Ofterdinger, whose love and help directly cherished my family's social life in Germany whenever needed. She was always open and supportive to make life enjoyable and easy for my wife and son. I would like to mention my beautiful wife- Mst Zinia Tasnim who has been accompanying me throughout this journey. I could not know how to express her contribution that has significant impact as she sacrificed her carrier as computer engineer just because to company me. Her unconditional support and love have been essential all these years. Thanks her so much to have such a precious gift-our child Ehan Qareeb Rahman who fulfil my life with joy and have been explored a different flavour and purpose of life to me.

Yet most importantly, I owe thank wholeheartedly to my all-time teachers and umbrella- my parents who always love, keep blessing and show me the ways of life to be a good person. As my father always said me, 'work hard and never disheartened your supervisor, since Prof. Adjaye has accepted you in his lab without knowing your scientific aptitude directly but based only on your documents'.

9. Curriculum Vitae

PERSONAL INFORMATION

Family Name: Rahman, First Name: Md Shaifur

Contact Address

Institute for Stem Cell Research and Regenerative Medicine, University Hospital Düsseldorf, Germany

+49015215712829 (Personal) +49 (0)211 81-08816 (Official)

msr.tbbru.bd@gmail.com (Personal)

Sex Male | Date of birth 21/09/1984 | Nationality Bangladeshi

ACADEMIC BACKGROUND

1. Doctoral candidate, Institute for Stem Cell Research and Regenerative Medicine, Heinrich Heine University Düsseldorf, Germany (Expected completion date December. 2020)
Thesis: Establishment of Human Amniotic Fluid and Urine as Sources for Mesenchymal Stem Cells of Renal Origin with Versatile Regenerative Potential
Lab: Prof. Dr. James Adjaye, Institute for Stem Cell Research and Regenerative Medicine, University Hospital, Heinrich Heine University Düsseldorf, Germany.

2. Erasmus Mundus Masters in Bio-Health Computing, Université Joseph Fourier, France (2013).
Thesis: Identification of the regions responsible for the interaction of MCPH proteins ASPM and CITK
Lab: Prof. Dr. med. Ferdinando Di Cunto, Neuroscience & Bioinformatics Group, Molecular Biotechnology Centre, Turin, Italy.

3. Master of Science in Biotechnology and Genetic Engineering, Khulna University, Bangladesh (2011).
Thesis: Characterization of putative interaction partner's (Ctc1 and Grcc10) of Zfp819.
Lab: Prof. Dr. med. Wolfgang Engel, Stem Cell Biology Group, Institute of Human Genetics, Göttingen, Germany.

4. Bachelor of Science in Biotechnology and Genetic Engineering, Khulna University, Bangladesh (2008).
Thesis: Potential of Fine Needle Aspiration Cytology (FNAC) in the Diagnosis of Tumor in Bangladesh.
Lab: Prof. Dr. med. Moni Mohan Saha, Lab of Onco-pathology, Khulna Medical College and Hospital, Bangladesh.

PUBLICATIONS

Rahman MS, Wruck W, Spitzhorn LS, Nguyen L, Bohndorf M, Martins S, Asar F, Ncube A, Erichsen L, Graffmann N, Adjaye J. The FGF, TGFβ and WNT axis Modulate Self-renewal of Human SIX2 (+) Urine Derived Renal Progenitor Cells. *Sci Rep.* 2020;10(1):739. doi: 10.1038/s41598-020-57723-2. PubMed PMID: 31959818. (IF 4.01).

Rahman MS, Akhtar N, Jamil HM, Banik RS, Asaduzzaman SM. TGF-β/BMP signaling and other molecular events: regulation of osteoblastogenesis and bone formation. *Bone Res.* 2015;3:15005. doi: 10.1038/boneres.2015.5. PubMed PMID: 26273537 (IF 12.34)

Jungbluth P, Spitzhorn LS, Grassmann J, Tanner S, Latz D, **Rahman MS**, Bohndorf M, Wruck W, Sager M, Grotheer V, Kröpil P, Hakimi M, Windolf J, Schneppendahl J, Adjaye J. Human iPSC-derived iMSCs improve bone regeneration in mini-pigs. *Bone Res.* 2019 Oct 24;7:32. doi: 10.1038/s41413-019-0069-4. PubMed PMID: 31667001 (IF 12.34)

Rahman MS, Islam R, Rana MM, Spitzhorn LS, Rahman MS, Adjaye J, Asaduzzaman SM. Characterization of burn wound healing gel prepared from human amniotic membrane and Aloe vera extract. *BMC Complement Altern Med*. 2019;19(1):115. doi: 10.1186/s12906-019-2525-5. PubMed PMID: 31159783 (IF 2.48)

Rahman MS, Spitzhorn LS, Wruck W, Hagenbeck C, Balan P, Graffmann N, Bohndorf M, Ncube A, Guillot PV, Fehm T, Adjaye J. The presence of human mesenchymal stem cells of renal origin in amniotic fluid increases with gestational time. *Stem Cell Res Ther.* 2018;9(1):113. doi: 10.1186/s13287-018-0864-7. PubMed PMID: 29695308 (IF 4.62)

Spitzhorn LS, **Rahman MS**, Schwindt L, Ho HT, Wruck W, Bohndorf M, Wehrmeyer S, Ncube A, Beyer I, Hagenbeck C, Balan P, Fehm T, Adjaye J. Isolation and Molecular Characterization of Amniotic Fluid-Derived Mesenchymal Stem Cells Obtained from Caesarean Sections. *Stem Cells Int.* 2017;2017:5932706. PMID: 29225627 (IF 3.94) (equal first author).

Hasan KM, **Rahman MS**, Arif KM, Sobhani ME. Psychological stress and aging: role of glucocorticoids (GCs). *Age* (Dordr). 2012;34(6):1421-33. doi:10.1007/s11357-011-9319-0. PubMed PMID: 21971999 (IF 6.44)

Spitzhorn LS, Megges M, Wruck W, **Rahman MS**, Otte J, Degistirici Ö, Meisel R, Sorg RV, Oreffo ROC, Adjaye J. Human iPSC-derived MSCs (iMSCs) from aged individuals acquire a rejuvenation signature. *Stem Cell Res Ther.* 2019;10(1):100. doi: 10.1186/s13287-019-1209-x. PubMed PMID: 30885246. (IF 4.62)

Rahman MS, Akhtar N, Hasan MZ, Asaduzzaman SM. Human tissue banking in Bangladesh: hope for the patients of massive burns, surgical wound and bone associated complications. *Int J Burns Trauma*. 2019;9(2):23-27. PubMed PMID: 31149389.

Rahman MS, Rana MM, Spitzhorn LS, Akhtar N, Hasan MZ, Choudhury N, Fehm T, Czernuszka JT, Adjaye J, Asaduzzaman SM. Fabrication of biocompatible porous scaffolds based on hydroxyapatite/collagen/chitosan composite for restoration of defected maxillofacial mandible bone. *Prog Biomater.* 2019;8(3):137-154. doi: 10.1007/s40204-019-0113-x. PubMed PMID: 31144260.

Akhtar N, **Rahman MS**, Jamil HM, Arifuzzaman M, Miah MM, Asaduzzaman SM. Tissue banking in Bangladesh: 12 years of experience (2003-2014). *Cell Tissue Bank*. 2016;17(2):189-97. doi: 10.1007/s10561-016-9549-6. PubMed PMID: 26915083. (IF 1.93)

Rana MM, **Rahman MS**, Ullah MA, Siddika A, Hossain ML, Akhter MS, Hasan MZ, Asaduzzaman SM. Amnion and collagen based blended hydrogel improves burn healing efficacy on rat skin wound model in presence of wound dressing bio-membrane. *Bio-Medical Materials and Engineering*. 2020.

Peter Brown, RELISH Consortium, Yaoqi Zhou. Large expert-curated database for benchmarking document similarity detection in biomedical literature search. *Database*, 2019. https://doi.org/10.1093/database/baz085. **Md Shaifur Rahman** as a co-author under RELISH Consortium.

Hasan MZ, **Rahman MS**, Diba F, Hossain ML, Akhtar N, Siddika A, Adnan MH, Jorge MP, Asaduzzaman SM. Human bone and amniotic membrane banking in Bangladesh for allografting: The impact of the International Atomic Energy Agency (IAEA). *Cell and Tissue Banking*. 2020.

Rahman MS, Spitzhorn LS, Bohndorf M, Tanja Fehm, Adjaye J. Spontaneous chromosome loss-gain-loss during iPSCs generation from full-term human AF-MSCs with chromosomes 18T. 2020. Manuscript in preparation.

Md Shaifur Rahman, Lucas Sebastian-Spitzhorn, Tanja Fehm, James Adjaye. Derivation of CK14+/CK5+ keratinocyte like cells from third trimester amniotic fluid cells. 2020. Manuscript in preparation.

Md Shaifur Rahman, Lucas-Sebastian Spitzhorn, James Adjaye. Human Mesenchymal Stem Cells (MSCs) with Enormous Regenerative Potential: A Quest for Non-invasive and Robust Sources of MSCs. 2020. Manuscript in preparation.

Book Chapter: Graffmann N, Spitzhorn LS, Martins S, **Rahman MS**, Nguyen L, Adjaye J (2020) Stem Cell Therapy. In: Hock F., Gralinski M. (eds). *Drug Discovery and Evaluation: Methods in Clinical Pharmacology*. Springer, Cham.

CONFERENCES ABSTRACTS / POSTERS / PRESENTATION

Poster/Abstract: **Md Shaifur Rahman**, Lucas-Sebastian Spitzhorn, Huyen-Tran Ho, Martina Bohndorf , Wasco Wruck, Laura Schwindt, Audrey Ncube, Carsten Hagenbeck, Percy Balan, Ines Beyer, Tanja Fehm, James Adjaye (2017) Dissecting the Complexity in Amniotic Fluid-Derived Cells Obtained from Caesarean Sections. 9th International Meeting, Muenster, NRW stem cell network, Germany.

Poster/Abstract: Lucas-Sebastian Spitzhorn, Pascal Jungbluth, Jan Grassmann, Stephan Tanner, **Md Shaifur Rahman**, Martina Bohndorf, Wasco Wruck, Martin Sager, Vera Grotheer, Joachim Windolf, Johannes Schneppendahl, James Adjaye (2018) Human fetal foreskin iPSC-derived iMSCs support regeneration in a Goettingen mini-pig bone defect model. Stem Cell Community Day, Duesseldorf, Germany.

Abstract/Presentation: **Md Shaifur Rahman**, Wasco Wruck, Lucas-Sebastian Spitzhorn, Lisa Nguyen, Martina Bohndorf, Soraia Martins, Fatima Asar, Audrey Ncube, Lars Erichsen, Nina Graffmann, James Adjaye (2019) The FGF, TGFβ and WNT axis modulate self-renewal of human SIX2+ urine derived renal progenitor cells. NRW stem cell network-retreat, Bonn, Germany.

Poster/Abstract: **Md Shaifur Rahman**, Lucas-Sebastian Spitzhorn, Wasco Wruck, Carsten Hagenbeck, Percy Balan, Nina Graffmann, Martina Bohndorf, Audrey Ncube, Pascale V Guillot, Tanja Fehm, James Adjaye. Third trimester amniotic fluid harbors mesenchymal stem cells of renal origin. 6th International meetings of GSCN, Heidelberg, Germany. 2018.

Poster/Abstract: Lucas-Sebastian Spitzhorn, Pascal Jungbluth, Jan Grassmann, Stephan Tanner, **Md Shaifur Rahman**, Martina Bohndorf, Wasco Wruck, Martin Sager, Vera Grotheer, Joachim Windolf, Johannes Schneppendahl, James Adjaye. Human iPSC-derived iMSCs improve regeneration in mini-pig. 6th International meetings of GSCN, Heidelberg. Germany.

PREVIOUS WORK EXPERIENCES

(2014-2016): **Scientific Officer,** Institute of Tissue Banking and Biomaterial Research, Atomic Energy Research Establishment, Ministry of Science and Technology, Bangladesh. Responsible for developing acceptable work policies and procedures that meet Tissue banking regulatory standards. Amniotic membrane and bone allograft processing and quality control. Human amniotic fluid derived molecules and cells isolation. Integral secondary job duties include hiring undergrad and master's students, training them for the specific research projects and supervising their research.

(2014-2015): **Lecturer (Part time)**, Department of Biotechnology and Genetic Engineering, Jahangirnagar University, Bangladesh. Mainly responsible for conducting cell Signalling and developmental biology course for Bachelor student.

PROFESSIONAL TRAINING / COURSES / WORKSHOP

Professional training on '*Tissue Banking and Advanced Therapies*'. DTI Barcelona, Spain. (3 months)
EMBL Course: Genome Engineering: CRISPR/Cas from Cells to Mice. Heidelberg, Germany. (8 days)
Training on '*Scientific Image Processing and Analysis*'. med RSD, Düsseldorf, Germany. (2 days)
EuroGTP II course: Good Practices for demonstrating safety and quality through recipient follow-up.
Seminar on '*Good Scientific Practice*'. iGRAD, Düsseldorf, Germany. (2 days)
Training on '*Optimizing Writing Strategies for Publishing Research in English*'. iGRAD, Düsseldorf, Germany. (2 days)
Workshop on '*Time Management*'. iGRAD, Düsseldorf, Germany. (2 days)
Workshop on '*The GMP-Quality Standard and Its Benefits for Research and Development*'. Essen, Germany. (1 day)
Seminar on '*The Two Faces of Processing ATMPs-Advanced Therapy Medicinal Products*'. Düsseldorf, Germany. (1 day)
Workshop on '*Get into Teaching*'. iGRAD, Düsseldorf, Germany. (2 days)
Workshop on '*Project Management in Science*. iGRAD, Düsseldorf, Germany. (2 days)
Course on *'Human Genetics'*. Institute of Human Genetics, University of Göttingen, Germany. (2 months)
Course on *'Developmental Biology of Vertebrates'.* MPI for Biophysical Chemistry, Göttingen, Germany. (2 months)

LAB INSTRUMENTAL, TEACHNICAL AND OTHER SKILLS

Cell Culture: Amniotic fluid-derived mesenchymal stem cells (AF-MSCs), Urine-derived renal progenitor cells (UdRPCs), uMSCs, BM-fMSCs, iPSCs, iMSCs, Human ESC, 3T3, HEK293T, and HaCat.

Assay and Techniques: Reprogramming (iPSC generation), Transfection, CRISPR-Cas base genome editing, qRT-PCR, Western blot, Co-IP, FACs, Immunostaining, Fluorescence microscopy and image analysis.

Scientific communication skills: Presented data clearly and confidently to both in small and large groups, at home or abroad in English. Wrote scientific articles in international peer-reviewed journals, as well as produced regular progression reports.

Laboratory managerial skills: Managed and planned work to achieve goals on time and set realistic objectives. Supervised Bachelor and Master Students, help to adapting with different scientific levels and backgrounds.

SCHOLARSHIP/AWARDS

DAAD Scholarship (91607303/ ST34), Heinrich Heine University Düsseldorf, Germany. (2016 to now)
Erasmus Mundus Scholarship, University of Joseph Fourier, Grenoble, France. (2012-2013)
Erasmus Mundus-EXPERT- Exchange Asia Scholarship, University of Göttingen. (2011-2012)
NSICT Masters Fellowship, Ministry of Science and Technology, Govt. of Bangladesh. (2010-2011)
USDA: Agro-Biotech Masters Fellowship, Khulna University, Bangladesh. (2009-2010)
BSc and MS Merit Scholarship with Distinction, Khulna University, Bangladesh. (2004-2010)

ADDITIONAL INFORMATION

Language skills: English (Proficient user as working language), Bengali (Mother language), and German (Basic user).

Memberships: Ex-Member of Erasmus Mundus Student Council, Grenoble, France.
Ex-Member, Tissue Engineering & Regenerative Medicine International Society (TERMIS), USA.
Member, Society for Experimental Biology and Medicine, USA.
Member, Bangladesh Association for Tissue Banking, Bangladesh.
Member, Bangladesh Biotechnologist Association, Bangladesh.
Ex-Divisional Editor, Medical and Molecular Biotechnology Division, Biotech Magazine, Bangladesh.

Leisure activity: Travelling, Fishing, Playing Football and Badminton.

REFERENCES

Prof. Dr. James Adjaye: Institute for Stem Cell Research and Regenerative Medicine, University Hospital Düsseldorf, Heinrich Heine Universität Düsseldorf, Moorenstr. 5, 40225 Düsseldorf, Germany. Tele: +49(0)21181–08191, Fax: +49(0)21181– 17858, Email: James.Adjaye@med.uni-duesseldorf.de

Prof. Dr. Ferdinando Di Cunto: Molecular Biotechnology Center, University of Torino, Via Nizza 52, 10126 Torino, Italy. Tele: +39-011-6706409, Fax: +39-011-6706432, Email: ferdinando.dicunto@unito.it

Prof. Dr. Eva Estebanez-Perpina: Parc Cientific de Barcelona, Institute of Biomedicine, University of Barcelona, Spain. Tele: (00-34) 93-403-11-19, Email: evaestebanez@ub.edu

Prof. Dr. Laura Herrero: Dept. of Biochemistry and Molecular Biology, University of Barcelona, Barcelona E-08028, Spain. Tele: (+34) 934 024 522, Fax: (+34) 934 024 520, Email: lherrero@ub.edu

CSO Dr. Sikder M Asaduzzaman: Institute of Tissue Banking and Biomaterial Research, Atomic Energy Research Establishment, Dhaka, Bangladesh. Tele: +88-02-7789034, Fax: +88-02-7789037, Email: sikderasad@yahoo.com

DECLARATION

I hereby certify that all information presented in the Curriculum Vitae is complete and correct to the best of my knowledge.

Date: 30.10.2020; Düsseldorf, Germany

Md Shaifur Rahman

10. Declaration of Authorship

I, Md Shaifur Rahman declare that this thesis and the work presented in it are my own and has been generated by me as the result of my own original research.

Title of thesis: Establishment of Human Amniotic Fluid and Urine as Sources for Mesenchymal Stem Cells of Renal Origin with Versatile Regenerative Potential

I confirm that:

1. This work was done wholly or mainly while in candidature for a PhD degree at Heinrich-Heine-Universität Düsseldorf.
2. Where any part of this thesis has previously been submitted for a degree or any other qualification at this University or any other institution, this has been clearly stated.
3. Where I have consulted the published work of others, this is always clearly attributed.
4. Where I have quoted from the work of others, the source is always given. With the exception of such quotations, this thesis is entirely my own work.
5. I have acknowledged all main sources of help.
6. Where the thesis is based on work done by myself jointly with others, I have made clear exactly what was done by others and what I have contributed myself.

Author name: Md Shaifur Rahman

Signed: 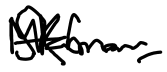

Date: 28.04.2021

Place: Duesseldorf, Germany.